INVESTIGATIONS OF URINARY ALPHA-1 ACID GLYCOPROTEIN.

by

KELSEY ELIZABETH JOYCE

A thesis submitted to the University of Birmingham for the degree of

DOCTOR OF PHILOSOPHY

School of Sport, Exercise, and Rehabilitation Sciences
College of Life and Environmental Sciences
University of Birmingham
February 2021

ABSTRACT

The primary objective of this thesis was to investigate the mechanisms of post-exercise and altitude-induced proteinuria by measuring urinary alpha-1 acid glycoprotein (α1-AGP), a sensitive marker of glomerular leak. Following a review of literature providing the rationale for urinalysis of α1-AGP (Chapters 1 and 2), initial experimental chapters outlined the development and validation of a novel immunoturbidimetric assay for low-concentration α1-AGP (Chapter 3), as well as, the application and analysis completed to establish a normative reference range from collected samples and a systematic literature review (Chapter 4). The novel immunoassay was further utilised to evaluate the contribution of hypoxia to post-exercise and altitude-induced α1-AGP excretion, combining data from field- and chamber-based studies (Chapters 5 and 6). The final experimental chapter (Chapter 7) examined α1-AGP excretion during ascent to high altitude, but without an acute exercise stimulus. The synthesis of the thesis findings and discussion of future directions (Chapter 8) highlighted that profound systemic hypoxaemia did not influence the degree of post-exercise proteinuria, which was more attributable to exercise intensity, however, nocturnal oxygenation during ascent did influence altitude-induced α1-AGP excretion. Collectively, this thesis advances techniques for the urinalysis of α1-AGP and increases understanding of the causes of post-exercise and altitude-induced proteinuria.

Dedication

This thesis is dedicated to Jo Bradwell and the fellowship from the Birmingham Medical Research Expeditionary Society.

"It is not the mountains we conquer, but ourselves."

– Sir Edmond Hillary

Acknowledgements

It has been with great honour that I have represented the JABBS Foundation over the last few years. Thank you to the foundation for the financial support that has funded this doctoral studentship at the University of Birmingham. Without this support I would not have gained the academic, professional, or life experiences that I had during these last few years.

I would also like to thank Gregg Wallis, Alex Cook, Amy Fountain, and Abi Cross from the Research and Development Department at The Binding Site, Ltd. for sharing their expertise (and lab bench space) related to immunoassay development and validation. In addition, I would like to thank Robert Williams and Jess Winfield from the Biochemistry Department at Heartlands Hospital Birmingham NHS Trust for their assistance with the secondary urinalysis. A very special thanks to Drs Courtney Wheatley-Guy and Bruce Johnson from the Johnson Lab (Rochester and Scottsdale campuses) at the Mayo Clinic for being gracious enough to lend the pulse oximeters for field-based data collections.

I would also like to thank Dr George Balanos for his kindness and support throughout the duration of this experience, as well as, sharing his expertise related to the dynamic end-tidal forcing system. I must also thank my incredibly supportive parents, for their positivity and encouragement throughout, despite being an ocean away.

A big thank you to Ms Amy Cogswell for her enthusiasm, positivity, and support (and sanity) leading up to our departure to Sikkim. I would also like to express my upmost appreciation for all Mountain Kingdoms and Rimo Expeditions team members, whom were all integral to the success and safety of the expedition to top camp near Zema Glacier in the northeast Indian Himalaya. A special thank you to Chewang Motup, Tsewang Sherpa, Jangu Sherpa, and Noah Sherpa from Rimo Expeditions for their elegance and grace en route to 4,800

m. A special thanks also to John Delamere for his dedication to expeditionary research, mentorship, and friendship throughout.

Last but not least, I am most grateful for Dr Sam Lucas and his patience, guidance, humour, and unwavering support throughout.

To all of those mentioned here and any whom I have forgot, thank you.

Publications and proceedings during PhD studies

Lucas SJE, Malein W, Thomas OD, Ashdown KM, Rue CA, **Joyce KE**, Newman C, Cadigan P, Johnson B, Myers SD, Myers FA, Wright AD, Delamere J, Imray CHE, Bradwell AR, Edsell M, and the Birmingham Medical Research Expeditionary Society. Effect of losartan on performance and physiological responses to exercise at high altitude (5,035 m). *BMJ Open Sport and Exercise Medicine.* 2020; 7(1). DOI: 10.1136/bmjsem-2020-000982.

Joyce KE, Delamere J, Ashdown K, Bradley C, Lucas RAI, Thomas O, Lock H, Talks B, Malein W, Lewis CT, Cross A, Letchford A, Bradwell AR, Lucas SJE and the Birmingham Medical Research Expeditionary Society. Nocturnal oxygen saturation is related to increased urinary alpha-1 acid glycoprotein during ascent to 4,800 metres. *25th Anniversary Congress European College of Sport Science.* 2020; Abstract-ID: 265.

Joyce KE, Weaver SR, Lucas SJE. Geographic components of SARS-CoV-2 expansion: a hypothesis. *J Appl Physiol.* 2020; 129: 257 – 262. doi: 10.1152/japplphysiol.00362.2020.

Joyce KE, Bradwell AR, Lucas SJE. Acetazolamide ***can*** impair exercise performance; it depends upon the studied cohort. *J Appl Physiol*. 2020; 128(5): 1457 – 1457.

Joyce KE, Delamere, J., Bradwell S, Myers SD, Ashdown K, Rue CA, Thomas O, Lucas SJE, Fountain A, Edsell M, Myers F, Malein W, Imray CHE, Clarke A, Lewis CT, Newman C, Johnson B, Cadigan P, Wright A, Bradwell AR, and the Birmingham Medical Research Expeditionary Society. Hypoxia is not the primary mechanism contributing to exercise-induced proteinuria. *BMJ Open Sport and Exercise Medicine.* 2020; 6(1). DOI: 10.1136/bmjsem-2019-000662.

Joyce KE, Bradwell S, Lucas SJE, Cook A, Fountain A, Delamere J, Bradwell AR. Comparison of sixty-minute urine excretion to 24-hours in determining proteinuria at altitude. *18th Annual International Conference on Environmental Ergonomics*, Amsterdam, Netherlands. 2019; abstract No. 101.

Joyce KE, Bradwell S, Lucas SJE, Cook A, Fountain A, Delamere J, Bradwell AR. Glomerular proteinuria increases as bicarbonate and carbon dioxide decrease at altitude. *18th Annual International Conference on Environmental Ergonomics,* Amsterdam, Netherlands. 2019; abstract No. 237.

Joyce KE, Balanos G, Fountain A, Bradwell AR, Lucas SJE. Hypoxia does not influence post-exercise proteinuria. *24th Annual European College of Sport Science Congress*, Prague, Czechia. 2019.

Babiker M, **Joyce KE**, Fenton A, Lasserson D, Ferro C, Bradwell AR, Cockwell P. Urinary alpha-1 acid glycoprotein and progression to end stage renal disease in chronic kidney disease. *UK Kidney Week*, Brighton, UK. 2019; P095.

Joyce KE, Lucas SJE, Bradwell S, Delamere J, Myers S, Thomas O, Fountain A, Bradwell AR, and the Birmingham Medical Expeditionary Society. Hypoxia is not the mechanism for exercise-induced proteinuria. *High Altitude Medicine & Biology*. 2018; 19(4): 0006.

Delamere JP, Bradwell AR, Bradwell SB, **Joyce KE**, Lewis C, Clarke A, Newman C, Shipman K and the Birmingham Medical Research Expeditionary Society. Losartan has no effect on hypoxic diuretic response to altitude. *High Altitude Medicine & Biology.* 2018; 19(4): 0005.

Joyce KE, Lucas SJE, Bradwell S, Delamere J, Myers S, Thomas O, Fountain A, Bradwell AR, and the Birmingham Medical Expeditionary Society. Urinary orosomucoid (alpha-1 acid glycoprotein) latex immunoassay is effective for the detection of increased proteinuria associated with altitude and sea-level exercise. *Proc Physiol Soc*, 2018; 41: PCA166.

Joyce KE, Lucas SJE, Bradwell S, Delamere J, Myers S, Thomas O, Fountain A, Bradwell AR, and the Birmingham Medical Expeditionary Society. Exercise proteinuria at altitude is reduced by acetazolamide. *Proc Physiol Soc,* 2018; 41: PCA167.

Joyce KE, Lucas SJE, Imray CHE, Balanos GM, and Wright, AD. Advances in the available non-biological pharmacotherapy prevention and treatment of acute mountain sickness and high altitude cerebral and pulmonary oedema. *Expert Opinion on Pharmacotherapy*, 2018; 1 – 12.

TABLE OF CONTENTS

CHAPTER 1: GENERAL INTRODUCTION

CHAPTER 2: BACKGROUND AND OVERVIEW

CHAPTER 3: DEVELOPMENTAL METHODS AND PRELIMINARY VALIDATION EXPERIMENTS FOR A LATEX-ENHANCED IMMUNOTURBIDIMETRIC ASSAY DESIGNED TO MEASURE LOW-CONCENTRATION ALPHA-1 ACID GLYCOPROTEIN (α1-AGP).

CHAPTER 4: EVALUATION OF URINARY ALPHA-1 ACID GLYCOPROTEIN (α1-AGP) IN HEALTH AND DISEASE.

CHAPTER 6: POST-EXERCISE URINARY ALPHA-1 ACID GLYCOPROTEIN IS DEPENDENT ON EXERCISE INTENSITY.

CHAPTER 7: URINARY ALPHA-1 ACID GLYCOPROTEIN AS A BIOMARKER OF ACCLIMATISATION DURING ASCENT TO ALTITUDE.

LIST OF FIGURES

CHAPTER 2

CHAPTER 3

CHAPTER 4

CHAPTER 5

CHAPTER 6

CHAPTER 7

LIST OF TABLES

CHAPTER 2

CHAPTER 3

CHAPTER 4

CHAPTER 5

CHAPTER 6

CHAPTER 7

LIST OF EQUATIONS

CHAPTER 3

CHAPTER 5

CHAPTER 7

LIST OF APPENDICES

LIST OF ABBREVIATIONS

2-DE	two-dimensional gel electrophoresis
4-PL	4-parameter logistic model
5-PL	5-parameter logistic model
Å	Angstrom
A-II	angiotensin-II
α1-AGP	alpha-1 acid glycoprotein
α1-AGP:CREA	alpha-1 acid glycoprotein-to-creatinine ratio (reported as mg/mmol or mg/g)
ACE	angiotensin-converting enzyme
AHI	apnoea-hypopnea index
AIDs	acquired immune deficiency syndrome
AKI	acute kidney injury
AMS	acute mountain sickness
ANOVA	analysis of variance
ANP	atrial natriuretic peptide
ARB	angiotensin II (type-1) receptor blocker
AT1	angiotensin type 1
AUC	area under the curve
AVR	aortic valve replacement
B-A	Bland-Altman
BLa	blood lactate
BMI	body mass index
BNP	brain natriuretic peptide

BP	blood pressure
bpm	beats per minute
BSA	bovine serum albumin
CABG	coronary artery bypass graft
Cl^-	chloride
CI	confidence interval
CKD	chronic kidney disease
CO_2	carbon dioxide
ConA	concanavalin A
COPD	chronic obstructive pulmonary disease
CREA	creatinine
CRP	C-reactive protein
CSF	cerebrospinal fluid
CT	cumulative time (e.g., CT <90%)
%CV	percent coefficient of variation
DBP	diastolic blood pressure
DD	deletion-deletion; in reference to ACE genotype
DEF	dynamic end-tidal forcing
DEXA	dual-energy X-ray absorptiometry
dH_2O	deionised water
DN	diabetic nephropathy
ECG	electrocardiogram
EDC	1-ethyl-3dimethylaminopropyl carbodiimide
eGFR	estimated glomerular filtration rate

ELISA	enzyme-linked immunosorbent assay
EMU	early morning urine
ERM	European Reference Material
ERN	ethical review number
ESL	endothelial surface layer
ET-1	enothelin-1
FDA	Food and Drug Administration
GBM	glomerular basement membrane
GCP	good clinical practices
GFR	glomerular filtration rate
GN	glomerular
GP	general practitioner
GXT	graded (maximal) exercise test
HACE	high-altitude cerebral oedema
HAPE	high-altitude pulmonary oedema
HCl	hydrochloric acid
HCO_3^-	bicarbonate
HF	heart failure
HIF-1α	hypoxia-inducible factor 1-alpha
HIV	human immunodeficiency virus
HR	heart rate
hs-CRP	high-sensitivity C-reactive protein
HSPGs	heparan sulphate proteoglycans
HVR	hypoxic ventilatory response

HYP	hypoxic
II	insertion-insertion (in reference to ACE genotype)
ID	insertion-deletion (in reference to ACE genotype)
IL-1	interlukin-1
IL-6	interlukin-6
IL-8	interlukin-8
IQR	interquartile range
IR	internal reference
IST	Indian Standard Time
K^+	potassium
kDa	kilodaltons
LLS	Lake Louise Score
LOA	Limits of Agreement
LOB	limit of blank
LOD	limit of detection
LLOQ	lower limit of quantification
LN	lupus nephritis
m	metres
MAP	mean arterial pressure
MDRD	Modification of Diet in Renal Disease
MES	2-(N-morpholino)ethanesulfonic acid
NaCl	sodium chloride
Na^+	sodium
NH_4Cl	ammonium chloride

NIRS	near-infrared spectroscopy
NO	nitric oxide
NOR	normoxic (or normoxia)
NS	nephrotic syndrome
O_2	oxygen
ODI	oxygen desaturation index
ORM1	orosomucoid-1
OSA	obstructive sleep apnoea
P_{GC}	glomerular capillary pressure or post-glomerular pressure
PETIA	particle-enhanced turbidimetric immunoassay
PCV	packed cell volume
PG	proteoglycan
pH	denoting the 'potential of hydrogen' or 'power of hydrogen)
p*I*	isoelectric point
PIS	patient information sheet
R^2	R-squared, goodness of fit or coefficient of determination
RAAS	renin-angiotensin-aldosterone system
RBF	renal blood flow
RID	radial immunodiffusion
RM-ANOVA	repeated-measures analysis of variance
ROC	receiver-operator characteristic
ROS	reactive oxygenated species
ROUT	robust regression and outlier removal
RPE	rating of perceived exertion

RR	respiratory rate
RSNA	renal sympathetic nerve activity
S_{dd}	between-day (or day-to-day) standard deviation
S^2_{dd}	between-day (or day-to-day) variance
S_{wr}	within-run standard deviation
S^2_{wr}	within-run variance
S_{rr}	between-run (or run-to-run) standard deviation
S^2_{rr}	between-run (or run-to-run) variance
S_T	total standard deviation
SaO_2	arterial oxygen saturation
SBP	systolic blood pressure
SD	standard deviation
SDI	Systemic Lupus International Collaborating Clinics/ACR Damage Index
SDS-PAGE	sodium dodecyl sulphate polyacrylamide gel electrophoresis
SLEDAI	systemic lupus erythematosus disease activity index
sLe^X	sialyl $Lewis^X$
SNS	sympathetic nervous system
SpO_2	peripheral oxygen saturation
SOP	standard operating procedure
T1DM	Type 1 Diabetes mellitus
T2DM	Type 2 Diabetes mellitus
TNF-α	tumor necrosis factor-α
TST	total sleep time
uORM	urinary orosomucoid

uORM/uCREA urinary orosomucoid-to-creatinine ratio

UV ultraviolet

$\dot{V}_E$ minute ventilation

VEGF vascular endothelial growth factor

W_{max} maximal exercise intensity measured in units for power output (Watts)

Chapter 1

GENERAL INTRODUCTION

This thesis explores the mechanism(s) and significance of proteinuria during acute physiologic challenge by analysing urinary alpha-1 acid glycoprotein (α1-AGP; or orosomucoid-1, ORM1). This thesis begins with this general introduction chapter (**Chapter 1**) that is initiated with a brief background about α1-AGP and a rationale for its analysis, which are followed by an outline of the thesis and an overview of the aims and objectives to be addressed within each of the experimental chapters.

1.1. Background and rationale

Plasma proteins are some of the main constituents of blood plasma. They have important physiologic functions that include transporting hormones, modulating immune responses, and regulating blood osmotic pressure, to name a few. Thus, it is no surprise that excessive plasma protein loss can be problematic. While the loss of plasma proteins can take on many forms, for the purposes of this thesis the focus will remain on their loss via excretion in the urine (i.e., proteinuria). Intrinsic properties (e.g., molecular weight, size, shape, or charge) of proteins can influence their propensity for leakage with the relative types and amounts of leaked proteins (in the urine) being reflective of the aetiology of the renal leak (i.e., tubular, glomerular, or both). Further, compared to urinary albumin (p*I*: 4.7 and ~66 kDa)[1] excretion the smaller and more negatively charged (i.e., anionic) plasma protein, α1-AGP (p*I*: 2.8 – 3.8, and 41 – 43 kDa)[2 3], has proven to be a more sensitive marker of glomerular leak. Specifically,

increased urinary α1-AGP can be indicative of pathophysiologic renal response(s) associated with disease (e.g., psoriatic arthritis[4] or Crohn's[5]), however, it is also observed in response to acute physiologic challenge (e.g., exercise[6] or ascent to altitude[7]). Despite these known occurrences of urinary α1-AGP under acutely altered physiologic conditions, the mechanism(s) underlying its excretion, and the potential significance for function, remain unclear. The main objective of this thesis is to investigate the mechanism(s) for and significance of urinary α1-AGP excretion in humans with acute physiologic challenge (e.g., exercise or altitude exposure).

1.2. Thesis outline

This general introduction chapter is followed by **Chapter 2**, which provides a general introduction for plasma proteins, as well as a comprehensive background for α1-AGP describing its structure(s), function(s), and regulation. **Chapter 2** also outlines the general significance of plasma protein loss with additional detail provided for the renal structures and their associated functions that may be relevant to α1-AGP excretion. **Chapter 2** finishes with descriptions of the dynamic interactions between α1-AGP and renal structures in relation to acute physiologic challenge (e.g., during physical exercise and ascent to altitude)* with potential mechanisms for α1-AGP excretion in each instance also highlighted. **Chapter 3** is a methodological chapter that begins with a discussion around the analytical techniques used to evaluate α1-AGP, followed by a description of the methods employed for immunoassay development and preliminary validation experiments of the novel particle- (latex-)enhanced immunoturbidimetric assay designed for the detection of low-concentration α1-AGP in human urine. The developed immunoassay will go on to be utilised in the remaining experimental

* Literature search strategy for this excerpt and contents of **Chapter 2** can be referred to in **Appendix 1**.

chapters (**Chapters 4 – 7**) to investigate urinary α1-AGP excretion during acute physiologic challenge. The aims of these individual chapters are outlined next.

1.3. Aims and objectives

Chapter 3 – To facilitate analyses of low ('subclinical') levels (and changes) of α1-AGP in human urine with precision, accuracy, and ease, the aim of this chapter was to develop and validate a highly sensitive latex-enhanced immunoturbidimetric assay for use on the Optilite™ auto-analyser (Model 1.2, Software version 6.0.1, The Binding Site, Ltd., Birmingham, UK).

Chapter 4 – Given the observed inconsistencies within the existing literature in relation to methodologies used for analysis and reporting of urinary α1-AGP, the aim of this chapter was to use the novel turbidimetric immunoassay to examine urinary α1-AGP excretion in healthy individuals across a range of specimen collection types (e.g., 24-hour timed, short-duration timed, and early-morning). Results were represented in various units of measurement (e.g., mg/l, μg/min, and mg/mmol) with statistical analyses conducted for each to assess the impact of age and sex. Urinary α1-AGP results were further compared to values observed in the existing literature and were intended to provide a foundation for updated reference ranges for urinary α1-AGP.

Chapter 5 and **6 –** Underlying mechanism(s) for and significance of post-exercise and altitude-induced proteinuria have remained allusive, although mechanistic hypotheses have been similar between the two. The suggestions have included: 1) haemodynamic determinants (pressure and flow); 2) hormonal influences; 3) acid-base disturbances[8 9]; and 4) hypoxia and oxidative stress[10-12]. Superimposition of exercise and altitude exposure presents a unique opportunity to explore and uncouple the relative mechanism(s) that may contribute to proteinuria[13]. The novel turbidimetric immunoassay (developed and validated in **Chapter 3**)

was utilised to measure α1-AGP excretion in urine specimens collected pre/post exercise tests conducted during field- (hypobaric hypoxia, **Chapter 5**) and chamber- (normobaric hypoxia, **Chapter 6**) based experiments. **Chapter 5** aimed to explore the effects of BP and hypoxia on urinary α1-AGP by comparing post-exercise urinary α1-AGP at altitude: 1) with vs without an angiotensin-II receptor blocker (e.g., losartan); and 2) with vs without acetazolamide. **Chapter 6** was designed to improve upon experiments from **Chapter 5** by adopting a less complex and more controlled design with altitude exercise tests conducted and urine specimens collected in an environmental chamber (normobaric hypoxia vs normobaric normoxia). Comparisons between urinary [α1-AGP] and urinary [albumin]* were also performed.

Chapter 7 – The final experimental chapter focused on mechanism(s) for altitude-induced (without exercise stimulus) α1-AGP excretion during ascent (and descent), specifically in the context of nocturnal oxygenation and sleep disturbances[14], as well as, alternate altitude-induced physiologic responses not yet explored (e.g., altered fluid balance or increases in systemic inflammation). The clinical significance of urinary α1-AGP during ascent was also evaluated in relation to the development and progression of acute mountain sickness (AMS; by Lake Louise Scores, LLS).

Chapter 8 – Based on findings from the preceding experimental chapters, this closing chapter will provide a synthesis of the thesis findings and discuss possible future directions.

* Bracketed shorthand will be utilised henceforward to refer to the concentration of an [analyte].

Chapter 2

BACKGROUND AND OVERVIEW

This thesis chapter begins with an introduction for plasma proteins that outlines their function(s) and regulation within the blood. This introduction is proceeded by a comprehensive background for α1-AGP, describing its structure(s), function(s), and regulation, which is further followed by a general overview for the significance of plasma protein loss. Additional detail is provided for the significance of plasma protein loss in the urine (i.e., proteinuria) with this being closely paired with descriptions of basic renal physiology and the potential origins of proteinuria (tubular vs glomerular). Further attention is then given to a comparison between α1-AGP and albumin, which establishes the basis for urinary α1-AGP being a more sensitive marker of glomerular responses compared to albumin. As such, additional detail is provided for the various glomerular structures and functions that may contribute to the development of urinary α1-AGP. Finally, the chapter finishes by outlining the dynamic interactions between renal structures and functions and α1-AGP during acute physiologic challenge (e.g., physical exercise or altitude exposure; see **Appendix 1** for literature search strategy) with the potential mechanisms underpinning urinary α1-AGP excretion during exercise or ascent to altitude highlighted.

2.1. PLASMA PROTEINS

Blood is comprised of four main components: red blood cells, white blood cells, platelets, and plasma[15]. The constituents of plasma include water, plasma proteins, and other solutes (e.g., electrolytes, dissolved gases, minerals, and carbohydrates)[15]. Further, the main

types of plasma proteins are albumins, immunoglobulins, (alpha, beta, and gamma), regulatory proteins (e.g., hormones and enzymes), and fibrinogens[1]. Plasma proteins are predominantly synthesised and secreted by the liver, except for gamma globulin which is synthesised by plasma cells[16]. Hepatic genes responsible for plasma protein synthesis are regulated by a multitude of stimulating factors, such as, interlukin-1 (IL-1), tumour necrosis factor alpha (TNF-α), interlukin-6 (IL-6), hepatocyte stimulating factor III, and corticosteroids, to name a few[17].

Plasma proteins serve many major functions and are, specifically, responsible for the binding and transport of lipids and other ligands, blood clotting, immune responses, and the maintenance of blood osmotic pressure[15]. Despite albumin being the most abundant plasma protein (~60% of all plasma proteins)[18], additional plasma proteins, such as, α1-AGP (discussed next) are also considered abundant, (~1% to 3% of all plasma proteins) and are no less important[19].

2.1.1. Alpha-1 acid glycoprotein (α1-AGP)

α1-AGP is a small-to-medium sized (molecular weight: 41 – 43 kDa, Stokes-Einstein radius*: 29 Å), anionic (p*I*, 2.8 – 3.8), acute phase, plasma protein[2 3] that plays a key role in immunomodulation, as well as, binding and transport of major basic-characteristic ligands and drugs[2] (as discussed in section **2.1.1.3**).

* Stokes–Einstein radius, also known as the hydrodynamic radius, of a molecule is the half-width (i.e., radius) of a sphere that diffuses at the same rate as the solute in question (i.e., macromolecule or colloid particle).

2.1.1.1. Structure of alpha-1 acid glycoprotein

In humans, α1-AGP consists of 183 amino acids forming a single-chain structure with two disulphide bridges[2 20 21 *]. As illustrated in **Figure 2.1** below, α1-AGP contains five *N*-linked glycosylation sites[†] each of which exhibit unique functional limitations and result in only 12 to 20 possible carbohydrate arrangements, or glycoforms[2].

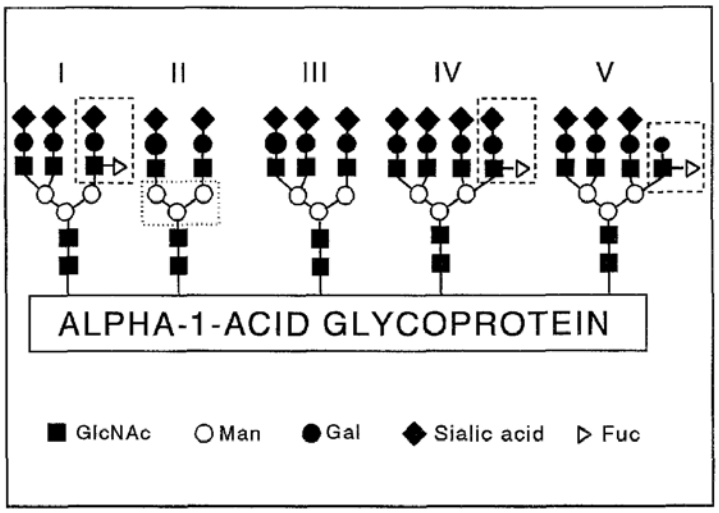

Figure 2.1 – Visual representations of the possible glycan arrangements (glycoforms) for human alpha-1 acid glycoprotein containing a single diantennary glycan. Roman numerals I – V indicate the five N-linked glycosylation sites with dashed boxes for moieties I and IV indicating sialyl Lewis^X (sLe^X) structures. The dashed boxed for moiety V indicates a Lewis^X (not sialylated) and the dashed box for moiety II surrounds the Con A binding site. Modified by van Dijk W, Havenaar EC, Brinkman-van der Linden EC. Alpha 1-acid glycoprotein (orosomucoid): pathophysiological changes in glycosylation in relation to its function. *Glycoconj J* 1995;12(3):227-33[22] from De Graaf TW, Van der Stelt ME, Anbergen MG, et al. Inflammation-induced expression of sialyl Lewis^X-containing glycan structures on alpha 1-acid glycoprotein (orosomucoid) in human sera. *J Exp Med* 1993;177(3):657-66[23].

The type (di-, tri-, or tetra-antennary) and extent (relative proportions of glycoforms present) of branching are determined by the degree of glycosylation, which can be influenced

[*] In humans, two disulfide bridges have been documented for α1-AGP between its cysteine residues (i.e. Cys5-Cys165 and Cys72-Cys147) and, effectively, increase the overall stability of the protein structure.

[†] N-linked glycosylation site refers to the nitrogen portion of an asparagine where oligosaccharides bind. Five N-linked sites should, in theory, allow for great diversity in the structure however, the unique limitations exhibited by α1-AGP's glycosylation sites only permit 12 to 20 possible glycoforms.

by the severity and stage of inflammation[22 24], as well as, various inflammatory mediators relative to the (patho)physiologic state. Also influencing α1-AGP's structure (and its functionality) is fucosylation, a type of glycosylation involving the addition of a fucose sugar. Levels of fucosylation appear to change independently of serum [α1-AGP], although high levels are observed in rheumatoid arthritis[25], cirrhosis and hepatitis[26], and cancer patients with poor prognoses[27]. Sialylation of α1-AGP, or the addition of a sialic acid to an oligosaccharide on the protein, often parallels fucosylation and results in increasing presentations of sialyl Lewis^X (sLe^X) (**Figure 2.1,** dotted line around the tetra-antennary). Sialylation of α1-AGP contributes largely to its anionic surface and its distinctly low p*I* (the pH at which its charge is neutralised); whereas desialylation stabilises α1-AGP and limits conformational change[24 28]. The degree of sialylation (i.e., amount of bound sialic acids) strongly influences the function of α1-AGP, particularly, its ability to bind and interact[22 29] and is influenced by the stage of inflammation. This can be observed in the sialic acid-dependent changes in binding between early-acute, late-acute, and chronic inflammation (**Figure 2.2**)[21 30].

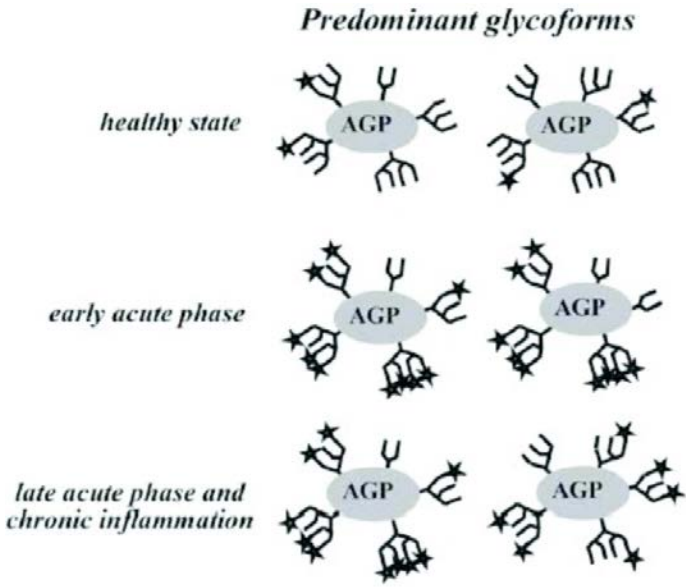

Figure 2.2 – Sialic acid-dependent changes in alpha-1 acid glycoprotein (α1-AGP) binding to E-selectin-IgG occurring in healthy persons and in various stages of inflammation (i.e., early acute, late acute, and chronic). Increased sialyl Lewis^{x} (or sLe^{X}) structures are observed with progressive inflammation and the presence of sLe^{X} alters the degree of binding (indicated using stars). Adopted from Van Dijk W, Do Carmo S, Rassart E, et al. The Plasma Lipocalins α1-Acid Glycoprotein, Apolipoprotein D, Apolipoprotein M and Complement Protein C8γ. *Madame Curie Bioscience Database* [Internet]. Austin, TX: Landes Biosciences 2000-2013[21].

2.1.1.2. Activation and regulation of alpha-1 acid glycoprotein

α1-AGP was first documented in the early 1950s[31] [32] with descriptions of its polymorphisms[33] and phenotypes[34] to follow. In humans, a series of three, closely linked genes (α1-AGP-*A, -B* and *-B'*) located on chromosome 9, encode for α1-AGP with the α1-AGP-*A* gene responsible for a majority of its synthesis[35]. Three common alleles (F1, F2, and S) contribute to the predominance of genetic variation of α1-AGP[36], although several additional alleles (e.g., A3 in Qataris; B10 in Sudanese; C3 in Egyptians)[37] have been identified. Geographical patterns also exist relative to allelic frequencies of the common alleles, with the most notable being the clinal increases (from west to east) in F1 and decreases in S allelic frequency[38] (**Table 2.1**). The world's highest F1 frequencies are observed amongst New Guineans (ORM1*F1 = 0.841), Thais (ORM1*F1 = 0.814), Gujarati Hindus (ORM1*F1 = 0.804), and Brazilian Indians (ORM1*F1 =

0.870) with little subcontinental variation evident worldwide[38]. The presence of these geographical patterns suggest an evolutionary origin for the variants however, functional differences between the allelic variations appear minimal apart from the notable differences in the number of binding sites per mmol of protein between common alleles (with S having the most)[39].

The predominance of α1-AGP synthesis occurs in liver hepatocytes[35]. α1-AGP has a half-life of approximately 2 to 3 days[40], with physiologic concentration in serum ranging from approximately 0.5 to 1.0 g/l[41] and pathophysiologic concentration rising anywhere from two- to ten-fold[42]. Hepatocyte production of α1-AGP can be stimulated by systemic injury or trauma (e.g., surgery[43]), viral[44] or bacterial infection[2], or 'non-specific inflammation' with production primarily influenced by interlukin-1 (IL-1), interlukin-6 (IL-6), and glucocorticoids[29 45]. Extra-hepatic expression of α1-AGP has also been demonstrated in epithelial cells[46], endothelial cells[47], pneumocyte II (alveolar type II epithelial cell)[2], and alveolar macrophages[24]. Extra-hepatic regulation however, is far less understood although the influences of cytokines[48], interlukin-8[49], retinoic acids[50], and glucocorticoids[51] have been demonstrated.

Table 2.1 – Serum orosomucoid-1 (ORM1) allele frequencies.

	N =	ORM1*F1	ORM1*F2	ORM1*S	Author
Arab (Arabe)	62	0.177	-	0.452	Nevo and colleagues[52]
Mexican (Teeneks)	44	0.205	0.568	0.227	García-Ortiz and colleagues[53]
Cheutas (Majorcan Jewish)	140	0.339	0.025	0.497	Picornell and colleagues[54]
Arab (Druzes)	139	0.369	0.011	0.388	Nevo and colleagues[52]
Mexican (Metizos)	101	0.406	0.455	0.139	García-Ortiz and colleagues[53]
Eastern European (Jewish)	141	0.436	0.014	0.436	Nevo and colleagues[52]
Bulgarian (Jewish)	212	0.455	0.028	0.434	Nevo and colleagues[52]
Central European (Jewish)	107	0.523	-	0.369	Nevo and colleagues[52]
British (Leicestershire)	103	0.529	-	0.471	Mastana and colleagues[38]
Indigenous Canadian	169	0.547	-	0.453	Escallcon and colleagues[55]
Aleuts	237	0.551	-	0.449	Escallcon and colleagues[55]
Portuguese	260	0.552	0.031	0.415	Montiel and colleagues[56]
Ecuadorian (Cayapa Indians)	3,600	0.554	-	0.446	Scacchi and colleagues[57]
Romanian (Jewish)	147	0.554	0.014	0.36	Nevo and colleagues[52]
North African (Jewish)	200	0.555	0.02	0.395	Nevo and colleagues[52]
Spanish (Galicia)	880	0.557	0.033	0.406	Montiel and colleagues[56]
American (US Whites)	228	0.559	-	0.386	Escallcon and colleagues[55]
French	112	0.563	0.049	0.388	Yuasa and colleagues[58]
Italian (Sardinian)	244	0.564	-	0.438	Scacchi and colleagues[59]
Sudanese	195	0.5641	0.0026	0.3897	Sebetan and colleagues[37]
Middle Eastern (Jewish)	140	0.568	0.011	0.364	Nevo and colleagues[52]
German	1,072	0.569	0.0368	0.3927	Dülmer and colleagues[60]
Spanish (Basque)	150	0.573	0.033	0.393	Montiel and colleagues[56]
Inuit	220	0.573	-	0.427	Escallcon and colleagues[55]
British (Northwest Derbyshire)	105	0.576	-	0.424	Mastana and colleagues[38]
German (Southwest/Bavaria)	407	0.5781	0.0195	0.3901	Luckenbach and colleagues[61]
Danes	215	0.581	0.033	0.386	Thymann and colleagues[62]
British (Northeast Derbyshire)	105	0.586	-	0.414	Mastana and colleagues[38]
Italian (Garfagnana, Tuscany)	238	0.586	0.021	0.393	Weidinger and colleagues[63]
Swiss	329	0.593	0.001	0.404	Eap and colleagues[64]
Qatari	400	0.5937	0.005	0.3787	Sebetan and colleagues[37]
Italian (Lombardy)	600	0.5992	0.015	0.386	Cerri and De Ferrari[65]
Egyptian	271	0.5996	0.0055	0.369	Sebetan and colleagues[37]
Senegalese (Wolof)	209	0.605	-	0.395	Corbo and colleagues[66]
Senegalese (Peul)	43	0.605	-	0.395	Corbo and colleagues[66]

Table 2.1 – Serum orosomucoid-1 (ORM1) allele frequencies (continued).

	N =	ORM1*F1	ORM1*F2	ORM1*S	Author
Swiss	220	0.607	-	0.393	Metzner and colleagues[67]
Senegalese (Tukulor)	14	0.607	-	0.393	Corbo and colleagues[66]
German (München)	272	0.610	0.04	0.348	Weidinger and colleagues[68]
German (South)	696	0.613	0.034	0.353	Thymann and Eiberg[62]
Nigerian	1	0.618	-	-	Moral and colleagues[69]
American (US African American)	181	0.619	-	0.384	Escallcon and colleagues[55]
Italian (all mainland)	567	0.621	-	0.379	Scacchi and colleagues[59]
Spanish (Madrid)	315	0.621	0.005	0.375	Alonso and colleagues[70]
German (West)	670	0.627	-	0.373	Metzner and Schiel[67]
British (South Derbyshire)	242	0.634	-	0.366	Mastana and colleagues[38]
Indian (Parsees)	180	0.636	0.008	0.356	Saha and colleagues[71]
Spanish (Tenerife/Canary Island)	108	0.639	-	0.361	Moral and colleagues[69]
Japanese (Izumo)	284	0.6426	0.0185	0.1812	Yuasa and colleagues[72]
Paraguayan	200	0.645	0.023	0.307	Umetsu and colleagues[73]
Libyan	105	0.650	0.009	0.309	Sebetan and Sagisaka[74]
Libyan Arab	1	0.659	-	-	Moral and colleagues[69]
Arab (Acre)	94	0.660	0.011	0.303	Nevo and colleagues[52]
Japanese (Myagi)	232	0.668	0.006	0.170	Sebetan and Sagisaka[75]
Turkish	93	0.673	-	0.327	Brega and colleagues[76]
Nepalese	141	0.674	0.014	0.312	Yuasa and colleagues[58]
Japanese (Yamaguchi)	200	0.680	0.022	0.163	Yuasa and colleagues[77]
Japanese (Yamaguchi)	184	0.680	0.0125	0.1525	Yuasa and colleagues[72]
Indian (Brahmin)	116	0.681	0.009	0.310	Mastana and colleagues[38]
Japanese (Okinawa)	364	0.688	-	0.166	Yuasa and colleagues[77]
Indian (Parsee)	51	0.696	-	0.304	Mastana and colleagues[38]
Burghers	100	0.700	0.01	0.290	Mastana and colleagues[38]
Sri Lankan	140	0.700	-	0.268	Umetsu and colleagues[73]
Han Chinese (Chengdu)	286	0.703	0.021	0.276	Yiping and colleagues[78]
Brazilian Indian (Pacaás Novos; Santo Andre)	112	0.705	0.009	0.236	Salzano and colleagues[79]
Han Chinese (Nanjing)	220	0.7068	0.0182	0.2750	Li and colleagues[80]
Indian (Maratha)	144	0.715	0.011	0.274	Mastana and colleagues[38]
Indian (Hyderabad Hindus)	115	0.717	0.026	0.270	Mastana and colleagues[38]
Taiwanese	200	0.726	-	0.181	Umetsu and colleagues[81]
Brazilian Indian (Pacaás Novos; Tanajura)	88	0.727	0.006	0.188	Salzano and colleagues[79]

Table 2.1 – Serum orosomucoid-1 (ORM1) allele frequencies (continued).

	N =	ORM1*F1	ORM1*F2	ORM1*S	Author
Indian & Sri Lankan (Tamils)	100	0.730	0.010	0.260	Mastana and colleagues[38]
Sri Lankan (Sinhalese)	88	0.733	0.017	0.250	Mastana and colleagues[38]
Moors	98	0.733	-	0.257	Mastana and colleagues[38]
Brazil Indian (Urubu-Kaapor)	77	0.734	-	0.266	Salzano and colleagues[79]
Malay	99	0.742	-	0.258	Mastana and colleagues[38]
Chinese	163	0.756	-	0.141	Mastana and colleagues[38]
Cambodian (Khmer)	31	0.758	-	0.242	Mastana and colleagues[38]
Japanese (Yamagata)	500	0.779	-	0.221	Umetsu and colleagues[82]
New Zealand (Cook Island)	318	0.7893	-	0.2107	Abe and colleagues[83]
Filipino	115	0.790	0.049	0.169	Umetsu and colleagues[84]
Indian (Gujarat Hindus)	84	0.804	-	0.196	Mastana and colleagues[38]
Thai	369	0.814	-	0.161	Umetsu and colleagues[73]
New Guinea highlanders	110	0.841	-	0.159	Escallcon and colleagues[55]
Brazilian Indian (Parakanã; born Jardim)	116	0.870	0.045	0.085	Salzano and colleagues[79]

Ethnic variation can be observed in the polymorphisms of ORM1 expressed as frequencies for the three major alleles (F1, F2, and S). Allele frequencies are presented in ascending order beginning with the lowest F1 frequency. ORM is used here instead of α1-AGP as this abbreviation is relevant to how alleles are typically named, and is utilised in the genetic literature (e.g., ORM1*F1).

2.1.1.3. Functions of alpha-1 acid glycoprotein

The full extent of α1-AGP's biologic functions are not clear, although its anti-inflammatory and immunoregulatory properties are undisputed[2]. α1-AGP's reactivity with concanavalin A (ConA), a lectin (a carbohydrate-binding protein), has however helped to elucidate connections between its structures and functions[23].

2.1.1.3.1. Immunoregulatory and anti-inflammatory properties

Remarkable immunoregulatory functions of α1-AGP can be observed in its inhibition of malarial parasites from invading erythrocytes[85], as well as, its inhibition of platelet aggregation[86 87]. Anti-neutrophil and anti-complement functions of α1-AGP[88] are particularly important to immunoregulation and can be observed in the prevention of polymorphonuclear neutrophil activation[89] and the modulation of cytokine excretion from monocyte-

macrophages[90]. An additional anti-inflammatory function of α1-AGP is its inhibition of histamine (via a cAMP-mediated pathway)[91]. These and other immunomodulatory and anti-inflammatory functions of α1-AGP are largely dose-dependent (within a physiologic range in serum) but are also related to the degrees of sialylation and glycosylation (and fucosylation)[22] [92]. For example, inhibition of platelet aggregation by α1-AGP is specifically related to sialylation (enhanced with desialylation)[87]. In addition, the presence of sialyl Lewis^X, a ligand for vital cell adhesion components (E-selectin and P-selectin), is dependent on inflammation that increases sialylation[23]. The efficacy of α1-AGP's anti-complement function is also dependent on the proportion of glycoforms present and can be demonstrated in its degree of inhibition of the anti-CD3-induced cellular proliferation (in lymphocytes)[93].

2.1.1.3.2. Regulation of capillary permeability

α1-AGP is also important for the maintenance of normal capillary permeability* [94] with this function best observed in its antagonistic effects on capillary leak[95]. In the context of the kidney and in the case of proteinuria, changes in [α1-AGP] within perfusate (i.e., plasma) may alter glomerular capillary permeability by influencing the permeability selectivity of the glomerular barrier[96]. For example, reductions in α1-AGP can promote capillary leak[47] [97] while local increases in epithelial[98] or endothelial α1-AGP production[47] can increase the anionic charge at the filtration barrier by adding of sialic acids that help limit glomerular permeability to water and plasma proteins[99]. The binding of α1-AGP to endothelial cells[91] or its interaction with the endothelial surface layer[98] may also add to the anionic properties of the filtration

* Alterations in capillary permeability by α1-AGP may have clinical significance in the context of high-altitude, specifically in regard to the development and progression of altitude illnesses (as discussed in subsection **2.2.1.1**).

barrier[100 101], however, the exact mechanism(s) by which α1-AGP modulates glomerular capillary permeability in this way are unclear.

2.1.1.3.3. Binding and transport

As a member of a lipocalin subfamily (immunocalin family[102]), α1-AGP also plays a large role in the binding of endogenous (e.g., glucocorticoids, steroid hormones) and exogenous (e.g., pharmaceuticals) compounds. The ligand binding site on α1-AGP in humans consists of three subsites (basic, acidic, and steroid binding sites), which contribute to its multiform biologic binding properties[103]. Binding properties of α1-AGP are also important to the pharmacokinetics and pharmacodynamics[104] of many drugs, especially where α1-AGP is the main serum binding protein[105] (e.g., propranolol[106 107]). As with capillary permeability, plasma [α1-AGP] can influence its binding properties with excessively elevated levels of α1-AGP potentially adversely impacting various drugs. For example, high levels of α1-AGP can reduce the anti-viral effects of protease inhibitors, drugs commonly used to prolong life among patients with acquired immunodeficiency (AIDs) and human immunodeficiency virus (HIV)[108 109].

2.2. SIGNIFICANCE OF PLASMA PROTEIN LOSS

Given the vital roles of plasma proteins, it is no surprise that excessive protein loss (or decreased plasma proteins, i.e., hypoproteinemia) can be problematic. To this point, a generalised reduction in plasma proteins (due to capillary wall leakage) can significantly alter the oncotic pressure of the blood and promote movement of fluid from the blood vessels into the interstitial space, which ultimately can result in oedema formation[110]. Such fluid exchange across the capillaries is governed by the physiologic properties (hydrostatic and oncotic pressures) known as Starling forces[110]. Reductions in plasma proteins can also negatively

impact the degree of binding for toxic substances (e.g., reactive oxygen species and lipid peroxidation products)[111], as well as, endogenous and exogenous ligands[112].

2.2.1. Proteinuria

While a variety of factors including increases in plasma water causing dilution, dietary changes, protein-losing enteropathy, excessive bleeding, medication, systemic inflammation, and decreased synthesis can cause reductions in plasma proteins[113], for the purposes of this thesis the focus shall remain on protein loss via excretion in the urine. Such excretion of plasma proteins (e.g., α1-AGP, albumin, or other) in the urine is, collectively, known as proteinuria. Proteinuria occurs as a result of acute or chronic renal stress or injury, such as, with acute physiologic challenge (e.g., exercise[6] or ascent to altitude[7]) or disease, respectively. The magnitude and duration of the renal stress/injury are likely continuous and dictate the degree and type of resultant proteinuria. Thus, it is no surprise that diseases are oftentimes associated with higher degrees of proteinuria (greater magnitudes and longer durations of renal stress/injury) compared to exercise or exposure to altitude, which are associated with lower total proteinuria (brief and transient renal stress without subsequent injury).

2.2.1.1. Tubular vs glomerular proteinuria

Proteinuria can originate from both the renal tubules and the glomerulus making plasma protein excretion* (into the urine) dependent upon filtration (by the glomerulus) and the amount of reabsorption (by the tubules). Filtration refers to the movement of molecules (i.e., water and small solutes) from the blood plasma in glomerular capillaries through the

* For substances that are neither metabolised or synthesised in the kidneys, the amount of the substance that enters the kidneys will be equal the amount that leaves the kidneys via excretion in the urine and via the renal vein (i.e., mass balanced). As such, urinary excretion rate of a substance is product of its concentration in urine and the urine flow rate (i.e., rate at which urine is formed).

layers of the glomerular filtration barrier (as discussed in the section **2.3.1**) and into Bowman's space to form the ultrafiltrate (**Figure 2.3**).

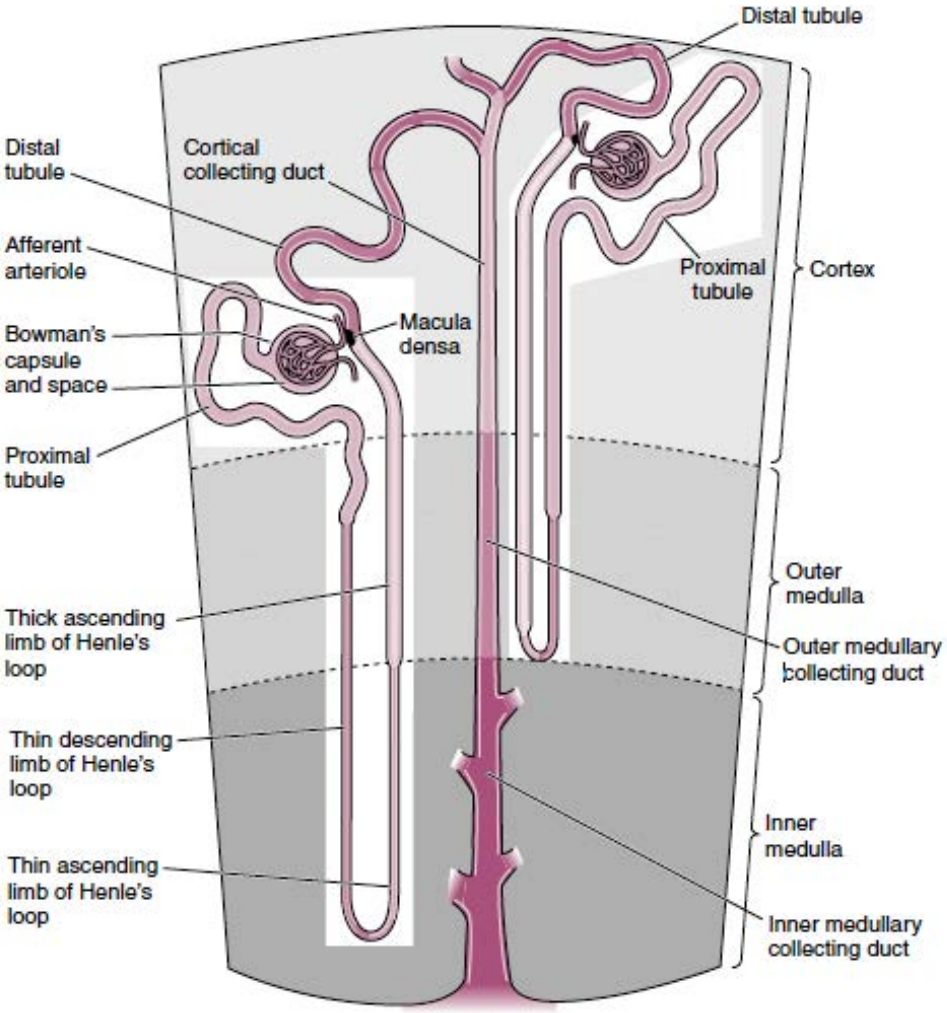

Figure 2.3 – Functional unit of the kidney (i.e., nephron). Adopted from Koeppen BM, Stanton BA: *Renal Physiology: Mosby Physiology Monograph Series*, ed 5, Philadelphia, 2013, Elsevier Mosby as modified from Boron WF, Boulpaep EL: *Medical Physiology*, ed 2, Philadelphia, 2009, Saunders Elsevier.

The glomerular filtration barrier restricts such movement of molecules based largely on size but, also on charge (i.e., size- and charge-selectivity, as also discussed in section **2.3.1**) with molecules measuring < 20 Å being freely filtered (not size restricted) and molecules measuring > 42 Å not being filtered[110]. Further, filtration of molecules between 20 to 42 Å is variable. Following filtration, the ultrafiltrate then passes through the tubules (i.e., proximal tubule, loop

of Henle, and distal tubule, and the collecting duct) where reabsorption and secretion occur. Reabsorption refers to the process(es) by which water* and other molecules† from the ultrafiltrate move through the tubular wall into the peritubular interstitium and are then returned to the blood‡. Thus, clearance of a substance refers to the volume of plasma from which a substance is completely removed (and excreted into the urine) per unit time (e.g., ml/min) whereas fractional clearance refers to the percentage of the substance that is filtered and then also excreted into the urine§

Low molecular weight proteins (less than ~40 kDa) are filtered in large amounts, albeit are generally (actively) reabsorbed by the tubules. As such, an abundance of low molecular weight proteins in urine implicates a tubular origin whereas an abundance of high(er) molecular weight proteins (e.g., albumin) in the urine implicates a glomerular origin[114]. Further, molecular weights of proteins are inversely related to their relative clearances[114]. For example, lysozyme (15 kDa, 19 Å)[115] has a substantially greater clearance compared to albumin (69 kDa, 37 Å), which is poorly filtered and if leaked, is largely reabsorbed by tubules[116].

Molecular shape (e.g., elongated) and charge can also influence plasma proteins' propensities to leak (sieving coefficient)[2] through the glomerular filter. For example, elongated proteins, such as bikunin and hyaluronan, exhibit higher glomerular sieving compared to albumin[117] despite being relatively similar in both, size and charge. Thus, characteristics (e.g., molecular weight and size, shape, and charge) of excreted proteins along with the relative

* Water is reabsorbed by passive diffusion from renal tubules however, this diffusion follows the concentration gradient created by NaCl, an actively reabsorbed molecule.

† Various other larger molecules (e.g. plasma proteins) are actively reabsorbed.

‡ The second step in the reabsorption process (i.e., movement from peritubular interstitium back into the blood) can also occur via active or passive transport.

§ Fractional clearance is expressed as a function of both, the plasma and urine concentration of the substance in question.

amounts of proteins excreted helps to distinguish between glomerular vs tubular origins, as well as, between intra-glomerular mechanisms contributing to proteinuria (as discussed in section **2.3.1**). For these reasons, the efficacies of urinary α1-AGP and albumin for the measurement of glomerular responses can be compared.

2.2.1.2. α1-AGP vs albumin

Plasma [albumin] (3.0 to 5.0 g/dl, ~60% of all plasma proteins) is substantially greater than plasma [α1-AGP] (0.5 to 1.0 g/dl, 1% to 3% of all plasma proteins) however, α1-AGP is slightly smaller in size (molecular weight: 41 – 43 kDa and Stokes-Einstein radius: 29 Å) compared albumin (molecular weight: 69 kDa and Stokes-Einstein radius: 37 Å) making it slightly less size restricted by the glomerular filter (i.e., by slit diaphragm pores, as discussed in the next section). Nevertheless, both albumin and α1-AGP are elongated proteins[117 118]. An important difference however, is that albumin is selectively reabsorbed by renal tubules[119] whereas α1-AGP is thought to be strictly limited to reabsorption by endocytosis (via megalin/cubilin pathway), which is relevant for the reabsorption of *all* filtered proteins passing through renal tubules[120]. The slightly greater clearance of α1-AGP compared to albumin (in a healthy kidney)[121] further confirms this. An additional important difference is that α1-AGP (p*I*, 2.8 – 3.8) is 'more' anionic than albumin (p*I*, 4.7)[98] making it more sensitive to changes in charge-selectivity within the glomerular filtration barrier. Taken together, these characteristics of α1-AGP have resulted in its consideration as a more sensitive or improved marker of glomerular leak compared to albumin*. However, to fully understand the dynamic

* The improved sensitivity of α1-AGP is supported by its successful use as a urinary biomarker (i.e., an analyte measured to detect the presence or progression of disease) for the early detection of various diseases (as highlighted in **Chapters 3** and **4**).

relationship between plasma proteins and 'fluctuating' properties of the glomerular filtration barrier, a thorough understanding of renal structures and functions must first be appreciated.

2.3. ORIGINS OF GLOMERULAR PERMEABILITY

To evaluate the relative contributions from the layers of the glomerular filtration barrier to glomerular leak, it is imperative to understand the dynamic structural and functional properties of these components, as well as, various local and systemic factors that can modulate such properties.

2.3.1. Structural and functional properties of the glomerulus

There are four major structural components of the glomerular filtration barrier (**Figure 2.4a – 2.4c**) that should be considered: 1) podocytes, foot processes, and slit diaphragms; 2) the glomerular basement membrane (GBM); 3) glomerular endothelial cells; and 4) mesangial cells.

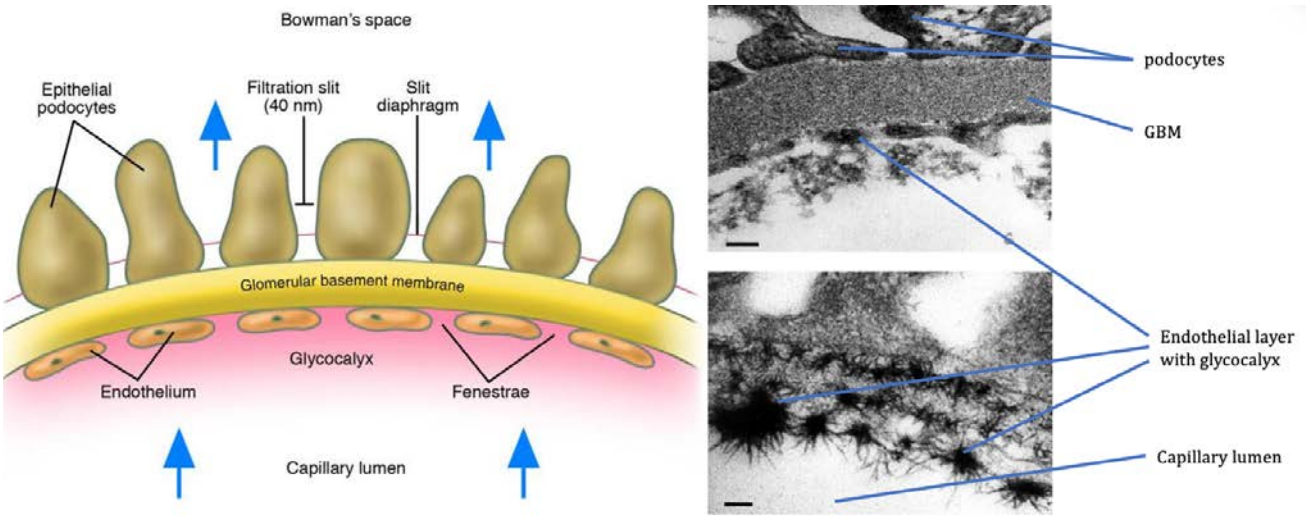

Figure 2.4 – Glomerular filtration barrier. Fig. 2.4a (left) – Graphical representation of the layers of the glomerular barrier to include: podocytes, filtration slits and slit diaphragms; glomerular basement membrane (GBM); endothelial cells, glycocalyx, and fenestrations. Blue arrows indicate the direction of ultrafiltration. Adopted from Deen WM. What determines glomerular capillary permeability? *Journal of Clinical Investigation* 2004;114(10):1412–14[122]. **Fig. 2.4b** and **Fig. 2.4c (both right) –** Electron microscope (EM) images of the filtration barrier before (top) and after (bottom) staining demonstrating the extensiveness of the glycocalyx (best shown following staining; bottom). Glomerular filtration barrier layers are highlighted to the right of the EM images. Adopted from Haraldsson B, Nystrom J, Deen WM. Properties of the glomerular barrier and mechanisms of proteinuria. *Physiol Rev* 2008;88(2):451-87[98].

2.3.1.1. Podocytes, foot processes, and slit diaphragms

Podocytes, separated by filtration slits and slit diaphragms, are the components of the glomerular barrier closest to the filtrate and are located on the 'outer' surface of the GBM. The filtration slits between neighbouring podocytes range in size (radii: 25 to 60 Å)[98] and are bridged with a thin layer of a series of proteins (nephrin, NEPH-1, podocin, p-cadherin, to name a few)[123], which is known as a slit diaphragm. The slit diaphragms function to span gaps between adjacent podocytes[110], limiting the free movement of macromolecules between them, and interact with proteins in podocytes and on the GBM[123]. Activation or inhibition of receptors on podocytes facilitates the 'opening' and 'closing' of the slits helping to regulate the passage of proteins and other macromolecules into Bowman's space, ultimately, contributing to the size-selective function of the filtration barrier[110]. Therefore, podocyte (or slit diaphragm) damage

or dysfunction, which may present as podocyte retraction[124], foot process effacement (or podocyte effacement), or GBM detachment, unsurprisingly can result in protein leakage. Experiments by Olson and colleagues[124] indicate such proteinuria may be attributed to the loss of sialic acids and anionic charge, although others show it may be a product of filtration under excessive intra-glomerular pressures. High filtration pressures increase angiotensin II (A-II) levels in podocytes and thereby reduce the expression of adhesion proteins (e.g., podocin and integrinβ_1), which can result in detachment[125].

2.3.1.2. Glomerular basement membrane (GBM)

The GBM is an extracellular matrix consisting of three primary layers: 1) the lamina interna (bordering the endothelial cells), 2) the lamina densa, and 3) the lamina externa (bordering the podocytes). These layers are comprised of important structural components including: laminin, integrin, type IV collagen, nidogen, and heparan sulphate proteoglycans (HSPGs)[126].

Accepted dogma has revered HSPGs (mainly argin and perlecan) of the GBM as crucial components believed to harbour fixed negative charges that contribute largely to the charge-selective function of the filtration barrier[126 127 128]. Heparan sulphate proteoglycans have a protein core with one or more covalently bonded glycosaminoglycan side chains (heparan sulphate) that are frequently altered by sulfation[129]. These negatively charged side chains are the components that contribute to HSPGs' inherent anionic charge[129] believed to contribute largely to the negative charge of the GBM, as mentioned, and thought to ultimately dictate the charge-selective function of the glomerular barrier. Studies demonstrating predominant leakage of cationic tracers paralleled by repulsion of anionic tracers[130] originally demonstrated this charge-selective function and also indicated possible GBM involvement in relation to

proteinuria. Nevertheless, conversations around the potential charge-selective function of the GBM's and any resultant contributions to proteinuria have been conflicting.

More recent knockout studies have challenged earlier experiments that attributed the filtration barrier's charge-selective function to the GBM. For example, when major contributors of the GBM's negative charge (argin and perlecan) have been knocked out or reduced by heparanase, the anionic charge of the GBM has been reduced, albeit permeability to negative tracers and proteins has remained unaffected[131 132 133]. Additional studies have argued that the charge-selective function may arise, not from the GBM, but from alternative layers within the glomerular filtration barrier, such as, the endothelial layer (see next section **2.3.1.3**)[98 134]. Thus, there is evidence to support and refute GBM involvement in the development of proteinuria by neutralising charges at the barrier and altering charge-selectivity. The involvement of other layers within the glomerular barrier in relation to charge-selectivity must also be considered (e.g., endothelial layer).

2.3.1.3. Glomerular endothelial layer

The glomerular endothelial layer is the inner most layer of the filtration barrier, lining the glomerular capillary wall and having contact with the blood (**Figure 2.5a** and **Figure 2.5b**). It is composed of endothelial cells, the empty space between endothelial cells (fenestrations), and the endothelial cell surface layer (ESL)[98]. The ESL is composed of the glycocalyx, rich in membrane-bound proteoglycans (PGs), and the attached endothelial cell coat[135], rich in secreted PGs, as well as, other secreted components including glycosaminoglycans, glycoproteins, and plasma proteins[98] (**Figure 2.5a** and **Figure 2.5b**). The fenestrations are unlike the spaces between podocytes and lack a 'gate-keeper' (**Figure 2.5a**), ultimately resulting in the 'free' passage of fluid and macromolecules (i.e., small proteins)[129 136].

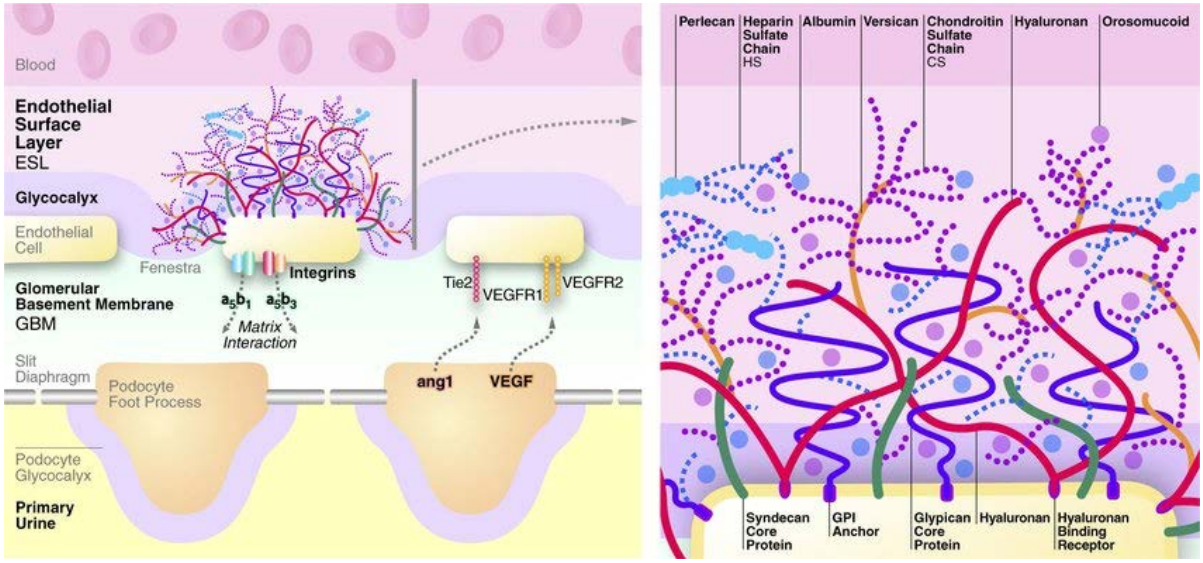

Figure 2.5 – Components within the glomerular filtration barrier. Fig. 2.5a (left) – Depiction of podocytes, slit diaphragms, glomerular basement membrane (GBM), endothelial cells, and the endothelial cell surface layer (ESL; endothelial cell coats and glycocalyx); **Fig. 2.5b (right)** – A close view of the endothelial cell coat and glycocalyx of the ESL. Note the bound alpha-1 acid glycoprotein (orosomucoid) to the chondroitin sulphate chain. Adopted from Haraldsson B, Nystrom J, Deen WM. Properties of the glomerular barrier and mechanisms of proteinuria. *Physiol Rev* 2008;88(2):451-87[98].

Considering the width of fenestrations (diameter, 600 to 700 Å or ~60 to 70 nm)[137] and the size of small proteins (e.g., radius of α1-AG, 29 Å, or radius of albumin, 37 Å) it would be reasonable to deduce that the endothelium contributes very little to the prevention/maintenance of permeability at the glomerular barrier[98]. On the contrary, however, recent studies have grown increasingly interested in the endothelial layer with regards to this function and have demonstrated contributions from both the endothelial cell coats and the dense network of negatively charged fibres (the glycocalyx)[98]. As previously mentioned, α1-AGP may bind to endothelial cells[138] adding to the anionic charge of the glomerular filter and may, therefore, help to repel anionic plasma proteins and prevent increases in permeability. Increased local production of α1-AGP by endothelial cells also remains possible[47] and would similarly contribute to the anionic charge. Conversely, a reduction in the anionic charge at the barrier would promote leakage into the urine. Inhibition of α1-AGP binding at endothelial cells,

due to the presentation of unfavourable glycoforms (activated by inflammation) or increased amounts of bound α1-AGP, would also be expected to limit its beneficial contributions to the glomerular barrier and could, furthermore, be expected to promote glomerular leak. The presence of urinary α1-AGP, in this case, may indicate endothelial cell dysfunction[47 139] or acute local physiologic disruption at the endothelial cell layer similar to that observed following experimental displacement (via infusion of hypertonic solution) of glomerular anions[135].

2.3.1.4. Mesangial cells

Mesangial cells are comprised of many components that are similar to those of other layers of the filtration barrier such as: collagen type II (and other types); laminin; and proteoglycans[98]; however, unlike other layers the mesangial cells are not in contact with either the perfusate (i.e., blood) or urinary lumen and exist in the glomerular matrix of differentiated cells (**Figure 2.6**). Mesangial cells form a contractile pole within renal functional units[140] that helps to regulate glomerular responses to pressure. Given this, it is unlikely that mesangial cells contribute to charge-selectivity. By contrast, mesangial cells more likely contribute to size-selectivity. Further, proteinuria possessing a mesangial component is most likely indicative of chronic pathophysiologic maladaptation as oppose to any transient physiologic response(s). Nevertheless, the possession of A-II receptors makes them vulnerable to acute involvement[141], which, along with other factors, will be discussed in the following sections related to the dynamic interactions between the glomerulus and α1-AGP during ascent.

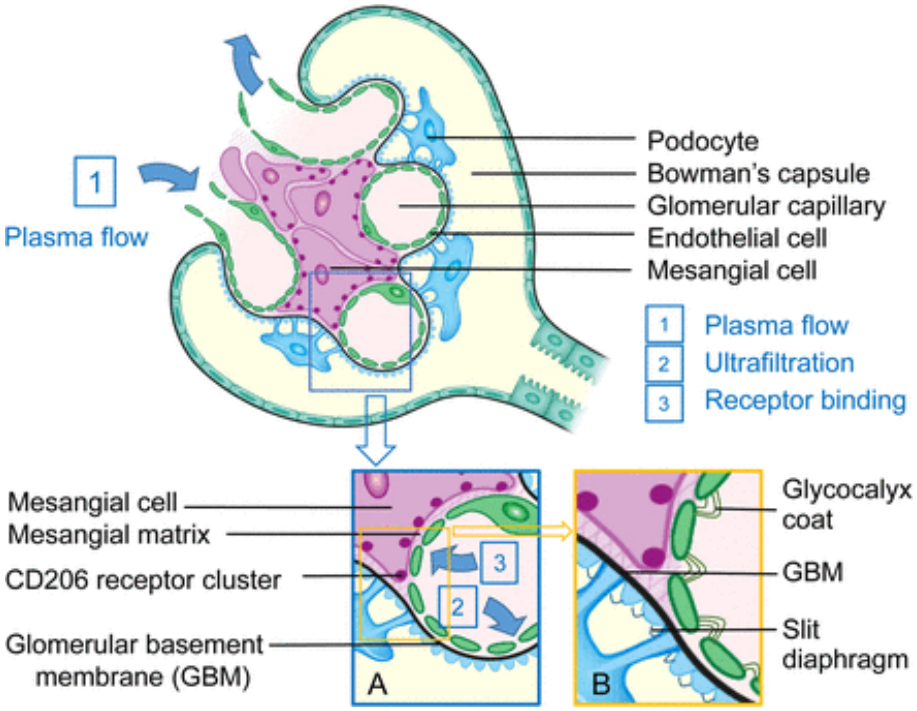

Figure 2.6 – Graphical representation of the glomerulus. The figure highlights the organisation of glomerular structural components relative to mesangial cells. Adopted from Qin Z, Hoh CK, Olson ES, et al. Molecular Imaging of the Glomerulus via Mesangial Cell Uptake of Radiolabeled Tilmanocept. *J Nucl Med* 2019;60(9):1325-32[142].

The comparison between α1-AGP and albumin (refer to **2.2.1.2**) taken together with the properties of the layers of the glomerular filtration barrier provide evidence to support α1-AGP as an improved marker of glomerular response compared to albumin. Further, α1-AGP stands to contribute greater insight into the aetiology of glomerular leakage (e.g., charge selectivity or recovery) and, therefore, may improve the understanding of proteinuria with acute physiologic challenge (e.g., physical exercise or altitude exposure) as discussed next.

2.4. ALTITUDE-INDUCED PROTEINURIA

2.4.1. Significance of α1-AGP loss during ascent

Plasma α1-AGP has been demonstrated to modulate capillary permeability at anatomical sites implicated in the progression of altitude illnesses (e.g., blood brain barrier[143],

and acute mountain sickness (AMS) or high-altitude cerebral oedema (HACE)[144]; or alveolar tissues[2] and high-altitude pulmonary oedema (HAPE)[145 146]). Thus, the significance for its loss (or blunted plasma increases) during ascent is emphasised by the potential instigation or perpetuation of oedema formation, which may result in the progression of altitude illness. Further, α1-AGP's generalised antagonistic effects on capillary leak[95] suggest that glomerular permeability (presenting as proteinuria) may provide insight into the leakiness of capillaries at other sites (e.g. brain).

2.4.2. Aetiology and mechanisms of altitude-induced proteinuria

Disruptions of physiologic homeostasis that occur with ascent and result in microvascular leak (presenting as transcapillary leak or oedema[147 148]) among lowlanders could, in part, begin to explain the acute transient altitude-induced proteinuria observed in these individuals[149 150]. By comparison, acute and chronic determinants of proteinuria among high-altitude natives[151] and residents[152] may be more difficult to distinguish. Nevertheless, the transient increases in proteinuria during ascent among lowlanders resolve with descent[153], much like the resolution of proteinuria following exercise cessation[11 154]; although the timeline for proteinuria to return to baseline following ascent is not well-established nor understood.

Until experiments by Winterborn and colleagues[155], altitude-induced proteinuria had been hypothesised to be a product of either the inhibition of tubular reabsorption by hypoxia or an alternate glomerular mechanism. With the infusion of lysine (a strong inhibitor of tubular protein reabsorption[156]) at altitude, Winterborn and colleagues were able to eloquently demonstrate that altitude-induced proteinuria was not only evident *before* the inhibition of tubular reabsorption (indicating a glomerular origin) but also was substantially increased following lysine infusion[155]. This evidence, indicating predominantly glomerular origins for

altitude-induced proteinuria, is further supported by studies examining protein excretion and lithium clearance with ascent that have showed unaltered tubular function at altitude[148]. The altitude-induced glomerular leak has been recently highlighted by Talks and colleagues[7], who also reported discrepant urinary leakages of similarly sized yet equally and oppositely charged proteins (e.g., α1-AGP vs lambda free light chains), as well as, additional differentials between anionic proteins (i.e., albumin vs α1-AGP). Given that albumin and α1-AGP are similar in size and α1-AGP being 'more' anionic[98], their differential leakages during ascent[7] indicate a perturbation of electrical forces within the glomerulus that is consistent with charge-selective mediated leakage. Thus, various physiologic factors that: 1) impact charge-selective properties; and 2) are altered with ascent (e.g., changes in acid-base balance, blood volume and composition changes, sympathetic nervous activity) can be considered and are discussed next.

Changes in serum [α1-AGP] may be considered as a factor that could influence urinary leakage however, increases in urinary α1-AGP do not correlate with changes in serum levels during ascent[149]. These results are consistent with earlier sea-level reports[157]. This is not to say, however, that upregulation of hepatocyte production of α1-AGP does not occur or is irrelevant during ascent to altitude as suggested in previous sections. Rather, the magnitude of hypoxia-induced hepatocyte production of α1-AGP does not appear to be indicative of the magnitude of its urinary excretion. Considering this, the stimulation of localised α1-AGP production, interaction, or altered function within the kidney due to hypoxia is more likely.

Anionic leakages during ascent have in fact been correlated with worsening SaO_2 (increasing hypoxaemia)[7], although this finding is not consistent[149]. It should be noted that the relative impact of hypobaria (altitude exposure associated with hypobaric-hypoxia), specifically, on responses that may contribute to altitude-induced proteinuria is not entirely clear[158]. Notwithstanding the potential independent effects of hypobaria and hypoxia with

regards to the stimulation of renal physiologic responses upon exposure to altitude[159], it can be suggested that hypoxia is the major contributor to proteinuria in the setting of high altitude[160]. As such, for the purposes of this thesis, and to improve understanding for the aetiology of altitude-induced increases in urinary α1-AGP, the focus shall remain on the direct effects of renal hypoxia, as well as, indirect mechanisms associated with physiologic responses to hypoxaemia (local or systemic). Existing hypotheses surrounding altitude-induced proteinuria have highlighted various potential mechanisms to include altered haemodynamics factors (e.g., flow or pressure changes) and acid-base disturbances (e.g., altered pH or local sialic acids), to name a few, although several additional factors may be influential (e.g., inflammation activation) during ascent.

2.4.2.1. Systemic and local acid-base disturbances

Alterations in acid-base balance upon exposure to altitude are well-documented[161 162]. These changes are a result of the hypoxic ventilatory response (HVR) induced by hypobaric hypoxia, which stimulates ventilation (an attempt to improve oxygenation). Such increases in ventilation result in concomitant reductions in both, arterial carbon dioxide ($PaCO_2$; hypocapnia) and hydrogen ion (H^+) concentration (increases in arterial/cerebral spinal fluid pH)[163]. The physiologic product of this response is known as respiratory alkalosis (as shown in **Figure 2.7**)[164] and is, in part, compensated for by increases in renal bicarbonate (HCO_3^-) excretion and H^+ retention (metabolic acidosis; via the proximal tubule) in an attempt to equilibrate pH (pH, ~7.4)[165].

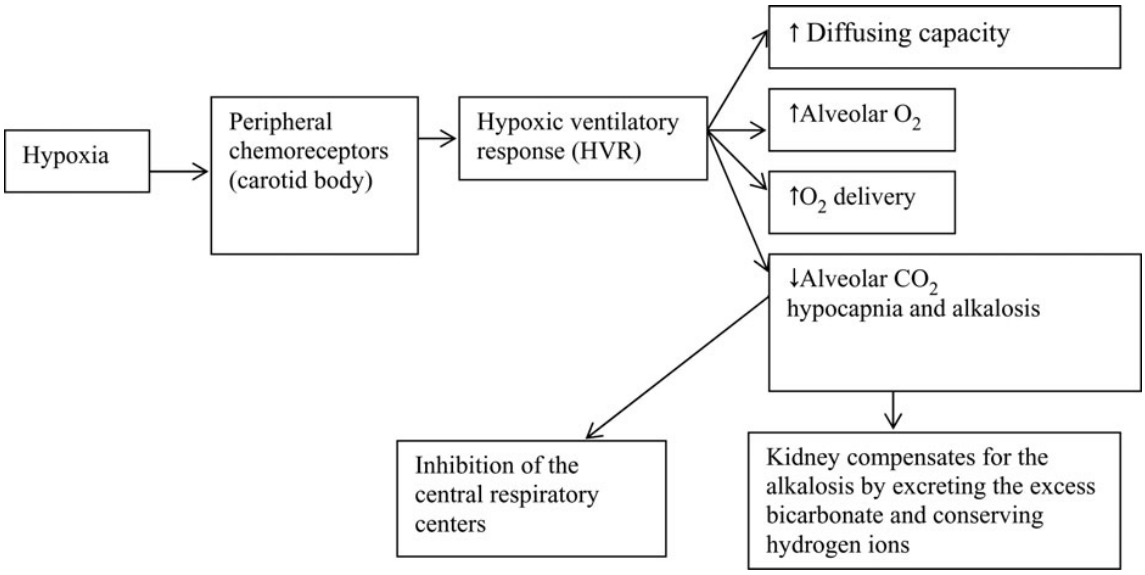

Figure 2.7 – Hypoxic stimulus (e.g., altitude) and resultant physiologic responses. Adopted from Goldfarb-Rumyantzev AS, Alper SL. Short-term responses of the kidney to high altitude in mountain climbers. *Nephrol Dial Transplant* 2014;29(3):497-506[164].

Hypotheses regarding the impact of acid-base disruptions on proteinuria during ascent may have, in part, been sparked by early results from exercise experiments that demonstrated a relationship between increases in blood lactate (or via increases in organic acid) and increases in post-exercise proteinuria[166]. Such hypotheses may have been further reinforced by those results observed following experimentally induced metabolic acidosis (via intravenous HCl)[167], as well as, the potential effects of pH on pore radii[168] that would promote increased proteinuria. Nevertheless, pH-induced alterations of pore radii alone cannot explain the variable changes in excretion rates between proteins of varying size and charge reported by Talks and colleagues[7] during ascent. Thus, an alternate mechanism of action of pH at the glomerular barrier must be considered. For example, a reduction in pH of the perfusate (i.e., the blood) may neutralise (via increased deposition of cations onto the anionic membrane) opposing charges between the blood and the filtration barrier, such that the barrier no longer favours repelling proteins back into the blood[169]. This is supported by experimentally induced glomerular permeability (and 'non-renal' microvascular permeability) to anionic proteins[170]

using protamine (a compound containing positive charges that associate with negative charges in the glomerular barrier)[171], which neutralises the predominantly negative GBM and effectively results in a net charge loss. Similarly, high- and low-ionic strength solutions have been used to demonstrate the influence of these electro-osmotic pressures exerted by perfusates on glomerular permeability. High-ionic strength solutions significantly increase the charge density of anionic proteins at the membrane while low-ionic strength perfusates significantly reduce the charge density of anionic proteins at the membrane[172]. Thus, charge neutralisation of the filtration barrier via a disruption of ionic equilibrium within the perfusate (the blood) could impact glomerular permeability and proteinuria with ascent as oppose to solely the charge of the leaking proteins in question[170 173].

Physiologic results observed with *progressive* ascent (as oppose to acute hypoxic exposure) however, are inconsistent with earlier hypotheses surrounding pH as potential mechanism contributing to altitude-induced proteinuria. More specifically, beyond initial exposure to high-altitude and with progressive ascent, reductions in $PaCO_2$ exceed HCO_3^- excretion, pH trends upwards, and alkalisation ensues[174 175]. Assuming the aforementioned theory to be true (i.e., reduced pH promotes charge-neutralisation-induced proteinuria), the alkalisation observed with progressive ascent would be expected to attenuate, rather than stimulate, proteinuria by limiting any charge neutralisation at the glomerular barrier or by limiting any pH-induced changes in pore radius. Nevertheless, the progressive increases in proteinuria with ascent clearly contradict this hypothesis[7]. A similar misalignment is evident with the administration of acetazolamide during ascent to altitude (as described next).

Acetazolamide is a potent carbonic anhydrase inhibitor* that is regularly administered for prophylaxis or treatment of AMS[176] as it helps to expedite acclimatisation[177], largely, by improving oxygenation[178 179]. Acetazolamide facilitates oxygenation by stimulating breathing through artificial acidification of the blood via inhibition of renal HCO_3^- reabsorption and reduction of renal H^+ excretion (prompting metabolic acidosis)[180], albeit additional mechanisms have been noted (e.g., reduction in hypoxic pulmonary vasoconstriction independent of carbonic anhydrase inhibition)[181 182]. In accordance with the aforementioned theory for the elevation in perfusate [H+] (lowering pH; metabolic acidosis) promoting charge neutralisation at the glomerular barrier, the acidotic effects of acetazolamide would be expected stimulate proteinuria. Contradictory to this, however, acetazolamide has been shown to attenuate proteinuria during ascent[183], albeit results have been conflicting[155]. Nevertheless, attenuation of proteinuria by acetazolamide during ascent indicates that altitude-induced proteinuria likely occurs independent of or secondary to changes in pH (or changes in $[H^+]$). Based on this, it could be further argued that altitude-induced proteinuria is largely attributable to downstream effects of hypoxaemia (e.g., inflammation) that can be mitigated by improvements in arterial oxygenation (e.g., with acetazolamide administration or with descent). Acetazolamide may work dually in this regard to limit altitude-induced rises in proteinuria by improving oxygenation and attenuating rises in pro-inflammatory cytokines (in the lung)[184]. To further elucidate the mechanisms by which acetazolamide may attenuate proteinuria during ascent, the examination of urinary α1-AGP from specimens collected during ascent and descent or with acclimatisation (i.e., multiple nights spent at same elevation) should

* Carbonic anhydrase is an enzyme that catalyses the reversible reaction between water (H_2O) and carbon dioxide (CO_2) and the dissociated ions of carbonic acid (H^+ and bicarbonate, HCO_3^-).

be considered alongside measurements for hypoxaemia, blood pH, and secondary factors (e.g., inflammatory markers) collected in parallel.

Although pH-induced alterations in glomerular permeability (via induced changes in pore radius or strictly changes in electrokinetic forces at various layers within the GBM) may contribute to proteinuria in certain scenarios, based on the presented evidence they do not appear to greatly contribute to altitude-induced rises in urinary α1-AGP. It remains possible that progressive increases in altitude (lower partial pressure of O_2) may increase either (or both) sialylation of α1-AGP (with sLe^X structure favoured; via some oxygen-sensitive pathways) or localised production or accumulation of renal cortical sialic acids, which can decrease anionic attributes of the electrostatic glomerular barrier, reducing its efficiency to repel anionic proteins[185]. Nonetheless, alternative mechanisms independent of acid-based changes that could promote urinary α1-AGP excretion during ascent should be considered and will be discussed in proceeding subsections.

2.4.2.2. Haemodynamic determinants

Haemodynamics within the glomerulus are complex with dissociated control observed for afferent (delivering) and efferent (receiving) arterioles. With regards to pressure and flow, vasoconstriction of the afferent arteriole reduces renal blood flow (RBF), reduces glomerular capillary pressure (P_{GC}), and reduces glomerular filtration rate (GFR); while vasodilation of the afferent arteriole increases RBF, increases P_{GC}, and increases GFR. By contrast, (mild) vasoconstriction of the efferent arteriole increases P_{GC} ('back-up' of blood) and GFR but reduces RBF; while vasodilation of the efferent arteriole reduces P_{GC} and GFR but increases RBF (**Figure 2.8**). Therefore, increases (or decreases) in GFR at altitude may be indicative of various changes in RBF or filtration pressure with increases in efferent vascular resistance during

ascent, potentially, resulting in high intraglomerular pressures (overly elevated P_{GC}) and possibly presenting as hyperfiltration.

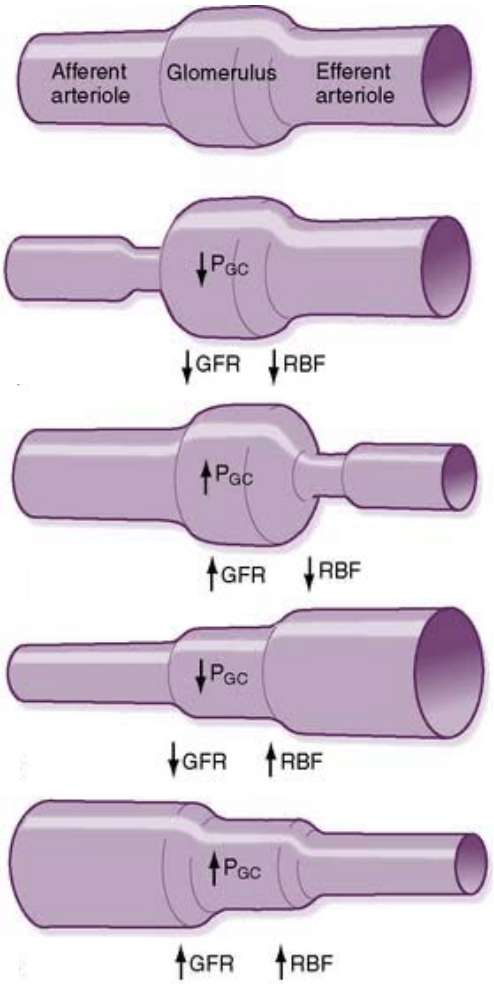

Figure 2.8 – Renal haemodynamics. Alterations in vasodilation or vasoconstriction of afferent and efferent arterioles are depicted in relation to the associated changes in glomerular filtration rate (GFR), renal blood flow (RBF), and glomerular capillary pressure (P_{GC}). Modified from Rennke, H. G., Denker, B. M., & Rose, B. D. (2007). *Renal pathophysiology: The essentials*. Philadelphia: Lippincott Williams & Wilkins[186].

Challenges to haemodynamic homeostasis, such as, reductions in blood flow (via redistribution to other tissues or reductions in total blood volume), vasoconstriction of the efferent arteriole (resulting in increased P_{GC}, intra-glomerular capillary, and filtration pressures), or elevations in systemic blood pressure (BP) promote proteinuria[11 12 187]. Therefore, alterations in haemodynamics that occur during ascent, such as, amplifications in

systemic BP[188], altered nocturnal dipping patterns[188], or increases in mean arterial pressure[189], could be expected to contribute to altitude-induced proteinuria. By contrast, afferent arteriole vasodilation (as observed with low blood pressure[110] or the administration of calcium channel blockers, CCBs[190]) during ascent could be expected to reverse any such afferent arteriole vasoconstriction-induced proteinuria. Attenuation of the vasoconstrictor effects by dihydralazine (an anti-hypertensive) during exercise supports this hypothesis[187] however, exacerbation of proteinuria despite vasodilation (via dopamine infusion)[189] at altitude is contradictory to it. These altitude results are further supported by the attenuation of altitude-induced increases in BP and hyperfiltration (by isradipine, a dihydropyridine class CCB) in the absence of concomitant reductions in altitude-induced proteinuria responses[148]. It is therefore suggested that altered filtration *pressure* (at the afferent arteriole) is not solely responsible for altitude-induced proteinuria and that pressure-independent (albeit still haemodynamically relevant) mechanisms may also be applicable.

2.4.2.2.1. Natriuretic peptides

Vasoconstriction of the afferent arterial (via exercise-[187 191] or altitude-induced[192] increases in noradrenaline and adrenaline) and subsequent reductions in RBF (or renal effective plasma flow)[189] during ascent may promote such altitude-induced proteinuria by amplifying reductions in O_2 delivery or altering the filtration-dependent potential difference along the glomerular barrier. The latter can be demonstrated with podocyte effacement[*], a response to injury that is characterised by changes in podocyte structure (e.g., retraction, flattening, widening, or shortening of foot processes) and function, that involves 'blocking' of

[*] Causes of podocyte effacement primarily relate to disarrangement of the cytoskeleton and may be product of: 1) systemic or local production of toxins, viral infection or activation of renin-angiotensin-aldosterone system; 2) abnormalities of structural proteins; 3) 'congenital or acquired' disorders associated with injury to the slit diaphragm; or 4) changes in GBM structure (refer to 193. Matovinović MS. Podocyte Injury in Glomerular Diseases. *EJIFCC* 2009;20(1):21-27.).

capillaries and subsequent reductions in filtration and disruptions of local electrochemical properties at the glomerular barrier (shown in **Figure 2.9**)[169]. While podocyte effacement is an unlikely cause of proteinuria during ascent, given the transient nature of altitude-induced proteinuria, alternate factors changing with ascent (as discussed next) may influence the filtration-dependent potential difference and could elicit the same end result.

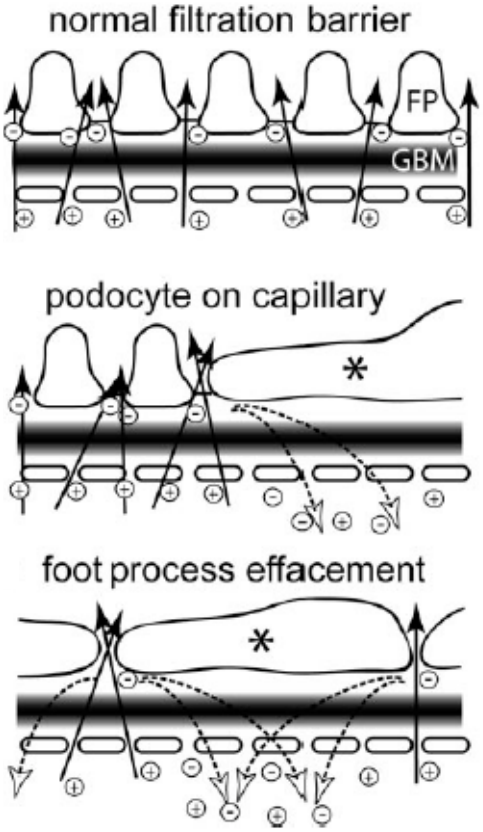

Figure 2.9 – Filtration-dependent electrokinetics. Normal electrical forces (top) with normal podocyte (or foot process, FP) function are depicted as are electrical forces with mild (middle) or severe (bottom) podocyte dysfunction (e.g., podocyte on capillary or foot process effacement, respectively). Electrical forces are shown to impede filtration and block the movement of ions, which can alter charge-selectivity. Solid arrows (top) indicate the expected attraction of cations to anions while hollow arrows (middle and bottom) indicate abnormal displacement of ions. GBM, glomerular basement membrane. * Damaged podocytes exhibiting effacement. Modified from Hausmann R, Kuppe C, Egger H, et al. Electrical forces determine glomerular permeability. *J Am Soc Nephrol* 2010;21(12):2053-8[169].

Hypoxia-induced reductions in venous return (via progressive contraction of plasma volume[194], large-scale reductions in venous drainage[195], or increased venous congestion[196]) may function similarly to the experimental obstruction of venous return from the legs when in the supine position. Such obstruction (e.g., thigh cuff occlusion) drastically reduces renal perfusion pressure and GFR, which reduce the filtration-dependent potential difference[169] (as with podocyte effacement described above). By contrast, experimental leg compression in the upright position limits pooling of blood in the legs and, thereby, promotes venous return, which enables the maintenance of normal renal perfusion pressure and GFR. Consequently, filtration-dependent potential difference is upheld, and proteinuria is prevented[169]. Venous return experiments provide evidence to support the potentiation of macromolecule diffusion (and proteinuria) with 'sluggish flow'[187] through the glomerulus (or dependence on GFR for filtration of molecules of certain charge and size[169 197]). The promotion of proteinuria during efforts to maintain renal perfusion (e.g., ascent to altitude) however, remains possible via alternate pathways (e.g., A-II, as discussed next) independent of alterations in the filtration-dependent potential difference.

2.4.2.2.2. Renin-angiotensin-aldosterone system (RAAS)

With regards to an alternative pathway (mentioned above), altitude-induced proteinuria may be considered in light of changes in levels of ACE and A-II or activation of A-II type 1 receptors[198] (AT1; via activation of renin-angiotensin-aldosterone system, RAAS). Administration of ACE inhibitors at sea-level has been observed to reduce both, BP and proteinuria[199], whereas the administration of ACE inhibitors[200] and A-II type-1 receptor blockers (ARBs or AT1 antagonists)[188 201] at altitude has only been shown to reduce BP. Furthermore, despite the expectation of attenuated proteinuria with the inhibition of vasoconstriction of the efferent arteriole and mesangial cells in these instances, alternative

pressure-independent mechanisms, such as, inhibition of A-II mediated pathways[198 202] appear possible with direct actions on the GBM likely[203]. Evaluations of altitude-induced proteinuria following administration an ARB, such as, telmisartan[200] (or similar, e.g., losartan) during ascent could help distinguish between pressure-dependent vs pressure-independent mechanisms and the relative contributions to proteinuria during ascent. To that end, consideration of ACE genotype[204 205] or other genetic factors[206] may also be warranted. The impact of renin on proteinuria has been implicated using renin injection[207], which results in increased proteinuria, as well as, renin inhibition, which results in reduced proteinuria[208]. However, altitude-induced proteinuria occurs in the presence of reductions in plasma renin (and catecholamines)[209 210] making this an unlikely mechanism.

Volumetric perturbations observed during ascent result in consequential increases in atrial natriuretic peptide (ANP)[211 212]. ANP and brain natriuretic peptide (BNP) are hormones that are secreted by atria and ventricles, respectively, in response to excessive stretch or loading due to volume overload. The primary function of ANP is to promote renal sodium excretion with a primary purpose of reducing extracellular fluid volume[110]. ANP can, however, elicit increases in permeability to plasma proteins resulting in proteinuria[213] and may do so by increasing the size (radius) and number of pores at the glomerular barrier[214], rather than altering the charge-selectivity at the endothelial level. However, ANP-induced increases in pore size and number cannot account for discrepancies between α1-AGP and albumin excretion previously observed at altitude, given their similarities with size (as discussed above). Therefore, direct effects of ANP on the endothelial glycocalyx must be considered, especially, with recent implications of ANP-induced capillary permeability being a crucial function of ANP[215].

2.4.2.2.3. Renal sympathetic nerve activity

The afferent arteriole is innervated by the sympathetic nervous system (SNS), while the efferent arteriole is not. Renal sympathetic nerve activity (RSNA) is increased in response to hypoxia[216] and further augmented among individuals whom develop severe altitude illness[217]. Increased RSNA elicits reductions in RBF and GFR by constricting the afferent arteriole, which results in a fall in renal perfusion and may reduce the filtration-dependent potential as previously mentioned[169]. Increased RSNA also enhances sodium reabsorption[110] promoting fluid retention that may further exacerbate pressure stress at the glomerular filter. Nevertheless, such pressure change would be more likely to result in altered pore radius and therefore, RSNA's alteration in ionic strengths (e.g., [Na^+]) may be more relevant to charge-selectivity[172].

2.4.2.3. Blood composition

Polycythemia can also induce proteinuria at altitude[202], however, this is generally observed with long-term residence at high altitude and would fail to explain the transient rises observed among high altitude sojourners. Sub-clinical elevations in haematocrit associated with ascent may provide some insight. Increases in haematocrit can be due to a multitude of factors that may include but are not limited to the well-established increases in erythrocytes (number and mass), haemoglobin (and other plasma proteins; hyperproteinemia), and plasma volume contraction (via multiple mechanisms)[218]. Physiologically, the increases in haematocrit are associated with increases in blood viscosity (hyperviscosity), which result in alterations in transglomerular hydraulic and oncotic pressure gradients, as well as, greater intraglomerular pressures in order to facilitate filtration and maintain flow into the post-glomerular vasculature[219]. Proteinuria associated with hyperviscosity and hyperproteinemia therefore, may be attributed to the associated alterations in pressure in surrounding vessels[220 221]. In

addition, high protein concentration in the blood may subtly modify the Donnan potential (i.e., the behaviour of charged particles at a permeable membrane) and, independently of filtration pressure, may subsequently alter electrical forces at the filtration barrier[169].

2.4.2.4. Kinin system

The involvement of the kinin system (kallikrein enzyme) in the development of proteinuria has also been proposed[167]. Specifically, the kinin system's mediation of proinflammatory effects (via bradykinin, a vasodilator), as well as, its promotion of natriuresis and diuresis, could be relevant to altitude-induced proteinuria[222]. While exercise studies indicate that proteinuria is more attributable to the RAAS[223 224], exercise- and altitude-induced proteinuria may occur by different mechanisms. Thus, exercise observations related to the role of the kinin system may not be equally applicable to altitude-induced proteinuria

2.4.2.5. Cytokines and circulating factors

Cytokines, such as, IL-6[225], IL-8, IL-10 are all known to increase during ascent to altitude[226]. Moderate increases in systemic cytokines with ascent are considered to be reflective of considerable local inflammation[227], with the local increases[228] likely to occur in the lungs as well as the kidneys, amongst other tissues. Oscillatory sleep patterns (e.g., Cheyne-Stokes breathing and sleep apnoea[229]) causing frequent desaturations may contribute to these pro-inflammatory responses that promote proteinuria (at sea-level)[230], notwithstanding that altitude-induced proteinuria likely occurs by multiple mechanisms[2]. For example, tumour necrosis factor-α (TNF-α), increased by altitude-associated sleep perturbations[231], can influence carbohydrate moieties of α1-AGP[22] and thus, may alter its efficacy in glomerular endothelial cells and thereby result in permeability.

Several additional circulating factors (e.g., hypoxia inducible factor 1α, HIF-1α) are also known to increase with ascent. Altitude-induced increases in HIF-1α may result in podocyte effacement or attenuated expression of integral structural components essential for podocyte integrity (podocin and nephrin), which could result in proteinuria[232]. Vascular endothelial growth factor (VEGF) may also be influential[233]. All in all, the effects of cytokines and circulating factors appear to alter a combination of both charge- and size-selectivity in glomeruli of healthy individuals.

2.4.2.6. Oxidative stress

Exaggerated intra-renal (cortical or medullary) hypoxia (by altitude or altitude-induced reductions in renal blood flow) may activate local hypoxia-sensitive pathways[234] that can induce proteinuria at different levels of the glomerular barrier (e.g., podocytes or GBM). Hypobaric-hypoxia associated with ascent to and residence at high-altitude[235] increases the production of reactive oxygenated species (ROS) and limits antioxidant repairing, which, in concert, results in greater oxidative stress that can confer cellular damage[236]. In the kidney, ROS production can damage integral proteins within the GBM (e.g., depolymerisation of the HSPG's into oligosaccharides)[237]. Degradation of laminin and heparan sulphate by ROS results in a decrease in the degree of the resting negative charge at the GBM, which is thought to increase its permeability to negatively charged molecules[136 238]. ROS scavenging helps to minimise this damage, limit increases in permeability, and reduce resultant proteinuria[239]. Factors that limit ROS scavenging during ascent could be important for limiting proteinuria. Nevertheless, while the production of uric acid (serum urate), an important and potent endogenous antioxidant defence mechanism[240], is elevated (hyperuricemia) during ascent[241], hyperuricemia has been shown to increase proteinuria in some cases[242]. Thus, the relevance of

excessive local ROS production or limited ROS scavenging to proteinuria during ascent requires further investigation.

2.4.2.7. Nitric oxide (NO)

Bioavailability of renal NO may also play a role in altitude-induced proteinuria. Decreased NO synthesis in the kidneys is known to precede proteinuria, with consequential elevations in proteinuria being reversible when NO is 'donated'[243]. While altitude is associated with generalised reductions in NO bioavailability (due to changes in amounts of isoforms or synthesis)[244], the consequential effects in relation to proteinuria are yet to be investigated.

2.5. EXERCISE-INDUCED PROTEINURIA

2.5.1. Significance of α1-AGP loss with exercise

Similar to albumin, stimulation of hepatic α1-AGP synthesis has been demonstrated in response to exercise with increased levels observed in blood, as well as, muscle and other tissues [245]. The significance for these increases in humans however, remains somewhat unclear. In exercising animals, the importance of α1-AGP (in plasma and muscle) has been demonstrated for muscle glycogen content[246] and muscular endurance[245]. Specifically, α1-AGP increases the dephosphorylation and activity of glycogen synthase promoting glycogen storage[246]. Considering this, low plasma α1-AGP (or α1-AGP loss) could conceivably be expected to contribute to muscular fatigue making α1-AGP excretion during exercise contradictory to its physiologic function. Nevertheless, post-exercise α1-AGP excretion appears to be a normal physiologic response that accompanies exercise[6].

2.5.2. Aetiology of exercise-induced proteinuria

Like, altitude-induced proteinuria, exercise-induced proteinuria is an acute, transient phenomenon peaking approximately 60 minutes after the cessation of (short-duration) maximal exercise, albeit having the potential to remain elevated above resting levels for up to 2 to 24 hours[11 154]. The intensity of exercise largely dictates the degree and type (glomerular vs tubular) of post-exercise proteinuria[247] with proteinuria following maximal exercise being of the glomerular/tubular mixed-type[248]. However, there is evidence to indicate that the glomerular component predominates. This has been shown using lysine infusions similar to altitude experiments concerning proteinuria[156] and is further emphasised by the predominance of albumin, transferrin, and IgG in post-exercise urine[249]. Nevertheless, the mode of exercise is also influential as evident in the differences between post-exercise proteinuria excretion rates after cycling and running (at comparable loads)[247]. There is also evidence to indicate a genetic component for post-exercise proteinuria[206].

As previously discussed for altitude-induced proteinuria, increases in glomerular permeability can be product of alterations in charge- (at the GBM or endothelial layer) and size-selectivity (e.g., widening of the slit diaphragm or failure of the podocytes) at the glomerular barrier. Like altitude-induced proteinuria, the overarching causes for such glomerular responses with exercise remain allusive. Nevertheless, hypothesised mechanisms for exercise- and altitude-induced proteinuria appear similar and have included: 1) haemodynamic determinants, 2) hormonal influences, 3) acid-base disturbance[8 9], and 4) hypoxia and oxidant stress[10-12].

2.5.2.1. Acid-base disturbances

Based on early animal experiments demonstrating elevated proteinuria with metabolic acidosis[250 251], the increased blood lactate (and reduction in serum pH) observed

with intense exercise has been suspected as a contributor to post-exercise proteinuria. As mentioned, acid-base disturbance is thought to contribute to proteinuria by neutralising the surface anionic charge at the filtration barrier[9], thereby increasing glomerular permeability. Studies of isolated perfused kidney have provided additional support for this by showing that kidneys are more permeable to albumin when perfused with low pH solution[169 173]. By contrast however, neither the administration of oral NH_4Cl or intravenous lactic-acid produce any proteinuric effect[187]. Further, different modes of exercise eliciting similar levels of blood lactate show no relationship with post-exercise proteinuria[247]. Thus, exercise intensity/workload appear to promote proteinuria independent from the ensuing lactate concentration.

Experiments with exercising dogs, however, have demonstrated that increased renal-cortical sialic acids (i.e., local acids) exhibited with exercise may decrease the efficacy of the electrostatic barrier and increase post-exercise proteinuria[185]. This is supported by the substantially greater post-exercise proteinuria observed among diabetics[156], whom exhibit increased glomerular sialic acids compared to healthy individuals[252]. Thus, local rather than systemic acid-base disturbance may be a contributing factor to post-exercise proteinuria.

2.5.2.2. Haemodynamic determinants

The haemodynamic responses associated with exercise, such as, reduced RBF, increased PG_C pressure, and increased systemic pressure all challenge renal homeostasis, which may contribute to exercise-proteinuria[11 12 187]. The contribution of reduced RBF (by way of renal arteriole vasoconstriction) to post-exercise proteinuria has been demonstrated by stimulating proteinuria with noradrenaline infusion[187 191] , which significantly increases (along with adrenaline) during exercise[253]. The attenuation of exercise-induced alterations in renal plasma flow and resultant proteinuria by dihydralazine (a direct vasodilator) further supports this hypothesis[187]. Although the mechanism(s) by which this occurs are not entirely clear, as

previously mentioned, it is suggested that the 'sluggish' glomerular flow may enhance the diffusion of macromolecules (e.g., α1-AGP and albumin)[187].

2.5.2.2.1. RAAS

While renin is an unlikely contributor to altitude-induced proteinuria, the opposite may be true for exercise. Exercise-induced proteinuria agrees with observations demonstrating increased proteinuria following renin injection as exercise is known to excite the RAAS and stimulate renin release from the kidneys[254 255] (via changes in renal perfusion and renal sympathetic nerve activity). Renin may stimulate proteinuria directly by acting on components within the glomerulus (e.g., mesangial cells)[256], or indirectly via downstream factors associated with renin release (e.g., effects of A-II or aldosterone)[187 257]. The latter of these two is most likely given the reduction in post-exercise proteinuria following the administration of captopril, an ACE inhibitor[258] whose anti-proteinuric effect has been attributed to its inhibition of A-II upregulation (rather than its inhibition of kininase)[218 219]. Further, animal models have demonstrated that A-II inhibition reduces post-exercise proteinuria[259]. The mechanism(s) underpinning A-II's involvement in post-exercise proteinuria, however, are not well-understood. It is suspected that A-II may increase glomerular permeability by increasing the space between endothelial cells (size of fenestrae) or reducing heparan sulphate expression[260].

2.5.2.2.2. Nitric oxide

Nitric oxide (NO) is one of the major vasodilators within the kidney. During exercise, its production increases in response to vascular shear stress with this being important for appropriate blood flow redistribution[261]. To this point, NO plays a key role in the appropriation efferent arteriole vasoconstriction by way of countering the vasoconstriction imposed by A-II during exercise[262 263]. Further, disruption or misappropriation of this balance may favour

exercise-induced α1-AGP excretion by way of moderating renal plasma flow and the subsequent diffusion of macromolecules, as previously discussed.

2.5.2.3. Prostaglandins

Evidence also indicates that prostaglandins influence α1-AGP[233], and may, therefore, have an impact on α1-AGP excretion during exercise. Vasodilatory prostaglandins may attenuate exercise-induced proteinuria by countering renal vasoconstriction associated with increases in renal sympathetic activity and A-II encountered during exercise. However, in healthy well-hydrated individuals, the haemodynamic effects of prostaglandins appear trivial in relation to the development post-exercise proteinuria[264] [265]. Rather, prostaglandin production may directly influence glomerular permeability during exercise via the actions of products from the cylcooxygenase pathway (i.e., arachidonic acid metabolism) on glomerular podocytes, endothelial cells, or mesangial cells [266] [267].

2.5.2.4. Hypoxia and oxidative stress

Considering previously proposed hypotheses, the stimulation of post-exercise proteinuria by exercise-induced hypoxaemia[268] is the least understood. This hypothesis may stem from altitude-based studies previously discussed that have shown relationships between reduced SaO_2 (or worsening PO_2) and increasing proteinuria, however, the underlying mechanisms for this are unclear.

The production of reactive oxygenated species (ROS) with intense exercise[269] may influence exercise-induced proteinuria due to the depolymerisation of glycosaminoglycan chains in the glomerular ESL[270], which increases permeability. ROS and nitrogen radicals may also degrade heparan sulphate and thereby reduce the resting negative charge at the GBM increasing its permeability to negatively charged molecules[136] [238]. Similarly, ROS may interact

with NO in such a way that results in the disruption of the vasoconstrictor-vasodilator balance as previously mentioned.

2.5.2.5. Other factors

Several alternative factors with known effects on the glomerular barrier (e.g., HIF-1α) that are altered during exercise may also be relevant to post-exercise proteinuria. For example, exercise-induced increases in HIF-1α (in an intensity-dependent fashion[247]) may function similarly to the experimental accumulation of HIF-1α. That is, exercise-induced increases in HIF-1α may promote post-exercise proteinuria by attenuating the expression of structural components essential for podocyte integrity (i.e., podocin and nephrin)[232]. The potential effects of the target genes of HIF-1α (e.g., VEGF[271], tissue-specific inhibitor of matrix metalloproteinases[272], or plasminogen activator inhibitor) must also be considered, as evidenced in the pathophysiologic presentation of proteinuria. However, the absence of any relationship between HIF-1α and exercise intensity or duration[232], despite exercise proteinuria being intensity-dependent, suggests that HIF-1α is unlikely to be the main contributor to post-exercise proteinuria. Afterall, HIF-1α plays a key role in normal redistribution of blood flow during exercise [273].

Like altitude-induced proteinuria, VEGF, increasing in response exercise, may also have an impact on post-exercise proteinuria. VEGF secreted from podocytes is key for the development and maintenance of glomerular endothelial cells[274] with glomerular endothelial cells being extremely sensitive to the level of VEGF[275]. More specifically, increased bioavailability of VEGF increases glomerular permeability by increasing the size of fenestrae (i.e., gap) between adjacent glomerular endothelial cells, and also altering the associated glycocalyx[276]. Although fenestrae are essential for the clearance of low-molecular-weight waste

products[98], VEGF blockade can also contribute to hypertension and proteinuria[277]. Thus, a balance likely exists for the VEGF-mediated glomerular permeability by way of endothelial fenestrae and the associated glycocalyx.

2.6. CONCLUSION

A background and overview of α1-AGP has been presented along with highlights of its structures and functions. Renal structures and functions have also been described in relation to the presentation of urinary α1-AGP, as have the potential mechanisms contributing to urinary α1-AGP during ascent to high-altitude, such as, hypoxia, local acid-base disturbance, altered haemodynamics, altered blood composition, and fluctuations in various circulating or local factors (e.g., ANP, BNP, cytokines, VEGF, TNF-α, ROS or NO).

To better, and more efficiently, assess the mechanism(s) for urinary α1-AGP, an accurate and precise, albeit not labour intensive or expensive, analytical technique would be advantageous. The next chapter of this thesis explores the development and preliminary validation of an immunoturbidimetric assay developed for detection of low-concentration α1-AGP in human urine.

Chapter 3

DEVELOPMENTAL METHODS AND PRELIMINARY VALIDATION EXPERIMENTS FOR A LATEX-ENHANCED IMMUNOTURBIDIMETRIC ASSAY DESIGNED TO MEASURE LOW-CONCENTRATION ALPHA-1 ACID GLYCOPROTEIN (α1-AGP).

Authors and affiliations:

Joyce KE[1 4], Cook A[2], Cross A[2], Fountain A[2], Wallis G[2], Bradwell AR[3 4], and Lucas SJE[1 4].

1. School of Sport, Exercise and Rehabilitation Sciences, University of Birmingham, Birmingham, UK
2. Research & Development, The Binding Site Group Ltd., Birmingham, UK
3. Medical School, University of Birmingham, Birmingham, UK
4. Birmingham Medical Research Expeditionary Society, University Birmingham, Birmingham UK

Statements of contribution:

KEJ – concept, execution, statistical analysis, and writing; AC, AF, AC, and GW – Guidance and support with for developmental methods and preliminary validation experiments; ARB, – concept; and SJEL, writing.

ABSTRACT

INTRODUCTION: Surmounting evidence exists for clinical and research applications of alpha-1 acid glycoprotein (α1-AGP) as a urinary biomarker. The most widely used analytical techniques for its detection, however, remain time consuming and laborious. Further, evidence of any automated particle-enhanced turbidimetric immunoassay (PETIA) specifically developed for the measurement of low [α1-AGP] in human urine remains limited. The purpose of this study was to describe: 1) developmental methodology of a PETIA optimised for a widely available auto-analyser to detect low [α1-AGP] in urine; and 2) preliminary validation experiments for this PETIA. **METHODS:** Monospecific polycolonal antibodies raised against human α1-AGP were affinity isolated with $F(ab')_2$ conjugated to latex particles to produce a latex-enhanced reagent optimised for use on the Optilite™ auto-analyser. Preliminary validation experiments were conducted to assess intra- and inter- assay imprecisions, inaccuracy, recovery, linearity, interference, stability, and comparison of methods (radial immunodiffusion, RID vs PETIA). **RESULTS:** Imprecisions did not exceed allowable limits (all within ± 4 SDs). The assay was considered linear within the range of 0.277 – 4.653 mg/l, although some nonlinearity was detected. Interference was detected for urea but not ascorbic acid. Stability duration was taken as 121 days, the maximum time point tested. Methods comparison demonstrated that urinary [α1-AGP] from PETIA was, on average, greater than RID, albeit there was a strong positive relationship between results produced by the two methods. **CONCLUSION:** Development of a PETIA for detection of low-concentration urinary [α1-AGP] was successful with preliminary validation experiments indicating good precision and stability. Further investigations of linearity and interference may be considered for improved performance.

3.1. INTRODUCTION

Urine and serum proteins have presented as useful biomarkers of disease and have enabled both detection and long-term monitoring. Urinary alpha-1 acid glycoprotein (α1-AGP) has recently gained ground in clinical practice and has been able to identify and distinguish between patients with: psoriasis[4], Crohn's disease[278], bladder cancer[279], pre-eclampsia[280], sepsis[281], and heart failure[282], to name a few (see **Chapter 4** for more). Urinary α1-AGP has also been used for research purposes as a biomarker of (patho)physiologic renal response(s) following exercise[6 11] and during ascent to altitude[7]. Despite these exquisite applications, current analytical techniques for urinary α1-AGP, such as, radial immunodiffusion (RID)[7], western blotting[5], enzyme-linked immunosorbent assay (ELISA)[283 284 285], immunoelectrophoresis[286], and nephelometry[287] are time consuming, laborious, and expensive, which do not make α1-AGP conducive to frequent or large scale analysis. Automated immunoturbidimetry however, could combat this problem and particle-enhanced immunoturbidimetric assays (PETIAs) may offer an additional advantage of being more sensitive for low [α1-AGP], particularly, in urine.

Immunoturbidimetric assays utilise an antigen-antibody reaction and sometimes couple antibodies with small (40 – 300 nm) polystyrene (latex) particles with known wavelengths[288] (particle-enhanced turbidimetric immunoassay; PETIA). These assays then measure the change in magnitude of light transmitted through solution containing the suspended particles, as a product of the light scattering effect[289 290]. These properties of PETIAs ultimately enable detection of proteins not measurable by traditional methods[291 292] and can do so with near-to complete automation. PETIAs' automation also offer the advantage of speed (~10-minute run times)[5] without compromising precision or accuracy, unlike conventional

methods. In fact, automated PETIAs have proven to be more sensitive (analysing [analytes] 10 to 100 times lower than conventional methods) with improved precision compared to previously used techniques, such as, western blotting[5 288]. The fast run times and nearly complete automation of PETIAs could accommodate large quantities of analysis per unit of time. For obvious reasons, an assay such as this would be advantageous for an analyte whose clinical relevancies and significance(s) have already been established and whose analytical loads (number of analyses) have the potential to become high (e.g., urinalysis of α1-AGP in hospital for disease screening or prognosis evaluation).

The application of a PETIA for human urinary α1-AGP was first described in 2004[15]. The immunoassay was optimised for use on the Cobas Integra 700 auto-analyser (Roche Diagnostics, Risch-Rotkreuz, Swtizerland) with subsequent validation experiments split between the Cobas Integra 700 and Cobas Mira Plus analysers (Roche Diagnostics, Risch-Rotkreuz, Switzerland)[288]. The most recent PETIA for urinary α1-AGP was optimised for the c502 module of the Cobas 8000 analyser (Roche Diagnostics GmbH, Mannheim, Germany)[5], however, it was validated using a calibrator that has since been recalled (N Protein Standard, SL for BN II systems, ref. no. OQIM13, Siemens Healthcare Diagnostics GmbH, Marburg, Germany)[293]. Validation of this assay and any follow-up studies using it (or the indicated calibration fluid), therefore, may be called into question and create a clear need for the development and validation of a new PETIA for the analysis of low-concentration α1-AGP in human urine. The purpose of the present study was to develop a latex-enhanced turbidimetric immunoassay for the detection of low-concentration of α1-AGP in human urine, optimise it for the Optilite™ turbidimetric auto-analyser (The Binding Site, Ltd., Birmingham, UK.), and execute a series of preliminary validation experiments (e.g., intra- and inter- assay imprecision, linearity, interference, and stability).

3.2. METHODS

Developmental methodologies for the novel immunoassay were initiated with the isolation of antibodies (section **3.2.1**), which was followed by conjugation of latex particles (section **3.2.2**) to yield a particle-enhanced reagent that was optimised (section **3.2.4**) for the OptiliteTM auto-analyser (section **3.2.3**). These processes were followed by preliminary validation experiments (section **3.2.5**; for reagent lots A and B) that included assessments of: intra- and inter- assay imprecisions (section **3.2.5.2**); inaccuracy and recovery (section **3.2.5.3**); linearity (section **3.2.5.4**); interference (section **3.2.5.5**); and assay stability (section **3.2.5.6**). Any methodologies that differed between reagent lots (A and B) were described individually.

3.2.1. Isolation of antibodies

Antigen preparation and antibody isolation, purification, and digestion/fragmentation were the essential first steps in the reagent development process, albeit remained independent and beyond the scope of the present thesis. Despite this, a brief description of these processes is provided.

Isolation of α1-AGP from human sera (antigen preparation) was the first developmental step with the purified sera then used for the immunisation of sheep (ovine). This was followed by collection of the sheep anti-serum (containing sheep anti-human immunoparticles) and affinity isolation of monospecific polyclonal* immunoglobulins, which

* Polyclonal (as opposed to monoclonal) antibodies are antibodies made by multiple different (non-identical) immune cells (i.e. the antibodies are also not clones) with monospecific (as opposed to polyspecific) antibodies of this type additionally having specificity that is singular through one of several ways: 1) antibodies with affinity for the same antigen; 2) antibodies that are specific to one antigen; or 3) antibodies specific to one tissue or type of cell.

were further digested to yield anti-α1-AGP antibody fragments (also known as F(ab')$_2$). These fragments were then conjugated to latex particles as described next.

3.2.2. Latex conjugation and reagent production

As part of the present thesis' methodologies, conjugation of α1-AGP F(ab')$_2$ to latex particles was performed in the Research and Development Laboratory at The Binding Site, Ltd., Birmingham, UK as described in the next sections.

3.2.2.1. Reagent lot A

To initiate reagent production, α1-AGP F(ab')$_2$ was conjugated to latex particles (200 nm diameter). To start this process, latex (40 μl) with solid content of 10% w/v and an acid content of 95.4 μeq/g was pipetted into 14 × 2 ml tubes (to contain 1 ml volume). Deionised (ultra-pure) water (dH_2O; 727.4 μl) and 2-(N-morpholino)ethanesulfonic acid (MES) buffer (50.0 μl; BT125) were then added to each tube and followed by the addition of 7.3 μl of 1-ethyl-3dimethylaminopropyl carbodiimide (EDC; dissolved in water to give 10 mg/ml and stored at -20 °C). Tubes were quickly vortexed (~5 seconds) and then incubated for 10 minutes on a roller mixer. The F(ab')$_2$ (in stock, 148.6 μl) was then added to the tubes, which were then sonicated for ~15 seconds and then incubated for 30 minutes on a tube roller mixer. Following mixing, 26.7 μl of bovine serum albumin (BSA; in stock 15% w/v) was then added to the tubes, which were then sonicated again for ~15 seconds and then incubated for 45 minutes on a roller mixer with sonication performed after both, 15 and 30 minutes. Tubes were then removed from the roller mixer and centrifuged for 30 minutes at 16,000 g. After centrifugation, the buffer was removed, and the latex pellet was resuspended into 1 ml of wash buffer (tris buffer in a 1/30 dilution into 18 ml; 600 μl of tris and 17.4 ml of dH_2O) and sonicated. Following sonication, centrifugation was repeated (30 minutes at 16,000 g). Next, the wash buffer was

removed, and the latex pellet resuspended into 1 ml of storage buffer (1.6 ml of tris buffer, 1.056 ml of BSA, and 45.344 ml of dH_2O) and then sonicated. Following this sonication, the latex and storage buffer products contained in each 2 ml tube were pooled into a single 50 ml tube. An additional 28 ml of storage buffer (2 ml for each of the 14 tubes) was then added to complete production process and yielded a single 'batch' of latex reagent. The conjugated latex reagent was then left to sit for 24 hours in light-limited refrigeration at 4 °C to ensure its stability prior to initial calibration. This concluded the production procedures for batch 1 with procedures repeated the following day (for 12 × 2 ml aliquots) to produce batch 2. Batches 1 and 2 were ultimately pooled (to form reagent lot A) to ensure adequate volume for validation experimentation (described in later sections).

3.2.2.2. Reagent lot B

Reagent lot B was manufactured in bulk at a later date with production, again, being preceded by the isolation of antibodies as previously described (refer to section **3.2.1**). Alternatively, for reagent lot B, dH_2O, MES coating buffer, and latex were added to a beaker and then mixed with a magnetic stirrer instead of adding to individual 2 ml aliquots. Following stirring, EDC (activation agent) was added and the mixture was stirred again for an additional 10 minutes. This was followed by the addition of BSA (blocking agent) and immediate sonication for ~12 seconds with additional sonication after 15 and 30 minutes (each sonication lasting ~12 seconds). The contents were then centrifuged at 18,000 rpm for 20 minutes. After centrifugation, the supernatant was removed and then resuspended into 5 ml of wash buffer (0.25 mol/l tris) and sonicated until the latex was uniformly dispersed. The resuspended mixture was diluted in wash buffer to its original volume with centrifugation and resuspension steps repeated. The final concentrated latex-reagent volume at this point was 200 ml (produced 24 October, 2019), which was stored in light-limited refrigeration at 4 °C until

diluted (1/3 dilution) into storage buffer (0.25 mol/l tris; 0.33% BSA; 0.1% EACA; 0.01% Benzamidine; 0.05% Proclin) fifteen days later (06 November, 2019).

3.2.3. Instrumentation and analyser specifications

The Optilite™ turbidimetric auto-analyser (Model 1.2, Software version 6.0.1, The Binding Site, Ltd., Birmingham, UK) is suitable for immunoturbidimetric analysis of serum, urine, plasma, and cerebrospinal fluid (CSF) and was chosen for the present experimentation. All experiments were performed using a single analyser at a single site (The Binding Site, Ltd., Birmingham, UK). The reagent disc onboard the Optilite™ was maintained between 2 to 4 °C with limited exposure to light throughout all experiments while specimen racks were maintained at ambient temperature (20 to 22 °C), also with limited exposure to light.

A daily maintenance check for the Optilite™ was performed and documented in accordance with site-specific Standard Operating Procedures (SOPs) at The Binding Site, Ltd each day prior to experimentation. Successful completion of the daily maintenance check was contingent upon absorbance results from water blank tests that were performed for all cuvette positions and at all measurable wavelengths (nm)*. Allowable standard deviations (SDs) for absorbance results were set to ± 2 SD (in units for milli-absorbance; mA). If water blank results exceeded these limits, an additional wash was performed, and water blank tests repeated until an acceptable result was achieved. Additional weekly, monthly, and quarterly maintenance checks, as well as, routine monthly and quarterly precision checks were also maintained for the Optilite™ throughout experimentation (in accordance with internal SOPs).

* Measurable wavelengths of the Optilite™ auto-analyser included the following wavelengths (nm): 340, 380, 405, 450, 510, 540, 575, 600, 620, 660, and 700 nm.

3.2.4. Assay optimisation and test parameters

The α1-AGP immunoassay described herein was designed for urinalysis of low-concentration (< 0.19 g/l)* human α1-AGP. Optimisation of the dose-response curve was performed by varying the sample dose and antibody concentration until an acceptable curve was generated (see section **3.2.4.1** for optimised standard dilutions)†. This was performed in accordance with internal SOPs at The Binding Site, Ltd. and with assistance from the Research and Development team.

The analyser required 88 µl of latex reagent (78 µl vol. used and 10 µl dead vol.), 61 µl of diluent (46 µl vol. used and 15 µl dead vol.), and 36 µl of sample (11 µl vol. used and 25 µl dead vol.) per test. Actual run time of the assay was 594 seconds (9.9 minutes), which consisted of two incubation phases performed at 37 °C. Additional analytical properties for the immunoassay are outlined next.

3.2.4.1. Calibration

The European Reference Material fluid DA470k (ERM DA470k/IFCC, 617 mg/l, α1-AGP) was used as a calibrator for both reagent lots A and B, as specific calibrators for these latex regents were not commercially available[294] (see Appendix 2 for the Certificate of Analysis). The reference material was reconstituted to form the calibration fluid ([α1-AGP]‡, 4.490 mg/l) and frozen at –20 °C in individual 2 ml polystyrene cryovials on two separate occasions (15 × 2 ml for reagent lot A; and 20 × 2 ml for reagent lot B) for use on subsequent days. No freeze-thaw cycles were permitted for the calibration fluid with thawed aliquots discarded after use.

* 0.19 – 6.0 g/l is the measuring range for the existing α1-AGP assay for serum.

† SOPs are property of The Binding Site, Ltd. and are not available for re-print.

‡ Brackets are used as shorthand to refer to the concentration of an [analyte] (e.g. [α1-AGP]).

Prior to calibration, the calibrator was thawed on a roller mixer at ambient temperature (20 to 22 °C) for approximately 30 minutes. A series of 7 standard dilutions of the calibration fluid ([α1-AGP], 4.940 mg/l) plus one blank (0.000 mg/l, NaCl saline solution, 154 mmol/l) were then analysed on the Optilite™ using a developmental research channel. The optimised dilutions for the 7-point curve were: (1 + 0), (1 + 1), (1 + 3), (1 + 7), (1 + 15), (1 + 31), and (1 + 63), which corresponded to the following [α1-AGP] targets: 4.940 mg/l 2.470 mg/l, 1.235 mg/l, 0.618 mg/l, 0.309 mg/l, 0.154 mg/l, and 0.077 mg/l, respectively.

Assay response was then estimated on device by subtracting the blank absorbance measurement from the end-point absorbance measurement (both performed at 600 nm wavelength) of the sample following the reaction. Standard curves were further fitted on device by applying a logit-log 4 model (or log 4-parameter logistic model, 4-PL) to response data (measured in units for absorbance, abs) for the standard dilutions outlined above. Graphically, standard curves were plotted with [α1-AGP] targets on the x-axis and assay response on the y-axis (on device) with these curves later recreated in Prism (v8.3.0 for Mac iOS, Graphpad Software Inc., San Diego, CA, USA)*.

3.2.4.1.1. Reagent lot A

Initial calibration was performed for both batches of reagent lot A (batches 1 and 2) following 24 hours of light-limited refrigeration (4 °C) with these calibrations compared prior to pooling (see section **3.3.2.1**), which was followed by an additional standard curve for the pooled reagent. Standard dilutions for the pooled reagent (reagent lot A) were repeated on 6 additional days thereafter (total of 7 non-consecutive days; see **Figure 3.1**) alongside preliminary validation experiments (see section **3.2.5**).

* Curves were recreated in Prism by first log-transforming target [α1-AGP] values (x-axis) and then applying a 4-PL model (fitted using least-squares regression) to the response data (y-axis).

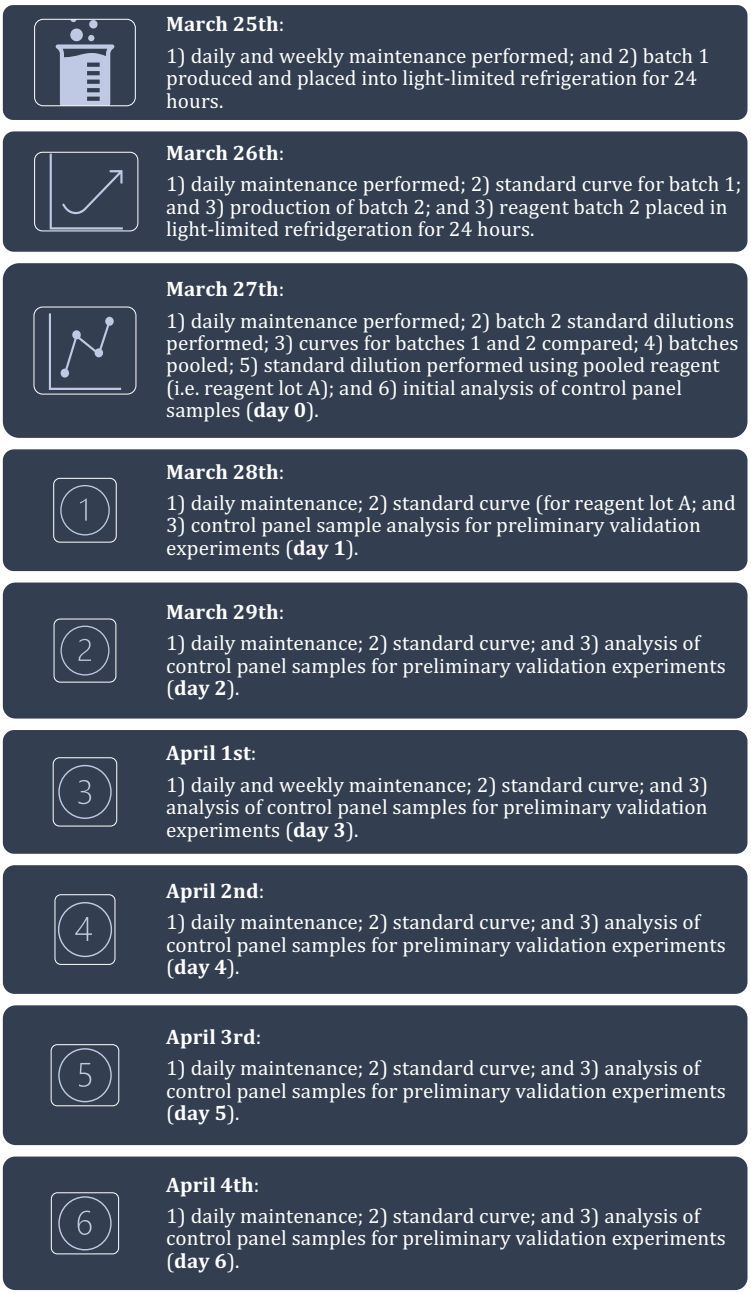

Figure 3.1 – Timeline of events for reagent batch production of and experimentation for reagent lot A. Reagent batch (1 and 2) 'production' (steps 1 and 2) referred to conjugation of $F(ab')_2$ (for alpha-1 acid glycoprotein) to latex particles. Numbering denoted on the left-hand side refers to the days following initial analysis, which was conducted on 27 March, 2019. All indicated dates refer to 2019.

3.2.4.1.2. Reagent lot B

Calibration was first performed following the dilution (1/3) of the concentrated latex reagent (200 ml) into 600 ml of diluent buffer (to yield ~800 ml of reagent in total) and subsequently each day for 6 non-consecutive days when validation experiments were

performed. Standard dilutions were also performed, and curves recorded, on each day of the longitudinal analysis for assay stability (for reagent lot B only; see section **3.2.5.6**).

3.2.4.2. Limit of the blank (LOB)

Limit of the blank was defined as the highest [α1-AGP] that could be expected when analysing a blank sample containing no analyte (dilution buffer consisting of saline). Limit of the blank is typically assessed by analysing 30 – 60 blank samples however, for the present study, analysis of 26 blank samples* was used to estimate the mean ± SD absorbance, which were further used in conjunction with **Equation 3.1** to calculate LOB[5 295] absorbance. This result was then plotted along the nonlinear curve (log 4-PL) to determine the corresponding [α1-AGP] for LOB (refer to **Appendix 3**).

Equation 3.1 – Limit of the Blank (LOB). The LOB result produced from this equation, in units for assay response (absorbance), was then be utilised in conjunction with the 4-PL standard curve to estimate the corresponding alpha-1 acid glycoprotein (α1-AGP) concentration (mg/l).

$$LOB = \bar{x}_{blank} + (1.645 \times SD_{blank})$$

Where:

$\bar{x}_{blank}$ = mean absorbance for analysis of blank samples (n = 26);
1.645 = LOB constant;
SD_{blank} = standard deviation of absorbance results from analysis of blank samples;
LOB = limit of the blank in units of absorbance (abs).

3.2.4.3. Limit of detection (LOD)

Limit of detection was defined as the lowest analyte (α1-AGP) concentration that could be reliably distinguished from a blank sample. Limit of detection can be estimated by analysing a blank sample and 10 different dilutions containing known [analyte] (each analysed 7 times)

* For logistical reasons, only 26 analyses were performed for LOB tests however, it is acknowledged that the most appropriate number of blank samples to be analysed for LOB quantification should be no less than 30 – 60 blank samples.

with the mean signals ± 3 SDs plotted against the [target][288 295 296]. More simply, LOD can be estimated using a standardised equation (**Equation 3.2**) together with the mean ± SD absorbance from repeat analyses of a blank (as used for LOB calculation)[295]. This estimation was performed for the present study with the absorbance result from **Equation 3.2** further plotted along a nonlinear curve in order to determine the corresponding [α1-AGP] for LOD (refer to **Appendix 3**).

Equation 3.2 – Limit of detection (LOD). The LOD result produced from this equation (in units for absorbance) was then plotted along a nonlinear curve (as described in **Appendix 3**) in order to determine the corresponding alpha-1 acid glycoprotein (α1-AGP) concentration (mg/l).

$$LOD = \bar{x}_{blank} + (3 \times SD_{blank})$$

Where:

- $\bar{x}$ = mean absorbance for analysis of blank samples (n = 26);
- 3 = constant;
- SD_{blank} = standard deviation of absorbance results from analysis of blank samples;
- LOD = limit of the detection with units for absorbance (abs).

3.2.4.4. Limits of quantification (LOQs)

Limits of quantification were defined as the measurement endpoints for the range of [α1-AGP] values over which the assay could accurately and precisely measure α1-AGP and reliably distinguish between different specimens. To determine the lower limit of quantification (LLOQ)[288 295], a series of dilutions slightly above the lower LOD can be analysed. Alternatively, mean absorbance ± SD from repeat analysis of a blank sample can be used in conjunction with **Equation 3.3**[5 295], which was used for the present study. The absorbance result produced by **Equation 3.3** was further plotted along the nonlinear curve to determine the corresponding [α1-AGP] for LLOQ (refer to **Appendix 3**).

Equation 3.3 – Lower limit of quantification (LLOQ). The LLOQ result from this equation, estimated in units for assay response (absorbance), was then plotted along the nonlinear curve to estimate the corresponding alpha-1 acid glycoprotein (α1-AGP) concentration (mg/l).

$$LLOQ = \bar{x}_{blank} + (10 \times SD_{blank})$$

Where:

$\bar{x}$ = mean absorbance for analysis of blank samples (n = 26);
10 = multiplier constant referring to 10 times the SD_{blank};
SD_{blank} = standard deviation of absorbance results from analysis of blank samples;
$LLOQ$ = lower limit of quantification with units for absorbance (abs).

3.2.5. Preliminary validation

Prior to initiating preliminary validation experiments, control panel samples were constituted from stock with individual aliquots made for each control (15 × 2 ml repeat polystyrene cryovials each) and frozen (at –20 °C[297]) for later use in validation trials. No freeze-thaw cycles for panel control samples were permitted and aliquots were discarded following analysis.

Preliminary validation tests were only initiated following successful calibration. Validation experiments were performed at independent timepoints for reagent lots A and B and aimed to examine immunoassay: intra- and inter-assay imprecisions (e.g., within-run, between-run, between-day); inaccuracy; recovery; linearity; interference, and stability (short- and long-term) as outlined in the proceeding subsections. Most all of these experiments were conducted for both reagent lots unless otherwise specified in-text (e.g., linearity tests were only executed using reagent lot A). Validation experiments were initiated with mass adjustments for panel control samples as described next.

3.2.5.1. Mass adjustments for control samples

Mass adjustments were performed for each panel sample (in accordance with procedures outlined next) in order to provide the most accurate [α1-AGP] (mg/l) for each sample and so that the most representative evaluations of the immunoassay could be conducted.

3.2.5.1.1. Reagent lot A

Three control samples (panel controls: 29, 36, and 39), containing known [α1-AGP] (911 mg/l, 356 mg/l, and 1560 mg/l, respectively), and a diluent (saline) were used for validation experiments for reagent lot A. Five repeat mass measurements (g) were performed for 100 µl of each panel sample and the diluent with the average masses (g) and coefficient of variation percentages (%CV) estimated (see 'Density replicates' in **Table 3.1**). Average masses for 100 µl of each sample and the diluent were estimated and then used to calculate the of density per ml (g/ml; average mass × 10) for each control sample (**Table 3.1**).

Table 3.1 – Panel control sample and diluent densities.

	Panel sample and diluent densities (*reagent lot A)*				Panel sample and diluent densities (*reagent lot B)*			
	Panel '29'	**Panel '36'**	**Panel '39'**	**diluent**	**Panel '24'**	**Panel '39'**	**Panel '239'**	**diluent**
Volume measured	100 µl	100 µl	100 µl	100 µl	100 µl	100 µl	100 µl	2 ml
Density replicates (g)	0.1084	0.1072	0.1090	0.1033	0.1055	0.1048	0.1052	2.0088
	0.1086	0.1072	0.1078	0.1028	0.1047	0.1061	0.1034	2.0131
	0.1089	0.1073	0.1075	0.1018	0.1046	0.1061	0.1040	2.0131
	0.1070	0.1072	0.1079	0.1006	0.1056	0.1056	0.1037	2.0175
	0.1073	0.1067	0.1080	0.1023	0.1050	0.1068	0.1034	2.0084
Average mass (g)	0.1080	0.1071	0.1080	0.1022	0.1051	0.1059	0.1039	2.0122
Density (g/ml)	1.0804	1.0712	1.0804	1.0216	1.0508	1.0588	1.0394	1.0609
%CV	0.78%	0.22%	0.53%	1.01%	0.43%	0.70%	0.72%	0.19%

Five repeat density measurements were performed for 100 µl of each control panel sample (obtained from stock; Panel controls: '24', '29', '36', '39', and '239') and 100 µl of diluent (or 2 ml for reagent lot B). Average mass was calculated from these replicates with this result then used to estimate the density (g/ml). %CV, coefficient of variation of the five density replicates.

A target dilution (1/500 into 15 ml) was then made for each of the three panel samples with the aim of fitting the target [α1-AGP] values onto various points of the standard curve (refer to section **3.2.4.1.1** for standard curve of reagent lot A). Masses of each panel sample and diluent required for the 1/500 dilutions were estimated as 14.9700 g and 0.0300 g, respectively, with the actual masses of sample (measured from 30 µl and 14.970 ml, respectively) added to the dilution recorded for each. With **Equation 3.4**, these measurements (i.e., 'actual sample mass' and 'actual diluent mass') were used in conjunction with estimated panel sample and diluent densities (shown in **Table 3.1**) and the stock [α1-AGP] of each panel sample (or '[sample conc.]' in **Equation 3.4**) to calculate the mass adjusted [α1-AGP] for each panel sample. Calculations were performed using Microsoft Excel (v16.0, Microsoft Corporation, Redmond, Washington, USA).

Equation 3.4 – Mass adjusted concentration (mg/l).

$$mass\ adj.value = [sample\ conc.]\left[\left(\frac{\frac{actual\ sample\ mass}{density}}{\left(\frac{actual\ diluent\ mass}{diluent\ density}\right)+\left(\frac{actual\ sample\ mass}{density}\right)}\right)\right]$$

Mass adjusted [α1-AGP] values for control samples (i.e., 0.732 mg/l, 1.863 mg/l, and 3.187 mg/l; **Table 3.2**) were then used as the reference [α1-AGP] values (unless otherwise indicated) for validation experiments that included assessments of assay imprecision (e.g., within-run, between-day, and total imprecisions) and interference (as described in next sections).

Table 3.2 – Mass adjustments for control panel samples.

	Sample [α1-AGP] (mg/l)	Target dilution	Target [α1-AGP] (mg/l)	Vol. required (ml)	Sample required (g)	Diluent required (g)	Actual sample mass (g)	Actual diluent mass (g)	Mass adj. [α1-AGP] (mg/l)
Control samples (reagent lot A)									
Panel 29	911	1/500	1.822	15	0.0300	14.9700	0.0327	15.0873	1.863
Panel 36	356	1/500	0.712	15	0.0300	14.9700	0.0328	15.1742	0.732
Panel 39	1560	1/500	3.120	15	0.0300	14.9700	0.0328	15.1482	3.187
Control samples (reagent lot B)									
Panel 239	920	1/500	1.840	15	0.0300	14.9700	0.0321	14.9038	1.914
Panel 24	442	1/500	0.844	15	0.0300	14.9700	0.0326	14.8268	0.929
Panel 39	1560	1/500	3.120	15	0.0300	14.9700	0.0311	14.8750	3.093

Stock alpha-1 acid glycoprotein (α1-AGP) concentration values (or [α1-AGP]) for panel control samples are presented (mg/l) and were diluted (1/500) for target [α1-AGP]. Density replicates and [stock] were utilised along with **Equation 3.4** to estimate the mass adjusted [α1-AGP] for each panel control that were further use for validation experiments.

3.2.5.1.2. Reagent lot B

Similar to panel samples used to evaluate reagent lot A, five replicate mass (g) measurements were performed for 100 µl of three panel control samples (panel controls: 239, 24, and 39) containing known amounts of α1-AGP (920 mg/l, 442 mg/l, and 1560 mg/l) and 2 ml of diluent. Replicate mass measurements (presented in **Table 3.1**) were then used to estimate the average mass (g) and %CV with the average mass used to calculate the density per ml (g/ml; average mass × 10) for each sample.

Target dilutions (1/500 into 15 ml) were then constituted from the stock panel samples with the intention of fitting [α1-AGP] values onto various points along the calibration curve (refer to section **3.2.4.1.2** for calibration curve of reagent lot B)*. Masses required for the dilution were 14.9700 g of diluent and 0.0300 g of panel sample with the actual diluent and sample masses added (for 30 µl and 14.970 ml) recorded for each (**Table 3.2**). These actual mass measurements (from **Table 3.2**) together with stock concentration values and densities previously estimated (refer to **Table 3.1**) were then used in order to make mass adjustments to the [α1-AGP] for each panel sample (using **Equation 3.4**). Mass adjusted [α1-AGP] values for these panel samples (0.929 mg/l, 3.093 mg/l, and 1.914 mg/l; **Table 3.2**) served as the reference [α1-AGP] values for subsequent validation experiments for reagent lot B (as described next).

3.2.5.2. Intra-assay and inter-assay imprecisions

Validation experiments were planned in accordance with the *NCCLS Approved Guidelines for the Evaluation of Precision Performance of Clinical Chemistry Devices*[298]. Appropriate equations (outlined next) were applied to triplicate [α1-AGP] results measured

* As for the controls used in conjunction with reagent lot A, replicate aliquots were made for the panel sample dilutions constituted from stock panel controls for reagent lot B and stored (at –20 °C) for later use.

from panel samples using the present immunoassay to estimate: intra-assay imprecision (or within-run SD and variance, SD^2), inter-assay imprecision (or between-day and between-run SDs and variances), total imprecision (SD and variance), and percent coefficient of variation (%CV) of each. Estimations were performed using Microsoft Excel.

3.2.5.2.1. Reagent lot A

3.2.5.2.1.1. Intra-assay imprecision

Panel samples (refer to **Table 3.2**) were analysed in triplicate (3 tests) once per day on 7 non-consecutive days* following the pooling of batches 1 and 2. Within-run SD (S_{wr}) and within-run variance (S_{wr}^2) were calculated for each of the three panel samples using triplicate [α1-AGP] results together with **Equation 3.5**[298]. Within-run %CV was also calculated for each panel control using **Equation 3.6**[299]. 'Acceptable imprecision' is a multifactorial dilemma, however, for the purposes of the present study this was set to ± 4 SDs of the total error[298 300] with allowable %CV for imprecision experiments set to < 5%[298].

Equation 3.5 – Within-run standard deviation. This equation was used for within-run standard deviation (S_{wr}) and within-run variance (S_{wr}^2) calculations when only a single run (with > 2 replicates) was performed each day[298]. Thus, this equation was utilised for imprecision estimates for reagent lot A only.

$$S_{wr} = \sqrt{\frac{\sum_{i=1}^{I}\sum_{j=1}^{N}\left(x_{ij}-\overline{x}_{i.}\right)^2}{I\times(N-1)}}$$

Where:

I	= total number of days;
N	= number of replicate analyses per run;
x_{ij}	= result on replicate j in run on day i;
$\overline{x_{i.}}$	= average (mean) of all replicates on day i;
S_{wr}	= within-run standard deviation;
S_{wr}^2	= within-run variance.

* The 7 non-consecutive days of triplicate analysis for calculations of intra- and inter-assay imprecision for reagent lot A occurred across a total of 10 days (refer to **Figure 3.1**, 27 March through 04 April, 2019).

Equation 3.6 – Percent coefficient of variation (%CV). Coefficient of variation was calculated using the standard deviation estimates of imprecision (e.g., S_{wr} or S_{dd}) and was presented as a percentage relative to the grand mean of triplicate results for alpha-1 acid glycoprotein concentration (or [α1-AGP]). Allowable %CV for imprecision experiments was set to < 5%.

$$\%CV = \frac{SD}{[grand\ mean]} \times 100$$

Where:

SD = standard deviation for relative imprecision (e.g., S_{wr} , S_{dd}, or S_T);

100 = constant rendering the result as a percentage of the grand mean;

$\%CV$ = percent coefficient of variation for the relative SD;

grand mean = mean [α1-AGP] for a panel control across all tests and days.

3.2.5.2.1.2. Inter-assay imprecision

Between-run and between-day imprecisions could not be distinguished for the reagent lot A, as only a single triplicate run was performed each day. Thus, appropriate equations for between-day and total precision SD were used as recommended in Appendix C of the *NCCLS Approved Guidelines for the Evaluation of Precision Performance of Clinical Chemistry Devices*. Between-day standard error (**Equation 3.7**), between-day SD and variance (**Equation 3.8**), and total SD (**Equation 3.9**) and the %CV (**Equation 3.6**) for each were estimated. Two-way repeated measures ANOVA (RM-ANOVA) with Dunnett's *post hoc* test was further used to detect any changes in assay performance over the course of imprecision experiments (across days and between control samples; time × condition) by comparing daily triplicate results for the three panel samples against the results obtained on the first of 7 non-consecutive days of experimentation (i.e., from 27 March, 2019 following pooling of batches 1 and 2). If a significant difference was detected (adjusted p-value < 0.05), further investigation was conducted by comparing standard curves.

Equation 3.7 – Standard error. Standard error was defined as the standard deviation of daily means[298] and estimated using the below equation. This equation was appropriate regardless of the number of runs performed per day and results were required for subsequent imprecision calculations (see next equation).

$$B = \sqrt{\left(\frac{\sum_{i=1}^{I}(\overline{x}_i - \overline{x}_{..})^2}{I-1}\right)}$$

Where:

I	= number of days;
$\overline{x_{i.}}$	= average replicates on day i;
$\overline{x_{..}}$	= average of all results over all days.

Equation 3.8 – Between-day imprecision. This between-day precision equation was used when only a single run was performed per day[298] and, therefore, was only used for imprecision calculations concerning reagent lot A. SD, standard deviation.

$$S_{dd} = \sqrt{B^2 - \frac{S_{wr}^2}{N}}$$

Where:

B	= result from **Equation 3.7**;
N	= number of replicates per run (e.g., 3 for triplicate);
S_{wr}^2	= squared result from **Equation 3.5** (within-run variance);
S_{dd}	= between-run (or day, in this case, between-day) SD;
S_{dd}^2	= between-run (or day, in this case) variance (SD^2 **Equation 3.8** result squared).

Equation 3.9 – Total standard deviation (S_T). This equation was used for the estimation of total precision standard deviation when only a single run per day was performed[298] (i.e., for reagent lot A only).

$$S_T = \sqrt{B^2 + \frac{N-1}{N} S_{wr}^2}$$

Where:

B	= result from **Equation 3.7**;
N	= number of replicate analyses per run;
S_{wr}^2	= square of the result from **Equation 3.5** (within-run variance);
S_T	= total standard deviation.

3.2.5.2.2. Reagent lot B

For each day of experimentation, reagent lot B was dispensed from a larger storage container into a smaller reagent vial that could be loaded onto the Optilite™. Following

analysis each day, any residual volume of reagent in the vial was replaced back into the main storage container. This process was performed to help preserve assay integrity and thus, to help yield the most representative results for validation experiments, as well as, to maximise the use of the reagent produced.

3.2.5.2.2.1. Intra-assay imprecision

In contrast to reagent lot A, panel samples were analysed in triplicate (3 tests) *twice* per day over 6 to 7 days. Thus, within-run imprecision (SD and variance) was calculated using (**Equation 3.10** opposed to **Equation 3.5**) albeit, using only 2 replicates from each triplicate; refer to 'Within-Run Precision Estimate' in *NCCLS Approved Guidelines for the Evaluation of Precision Performance of Clinical Chemistry Devices*). Within-run %CV was calculated using **Equation 3.6** and the output from **Equation 3.10**.

Equation 3.10 – Within-run standard deviation. This equation was used (opposed to Equation 3.5) when multiple (at least 2) runs having 2 replicates/run were performed per day[298] . Thus, this equation was only used for imprecision estimates for reagent lot B with 2 replicates from triplicates used for the calculation.

$$S_{wr} = \sqrt{\frac{\sum_{i=1}^{I}\sum_{j=1}^{2}\left(x_{ij1} - \overline{x}_{ij2.}\right)^2}{4 \times I}}$$

Where:

I	= total number of days;
j	= run number within a given day (1 or 2);
x_{ij1}	= result on from replicate 1, run j on day i;
x_{ij2}	= result from replicate 2, run j on day i;
S_{wr}	= within- run standard deviation;
S_{wr}^2	= within-run variance.

3.2.5.2.2.2. Inter-assay imprecision

In contrast to reagent lot A, between-day and between-run imprecisions (SDs and variances) were distinguishable for reagent lot B and, therefore, calculated separately. Between-run imprecision was calculated using **Equation 3.7**, **Equation 3.11**, and **Equation**

3.13, while between-day imprecision was calculated using **Equation 3.7, Equation 3.11**, and **Equation 3.12**. Using results from **Equation 3.11**, **Equation 3.12**, and **Equation 3.13**, total SD and total variance were calculated using **Equation 3.14**. Between-day, between-run, and total %CVs were calculated using the appropriate results produced from the above equations and in conjunction with **Equation 3.6**. Two-way RM-ANOVA was also used to compare triplicate results between days. If significant differences were detected further comparison was performed between the standard curves and measured concentration for standard dilutions obtained on different days.

Equation 3.11 – Intermediate step for imprecision calculations. This equation functioned as an intermediate step that yielded values required by subsequent equations to estimate: between-run variance (S_{rr}^2), between-day variance (S_{dd}^2), and total standard deviation (S_T)[298].

$$A = \sqrt{\left(\frac{\sum_{i=1}^{I}(\overline{x}_{i1}-\overline{x}_{i2})^2}{2I}\right)}$$

Where:

I = number of days (with two runs);
$\overline{x_{i1}}$ = average result of run 1 on day *i* (mean of the 2 results);
$\overline{x_{i2}}$ = average result of run 2 on day *i* (mean of the 2 results).

Equation 3.12 – Between-day variance. This equation was used instead of **Equation 3.8** to calculate between-day variance from panel control sample results analysed with reagent lot B only[298].

$$S_{dd}^2 = B^2 - \frac{A^2}{2}$$

Where:

B = result from **Equation 3.7** squared;
A = result from **Equation 3.11** squared;
S_{dd}^2 = between-day variance;
$\sqrt{S_{dd}^2}$ = between-day standard deviation.

Equation 3.13 – Between-run variance. This equation was used to calculate the between-run variance from days when more than one run was performed (reagent lot B only)[298].

$$S_{rr}^2 = A^2 - \frac{S_{wr}^2}{2}$$

Where:

S_{wr}^2 = result from **Equation 3.10** (within-run variance);
A = result from **Equation 3.11**;
S_{rr}^2 = between-run variance;
$\sqrt{S_{rr}^2}$ = between-run standard deviation.

Equation 3.14 – Total standard deviation (S_T). This equation was used to estimate total precision standard deviation[298] in place of **Equation 3.9** when more than one run was performed per day. This equation was only used for S_T calculations related to reagent lot B.

$$S_T = \sqrt{S_{dd}^2 + S_{rr}^2 + S_{wr}^2}$$

Where:

S_{wr}^2 = within-run variance; result from **Equation 3.10**;
S_{dd}^2 = between-day variance; result from **Equation 3.12**;
S_{rr}^2 = between-run variance; result from **Equation 3.13.**

3.2.5.3. Inaccuracy and recovery

Inaccuracy and recovery were calculated for reagent lots A and B from the relevant panel sample results for each. Inaccuracy was calculated as the mean difference between the observed and target [α1-AGP] (mg/l) for each panel sample. Recovery was calculated as the percentage of the target [α1-AGP] successfully 'identified' or 'recovered' by the assay (using **Equation 3.15**).

Equation 3.15 – Recovery. Recovery was estimated as the percentage of alpha-1 acid glycoprotein concentration (i.e., [α1-AGP]; mg/l) 'identified' or recovered by the immunoassay relative to the target [α1-AGP] in the sample. Recovery of [α1-AGP] was estimated for panel control samples that were analysed as part of validation experiments. Brackets shorthand for concentration of an [analyte].

$$recovery = \frac{[O]}{[T]} \times 100$$

Where:

[O] = observed concentration (mg/l) for α1-AGP measured by the assay;

[T] = target concentration (mg/l) for α1-AGP in the panel control.

3.2.5.4. Linearity

Linearity tests were performed using reagent lot A only and were planned for a range of [α1-AGP] as described next. To begin, five repeat mass measurements were performed for 100 μl of diluent (saline) and 100 μl of an internal reference (IR) fluid containing α1-AGP (570 mg/l). Replicate measurements were then used to estimate average mass (g), density (g/ml), and %CV for the diluent and IR (**Table 3.3**).

Table 3.3 – Average masses and densities of 100 μl of an internal reference (IR) fluid containing alpha-1 acid glycoprotein (α1-AGP).

	100 μl IR density	**100 μl diluent density**
Density replicates	0.1080	0.1020
	0.1064	0.1050
	0.1063	0.1011
	0.1071	0.1015
	0.1065	0.1019
Average mass (g)	0.1069 ± 0.0007	0.1023 ± 0.0016
Density (g/ml)	1.0686	1.023
%CV	0.66%	1.52%

Five repeat mass measurements were performed for 100 μl of a diluent (saline) and the IR fluid for α1-AGP. Replicates were used to estimate the average mass (g) for each (mean ± standard deviation), which were then used to calculate density (g/ml). These density estimates were further used to calculate the mass adjusted [α1-AGP] for each dilution made for linearity tests (see **Table 3.4** for dilutions). %CV, percent coefficient of variation (for density replicates).

As per the *NCCLS Approved Guideline EP6-A*[301], a high pool (target [α1-AGP], 4.940 mg/l)[*] and a low pool (target [α1-AGP], 0.000 mg/l; in 7.630 ml) were then constituted from the diluent and IR. The actual diluent and IR masses combined to form each pool were recorded and used along with the average masses estimated from the five density replicates (refer to **Table 3.3**) in order to calculate the mass adjusted [α1-AGP] in each pool (low pool: saline, 0.000 mg/l; high pool: IR 4.807 mg/l) as previously described (see section **3.2.5.1**). A series of 13 dilutions (~800 µl by volume or 0.800 g each) were then constituted from these high and low pools, which were analysed for linearity experiments[301]. Target [α1-AGP] for each dilution was determined by the proportion (by mass) of high pool added. Actual masses (g) of the high and low pools combined to form each dilution were recorded and used to calculate the mass adjusted portion of the dilution made from the high pool, as well as, the mass adjusted [α1-AGP] target (mg/l) for each dilution (**Table 3.4**). All dilutions were analysed in triplicate on the Optilite™ using reagent lot A.

Linear and nonlinear (3rd order polynomial) fits were applied to triplicates (i.e., 'observed results') using the Analyse-it Microsoft Excel extension (Analyse-it Software, Ltd., Leeds, UK) with nonlinearity detected by testing whether nonlinear coefficients were significantly different from zero ($\alpha < 0.05$) as described in the *NCCLS Approved Guideline EP6-A*[301]. Deviation from linearity was calculated for each dilution with allowable nonlinearity set to ± 10%, relative to the mass adjusted [α1-AGP] of the dilution in question.

[*] 0.0474 g of IR + 5.4226 g of diluent equated to approximately 5.470 ml of high pool containing a target [α1-AGP] of 4.940 mg/l.

Table 3.4 – Dilution series for linearity tests.

IR dilution No.	High pool target (%)	Low pool target (%)	Mass adj. high pool (%)	Mass adj. target [α1-AGP] (mg/l)
1	0%	100%	0.00%	0.000
2	2%	98%	2.03%	0.097
3	5%	95%	5.53%	0.266
4	10%	90%	10.17%	0.489
5	20%	80%	20.17%	0.969
6	30%	70%	30.92%	1.486
7	40%	60%	40.30%	1.937
8	50%	50%	50.27%	2.416
9	60%	40%	59.98%	2.883
10	70%	30%	69.78%	3.354
11	80%	20%	79.55%	3.824
12	90%	10%	90.92%	4.370
13	100%	0%	100.00%	4.807

Concentration of alpha-1 acid glycoprotein (or [α1-AGP]; mg/l) contained within the high pool target was 4.807 mg/l. Target proportions of high and low pools to be combined to form each dilution are presented as percentages. Mass adjusted proportions (and mass adjusted target [α1-AGP]) of high pool added were then estimated were calculated using densities of the internal reference (IR) and diluent (refer to **Table 3.3**), as well as, the actual masses of the high and low pools added to each dilution.

3.2.5.5. Interference

Interference of urea and ascorbic acid were tested (individually) for reagent lot A only. Urea (1.25 g) was diluted from stock into 2.5 ml of diluent (saline) to form an initial solution containing 500 g/l of urea. Ascorbic acid (12.0466 mg) was diluted from stock into 10 ml of diluent to form an initial solution containing 6,840 μmol/l of ascorbic acid. Two 10 ml pools (0% and 100% pools) were then constituted for each interferent using these initial interferent solutions together with a control panel sample containing α1-AGP (as outlined next). Dilution series were then created for each interferent using relative amounts of the 0% and 100% pools (also outlined next).

To create the 100% pool for urea, 1 ml of the initial urea solution (500 g/l) was combined with 1 ml of an α1-AGP dilution (created from a stock control sample containing 356

mg/l [α1-AGP]* and 8 ml of diluent to form 10 ml containing: 50 g/l urea and 0.712 mg/l α1-AGP. To create the 100% pool for ascorbic acid, 500 μl of the initial ascorbic acid solution (6,840 μmol/l) was combined with 1 ml of the α1-AGP dilution and 8.5 ml of diluent to form 10 ml containing: 342 μmol/l ascorbic acid and 0.712 mg/l α1-AGP. The 0% pools for both interferents were constituted by combining 1 ml of the α1-AGP dilution from the control sample with 9 ml of diluent to yield 10 ml containing: 0.712 mg/l of α1-AGP. A series of further dilutions (e.g., 80%, 60%, 40%, and 20% pools) were then constituted for both interferents by combining relative amounts of the 0% and 100% pools. Interferent (urea or ascorbic acid) concentration was estimated for serial dilutions (presented in **Table 3.12** alongside results) while target [α1-AGP] remained the same (i.e., 0.712 mg/l) for all dilutions.

As a general rule, deviations of 3 to 10%, relative to the initial [analyte], for measured results can indicate interference[302 303]. More specifically, results ± 3 SD (but < 5 SD) relative to the initial [analyte] indicate potential interference, whereas results ≥ 5 SD relative to the initial [analyte] indicate definite interference. Therefore, the latter has been recommended as the allowable deviation cut-off for interference tests[304]. Statistical methods comparing [analyte] between initial vs serial interferent dilutions, have also been recommended for tests of interference (with significant comparisons; set to $\alpha < 0.05$)[303]. With the above in mind, the present study adopted a statistical approach to assess interference by comparing the initial [α1-AGP] measured from the 0% dilution (in triplicate) to the [α1-AGP] from serial interferent dilutions (20% – 100% dilutions). This approach utilised a one-way RM-ANOVA with Dunnett's

* 200 μl of a stock sample containing [α1-AGP] (356 mg/l) was diluted (1/50) to produce a solution containing ~7.12 mg/l [α1-AGP]. This pool would be added to (and further diluted) the 0% and 100% interferent pools (i.e. 1ml added to 0% and 100% pools). Thus, the control sample would be ultimately diluted 1/500. Given that dilutions were constituted by volume rather than actual masses added, the target [α1-AGP] was estimated for the interferent dilutions as 0.712 mg/l (opposed to mass adjusted [α1-AGP] of 0.732 mg/l).

post hoc test to account for repeat pairwise comparisons of [α1-AGP] between the 0% dilution (triplicate mean) and the additional interferent dilutions (20%, 40, 60%, 80% and 100% dilutions). Interference was considered occurring if [α1-AGP] from any serial interferent dilution (20% – 100%) was significantly different (any adjusted *p*-value < 0.05) in comparison to the initial [α1-AGP] from the 0% dilution. These findings were cross-checked with SD percentages for triplicate [α1-AGP] measurements from interferent dilutions (20% – 100%), which were estimated relative to the average [α1-AGP] for the 0% pool. %CV and recovery of triplicate [α1-AGP] measurements were also estimated for each interferent dilution (0% – 100%). Recovery was estimated as a percentage relative to the target [α1-AGP] (as oppose to estimated relative to the 0% dilution [α1-AGP]).

3.2.5.6. Stability

The CLSI Evaluation of in vitro diagnostic reagents Approved Guideline EP25-A was utilised to plan 'in-use' stability (or 'open-vial' stability) testing. The purpose of stability experiments was to assess the duration of time over which the performance of latex-enhanced reagent remained within acceptable limits while stored in light-limited refrigeration at 4 °C. The purpose of stability experiments was not to examine the stability of [α1-AGP] in controls or human specimens, which has already been examined[5 288]. Given that the product under evaluation could not tolerate freezing, a real-time, classical stability study design was adopted with testing scheduled at pre-determined timepoints (outlined below). A single Optilite™ analyser was utilised for the duration of stability experiments while two operators were involved in analysis, albeit adhering to the same reagent and sample handling and analysis procedures.

Sufficient amounts of reagent (lot B; +20% of required amount), panel control samples, and the calibrator were prepared in advance of stability trials with freshly thawed (from –20 °C) calibrator and sample aliquots used for each stability trial (i.e., no freeze-thaw cycles permitted). Each stability trial began with standard dilutions of the calibrator with responses (i.e., absorbances) fitted using a nonlinear method on-device (logit-log 4 model). Standard dilutions would be followed by analysis of three panel control samples (indicated in **Table 3.2**) in triplicate (once per day) with the mean [α1-AGP] then utilised for analysis (as described next).

Power analysis was performed according to EP25-A Appendix C to determine the sampling plan that would achieve power $1 - \beta = 0.80$ with the allowable drift limit set to ± 5% of the initial mean triplicate. Assuming three replicates would be performed and utilising %CVs from previous estimations (**Table 3.9**), this analysis indicated that a single triplicate run (i.e., one 'repeat' performed using reagent lot B only) would be appropriate for the application of a 10- or 13-point regression (i.e., 10 or 13 days). Thus, in-use stability trials were planned for the days of preliminary validation experiments (on 06, 07, 08, 11, 12, 13, and 14 November, 2019) and at pre-specified timepoints thereafter (i.e., post- 4, 5, 6, 7, 8, 10, 12, and 16 weeks).

At the end of the scheduled study period, a linear regression was performed individually for mean [α1-AGP] results (y-axis) vs time (days; x-axis) for each panel sample. If the slope of the linear regression was significant (i.e., $\alpha < 0.05$), the stability duration was taken as x-coordinate (in days) for the point of intersection between the one-sided 95% confidence interval (CI; upper if slope is positive or lower if slope is negative)[305]. If the slope was not significant ($\alpha \geq 0.05$), the stability duration was considered as the maximum time point tested[305].

Within-run (**Equation 3.5**), between-day (**Equation 3.7** and **Equation 3.8**), and total (**Equation 3.7** and **Equation 3.9**) imprecisions (SDs and variances) were also calculated from triplicate panel sample results using equations that appropriately accounted for 1 triplicate/day (i.e., 3 tests × 1 run/day) as previously described (refer to section **3.2.5.2**). Imprecisions were calculated as the 'cumulative' value for each timepoint using panel sample results analysed on and up to the timepoint in question. Within-run, between-day, and total %CVs (**Equation 3.6**), as well as, inaccuracies and recoveries were also calculated for each timepoint.

3.2.5.7. Methods comparison

Methods comparison between the newly developed PETIA and radial immunodiffusion (RID) was performed and reported in accordance with NCCLS Approved Guideline E9-A2[306]. [α1-AGP] was analysed in triplicate using PETIA (on the Optilite™ auto-analyser) from stored human urine specimens (n = 126)[*]. Successful triplicates were matched to corresponding RID[†] results previously published[7], albeit with a different *a priori* question in mind, and triplicate mean [α1-AGP] (from PETIA results) calculated. Distribution of these data was assessed for normality/lognormality with unmatched results (e.g., sample failure or [α1-AGP] less than lower limit, < 0.08 mg/l) and outliers removed (using Grubbs' test[307 308] due to uncertainty of true outliers) prior to statistical analysis.

[*] Twenty-four-hour urine specimens (containing sodium azide as preservative) were collected (see **Chapter 5** for urine collection procedures) and kept frozen (–80 °C) until RID and PETIA analysis with a fresh (previously unthawed) replicate aliquot analysed for each analytical method.

[†] RID for urinary [α1-AGP] was performed in singlet approximately 18 months after specimen collection and PETIA for urinary [α1-AGP] performed in triplicate approximately 6 months after RID. Triplicate PETIA results included for the purposes of the methods comparison were produced using a single reagent lot across two days with calibration curves performed each day.

Minimum and maximum [α1-AGP] results measured from all specimens by each method were reported, with methods (RID and PETIA) further compared based on measured [α1-AGP] values using three plots: 1) a Bland-Altman (B-A) plot[309]; 2) a scatter plot of all individual PETIA results from triplicates (y-axis) vs RID results (x-axis); and 3) a scatter plot of the triplicate mean from PETIA (y-axis) vs RID (x-axis)[306]. All plots were constructed using Prism (v8.3.0 for Mac iOS, Graphpad, San Diego, CA, USA). For the B-A plot, data were plotted as the difference in [α1-AGP] between methods (RID – PETIA; y-axis) vs the average [α1-AGP] of the two results (x-axis)[310] with the bias and Limits of Agreement (95% limits of agreement, 95% LOAs)[311] reported and a simple linear regression also fitted to these data. Further, slope ± 95% CIs, y-intercept ± 95% CIs, and goodness of fit (R^2 and Sy.x)[306] for the best-fit line of the simple linear regression were also estimated.

3.2.5.8. Statistical analyses

Statistical analyses were largely specific to each experiment and therefore have been outlined in-text. All statistical tests were two-tailed with significance set to $\alpha < 0.05$ (with adjusted *p*-values presented where appropriate) unless otherwise indicated. IBM SPSS Statistics (v25.0 for Mac iOS, Armonk, NY, USA) and Prism (v8.3.0, GraphPad, San Diego, CA, USA) were used for these statistical analyses unless otherwise indicated.

3.3. RESULTS

3.3.1. Latex conjugation – reagent lots A and B

Individual reagent batches were successfully produced on two separate occasions for reagent lot A (batches 1 and 2) taking approximately 6 hours with the time including general

preparation, production SOPs, and clean up. Once combined, batches yielded approximately 104 ml of reagent in total (to include the storage buffer) from 26 × 1 ml individual test coats.

A new batch of isolated antibodies was required for the production of reagent lot B. Following the 1/3 dilution of the concentrated reagent (200 ml, reagent lot B), bulk production yielded ~800 ml of latex-enhanced reagent.

3.3.2. Assay optimisation and test parameters

3.3.2.1. Calibration

In total, each calibration (7-point plus one blank) for the α1-AGP immunoassay required only 704 µl of reagent. No calibrations failed throughout any of the experiments. Thus, to avoid undue repetition, only calibration curves from select timepoints were presented (**Figure 3.2** and **Figure 3.3**) with these results outlined next.

3.3.2.1.1. Reagent lot A

A comparison of assay responses for standard dilutions for the two original test coat batches (subsequently pooled to form reagent lot A) is presented in **Figure 3.2a** to demonstrate repeatability of small batch production and the consistency between batch performance. An additional comparison of calibrations performed immediately following pooling and 1-week later is presented in **Figure 3.2b**.

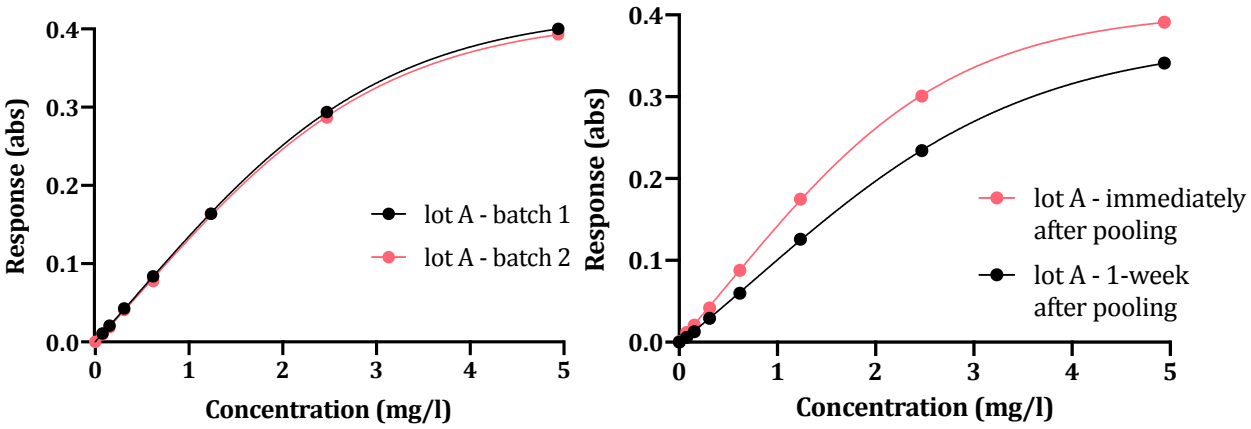

Figure 3.2 – Calibration curves for reagent lot A. Fig. 3.2a (left). Standard curves generated from assay response to standard dilutions of a calibration fluid containing alpha-1 acid glycoprotein (α1-AGP; 4.940 mg/l) for two individual batches (1 and 2) of latex reagent (combined to form reagent lot A); **Fig. 3.2b (right)** – Standard curves generated from assay response to standard dilutions of a calibration fluid containing α1-AGP (4.940 mg/l) and were reflective of calibration performed 'immediately after pooling' (of batches 1 and 2) on 27 March, 2019 and ~1-week later on 04 April, 2019. Logit-log 4 nonlinear regression was applied to response data (absorbance, abs) for the standard dilutions (7-point plus one blank) with these data plotted (y-axis) relative to target [α1-AGP] for each of the standard dilutions (x-axis).

3.3.2.1.2. Reagent lot B

Latex production for reagent lot B took place on 24 October, 2019 with the concentrated dilution (from 200 ml) performed on 06 November, 2019 to yield the latex-enhanced reagent ready for use. This was immediately followed by standard dilutions. These initial standard dilutions were compared to further calibration curves (e.g., obtained 8 days later on 14 November, 2019) and are shown in **Figure 3.3a**. Assay responses to standard dilutions for reagent lot B (from 06 November, 2019) were further compared to those from reagent lot A (as shown in **Figure 3.3b**) in order to demonstrate consistency of response between reagents produce in small batches and in bulk.

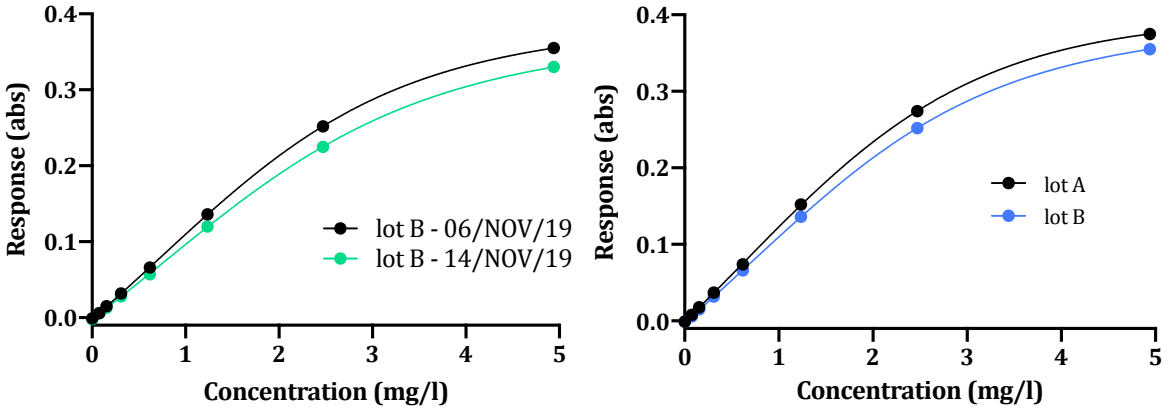

Figure 3.3 – Calibration curves generated from standard dilutions for reagent lots B (and A). Fig. 3.3a (left) – Standard curves for reagent lot B compared between calibrations performed eight days apart using standard dilutions of a calibration fluid (containing alpha-1 acid glycoprotein, α1-AGP; 4.940 mg/l); **Fig. 3.3b (right)** – Standard curves generated from the initial standard dilutions of each reagent lot, specifically: 'immediately following pooling' (or 27 March, 2019) for reagent lot A and 06 November, 2019 for reagent lot B. Curves were fitted by applying a logit-log 4 nonlinear regression (4-parameter logistic, 4-PL) method to response data for standard dilutions (7-point plus one blank, saline). Assay response (in units of absorbance abs; y-axis) was plotted relative to the target [α1-AGP].

3.3.2.2. Analytical limits (LOB, LOD, and LLOQ)

Analytical limits for LOB (0.01980 mg/l for -7.946×10^{-5} abs), LOD (0.029 mg/l for 0.00089 abs), and LLOQ (0.076 mg/l for 0.00581 abs) were successfully calculated for the present immunoassay. The rounded LLOQ result (i.e., 0.08 mg/l) was entered as the lower limit for the detection range for Optilite™ test parameters, which could only accommodate up to two decimal places. The maximum limit of the (working) measuring range for the primary dilution (at neat) was further identified in linearity experiments (see section **3.3.3.2**) with the final extended measuring range determined independent of the present experiments, albeit calculated as 0.08 – 148.2 mg/l (with serial dilutions set to 1 + 5 and 1 + 29).

3.3.3. Preliminary validation

3.3.3.1. Intra- and inter- assay imprecisions

3.3.3.1.1. Reagent lot A

Triplicate results for panel control samples analysed using one reagent batch (batch 2) were compared to results produced by using the final pooled product (reagent lot A) and are presented as mean ± SD and %CV in **Table 3.5** (comparison of pre- and post- pooling). Daily triplicate results for panel samples analysing using reagent lot A (as the pooled product), are presented as mean ± SD with recovery, %CV, and inaccuracy in **Table 3.6.**

Table 3.5 – Comparison of recovery and inaccuracy between an individual test coat (batch 2) and pooled reagent (batches 1 and 2; reagent lot A).

Target [α1-AGP] (mg/l)	Mean [α1-AGP] (mg/l)		Recovery (%)		CV (%)		Inaccuracy (mg/l)	
	batch 2	*lot A*	*batch 2*	*lot A*	*batch 2*	*lot A*	*batch 2*	*lot A*
0.732	0.69 ± 0.01	0.69 ± 0.03	95%	94%	2.20	3.66	–0.04 ± 0.02	–0.05 ± 0.03
1.863	2.22 ± 0.04	2.10 ± 0.01	119%	112%	1.71	0.55	0.35 ± 0.04	0.23 ± 0.01
3.187	3.75 ± 0.10	3.70 ± 0.02	117%	116%	2.74	0.56	0.56 ± 0.10	0.52 ± 0.02

Results were calculated from triplicate analysis performed 24-hours after the production of batch 2 and immediately following pooling of batches 1 and 2, on the same day. Recovery was calculated as the percentage of the target alpha-1 acid glycoprotein (α1-AGP) concentration successfully measured by the assay while mean inaccuracy (mg/l) was estimated as the difference in [α1-AGP] between the measured and [target]. Mean [α1-AGP] and inaccuracy results presented as mean ± standard deviation (SD) and percent coefficient of variation (%CV) and recovery as percentages (%).

Table 3.6 – Daily triplicate alpha-1 acid glycoprotein (α1-AGP) results analysed from panel samples.

Day	Target [α1-AGP] (mg/l)	Mean ± SD (mg/l)	Mean recovery (%)	%CV	Mean inaccuracy (mg/l)
0		0.693 ± 0.025	95%	2.20	–0.039 ± 0.015
1		0.697 ± 0.012	95%	1.66	–0.035 ± 0.012
2		0.677 ± 0.012	92%	1.71	–0.055 ± 0.012
3	**0.732**	0.710 ± 0.010	97%	1.41	–0.022 ± 0.010
4		0.700 ± 0.010	96%	1.43	–0.032 ± 0.010
5		0.680 ± 0.010	93%	1.47	–0.052 ± 0.010
6		0.710 ± 0.000	97%	0.00	–0.022 ± 0.000
0		2.217 ± 0.038	119%	1.71	0.354 ± 0.038
1		2.183 ± 0.025	117%	1.15	0.320 ± 0.025
2		2.307 ± 0.047	124%	2.05	0.444 ± 0.047
3	**1.863**	2.223 ± 0.021	119%	0.94	0.360 ± 0.021
4		2.233 ± 0.040	120%	1.81	0.370 ± 0.040
5		2.213 ± 0.035	119%	1.59	0.350 ± 0.035
6		2.240 ± 0.078	120%	3.49	0.377 ± 0.078
0		3.747 ± 0.103	118%	2.74	0.560 ± 0.103
1		3.820 ± 0.036	120%	0.94	0.633 ± 0.036
2		4.000 ± 0.066	126%	1.64	0.813 ± 0.066
3	**3.187**	3.847 ± 0.055	121%	1.43	0.670 ± 0.055
4		3.897 ± 0.078	122%	1.99	0.710 ± 0.078
5		3.790 ± 0.069	119%	1.83	0.603 ± 0.069
6		3.910 ± 0.053	123%	1.35	0.723 ± 0.053

Daily [α1-AGP] results and inaccuracies are presented as mean ± standard deviation (SD) with all results estimated from triplicate analysis (of α1-AGP) performed once per day utilising reagent lot A. Inaccuracy was estimated as the mean difference ± SD between the measured and target [α1-AGP]. Day 0 represented measurements performed immediately following pooling of reagent batches (i.e., 27 March, 2019; refer to **Figure 3.1**). %CV, percent coefficient of variation.

Triplicate [α1-AGP] results were used in conjunction with appropriate equations (as outlined in section **3.2.5.2**) to estimate within-run (intra-assay imprecision; SD and variance), between-day (inter-assay imprecision; variance and standard error), and total (SD and variance) imprecisions. Imprecision estimates are presented in **Table 3.7** with within-run and between-day %CVs, mean recoveries, and inaccuracies presented in **Table 3.8**.

Table 3.7 – Intra- (within-run) and inter-assay (between-run/between-day) imprecisions.

Target [α1-AGP] (mg/l)	Within-run imprecision		Between-day Imprecision			Total imprecision	
	SD	*Variance*	*SE*	*SD*	*Variance*	*SD*	*Variance*
0.732	0.010	< 0.001	0.014	0.013	0.0002	0.016	0.0003
1.863	0.045	0.002	0.041	0.031	0.0020	0.055	0.0030
3.187	0.061	0.004	0.075	0.067	0.0060	0.090	0.0080

Calculations were performed in accordance with NCCLS guidelines (as outlined in-text) for within-run (**Equation 3.5**), standard error (**Equation 3.7**), between-day (**Equation 3.8**), and total (**Equation 3.9**) imprecisions using triplicate results for alpha-1 acid glycoprotein (α1-AGP) analysed from panel control samples (on 7 non-consecutive days) utilising reagent lot A. SE, standard error. SD, standard deviation.

Table 3.8 – Percent coefficient of variation (%CV), inaccuracy, and recovery estimates.

Target [α1-AGP] (mg/l)	Within-run %CV	Between-day %CV	Total %CV	Inaccuracy (mg/l)	Recovery (%)
0.732	1.40%	1.91%	2.36%	0.036 ± 0.016	95.0%
1.863	2.02%	1.42%	2.47%	0.370 ± 0.054	119.4%
3.187	1.58%	1.72%	2.33%	0.690 ± 0.088	121.7%

%CV results for panel samples analysed using reagent lot A were estimated using **Equation 3.6** and imprecisions presented in **Table 3.7**. Similarly, inaccuracies were estimated for each panel control sample analysed in triplicate and are presented as mean ± standard deviation (SD) of the difference between the measured and target concentration for alpha-1 acid glycoprotein (or [α1-AGP]; mg/l). Recovery results are presented as the average percentage relative to the target [α1-AGP] successfully measured by the assay (estimated using **Equation 3.15**).

Imprecisions for reagent lot A did not exceed allowable limits (all %CVs < 5%), although 3 individual tests yielded [α1-AGP] results that fell outside ± 4 SDs of the total error (2 below, 1 above) for the 1.863 mg/l target [α1-AGP]. Despite this, a two-way RM ANOVA did not detect a significant effect of time (p = 0.126) nor was any interaction effect (panel control × time; p = 0.077) observed for immunoassay performance (27 March, 2019 vs additional non-consecutive days). Further, parameters from the log-4-PL fits for the response data were also not significantly different between days.

3.3.3.1.2. Reagent lot B

Estimates of within-run, between-run, between-day, and total imprecisions (SDs and variances for each) calculated from triplicate results for panel controls analysed using reagent lot B are presented in **Table 3.9**. Results for corresponding %CVs, mean recoveries, and inaccuracies are presented in **Table 3.10**.

Table 3.9 – Intra- and inter-assay imprecisions for reagent lot B.

		Within-run imprecision		Between-run imprecision		Between-day imprecision		Total imprecision	
Target [α1-AGP] (mg/l)		*SD*	*Variance*	*SD*	*Variance*	*SD*	*Variance*	*SD*	*Variance*
Panel 24	0.929	0.0101	0.0001	0.014	0.0002	0.014	0.0002	0.017	0.0101
Panel 39	3.093	0.1130	0.0128	0.050	0.0025	0.087	0.0076	0.120	0.1133
Panel 239	1.914	0.0267	0.0007	0.015	0.0002	0.029	0.0008	0.034	0.0267

Within-run (**Equation 3.10**), between-run (**Equation 3.7, Equation 3.10**, **Equation 3.11**, and **Equation 3.13**), between-day (**Equation 3.7**, **Equation 3.11**, and **Equation 3.12**), and total (**Equation 3.9**) imprecisions (standard deviation, SD; and variances, SD^2) were calculated using the indicated equations (and as outlined in-text) in conjunction with triplicate results for alpha-1 acid glycoprotein (α1-AGP) concentrations analysed across 6 non-consecutive days (06, 07, 11, 12, 13, and 14 November, 2019) from panel control samples.

Table 3.10 – Percent coefficient of variation (%CV), recovery, and inaccuracy estimates for reagent lot B.

Target [α1-AGP] (mg/l)		Within-run %CV	Between-run %CV	Between-day %CV	Total %CV	Inaccuracy (mg/l)	Recovery (%)
Panel 24	0.929	1.15%	1.65%	1.62%	2.00%	−0.057 ± 0.018	93.8%
Panel 39	3.093	3.32%	1.48%	2.55%	3.53%	0.317 ± 0.129	110.3%
Panel 239	1.914	1.40%	0.78%	1.51%	1.79%	−0.006 ± 0.046	99.7%

The target alpha-1 acid glycoprotein (α1-AGP) concentration (mg/l) is presented for each control sample analysed in triplicate on 6 non-consecutive days (06, 07, 11, 12, 13, and 14 November, 2019). Inaccuracies are presented as mean ± standard deviation (SD) of the differences between target and measured [α1-AGP] while within-run, between-run, between-day, and total %CV are presented as percentages relative to target [α1-AGP] (calculated using **Equation 3.6**).

Imprecision estimates calculated from panel sample triplicates analysed using reagent lot B did not exceed the allowable limits (all %CVs < 5%) and no measurements fell outside ± 4 SDs of the total error (**Table 3.10**). Further, when comparing initial [α1-AGP] results (from 06 November, 2019) to panel sample results obtained during imprecision experiments (through 14 November, 2019), two-way RM-ANOVA did not detect a significant effect of time (between days, p = 0.058) nor was a significant interaction effect observed (panel control × time; p = 0.170).

3.3.3.2. Linearity

Linearity results (linear and nonlinear, 3rd order polynomial, fits; and relative nonlinearity and 95% CIs) are presented in **Table 3.11** along with the observed mean [α1-AGP] results and %CVs (from triplicate analysis) for the mass adjusted targets.

Table 3.11 – Internal reference (IR) dilution and linearity results.

Dilution No.	Mass adj. target (mg/l)	Observed mean (mg/l)	%CV	High pool (%)	Linear fit	Nonlinear fit (3rd order polynomial)	Non-linearity	95% CIs	Allowable non-linearity
1	0.000	n/a	n/a	n/a	n/a	n/a	n/a	n/a	n/a
2	0.097	< 0.080	< 0.08	-	-	-	-	-	-
3	0.266	0.277	2.09%	0.055	0.312	0.303	–2.8%	–12.7 to 7.0%	± 10.0%
4	0.489	0.550	0.00%	0.102	0.558	0.520	–6.9%	–9.4% to 4.3%	± 10.0%
5	0.969	1.037	0.56%	0.202	1.088	1.032	–5.1%	–6.8% to 3.4%	± 10.0%
6	1.486	1.633	1.54%	0.309	1.658	1.633	–1.5%	–3.0% to –0.1%	± 10.0%
7	1.937	2.187	0.26%	0.403	2.156	2.179	1.0%	0.0% to 2.0%	± 10.0%
8	2.416	2.730	2.04%	0.503	2.685	2.758	2.7%	2.0% to 3.4%	± 10.0%
9	2.883	3.290	2.13%	0.600	3.200	3.302	3.2%	2.5% to 3.9%	± 10.0%
10	3.354	3.830	2.52%	0.698	3.720	3.810	2.4%	1.8% to 3.0%	± 10.0%
11	3.824	4.270	0.62%	0.796	4.238	4.254	0.4%	0.0% to 0.7%	± 10.0%
12	4.370	4.653	0.75%	0.909	4.841	4.666	–3.6%	–4.4% to –2.8%	± 10.0%
13	4.807	n/a	n/a	n/a	n/a	n/a	n/a	n/a	n/a

Observed mean alpha-1 acid glycoprotein concentration (or [α1-AGP]; mg/l) was calculated from triplicate analysis performed on the Optilite™ analyser and is presented alongside the mass adjusted target concentration calculated for each dilution. Percentage of the high pool (% high pool) contained within each dilution is indicated along with the 95% confidence intervals (CIs) and the relative differences between linear and nonlinear fits (nonlinearity; allowable nonlinearity was set to ± 10%). IR, internal reference (for α1-AGP); %CV, percent coefficient of variation (of triplicate analyses); 'n/a', dilutions not tested; '< 0.08' assay unable to quantify α1-AGP in the dilution (measured result fell below lower end of the measuring range).

Linear and non-linear (3rd order polynomial) fits plotted from triplicate means for each dilution are presented in **Figure 3.4**. Nonlinearity was plotted as the difference between linear and nonlinear fits as shown in **Figure 3.5**. Upon examination of the regression coefficients, nonlinearity was detected (β2 and β3, both $p < 0.05$) however, the degree of nonlinearity did not exceed allowable limits (i.e., ± 10% of [α1-AGP] in the high pool dilution; **Table 3.4**) and the assay was considered to be linear ($R^2 = 0.998$) in the range of 0.277 – 4.653 mg/l* (slope, 0.053 and y-int., 0.019).

* The observed measuring interval for linearity noted in-text corresponded to a mass adjusted target range of 0.2658 – 4.3698 mg/l for [α1-AGP].

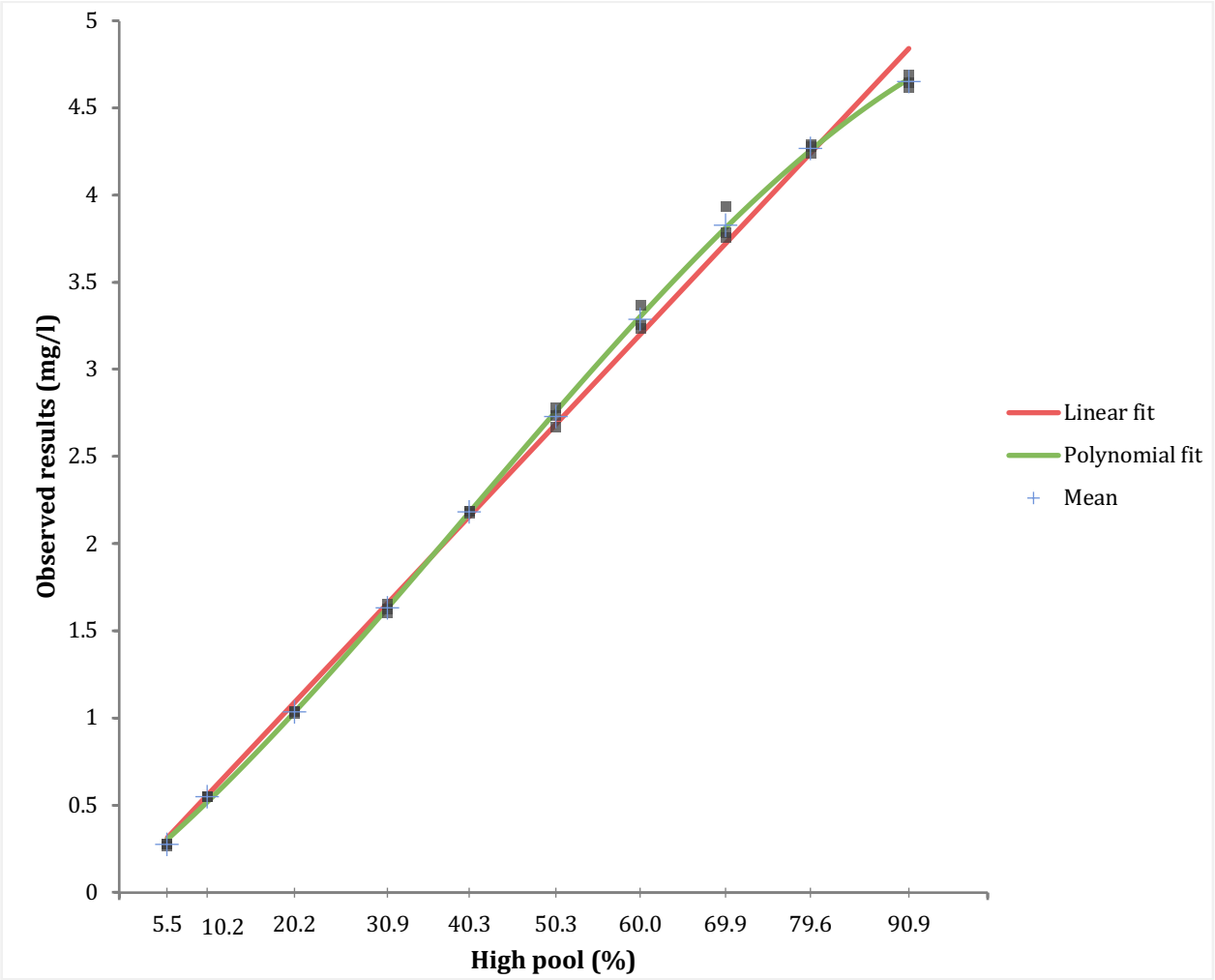

Figure 3.4 – Linear and nonlinear fits. Alpha-1 acid glycoprotein (α1-AGP) was analysed in triplicate using the immunoturbidimetric assay for each dilution (refer to **Table 3.11**) with the triplicate mean [α1-AGP] (mg/l) plotted (y-axis) relative to the proportion of high pool added to that dilution (x-axis; percentages were rounded). Linear and nonlinear (3rd order polynomial) fits were applied to these data. The assay was found to be linear (R^2 = 0.998) in the range of 0.277 – 4.653 mg/l (slope, 0.053 and y-intercept, 0.019).

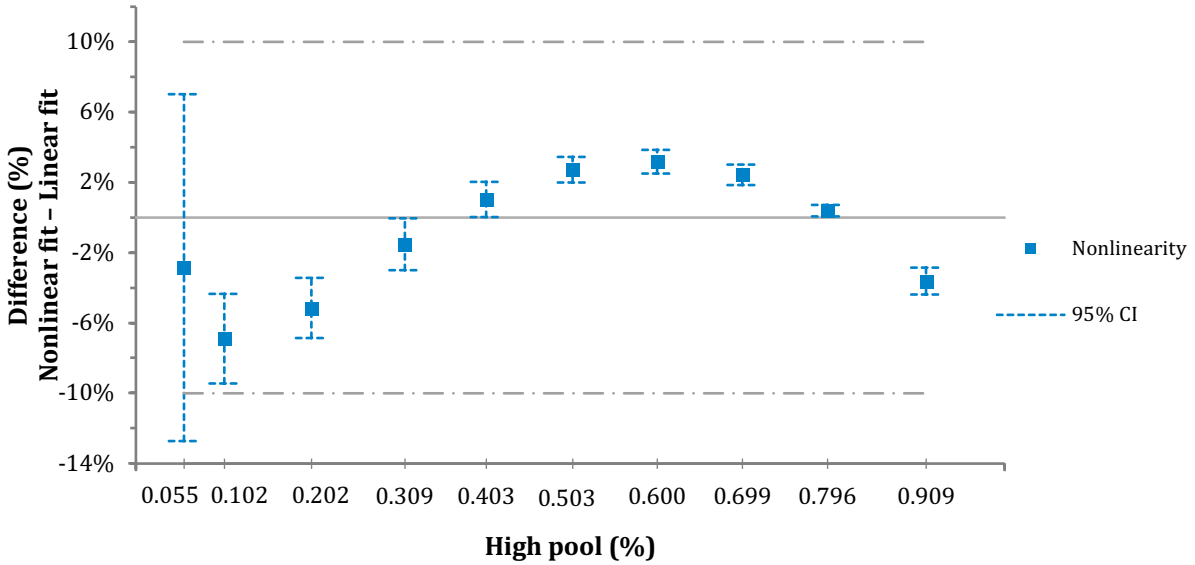

Figure 3.5 – Nonlinearity results. Nonlinearity was examined for the particle-enhanced turbidimetric immunoassay (reagent lot A only) by analysing triplicate dilutions containing alpha-1 acid glycoprotein (α1-AGP). Linear and nonlinear fits were applied to triplicate [α1-AGP] results with data then plotted as percent difference (%) between the nonlinear and linear fits (y-axis; relative to the mass adjusted target [α1-AGP]) for each high pool dilution (x-axis). Dashed error bars represented 95% confidence intervals (95% CIs) the differences between fits. Allowable nonlinearity was set to ± 10% (relative to the target [α1-AGP] contained within each dilution) and was marked by horizontal dashed lines. Only the 95% CIs for the lowest [α1-AGP] (or the 5.53% high pool dilution) exceeded allowable limits (95 CIs: –12.7 to 7.0%).

3.3.3.3. Interference

Results from interference experiments are presented in **Table 3.12** and **Figure 3.6a – 3.6c**. No %CVs for any interferent dilutions for either, ascorbic acid or urea, exceeded 5%. From **Table 3.12**, it was clear that, when analysed from ascorbic acid and urea interferent dilutions, [α1-AGP] was lower than the target (i.e., less than 0.712 mg/l).

Table 3.12 –Interferences of urea and ascorbic acid.

[Interferent]	Percentage of [high pool]	Measured [α1-AGP] (mg/l)	CV (%)	Recovery (%)	Percent Δ (%)	adj. *p*-value
Urea						
50 g/l	100%	0.583 ± 0.012	1.98%	81.9%	7.4%	0.048*
40 g/l	80%	0.593 ± 0.010	0.97%	83.3%	5.8%	0.020*
30 g/l	60%	0.600 ± 0.010	1.67%	84.3%	4.8%	0.084
20 g/l	40%	0.610 ± 0.000	0.00%	85.7%	3.2%	< 0.001*
10 g/l	20%	0.610 ± 0.000	0.00%	85.7%	3.2%	< 0.001*
0 g/l	0%	0.630 ± 0.000	0.00%	88.5%	-	-
Ascorbic acid						
342.0 μmol/l	100%	0.630 ± 0.017	2.75%	88.5%	1.1%	0.987
273.6 μmol/l	80%	0.613 ± 0.010	0.94%	86.1%	1.6%	0.484
205.2 μmol/l	60%	0.620 ± 0.000	0.00%	87.1%	0.5%	0.969
136.8 μmol/l	40%	0.623 ± 0.001	0.93%	87.5%	< 0.0%	> 0.999
68.4 μmol/l	20%	0.613 ± 0.010	0.94%	86.1%	1.6%	0.783
0.00 μmol/l	0%	0.623 ± 0.012	1.85%	87.6%	-	-

Results are presented as mean ± standard deviation (SD) for concentration (mg/l) of alpha-1 acid glycoprotein (α1-AGP, mg/l) measured in triplicate using the particle-enhanced immunoturbidimetric assay (reagent lot A). The target [interferent] for each dilution was estimated as a percentage of the [high pool interferent] (i.e., 50 g/l for urea or 342 μmol/l for ascorbic acid). Percent coefficient of variation (%CV) was calculated from triplicate [α1-AGP] measurements (SD/triplicate mean × 100). Relative difference of triplicate mean [α1-AGP] compared to the initial [α1-AGP] (i.e., estimated relative target, 0.712 mg/l) from the 0% interferent dilution (i.e., 0.630 ± 0.000 mg/l for urea; or 0.623 ± 0.012 mg/l for ascorbic acid) was reported as was recovery of [α1-AGP] for each dilution. This relative difference is referenced as 'Percent Δ'. All statistical tests were two-tailed with significance set to $\alpha < 0.05$ (marked by asterisk, *) and adjusted *p*-values presented for comparisons against the 0% dilution (from one-way ANOVA with Dunnett's *post hoc* test).

Nevertheless, when [α1-AGP] from the 0% interferent dilution for ascorbic acid (0.623 ± 0.012 mg/l) was compared to triplicate means from 20% – 100% dilutions for ascorbic acid, no significant differences were detected (see **Figure 3.6b**) nor did any of the relative differences fall outside ± 3 SD percentages (**Table 3.12**). When [α1-AGP] from the 0% interferent dilution for urea (0.630 ± 0.000 mg/l) was compared triplicate means from 20% – 100% dilutions, significant differences were detected for the 20%, 40%, 80, and 100% dilutions as indicated in **Figure 3.6a**. Unsurprisingly, relative differences compared to the

initial [α1-AGP] for the 100% and 80% dilutions for urea were > 5% with relative differences for all the dilutions (except 60% dilution) being > 3% (**Table 3.12**).

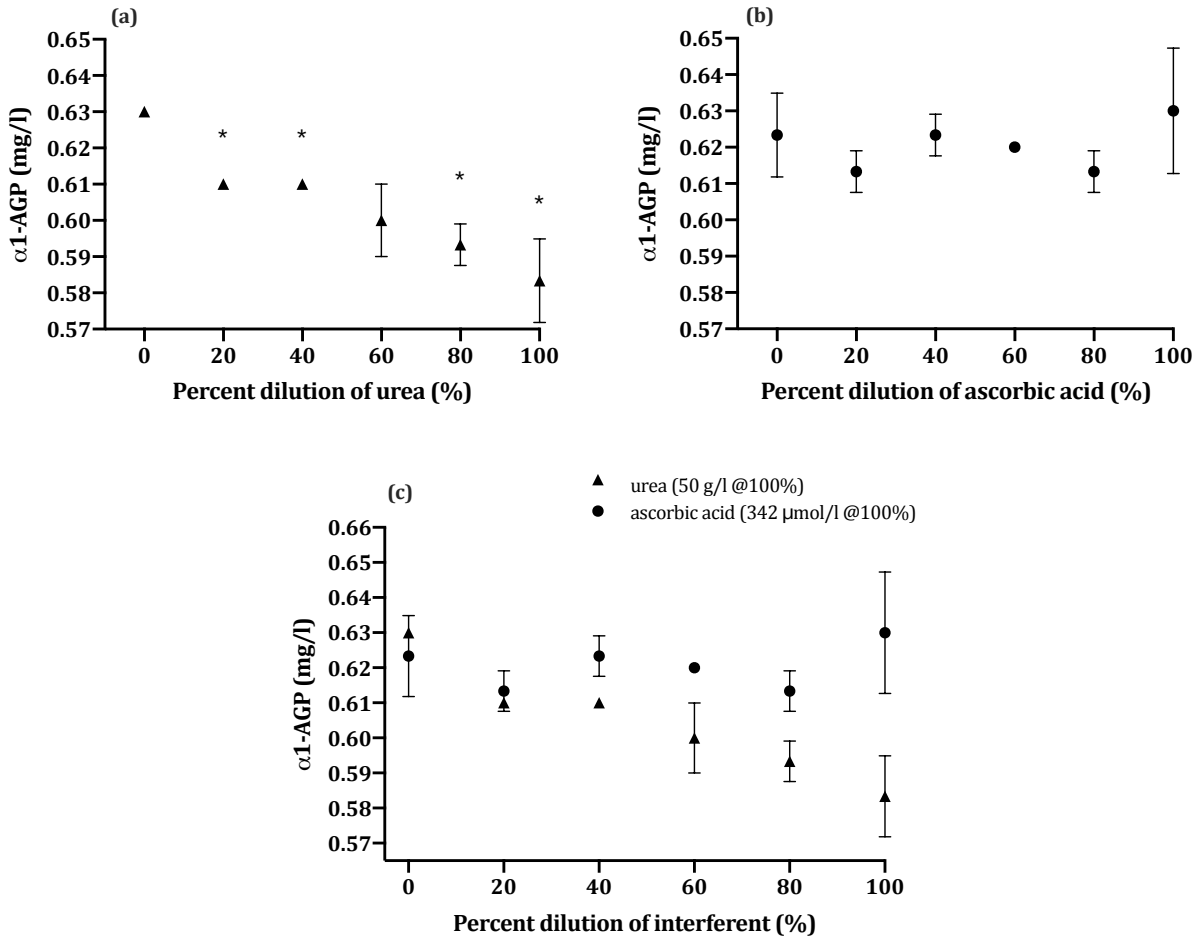

Figure 3.6 – Immunoassay interference. Fig 3.6a (top left) – Interference of ascorbic acid; **Fig. 3.6b (top right)** – Interference of urea; **Fig. 3.6c (bottom)** – Urea and ascorbic acid interference for the alpha-1 acid glycoprotein (α1-AGP) immunoassay. Mean [α1-AGP] (mg/l) estimated from triplicate measurements was plotted (*y*-axis) as mean ± standard deviation (SD; represented by error bars) for each interferent dilution. [α1-AGP] from 20% – 100% dilutions were compared to the [α1-AGP] from the 0% dilution using one-way repeated measures ANOVA with Dunnett's post hoc test. Significance differences from the 0% dilution were observed for urea for the following dilutions: 100% ($p = 0.048$), 80% ($p = 0.020$), 40% ($p < 0.001$), and 20% ($p < 0.001$). No significant differences from the 0% dilution were observed for ascorbic acid (all *p*-values > 0.05). All statistical tests were two-tailed with significance set to $\alpha < 0.05$ and marked by asterisk, *.

3.3.3.4. Stability

Stability trials were successfully completed at the indicated timepoints in **Table 3.13** with in-use stability evaluated using triplicate means for [α1-AGP] from the three panel

samples (on these days). No slopes for any of the linear regressions applied to triplicate mean [α1-AGP] results for the three panel samples were significant (all *p*-values > 0.05; **Table 3.13**). Thus, the maximum timepoint (i.e., 121 days) was accepted as the in-use stability duration.

Table 3.13 – Timeline and results for stability trials.

		Panel 24 0.929 mg/l	**Panel 39** 3.093 mg/l	**Panel 239** 1.914 mg/l
Date	**Days**	**Triplicate means**		
06 November, 2019	0	0.857	3.343	1.860
07 November, 2019	1	0.863	3.213	1.923
08 November, 2019	2*	-	-	-
11 November, 2019	5	0.870	3.510	1.943
12 November, 2019	6	0.857	3.287	1.830
13 November, 2019	7	0.863	3.357	1.883
14 November, 2019	8	0.900	3.490	1.957
19 November, 2019	13	0.883	3.392	1.924
3 December, 2019	27	0.863	3.347	1.915
11 December, 2019	35	0.863	3.367	1.890
19 December, 2019	42	0.866	3.465	1.805
8 January, 2020	63	0.885	3.301	1.917
7 February, 2020	93	0.879	3.401	1.923
06 March, 2020	121	0.868	3.358	1.855
09 April, 2020	incomplete**	-	-	-
		Regression statistics		
	Slope	5.478×10^{-5}	4.689×10^{-5}	-1.835×10^{-4}
	y-int.	0.8687	3.370	1.900
	SE slope	9.747×10^{-5}	6.497×10^{-4}	3.353×10^{-4}
	p-value	0.5854	0.6130	0.9438

Data are presented as mean alpha-1 acid glycoprotein (α1-AGP) concentration (mg/l) from triplicate analysis (performed on indicated dates) for 3 panel samples (i.e., Panel 24, 39, and 239). 'Regression statistics' are also presented for linear regression analysis applied to mean data and were used to evaluate stability duration[305]. If the slope was: 1) significant, stability duration taken as the x-coordinate for the point of intersection between the one-sided 95% confidence interval and the maximum acceptance drift limit (± 5% of the mean [α1-AGP] from 06/NOV/2019) for the respective measurand; or 2) not significant, stability duration was taken as the maximum time point included. *Panel sample results were not successfully recovered from the Optilite™ (auto-analyser) memory due to human error. **Stability trial was not completed due to COVID-19 related factors[312], which also prevented any possibility to extend stability experiments. All statistical tests were two-tailed with significance set to $\alpha < 0.05$. SE, standard error.

Results for the cumulative within-run, between-day, and total imprecisions are presented in **Table 3.14**. Within-day, between-day, and total %CVs and overall recovery and inaccuracy are presented in **Table 3.15**. No triplicate [α1-AGP] results fell outside $\pm$ 4 SDs of the calculated (cumulative) total error at the respective timepoint (or for prior timepoints) nor did any of the (cumulative) total CVs exceed 5% (max 4.58%).

Table 3.14 – Imprecision results for stability trials.

	Within -run		Between-day		Total imprecision	
Day	*SD*	*Variance*	*SD*	*Variance*	*SD*	*Variance*
	Panel 24: 0.929 mg/l					
Day 1	0.0047	2.17×10^{-5}	0.0056	4.57×10^{-5}	0.0068	3.12×10^{-5}
Day 5	0.0041	1.69×10^{-5}	0.0098	0.0001	0.0104	9.64×10^{-5}
Day 6	0.0039	1.53×10^{-5}	0.0084	8.12×10^{-5}	0.0090	7.10×10^{-5}
Day 7	0.0034	1.13×10^{-5}	0.0072	5.87×10^{-5}	0.0077	5.12×10^{-5}
Day 8	0.0028	7.95×10^{-5}	0.0168	0.0003	0.0170	0.0003
Day 13	0.0026	6.94×10^{-6}	0.0162	0.0003	0.0164	0.0003
Day 27	0.0029	8.54×10^{-6}	0.0153	0.0002	0.0155	0.0002
Day 35	0.0030	8.75×10^{-6}	0.0144	0.0002	0.0146	0.0002
Day 42	0.0028	7.76×10^{-6}	0.0136	0.0002	0.0138	0.0002
Day 63	0.0026	6.53×10^{-6}	0.0137	0.0002	0.0139	0.0002
Day 93	0.0024	5.97×10^{-6}	0.0133	0.0002	0.0134	0.0002
Day 121	0.0025	6.00×10^{-6}	0.0128	0.0002	0.0129	0.0002
	Panel 39: 3.093 mg/l					
Day 1	0.0724	0.0052	0.0907	0.0082	0.1082	0.0117
Day 5	0.0511	0.0026	0.1480	0.0219	0.1537	0.0236
Day 6	0.0385	0.0015	0.1255	0.0157	0.1293	0.0167
Day 7	0.0311	0.0010	0.1090	0.0119	0.1119	0.0125
Day 8	0.0261	0.0007	0.1149	0.0132	0.1168	0.0137
Day 13	0.0239	0.0006	0.1050	0.0110	0.1068	0.0114
Day 27	0.0223	0.0005	0.0975	0.0095	0.0992	0.0098
Day 35	0.0218	0.0005	0.0915	0.0084	0.0932	0.0087
Day 42	0.0197	0.0004	0.0870	0.0077	0.0885	0.0078
Day 63	0.0185	0.0003	0.0872	0.0076	0.0885	0.0078
Day 93	0.0177	0.0003	0.0858	0.0074	0.0870	0.0076
Day 121	0.0177	0.0003	0.0825	0.0068	0.0838	0.0070
	Panel 239: 1.914 mg/l					
Day 1	0.0316	0.0010	0.0307	0.0010	0.0401	0.0016
Day 5	0.0488	0.0024	0.0436	0.0019	0.0591	0.0035
Day 6	0.0301	0.0009	0.0529	0.0028	0.0583	0.0034
Day 7	0.0288	0.0008	0.0458	0.0021	0.0515	0.0027
Day 8	0.0276	0.0008	0.0495	0.0025	0.0544	0.0030
Day 13	0.0263	0.0007	0.0463	0.0021	0.0510	0.0026
Day 27	0.0251	0.0007	0.0431	0.0019	0.0480	0.0023
Day 35	0.0244	0.0006	0.0405	0.0016	0.0405	0.0016
Day 42	0.0249	0.0006	0.0491	0.0024	0.0491	0.0024
Day 63	0.0242	0.0006	0.0472	0.0022	0.0471	0.0022
Day 93	0.0239	0.0006	0.0458	0.0021	0.0457	0.0021
Day 121	0.0234	0.0006	0.0453	0.0021	0.0453	0.0021

Within-run, between-day, and total imprecisions (standard deviations, SDs, and variances) were calculated utilising daily triplicate alpha-1 acid glycoprotein concentration results (analysed using reagent lot B) analysed up to and on the indicated day (occurring between November 2019 – March 2020). 'Day' referred to days following 06 November, 2019 (i.e., 'Day 0'). Imprecision estimates utilised: **Equation 3.5, Equation 3.7**, **Equation 3.8**, and **Equation 3.9**.

Table 3.15 – Estimates of immunoassay imprecision for stability experiments.

	Within-run %CV	Between-day %CV	Total %CV	Inaccuracy (mg/l)	Recovery (%)
	Panel 24: 0.929 mg/l				
Day 1	0.54	0.65	0.79	–0.067	92.8
Day 5	0.48	1.14	1.20	–0.056	94.0
Day 6	0.45	0.98	1.04	–0.070	92.5
Day 7	0.39	0.83	0.89	–0.066	92.9
Day 8	0.33	1.94	1.95	–0.029	96.9
Day 13	0.30	1.87	1.88	–0.046	95.0
Day 27	0.34	1.76	1.78	–0.066	92.9
Day 35	0.34	1.65	1.68	–0.064	93.2
Day 42	0.32	1.56	1.58	–0.063	93.2
Day 63	0.29	1.58	1.60	–0.044	95.2
Day 93	0.28	1.53	1.54	–0.051	94.6
Day 121	0.28	1.47	1.48	–0.061	93.5
	Panel 39: 3.093 mg/l				
Day 1	2.22	0.11	3.32	0.121	103.9
Day 5	1.52	0.15	4.58	0.416	113.4
Day 6	1.15	0.13	3.88	0.193	106.3
Day 7	0.93	0.11	3.35	0.263	108.5
Day 8	0.78	0.12	3.47	0.400	112.8
Day 13	0.71	0.11	3.17	0.300	109.7
Day 27	0.66	0.10	2.95	0.254	108.2
Day 35	0.65	0.09	2.77	0.275	108.9
Day 42	0.58	0.09	2.62	0.372	112.0
Day 63	0.55	0.09	2.63	0.208	106.7
Day 93	0.52	0.09	2.58	0.308	110.0
Day 121	0.53	0.08	2.48	0.265	108.6
	Panel 239: 1.914 mg/l				
Day 1	1.67	1.63	2.12	0.006	100.3
Day 5	2.56	2.29	3.10	0.029	101.5
Day 6	1.59	2.80	3.09	–0.085	95.6
Day 7	1.52	2.43	2.730	–0.030	98.4
Day 8	1.46	2.61	2.87	0.041	102.2
Day 13	1.38	2.43	2.68	0.010	100.5
Day 27	1.32	2.26	2.51	0.001	100.0
Day 35	1.29	2.13	2.13	–0.022	98.9
Day 42	1.32	2.59	2.59	–0.109	94.3
Day 63	1.28	2.49	2.49	0.003	100.2
Day 93	1.26	2.41	2.41	0.009	100.5
Day 121	1.24	1.33	2.39	–0.059	96.9

Percent coefficient of variation (%CV), inaccuracy, and recovery are presented for triplicate measurements of 3 control (panel) samples containing known amounts of alpha-1 acid glycoprotein (α1-AGP). Results were calculated using **Equation 3.6** and **Equation 3.10** in conjunction with the corresponding SD results presented in **Table 3.14**. Day 0 (not shown) was 06 November, 2019 (as between-day values were not calculated for Day 1). Inaccuracy and recovery were calculated relative to the target [α1-AGP] indicated for each panel sample. All dates were in reference to November 2019 – March 2020.

3.3.3.5. Methods comparison

From the 126 urine specimens analysed, [α1-AGP] results from a total of 115 specimens were matched (having both PETIA and RID results) and included for analysis. The overall %CV (1.61%) for [α1-AGP] measurements using PETIA was well below the allowable %CV (set to < 5%). Similarly, all individual triplicate %CVs remained less than 15% (max, 11.95%; min, 0.00%). Urinary [α1-AGP] results produced from PETIA (0.09 – 9.45 mg/l for individual values or 0.09 – 9.387 mg/l for triplicate means) were more sensitive (having a lower minimum) than those produced by RID (0.120 – 6.101 mg/l). Urinary [α1-AGP] measurements from RID however, were, on average, lower than PETIA (bias, –0.131 ± 0.711; 95% LOAs, –1.525 to 1.263) as observed in the B-A plot in **Figure 3.7**. This difference was significant evident from the significantly non-zero slope (–0.210 ± 0.043; $p < 0.001$) of the best fit line (y int. 0.159 ± 0.085) plotted from the simple linear regression. Despite these differences, a significant strong positive relationship was observed between urinary [α1-AGP] results measured by RID and PETIA (individual results, **Figure 3.8a**; and triplicate means, **Figure 3.8b**).

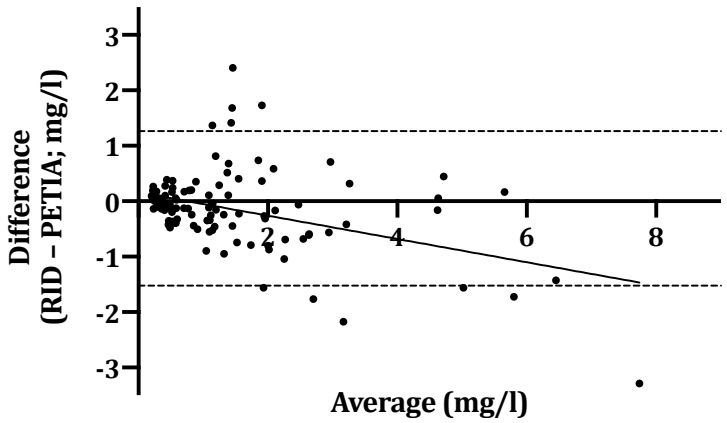

Figure 3.7 – Bland-Altman (B-A) plot. B-A plot compares urinary alpha-1 acid glycoprotein (α1-AGP, mg/l) results between radial immunodiffusion (RID) and particle-enhanced turbidimetric immunoassay (PETIA) methods. Data are plotted as the difference (y-axis) between RID – PETIA (triplicate mean from PETIA) vs the average (x-axis) [α1-AGP] for matched urinary measurements (n = 115 pairs). Bias was estimated as −0.131 ± 0.711 and the 95% Limits of Agreement (95% LOAs) observed from −1.525 to 1.263 (represented by horizontal dashed lines). The best-fit line (significantly non-zero slope; −0.210 ± 0.043, $p < 0.001$) was plotted from the simple linear regression (y = −0.210*x + 0.159) with the goodness of fit also estimated (Sy.x = 0.648; and $R^2 = 0.177$). All statistical tests were two-tailed with significance set to $\alpha < 0.05$.

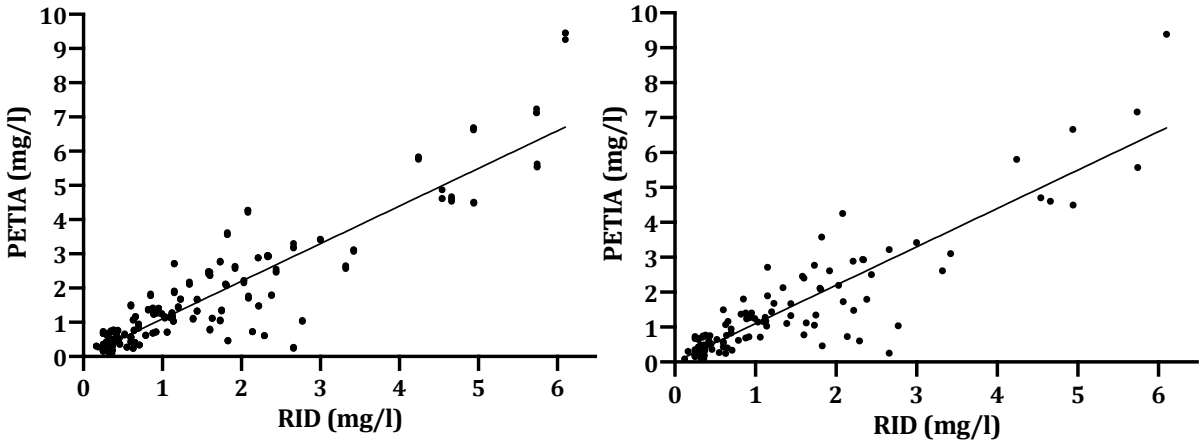

Figure 3.8 – Scatter plots for methods comparison. Urinary alpha-1 acid glycoprotein (α1-AGP) concentration ([α1-AGP]; mg/l) was measured using particle-enhanced turbidimetric immunoassay (PETIA) and radial immunodiffusion (RID). **Fig. 3.8a (left)** – Individual urinary [α1-AGP] results from triplicates analysed using PETIA (y-axis) are plotted against the corresponding RID results (x-axis) with correlation analysis (Pearson r = 0.900, $p < 0.001$) and linear regression applied ($R^2 = 0.809$); **Fig. 3.8b (right)** – Triplicate mean [α1-AGP] from PETIA (y-axis) is plotted against the corresponding RID result with correlation analysis (Pearson r = 0.900, $p < 0.001$) and linear regression applied ($R^2 = 0.811$). All statistical tests were two-tailed with significance set to $\alpha < 0.05$.

3.4. DISCUSSION

3.4.1. Latex conjugation and test coat production

Production processes for the present immunoassay were facilitated using monospecific polyclonal sheep antisera while previous studies utilised rabbit antisera[5]. It was evident that a substantially larger volume of reagent could be produced by manufacturing this reagent in bulk (~104 ml vs ~800 ml), which is obviously more time efficient and also more appropriate for large quantities of analyses (e.g., clinical chemistry lab in a hospital). Small batch production, however, is repeatable and sufficient for small-scale research applications.

3.4.2. Assay optimisation and test parameters

The run time of the present PETIA on the Optilite™ (~10 minutes) was comparable to earlier studies using alternative auto-analysers (**Table 3.16**). Similarly, LOB, LOD, and LLOQ were comparable to earlier assays[5 288], although the present PETIA embodied an exceptionally wider measuring range compared to previous immunoassays used for urinalysis α1-AGP[5] (**Table 3.16**). Nevertheless, LLOQ of present immunoassay for use on the Optilite™ was far more sensitive (down to 0.08 mg/l) compared to the existing serum α1-AGP immunoassay (0.19 – 6.0 g/l, at neat).

Table 3.16 – Analytical limits for turbidimetric immunoassays used for urinalysis of alpha-1 acid glycoprotein (α1-AGP).

	Kustán and colleagues[5]	Christiansen and colleagues[288]	present immunoassay
Analyser used	Cobas 8000	Cobas Integra 700 (and Cobas Mira)	Optilite™
Calibration working range (mg/l)	0.16 – 5.25	0.20 – 5.00	0.08 – 4.94
Extended measuring range (mg/l)	0.10 – 31.5	0.07 – 50.0	0.08 – 148.20
Limit of the blank (mg/l)	0.01	-	0.0198 (-7.94 x 10^{-5})*
Limit of detection (mg/l)	0.02	0.05	0.029 (0.0009)*
Limit of quantification (mg/l)	0.08	-	0.076 (0.0058)*
Linearity range (mg/l)	0.1 – 4.48	0.10 – 37.50 (0.5 – 5.00)	0.277 – 4.653**
Linearity (R^2)	0.999	0.998† (1.001†)	0.998

The particle-enhanced immunoturbidimetric assay outlined in the chapter text is represented as the 'present immunoassay'. Different [target] of α1-AGP were incorporated for standard dilutions for all immunoassays, which were all also performed on different analysers (i.e., Cobas Integra 700, Cobras 8000, and Optilite™). Results from Christiansen and colleagues[288] were produced on two separate machines, thus, results for the Cobas Mira are represented in parenthesis where possible. † Mean recovery in the range of linearity. * [α1-AGP] values were reported in mg/l with the response (absorbance, abs) indicated in parenthesis. ** The measuring interval (or range of linearity) corresponded to mass adjusted target range of 0.2658 – 4.3690 mg/l for [α1-AGP].

3.4.2.1. Calibration

Standard dilutions were executed using a human serum reference fluid (617 mg/l) as the calibrator, which was similar to previously used calibrators (human serum reference fluid, 656 mg/l)[288]. Absorbance data for standard dilutions analysed using reagents A and B were fitted on-device utilising a logit-log 4 method with these standard curves successfully recreated in Prism from the raw response data. Despite evidence of a potential reduction in assay response (absorbance) along the entire curve ~1 week following pooling of reagent batches for lot A (1 and 2; as observed in **Figure 3.2b**), this was not sufficient evidence to support a decrement in assay performance, which must also consider analytical results for control

samples (as described in the next section). The limited difference between calibration curves for the two reagent lots A and B demonstrated the repeatability of PETIA production (outlined in section **3.2.2**) and the consistency between small and bulk reagent production.

Application of the logit-log 4 method to standard dilutions was in contrast to previous studies that used either the cubic spline method[5] or a logit-log 5 model[288]. Compared to the cubic spline method, the logit-log 4 model is more accurate, deals better with asymmetries and, specifically, better handles data points that may fall in between standard dilutions[313]. For these reasons, the logit-log 4 method was more appropriate than the cubic spline method for use with bioassays[313]. Nevertheless, application of a 5-PL model could, potentially, offer some advantages (e.g., eliminate any lack-of-fit error[313]) and, therefore, should be considered in future investigations.

3.4.3. Preliminary validation

The present PETIA designed for analysis of low-concentration α1-AGP was preliminarily validated in accordance with the 2nd Edition of Eurachem guidelines[314] and various NCCLS approved guidelines (with minor exceptions*) for assessments of: intra- and inter- assay imprecision[298], linearity[315], accuracy[316], interference, assay stability, and methods comparison[306 317].

* Preliminary validation experiments were performed in accordance with all referenced guidelines with the single exception of not being conducted for 20 days using a single reagent lot. Given that preliminary validation results were not intended for use as part of any manufacturer's precision claims (i.e. minimum of 20 days of experimentation using a single lot of reagent is recommended) and the rise of the global pandemic, validation tests were not repeated nor continued beyond March 2020. Further validation experiments would be required prior to commercialisation and should aim to conduct validation experiments over the no less than 20 – 21 days as per the NCCLS guidelines prior to commercialisation (refer to 298. NCCLS Approved Guideline EP5-A. Evaluation of Precision Performance of Clinical Chemistry Devices. Wayne, PA1999.).

3.4.3.1. Intra- and inter- assay imprecisions

Imprecisions of the current assay were compared to similar existing assays in **Table 3.17**. Previous evaluations of intra-assay (within-run) imprecision have been conducted by diluting a sample with a known [α1-AGP] (e.g., 845 mg/l, PC2, ref. no. 05117216 190, Roche Diagnostics GmbH, Mannheim, Germany) into four different dilutions and, subsequently, performing 10 parallel measurements of each dilution on the same day[5]. Evaluations of intra-assay imprecision have also been demonstrated by analysing three control samples for [α1-AGP] in duplicate twice per day for 19 – 20 days[288]. Most similar to the latter approach, the present study analysed three control samples in triplicate once or twice per day (depending on reagent lot in question) for evaluations of assay imprecisions.

Table 3.17 – Comparison of immunoassay imprecisions.

Target [α1-AGP] (mg/l)	Within-run imprecision		Total imprecision		Analyser	Author(s)
	SD	*%CV*	*SD*	*%CV*		
0.23	0.015	6.7%	0.024	10.4%	Cobas Integra 700	Christiansen and colleagues[288]
1.08	0.011	1.0%	0.042	3.9%		
4.69	0.047	1.0%	0.016	3.4%		
0.68	0.039	5.7%	0.048	7.00%	Cobas Mira	Christiansen and colleagues[288]
1.34	0.064	5.8%	0.088	6.60%		
2.57	0.120	4.6%	0.12	4.80%		
0.30	0.30 ± 0.01*	4.44%	0.30 ± 0.01*	3.50%	Cobas 8000	Kustán and colleagues[5]
0.64	0.62 ± 0.01*	1.92%	0.63 ± 0.03*	1.77%		
2.11	2.06 ± 0.01*	0.45%	2.17 ± 0.04*	4.29%		
3.86	3.73 ± 0.08*	2.01%	3.83 ± 0.13*	4.55%		
0.732	0.010	1.40%	0.016	2.36%	Optilite™	Reagent lot A**
1.863	0.045	2.02%	0.055	2.47%		
3.187	0.061	1.58%	0.090	2.33%		
0.929	0.010	1.15%	0.017	2.00%	Optilite™	Reagent lot B**
1.914	0.027	1.40%	0.034	1.79%		
3.093	0.113	3.32%	0.120	3.53%		

Comparisons of imprecisions from previously described turbidimetric immunoassays used for the analysis of urinary alpha-1 acid glycoprotein (α1-AGP) compared to the immunoassay outlined in the present study. Within-run and total imprecisions are presented as standard deviation (SD) unless otherwise indicated by asterisk (*), where results are presented as the mean [α1-AGP] measured ± within-run or total SD, and as reported by the authors indicated. ** Reagent lots from the present study.

3.4.3.1.1. Reagent lot A

Despite the brevity of imprecision experimentation (i.e., < 21 days) and the inability to separate between-day and between-run imprecisions for reagent lot A, imprecision estimates were comparable to those exhibited by Kustán and colleagues[5], whom executed experiments over a similar time interval (e.g., 10-day precision). In addition, total imprecision for reagent lot A was lower than that of a previously developed assay optimised for use on the Cobas Integra 700[288]. Importantly, two-way RM-ANOVA analysis of control sample results did not detect a significant difference between [α1-AGP], which indicated that the apparent reduction in assay

response (as mentioned in section **3.3.2.1**) observed following batch pooling did not influence assay performance (i.e., measured [α1-AGP] results). Thus, valuable information was gained from imprecision evaluations in spite of the less than optimal duration of experimentation[5]. Future analyses conducted along a similar time interval (i.e., 7 to 10 days) could be reasonably expected to produce results having comparable within-run precision.

3.4.3.1.2. Reagent lot B

Within-run imprecisions were improved (i.e., reduced) for reagent lot B compared to reagent lot A for the low- and mid-range panel samples, albeit slightly elevated for the highest control [α1-AGP] (i.e., 3.093 mg/l). This was evident from the within-run SDs and the associated %CVs (refer to **Table 3.9** and **Table 3.10**). As a consequence, a similar observation was made for the total imprecisions. Between-day, between-run, and total imprecision did not exceed allowable limits, indicating good precision. Future evaluations of assay imprecision for the present immunoassay could be strengthened by analysing more control samples that span a wider range of target [α1-AGP].

3.4.3.2. Inaccuracy and recovery – reagent lots A and B

Recovery for the present immunoassay was lowest at the low end of the working range and was lower than previous assays at a similar [α1-AGP][5] (see **Table 3.18**). Nevertheless, recovery at this [α1-AGP] was still well within the acceptable range (i.e., 80% – 120%)[318]. By contrast, recovery at the higher end of the working range (> 3.0 mg/l) was consistently > 100% (and inaccuracies were positive) with results at this level being the only time when the acceptable recovery range was exceeded. Reagent lot B appeared to improve upon these inaccuracies, although the reason for this difference was not clear. Further studies are required

to confirm the present results observed at the high end of the working range, and also to assess recovery across a wider range of [α1-AGP] (opposed to only 3 controls).

Table 3.18 – Comparisons of recoveries and inaccuracies between automated turbidimetric immunoassays for urinalysis of human alpha-1 acid glycoprotein (α1-AGP).

Target [α1-AGP] (mg/l)	Recovery (%)	Inaccuracy (mg/l)	Analyser used	Author
3.26	101%	-	Cobas Integra 700	Christiansen and colleagues[288]
1.64	105%	-		
1.09	107%	-		
0.66	108%	-		
0.22	107%	-		
0.30	99.24%	-	Cobas 8000	Kustán and colleagues[5]
0.64	102.51%	-		
2.11	98.31%	-		
3.86	100.18%	-		
0.732	95.0%	-0.036 ± 0.016	Optilite™	Reagent lot A*
1.863	119.4%	0.690 ± 0.088		
3.187	121.7%	0.370 ± 0.054		
0.929	93.8%	-0.057 ± 0.018	Optilite™	Reagent lot B*
1.914	99.7%	-0.006 ± 0.046		
3.093	110.3%	0.317 ± 0.129		

Recovery results reported by Kustán and colleagues[5] are reported for the 'Total recovery' as cited in-text. Recovery is presented as percentage (%) relative to the target [α1-AGP] (mg/l). Inaccuracy results are presented as mean ± standard deviation (SD) and were estimated as the difference between measured and target [α1-AGP] (mg/l). Reagent lots A and B described in the present study are marked by asterisk (*).

The degree to which any such over- or underestimations may influence any significance of sub-clinical (i.e., low [α1-AGP] that is not pathologic but has demonstrated physiologic significance; refer to **Chapter 2**) or clinical observations remains unclear. To better understand this, a more in-depth evaluation of existing ranges published for [α1-AGP] will be explored in subsequent chapters (see **Chapter 4**).

3.4.3.3. Linearity

Linearity experiments utilised similar methods to the only other two existing immunoassays capable of urinalysis of [α1-AGP] (e.g., 2 to 4 parallel measurements of 10 different dilutions of control samples). Similarly, the present linearity results were comparable to linearity observed for similar immunoassays (R^2 = 0.999 and R^2 = 0.998) evaluated across similar ranges[5 288] (see **Table 3.16**). Although the degree of nonlinearity for the current assay did not exceed allowable limits, given the detection of some nonlinearity and noting the 95% CIs for the 5.53% dilution (refer to **Table 3.4**), which did exceed allowable nonlinearity (–12.7 to 7.0%; **Figure 3.5**), it was clear that additional attention is required. Similarly, the result from Dilution No. 2 (refer to **Table 3.11**), which went 'undetected' (falling below the lower limit of quantification, < 0.08 mg/l), despite the mass adjusted concentration (0.0974 mg/l) falling within the assay's measuring range, also requires further investigation. Taken together, these results indicate that the range of linearity may require revaluation.

As linearity experiments were not repeated, it could not be confirmed whether the above results were repeatable for both reagent lots or whether the result may have been attributed to the high pool dilution in question (or related calculations). Clarity related to this may be provided by future linearity experiments utilising and diluting a urine control as opposed to a serum control and would help ensure such a factor did not contribute to the present findings of 'good' linearity. Future studies may also be improved by measuring dilutions containing [α1-AGP] that are 20 to 30% wider than the expected measuring range in order to explore the widest possible linear range[301].

3.4.3.4. Interference

Despite being purported as an admitted limitation of previous studies, interferences have only been theorised at best and none have analysed the interferences of urea and ascorbic

acid, specifically[5]. Target [α1-AGP] of 0.712 mg/l was chosen for assessments of interference (for urea and ascorbic acid) given that the assay appeared to be most accurate and precise near this concentration (as observed in **Table 3.7**). Thus, it was hoped that by using this [α1-AGP], even the subtlest deviations from the target [α1-AGP] would be detected.

A proactive approach was adopted to stem any interference(s) (via use of blocking agent; use of F(ab)'$_2$[319]) and to help limit the generation of erroneous results that can occur as a product (e.g., cross-reactivity[320]) however, results still demonstrated evidence of interference. Despite %CVs not exceeding the allowable limit (remaining < 5%), results for the relative differences compared to initial measurements indicated that substances abundantly found in urine (i.e., urea[321]) have the potential to influence [α1-AGP] results when analysed using the present PETIA (refer to **Figure 3.6**). The observed interference of urea remains relevant when considered with respect to the physiologic range of excretion (12 – 20 g of urea/day)[322] and the expected 24-hour urine production (e.g., anywhere from 0.50 – 3.00 litres)*. Nevertheless, the observed interference of urea must be considered with respect to clinically significant cut-off values (or normal reference ranges) with additional consideration given to different magnitudes of deviation that may be exhibited across a range of [α1-AGP].

For this reason, additional experimentation related to interference is required and would be strengthened by performing analysis: 1) across a wider range of α1-AGP and interferent concentrations; and 2) for alternative interferents. Additional interferents for consideration may include but shall not be limited to: preservatives commonly used in urine specimen collections[323] (e.g., sodium azide, 2 ml of 0.1%, total 4 mg in solution, 1/500 dilution from stock); alternative protease inhibitors or other preservatives used in urine specimens[324]

*For example, 20 g urea excreted over 24-hours in 2 litres of urine would equal 10 g/l. Similarly, 20 g urea excreted of 24-hours in 0.5 litres would equal 40 g/l.

[325]; various excreted drug compounds[326]; or other regularly occurring compounds found in urine[327].

3.4.3.5. Stability

The classical design used for the assessment of in-use stability in the present study has a drawback of introducing long-term variability or bias into stability results through many potential factors, such as, laboratory environment fluctuations; multiple calibrations; and device hardware maintenance, changes or, replacements[305]. Nevertheless, reagent lot B was considered stable over the course of experimentation (i.e., 121 days).

In hindsight, it would have been more appropriate if all stability trials were evenly spaced. It should also be noted, however, that the sole use of panel control samples for stability tests could have played a part as some diagnostic reagents have exhibited little or no drift with controls but significant drift if human specimens are tested[305]. Further experimentation across a longer period of time (e.g., 13 months) is required to determine the full duration of in-use stability. Future stability studies may also be strengthened by adopting proposed improvements presented by Holland and colleagues[328] for the statistical methodologies.

3.4.3.6. Methods comparison

Consistent with previous methods comparisons[5] [288], the present analysis demonstrated that PETIA yielded urinary [α1-AGP] results that were, on average, greater than those produced by traditional methods, such as, western blotting or, in this case, RID. Given that urine specimens were stored at –80 °C prior to analysis using both methods, the time between specimen collection and analysis (using either, RID or PETIA) should not have influenced observed results[5] [288] [329] and, therefore, cannot explain observed differences in [α1-AGP] results between the two methods. Use of a warming cupboard to thaw specimens prior

to PETIA analysis could provide an explanation, in part, but would fail to explain the improved sensitivity (i.e., lower minimum) observed for PETIA. Methods comparison could have been strengthened with the parallel analysis of panel control samples throughout analysis of human specimens.

3.4.4. Limitations

The brevity of the validation experiments was an obvious limitation however, meaningful results were still gained from and were sufficient for the formation of preliminary conclusions and ideas for future directions. It is unclear whether, and to what degree, the presence of different types and amounts of α1-AGP glycoforms could have influenced immunoassay performance. Nevertheless, given established associations between the types or amounts of α1-AGP glycoforms[2] (in serum) and relative function(s) (e.g., immunomodulating properties and binding abilities[104]) or clinical presentation, it is clear this deserves further investigation. This is, particularly, relevant for instances when the use of urinary α1-AGP as a diagnostic biomarker may be indicated (e.g., Crohn's; see next chapter for more) and even more so when low levels of urinary [α1-AGP] are being analysed as they more sensitive to subtle incorrectness.

3.5. CONCLUSION

When used together with automated immunoturbidimetry, the present latex-enhanced reagent developed for the analysis of [α1-AGP] was exhibited to be: 1) precise (i.e., within-run, between-run, between-day, and total imprecisions did not exceed allowable limits); 2) linear in the range of 0.277 – 4.653; and 3) stable for (at least) 121 days. Urinary [α1-AGP] results were also more sensitive than, albeit consistent with, results produced by RID.

Therefore, subsequent experimental chapters of this thesis go on to utilise this immunoassay for the urinalysis of α1-AGP in human specimens.

Chapter 4

EVALUATION OF URINARY ALPHA-1 ACID GLYCOPROTEIN (α1-AGP) IN HEALTH AND DISEASE.

A full manuscript for data presented in this chapter is currently being prepared for submission to the Journal of Clinical Chemistry.

Authors and affiliations:

Joyce KE[1 4], Delamere J[2 4], Ashdown K[3 4], Bradwell AR[2 4], and Lucas SJE[1 4].

1. School of Sport Exercise and Rehabilitation Sciences, University of Birmingham
2. Medical School, University of Birmingham, Birmingham, UK
3. Occupational Performance Research Group, University Chichester, Chichester, UK
4. Birmingham Medical Research Expeditionary Society. University of Birmingham, Birmingham, UK

Statement of contribution:

KEJ – concept, design, data collection, statistical analysis, and writing; JD – concept, design, and data collection; KA – data collection and writing; ARB – concept and design; and SJEL – concept, data collection, and writing.

ABSTRACT

INTRODUCTION: Recent applications of urinary alpha-1 acid glycoprotein (α1-AGP) as a disease biomarker have resulted in the use of multiple analytical techniques for its quantification, without consensus or guidelines for the standardisation of its reporting. The purpose of this study was to evaluate normative ranges of urinary α1-AGP in humans (healthy and diseased) by: 1) examining existing literature, and 2) analysing human specimens utilising a novel immunoturbidimetric assay. **METHODS:** A PRISMA-based literature search included studies (n = 53) reporting urinary α1-AGP in units including: absolute concentration (mg/l), excretion (μg/min or mg/24-hours), α1-AGP-to-creatinine ratio, ($mg/mmol_{\alpha1\text{-}AGP:CREA}$), percentage of total urinary protein (%), and clearance (μl/min). Data from the literature were compiled and presented with results from urinalysis of twenty-four-hour (n = 25), short-duration (30-minutes to 2-hours; n = 31), and early-morning urine (EMU, n = 18) specimens collected as part of this thesis. Immunoturbidimetric urinalysis for α1-AGP was conducted using a novel latex-enhanced assay (0.08 – 148.2 mg/l) on the Optilite™ auto-analyser. Statistical analysis compared urinary α1-AGP units between specimen types, age groups, and sexes. **RESULTS:** Urinary [α1-AGP] was most commonly reported in the literature. $mg/l_{24\text{-}hours}$ was, on average, 0.283 mg/l greater than mg/l_{EMU} with the difference being significant (p = 0.015), despite mg/l_{EMU} and $mg/l_{24\text{-}hours}$ being related (p = 0.026, r = 0.523). Also related were log-transformed values for mg/24-hours and $mg/mmol_{\alpha1\text{-}AGP:CREA}$ (p = 0.041, r = 0.486). No difference was observed between 24-hour and short-duration specimens (all intervals, $p > 0.05$) for α1-AGP excretion. Multiple linear regression based on age and sex was not significant for any urinary α1-AGP units from 24-hour or EMU specimens (all $p > 0.05$). **CONCLUSION:** Latex-enhanced immunoturbidimetry is successful for the detection of α1-AGP in human urine with

experimental results comparable to the existing literature. Although certain urinary α1-AGP units are related (e.g., mg/$l_{24\text{-hour}}$ vs mg/l_{EMU}), this must be considered in the context of the healthy cohort studied here. Despite no observable impact of age or sex in experimental urinalysis, it was clear from the literature that age warrants further investigation, particularly, in relation to whether age-specific reference values in healthy and diseased individuals are required.

4.1. INTRODUCTION

Alpha-1 acid glycoprotein (α1-AGP; or orosomucoid-1) is an acute phase plasma protein that increases in response to inflammation[2]. Serum fluctuations in α1-AGP have been well studied, whereas evaluations of its presence and significance in urine have been relatively limited until recently. Urinary α1-AGP has proven to be a sensitive clinical biomarker of several diseases including: heart failure[282], type 2 diabetes mellitus (T2DM)[330], chronic kidney disease[285], acute kidney injury[331], sepsis[281], irritable bowel syndrome[5], Crohn's disease[5 278], pre-eclampsia[280], bladder cancer[279], prostate cancer[332], acute paediatric appendicitis[333], and psoriasis[4], to name a few. Urinary α1-AGP has also demonstrated predictive abilities related to disease outcomes[334], with additional reports evident in relation to physiologic responses(s) (e.g., exercise[335] or ascent to altitude[7]).

Novel applications of urinary α1-AGP have resulted in the use of multiple analytical techniques for its quantification, which have included: radial immunodiffusion (RID)[7], western blotting[5], enzyme-linked immunosorbent assay (ELISA)[285 283 284], immunoelectrophoresis[286], nephelometry[287], and high accuracy mass spectrometry[333]. Similarly, methods of collection and units of measure reported for urinary α1-AGP have taken on many forms. Methods of collection have included early morning midstream[282 279], spontaneous[5], and timed (e.g., 5-[336], 24-[7], or 48-hour[6]) urine collections, with accompanying results presented in various measurement units including: excretion rate (μg/min or mg/24-hours), absolute concentration (mg/l), α1-AGP-to-creatinine ratio (α1-AGP:CREA or; $mg/mmol_{\alpha 1\text{-}AGP:CREA}$), percentage of total urinary protein (%), and clearance (μl/min). Evidence and consensus for the most appropriate analytical methods and collection procedures for the examination of urinary α1-AGP are limited[337], with additional

gaps evident in regards to any healthy reference ranges or disease cut-offs, as well as, recommendations for the standard units of measure to be reported.

Given this, the objective of the present study was to examine and evaluate collection, processing, and reporting procedures for human urine specimens analysed for α1-AGP (among healthy and diseased individuals), with an ultimate goal of establishing normative ranges. To achieve this, published results for urinary α1-AGP (any and all units) were compiled from the existing literature and combined with particle-enhanced immunoturbidimetry urinalysis (as outlined in **Chapter 3**) of various types of urine specimens (i.e., early morning midstream, timed-spot, and 24-hour urine specimens) collected within this thesis. We hypothesised that the immunoturbidimetric assay would successfully detect α1-AGP in various types of human urine specimens and across a wide concentration range. In addition, results were unlikely to exceed the upper or lower limits of detection, and be within the range of values reported in literature for comparable cohorts and units of measure. Age and sex were considered to have the potential to influence urinary results, although the propensity for any such impact on the various units of measure was uncertain. Finally, EMUs and timed-spot urine specimens were expected to potentially under- or over-estimate α1-AGP values measured from 24-hours specimens.

4.2. METHODS

Methodology will be divided between urinalysis performed as part of experimental studies within this thesis (see section **4.2.1**) and the literature search that was conducted as part of this chapter (see section **4.2.2**).

4.2.1. Methodology for experimental studies within the thesis

4.2.1.1. Ethical approval and standardisation procedures for participants

This study was included as a part of two larger studies (outlined in detail in **Chapter 6** and **7**) both having received ethical approval through the University of Birmingham (ERN_18-1270 and ERN_19-0325) for identical collection procedures and analytical procedures. Written informed consent was obtained prior to voluntary participation. Samples included in the current study were from healthy individuals without any pre-existing cardiac, pulmonary, or metabolic conditions (assessed via a University-approved health history questionnaire that was completed following written consent). Participant characteristics can be found alongside results in section **4.3.1.**

Participants were asked to refrain from: 1) engaging in vigorous activities[338] * or consuming alcohol in the 24-hours prior, and 2) consuming caffeine in the 4-hours prior to all urine specimen collections (24-hour, EMU, and timed-spot) and also *during* the 24-hour urine specimen collections.

4.2.1.2. Urine specimen collection and processing

Twenty-four-hour (see section **4.2.1.2.1**, short-duration timed spot (30-minute to 2-hour; see section **4.2.1.2.2**), and early-morning midstream urine (EMU; see section **4.2.1.2.3**) specimens were collected for the present study.

4.2.1.2.1. Twenty-four-hour urine specimens

Twenty-four-hour urine specimens were collected by participants external to the laboratory with collections occurring at a time convenient to participants. Twenty-four-hour

* Vigorous activity was defined, and described to participants (based on the American College of Sport Medicine guidelines for exercise testing and prescription), as any activity having an intensity that prevented singing or talking for any more than a few words due to the need to breathe.

collections were initiated following a voluntary urination (with the precise time of this recorded and reported) after which participants were instructed to collect all urine for a duration of 24-hours. Specimens were collected in provided 3,000 ml UV-protected vesicles (SARSTEDT, Nümbrecht, Germany) designed for human urine collection, containing 2 ml of sodium azide (0.1% in solution) as a preservative.

Upon completion of the 24-hour urine collection, participants were asked to record the precise time of completion (to the minute) and contact the laboratory to arrange specimen return. Upon return of the 24-hour specimens to the laboratory, collection start and end times were recorded with specimens then measured for: volume (ml), weight (g), and total collection duration (in minutes). Approximately 20 ml of urine was then pipetted into a conical, polypropylene[339] centrifuge tube and centrifuged for 10 minutes[5] (4,300 – 5,400 rpm or 2,660 – 3,500 rcf at 4 °C) for the sole purpose of rendering specimens acellular[*]. Following centrifugation, the supernatant was pipetted into four repeat 2 ml aliquots (containing ~1.5 ml in each) and stored at –80 °C until urinalysis.

4.2.1.2.2. Timed-spot urine specimens

Timed-spot urine specimens were collected at the University of Birmingham in the School of Sport, Exercise, and Rehabilitation Sciences' Human Performance Laboratory as part of the control arm of a larger study (outlined in **Chapter 6**). **Figure 4.1** below shows the timeline of the sampling timepoints, spanning 30 min, 1- and 2-hour collection durations. Similar to 24-hour specimens, timed-spot specimens were measured for volume (ml), weight

[*] Specimens were centrifuged to render them acellular for the purposes of storage in compliance with the Human Tissue Act. Variability in the centrifugal forces was due to the use of two different centrifuges as the data collections were effectively divided into two portions.

(g), and collection duration (mins) and then centrifuged, pipetted into four repeat 2 ml aliquots, and frozen (at –80 °C) until urinalysis (as described in section **4.2.1.3**).

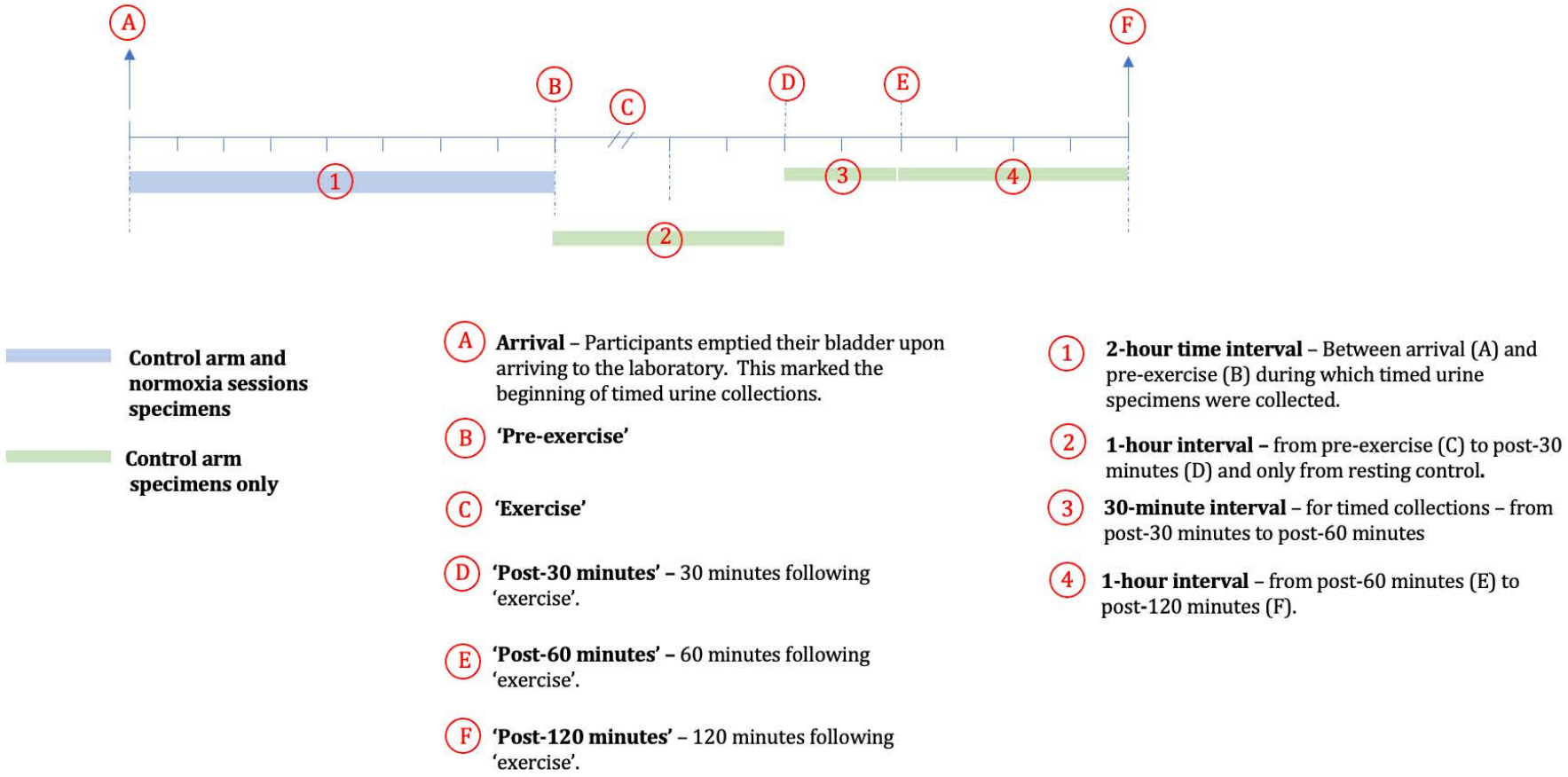

Figure 4.1 – Schematic of the sampling timepoints for timed spot-urine collections. Downward tick marks are representative of 15-minute intervals. Numbered items are indicative of durations over which timed spot-urine specimens were collected while lettered items are indicative of events occurring during the session.

4.2.1.2.3. Early morning urine (EMU) specimens

Similar to 24-hour specimens, EMU specimens were collected outside of the laboratory on a pre-determined day chosen by the participant. EMU specimens were collected upon waking from mid-stream urine into a 100 ml, clear, polypropylene specimen cup fitted with a high-density polyethylene screw cap (SARSTEDT, Nümbrecht, Germany). Unlike 24-hour and timed-spot urine specimens, the volumes and collection durations of EMU specimens were not recorded. Rather, 10 ml of urine from the EMU specimen was centrifuged within ~30 minutes of collection with the supernatant immediately aliquoted (into four repeat 2 ml cryovials) and frozen as previously described.

4.2.1.3. Urinalysis and units of measurement

All urine specimens were freshly thawed (i.e., no previous thaw-refreeze cycles) in a heating cupboard at 37 °C[5 288] for one hour immediately prior to triplicate analysis for α1-AGP utilising a novel immunoturbidimetric assay (described in **Chapter 3**; measuring range: 0.08 – 148.20 mg/l) performed on the Optilite™ auto-analyser (The Binding Site, Ltd., Birmingham, UK). Measurement outputs for α1-AGP from the Optilite™ were reported in units of concentration (mg/l), which were presented and further utilised in conjunction with the recorded specimen volumes and collection durations to estimate urinary α1-AGP excretion rate for 24-hour and timed-spot urine specimens (mg/24-hours and μg/min). Measurement units for 24-hour and timed-spot urine specimens, including concentration ($mg/l_{24\text{-}hours}$) and excretion rate (mg/24-hours and μg/min) were then compared with the existing literature (as described in later sections).

Only EMU specimens were additionally analysed for urinary creatinine, following a single freeze-thaw cycle, using a commercially available kit on the Alinity auto-analyser (v2.6.2,

ci-series, Abbott Laboratories, Lake Bluff, Illinois, USA)*. Urinary creatinine results were further utilised in conjunction with urinary [α1-AGP] results from EMUs to calculate the α1-AGP-to-creatinine ratio (α1-AGP:CREA; $mg/mmol_{\alpha1\text{-}AGP:CREA}$). Only concentration ($mg/l_{EMU}$) and $mg/mmol_{\alpha1\text{-}AGP:CREA}$ from EMU specimens were compared with α1-AGP units from the existing literature.

4.2.1.4. Statistical analysis

All statistical analyses were performed using Prism (v8.3.0 for Mac iOS, Graphpad Software Inc., San Diego, CA, USA). Distributions of urinary α1-AGP units data were assessed for normality or lognormality prior to analysis with log-transformed values utilised for statistical analysis where appropriate (i.e., when distributions were skewed). Descriptive statistics were reported for each of the various units of measure for urinary α1-AGP and included the following: mean ± standard deviation (SD); range; upper and lower 95% confidence intervals (95% CIs); and percent coefficient of variation (%CV). All statistical tests were two-tailed with significance set to $\alpha < 0.05$.

4.2.1.4.1. Twenty-four-hour and EMU specimens

A priori comparisons were performed between sexes for all units of measure of urinary α1-AGP and were facilitated using unpaired t-tests comparing log-transformed α1-AGP values from 24-hour and EMU specimens†. Simple linear regressions were also utilised to model log-based units (individually) based on age or sex (separately), whereas a multiple linear regression was used to predict each log-transformed unit of measurement based on both age

* Urinalysis for creatinine was assisted by the Biochemistry Department at Birmingham Heartlands Hospital, University Hospitals Birmingham, NHS Trust.

†Only $mg/mmol_{\alpha1\text{-}AGP:CREA}$ results for EMU specimens required log-transformation prior to analysis as mg/l_{EMU} results exhibited a normal distribution.

and sex. Goodness of fit (R_y^2) for both of these models was reported with $R_y^2 > 0.5$ desired. Also reported for multiple linear regressions only were the F ratio and multicollinearity (R_i^2) between variables included in the model. As a general rule, multicollinearity was considered not to be problematic when R_i^2 was < 0.6[340].

Paired t-tests were used to compare [α1-AGP] between 24-hour and EMU specimens (i.e., $mg/l_{24\text{-hours}}$ vs mg/l_{EMU}, respectively) within individuals. A Bland-Altman (B-A) plot[310] was constructed to assess the bias and agreement (95% limits of agreement, 95% LOAs) between these two measurements of [α1-AGP] (($mg/l_{24\text{-hours}}$ – mg/l_{EMU})/average). A simple linear regression was applied to the differences vs averages, with slope of the regression and goodness of fit (R^2) assessed.

Lastly, linear regression analysis was performed to evaluate any relationship between mg/24-hours (estimated from 24-hour specimens) and $mg/mmol_{\alpha1\text{-AGP:CREA}}$ (estimated from EMU specimens) to determine whether they may, potentially, be used interchangeably. Goodness of fit (R_y^2) for this model was desired to be > 0.5.

4.2.1.4.2. Timed spot-urine specimens

Log-transformed values of α1-AGP excretion and concentration from timed spot-urine specimens were compared to values from 24-hour specimens using a mixed-effects model with Dunnett's post *hoc* test to account for multiple comparisons between 24-hour α1-AGP and timed-spot urine measurements (from the different time intervals included). Similar to the previous section, B-A plots were constructed (individually) for [α1-AGP] and α1-AGP excretion (μg/min) in order to compare results between 24-hour and timed spot-urine specimens. These data (for the various units) were plotted as the difference (24-hour – timed spot-urine) vs the average and evaluated as described in previous sections.

4.2.2. Methodology for evaluation of the existing literature

As outlined in the introduction, previous studies have analysed urinary α1-AGP excretion among diseased individuals with similar analysis among healthy controls often occurring in parallel. However, no systematic review or meta-analysis for the collective examination of urinary α1-AGP results from healthy individuals and/or between different disease groups appears in the literature. As a part of the present study, a meta-analysis was conducted in order to examine the range of urinary α1-AGP results reported in the literature for both, healthy and diseased individuals (examined separately). Methods for the search strategy, data extraction, and evaluation are described next.

4.2.2.1. Search strategy and screening

The search strategy was conducted in accordance with the 2009 PRISMA guidelines for meta-analyses[341] (see **Figure 4.2**), albeit the search protocol was not prospectively registered. Databases searched included MEDLINE, Web of Science, and Cochrane Central Register of Control Trials (CENTRAL). For these databases, "(('urine' OR 'urinary') AND ('orosomucoid' OR 'alpha-1 acid glycoprotein'))" was an example of the search formula used (see **Appendix 4** for full list of search terms). Searches were not limited to the English language, years searched, or publication status. The total number of studies identified from database searches and from alternative sources (e.g., referenced by selected studies) were reported with duplicates then removed. The remaining studies were then screened for cohort species (human vs animal) with only human studies included for further screening, which aimed to identify and exclude studies that were wrongfully identified. Reasons for these erroneous flags included: use of α1-AGP within the methods; analysis of serum or plasma α1-AGP; or analysis of urinary α1-AGP but presentation of unitless results (e.g., area-under the curve, AUC, or receiver-

operator characteristic, ROC, only), to name a few (see section **4.3.2** for full list). The final search was conducted on 30 November, 2020.

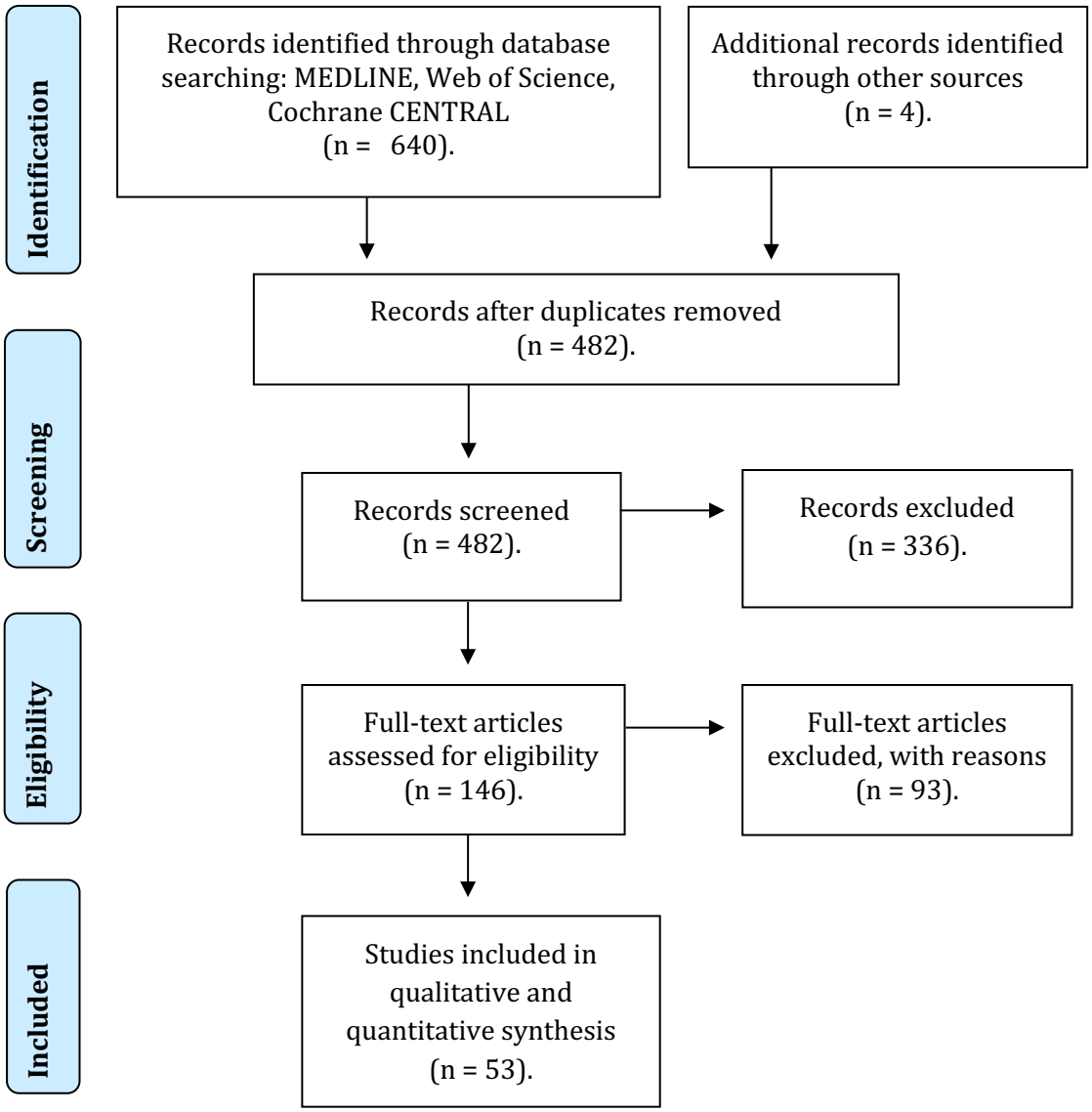

Figure 4.2 – Identification, screening, eligibility, and inclusion criteria for meta-analysis. Databases searched included MEDLINE, Web of Science, and Cochrane Central Register of Controlled Trials (CENTRAL). For the purposes of the present study, the number of final studies included was the same for qualitative and quantitative analysis (n = 53).

4.2.2.2. Data extraction and analysis

The following data were extracted from each included study for healthy* and diseased cohorts:

1) cohort type (control/healthy or disease; with the disease category further distinguished);
2) number of participants;
3) cohort age;
4) type of urine collection (e.g., random/spot urine, early-morning urine, timed (e.g., 24 hours);
5) whether a preservative was used (e.g., sodium azide, Tween-20, or other);
6) specimen storage temperature;
7) analytical method used for urinalysis (e.g., PETIA, RID, ELISA, western blotting, or other);
8) units of measure reported for urinary α1-AGP (e.g., [α1-AGP], mg/l; excretion rate, μg/min or mg/24-hours; ratio-to-creatinine, mg/mmol or mg/g; clearance, μl/min; and percentage of total protein, %);
9) and whether the impact of sex had been evaluated.

Original units data for urinary α1-AGP were extracted and reported in their published form (e.g., median ± interquartile ranges, IQRs; mean ± SD; or mean (95% confidence intervals)) and then converted to produce a uniform format across all studies (i.e., mean ± SD). The purpose of establishing a uniform format across all studies was so that results could be plotted and compared between studies and against results from urinalysis conducted as part of sections **4.2.1.2** and **4.2.1.4**. Conversions utilised equations outlined in Chapter 6 of the

* Healthy cohorts may have been the main group of interest or included as part of a larger study as the control group.

Cochrane Handbook[342] with recommended improvements, outlined by Hozo and colleagues[343*] and Wan and colleagues[344], also applied where appropriate.

4.3. RESULTS

As with the methods section, results are divided between those obtained as part of experimental studies within this thesis (section **4.3.1**) and those from the literature search (section **4.3.2**). An additional section is also presented bringing these data together (section **4.3.3**).

4.3.1. Results from experimental studies within the thesis

4.3.1.1. Participant characteristics and specimen collections

Twenty-eight individuals were initially recruited, with: 1) 25 individuals (13 females and 12 males; 32 ± 15 years (range: 20 – 74 years)) successfully completing 24-hour urine collections (no spills reported); 2) 18 individuals (7 females and 11 males; 36 ± 16 years (range: 23 – 74 years)) completing EMU collections; and 3) 7 individuals (5 females and 2 males; 21 ± 1 years (range: 20 – 22 years)) completing timed spot-urine collections. Attrition (n = 3) was due to participant-initiated withdrawal for personal reasons unrelated to the study.

4.3.1.2. Urinalysis

Descriptive statistics for successful urinalysis of α1-AGP in triplicate from 24-hour (n = 25; 100% success) and EMU (n = 18; 100% success) specimens are presented in **Table 4.1a**, with results further divided by sex and presented in **Table 4.1b.**

[*] For the purpose of these estimations, original results presented as 2.5 – 97.5 percentiles were assumed as the 95% CIs whereas, 25 and 75 percentiles were assumed as the first and third interquartile ranges (i.e. q1 and q3, respectively).

Table 4.1 – Descriptive statistics for various units of urinary alpha-1 acid glycoprotein (α1-AGP).

Tab. 4.1a – Urinary α1-AGP results for entire cohort

Measurement unit	Mean ± SD	Minimum – maximum (range)	Upper and lower 95% CIs	CV (%)
mg/24-hours	1.416 ± 1.342	0.386 – 7.019 (6.632)	0.862 to 1.970	94.8
μg/min	0.983 ± 0.932	0.269 – 4.875 (4.605)	0.599 to 1.368	94.8
mg/l$_{24\text{-hours}}$	0.882 ± 0.845	0.257 – 3.343 (3.087)	0.533 to 1.231	95.9
mg/mmol$_{\alpha1\text{-AGP:CREA}}$	0.030 ± 0.029	0.009 – 0.130 (0.121)	0.016 to 0.045	96.0
mg/l$_{EMU}$	0.349 ± 0.208	0.082 – 0.799 (0.717)	0.246 to 0.453	59.6

Tab. 4.1b – Urinary α1-AGP results divided by sex

Measurement unit	Mean ± SD		*p*-value	CV (%)
	Males	***Females***		***M vs F***
mg/24-hours	1.480 ± 1.842 (–0.001)	1.358 ± 0.697 (0.074)	0.537	124.5 vs 51.3
μg/min	1.028 ± 1.279 (–0.160)	0.943 ± 0.484 (–0.008)	0.537	124.5 vs 51.3
mg/l$_{24\text{-hours}}$	0.694 ± 0.657 (–0.260)	1.069 ± 1.012 (–0.113)	0.256	94.6 vs 94.7
mg/mmol$_{\alpha1\text{-AGP:CREA}}$	0.024 ± 0.016 (–1.690)	0.038 ± 0.040 (–1.586)	0.508	67.0 vs 105.3
mg/l$_{EMU}$	0.364 ± 0.185	0.331 ± 0.246	0.749	50.6 vs 74.4

Urinary results from 24-hour and early morning urine (EMU) specimens are presented in **Tab. 4.1a** as the mean ± standard deviation (SD); minimum – maximum (range); and upper and lower 95% confidence intervals (95% CIs) for each measurement unit. These results are divided by sex in **Tab 4.1b** with urinary results presented as the mean ± SD with the mean log-transformed value in parenthesis*. EMU and 24-hour results are separated by a dotted line in **Tab 4.1a** and **4.1b**. Twenty-four-hour α1-AGP excretion is presented in two units, mg/24-hours and μg/min. [α1-AGP] from 24-hour specimens is represented as mg/l$_{24\text{-hours}}$ while [α1-AGP] from EMU specimens is represented as mg/l$_{EMU}$. The ratio of urinary α1-AGP-to-creatinine (α1-AGP:CREA; mg/mmol$_{\alpha1\text{-AGP:CREA}}$) is presented only for EMU specimens. Percent coefficient of variation (%CV), a measure of inter-individual variation, was estimated (from absolute, not log-transformed results) relative to the mean ± SD estimates for the group or for each sex. *p*-values in **Tab 4.1b** are representative of unpaired t-tests comparing log-transformed urinary measurements between sexes*. Significance was set to $\alpha < 0.05$. *All distributions for urinary results were skewed except mg/l$_{EMU}$ thus, statistical analyses were performed on log-transformed values for all results except mg/l$_{EMU}$.

4.3.1.2.1. Twenty-four-hour specimens

All units of measure for 24-hour urinary α1-AGP exhibited lognormal distributions and therefore, all statistical tests were performed on the log-transformed data for these specimens. No significant differences were observed between males and females for any unit of urinary α1-AGP from 24-hour specimens (all *p*-values > 0.05, see **Table 4.1a**).

Results from the simple linear regression were also not significant for either age or sex for any units of urinary α1-AGP from 24-hour specimens (**Table 4.2**). Similarly, multiple linear regression based on age and sex was also not significant for any units of urinary α1-AGP from 24-hour specimens (**Table 4.2**) with multicollinearity (between age and sex) being low (R^2 = 0.116).

Table 4.2– Results from simple linear regression and multiple linear regression analyses based on age and sex for units of measure of urinary alpha-1 acid glycoprotein (α1-AGP).

	Simple linear regression				Multiple regression			
	Age		Sex		Age and Sex			
Measurement unit	**R^2**	***p*-value**	**R^2**	***p*-value**	**F(DFn, DFd) = F**	**R^2**	***p*-value**	**Multi-collinearity (R_i^2)**
log(mg/24 hours) and **log(μg/min)**	0.030	0.421	0.017	0.537	F(2, 21) = 0.371	0.034	0.695	0.116
log(mg/$l_{24\text{-hours}}$)	0.038	0.364	0.055	0.259	F(2, 21) = 0.680	0.061	0.517	0.116
log(mg/$mmol_{α1\text{-AGP:CREA}}$)	0.003	0.842	0.028	0.508	F(2, 15) = 0.333	0.043	0.722	0.102
mg/l_{EMU}	0.003	0.826	0.007	0.749	F(2, 15) = 0.538	0.009	0.946	0.102

The ratio of urinary α1-AGP to urinary creatinine is represented as mg/$mmol_{α1\text{-AGP:CREA}}$. F ratio is presented for multiple linear regression models. R^2 is representative of the goodness of fit for the relative model. By contrast, R_i^2 was reported for multicollinearity to evaluate the relationship between included variables (i.e., sex and age). Statistical analysis was performed for log-transformed units of urinary α1-AGP except [α1-AGP] from early morning urine (EMU) specimens (i.e., mg/l_{EMU}), which were normally distributed. All statistical tests were two-tailed with significance was set to $\alpha < 0.05$.

4.3.1.2.2. EMU specimens

Data for [α1-AGP] from EMUs (mg/l_{EMU}) were normally distributed while the α1-AGP:CREA data (mg/$mmol_{α1\text{-}AGP:CREA}$) from EMUs were lognormal. No significant differences were observed between males and females for either mg/l_{EMU} or mg/$mmol_{α1\text{-}AGP:CREA}$ from EMU specimens, however, %CV appeared higher in females compared to males for both mg/$mmol_{α1\text{-}AGP:CREA}$ and mg/l_{EMU} (**Table 4.1b**). Simple linear regression was not significant for either age or sex for any units of urinary α1-AGP for EMU specimens (refer to **Table 4.2**). Multiple linear regression based on age and sex was also not significant for either mg/l_{EMU} or mg/$mmol_{α1\text{-}AGP:CREA}$ (refer to **Table 4.2**) and multicollinearity was low (R_i^2 = 0.102).

4.3.1.2.3. 24-hour vs EMU specimens

Urinary [α1-AGP] from 24-hour was, on average, greater (mean difference: 0.283 mg/l [CIs: 0.062 to 0.505 mg/l]) than values from EMU specimens (p = 0.015) with this difference emphasised by the significant difference between log-transformed values for these specimens (p = 0.001). However, these differences were not echoed by the B-A plot for concentration values (i.e., differences vs averages of mg/$l_{24\text{-}hours}$ vs mg/l_{EMU}; see **Figure 4.3**). Moreover, exploratory analysis demonstrated a significant relationship between both, log-transformed concentration values (p = 0.026, r = 0.523), as well as, between log(mg/24-hours) and log(mg/$mmol_{α1\text{-}AGP:CREA}$) results ($p$ = 0.041; r = 0.486).

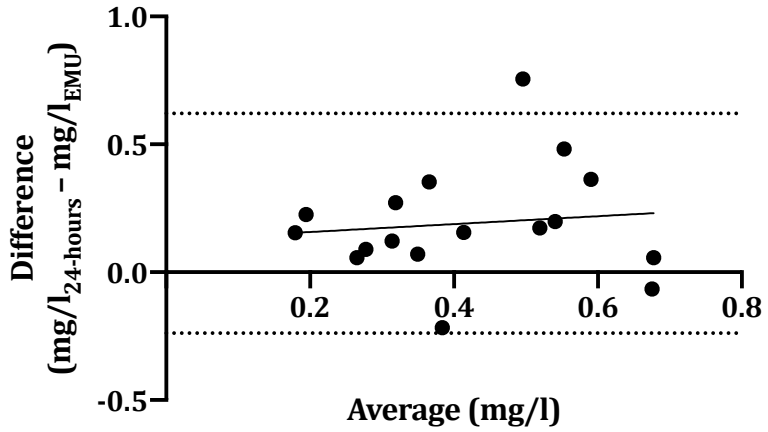

Figure 4.3 – Bland-Altman plot comparing the agreement between urinary alpha-1 acid glycoprotein (α1-AGP) concentration from 24-hour and early morning urine (EMU) specimens. Data are plotted as the difference vs the average ($mg/l_{24\text{-hour}}$ – mg/l_{EMU})/average for [α1-AGP] with outliers removed. Bias was estimated as 0.191 ± 0.219 with the 95% limits of agreement from –0.239 to 0.621 (dashed horizontal lines). Slope of the best fit line was not significantly non-zero (0.155 ± 0.126, p = 0.673) and the goodness of fit was low (R^2 = 0.012).

4.3.1.2.4. Timed-spot vs 24-hour specimens

A total of 31 timed spot-urine specimens were successfully collected from the subset of individuals (n = 7) over the five separate time intervals (total 35 possible collections, 88.6% success). Urinary α1-AGP was successfully analysed in triplicate (and excretion subsequently estimated) for 29 out of 31 of these specimens (93.6% success)*.

Urinary α1-AGP excretion rates (μg/min) estimated from timed-spot urine specimens were not significantly different from 24-hour excretion for any of the outlined intervals (all adj. p-values > 0.05) when compared within-individuals. Similarly, the slope of the linear regression for the B-A plot of excretion data was not significant (see **Figure 4.4a**). By contrast, the slope for the linear regression applied to B-A data for urinary [α1-AGP] was significantly different from zero (p = 0.008; **Figure 4.4b**).

* Overall success for all urinalysis of α1-AGP when considering 24-hour, EMU, and timed spot urine specimens was 97.3%.

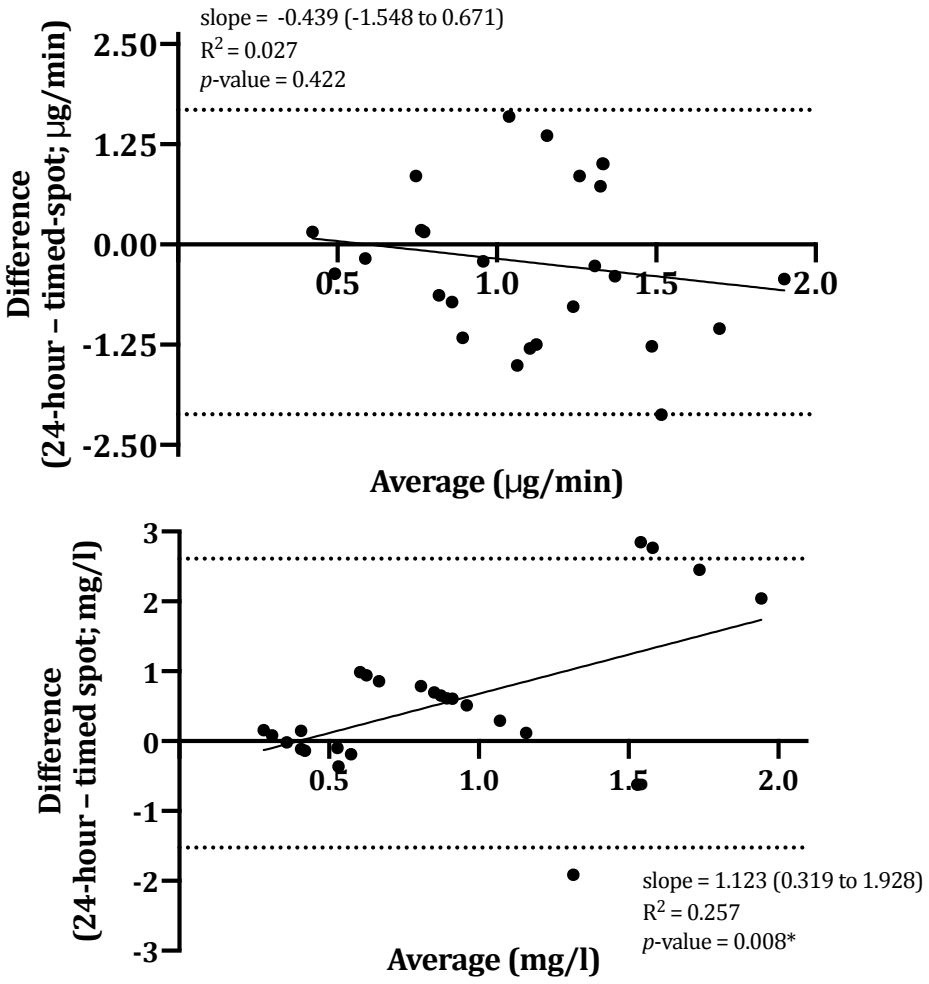

Figure 4.4 – Bland Altman (B-A) plot comparing urinary alpha-1 acid (α1-AGP) values between 24-hour and timed-spot urine specimens. Fig. 4.4a (top) – Urinary α1-AGP excretion rates (µg/min); and **Fig 4.4b (bottom)** – Urinary α1-AGP concentration (mg/l). Excretion rates were estimated from specimen volume and [α1-AGP] measured using the particle-enhanced turbidimetric immunoassay (PETIA) described in **Chapter 3**. Timed-spot urine specimens were collected over pre-determined intervals (i.e., 30, 60, and 120 minutes; refer to **Figure 4.1**). Data are plotted as the difference (24-hour – timed-spot) vs average for both concentration and excretion rate B-A plots. Bias (0.220 ± 0.969 µg/min and 0.543 ± 1.055 mg/l) and 95% Limits of Agreement (–1.678 to 2.119 µg/min and –1.525 to 2.610mg/l; dashed horizontal lines) were estimated from the B-A plot with a simple linear regression applied to these data and the slope (upper and lower 95% confidence intervals) and goodness of fit reported. All statistical tests were two-tailed with significance set to $\alpha < 0.05$.

4.3.2. Results from search of the existing literature

Total number of studies identified from database searches and alternative sources (n = 644), as well as, the final number of studies included (n = 53) are shown in **Figure 4.2** with a full list of exclusion criteria provided below:

1) Duplicate studies retrieved from multiple databases or data dually reported (e.g., abstract and full-length paper; n = 169).
2) Cohort type was animal, not human (n = 62).
3) Erroneously flagged (e.g., serum measurements; use in methodologies; review article mentioning α1-AGP or other irrelevant mention) with urinary α1-AGP not actually reported as an outcome measure (n = 274).
4) Neither the abstract nor the full-length publication were retrievable despite exhaustive efforts (e.g., University access, Interlibrary loan, or other unofficial sources; n = 11).
5) Urinalysis was conducted for α1-AGP, however, results were not presented in a format that could be extracted for further comparison (e.g., only graphical format or only AUCs or ROCs reported) (n = 75).

Characteristics of the included studies are presented in **Table 4.3** with the extracted urinary α1-AGP results (in their original forms) presented in **Table 4.4** (for healthy) and **Table 4.5** (for disease). These results were further converted (refer to section **4.2.2.2**) to produce a uniform format (i.e., mean ± SD) across all datasets, which were then plotted and compared for each unit as depicted* in **Figure 4.5a – 4.5e**.

* Outliers (for mean results) from healthy and disease cohorts were removed (separately) using Grubb's method (identifying only one outlier per measurement unit) prior to plotting.

Table 4.3 – Summary of included studies.

Number of studies that…	
1. Collected…	
24-hour or other timed urine specimens	16
Early-morning urine specimens	12
Random spot-urine (daytime) specimens	19
Not specified	6
2. Stored samples at…	
2 to 8 (or higher) °C	11
–20 to 25 °C	10
–70 to –80 °C	19
Not specified	13
3. Performed urinalysis using…	
ELISA	18
RID	10
PETIA	16
Other	9
4. Used preservative.	
Yes	14
No	14
Not specified	25
5. Reported urinary results for…	
Urinary [α1-AGP] (mg/l)	25
Urinary α1-AGP excretion rate (μg/min)	11
Urinary α1-AGP excretion rate (mg/24-hours)	5
Urinary α1-AGP-to-creatinine ratio ($mg/mmol_{\alpha 1\text{-}AGP:CREA}$)	12
Urinary α1-AGP-to-creatinine ratio (mg/g)	13
α1-AGP clearance (μl/min)	7
Urinary α1-AGP relative to total protein (%)	2
6. Reported…	
Number of males/females*	17
Evaluating the impact of sex on a1AGP results*	11
α1-AGP results separately by sex*	6
Significant difference between sex for any unit*	2

Study characteristics are presented for all included studies (n = 53). Some studies reported multiple units for urinary alpha-1 acid glycoprotein (α1-AGP), thus, the total exceeded 53 for this category (item No. 5). * Indicates that only healthy studies (n = 29) were considered for characteristics related to sex (see entries for item No. 6). Enzyme-linked immunosorbent assay, ELISA; radial immunodiffusion, RID; and particle-enhanced turbidimetric immunoassay, PETIA.

Table 4.4 – Urinary alpha-1 acid glycoprotein (α1-AGP) among healthy humans.

Age (years)	N =	Concentration (mg/l)	Excretion rate (µg/min)	Excretion rate (mg/24hrs)	α1-AGP:CREA ratio (mg/mmol or mg/g)	Clearance (µl/min)	Percentage of total protein (%)	Analytical method	Author
-	6	0.36 ± 0.11	0.287 ± 0.095	0.413 ± 0.136	-	-	1.3%	RID	Poortmans et al. 1968[249]
-	20	-	-	-	1.697 ± 3.369*	-	-	ELISA	Jerebtsova et al. 2018[285]
-	11	-	-	-	-	-	0.161 ± 0.072	Mass spec. + 2 DE	Mu et al. 2012[345]
-	33	-	-	-	6 (1 – 44)*	-	-	ELISA	Bonde & Vittinghus 1996[346]
-	5	0.2 – 1.1	-	-	0.23 – 0.89	-	-	ELISA	Phillips et al. 1988[347]
< 1 month	14	63.5 (13.4 – 75.0)‡	-	-	7.4 (4.5 – 29.0)‡	-	-	RID	Hjorth et al. 2000[348]
1 – 12 months	35	0.8 (0.50 – 1.5)‡	-	-	0.5 (0.3 – 1.4)‡	-	-	RID	Hjorth et al. 2000[348]
1 – 5	66	1.7 (1.5 – 2.4)‡	-	-	0.3 (0.3 – 1.2)‡	-	-	RID	Hjorth et al. 2000[348]
3.9 ± 5.3	15	5.5 ± 8.0◊	-	-	-	-	-	SDS-PAGE	Devarajan et al. 2010[331]
3.9 ± 4.5	230	6.0 ± 15.0◊	-	-	-	-	-	SDS-PAGE	Devarajan et al. 2010[331]
6.6 ± 0.4	30		-	-	$2.5 \times 10^{-5} \pm 0.18 \times 10^{-5}$*	-	-	PETIA	Gozal et al. 2009[230]
6 – 10	61	2.3 (1.3 – 3.1)‡	-	-	0.4 (0.2 – 0.9)‡	-	-	RID	Hjorth et al. 2000[348]
8.83 ± 0.21	41	-	-	-	0.191 ± 0.020*	-	-	ELISA	Selvaraju et al. 2019[349]
11 – 15	71	1.9 (1.3 – 2.7)‡	-	-	0.2 (0.1 – 0.3)‡	-	-	RID	Hjorth et al. 2000[348]
11 (10.1 – 12.0)	18	-	-	-	0.605 (0.408 – 1.458)*	-	-	ELISA	Smith et al. 2018[350]
12.3 ± 3.3	60	0.575 (0.450)**	-	-	-	-	-	ELISA	El-Beblawy et al. 2016[351]
13 (9.8 – 14.8)	23	-	-	-	0.313 (0.108 – 0.729)*	-	-	ELISA	Watson et al. 2012[352]
14 (10 – 17)††	30	-	-	-	0.09 (0.07 – 0.15)	-	-	PETIA	Szirmay et al. 2019[278]
14 (10 – 18)††	30	0.56 (0.10 – 2.96)†	-	-	0.09 (0.02 – 0.19)†	-	0.91	PETIA	Kustán et al. 2016[5]
23 – 78	23	-	0.424 ± 0.257‡‡	0.61 ± 0.37**	-		-	RID	Talks et al. 2018[7]
23 (10 – 58)††	72	0.69 (0.13 – 2.96)†	-	-	0.08 (0.01 – 0.24)†	-	1.00	PETIA	Kustán et al. 2016[5]
25 – 55	6	0.55 ± 0.58	-	-	0.02 (0.003 – 0.28)	-	-	ELISA	Vittinghus et al. 1990[283]
25 – 69	12	-	0.292 (0.083 – 0.569)‡‡†	0.42 (0.12 – 0.82)††	-	-	-	Immuno-electrophoresis	Jensen et al. 1972[353]
26 ± 5	10	-	0.237 ± 0.126	0.34128 ± 0.18144‡‡	-	-	-	RID	Koshimura et al. 2005[119]
29 (21 – 39)††	19	0.71 (0.25 – 2.30)†	-	-	0.07 (0.01 – 0.35)†	-	1.09	PETIA	Kustán et al. 2016[5]
29 – 81	11	-	1.02 ± 0.69	1.468 ± 0.994‡‡	-	1.645 ± 1.541†	-	RID	Poortmans et al. 1979[354]
30 ± 4	153	0.43 (0.06 – 27.12)††	-	-	-	-	-	PETIA	Christiansen et al. 2010[280]
36.5 (19.8 – 64.5)	77	-	-	-	0.98 (0.36 – 3.86)***	-	-	Nephelometry	Bernard et al. 1979[336]

Table 4.4 – Urinary alpha-1 acid glycoprotein (α1-AGP) among healthy humans (continued).

Age (years)	N =	Concentration (mg/l)	Excretion rate (μg/min)	Excretion rate (mg/24hrs)	α1-AGP:CREA ratio (mg/mmol or mg/g)	Clearance (μl/min)	Percentage of total protein (%)	Analytical method	Author
39 (20 – 62)††	95	2.9 (2.4 – 21.0)‡‡‡	-	-	0.2 (0.1 – 2.0)‡‡‡	-	-	RID	Tencer et al. 1996[337]
39 (20 – 62)††	95	10.9 (8.3 – 24.9)‡‡‡	-	-	0.8 (0.6 – 3.3)‡‡‡	-	-	RID	Tencer et al. 1996[337]
39 (21 – 58)††	38	-	-	-	0.07 (0.04 – 0.15)	-	-	PETIA	Szirmay et al. 2019[278]
40 ± 6	28	-	0.295 (0.136 – 0.799)†	0.425 (0.196 – 1.151)‡‡	-	5.6 (2.85 – 12.75)	-	RID	Ito et al. 1989[355]
43 ± 13	69	0.26 (0.08 – 1.99)††	0.36 (0.07 – 2.04)††	0.518 (0.101 – 2.938)‡‡	0.040 (0.008 – 0.180)††	0.43 (0.10 – 2.43)††	-	PETIA	Christiansen et al. 2004[288]
43 ± 13	69	0.08 (0.06 – 0.10)†††	0.07 (0.06 – 0.10)†††	0.101 (0.086 – 0.144)‡‡	0.009 (0.007– 0.012)†††	0.12 (0.09 – 0.15)†††	-	PETIA	Christiansen et al. 2004[288]
43 ± 13	69	1.98 (1.55 – 2.52)†††	2.04 (1.53 – 2.73)†††	2.938 (2.203 – 3.931)‡‡	0.17 (0.13 – 0.23)†††	2.36(1.80 – 3.08)†††	-	PETIA	Christiansen et al. 2004[288]
44 (30 – 53)	41	0.82 (0.33 – 1.14)	-	-	0.07 (0.04 – 0.15)	-	-	PETIA	Kustán et al. 2018[4]
45 (32 – 53)	40	0.79 (0.36 – 1.16)	-	-	0.08 (0.06 – 0.15)	-	-	PETIA	Kustán et al. 2017[356]
46.7 ± 7.1	17	-	2.083 ± 0.694	3 ± 1	-	3 ± 1.2	-	Nephelometric immunoassay	Vasson et al. 1993[357]
48.5 ± 2.8	6	-	0.39 ± 0.28	0.562 ± 0.40‡‡	-	-	-	PETIA	Jiang et al. 2009[139]
51 (40 – 58)††	23	0.76 (0.14 – 2.64)†	-	-	0.08 (0.02 – 0.24)†	-	1.36	PETIA	Kustán et al. 2016[5]
51.9 ± 4.1 (44 – 58)	17	-	0.17 (0.028 – 5.10)	0.245 (0.040 – 7.344)‡‡	-	-	-	RID	Narita et al. 2004[358]
53 ± 11 (30 – 67)	21	-	0.54 (0.18 – 2.04)	0.778 (0.259 – 2.938)‡‡	-	-	-	PETIA	Christiansen et al. 2009[330]
53 ± 11 (30 – 67)♦	21	-	0.5 (0.1 – 1.9)††	0.72 (0.144 –2.736)†† ‡‡	-	-	-	PETIA	Christiansen et al. 2010[359]
53 ± 11 (30 – 67)♦	21	-	1.6 (0.6 – 5.2)††	2.3 (0.864 – 7.488)†† ‡‡	-	1.54 (0.55 – 5.96)††	-	PETIA	Christiansen et al. 2010[359]
54.43 ± 11.88	155	0.95 (0.40 – 2.05)	-	-	1.14 (0.46 – 2.14)*	-	-	PETIA	Wang et al. 2020[360]
59.82 ± 13.17	62	-	-	-	2.102 ± 1.069*	-	-	ELISA	Hou et al. 2014[282]
65.33 ± 10.57	53	-	-	-	2.243 ± 0.970*	-	-	ELISA	Li et al. 2016[279]

Urinary α1-AGP Data are presented in their original published format (e.g., mean ± standard deviation, median ± interquartile ranges, etc) in ascending order by mean age of the relative cohort. Published formats are indicated by markings described next with any data presented without markings presented as the minimum – maximum (predominately for age), median (25% and 75% interquartile ranges, IQRs), or mean ± SD. Markings indicate: * α1-AGP-to-creatinine ratio (α1-AGP:CREA) presented as mg/g instead of mg/mmol; ** median (50% IQR); † median (2.5 – 97.5% percentiles or 95% confidence intervals, CIs); *** median (5th to 95th percentiles); †† median (range); ††† secondary to median (range) for the 2.5 and 75 percentiles and associated 90% CIs; ‡ 90th percentile (90% CIs); ‡‡ post-publication estimates for excretion rates presented as μg/min (opposed to mg/24-hours); ‡‡‡ upper (95%) reference limit (90% CIs) with duplicate rows representing overnight and random samples; ♦ duplicate rows represented overnight vs daytime results; and ◊ mean ± SEM. Particle-enhanced turbidimetric immunoassay, PETIA; radial immunodiffusion, RID; sodium dodecyl sulphate polyacrylamide gel electrophoresis, SDS-PAGE; and enzyme-linked immunosorbent assay, ELISA.

Table 4.5 – Urinary alpha-1 acid glycoprotein (α1-AGP) in humans with disease.

Disease population	Age (years)	N =	Concentration (mg/l)	Excretion rate (μg/min)	Excretion rate (mg/24hr)	α1-AGP:CREA ratio (mg/mmol or mg/g)	Percentage of total protein (%)	Clearance (μl/min)	Analytical method	Author
Crohn's disease	27 (12 – 62) ††	28	4.15 (1.97 – 10.30)	-	-	0.40 (0.20 – 1.08)	3.7 (2.5 – 6.4)	-	PETIA	Kustán et al. 2016[5]
Sepsis	67 (30 – 82) ††	30	90.20 (42.01 – 137.23)	-	-	19.13 (13.4 – 32.8)	18.7 (11.9 – 34.9)	-	PETIA	Kustán et al. 2016[5]
Sepsis	68 (47 – 84) ††	7	-	-	-	25 (7.0 – 48.0)††	-	-	PETIA	Magid et al. 2005[361]
Chronic HF	< 65	93	-	-	-	6.4 ± 4.4*	-	-	ELISA	Hou et al. 2014[282]
Chronic HF	≥ 65	83	-	-	-	6.6 ± 4.2*	-	-	ELISA	Hou et al. 2014[282]
Systolic HF	68.2 ± 11.3	52	10.4 ± 21.8	-	-	-	-	-	Turbidimetric method	Prescott et al. 2009[362]
Psoriatic arthritis	66 (61 – 70) ††	56	1.08 (0.60 – 1.65)	-	-	0.12 (0.07 – 0.28)	-	-	PETIA	Kustán et al. 2018[4]
Mild Psoriasis	63 ± 9.98•	78	0.598 (0.26 – 1.29)	-	-	0.06 (0.02 – 0.17)	-	-	ELISA	Németh et al. 2019[363]
Mod. psoriasis	63 ± 9.98•	20	1.87 (0.54 – 4.12)	-	-	0.17 (0.09 – 0.31)	-	-	ELISA	Németh et al. 2019[363]
Severe Psoriasis	63 ± 9.98•	16	0.99 (0.28 – 2.81)	-	-	0.10 (0.04 – 0.17)	-	-	ELISA	Németh et al. 2019[363]
Bladder cancer	64.9 ± 18.9	112	7.172 ± 3.05	-	-	-	-	-	ELISA	Li et al. 2016[279]
T1DM w/ early decline	36 ± 10	15	1.071 ± 0.219	-	-	-	-		ELISA	Schlatzer et al. 2012[364]
T1DM	13.4 ± 2.8	60	3.45 (2.637)***	-	-	-	-	-	ELISA	El-Beblawy et al. 2016[351]
T1DM	40 ± 16	148	-	7.8 (3.8 – 19.4)	11.23 (5.47 –27.94)‡‡	-	-	-	Immuno-turbidimetry	Christiansen et al. 2005[334]
T2DM	52.7 ± 7.0	61	-	0.370 (0.071 – 6.40)††	0.533 (0.102 –9.216)†† ‡‡	-	-	-	RID	Narita et al. 2004[358]
T2DM	56 ± 9 (33 – 68)	24	-	4.36 (1.30 – 41.16)	6.34 (1.87 – 59.33)‡‡	-	-	-	PETIA	Christiansen et al. 2009[330]
T2DM (overnight)	56 ± 9 (33 – 68)	24	-	4.50 (1.80 – 37.10)††	6.48 (2.595 – 53.424)‡‡	-	-	-	PETIA	Christiansen et al. 2010[359]
T2DM (daytime)	56 ± 9 (33 – 68)	24	-	7.0 (3.2 – 20.3) ††	10.08 (4.61 – 29.23)†† ‡‡	-	-	7.33 (2.85 – 14.21)††	PETIA	Christiansen et al. 2010[359]
T2DM	60 (49 – 71)††	242	-	10.7 (5.7 – 22.0)	15.408 (8.208 – 31.68)‡‡	-	-	-	Immuno-turbidimetry	Christiansen et al. 2002[365]
T1DM & T2DM	50 ± 7.5	30	-	0.71 ± 0.41	1.022 ± 0.590‡‡	-	-	-	Immuno-turbidimetry	Jiang et al. 2009[139]
T2DM w/ CKD (all stages)	62.9 ± 11.3	85	-	-	-	$3.85 \times 10^{-5} \pm 5.7 \times 10^{-5}$	-	-	ELISA	Inoue et al. 2013[366]
DN w/ microalbuminuria	52 ± 2.9	30	-	1.93 ± 0.68	2.779 ± 0.979‡‡	-	-	-	Immuno-turbidimetry	Jiang et al. 2009[139]
DN w/ macroalbuminuria	53.5 ± 4.0	30	-	2.88 ± 0.94	4.147 ± 1.354‡‡	-	-	-	Immuno-turbidimetry	Jiang et al. 2009[139]
Overweight	8.44 ± 0.25	24	-	-	-	0.3635 ± 0.03764*	-	-	ELISA	Selvaraju et al. 2019[349]
Obese	8.54 ± 0.26	23	-	-	-	0.3583 ± 0.04155*	-	-	ELISA	Selvaraju et al. 2019[349]
Pre-eclampsia	29 ± 4	20	0.84 (0.21 – 7.65)††	-	-	-	-	1.47 (0.35 – 7.47)††	PETIA	Christiansen et al. 2010[280]
1st tri. Gest. diabetes + pre-term birth	29 ± 4	65	0.53 (0.06 – 27.12)††	-	-	-	-	1.05 (0.18 –18.69)††	PETIA	Christiansen et al. 2010[280]
1st tri. Gest. diabetes w/o pre-term birth	30 ± 4	108	0.39 (0.06 – 20.44)††	-	-	-	-	0.85 (0.14 – 10.6)††	PETIA	Christiansen et al. 2010[280]

Table 4.5 – Urinary alpha-1 acid glycoprotein (α1-AGP) in humans with disease (continued).

Disease population	Age (years)	N =	Concentration (mg/l)	Excretion rate (µg/min)	Excretion rate (mg/24hr)	α1-AGP:CREA ratio (mg/mmol or mg/g)	Percentage of total protein (%)	Clearance (µl/min)	Analytical method	Author
Hepatocelluar carcinoma	45 ± 14	48	1.37 (0.522 – 10.91 ††)	-	-	-	-	-	ELISA	Zhan et al. 2020[367]
Cirrhosis	22 – 56	37	-	-	-	-	-	0.79 (0.12 – 1.83)	Rocket electrophoresis	Milani et al. 1982[368]
Liver cirrhosis	54 ± 12.9	51	0.575 (0.320 – 1.056)	-	-	-	-	-	ELISA	Zhan et al. 2020[367]
Burn patients	-	3	160	-	-	-	-	-	ELISA	Sviridov et al. 2009[287]
Sickle cell	-	20	-	-	-	5.192 ± 1.102*	-	-	ELISA	Jerebtsova et al. 2018[285]
SC (HbSS) - Stage 0	36 (18 – 67)††	51	-	-	-	7.6 ± 8.25*	-	-	ELISA	Jerebtsova et al. 2020[369]
SC (HbSC) - Stage 1+ CKD	39 (20–61) ††	15	-	-	-	52.9 ± 99.6*	-	-	ELISA	Jerebtsova et al. 2020[369]
Active LN	13.0 (11.4 – 15.2)	9	-	-	-	145.44 (54.75 – 250.37)*	-	-	ELISA	Smith et al. 2018[350]
LN (+ SLEDAI renal)	15.4 ± 0.49‡	98	2.53 (1.74 – 3.68)†††	-	-	-	-	-	ELISA	Suzuki et al. 2009[370]
LN (+ SDI renal)	15.4 ± 0.49‡	98	9.65 (2.23 – 41.65)†††	-	-	-	-	-	ELISA	Suzuki et al. 2009[370]
LN (responders)	15.6 ± 2.9•	37	0.01024 ± 0.0023‡	-	-	-	-	-	ELISA	Brunner et al. 2017[371]
LN (non-responders)	15.6 ± 2.9•	50	0.01144 ± 0.0025‡	-	-	-	-	-	ELISA	Brunner et al. 2017[371]
Steroid-sensitive NS	7.5 ± 0.8	30	82.89 (17.38 – 395.22)	-	-	-	-	-	ELISA	Bennett et al. 2017[372]
Steroid-resistant NS	12.3 ± 1.2	20	90.97 (13.43 – 616.16)	-	-	-	-	-	ELISA	Bennett et al. 2017[372]
Haemodialysed patients	50.7 ± 12.9	30	-	13.89 ± 9.729‡‡	20 ± 14	-	-	78 ± 90‡‡	Nephelometric immunoassay	Vasson et al. 1993[357]
Uremia patients	58.4 ± 12.3	25	1.37 (0.522 – 10.91)	87.50 ± 111.11‡‡	126 ± 160	-	-	12 ± 9‡‡	Nephelometric immunoassay	Vasson et a. 1993[357]
GN w/o preservative	27 – 80	10	53 (13 – 136)††	-	-	-	-	-	RID	Tencer et al. 1994[297]
GN w/ preservative	27 – 80	10	56 (11 – 140)††	-	-	-	-	-	RID	Tencer et al. 1994[297]
CABG + AVR	67 (60 – 73)	38	1.92 (0.64 – 4.56)	-	-	0.29 (0.16 – 0.42)	-	-	PETIA	Kustán et al. 2017[356]
AVR surgery	68 (62 – 74)	18	-	-	-	0.33 (0.13 – 0.49)	-	-	PETIA	Kustán et al. 2017[356]
CABG surgery	65 (54 – 72)	20	-	-	-	0.27 (0.17 – 0.36)	-	-	PETIA	Kustán et al. 2017[356]
HIV (Cluster1)	40 (36 – 45)	301	1.2 (0.6 – 2.8)	-	-	-	-	-	ELISA	Scherzer et al. 2016[373]
HIV (Cluster2)	41 (36 – 45)	407	3.2 (1.2 – 6.6)	-	-	-	-	-	ELISA	Scherzer et al. 2016[373]
HIV (Cluster3)	43 (38 – 48)	131	22.4 (7.4 – 38.6)	-	-	-	-	-	ELISA	Scherzer et al. 2016[373]
Stable CKD	71.2 ± 14.5	106	-	-	-	32.6 ± 71.5*	-	-	Immuno-nephelometry	Nickolas et al. 2008[374]
Acute kidney injury	58.1 ± 16.7	30	-	-	-	201 ± 274*	-	-	Immuno-nephelometry	Nickolas et al. 2008[374]
AKI 2 hr post CABG	3.6 ± 4.6	135	75 ± 70◊	-	-	-	-	-	SDS-PAGE	Devarajan et al. 2010[331]
AKI post-surgical	4.0 ± 7.8	15	81 ± 54◊	-	-	-	-	-	SDS-PAGE	Devarajan et al. 2010[331]
Pre-renal azotemia	65.1 ± 16.4	88	-	-	-	73.3 ± 103*	-	-	Immuno-nephelometry	Nickolas et al. 2008[374]

Table 4.5 – Urinary alpha-1 acid glycoprotein (α1-AGP) in humans with disease (continued).

Disease population	Age (years)	N =	Concentration (mg/l)	Excretion rate (μg/min)	Excretion rate (mg/24hr)	α1-AGP:CREA ratio (mg/mmol or mg/g)	Percentage of total protein (%)	Clearance (μl/min)	Analytical method	Author
Patients w/normal kidney fx.	56.3 ± 18.5	411	-			31.8 ± 65.2*	-	-	Immuno-nephelometry	Nickolas et al. 2008[374]
OSA	6.6 ± 0.7	60	-	-	-	$6.71 \times 10^{-5} \pm 3.9 \times 10^{-5}$*	-	-	PETIA	Gozal et al. 2009[230]
Cadmium exposed	54.1 (41.8 – 64.3)*	42	-			15.5×10^{-5}* ± 3.5×10^{-5}*	-	-	Nephelometry	Bernard et al. 1979[336]
Stainless steel welders	-	35	-	-	-	9 (2 – 108)* ††	-	-	ELISA	Bonde & Vittinghus 1996[346]
mild steel welders	-	46	-	-	-	12 (2 – 72)* ††	-	-	ELISA	Bonde & Vittinghus 1996[346]
ex-welders	-	21	-	-	-	6 (2 – 117)* ††	-	-	ELISA	Bonde & Vittinghus 1996[346]
'patients'	-	7	257.14 ± 118.8	-	-	-	-	-	RID	Beilby et al. 1990[375]

Various units of measures were included: excretion rate (μg/min or mg/24-hours); concentration (mg/l); ratio-to-creatinine (α1-AGP:CREA, mg/mmol or mg/g); and percent of total urinary protein (% total protein). Age and urinary results were presented as median (interquartile ranges, IQRs) or mean ± SD unless otherwise marked by the following symbols to indicate: †† age or urinary results presented as median (minimum – maximum); * α1-AGP:CREA units presented as mg/g instead of mg/mmol; ♦ age presented as mean across the cohort, which included all severities of psoriatic arthritis (mild, moderate, and severe) or lupus nephritis (LN) non-responders and responders; ** median (25 – 75% percentiles); *** median (50% IQR); † median (2.5 – 97.5% percentiles); ††† geometric mean (95% confidence intervals); ǂ mean ± standard error; ◊ mean (5^{th} – 95^{th} percentiles); ǂǂ estimated (post-publication) from the corresponding μg/min excretion rates presented. Acute kidney injury, AKI; aortic valve replacement, AVR; chronic kidney disease, CKD; coronary artery bypass graft, CABG; diabetic nephropathy, DN; enzyme-linked immunosorbent assay, ELISA; glomerular nephritis, GN; heart failure, HF; human immunodeficiency virus, HIV; HbSS and HbSC, genotypes for sickle cell disease; nephrotic syndrome, NS; obstructive sleep apnea, OSA; particle-enhanced turbidimetric immunoassay, PETIA; radial immunodiffusion, RID; sodium dodecyl sulphate polyacrylamide gel electrophoresis, SDS-PAGE; Systemic lupus erythematosus disease activity index, SLEDAI; Systemic Lupus International Collaborating Clinics/ACR Damage Index, SDI; Type 1 diabetes mellitus, T1DM; and Type 2 diabetes mellitus, T2DM.

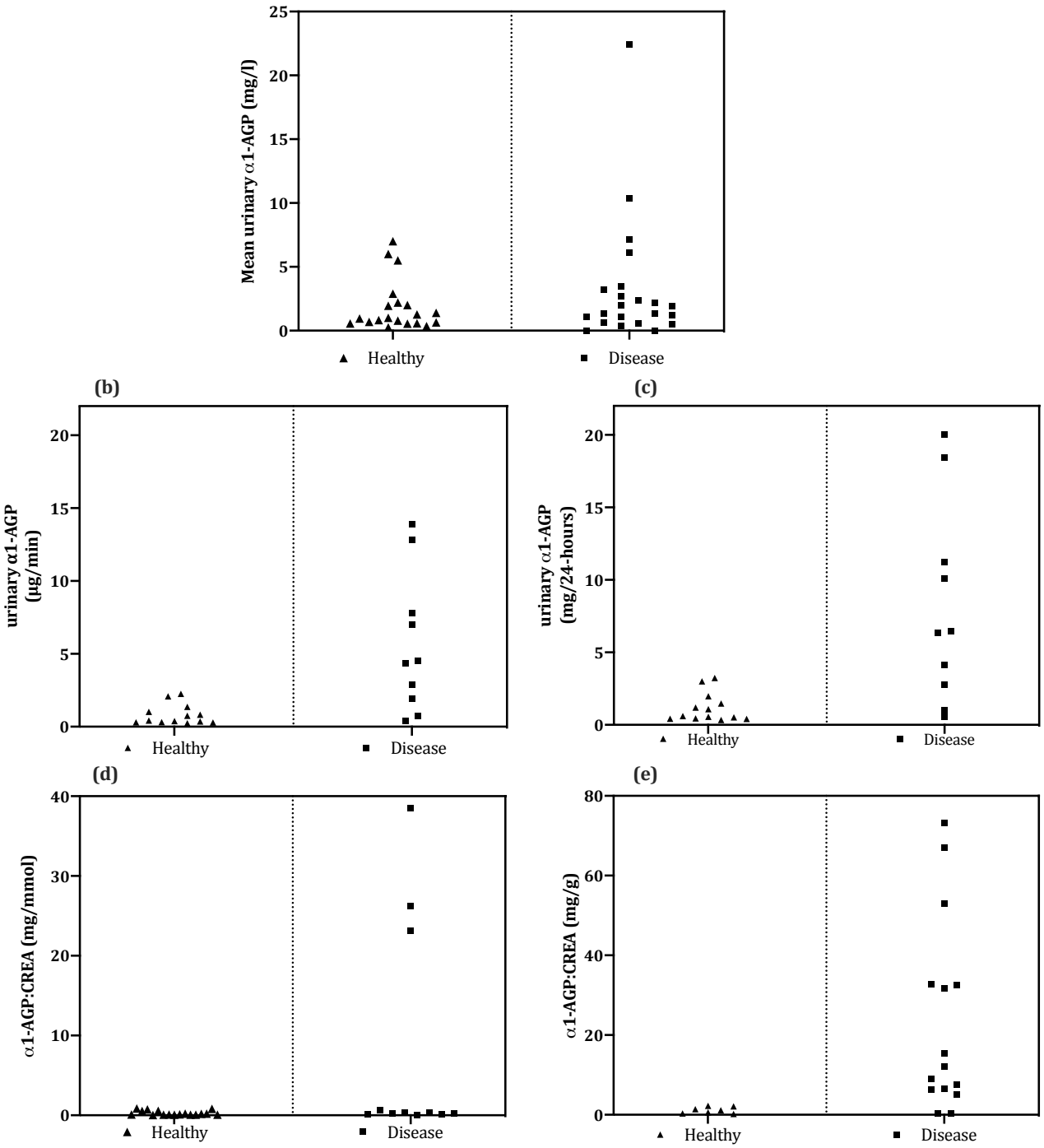

Figure 4.5 – Units of measure for urinary alpha-1 acid glycoprotein (α1-AGP) among healthy and diseased cohorts. Fig 4.5a (top) – Urinary α1-AGP concentration (mg/l); **Fig 4.5b (middle left)** – Urinary α1-AGP excretion rate (µg/min); **Fig 4.5c (middle right)** – Urinary α1-AGP excretion rate (mg/24-hours); **Fig 4.5d (bottom left)** – Urinary α1-AGP-to-creatinine ratio (mg/mmol); and **Fig 4.5e (bottom right)** – Urinary α1-AGP-to-creatinine ratio (mg/g). Data are plotted (healthy vs disease) as the estimated mean urinary α1-AGP result (refer to **Table 4.4** and **Table 4.5** for the original unit formats) for included studies (n = 53) after outlier removal (using Grubb's method).

4.3.3. Experimental urinalysis from thesis compared to existing literature

As presented in see **Figure 4.6a – 4.6d**, the most commonly reported units for urinary α1-AGP among healthy cohorts in the existing literature (refer to **Table 4.4** and **Figure 4.5**) were plotted as a function of mean cohort age with these data compared to results from experimental urinalysis results (upper and lower 95% CIs presented in **Table 4.1**).

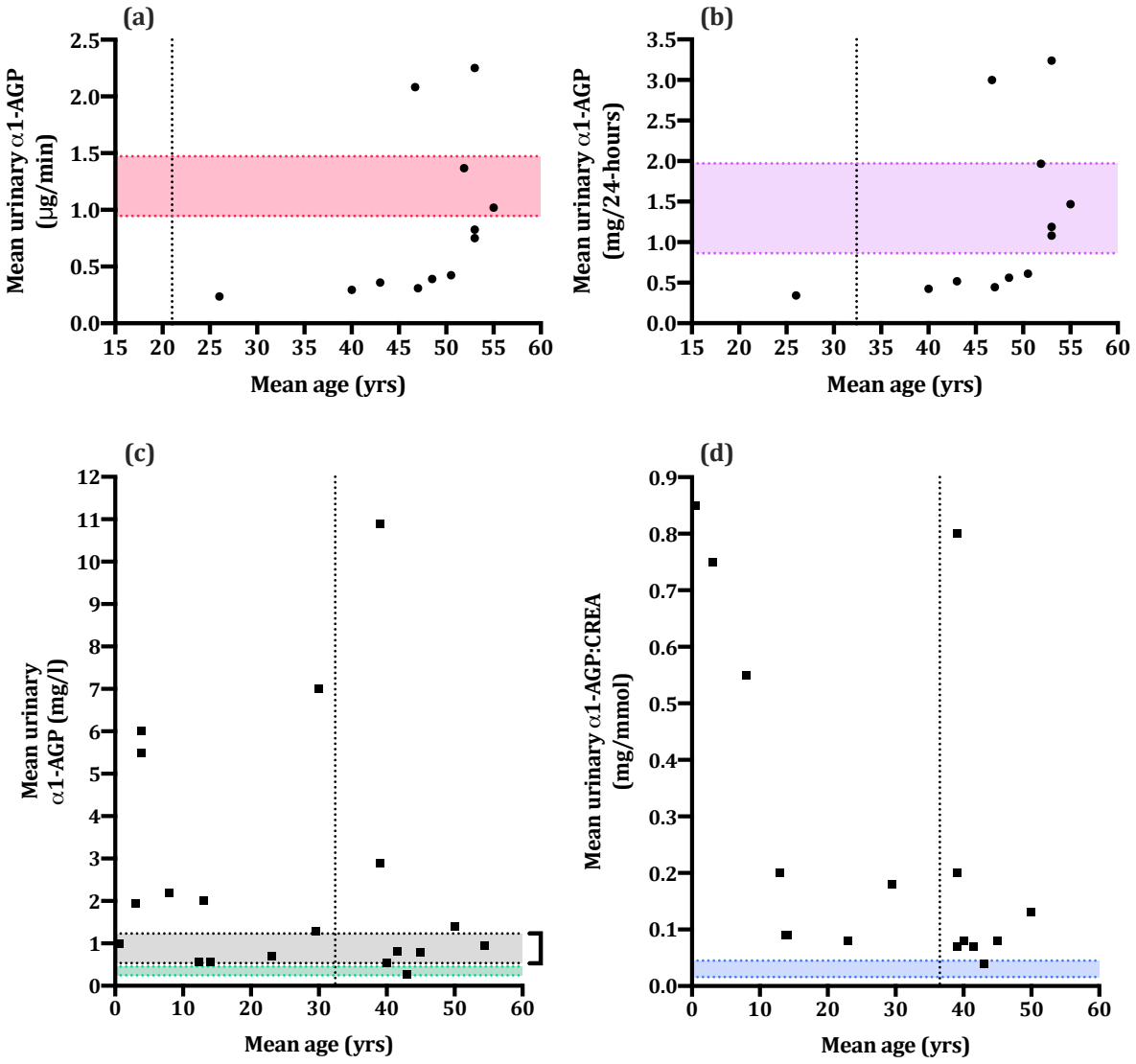

Figure 4.6 – Urinary alpha-1 acid glycoprotein (α1-AGP) among healthy individuals. Fig 4.6a (top left) – Urinary α1-AGP excretion rate (mg/min); **Fig 4.6b (top right)** – Urinary α1-AGP excretion rate (mgs/24-hours); **Fig. 4.6c (bottom left)** – Urinary α1-AGP concentration (mg/l); **Fig. 4.6d (bottom right)** – Ratio of urinary α1-AGP to urinary creatinine (α1-AGP:CREA; $mg/mmol_{\alpha 1\text{-}AGP:CREA}$). Data are plotted as the estimated means from original results presented in **Table 4.4** (refer to section **4.2.2.2**). Horizontal shaded colour areas represent the upper and lower 95% confidence intervals (CIs) for α1-AGP results from experimental urinalysis (as presented in **Table 4.1**) and are indicated for the following units: concentration (from 24-hour and early morning urine specimens; grey and green areas, respectively); excretion rates (from timed spot-urine, μg/min, and 24-hour specimens, mg/24-hours; pink and purple, respectively); and ratio-to-creatinine ($mg/mmol_{\alpha 1\text{-}AGP}$ from early morning specimens, blue). Vertical dotted lines represent mean age of individuals for data in shaded regions (as indicated in section **4.3.1.1**). The 95% CIs [0.520 to 1.171 mg/l] for urinary [α1-AGP] from timed-spot urine specimens are represented with a bracket to the left of **Fig. 4.6c**, as values overlapped with those already plotted.

4.4. DISCUSSION

Earlier evaluations of 'normal' reference ranges for urinary α1-AGP among healthy individuals were performed 25 years ago using methods that were approximately 6.25 times less sensitive (refer to **Chapter 3**) than the present assay, having a lower limit of detection of 0.5 mg/l[337]. Revaluation of these 'standards' utilising a more sensitive (< 0.5 mg/l) and automated method was therefore warranted. The objective of the present study was to evaluate low-concentration urinary α1-AGP using a novel PETIA optimised for the Optilite™ auto-analyser with the aim of comparing results for several units to results found in the existing literature. As a part of this aim, the impact of age and sex on urinary α1-AGP results were also assessed.

4.4.1. Specimen handling, processing, and analytical methods

Analysis of the urinary proteome is dependent upon the collection of a viable specimen that has been safeguarded against contamination and molecular damage (e.g., protein breakdown). Thus, it is no surprise that specimen collection- (e.g., inclusion of preservative) and processing-related (e.g., storage temperature or analytical technique) factors can have an impact on urinary α1-AGP measurements. For example, compared to fresh specimens, α1-AGP appears stable in human urine specimens stored between 2 to 8 °C for up to 7 to 10 days[5 288] with and without preservatives[329 297]. By contrast, storage between 18 to 22 °C for the same duration may produce significantly different results[288]. Moreover, the influences of storage temperature and duration on urinary α1-AGP measurements have only been detectable when using automated immunoturbidimetry (2 to 8 °C for 60 days vs –20 °C for 30 and 300 days)[288] for urinalysis and not when utilising RID (after 180, 365, and 730 days)[329].

For the establishment of the most accurate urinary α1-AGP reference values or clinical cut-offs, and based on the presented evidence, it could be argued that urine specimens (to be analysed for α1-AGP) should be stored with preservative, at a temperature of –20 °C or colder, thawed in a heating cupboard immediately prior to analysis, and analysed within 60 days of collection utilising PETIA, consistent with the methodology of the present study. It was evident from **Table 4.3** however, that only 29 out of 53 studies stored specimens at temperatures consistent with this. While even fewer studies reported to have both stored specimens with preservative (i.e., not specified within the study) and analysed α1-AGP utilising PETIA (i.e., specified using an alternate analytical technique). In addition, the present PETIA was successful in detecting urinary α1-AGP in a predominance of specimens (97.3% of all analysed urine specimens), consistent with evaluations presented in **Chapter 3**, which was superior than evaluations described in earlier studies (i.e., 70% success)[337]. Thus, the present study may be referred to as a guide for future research aiming to analyse urine specimens for α1-AGP.

4.4.2. Units of measure

From the summary tables presented in **Table 4.4** and **Table 4.5** it was clear that a lack of consistency exists in regards to the units reported for urinary α1-AGP. Additional inconsistencies were evident in the formats of reported results (e.g., mean ± SD, median ± IQR, or mean ± 95 CIs). These differences made statistical comparisons between studies, as well as, against the present urinalysis, somewhat difficult. Nevertheless, observations related to each unit of urinary α1-AGP are discussed next.

4.4.2.1. Concentration

As shown in **Table 4.4** and **Table 4.5**, values of urinary α1-AGP among healthy and diseased populations were most commonly reported as concentration, with results not often

further subjected to a creatinine correction. This was similar to previous issues encountered for the reporting of urinary albumin[376]. Despite the small sample size and the wide age range for the present cohort, urinary [α1-AGP] measurements from EMU and 24-hour specimens were largely comparable to results presented in **Table 4.4** (see also **Figure 4.6c**). Results from the B-A plot (refer to **Figure 4.3**) provided support for the agreement in urinary [α1-AGP] values between 24-hour and EMU specimens (e.g., mg/l_{EMU} vs mg/$l_{24\text{-hours}}$). However, mg/l_{EMU} (or 'overnight') measurements appeared lower in comparison to 24-hour measurements with comparison of log-transformed values indicating a significant difference between the two. These differences were similar to those observed between 24-hour and timed-spot urine specimens as indicated in B-A plot (refer to **Figure 4.4b**).

The 'day-night' difference mentioned above was consistent with that previously described[337] and also congruent with the circadian pattern observed for other urinary proteins (e.g., albumin)[377] [378]. Although several plausible mechanisms have been hypothesised to explain the diurnal variation exhibited for urinary α1-AGP (e.g., changes in haemodynamics or alterations in the glomerular barrier itself[379]; refer to **Chapter 2**), conclusions regarding these mechanisms could not be reached based solely on the present urinalysis results. Importantly, what could be concluded, was that morning or daytime urine specimens may underestimate the (uncorrected) [α1-AGP] exhibited in 24-hour specimens. This is significant given that urinary [α1-AGP] was most commonly reported and that many disease cut-offs are based solely on concentration values. Further, it appears possible that erroneous diagnostic conclusions could occur as a result of the urine specimen type not being explicitly stated in conjunction with the established urinary cut-off value for α1-AGP. Also observed was the vast degree of variation in urinary [α1-AGP] values between different types of pathophysiologic responses (e.g., sepsis

being extremely high by comparison). This could become extremely important in the presence of multiple comorbidities and should be taken into account in future clinical research.

4.4.2.2. Excretion rate

Unlike concentration values, excretion rates standardise urinary α1-AGP measurements by correcting for specimen volume and collection duration, which can contribute to significant differences. Compared to other units, however, urinary α1-AGP excretion rates (mg/24-hour and μg/min) were reported least in the literature. Even so, it was clear from **Figure 4.5b** and **4.5c** that α1-AGP excretion was greater among diseased individuals compared to healthy individuals, notwithstanding that the range of urinary values was wide for diseases included.

Results from the present urinalysis for 24-hour excretion appeared consistent with results from previous studies (**Figure 4.6a** and **4.6b**), as evident in the overlap of values with the measured range (mean ± 95% CIs). However, given the limited reporting of excretion rates in the literature, no definitive conclusions could be reached regarding the consistency between the present results and the wider population. Nevertheless, there was no difference in the α1-AGP excretion rate between 24-hour and timed-spot urine specimens with this result solidified by the improved sensitivity (i.e., lower limit of 0.08 mg/l) of the present assay in comparison to earlier methods conducting similar evaluations[337], which had a lower limit of 0.5 mg/l.

4.4.2.3. Ratio-to-creatinine

As shown in **Table 4.4** and **Table 4.5**, it was clear that urinary α1-AGP:CREA results were less commonly reported compared to [α1-AGP] and that inconsistencies existed for the ways in which α1-AGP:CREA was reported (mg/mmol vs mg/g). Results from the present

urinalysis appeared lower in comparison to results from the literature (see **Figure 4.6d**), although the reason for this difference is not immediately clear.

The observed lack of application of correction factors (e.g., creatinine) to urinary [α1-AGP] results is problematic as uncorrected values fail to account for specimen volume or collection duration, which can easily influence results[380], as well as, additional factors that may be somewhat explained with creatinine levels (e.g., age or sex differences[5]). α1-AGP:CREA has therefore been suggested as the most appropriate unit of measurement as it helps to minimise the degree of variation exhibited[380], making it easier to interpret across a range of populations. Creatinine correction however, can be vulnerable to alterations in creatinine levels that occur with physiologic renal responses (e.g., following exercise[381]) and pathophysiologic renal adaptations (e.g., reduced kidney function or low muscle mass[382]).

Given the potentiation of high inter-individual variation for urinary α1-AGP, it seems inappropriate to solely utilise or report uncorrected units (i.e., concentration), yet clinical studies have predominantly reported urinary α1-AGP results as concentration, and have produced meaningful data with implications for clinical practice (e.g., detection/prediction of T1DM with early decline or detection of bladder cancer; refer to **Table 4.5**). Consistent with this, and when evaluated collectively (i.e., males and females), creatinine correction performed in the experimental portion of the present study did not appear to reduce the degree of inter-individual variation that was observed for urinary [α1-AGP] values. In fact, the %CVs for urinary [α1-AGP] values from EMUs were substantially lower than those for α1-AGP:CREA ($mg/mmol_{\alpha1\text{-}AGP:CREA}$). Notwithstanding the practicality of concentration-only values, there may still be a need to explore improved approaches for reporting creatinine-corrected values[383]. Incorporation of alternative correction factors (e.g., urinary cystatin C) may also be considered in the future to enhance non-clinical and clinical significance for this unit of urinary α1-AGP.

4.4.2.4. Influence of age and sex

Variation in urinary α1-AGP between individuals is thought to be greater than intra-individual variation[384] (85% vs 40%, respectively), which is consistent with the established inter- and intra-individual variability (e.g., across ages or between sexes vs between-days for a single individual) known to exist within the urinary proteome[385]. This inter-individual variation for urinary α1-AGP has largely been thought to be product of age[348] and sex[278], although many studies have demonstrated no effect of age or sex on urinary α1-AGP excretion[337]. In support of the latter, the present study showed no evidence of a significant effect for sex or age on any units of urinary α1-AGP. Similarly, %CVs, serving as measures of inter-individual variability[384], for urinary [α1-AGP] measurements were most consistent between males and females for 24-hour specimens (opposed to EMU specimens). By contrast, there was a greater difference between the two sexes for units obtained from EMU specimens, despite the %CVs being smaller than those from 24-hour specimens. It remains unclear whether the null relationships between urinary α1-AGP and sex or age remain unaltered with disease. The cohort data presented in **Table 4.5** may be further explored in order to evaluate this question, however, this was beyond the scope of the present study.

With regards to age, and in reference to the existing literature, there appeared to be a certain degree of age-related effects on urinary α1-AGP. This was most pronounced when observed graphically (e.g., young cohorts, < 12-months old[348] vs older cohorts; refer to **Table 4.4**, **Table 4.5,** and **Figure 4.6a – 4.6d**). While no individuals < 12-months old were included as part of the present urinalysis, it was clear from the indicated tables and figures that age requires further investigation (specifically to include individuals < 15 years old) in regards to the diagnostic accuracy (and associated cut-off values) of urinary α1-AGP. More in-depth

evaluations of α1-AGP excretion in older individuals are also warranted given the known age-related changes in glomerular permeability and overall renal structure and function[386], which could influence urinary α1-AGP[387]. Similarly, further investigation is required in order to determine whether age-appropriate reference ranges or cut-off values are required for various diseases (e.g., Crohn's disease[278], T1DM[364], or T2DM[351]; refer to **Table 4.5**).

While Deming regression (and Passing-Bablock regression) analysis was considered in evaluating any relationship between urinary α1-AGP results and age for original data from existing literature (presented in **Table 4.4**), the observed inconsistencies for urinary reporting and the necessitation of multiple conversions of the published results ultimately led to this not being performed or included, and was deemed beyond the original purpose of identifying basic normative data for urinary α1-AGP. An improved strategy may be to perform a large population-based study or to analyse a large number of biobank specimens from healthy and diseased individuals. In addition, and to help confirm or deny any confound of age or sex in relation to urinary α1-AGP exhibited with disease, studies that have previously established clinical cut-offs for urinary α1-AGP, albeit may have been excluded here (e.g., due to presentation of only ROCs or AUCs), could be explored.

4.4.3. Limitations and future work

Although the intra-individual variation is considered to be lower than inter-individual variability for urinary α1-AGP excretion, this was not measured in the present study nor was it commonly reported in the existing literature. Thus, it is unclear whether intra-individual variation could have impacted results and whether alternate factors (e.g., ethnicity) may additionally influence such variation, which has previously been demonstrated for other types of proteinuria (e.g., albuminuria)[388]. Future studies could benefit from including repeat 24-

hour and early morning specimens to better understand intra- and inter-individual variation of urinary α1-AGP and any relative impact on results among healthy or diseased individuals. Similarly, clinical diagnostic or predictive usages of urinary α1-AGP that are highly sensitive[351] (i.e., when urinary α1-AGP values are low or where cut-off values fall close to normative reference values) or those applications that lack definitive cut-off values may consider comparing urinary α1-AGP units from both, 24-hour and EMU specimens in efforts to ensure accuracy and validity. The practicality of utilising EMU specimens however, must not be discounted[360].

Measures of α1-AGP clearance were also not assessed in the present study, and were rarely reported in the literature for healthy or diseased cohorts. Evaluations of serum and urinary α1-AGP in concert may also be useful in distinguishing between systemic and local mechanisms contributing to proteinuria. While serum α1-AGP has not dictated urinary α1-AGP excretion in healthy individuals in the past[7], it is unclear whether this remains true for diseased individuals. Additional investigations are required to assess the clinical utility and applicability of α1-AGP clearance to disease onset or progression.

4.5. CONCLUSION

The present study provides recommendations for the collection, processing, and analysis of urinary α1-AGP in human specimens, which were required due to existing literature being outdated and utilising less sensitive analytical techniques. These practices may be adopted by future investigators in order to produce a pool of research that is more consistent. While no significance of age or sex was observed, from the literature it was clear that the establishment of age-specific reference ranges for urinary α1-AGP measurements may be

required. Similarly, the establishment of disease cut-off values for all units of measure are required to improve the diagnostic ability of urinary α1-AGP. Thus, deployment of urinalysis for α1-AGP in clinical practice should be implemented carefully with close consideration of published research and with caution where no definitive cuff-offs currently exist. The next chapter utilises the developed immunoassay to analyse urinary α1-AGP from human urine specimens collected pre/post exercise tests conducted at sea-level and twice at altitude.

Chapter 5

USE OF AN IMMUNOTURBIDIMETRIC ASSAY FOR ANALYSIS OF POST-EXERCISE URINARY ALPHA-1 ACID GLYCOPROTEIN.

Data from this chapter gave rise to several scholarly publications (e.g., conference abstracts and peer-reviewed papers) that are listed below (with appropriate links provided) and followed by statements of co-authors' contribution(s):

i. **Joyce KE**, Delamere JP, Bradwell SB, Myers S, Ashdown K, Rue CA, Thomas O, Lucas SJE, Fountain A, Edsell M, Myers F, Malein W, Imray C, Clarke A, Lewis CT, Newman C, Johnson B, Cadigan P, Wright A, Bradwell AR, and Birmingham Medical Research Expeditionary Society. Hypoxia is not the primary mechanism contributing to exercise-induced proteinuria. *British Journal of Medicine Open Sport and Exercise Medicine.* 2020; 6(1).

ii. **Joyce KE**, Lucas SJE, Bradwell S, Delamere JP, Myers SD, Thomas O, Fountain A, Bradwell AR, and the Birmingham Medical Research Expeditionary Society. Hypoxia is not the mechanism for exercise-induced proteinuria. *High Altitude Medicine & Biology.* 2018; 19(4): 0006. https://doi.org/10.1089/ham.2018.29015.abstracts

iii. **Joyce KE**, Lucas SJE, Bradwell S, Delamere JP, Myers SD, Thomas O, Fountain A, Bradwell AR, and the Birmingham Medical Research Expeditionary Society. Urinary orosomucoid (alpha-1 acid glycoprotein) latex immunoassay is effective for the detection of increased proteinuria associated with altitude and sea-level exercise. Europhysiology, London, UK. 2018; *Proc Physiol Soc* 41: PCA166.

iv. **Joyce KE**, Lucas SJE, Bradwell S, Delamere JP, Myers S, Thomas O, Fountain A, Bradwell AR, and the Birmingham Medical Research Expeditionary Society. Exercise proteinuria at altitude is reduced by acetazolamide. Europhysiology, London, UK. 2018; *Proc Physiol Soc 41: PCA167.*

v. Delamere JP, Bradwell AR, Bradwell SB, **Joyce KE**, Lewis CT, Clarke A, Newman C, Shipman K and Birmingham Medical Research Expeditionary Society. Losartan has no effect on hypoxic diuretic response to altitude. *High Altitude Medicine & Biology.* 2018; 19(4): 0005. https://doi.org/10.1089/ham.2018.29015.abstracts

vi. Lucas SJE, Malein W, Thomas OD, Ashdown KM, Rue CA, **Joyce KE**, Newman C, Cadigan P, Johnson B, Myers SD, Myers FA, Wright AD, Delamere J, Imray CHE, Bradwell AR, Edsell M, and the Birmingham Medical Research Expeditionary Society. Effect of losartan on performance and physiological responses to exercise at high altitude (5,035 m). *BMJ Open Sport and Exercise Medicine.* 2020; 7(1). DOI: 10.1136/bmjsem-2020-000982.

Statements of contribution(s):

Given the expedition's rise to multiple publications with different co-authors, statements of co-authors' contribution(s) were provided for the publications listed above. Items i – iv were associated with the following contributions and involvements: KEJ – Immunoturbidimetric urinalysis, statistical analysis, writing, and academic communications; SJE – Exercise tests and writing; ARB – Concept, study design, and writing*; ME,* CI, WM, OT, BJ, and CN – Physiologic data collection and daily medical examinations; AF – Assistance with immunoturbidimetric analysis; JPD and AW – Concept and urine specimen collection; SBB – Urine specimen collection; KA, CAR, and SDM – Exercise tests; FM – ACE genotyping; and the BMRES – Provided additional assistance to make the expedition possible. Item five was associated with the following contributions and involvements: JPD – Concept, specimen collection, analysis, and writing; ARB – Concept, analysis, and writing; KEJ – Writing and academic communication; CN – Analysis and writing; SBB, AC, and CTL – Specimen collection; and KS – Clinical chemistry analysis for aldosterone and copeptin (published elsewhere).

Note that this published chapter has been formatted and edited for this thesis. Specifically, **Chapter 5** applies a format that is more consistent with preceding chapters and with redundant information omitted and the reader referred to the appropriate preceding information (e.g., immunoassay specifications outlined in **Chapter 3**). References were also added where indicated.

ABSTRACT

INTRODUCTION: Proteinuria increases at altitude and with exercise, potentially as a result of hypoxia. Using urinary alpha-1 acid glycoprotein (α1-AGP) levels as a sensitive marker of proteinuria, we examined the impact of relative hypoxia due to high altitude and blood pressure-lowering medication, on post-exercise proteinuria. **METHODS**: Twenty individuals were pair-matched for sex, age, and angiotensin-converting enzyme (ACE) genotype. They completed maximal exercise tests once at sea-level and twice at altitude (5,035 m). Losartan (100 mg/day; angiotensin-receptor blocker) and placebo were randomly assigned within each pair 21 days before ascent. The first altitude exercise test was completed within 24–48 hours of arrival (each pair within ~1 hour). Acetazolamide (125 mg twice daily) was administrated immediately after this test for 48 hours until the second altitude exercise test. **RESULTS:** With placebo, post-exercise α1-AGP levels were similar at sea-level and altitude. Odds ratio for increased resting α1-AGP at altitude vs sea-level was greater without losartan (2.16 times greater). At altitude, odds ratio for reduced post-exercise α1-AGP (58% lower) was higher with losartan than placebo (2.25 times greater, $p = 0.059$) despite similar SpO_2% ($p = 0.95$) between groups. Acetazolamide reduced post-exercise proteinuria by approximately threefold (9.3 ± 9.7 vs 3.6 ± 6.0 μg/min; $p = 0.025$) although changes were not correlated ($r = -0.10$) with significant improvements in SpO_2% ($69.1 \pm 4.5\%$ vs. $75.8 \pm 3.8\%$; $p = 0.001$). **DISCUSSION:** Profound systemic hypoxia imposed by altitude does not result in greater post-exercise proteinuria than sea-level. Losartan and acetazolamide may attenuate post-exercise proteinuria, however further research is warranted.

5.1. INTRODUCTION

Proteinuria typically results from protein leakage from the capillary lumen through the glomerular filter[155], with some removal in the tubules, as shown by studies inhibiting renal tubular reabsorption with lysine infusions[187]. Comparisons between albumin, a selectively reabsorbed[120], 66 kDa, negatively charged (p*I* 4.7) protein that passes through the glomerular membrane via the slit diaphragm pores[389], and alpha-1 acid glycoprotein (α1-AGP)[11 249 7], a smaller (41 – 43 kDa) and more negatively charged protein (p*I* ~2.7)[11 7] indicate that urinary α1-AGP is a more sensitive marker of glomerular leakage than albumin[7 285 157]. Urinary α1-AGP excretion has implicated the glomerular origin of the proteinuria exhibited post-exercise[11] and with ascent to altitude[7]. Hypothesised mechanisms for such glomerular leak have included changes in renal blood flow[11 390], increases in peritubular and blood pressures[187] (BP), hypoxia[10], and acid-base disturbances[187], although the mechanisms remain unclear[391]. The contributions of BP and hypoxia, specifically, to post-exercise proteinuria may be uniquely evaluated by superimposing exercise and altitude exposure.

At altitude, exercise BP is amplified[392 201] and such exaggerations are responsive to antihypertensive therapies such as, angiotensin II type 1 receptor (AT1) antagonists or, blockers (ARBs)[188 392]. ARBs reduce BP via several mechanisms, to include selectively blocking angiotensin II (A-II) from binding to AT1s within the vasculature[198], promoting vasodilation. Specific to the kidney, ARBs (e.g., losartan) 'block' vasoconstriction imposed by A-II on afferent arterioles[110]. ARBs also limit both, vasopressin secretion and aldosterone production further adding to its BP lowering effect[198]. Considering these factors, it would be reasonable to expect post-exercise proteinuria at altitude to be greater than at sea-level and that AT1 blockers such as losartan could attenuate the post-exercise response. To evaluate this, comparisons for post-

exercise α1-AGP excretion were planned between: 1) sea-level and altitude exercise and 2) losartan and placebo groups following exercise at altitude.

Exercise oxygen saturation is also altered at altitude and is profoundly lower compared to sea-level[393] but can be improved by acetazolamide[394], a carbonic anhydrase inhibitor commonly used to prevent altitude illness[176 179]. By inhibiting carbonic anhydrase, a catalyst of the reversible CO_2 hydration reaction, acetazolamide promotes carbonic acid formation and dissociation of hydrogen ions (H^+) and bicarbonate in the blood[179], which limits hypoxia induced alkalosis and improves oxygen saturation[179]. Assuming hypoxia as the main mechanism of post-exercise proteinuria, altitude exercise would be expected to produce larger increases in post-exercise proteinuria compared to sea-level. In addition, subsequent improvements in arterial oxygenation would be expected to have the 'reverse' effect. To evaluate this, comparisons of post-exercise α1-AGP were planned between: 1) sea-level and altitude and 2) placebo and placebo + acetazolamide groups at altitude.

We hypothesised that exercise at altitude would increase post-exercise α1-AGP levels compared with sea-level, primarily due to greater systemic hypoxia, and that losartan and acetazolamide would attenuate the observed increases by improving blood and peritubular pressures[198] and alleviating renal hypoxia[183], respectively.

5.2. MATERIALS & METHODS

As part of an expedition to Quito, Ecuador, post-exercise urinary α1-AGP excretion was measured in twenty pair-matched individuals once at sea-level (before placebo or losartan administration) and twice at altitude as outlined in the following sections.

5.2.1. Design and participants

Twenty participants (14 male, 6 female) free of any pre-existing conditions were included in the study. Angiotensin converting enzyme (ACE) genotyping (II, ID, or DD) was performed to limit potential differences between groups that could be attributed to ACE genotype (e.g., response to losartan[204] or response to altitude[205]). Participants were pair-matched for ACE genotype, age, sex, previous altitude exposure, and glomerular filtration rate (GFR, obtained 4 weeks prior to ascent) (see **Figure 5.1**).

Following matching, a double-blind, randomised, placebo-controlled trial design was adopted. Individuals within each pair were randomly assigned to either placebo or losartan groups (**Figure 5.1a**). Losartan administration (100 mg/day or placebo) began in the UK 21 days prior to departure for Quito, Ecuador (2,850 m). Upon arrival at Quito, participants ascended over 10 days to the Whymper Hut on the flank of Chimborazo volcano (5,035 m, **Figure 5.1b**).

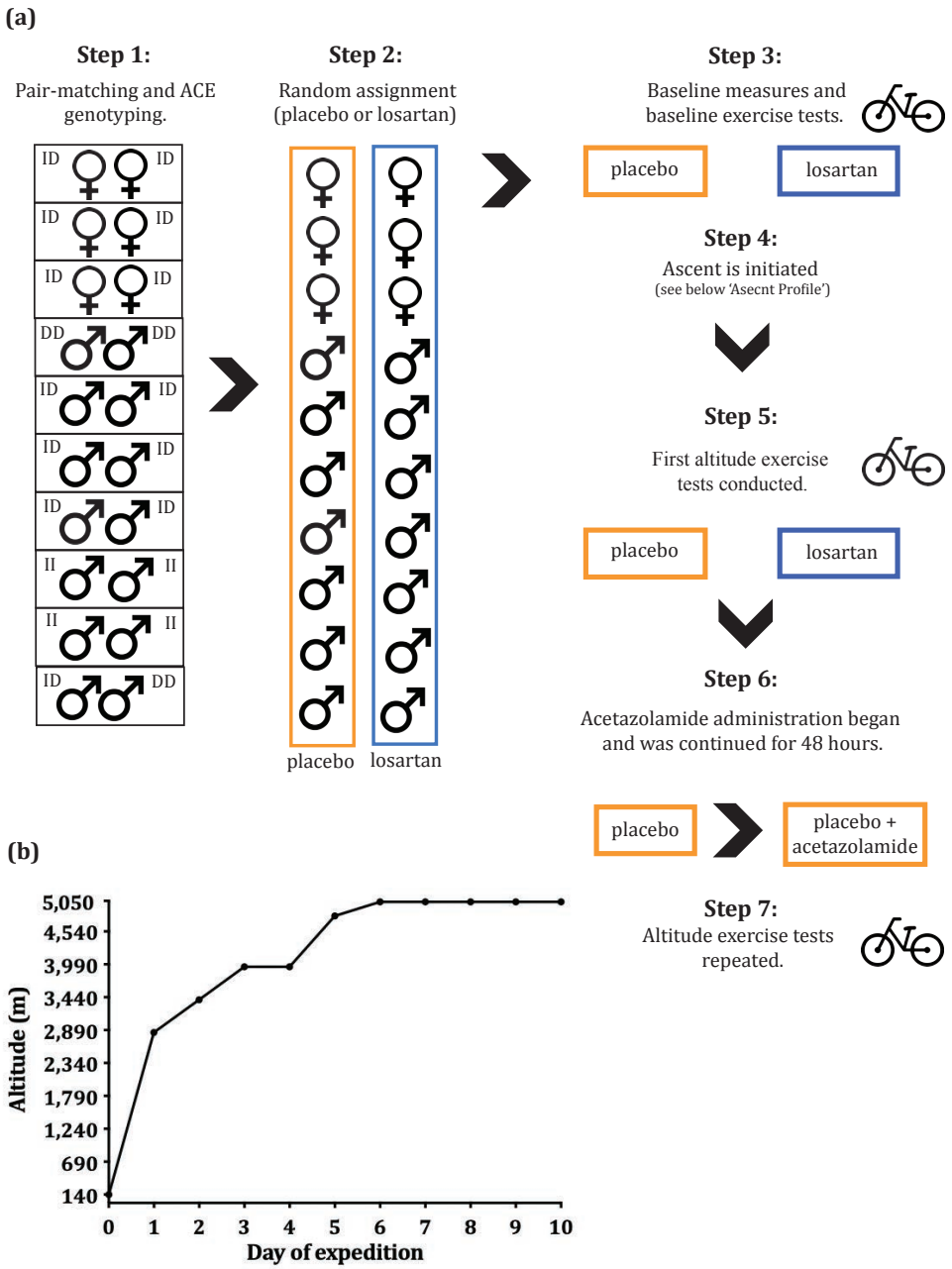

Figure 5.1 – Study design and ascent profile. Fig 5.1a – *Step 1*: Participants pair-matched for angiotensin converting enzyme (ACE) genotype (II, ID, or DD; see), age, sex (male, ♂; female, ♀), glomerular filtration rate (GFR), and previous altitude exposure; ***Step 2:*** Within pairs, participants randomly assigned to placebo or losartan group; ***Step 3*:** Baseline characteristics collected and baseline exercise tests executed (4 weeks before ascent), which were followed by commencement of losartan administration (21 days before ascent); ***Step 4:*** Groups ascended together in accordance with **Fig. 5.1b; *Step 5:*** First altitude exercise tests executed in both groups (5,035 m); ***Step 6*:** Following the first altitude exercise test, acetazolamide (125 mg p.o. BID) was administered for 48 hours; ***Step 7:*** Repeat altitude exercise test (only placebo group data reported); **Fig 5.1b –** Expedition ascent profile. Day 0: Birmingham, UK (140 m); Days 1 and 2: Quito, Ecuador (2,850 m); Day 3: Chunquiragua in Chaupi (3,400 m); Days 4 and 5: Estrella del Chimborazo Marco Cruz (3,950 m) with hike to 5,000 m on Day 5; Day 6: Carrel Hut (4,800 m); and Days 7 – 10: Whymper Hut (5,035 m).

5.2.2. Baseline and daily measures

Baseline measures of height, body mass (kg), GFR, estimated GFR (eGFR; calculated using the Modification of Diet in Renal Disease (MDRD) study equation[395] (see **Equation 5.1**), and serum creatinine (μmol/l) were recorded 4 weeks prior to ascent (**Figure 5.1a**) whereas resting measures of systolic blood pressure (SBP) and diastolic blood pressure (DBP) were collected each morning during ascent (**Figure 5.1b**; using a manual sphygmomanometer).

Equation 5.1– Modification of Diet in Renal Disease (MDRD) study equation[395].

$$eGFR = 32{,}788 \times SCr^{-1.154} \times Age^{-0.203} \times 0.742_{if\ female}$$

Where:

eGFR = estimated glomerular filtration rate (ml/min/1.73 m$^{2)}$;
SCr = serum creatinine in units for μmol/litre;
Age = age in years;
0.742 = constant used to further correct values for females.

5.2.3. Exercise protocols and measures

5.2.3.1. Sea-level exercise

Baseline sea-level graded maximal exercise tests were performed 4 weeks prior to ascent on a cycle ergometer (Alticycle) designed for altitude studies[396] (**Figure 5.1a**). Volitional fatigue was used as the primary endpoint criterion for test termination[397]. Maximal power output (W_{max}) was measured by the Alticycle. Heart rate (HR) recordings were facilitated by telemetry (Polar Electro, UK Ltd).

5.2.3.2. Altitude exercise

The first altitude exercise tests were commenced on arrival to the Whymper Hut (day 7) for five pairs and completed on the following day (day 8) for remaining pairs (**Figure 5.1b**). These initial tests were immediately followed by acetazolamide administration (125 mg orally, twice daily), which occurred 48 hours prior to the second round of altitude exercise tests in all

participants. Similar to the first tests, the second round of altitude exercise tests were performed across two days (on days 9 and 10, **Figure 5.1b**).

At altitude, pre-exercise measurements of oxygen uptake (VO_2), carbon dioxide production (VCO_2), ventilation (V_E), HR, SBP, and DBP were collected. Participants undertook a 5-minute self-paced warm-up followed by a modified graded exercise test on the Alticycle, which was commenced at 30% of sea-level W_{max}. Intensity was increased every 3 minutes by 10% until the participant reached 80% of sea-level W_{max}. From this point, intensity was increased by 10% each minute until volitional fatigue. Expired respiratory gases were analysed breath-by-breath using a Cosmed K4b² (Metabolic Company, Rome, Italy) portable metabolic system alongside continuous measurements of HR (via three-lead ECG), oxygen saturation (SpO_2; via pulse oximetry, Datex Ohmeda 3900, GE Healthcare USA), and beat-to-beat measurements of SBP and DBP by photoplethysmography (Portapres, Finapres Medical Systems BV, Netherlands). Changes (Δ) in SBP and DBP were calculated as the difference between pre-exercise and W_{max} measurements. Urine specimens were collected surrounding exercise as outlined below (see section **5.2.4**).

5.2.4. Urine collection and storage

Twenty-four-hour urine samples were collected over one day at sea-level and on each day of the expedition (10 days) with four aliquots (2 ml each) taken from each daily collection and frozen on dry ice.

For pre-exercise collections, participants were instructed to drink 500 ml of water between 90 and 30 minutes pre-exercise and to provide a timed (60 minute) urine specimen immediately prior to exercise. Post-exercise urine specimens were collected at 60, 120 and 180 minutes. Four aliquots (2 ml each) were taken from exercise specimens and frozen on dry ice,

with the residual volumes returned to each individual's 24-hour collection bottle. Urine samples were transported back to Birmingham, UK and stored at –80 °C until urinalysis.

5.2.5. Urinalysis

Urine specimens were thawed at room temperature for one hour prior to urinalysis for α1-AGP. All exercise urine samples were analysed using the latex-enhanced immunoturbidimetric assay described in **Chapter 3** using the Optilite™ auto-analyser (The Binding Site Ltd., Birmingham, UK). Results were yielded as concentration of α1-AGP (mg/l), which was then converted to excretion rate (mg/24-hours or μg/min) based on specimen volumes and collection durations. By contrast, the 24-hour urine samples were initially analysed for α1-AGP using radial immunodiffusion (RID; by Talks and colleagues[7]) with only a subset of these specimens also analysed (in triplicate) using the turbidimetric immunoassay and further used for methods comparison (as outlined in **Chapter 3**).

5.2.6. Statistical analysis

Statistical analyses were performed using SPSS Statistics (v25 for Mac iOS, IBM, Armonk, NY, USA). Normality of distribution was determined by the Shapiro-Wilk test, with data (24-hour urinary α1-AGP excretion) log-transformed where possible. Continuous variables are presented as mean ± standard deviation (SD) or median ± interquartile range (IQR) where appropriate. All tests for significance were two-tailed with statistical significance set at $p \leq 0.05$ unless otherwise indicated.

Independent *t*-tests were used to compare group means (placebo vs losartan) where data were normally distributed and when measures were not repeated (e.g., age and other baseline characteristics). Repeated-measures ANOVA with pairwise comparisons (Bonferroni corrected) was used to evaluate group (placebo vs losartan) and interaction effects (where

appropriate) across days for normally distributed data (e.g., transformed 24-hour α1-AGP, DBP, and SBP). Friedman test was used to determine the main effect of time on α1-AGP excretion surrounding exercise (i.e., pre, post-60, post-120, and post-180 minutes) where data were not normally distributed. These results are presented as: "χ^2(df), *p*-value". When appropriate, the post-hoc Wilcoxon signed rank test with Bonferroni correction for repeated measures was used to distinguish significance between time points (significance set at $p \leq 0.0125$; i.e., corrected for three comparisons). Mann-Whitney U test was used to compare significant time points between groups (i.e., placebo vs losartan at post-60 minutes).

To avoid any superimposed effects of the two drugs on results, comparisons between the two altitude tests (before and after acetazolamide administration, placebo vs placebo + acetazolamide) were limited to individuals from the placebo group completing both tests (n = 9, **Figure 5.1** and **Table 5.3**). For these comparisons, Friedman test and Wilcoxon signed rank test were applied as previously described with additional use of the Wilcoxon signed rank test to compare α1-AGP excretion (within-individuals) between placebo and placebo + acetazolamide at post-60 minutes. Spearman's correlation was used to evaluate relationships between daily measures (e.g., DBP and 24-hour α1-AGP excretion) and exercise measures (e.g., SpO_2 and post-exercise α1-AGP excretion).

Odds ratios were calculated for urinary α1-AGP excretion in placebo and losartan groups at rest (pre-exercise and post-exercise at 120 and 180 minutes) and with exercise (at post-60 minutes) based on the relative changes [relative increase (+) or decrease (–)] from baseline sea-level measures within each individual.

5.2.7. Patient and public involvement

The study was supported by the Birmingham Medical Research Expeditionary Society, which provided input for the conduct of the research. Patients were not included. Public involvement was limited to recruitment. Notification was given to participants at the time of consent that acquisition of personal data was permitted upon request. Permission was also obtained at this time for the dissemination of de-identified data within the research team and only externally when a reasonable request was submitted directly to the corresponding author(s) of the present study within 6 months of its publication. A portion of the cohort was invited to review the research methods for accuracy and readability.

5.2.8. Ethical approval

This observational study was approved by the Chichester University Research Ethics Committee (protocol number: 1314 42) and was performed according to the Declaration of Helsinki. This study did not aim to investigate any safeties or efficacies of the already FDA approved drugs included thus, no clinical trial approval was obtained. There were no active FDA recalls for either drug for the duration of the study.

5.3. RESULTS

5.3.1. Baseline measures

Baseline data are presented in **Table 5.1**. Placebo and losartan groups were not significantly different at baseline for measures of age, body mass, height, GFR, eGFR, or creatinine. ACE genotype was exactly matched in 9 out of 10 pairs, with all allelic variations represented (ID, n = 13; II, n = 4; and DD, n = 3; see **Table 5.1**).

Table 5.1 – Baseline sea-level characteristics.

	placebo	losartan	*p*-value	ACE genotype pairs					
				female pairs			*male pairs*		
Age (yrs)	38.6 ± 18.5	40.4 ± 18.0	0.83	*1*	ID	ID	*4*	II	II
Body mass (kg)	74.1 ± 11.5	66.7 ± 13.3	0.71	*2*	ID	ID	*5*	II	II
Height (cm)	172.6 ± 8.4	176.4 ± 8.9	0.83	3	ID	ID	*6*	ID	ID
GFR (ml/min/1.73 m²)	88.0 ± 15.2	90.8 ± 15.8	0.69				*7*	ID	ID
eGFR (ml/min/1.73 m²)	87.8 ± 15.3	90.8 ± 15.9	0.68				*8*	ID	ID
Creatinine (μmol/l)*	84.5 ± 24.0	81.0 ± 31.0	0.58				*9*	DD	ID
							10	DD	DD

Baseline results were obtained at sea-level and *prior* to the administration of placebo and losartan. Continuous variables are presented as mean ± standard deviation (SD) unless indicated by *, where data are presented as median ± interquartile range (IQR). All allelic variations (insertion/deletion (I/D) alleles; II, ID, and DD) for the angiotensin-converting enzyme (ACE) gene were represented with 90% matched within pairs. Participants were equally matched for sex (male and female). Significance was set to $\alpha < 0.05$ with no differences observed between groups at baseline sea-level. GFR, glomerular filtration rate; eGFR, estimated glomerular filtration rate (calculated using the MDRD study equation[395]; refer to **Equation 5.1** or section **5.2.2**).

5.3.2. Daily measures

Results for daily measures are presented in **Figure 5.2**. Collectively with ascent, daily DBPs increased significantly ($p = 0.04$) while SBP increased, albeit not significantly ($p = 0.17$). Daily SBPs and DBPs remained similar between groups with ascent (SBP, $p = 0.71$ and DBP, $p = 0.72$; **Figure 5.2a** and **5.2b**).

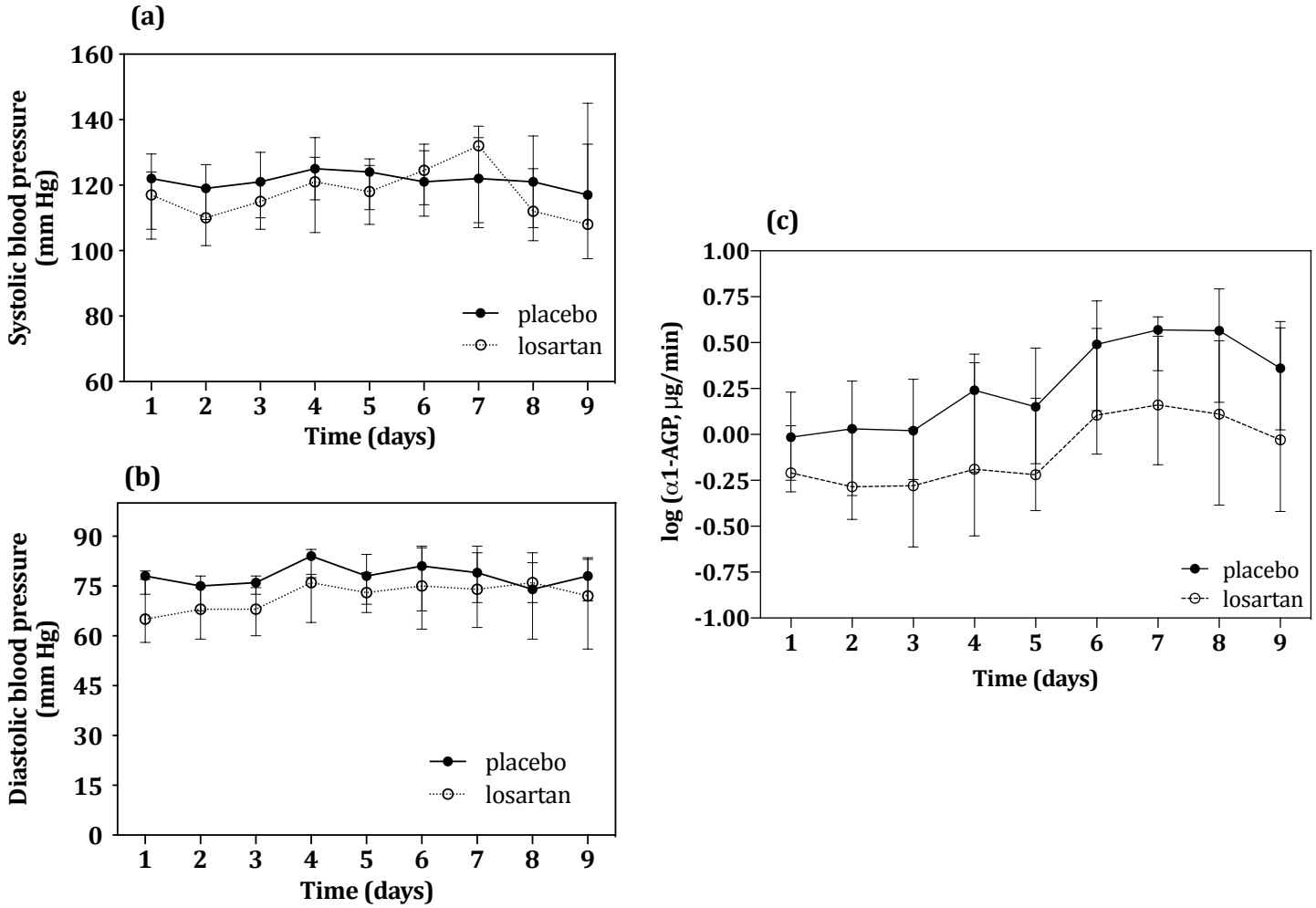

Figure 5.2 – Daily measures of blood pressure and twenty-four-hour urinary alpha-1 acid glycoprotein (α1-AGP) excretion rates with ascent. Fig. 5.2a (top left) – Daily systolic blood pressures (SBPs; mm Hg); **Fig. 5.2b (bottom left)** – Daily diastolic blood pressures (DBPs; mm Hg). Data are plotted as daily medians ± interquartile ranges (IQRs; represented by error bars); **Fig. 5.2c (right)** – Logarithmic-transformed 24-hour urinary α1-AGP excretion rates (μg/min) by days with ascent. Data are plotted for each day as the mean log of 24-hour α1-AGP ± standard deviation (SD; represented by error bars). Twenty-four-hour urinary α1-AGP excretion collectively increased with ascent ($p < 0.01$) with no difference observed between groups with ascent ($p = 0.97$). rates (μg/min) by days with ascent.

5.3.3. Exercise studies

5.3.3.1. Baseline sea-level exercise

Baseline exercise data are presented in **Table 5.2**. All 20 participants achieved exhaustion during baseline sea-level exercise tests. Baseline measures of HR_{max}, absolute W_{max}, and relative W_{max} were no different between groups (**Table 5.2**).

Table 5.2 – Maximal exercise test results compared between groups at baseline and twice at altitude.

	Sea-level exercise				
	placebo	**losartan**	***p*-value**		
HR_{max} (bpm)	172 ± 17	174 ± 23	0.82		
Absolute W_{max} (W)	243 ± 66	238 ± 70	0.89		
Relative W_{max} (W/kg)	3.3 ± 0.5	3.1 ± 0.5	0.41		
	Altitude exercise				
	placebo	**losartan**	***p*-value**	**placebo + acetazolamide**	***p*-value**
	pre-exercise				
HR (bpm)	80 ± 12	76 ± 15	0.50	78 ± 14	0.10
SBP (mm Hg)	162 ± 28	159 ± 22	0.82	149 ± 22	0.17
DBP (mm Hg)	79 ± 6	76 ± 12	0.22	76 ± 8	0.61
SpO_2 (%)	76 ± 7	78 ± 5	0.40	84 ± 4	< 0.01*
	maximal exercise				
HR_{max} (bpm)	152 ± 24	143 ± 35	0.78	147 ± 21	0.63
SBP at W_{max} (mm Hg)	229 ± 47	221 ± 50	0.81	232 ± 47	0.43
Δ SBP (mm Hg)	70 ± 31	66 ± 42	0.80	82 ± 46	0.26
DBP at W_{max} (mm Hg)	87 ± 13	85 ± 19	0.81	96 ± 15	0.08
Δ DBP (mm Hg)	8 ± 10	9 ± 11	0.93	19 ± 14	0.04*
SpO_2 at W_{max} (%)	70 ± 5	71 ± 7	0.89	77 ± 4	< 0.01*
Absolute W_{max} (W)	155 ± 52	138 ± 55	0.53	149 ± 46	0.71
Relative W_{max} (W/kg)	2.1 ± 0.6	1.8 ± 0.5	0.23	2.0 ± 0.5	0.18

Values are presented as mean ± standard deviation (SD). * Significant ($p \leq 0.05$) difference between placebo and placebo + acetazolamide altitude exercise tests (n = 9; within-individual comparisons). HR, heart rate (bpm); HR_{max}, maximal heart rate; SBP, systolic blood pressure; DBP, diastolic blood pressure; Δ SBP or Δ DBP, change between measurements obtained pre-exercise vs at W_{max}; SpO_2, peripheral oxygen saturation by pulse oximetry (%); and W_{max}, absolute (W) or relative (W/kg) power output at volitional fatigue.

5.3.3.2. Altitude exercise (losartan vs placebo)

Altitude exercise data are presented in **Table 5.2**. Pre-exercise measures of SpO_2, HR, SBP, and DBP were not different between groups. All participants achieved exhaustion during

the first altitude exercise tests. At altitude, absolute W_{max} and relative W_{max} were both reduced by ~40% compared to sea-level, but remained similar between groups. HR_{max}, SpO_2 at W_{max}, SBP at W_{max}, and DBP at W_{max} were also similar between groups. Changes in SBP and changes in DBP did not differ between groups.

5.3.3.3. Altitude exercise (placebo vs placebo + acetazolamide)

Nine individuals from the placebo group went on to complete the second altitude exercise test following acetazolamide administration. These data are presented in **Table 5.2**. Pre-exercise HR, SBP, and DBP were no different than before acetazolamide, although pre-exercise SpO_2 was significantly improved with acetazolamide ($p < 0.01$).

Altitude exercise measures of absolute W_{max}, relative W_{max}, SBP at W_{max}, DBP at W_{max}, and HR_{max} were similar before and after acetazolamide, as were the changes in SBP. By contrast, changes in DBP were significantly greater with acetazolamide ($p = 0.04$). SpO_2 at W_{max} was significantly increased with acetazolamide ($p < 0.01$).

5.3.4. Urine studies

5.3.4.1. Twenty-four-hour excretion

Twenty-four-hour urinary α1-AGP excretion (μg/min) significantly increased with ascent ($p < 0.01$), although no differences were observed between groups for logarithmic transformed excretion rates ($p = 0.97$, **Figure 5.2c**). Twenty-four-hour urinary α1-AGP excretion correlated with DBP but not SBP on days 1 (*rho* = 0.63, $p = 0.05$), 6 (*rho* = 0.75, $p = 0.01$) and 9 (*rho* = 0.90, $p = 0.04$) of the expedition in the losartan group only.

5.3.4.2. Baseline sea-level

Baseline urine results are presented in **Table 5.3** and **Figure 5.3a**. Urinary α1-AGP excretion rates were no different between groups before exercise. Exercise increased urinary

α1-AGP excretion in both placebo groups with excretion rates peaking at post-60 minutes (**Figure 5.3a**). Urinary α1-AGP excretion at post-60 minutes was similar between groups (p = 0.63) and resolved after 120 minutes in both groups (**Figure 5.3a**).

Table 5.3 – Comparisons of pre- and post-exercise alpha-1 acid glycoprotein (α1-AGP) excretion between groups at sea-level and twice at altitude.

	Baseline α1-AGP excretion (μg/min)					
	placebo	***p*-value (*Z*-score)**	**losartan**	***p*-value (*Z*-score)**		
pre-exercise	3.5 ± 4.4	0.038 (–2.07)	1.4 ± 2.8	0.028 (–2.20)		
Δ pre- to post-60	8.4 ± 16.3	-	13.8 ± 22.5	-		
post-60 min	13.7 ± 13.8	-	13.5 ± 33.3	-		
post-120 min	1.8 ± 1.2	0.008 (–2.67)*	1.6 ± 2.7	0.013 (–2.50)*		
post-180 min	1.5 ± 2.2	0.008 (–2.67)*	1.2 ± 1.7	0.017 (–2.38)		
	Altitude α1-AGP excretion (μg/min)					
	placebo	***p*-value (*Z*-score)**	**losartan**	***p*-value (*Z*-score)**	**placebo + acetazolamide**	***p*-value (*Z*-score)**
pre-exercise	3.1 ± 5.3	0.022 (–2.29)	2.4 ± 3.4	0.009 (–2.60)*	4.4 ± 5.7	0.160 (–1.40)
Δ pre- to post-60	7.9 ± 14.3	-	4.8 ± 9.9	-	1.2 ± 11.0**	0.160 (–1.40)
post-60 min	11.5 ± 19.2	-	8.2 ± 5.9	-	7.7 ± 12.1	-
post-120 min	3.2 ± 2.4	0.007 (–2.70)*	2.8 ± 4.4	0.012 (–2.52)*	3.4 ± 5.0	-
post-180 min	1.3 ± 4.3	0.011 (–2.55)*	1.5 ± 1.5	0.018 (–2.4)	2.7 ± 4.2	0.025 (–2.24)

Urinary α1-AGP excretion rates (μg/min) are presented as median ± interquartile range (IQR) before (pre-exercise, 0 min) and after (post-60, post-120, and post 180 minutes) exercise initiation. Results are presented for placebo vs losartan (baseline), placebo vs losartan (first altitude exercise), and placebo vs acetazolamide (first compared to second altitude exercise). Significance was set to $\alpha \leq 0.05$ (unless otherwise indicated) with *Z*-scores presented in parenthesis where appropriate. Significance was marked by the following: * post-60 min α1-AGP excretion vs repeated comparisons to other time points time points (significance set to $\alpha \leq 0.0125$); ** difference between groups (i.e., placebo vs losartan or placebo vs placebo + acetazolamide) at the respective time point.

5.3.4.3. Altitude (placebo vs losartan)

Altitude exercise results are presented in **Table 5.3** and **Figure 5.3b**. Pre-exercise α1-AGP excretion rates were similar between groups (p = 0.62), although the odds ratio for a relative increase in α1-AGP excretion at rest (pre-, post-120 minutes, post-180 minutes) was 2.16 times greater without losartan at altitude. Altitude exercise significantly increased urinary α1-AGP excretion in both placebo ($\chi^2(3)$ = 10.73, p = 0.013) and losartan ($\chi^2(3)$ = 15.86, p < 0.01) groups (**Figure 5.3b**). Post-60 minutes α1-AGP excretion was lower with losartan compared to placebo, although the difference was not statistically significant (p = 0.28, **Figure 5.3b** and **Table 5.3**). In the losartan group only, the change in α1-AGP excretion from pre- to post-60 minutes was lower compared to those changes observed at baseline, although this difference was not significant (p = 0.059, **Figure 5.3d**). The odds ratio for reduced urinary α1-AGP excretion at post-60 minutes (sea level vs 1st altitude test) was 2.25 greater with losartan.

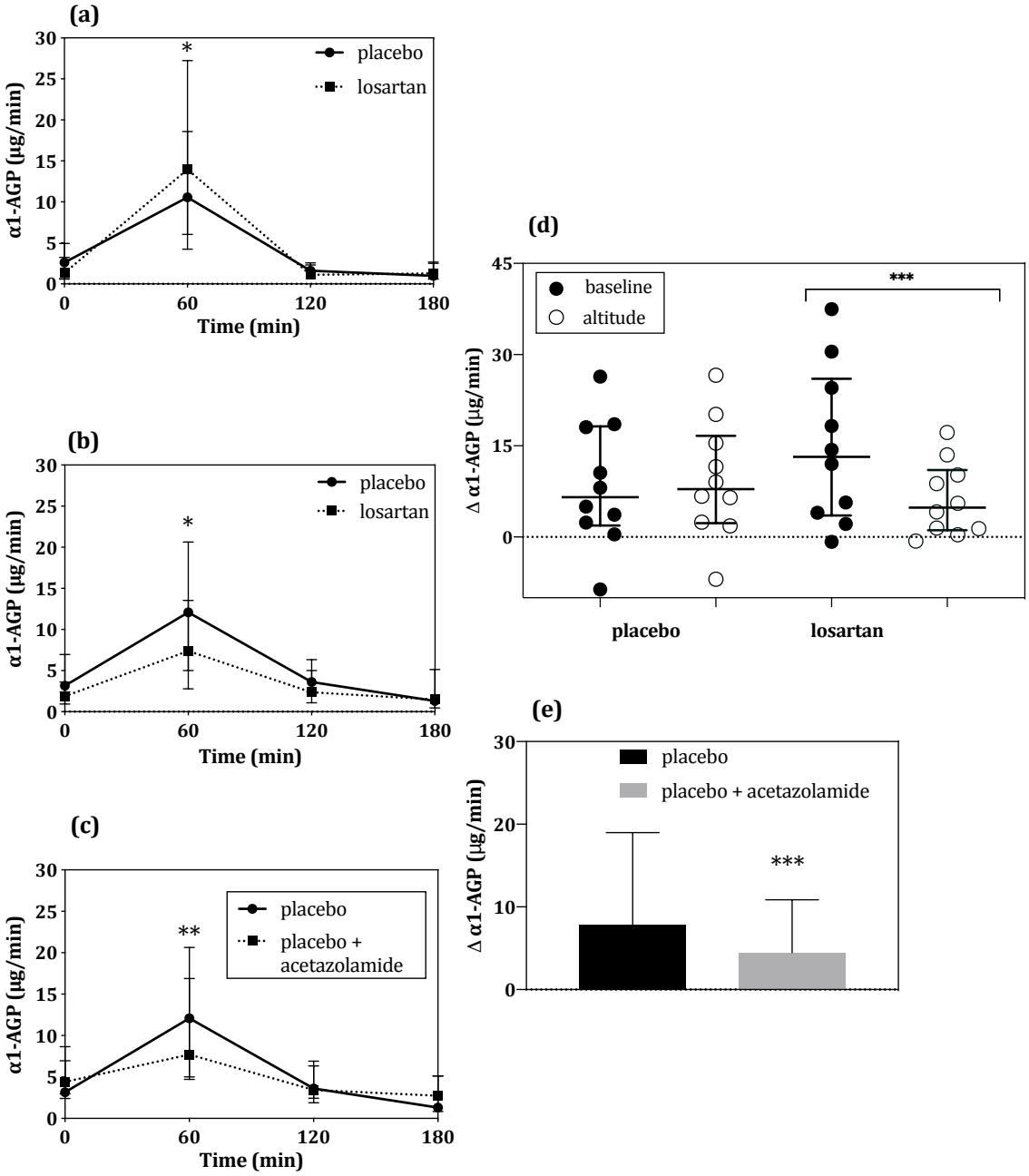

Figure 5.3 – Pre- and post-exercise urinary alpha-1 acid glycoprotein (α1-AGP) excretion (µg/min). Fig. 5.3a – Comparisons between placebo vs losartan groups at baseline sea-level; **Fig. 5.3b –** Comparisons between placebo vs losartan groups at altitude (first altitude exercise); **Fig. 5.3c –** Comparisons between placebo vs placebo + acetazolamide at altitude (second altitude exercise); **Fig. 5.3d** – Individual data for change in α1-AGP (Δ α1-AGP; pre- to post-60 min) for losartan and placebo groups at baseline and for the first altitude exercise; **Fig. 5.3e** – Comparisons between placebo vs placebo + acetazolamide. Results are plotted as group median (or individual values, **Fig. 5.3d**) ± interquartile ranges (IQRs; represented by error bars). Significance was set to $\alpha < 0.05$ and is indicated by: * effect of exercise on urinary α1-AGP excretion; ** difference between groups at post-60 minutes; and *** difference between placebo and placebo + acetazolamide for Δ α1-AGP (**Fig. 5.3e**) or trend ($p = 0.059$) of difference (for Δ α1-AGP) between baseline and first altitude exercise tests in the losartan group (**Fig. 5.3d**).

5.3.4.4. Altitude (placebo vs placebo + acetazolamide)

Results for comparisons of post-exercise α1-AGP between placebo and placebo + acetazolamide are presented in (**Table 5.2** and **Table 5.3**; **Figure 5.3c** and **Figure 5.3e**). As with placebo, altitude exercise tests, placebo + acetazolamide exercise resulted in an increase in urinary α1-AGP excretion ($\chi^2(3) = 10.73$, $p = 0.01$, **Figure 5.3c**). Despite similar exercise peak power outputs (**Table 5.2**) between placebo and placebo + acetazolamide tests, post-exercise α1-AGP excretion (at 60 min post-exercise) was significantly lower following placebo + acetazolamide exercise ($p = 0.025$, **Figure 5.3c**). Exercise-induced increases in α1-AGP excretion (Δ α1-AGP from pre- to post-60 minutes) were significantly reduced ($p = 0.036$) with acetazolamide by nearly three-fold (**Figure 5.3e**). These changes were not correlated (r = -0.10, $p = 0.82$) with the significant improvements in pre-exercise SpO_2 or SpO_2 at W_{max} with acetazolamide administration (**Table 5.3**).

5.4. DISCUSSION

Compared to sea-level and despite substantial systemic hypoxia at W_{max}, post-exercise α1-AGP excretion was not greater at altitude suggesting that hypoxia is not the primary mechanism. Altitude-related reductions in exercise intensity could, in part, explain this result[398], but would fail to explain the increased likelihood for post-exercise α1-AGP to be lower with losartan compared to placebo when exercise intensities were similar. It had been expected that losartan would mitigate BP amplifications and thus lower post-exercise α1-AGP, however no difference in the BP response to exercise was observed between groups. Therefore, there was no evidence to attribute post-exercise α1-AGP responses to alterations in blood[399] or peritubular pressures[400].

The direct action of ARBs within the glomerular filtration barrier on AT1s of podocytes[198] could provide an alternative explanation. Activation of AT1s on podocytes induces heparanase expression, which promotes the cleavage of heparan sulphate and inhibits the production and secretion of heparan sulphate proteoglycans (HSPGs)[401]. The net result is neutralisation of the negatively charged HSPGs, which limits the charge-selective function of the glomerular basement membrane (GBM)[402]. Blocking AT1s with losartan thus, promotes the localised retention of negatively charged proteins at the GBM[203] and limits the charge-selectivity impairment[403] which, in the present study, manifests as a reduction in the extent of post-exercise α1-AGP. This hypothesis is consistent with findings related to the intensity-dependent increases in angiotensin-II[404] and exercise-related increases in α1-AGP[405], although further investigations are required.

Despite being performed at similar workload, post-exercise α1-AGP appeared lower following acetazolamide with these reductions being, curiously, unrelated to the significant improvement in SpO_2 observed during exercise. On its own, this could provide further support indicating that hypoxia was not the primary mechanism for post-exercise proteinuria. Unfortunately, the effects of acetazolamide on post-exercise α1-AGP could not be separated from any acclimatisation effect. Thus, no definitive conclusion regarding acetazolamide's effects on post-exercise proteinuria can be provided. Nonetheless, unchanged exercise performance following acetazolamide administration despite improvements in oxygen saturation supports the possibility that acetazolamide may limit performance[396 406 407]. Future research is required to evaluate acetazolamide-related changes in: 1) post-exercise proteinuria; and 2) exercise performance during ascent. The latter question was addressed in a follow-up publication from this expedition[408].

5.4.1. Limitations and future directions

The inability to control for extraneous variables (e.g., activity, sleep, environmental conditions), as well as, low participant numbers were weaknesses of the present study but are common limitations for such field-based research[409]. Not controlled for were the inter-individual variability[7] and between-day variations in α1-AGP excretion, which could have impacted results. Future research could be strengthened by incorporating a sea-level control arm that compared post-exercise proteinuria between exercise tests executed 48-hours apart. Benefit could also be gained by using a less complex design and avoiding overlapping factors (e.g., acclimatisation status and time course of exercise tests in this case). Lastly, further research is needed in order to confirm the relationship between DBP and 24-hour α1-AGP excretion.

5.5. CONCLUSION

The present findings suggest that post-exercise urinary α1-AGP is: 1) more related to exercise intensity rather than degree of hypoxia or BP, and 2) possibly influenced by the activation or inhibition of AT1 receptors (via administration of losartan). Losartan may act to limit post-exercise proteinuria by helping to maintain the charge-selectivity function in the glomerular filter, although further investigations are required to confirm this.

Given the complexity of the present design (e.g., administration of two drug treatments; two exercise sessions performed days apart at altitude) and limitations associated with field-based research it was difficult to distinguish between the relative mechanism(s) for exercise- and altitude-induced urinary α1-AGP excretion. Therefore, a chamber-based cross-over comparison (normoxia vs hypoxia) was planned and will be described in the next chapter.

Chapter 6

POST-EXERCISE URINARY ALPHA-1 ACID GLYCOPROTEIN IS DEPENDENT ON EXERCISE INTENSITY.

Data from this chapter was presented at the 24th Annual European College of Sport Science Congress in Prague, Czechia in 2019 (see reference below) with the full manuscript from this chapter currently being prepared for Journal of Exercise Physiology.

Joyce KE, Balanos G, Fountain A, Bradwell AR, Lucas SJE. Hypoxia does not influence post-exercise proteinuria. *24th Annual European College of Sport Science Congress*, Prague, Czechia. 2019.

Statement of contribution:

Author contributions for the above abstract were as follows. KEJ – Design, recruitment, data collection, statistical analysis, and writing; SJEL – Concept and design, data collection, and writing; GB – Concept and design, delivery of hypoxic ventilatory response tests, and data collection; AF – Assistance with immunoturbidimetric urinalysis; ARB – writing. Additional contributions to the full-length manuscript were made by Mr Chris Bradley, who led the delivery and analysis of hypoxic ventilatory response tests.

ABSTRACT

INTRODUCTION: Proteinuria is a transient physiologic phenomenon that occurs with a range of physical activities and during ascent to altitude. Exercise intensity appears to largely dictate the magnitude of post-exercise proteinuria, however evidence also indicates possible contributions from exercise-induced hypoxaemia or reoxygenation. Utilising an environmental hypoxic chamber, this crossover designed study aimed to evaluate urinary alpha-1 acid glycoprotein (α1-AGP) excretion surrounding exercise experiments to assess the contribution(s) of hypoxia to post-exercise proteinuria. We hypothesised that the systemic hypoxia would augment post-exercise urinary α1-AGP compared to normoxic exercise despite lower absolute exercise intensity. **METHODS**: Sixteen individuals underwent experimental sessions in normoxia (NOR; 20.9% O_2) and hypoxia (HYP; 12.0% O_2). Sessions began with a 2-hour priming period before completing a graded maximal exercise test (GXT) on a cycle ergometer, which was followed by continuation of exposure for an additional 2 hours. Physiologic responses (i.e., systolic and diastolic blood pressure; heart rate; and peripheral oxygenation, SpO_2) and Lake Louise Scores were recorded with urine specimens also collected (analysed for albumin and α1-AGP) surrounding GXT at 30-minute intervals (e.g., pre- and post-exercise at 30, 60, and 120 minutes). **RESULTS:** As expected, exercise intensity was significantly reduced in HYP (193 ± 45 W) compared to NOR (249 ± 59 W; $p < 0.001$). Contrary to our hypothesis, post-exercise urinary α1-AGP was greater in NOR (20.04 ± 14.84 μg/min) compared to HYP (15.08 ± 13.46 μg/min), albeit the difference at post-30 minutes was not significant ($p = 0.233$). Changes in post-exercise urinary α1-AGP (from pre- to post-30 minutes) were not related to physiologic responses or performance outcomes observed during exercise in NOR or HYP. **CONCLUSION**: Profound systemic hypoxia does not alter exercise-induced increases in urinary α1-AGP.

6.1. INTRODUCTION

Glomerular proteinuria is a transient physiologic phenomenon that occurs in healthy individuals following exercise[6] and during ascent to altitude[149 155]. Exhibited across a range of physical activities (e.g., swimming[410], running[411], boxing[412], and rowing[413]), it can be characterised by increases in urinary albumin or alpha-1 acid glycoprotein (α1-AGP)[6 7 335], a potentially more sensitive marker[155]. Exercise intensity ultimately dictates the degree of the post-exercise increases[398 11], although the mechanism(s) for this are not well understood. Intermittent exercise has been shown to elicit greater increases in proteinuria compared to continuous exercise[414], implicating a possible contribution from exercise-induced hypoxaemia[268 415] (or reoxygenation). This is supported by findings from altitude studies that have shown relationships between urinary α1-AGP and arterial oxygenation (SaO_2)[7] and arterial blood gases (PO_2, PCO_2, and HCO_3^-)[335].

Altitude exercise has presented a way to explore the involvement of hypoxaemia in the development of post-exercise glomerular proteinuria. Given that hypoxia may potentiate additional contributors proposed for post-exercise proteinuria, such as, disruptions in acid-base balance[398 9], increases in blood pressure (via changes in catecholamines[416] or renin-angiotensin-aldosterone-system components[335 404 187]), or increases in oxidative stress[417 12], proteinuria following altitude exercise could be expected to exceed that after a sea-level equivalent bout. Some studies support this notion[13] while other, more recent, altitude field-based studies do not[335]. Thus, further evaluation is required for improved understanding of the impact of hypoxaemia on post-exercise glomerular proteinuria. In these pursuits, hypoxic ventilatory response (HVR) may be worthy of consideration, especially since it relates to the degree of hypoxaemia exhibited with exercise at altitude[418].

The objective of the present study was to evaluate the contribution(s) of hypoxia to post-exercise proteinuria by measuring urinary α1-AGP excretion following maximal exercise in an environmental chamber. Investigations aimed to examine: 1) the time course and degree of urinary α1-AGP excretion surrounding exercise in normoxia (NOR) and hypoxia (HYP); 2) physiologic responses to exercise in NOR and HYP in relation to post-exercise urinary α1-AGP excretion; and 3) whether any associations existed between hypoxic ventilatory response (HVR) test outcomes and the degree of post-exercise urinary α1-AGP (exhibited in NOR vs HYP).

6.2. METHODS

6.2.1. Ethical approval and recruitment

Ethical approval was granted by the University of Birmingham (ERN_18-1270). Participants were recruited from the public via advertising or by word of mouth. Written informed consent was obtained prior to participation with consented participants completing a general health history questionnaire prior to inclusion. Only healthy individuals without any signs, symptoms, or history of cardiovascular, pulmonary, renal, or metabolic disease were included. Individuals who reported: 1) active pharmacotherapy; 2) actively being under the care of a GP (for any reason); or 3) current smoking (or recent history of quitting) were also excluded[419]. If a participant became hypertensive (systolic or diastolic blood pressure, SBP or DBP, ≥ 140 mm Hg or ≥ 90 mm Hg, respectively)[420] or tachycardic (heart rate > 100 bpm) at rest (following repeat measurements)* during any session, they were withdrawn. Participants were also free to withdrawal at any time on their own volition.

* If the average of two automated sphymomanometry measurements (performed ≥ 5 minutes apart) exceeded indicated limits, manual sphymomanometry was used to confirm. If manual measurements were also greater than the upper limit, the participant was withdrawn. The purpose of using the automated cuff was to promote uniformity of repeat measurements performed throughout the session. For consistency, the first automated measurement was included in analysis.

6.2.2. Study design

All participants first completed a familiarisation session that included a graded incremental maximal exercise test (GXT) in ambient conditions (see section **6.2.3**). A randomised crossover design was then adopted with all participants completing two experimental sessions (NOR and HYP; see next section) each consisting of physiologic response measurements, a GXT, and timed urine collections (see section **6.2.5**). Resting control trials and an HVR tests were also completed, albeit only in a subset of participants (see section **6.2.6**) in order to balance realism with the expectations of each participant (e.g., time commitments; familiarisation: ~1 hour + NOR and HYP sessions: ~4.5 hours ea.). For all sessions participants were asked to refrain from: 1) partaking in strenuous exercise or consuming alcoholic beverages in the 24-hours prior; and 2) consuming caffeine in the 4-hours prior. All sessions were separated by no less than 48-hours.

6.2.3. Experimental and control sessions

The intervention timeline for experimental sessions (NOR, 20.9% O_2; and HYP, ~12.0% O_2)* performed in an environmental chamber (Sporting Edge UK, Basingstoke, UK) is outlined in **Figure 6.1**. Participants were blinded to condition wherever possible (e.g., by using sham hypoxia for NOR sessions[421]). Sessions consisted of a pre-exercise 2-hour priming exposure (upright seated) before completing a GXT that lasted ~15 min, which was followed by a continuation of exposure for an additional 2 hours (total session duration, ~4.5 hours). Resting control sessions were identical to experimental sessions with the exception of GXT, which was substituted by a time-controlled resting period (familiarisation GXT duration used as duration for this resting period). If at any point a participant felt too unwell to continue, presented with

* Refer to **Appendix 5** and accompanying **Supplemental Equation 1** (***Steps 1 – 4***) for target O_2 estimations for HYP sessions.

moderate or severe symptoms of acute mountain sickness (AMS; Lake Louise Score, LLS, > 5[422]), or requested to leave the chamber for any reason, they were removed immediately.

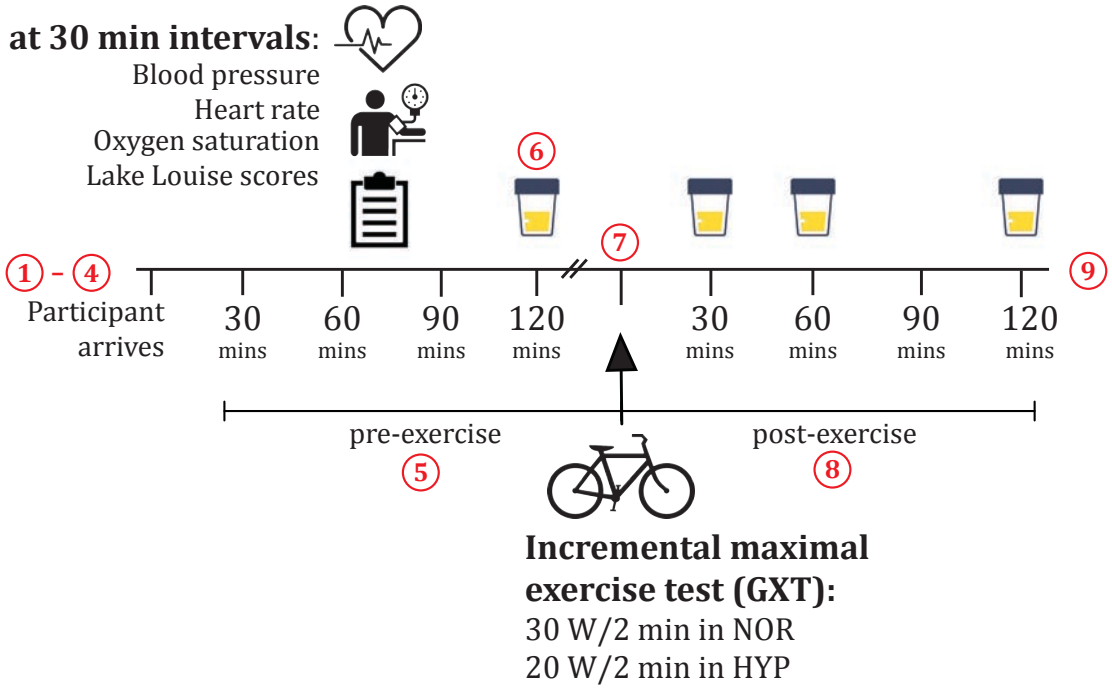

Figure 6.1 – Experimental session timeline. Detailed schematic for the conduct of resting control trials and experimental sessions in normoxia (NOR) and hypoxic (HYP). Sessions were identical other than graded incremental maximal exercise (GXT) being substituted by a resting period (length of familiarisation GXT) for resting control trials. Each session was conducted in accordance with the following: 1) participant arrived and underwent 10 to 15 minutes of seated rest; 2) 'baseline' (sea-level) physiologic response outcomes (heart rate, systolic and diastolic blood pressures, peripheral oxygenation, and Lake Louise Scores) were recorded; 3) participant asked to empty their bladder in order to start clock for timed urine collections; 4) participant entered the chamber; 5) participant encouraged to drink at least 500 ml in the 2 hours leading up to GXT during which physiologic response outcomes were recorded at 30-minute intervals; 6) urine specimens collected immediately pre-exercise; 7) GXT was administered with staged increases adjusted for condition (30 W vs 20 W/2 min; NOR and HYP, respectively; to standardise test duration between conditions) and physiologic response outcomes recorded throughout (every 1 to 2 minutes; refer to section **6.2.4**); 8) post-exercise physiologic response outcomes and timed urine specimens collected 30, 60, and 120 minutes following GXT; and 9) participant exited the environmental chamber and was monitored for approximately 15 minutes (and up to one hour) prior to departure.

Peripheral oxygenation (SpO_2; via finger pulse oximetry; $WristOx_2$, Model 3150, Nonin Medical Inc., Plymouth, MN, USA), heart rate (HR; via 3-lead electrocardiogram, ECG), SBP and DBP (via automated sphygmomanometry of the brachial artery; Tango M2 Stress Monitor,

SunTech Medical, Morrisville, NC, USA), mean arterial pressure (MAP, mm Hg; estimated as, (SBP + 2 × DBP) ÷ 3), and LLS[422] were measured: upon arrival; at 30-minute intervals throughout experimental sessions; and for at least 15 minutes (and up to 1 hour) following each session. Urine specimens were also collected throughout these sessions as outlined in section **6.2.5.1**.

6.2.4. Graded incremental maximal exercise tests (GXTs)

Graded exercise tests were conducted on an upright cycle ergometer (Velotron, Quarq Technology, Spearfish, SD, USA) and initiated with a 3-minute warm-up performed at 50 watts (W) with a target rating of perceived exertion (RPE) of 14 using the Borg Scale[423]. This warm-up was followed by the first 2-minute stage (at 60 W) with wattage increased every two minutes thereafter by 30 W or 20 W (for NOR or HYP, respectively) until volitional fatigue[424] or an RPE of 20 was achieved. Exercise tests were ended with an unloaded, self-paced cool-down lasting approximately 3 to 5 minutes*.

Blood lactate (BLa) was measured immediately before and after GXT from blood obtained by finger prick (Lactate Plus, Nova Biomedical, Waltham, MA, USA). SpO_2 and HR were recorded each minute throughout GXT while power output (in watts), SBP, DBP, and RPE were recorded at the end of each 2-minute stage. Performance (maximal power output, W_{max}) and physiologic response outcomes (SBP, DBP, MAP, HR_{max}, and SpO_2) were recorded at max with 'peak' (maximum) and 'nadir' (minimum) values (e.g., SBP_{peak}, DBP_{peak}, RPE_{peak}, and SpO_{2nadir}) encountered during GXT also reported.

* To ensure maximal effort was achieved for NOR and HYP exercise tests, the anticipated W_{max} for each condition was estimated from familiarisation W_{max} (NOR = 100% of familiarisation W_{max} and HYP = ~70 – 80% of familiarisation W_{max}).

6.2.5. Urine experiments

6.2.5.1. Specimen collection and handling

To mark the start of timed collections, participants were asked to empty their bladder (not collected) within 15 to 20 minutes of arrival and prior to entering the environmental chamber. All urine produced thereafter was collected into 3,000 ml, UV-protected, polyethylene, vesicle designed for human urine collections (SARSTEDT, Nümbrecht, Germany). Separate containers used for each timed collection with specimens collected immediately pre-exercise (arrival to pre-exercise; ~2 hours) and at the following timepoints following exercise: post-30 minutes (pre-exercise to post-30 minutes; length of GXT + 30 minutes); post-60 minutes (post-30 to post-60-minutes; 30 minutes), and post-120 minutes (post-60 to post-120 minutes; 60 minutes; see **Figure 6.1**). Volume (ml), weight (g), and time of collection were recorded immediately following collection for each specimen with a sample (20 ml) then aliquoted into a conical centrifuge tube and temporarily stored on ice (~0 °C) until the end of the session, when all samples were centrifuged (5,400 rpm at 21 °C) for 10 minutes[425], rendering them acellular. Supernatants from these samples were further aliquoted into 2 ml microcentrifuge tubes (4 × replicates) and frozen at –80 °C until urinalysis.

6.2.5.2. Urinalysis

Urine specimens were thawed in a warming cabinet (37 °C)[283 288] for approximately 1 hour prior urinalysis. Specimens were analysed: 1) in triplicate for α1-AGP utilising an immunoturbidimetric assay (measuring range: 0.08 to 148.20 mg/l; refer to **Chapter 3** for assay details) and 2) in singlet for albumin using commercially available kits (The Binding Site, Ltd., Birmingham, UK), which contained high- and low- controls, calibrator, and the reagent (measuring range: 11 – 66,500 mg/l). Both assays were performed on the Optilite™ auto-

analyser (The Binding Site, Ltd., Birmingham, UK). Triplicate [α1-AGP] results were used in conjunction with specimen volume (or weight) and collection duration to estimate α1-AGP excretion rate (μg/min). Triplicate excretion rates for each specimen were then averaged with this result used for statistical analysis. Change (Δ) in α1-AGP was estimated as the difference between pre-exercise and post-30 minutes excretion rates.

6.2.6. Hypoxic ventilatory response (HVR) tests

An additional visit was undertaken among a subset of participants (n = 6) to assess their HVR. HVR tests were administered via a dynamic end-tidal forcing (DEF) system (v1, BreathDP, University of Oxford) using a stepped, isocapnic-hypoxia protocol[426 427] (see **Figure 6.2**). Tests began with participants seated at rest while breathing ambient room air for 5 minutes via a mouthpiece connected to the DEF, which allowed ventilation to stabilise. During this resting period, 'baseline' partial pressure of end-tidal CO_2 ($P_{ET}CO_2$) was recorded. Next, a series of 3-minute stepped decreases in the partial pressure of end-tidal oxygen ($P_{ET}O_2$) were administered (at 100 mm Hg, 65 mm Hg, and 55 mm Hg) with $P_{ET}CO_2$ clamped ~1 mm Hg above 'baseline' throughout. Three-minute steps were followed by a final 5-minute step at 100 mm Hg $P_{ET}O_2$ with (total test duration, ~20 minutes). Measures of ventilation (tidal volume; respiratory rate; and minute ventilation, $\dot{V}_E$), SpO_2, and HR (via 3-lead ECG) were recorded continuously throughout.

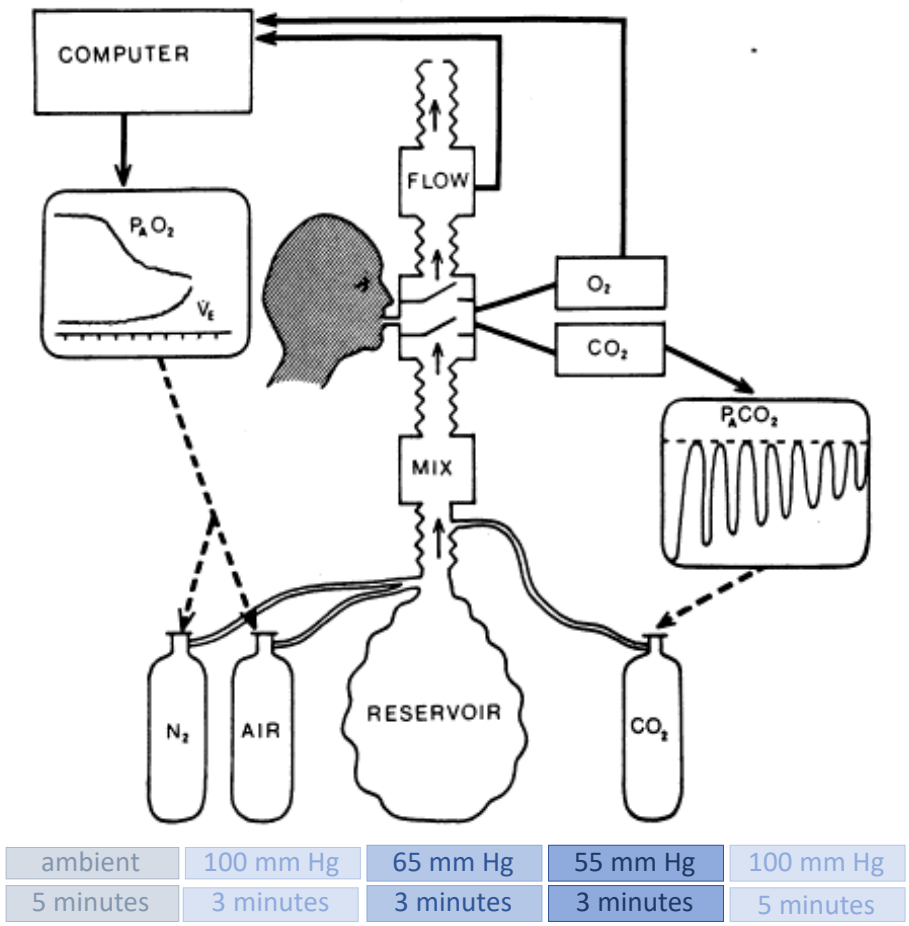

Figure 6.2 – Hypoxic ventilatory response (HVR) test. Fig 6.2a (top) – Depiction of the method used to administer HVR tests executed using the dynamic end-tidal forcing system*; **Fig. 6.2b (bottom)** – Timeline of isocpanic-hypoxia steps administered during HVR tests occurring at the following partial pressures of end-tidal oxygen ($P_{ET}O_2$; mm Hg): 100 mm Hg, 65 mm Hg, and 55 mm Hg. Partial pressure of end-tidal carbon dioxide ($P_{ET}CO_2$) was clamped at ~1 mm Hg above the observed resting $P_{ET}CO_2$ throughout all hypoxic steps. * Adopted from Weil JV, Byrne-Quinn E, Sodal IE, et al. Hypoxic ventilatory drive in normal man. *J Clin Invest*. 1970;49(6):1061-1072[426].

Thirty-second averages were estimated for $\dot{V}_E$, SpO_2, and V_E/SpO_2 (l/min/%) and plotted as a function of time for the three isocapnic-hypoxic steps. V_E/SpO_2 represented the relationship between the 30-second average values for $\dot{V}_E$ and SpO_2 at each 30-second interval, whereas $\dot{V}_E/SpO_2$ slope (or $\Delta\dot{V}_E/\Delta SpO_2$) represented the slope of the best-fit line plotted (within individuals) from the linear regression ($\dot{V}_E$, y-axis; and SpO_2, x-axis) across all steps[428 429 430]. Peak $\dot{V}_E$ (l/min), minimum SpO_2 (%), and mean values for $\dot{V}_E$, SpO_2, and $\dot{V}_E/SpO_2$ were reported for each step while $\dot{V}_E/SpO_2$ slope ($\Delta\dot{V}_E/\Delta SpO_2$) was reported for the entire HVR test

(accounting for all three steps). By convention, $\dot{V}_E/SpO_2$ slopes were presented as absolute values with actual values used for statistical analysis. Void of missing data for all steps, repeated measures ANOVA with Tukey's *post hoc* test was used to compare HVR outcomes between isocpanic-hypoxic steps.

6.2.7. Statistical analysis

Normality of distribution was assessed using Shapiro-Wilk test for each outcome measure with data log-transformed where possible and outliers removed (using ROUT method) where appropriate (for normally distributed data) prior to analysis. Analysis of urinary α1-AGP excretion was performed for log-transformed values (as described in **Chapter 5**) with absolute excretion rates also reported.

Mixed-effects model was utilised to evaluate the main effects of condition (i.e., NOR vs HYP) and time for physiologic responses (e.g., SBP, DBP, HR, and SpO_2) and urinary proteins (i.e., α1-AGP or albumin) with: 1) Tukey's *post hoc* test for multiple comparisons between 30-minute interval measurements; 2) Šidák's correction for multiple comparisons between conditions at 30-minute intervals; or 3) Dunnett's test for multiple comparisons against an initial measurement (e.g., pre-exercise vs post- 30, 60, and 120 minutes). To compare GXT outcomes between conditions, singular physiologic (e.g., SBP_{peak} or HR_{max}), performance (e.g., W_{max}), and urinary measures (e.g., Δ α1-AGP) were compared using paired t-tests (or Wilcoxon signed ranks tests). Statistical analysis for HVR test outcomes is outlined in section **6.2.6**.

Correlation analysis (Pearson or Spearman where appropriate*) was performed for log(post-30) and log(Δ) α1-AGP excretion with *a priori* comparisons facilitated between

* Pearson correlation was used for parametric data while Spearman rho was used for nonparametric data or variables with a small dataset (i.e. HVR test outcomes for the subset only).

performance and physiologic response outcomes from GXTs (e.g., $W_{max,}$ SBP_{peak}, DBP_{peak}, or HR_{max}), as well as, HVR test outcomes (e.g., peak $\dot{V}_E$ or $\Delta\dot{V}_E/\Delta SpO_2$). *p*-values were presented in table format with corresponding Pearson r (or Spearman rho) and R^2 (from linear regression) reported only for significant results.

Statistical tests were performed using SPSS Statistics (v25 for Mac iOS, IBM, Armonk, NY, USA) or Prism (v8.3.0 for Mac iOS, Graphpad Software Inc., San Diego, CA, USA) with data presented as mean ± standard deviation (SD) unless otherwise indicated. All statistical tests were two-tailed with significance set to $\alpha < 0.05$ and adjusted *p*-values presented with appropriate corrections applied (as outlined above).

6.3. RESULTS

Eighteen individuals were enrolled with sixteen (n = 16; 8 males, 8 females) university-aged (21.1 ± 1.3 years) participants successfully completing both exercise experimental sessions. Attrition was attributed to dropout (× 1; for personal reasons) and researcher-initiated withdrawal (× 1; hypertension at rest during HYP session) with data collected from withdrawn participants excluded from statistical analysis. A subset of seven individuals also completed resting control trials with 6 of 7 also completing the HVR test.

6.3.1. Experimental and control session

Physiologic responses for the entire cohort (n = 16) from NOR and HYP sessions are presented in **Figure 6.3** with measurements from resting control trials (for the subset) outlined in **Appendix 6.** Despite the significant effect of condition for SpO_2 ($p < 0.001$; **Figure 6.3a**), HYP sessions were well tolerated with AMS symptoms at 30-minute intervals mostly being minimal (i.e., LLS < 3; mean of all measurements, 0.714 ± 0.781) or mild (i.e., LLS of 3 to 5 points)

apart from one moderate score (i.e. LLS of 6 to 9 points) reported at the end of an HYP session (i.e., at post-120 minutes). No participants required premature removal from the environmental chamber. A significant effect of time ($p < 0.001$) and condition ($p = 0.006$), but not interaction ($p = 0.054$), were observed for HR (**Figure 6.3b**). A significant effect of time ($p = 0.017$) but not condition ($p = 0.771$) or interaction ($p = 0.242$) were observed for DBP (**Figure 6.3c**). No significant effects of condition, time, or interaction (all $p > 0.05$) were observed for SBP (**Figure 6.3d**).

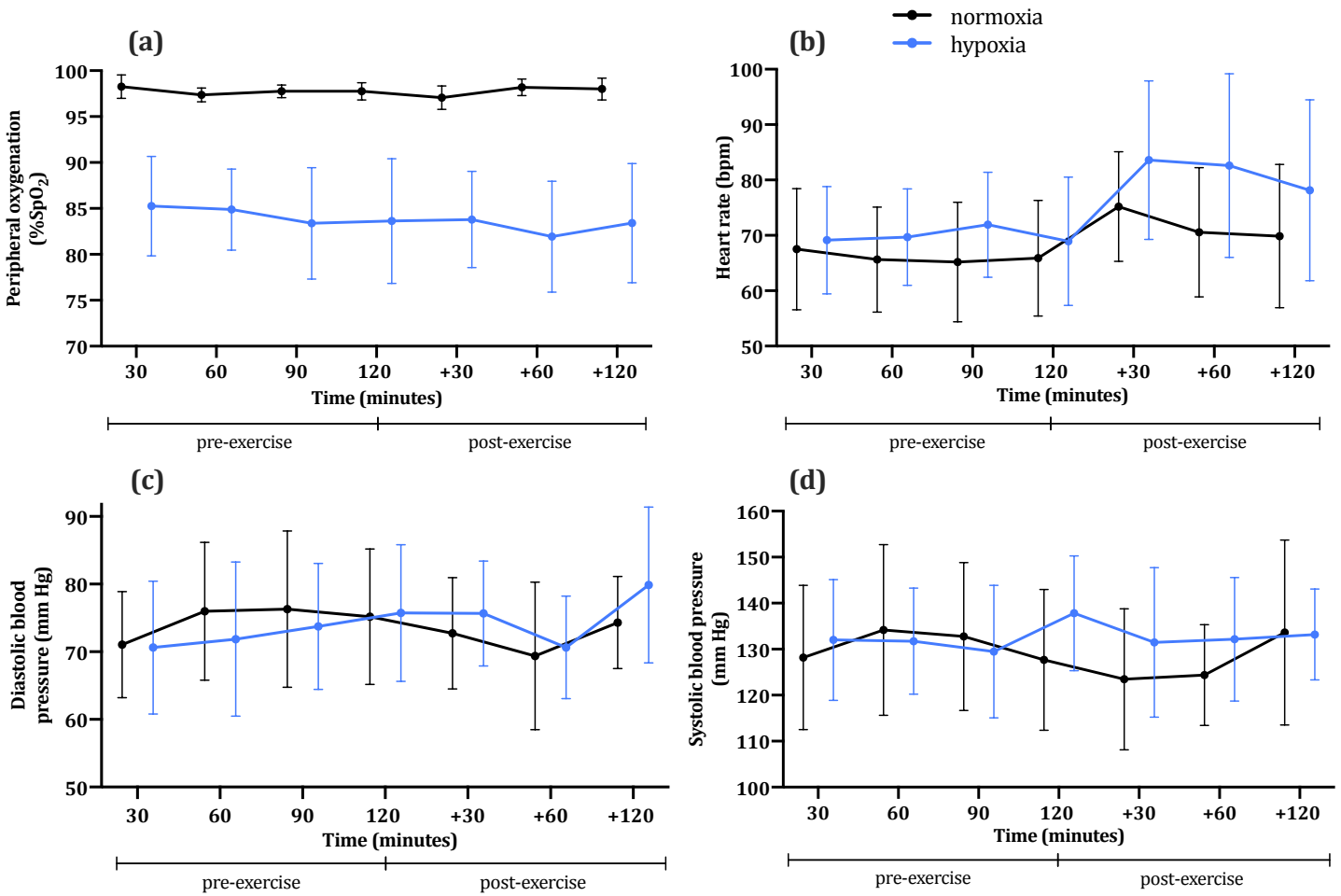

Figure 6.3 – Physiologic measurements during normoxic (NOR) vs hypoxic (HYP) sessions. Fig. 6.3a (top left) – Peripheral oxygenation (SpO_2). A significant effect of condition ($p < 0.001$) but not time ($p = 0.368$) or interaction ($p = 0.161$) was observed for SpO_2; **Fig. 6.3b (top right)** – Heart rate (HR). Significant effects of time ($p < 0.001$) and condition ($p = 0.006$), but not interaction ($p = 0.054$), were observed for HR; **Fig. 6.3c (bottom left)** – Diastolic blood pressure (DBP). A significant effect of time ($p = 0.017$) but not condition ($p = 0.771$) or interaction ($p = 0.242$) were observed for DBP; **Fig. 6.3d (bottom right)** – Systolic blood pressure (SBP). No significant effects of condition ($p = 0.181$), time ($p = 0.398$), or interaction ($p = 0.149$) were observed for SBP. Mixed effects analysis was used to evaluate main effects of condition (NOR vs HYP) and time (across 30-minute intervals). Data are presented as mean ± standard deviation (SD; error bars) with NOR and HYP data interleaved for clarity. All statistical tests were two-tailed with significance set to $\alpha < 0.05$.

6.3.2. Maximal exercise tests

Results from paired *t*-tests (or Wilcoxon tests) for GXT performance and physiologic response outcomes are presented in **Table 6.1**. As expected, SpO_{2max}, SpO_{2nadir}, and W_{max} were significantly lower in HYP compared to NOR (both, $p < 0.001$) while SBP_{max} and MAP_{max} were significantly greater in HYP compared to NOR (both, $p < 0.05$). DBP_{max}, **DBP_{peak}, SBP_{peak}** HR_{max}, RPE, Δ BLa, and ambient CO_2 were no different between NOR and HYP.

Table 6.1 – Performance and physiologic response outcomes from maximal exercise tests performed in normoxia and hypoxia.

	Normoxia	Hypoxia	*p*-value
W_{max} (W)	249 ± 59	193 ± 45	< 0.001*
SpO_{2max}(%)	95 ± 3	80 ± 5	< 0.001* †
SpO_{2nadir} (%)	94 ± 3	75 ± 5	< 0.001* †
HR_{max} (bpm)	183 ± 15	183 ± 13	0.942†
SBP_{max} (mm Hg)	175 ± 36	198 ± 25	0.039*
SBP_{peak} (mm Hg)	188 ± 31	203 ± 29	0.172
DBP_{max} (mm Hg)	78 ± 12	80 ± 16	0.605
DBP_{peak} (mm Hg)	79 ± 14	90 ± 18	0.091†
MAP_{max} (mm Hg)	110 ± 14	119 ± 16	0.049*
RPE	19 ± 2	19 ± 2	0.973†
Ambient CO_2 (ppm)	868 ± 200	837 ± 413	-
Δ BLa (mmol/l)	6.23 ± 7.37	6.24 ± 4.02	0.996

Data are presented as mean ± SD. 'Max' subscript is representative of measurements that were obtained at the time maximal power output was achieved while 'peak' and 'nadir' values are representative of maximum or minimum measurements, respectively, encountered throughout the exercise test. Δ BLa referred to the change in blood lactate from pre- to post-exercise. Paired samples *t*-tests (or Wilcoxon's signed rank test, indicated by '†') were used to perform comparisons between normoxia vs hypoxia with significant differences marked by asterisk (*). All statistical tests were two-tailed with significance set to $\alpha < 0.05$. W_{max}, maximal power output; SpO_2, peripheral oxygenation; HR, heart rate; SBP, systolic blood pressure; DBP, diastolic blood pressure; MAP, mean arterial pressure; RPE, rating of perceived exertion (Borg Scale[423]); and CO_2, ambient carbon dioxide.

6.3.3. Urinalysis

A total of 112 urine specimens were successfully collected from the 128 possible timepoints for experimental sessions* with an additional 24 specimens collected from the 28 possible timepoints for resting control sessions†. From the grand total of 136 specimens (from the total 156 possible timepoints), urinalysis for α1-AGP was successful in 95.6% of specimens while urinalysis for albumin was only successful in 23.7% of specimens.

Urinary α1-AGP excretion rates from resting control trials and NOR and HYP sessions are presented in **Table 6.2**‡. Pre-exercise urinary α1-AGP was no different between conditions (NOR, 2.80 ± 2.18 μg/min vs HYP, 2.93 ± 3.76 μg/min; $p = 0.959$, **Table 6.2**). By comparison, urinary α1-AGP was significantly greater at post-30 minutes in both NOR (20.04 ± 14.84 μg/min; $p < 0.001$) and HYP (15.08 ± 13.46 μg/min; $p = 0.001$; **Figure 6.4a**) making the significant main effect of time ($p < 0.001$) unsurprising. Despite urinary α1-AGP being greater at post-30 minutes in NOR, the difference between conditions was not significant ($p = 0.532$; **Table 6.2**) nor was a main effect of condition ($p = 0.223$; **Figure 6.4a**) or interaction ($p = 0.802$) observed. Similarly, Δ α1-AGP was no different between conditions, despite being greater in NOR (15.09 ± 14.77 μg/min) compared to HYP (11.22 ± 14.71 μg/min; $p = 0.233$; **Figure 6.4b**).

* NOR and HYP sessions: 16 participants × 4 timepoints/session × 2 sessions (NOR and HYP) = 128 possible timepoints.

† Resting control: 7 participants × 4 possible timepoints × 1 session = 28 possible timepoints.

‡ It would be remiss to present only log-transformed values for urinary α1-AGP excretion rates as this would limit practical applications, as well as, comparisons with existing literature. Likewise, it would be inappropriate to perform statistical analysis that assumes normality of the distribution for those data that are known to be lognormal. Thus, to balance these factors the absolute urinary α1-AGP excretion rates were presented with *p*-values presented for corresponding statistical analysis of the log-transformed data.

Table 6.2 – Urinary alpha-1 acid glycoprotein (α1-AGP) excretion surrounding exercise tests.

Collection timepoint	Rest (n = 7)	Normoxia (n = 16)	Hypoxia (n = 16)	*p*-value
pre-exercise	2.36 ± 3.92	2.80 ± 2.18	2.93 ± 3.76	-
		(0.32 ± 0.37)	(0.23 ± 0.47)	0.959
post-30 minutes	1.16 ± 0.70	20.04 ± 14.84	15.08 ± 13.46	-
		(1.19 ± 0.34)	(0.97 ± 0.48)	0.532
post-60 minutes	1.29 ± 0.66	6.66 ± 5.47	3.93 ± 2.52	-
		(0.62 ± 0.50)	(0.51 ± 0.30	0.956
post-120 minutes	1.47 ± 0.52	3.79 ± 2.04	3.34 ± 1.97	-
		(0.47 ± 0.39)	(0.42 ± 0.37)	0.995

Urinary α1-AGP excretion rates (μg/min) are presented as mean ± standard deviation (SD) with the corresponding log-transformed mean ± SD indicated below in parenthesis. Mixed-effects analysis with relevant *post hoc* tests (see section **6.2.7**) was used to compare log(α1-AGP) excretion between conditions and timepoints (across 30-minute intervals). All statistical tests were two-tailed with significance set to $\alpha < 0.05$ and adjusted *p*-values presented.

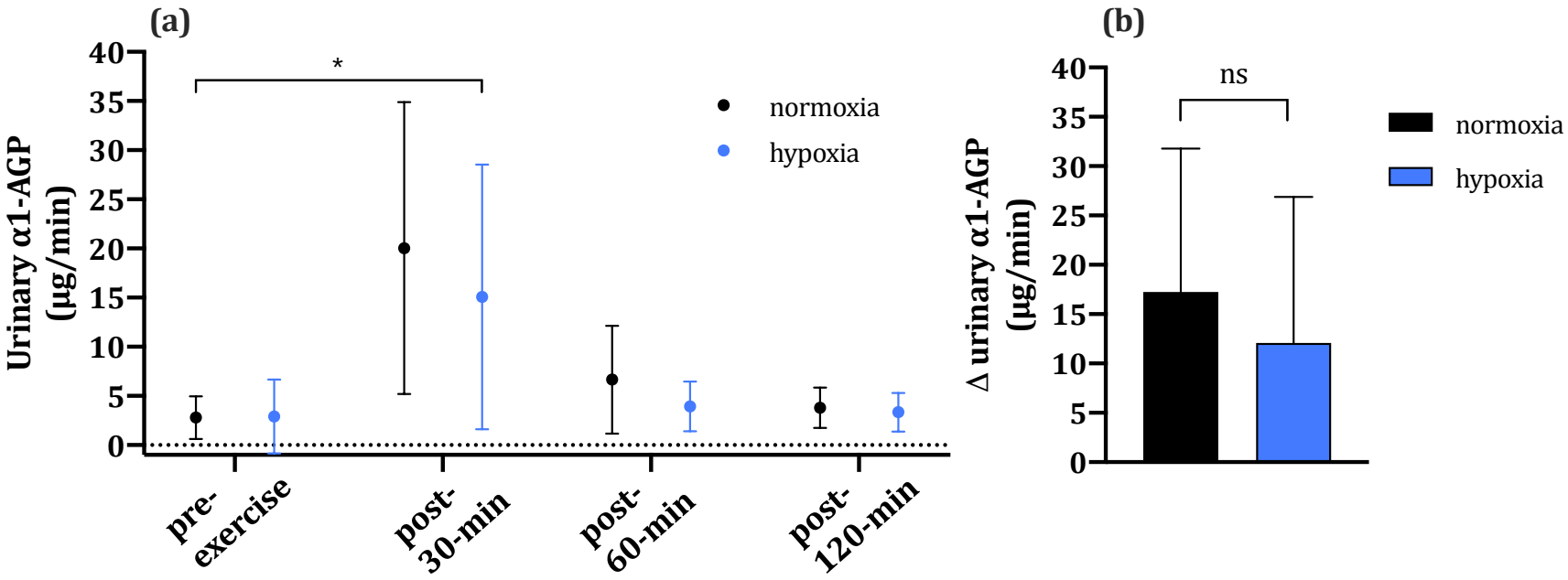

Figure 6.4 – Urinary alpha-1 acid glycoprotein (α1-AGP) excretion before and after maximal exercise. Fig 6.4a (left) – Urinary α1-AGP excretion rates (μg/min) from 30-minute interval collections surrounding exercise tests performed in normoxia (NOR) and hypoxia (HYP) are plotted as mean ± standard deviation (SD; error bars). Mixed-effects analysis (with Dunnett's test; see section **6.2.7**) was applied to corresponding log-transformed data for comparisons against pre-exercise excretion (for post- 30, 60, and 120 minutes) and between conditions at each timepoint (with Šidák's correction). Significant increases in α1-AGP excretion compared to pre-exercise were detected at post-30 minutes only for both, NOR ($p < 0.001$) and HYP ($p = 0.001$) sessions (marked by asterisk, *); **Fig. 6.4b (right)** – Change (Δ) in urinary α1-AGP excretion (μg/min) from pre- to post-30 minutes. Δ α1-AGP was greater in NOR (15.09 ± 14.77 μg/min) vs HYP (11.22 ± 14.71 μg/min), albeit the difference between conditions for log(Δ α1-AGP) was not significant (ns; $p = 0.233$). All statistical tests were two-tailed with significance set to $\alpha < 0.05$ and adjusted p-values presented.

6.3.4. HVR tests

Individual data for 30-second averages of $\dot{V}_E$, SpO_2, and $\dot{V}_E/SpO_2$ were plotted across time for the three isocapnic-hypoxic steps and are presented in **Figure 6.5a – 6.5c**.

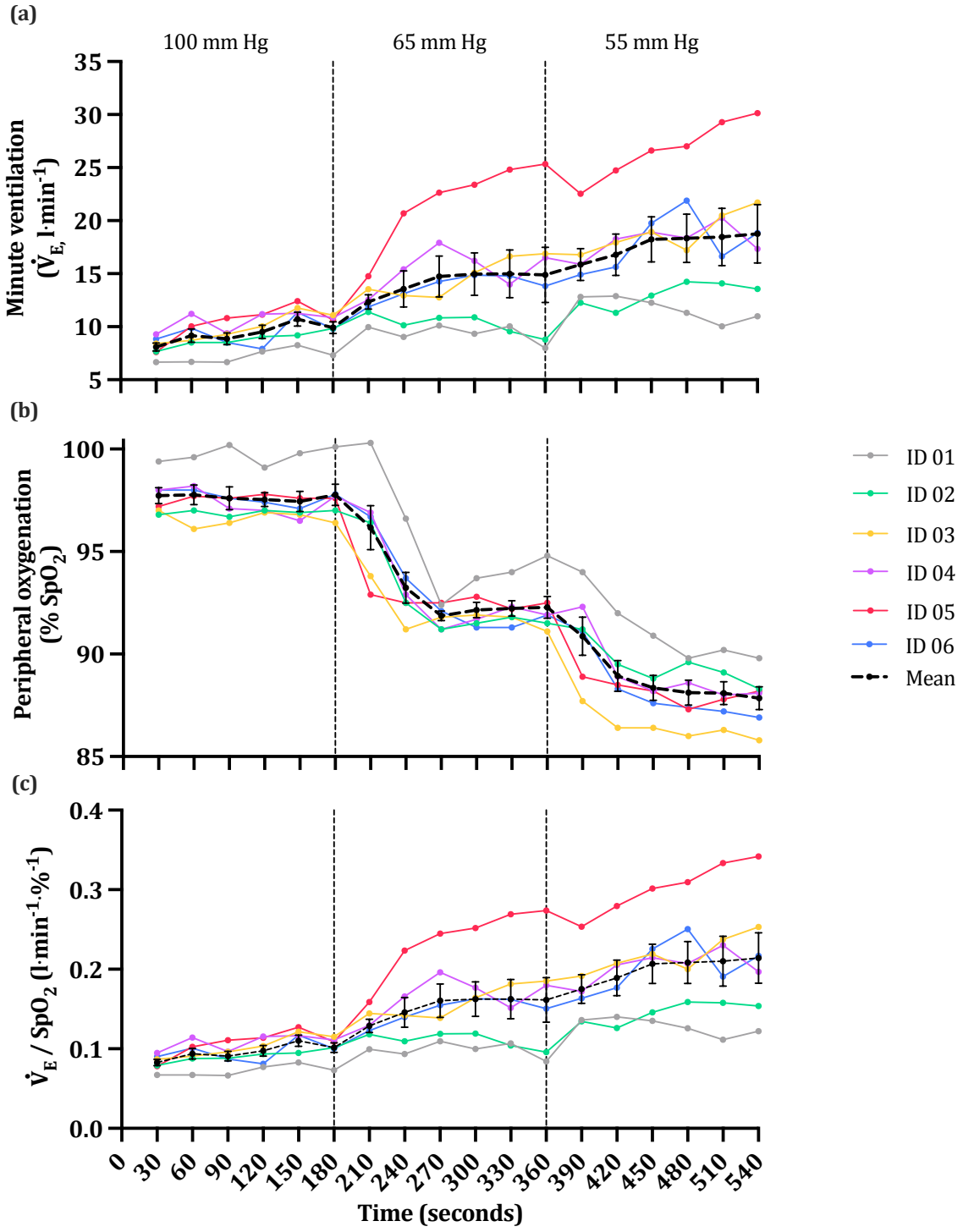

Figure 6.5 – Hypoxic ventilatory response (HVR) tests. Fig. 6.5a (top) – Minute ventilation ($\dot{V}_E$; **Fig. 6.5b (middle)** – Peripheral oxygen saturation (SpO_2); and **Fig. 6.5c (bottom)** – $\dot{V}_E/SpO_2$ (l/min/%). Data are plotted as the 30-second averages across three isocapnic-hypoxic steps at the following partial pressures of end-tidal oxygen ($P_{ET}O_2$): 100 mm Hg, 65 mm Hg, and 55 mm Hg.

Descriptive statistics for V_E and SpO_2 from isocpanic-hypoxic steps are presented in **Table 6.3**. Mean $\dot{V}_E$ (17.74 ± 5.30 l/min) and peak $\dot{V}_E$ (23.18 ± 7.43 l/min) were greatest for the 55 mm Hg whereas mean SpO_2 (89 ± 2%) and minimum SpO_2 (88 ± 1%) were lowest for the 55 mm Hg step. V_E/SpO_2 was greatest for the 55 mm Hg step (0.201 ± 0.061 l/min/%).

Table 6.3 – Hypoxic ventilatory response (HVR) test outcomes.

	$\dot{V}_E$ (l/min)		SpO_2 (%)		$\dot{V}_E/SpO_2$ (l/min/%)
	Peak	*Mean*	*Minimum*	*Mean*	*Mean*
100 mm Hg	12.51 ± 2.01	9.37 ± 1.25	96 ± 1	98 ± 1	0.096 ± 0.016
65 mm Hg	19.34 ± 7.19	14.25 ± 4.47	91 ± 1	93 ± 1	0.154 ± 0.050
55 mm Hg	23.18 ± 7.43	17.74 ± 5.30	88 ± 1	89 ± 2	0.201 ± 0.061
***p*-value**	0.007*	0.006*	< 0.001*	< 0.001*	0.008*

HVR test outcomes included: minute ventilation (V_E) and peripheral oxygenation (SpO_2). Data are presented as mean ± standard deviation (SD; unless otherwise indicated) for a subset (n = 6) of participants. 'Peak' and 'minimum' values were recorded from unaveraged recordings for all isocapnic-hypoxic steps (partial pressures of end-tidal oxygen ($P_{ET}O_2$): 100 mm Hg, 65 mm Hg, and 55 mm Hg) while 'mean' values represented the average ± SD of 30-second measurements within the respective step. $\dot{V}_E/SpO_2$ data in this table represented the direct relationship between $\dot{V}_E$ and SpO_2 for each step (estimated from 30-second interval data). By contrast, $\dot{V}_E/SpO_2$ slope (or $\Delta\dot{V}_E/\Delta SpO_2$; as shown in **Figure 6.6**) represented the relationship between these two variables by applying a linear regression to 30-second interval data for all steps. Repeated measures ANOVA with Tukey's *post hoc* test was used to compare outcomes between isocapnic-hypoxic steps. All statistical tests were two-tailed with significance set to $\alpha < 0.05$ and differences between steps marked by asterisk, *.

The dynamic relationship between $\dot{V}_E$ and SpO_2 for HVR tests was best illustrated by plotting $\dot{V}_E$ (y-axis) as a function of SpO_2 (x-axis) across all steps and applying a linear regression analysis for individual data (see **Figure 6.6**).

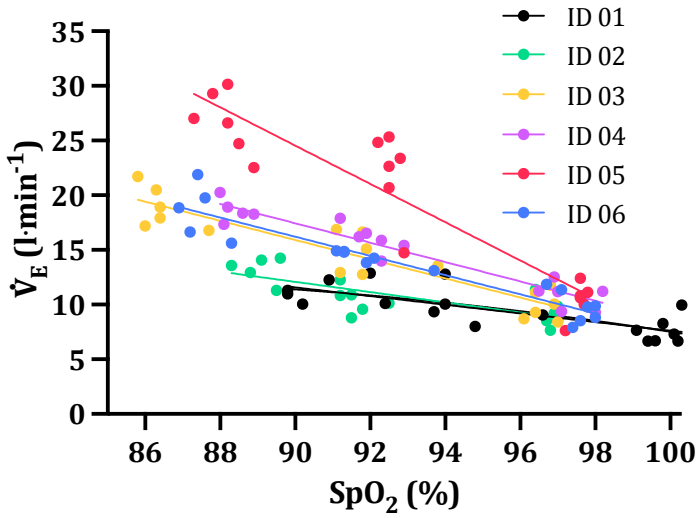

ID No.	$\dot{V}_E$/SpO2 slope	y-intercept	R^2
ID 01	0.396 (–0.57 to -0.22)	47.19 (30.54 to 63.85)	0.591
ID 02	0.468 (–0.67 to -0.27)	54.22 (35.63 to 72.80)	0.607
ID 03	0.877 (–1.07 to -0.69)	94.83 (77.40 to 112.30)	0.857
ID 04	0.887 (–1.03 to -0.75)	97.24 (84.38 to 110.10)	0.921
ID 05	1.751 (–2.14 to -1.37)	182.10 (146.30 to 217.90)	0.853
ID 06	0.877 (–1.05 to -0.71)	95.14 (79.26 to 111.00)	0.881

Figure 6.6 – Linear regression analysis for minute ventilation ($\dot{V}_E$) and peripheral oxygenation (SpO_2). Thirty-second averages for V_E (y-axis) and SpO_2 (x-axis) from hypoxic ventilatory response (HVR) tests are plotted for all isocapnic-hypoxic steps (partial pressures of end-tidal oxygen: 100 mm Hg, 65 mm Hg, and 55 mm Hg). Linear regression was applied to individual data (indicated by colour) with the slopes, y-intercepts, and R^2 values (indicated in legend) of the best-fit lines representative of $\dot{V}_E/SpO_2$ slope (or $\Delta\dot{V}_E/\Delta SpO_2$). By convention, $\dot{V}_E/SpO_2$ slopes are presented (in the legend) as absolute values (positive integers), although y-intercepts and 95% confidence intervals (CIs) are presented as actual values.

6.3.5. Correlation analysis

Results from correlation analyses are presented in **Table 6.4**. Significant positive relationships were observed between log(Δ α1-AGP) and SBP at max (p = 0.045; R^2 = 0.317) and MAP at max (p = 0.044; R^2 = 0.319) in HYP only. No other performance, physiologic response, or HVR test outcomes were related to α1-AGP for either condition (**Table 6.4**). Of note, however, was the participant exhibiting the uncharacteristically elevated HVR ('ID 05' shown in red in **Figure 6.5a – 6.5c** and **Figure 6.6**) whom also was the only participant to exhibit greater post-30-minute α1-AGP excretion in HYP (absolute, 33.70 μg/min; Δ 31.56 μg/min;) than NOR (absolute, 27.74 μg/min; Δ 26.26 μg/min), despite a reduction in W_{max} (33% reduction) that was greater than that of the group (23 ± 7% reduction). This participant also exhibited the highest MAP at max (148 mm Hg) out of group in HYP.

Table 6.4 – Correlation analysis results for post-exercise alpha-1 acid glycoprotein (α1-AGP) excretion.

	Normoxia		**Hypoxia**	
	log(post-30)	log(Δ)	log(post-30)	log(Δ)
Exercise tests				
W_{max}	0.347	0.450	0.234	0.129
SpO_{2max}	0.520†	0. 508†	0.184†	0.398†
SpO_{2nadir}	0.533†	0.533†	0.961	0.438†
HR_{max}	0.816†	0. 573†	0.892†	0.867†
SBP_{max}	0.674	0.726	0.072	0.045**
SBP_{peak}	0.436	0.489	0.176	0.121
DBP_{max}	0.458	0.477	0.554	0.501
DBP_{peak}	0.586†	0. 713†	0.849†	0.539†
MAP_{max}	0.996	0.954	0.069	0.044**
HVR tests				
Peak $\dot{\mathbf{V}}_{\mathbf{E}}$	0.564†	0.497†	0.714†	0.714†
Minimum SpO_2	0.803†	0.919†	0.497†	0.497†
$\dot{\mathbf{V}}_{\mathbf{E}}/SpO_2$ slope	0.497†	0.419†	0.564†	0.564†

Pearson or Spearman (*p*-values marked by †) correlation was performed for log-transformed post-30-minute or change (Δ; from pre- to post-30 minutes) α1-AGP excretion rates and performance and physiologic response outcomes from exercise tests, as well as, hypoxic ventilatory responses (HVR) test outcomes. Linear regression was applied for those variables demonstrating a significant relationship in order to further assess. Significant relationships were evident between log(Δ) and SBP at max ($r = 0.563$, $R^2 = 0.317$), as well as, MAP ($r = 0.564$; $R^2 = 0.319$) for hypoxia only. All statistical tests were two-tailed with significance set to $\alpha < 0.05$. Significant results were marked by double asterisk, **. W_{max}, maximal power output; HR_{max}, maximal heart rate; SBP, systolic blood pressure; DBP, diastolic blood pressure; MAP, mean arterial pressure; and $\dot{V}_E$, minute ventilation; peripheral oxygenation, SpO_2; $\dot{V}_E/SpO_2$ slope (or $\Delta\dot{V}_E/\Delta SpO_2$), slope of the best-fit line plotted from the simple linear regression for data from all three isocapnic-hypoxic steps.

6.4. DISCUSSION

The purpose of this study was to assess the contribution(s) of hypoxia to post-exercise proteinuria by evaluating urinary α1-AGP excretion surrounding exercise. To facilitate this, physiologic responses and urinary α1-AGP excretion were measured during and surrounding

exercise tests performed in NOR and HYP. An additional aim was to determine whether any association existed between HVR and the degree of post-exercise urinary α1-AGP exhibited (in NOR or HYP).

The superior sensitivity of urinary α1-AGP over albumin for evaluations of post-exercise glomerular proteinuria was demonstrated and enabled by the novel turbidimetric immunoassay for urinary α1-AGP (described in **Chapter 3**), notwithstanding the unknown reason for low measurability of urinary albumin. As expected, HYP exercise potently stimulated hypoxaemia. However, despite marked reductions in SpO_2 with HYP exercise and controlling for exercise duration, post-exercise urinary α1-AGP excretion was, on average, lower in HYP compared to NOR (refer to **Table 6.2**). Further, no correlations were observed between post-exercise α1-AGP excretion and the degree of desaturation during exercise or any HVR test outcomes (refer to **Table 6.4**). Despite HVR outcomes not being correlated with post-exercise α1-AGP excretion, findings from HVR tests were interesting with three types of responders reflected (as highlighted in **Figure 6.5a – 6.5c**). Taken together, this evidence indicates that post-exercise urinary α1-AGP excretion cannot be directly attributed to hypoxia.

The coupling between desaturation and attenuated post-exercise α1-AGP excretion in HYP observed in this study supports earlier cycling-based studies that have demonstrated similar reductions[335] (refer to **Chapter 5**) or unchanged[148] post-exercise excretion in hypoxia. The present observations were attributed to the concomitant reductions in exercise performance that are known to accompany hypoxic exercise[431], which have, in part, been attributed to reductions in blood flow to the working limbs[432]. It could be suggested that in response to vigorous hypoxia (i.e., with maximal exercise in HYP), an alteration in the redistribution of blood flow occurs, promoting such a balance between glomerular blood flow and pressure[433 110] that proteinuria is not favoured to the same extent as with NOR exercise (or

different exercise intensities[13]). This implicates the likely role of renal haemodynamics (or closely associated factors) in the progression of post-exercise glomerular proteinuria[390]. Development of significant relationships between post-exercise α1-AGP and SBP at max, as well as, MAP at max in HYP, despite attenuated α1-AGP excretion in the face of higher pressures (SBP and MAP at max), further supports this and highlights the appropriation of intrinsic control. This should, however, be considered on balance with findings from **Chapter 5** (i.e., the absence of any significant difference between losartan and placebo for post-exercise α1-AGP in HYP). As such, a delicate balance likely exists between the many factors that govern renal haemodynnamics with one or more of these factors having the potential to also, independently, influence post-exercise proteinuria.

Misappropriation of renal haemodynamics (or related physiologic factors) can provide an explanation for the *increase* in post-exercise α1-AGP in HYP (compared to NOR) that occurred in the participant with the highest HVR (and greatest LLS), despite a reduction in power output. It was assumed that an augmented HVR would minimise post-exercise proteinuria in HYP by limiting the degree of hypoxaemia[418] or increasing exercise performance limitations[434]. However, in HYP, a high HVR may perpetuate post-exercise proteinuria by heightening the competition for blood flow[435] [436] between exercising muscles, ventilatory muscles, and the kidneys, and by disrupting the balance between factors closely linked with renal haemodynamics (e.g., . Whether this pattern was physiologic or pathophysiologic[437] [438] remains unclear and further investigations are required for any such distinction.

6.4.1. Limitations and future directions

Inability to report performance outcomes (e.g., exercise intensity) in relative measures (e.g., W/kg or VO_{2max} in ml/kg/min) is an obvious limitation and likely the cause for the absence

of any significant relationship between power output and post-exercise α1-AGP. Nevertheless, the purpose of this study was not to specifically evaluate the effect of intensity but rather to evaluate the effect of hypoxaemia by delivering a potent hypoxic stimulus (i.e., maximal exercise in hypoxia). Moreover, the proteinuric effect of such hypoxic exercise was expected to transcend that of intensity.

BLa measurements were repeatedly unsuccessful, being particularly problematic in HYP. Frequency of device failure in both conditions contributed to many missing data points with measurements for pre- and post-exercise in both NOR and HYP only successful in a subset of participants (n = 7). Notwithstanding the known biases of the Lactate Pro[439] [440], device performance was disappointing and future studies wishing to evaluate any contribution from BLa (or acid-base disruptions) to glomerular proteinuria would be advised to utilise alternative devices or methods[441].

Building upon the findings herein and to improve the understanding surrounding the contribution of renal haemodynamics, future researchers may consider: 1) analysing additional physiologic markers of sympathetic nerve activation (e.g., plasma epinephrine or norepinephrine)[442] [443], glomerular endothelial permeability (e.g., urinary glycosaminoglycans)[444] [445], and renal oxidative stress or antioxidant status (e.g., antioxidant enzymes or total antioxidant capacity)[446] [447]; and 2) measurements of renal blood flow (e.g., non-radioactive microsphere[448] [449]), perfusion[390] (e.g., using near-infrared spectroscopy, NIRS[450]) or oxygen demand[451].

6.5. CONCLUSION

Findings demonstrate the utility of immunoturbidimetric analysis for urinary α1-AGP and examinations of post-exercise proteinuria. Despite profound systemic hypoxaemia,

exercise-induced increases urinary α1-AGP excretion appear to be dictated by exercise intensity. With this, closer examinations of altitude-induced proteinuria during ascent were planned with additional consideration given to nocturnal oxygenation (as described in the next chapter).

Chapter 7

URINARY ALPHA-1 ACID GLYCOPROTEIN AS A BIOMARKER OF ACCLIMATISATION DURING ASCENT TO ALTITUDE.

Data presented within this chapter was submitted as an abstract and accepted for oral presentation at the 2021 International Society of Mountain Medicine conference. The full-length manuscript is currently being prepared for the SLEEP Journal:

> **Joyce KE**, Delamere J, Ashdown K, Bradley C, Malein W, Letchford A, Lock H, Thomas O, Bradwell AR, and Lucas SJE. 'Nocturnal saturation variance is related to Lake Louise Scores during ascent to 4,800 m'. *In preparation.*

Statement of contribution:

KEJ – concept, design, data collection (urine and arterialised specimens and nocturnal oximetry recordings), biomarker analysis (for serum and urine), statistical analysis, and writing; JD – concept and data collection; KA – data collection and writing; CB – data collection; WM and AL – morning medical examinations; OT, data collection and medical oversight; HL – data collection and morning medical examinations; AR – concept and design; and SJEL – concept, data collection, and writing.

ABSTRACT

INTRODUCTION: Utilising urinary alpha-1 acid glycoprotein (α1-AGP) as a sensitive marker of altitude-induced proteinuria, the objective of this study was to evaluate 24-hour and early-morning α1-AGP excretion during ascent to HA along with physiologic responses, blood and urine biomarkers, and nocturnal pulse oximetry. **METHODS:** Eighteen participants (36 ± 16 years) ascended over 11 days to 4,800 m near the Zema Glacier at the base of Kanchenjunga. Twenty-four-hour and early morning urine (EMU) specimens were collected daily and frozen (–80 °C) until urinalysis, which was conducted for α1-AGP utilising automated immunoturbidimetry (0.08 – 148.20 mg/l). Physiologic responses (e.g., heart rate and BP) were recorded daily with additional physiologic measurements (e.g., arterial blood gases) performed on select days. Peripheral oxygenation (%SpO_2) was recorded continuously overnight throughout (WristOx, Model 3150, Nonin Medical) with artifact-free recordings used to generate relative and cumulative frequency plots, assess statistical moments (e.g., mean, kurtosis proper, skew, variance), and evaluate desaturation characteristics (e.g., oxygen desaturation index, ODI). **RESULTS:** α1-AGP excretion in 24-hour (mg/24-hours) and EMU (mg/mmol$_{\alpha1\text{-AGP:CREA}}$) specimens were significantly elevated throughout ascent compared to baseline (1.093 ± 0.582 mg/24-hours and 0.025 ± 0.016 mg/mmol$_{\alpha1\text{-AGP:CREA}}$, respectively; both, $p < 0.001$). Twenty-four-hour excretion was greatest (6.461 ± 5.212 mg/24-hours) during the first 24 hours at 4,800 m and EMU excretion was greatest (0.205 ± 0.169 mg/mmol$_{\alpha1\text{-AGP:CREA}}$) the first morning at 4,800 m. Twenty-four-hour and EMU α1-AGP excretion measurements correlated well ($p < 0.001$, r = 0.758). Mean nocturnal SpO_2 decreased with ascent ($p < 0.001$) while nocturnal SpO_2 variance ($p < 0.001$), skew ($p = 0.034$), kurtosis proper ($p = 0.029$), and ODI ($p < 0.001$) increased. mg/24-hours was strongly correlated with altitude ($p < 0.001$, r =

0.824) and nocturnal pulse oximetry measures; specifically: mean SpO_2 ($p < 0.001$, r = –0.932), ODI ($p < 0.001$, r = 0.945), and SpO_2 variance ($p < 0.001$, r = 0.825). Similarly, $mg/mmol_{\alpha 1\text{-}AGP:CREA}$ was correlated with nocturnal measures; specifically: mean SpO_2 ($p = 0.023$, r = –0.548), SpO_2 variance ($p = 0.001$, r = 0.523, and ODI ($p = 0.004$, r = 0.665). A significant difference between individuals scoring positive vs negative for acute mountain sickness (AMS) was observed for α1-AGP excretion (AMS^+: 5.91 [1.55 – 9.17] mg/24-hours vs AMS^-: 1.99 [1.26 – 3.67] mg/24-hours; $p = 0.001$). **DISCUSSION:** Glomerular proteinuria, marked by α1-AGP excretion (mg/24-hours and $mg/mmol_{\alpha 1\text{-}AGP:CREA}$), is significantly increased during ascent to altitude. These increases are related to alterations in nocturnal oxygenation also observed during ascent, and showed potential clinical significance in relation to the presentation of AMS during ascent.

7.1. INTRODUCTION

Excretion of plasma proteins into the urine (i.e., proteinuria) can occur as a product of acute or chronic (patho)physiologic response to glomerular or tubular compromise. Urinary alpha-1 acid glycoprotein (α1-AGP) is but one of such proteins and has proven to be a sensitive marker of glomerular leak during ascent to high-altitude (HA)[7 154]. Many potential mechanisms have been outlined for altitude-induced proteinuria[155] with the role of hypoxia having been suggested[7 183].

Associations between hypoxia-related sleep disturbances and proteinuria have been demonstrated at sea-level[452]. Further, these nocturnal disturbances are exacerbated with ascent[229 453], potentially, due to the greater hypoxia exhibited overnight[454]. The magnitude of hypoxia, exaggerated with HA-exercise, however, has produced conflicting results (refer to **Chapter 5** and **6**) making the mechanisms for altitude-induced proteinuria unclear. Despite this, no investigations of the relationship between nocturnal oxygenation and altitude-induced proteinuria during ascent appear in the literature. This literature gap is likely a product of the feasibility and practicality of measuring the necessary components to evaluate this question (e.g., 24-hour urine specimens) and presents a unique challenge for this type of field-based research.

Previous altitude studies related to urinary α1-AGP have collected 24-hour urine specimens[7], although early morning urine (EMU) specimens may, more appropriately, assess the impact of hypoxia, which is greatest overnight. EMU specimens are also more feasible and practical in the HA environment. Despite the agreement between 24-hour and EMU measurements of urinary α1-AGP at sea-level (described in **Chapter 4**), the consistency between these two specimens for urinary α1-AGP measurements in the context of

(patho)physiologic adaption(s) that occur during ascent is largely unknown. Thus, a comparison of urinary α1-AGP measurements between 24-hour and EMU specimens collected during ascent is also warranted.

In addition to urinary measures, evaluation of the impact of hypoxia on altitude-induced proteinuria requires the direct assessment of the hypoxic stimulus. Pulse oximetry presents a simple way to measure peripheral oxygenation (SpO_2) and has previously proven useful during ascent[455 456]. The most appropriate methodology for collecting pulse oximetry data at HA, however, is less clear. In the past, collections at HA have largely been performed over short-durations (30 to 60 seconds[457]) with these measurements being further limited to a singular metric (e.g., 95% SpO_2). Such short-duration measurements unfortunately fail to capture vital data (e.g., nocturnal oxygenation) that are relevant to HA illnesses[458 459], and that are of interest in relation to altitude-induced proteinuria. By contrast, longer duration measurements (e.g., nocturnal recordings), which appear to be feasible at HA[460 461], would be more advantageous. Specifically, nocturnal SpO_2 recordings enable the capture of data related to oxygenation patterns[14 462 463] and saturation morphology[464 465 466 467], which may assist the detection of (mal)adaption to altitude[456 468 14]. Additional derivatives of these nocturnal recordings (e.g., total sleep time spent below 80% saturation, TST < 80%[460 468]) may also be useful.

Therefore, the objective of the present study was to assess the impact of hypoxia on altitude-induced proteinuria. To do this, day-time physiologic responses (e.g., heart rate, blood pressure, serum inflammatory markers[469 149], and Lake Louise Scores, LLS), early-morning and 24-hour urinary proteins, and nocturnal $\%SpO_2$ (via finger pulse oximetry[470]) were measured during ascent to and descent from 4,800 m. Further, a specific aim of this study was to determine whether altitude-induced α1-AGP excretion is related to: 1) physiologic responses;

2) nocturnal oxygenation derivatives (e.g., oxygen desaturation index, mean SpO_2, nocturnal SpO_2 skew, kurtosis proper, or variance, to name a few); or 3) the presentation of acute mountain sickness (AMS; determined by LLS)[471] during ascent to HA. An additional aim was to determine whether measurements of urinary α1-AGP during ascent were comparable between early-morning and 24-hour urine specimens.

7.2. METHODS

Ethical approval for the present study was obtained through the University of Birmingham (ERN_19-0325) and was conducted in accordance with guidelines set by the Declaration of Helsinki, as well as, the '*STAR Data Reporting Guidelines for Clinical High Altitude Research*'[472], which is specific to HA research.

7.2.1. Location, setting, and ascent profile

Expedition profile and accompanying camp altitudes are presented in **Figure 7.1**. Participants ascended to 4,800 m in the northeastern Indian Himalaya near the Zema Glacier at the base of Kanchenjunga. The expedition began with an 11-day ascent from Gangtok (1,650 m), Sikkim, India (morning 06 October – morning 18 October, 2019), which was followed by a 6-day descent from top camp (4,800 m) back to Gangtok (late-morning 18 October to end-of-day 23 October, 2019). Ascent and descent both included some vehicular transport (as indicated in **Figure 7.1**), although transit was predominantly biped (per unit time). Trekking duration and load carriages were variable between days and individuals. A vegetarian diet (low-to-moderate protein) was adopted by all participants from 10 to 19 October, 2019* and fluid intake was ad libitum throughout (not recorded).

* Meat options were available on 2 to 3 days throughout.

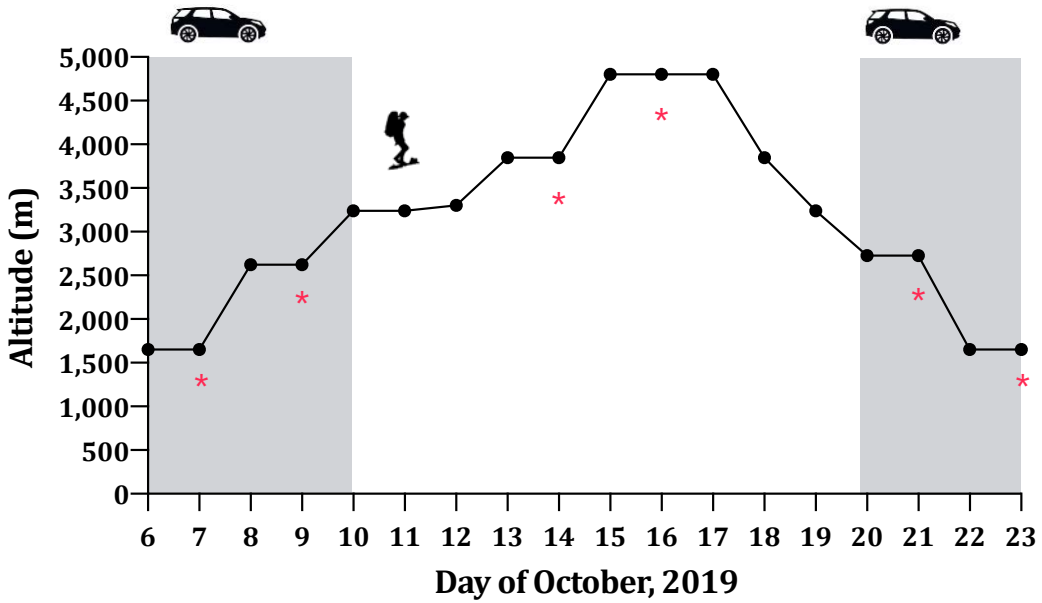

Day of October	Location	Waking altitude (m)	Sleeping altitude (m)
Baseline	Birmingham	~130	~130
6	Gangtok	440	1,650
7	Gangtok	1,650	1,650
8	Lachung	1,650	2,624
9	Lachung	2,624	2,624
10	Thalem	2,624	3,240
11	Thalem	3,240	3,240
12	Jakthang	3,240	3,300
13	Yabuk	3,300	3,850
14	Yabuk	3,850	3,850
15	top camp	3,850	4,800
16	top camp	4,800	4,800
17	top camp	4,800	4,800
18	Yabuk	4,800	3,850
19	Thalem	3,850	3,240
20	Lachen	3,240	2,728
21	Lachen	2,728	2,728
22	Gangtok	2,728	1,650
23	Gangtok	1,650	1,650

Figure 7.1 – Expedition profile. This figure outlines the 11-day ascent to a top camp (4,800 m) near the Zema glacier at the base of Kanchenjunga in northeastern Indian Himalaya (Sikkim, India) followed by a 6-day descent. Expedition dates were 06 October – 23 October, 2019 with morning 06 October, 2019 initiated from Bagdogra, India (440 m). Shaded areas indicate vehicular transit days (by land) with all other transit days being biped. Nightly camp altitudes are presented in the accompanying legend. * Red asterisks indicate days on which arterialised blood samples were collected.

7.2.2. Participants and study design

Eighteen (7 females, 11 males) healthy lowland individuals (native to UK, USA, and New Zealand all with residence altitudes < 200 m) were included in the present study. Baseline characteristics were recorded in Birmingham, UK (~130 m) approximately 1 to 2 weeks prior to departure for Sikkim, and included: age, height, body weight, body mass index (BMI), estimated glomerular filtration rate (eGFR, **Equation 7.1**) [473], previous altitude exposures (exposure to > 2,500 m within the 3 to 5 months preceding the expedition), and history of severe altitude illness.

Equation 7.1 – Estimated glomerular filtration rate (eGFR). Adopted from Stevens LA, Coresh J, Schmid CH, et al. Estimating GFR using serum cystatin C alone and in combination with serum creatinine: a pooled analysis of 3,418 individuals with CKD. Am J Kidney Dis 2008;51(3):395-406[473].

$$eGFR = (127.7 \times CysC) - (1.17 \times age) - (0.13 \times 0.91_{if\ female} \times 1.06_{if\ black})$$

Where:

eGFR	= estimated glomerular filtration rate in units of ml/min/1.73 m^2;
CysC	= serum [cystatin C] (mg/l);
age	= age (in years) of participant;
0.91	= correction factor for sex;
1.06	= correction factor for ethnicity.

Altitude collections were initiated evening 06 October, 2019 (**Figure 7.1**) and were continued throughout the expedition (as outlined in proceeding sections) in accordance with the 'typical daily collection' presented in (**Figure 7.2**). Daily collections included: physiologic measures, venous blood specimens, urine specimens (24-hour and early morning mid-stream) and nightly pulse oximetry recordings (two nights for baseline) with arterialised earlobe specimens collected on pre-selected days as indicated in **Figure 7.1**. Each collection is outlined in the following sections.

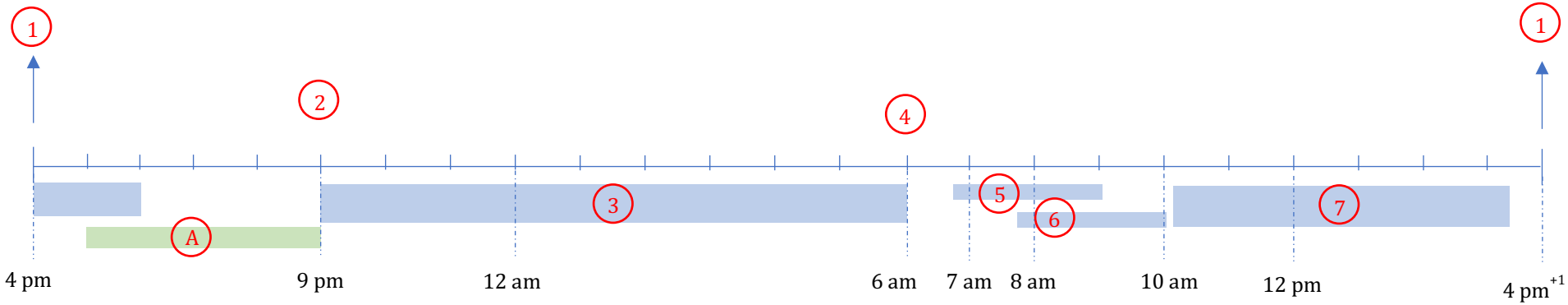

Blue shaded areas indicate research activities (and represented using numbers).

Green shaded areas indicate non-research activities, which were also important to the daily flow (and represented using letters).

1. **24-hour urine specimen collection** initiated (at 4 pm each day) with the previous day's specimen also collected and processed (typically took 1 to 2 hours).

A. **Evening camp routine** to include meals and social time.

2. **Evening Lake Louise Scores**; collected prior to going to bed (i.e. between 8 to 10 pm depending).

3. **Nocturnal pulse oximetry**. Collected for the duration of the night whilst asleep.

4. **Early morning urine** specimens; collected as mid-stream catch from the first void upon waking.

5. **Venous blood sample collection.**

6. **Morning medical evaluations** during which HR, BP, and SpO_2 measurements were collected.

7. **Trekking or other daily activities.** Daily trekking was initiated after completion of morning medical evaluations.

Figure 7.2 – Timeline of daily activities. Timeline presented illustrates a typical day on the expedition. Daily experimentation included: 24-hour urine collections (from 4pm to 4pm^{+1}), early morning mid-stream urine collections, medical evaluations, venous blood collections. Medical evaluations included measurements for: blood pressure (BP), heart rate (HR), 30 to 90-second momentary peripheral oxygenation (SpO_2), morning Lake Louise Scores (LLS), respiratory rate, and collection of the PM self-report LLS questionnaires from previous nights (recorded each night, collected every other morning). Morning iSTAT measurements (not pictured) were collected in rotation with venous blood collections on days indicated in **Figure 7.1**.

7.2.3. Daily physiologic measurements and Lake Louise Scores (LLS)

Morning medical evaluations began on the morning of 07 October, were conducted daily, and continued through to the morning of 22 October, 2019. Measures obtained during these examinations included: systolic and diastolic blood pressures (SBP and DBP, respectively) (via manual sphygmomanometer), respiratory rate (RR, counted by visual examination of chest rise and fall over 30 seconds), body weight (Salter Scales), and heart rate (via pulse oximetry and verified with 30-second palpation). For medical safety, lung auscultations were also recording during these visits.

AMS was also assessed during these morning medical examinations via LLS[422] with participants recording an additional LLS each evening and these scores collected the following morning. Morning AMS scores were used to distinguish between AMS-positive (AMS^+), recognised as a total LLS > 3 including at least one (≥ 1) point for headache, and AMS-negative (AMS^-), recognised as a total score of < 3 with a headache score of 0[422].

7.2.4. Collection, processing, and analysis of biological specimens

7.2.4.1. Urine specimens

Early morning urine (EMU; midstream) and 24-hour urine specimens were collected at baseline and each day during the expedition. EMU specimens were collected upon waking from mid-stream urine into a 100 ml, clear, polypropylene specimen cup fitted with a high-density polyethylene screw-on lid (SARSTEDT, Nümbrecht, Germany). Approximately 10 ml of the EMU specimen was immediately pipetted into a centrifuge tube (conical, polypropylene[339]) and then centrifuged for approximately 10 minutes* at approximately 2,000 g (4,300 to 5,000

* In compliance with the Human Tissue Act 2004, urine specimens were centrifuged immediately following collection rendering them acelluar and thus, able to be stored upon return to the University of Birmingham.

rpm[425]) in the Heraeus® Labofuge® 200 centrifuge (Thermo Scientific, Waltham, Massachusetts, USA). Following centrifugation, 1.5 ml of specimen was aliquoted into four repeat 2 ml microcentrifuge tubes (polypropylene, with screw cap, freeze-able down to–90 °C) and frozen (using solid CO_2 at –80°C) within 30 to 90 minutes of collection[474]. Residual volumes from EMU collections were replaced into individuals' 24-hour urine collection pots.

Twenty-four-hour specimens were collected into 3,000 ml dark-brown, UV-protected, polyethylene containers fitted with a screw cap (SARSTEDT, Nümbrecht, Germany) containing 2 ml of sodium azide (0.1% solution) as a preservative. Twenty-four-hour collections began each day at 4 pm and continued until 4 pm the following day (4 pm^{+1}) (refer to **Figure 7.2**). Upon completion of 24-hour collections, specimen volumes (ml), weights (g) (Salter Kitchen weighing scales, calibrated prior to each weighing session), and collection durations were recorded. Following this, 10 ml of urine from each specimen was pipetted into 12 to 15 ml centrifuge tubes and centrifuged in accordance with the procedures outlined for EMU specimens. Following centrifugation, 1.5 ml of specimen was also aliquoted into four repeat 2 ml microcentrifuge tubes (polypropylene, with screw cap, freeze-able down to approx. –90 °C) and immediately frozen at –80 °C (using solid CO_2).

EMU and 24-hour specimens remained frozen at –80 °C (and out of sunlight) for the duration of the expedition and throughout transport back to the UK. Upon return, specimens were replaced into long-term freezer storage (also at –80 °C) where they remained for 2 to 6 weeks[329] until urinalysis.

7.2.4.1.1. Urinalysis for alpha-1 acid glycoprotein (α1-AGP)

Urinalysis for α1-AGP was conducted for 24-hour and EMU specimens using an immunoturbidimetric assay designed for the detection of low-concentration α1-AGP in human

urine (measuring range: 0.077 – 148.2 mg/l; refer to **Chapter 3**). No freeze-thaw cycles were permitted prior to urinalysis for α1-AGP.

Specimens were thawed for approximately 60 minutes in a warming cabinet (at 37°C)[283 288] prior to urinalysis of 24-hour specimens whilst the latex-enhanced reagent for the immunoturbidimetric assay was calibrated using the Optilite™ auto-analyser (Model 1.2, Software version 6.0.1, The Binding Site, Ltd., Birmingham, UK). European Reference Material DA470k/IFCC (α1-AGP, 617 mg/l; see **Appendix 2**) was used as calibrator. Control panel samples (three levels) were also analysed each day prior to initiation of urinalysis. All tests were performed using a single reagent lot, on a single Optilite™ analyser, at a single location, and by the same technician. Reagent disc temperatures were maintained between 3.0 to 5.0 °C throughout urinalysis.

Following calibration and analysis of control samples, thawed specimens were inverted, vortexed, aliquoted into specimen cups, and loaded into rack discs that were then loaded into the Optilite™ at ambient temperature (20 to 22 °C). Urine specimens (24-hour and EMU) were then analysed in triplicate for α1-AGP using the assay indicated above (run time, ~10 minutes). Individual participants' urine specimens (both, 24-hour and EMU) were analysed for α1-AGP together on a single day in order to limit any confounding influence of between-day imprecision on urinary results. Percent coefficient of variation (%CV) was calculated for each triplicate by dividing the standard deviation (SD) of the triplicate values by the triplicate mean and then multiplying by 100. If the %CV for any triplicate was > 4% the specimen was re-analysed (in triplicate). Following urinalysis for α1-AGP, EMU and 24-hour specimens were replaced into long-term freezer storage (at –80°C) until further urinalysis for electrolytes and creatinine (CREA; described next in section **7.2.4.1.2**).

Within-run imprecision (standard deviation, S_{wr}; variance, S^2_{wr}) for the latex-enhanced immunoturbidimetric assay was calculated for each triplicate with estimates accounting for six total days of analysis. Since analyses were not repeated between-days nor were there any reference values for the human specimens, estimates were calculated using modified versions of **Equation 3.5** and **Equation 3.8** (refer to **Chapter 3**). S_{wr} was averaged across all triplicates and further used to determine the within-run variance and the within-run %CV for the assay. Allowable within-run %CV for the assay was set to 10%. As there was no real reference for the biologic samples nor were tests repeated on multiple days, inaccuracy and recovery and other estimates of imprecision were not included.

7.2.4.1.2. Urinalysis for electrolytes and creatinine

Urinalysis for electrolytes (from 24-hour specimens) and CREA (mmol/l, from EMU specimens) was performed using the Alinity auto-analyser (v2.6.2, ci-series, Abbott Laboratories, Lake Bluff, Illinois, USA) by the Biochemistry Department at Birmingham Heartlands Hospital, University Hospitals Birmingham, NHS Trust, UK following a single freeze-thaw cycle. The maximum time between collection and this analysis was ~4 months[475]. Electrolytes analysed included: sodium (Na^+, mmol/l), potassium (K^+, mmol/l), chloride (Cl^-, mmol/l). Urinary [electrolyte] (mmol/l) was used to calculate the total mmol of each electrolyte excreted over a 24-hour period (mmol/24-hours). Urinary CREA (mmol/l) was used to correct [α1-AGP] from EMU specimens (i.e., to produce α1-AGP:CREA ratio; $mg/mmol_{\alpha1\text{-AGP:CREA}}$)[5], as specimen volume and collection duration were not recorded for these specimens. On days when iSTAT measurements were also collected (i.e., baseline, 07, 09, 14, 16, 21, and 23 October, 2019), the total amount of Na^+ and K^+ filtered through the kidneys and reabsorbed by renal tubules was calculated using blood [electrolyte] and total mmol excreted in 24-hour specimens (as outlined in **Equation 7.2, *Steps 1 – 2***).

Equation 7.2 – Calculation of electrolyte reabsorption. Calculations utilised blood [electrolyte] measured using the iSTAT analyser, eGFR (ml/min/1.73 m^2) calculated from serum cystatin C, and the total mmol of electrolyte measured from 24-hour urine specimens[110].

$$\textbf{\textit{Step 1:}}\ filtered\ load_{i\,j} = [electrolyte]_{i\,j} \times \frac{eGFR_j \times 60\ \text{min} \times 24\ \text{hours}}{1000\ \text{ml}}$$

$$\textbf{\textit{Step 2:}}\ percentage\ reabsorbed_{i\,j} = \frac{filtered\ load_{i\,j} - mmol\ excreted_{i\,j}}{filtered\ load_{i\,j}} \times 100$$

Where:

[electrolyte] = concentration (mmol/l) of electrolyte (Na^+ or K^+) in the blood measured by iSTAT;

i = blood electrolyte (e.g., sodium or potassium, in this case);

j = day of the expedition;

eGFR = estimated glomerular filtration rate (ml/min/1.73 m^2) calculated from cystatin C-based equation (refer to **Equation 7.1**).

filtered load = total mmol of electrolyte (i) filtered through the kidney on day (j);

reabsorbed load = percentage of electrolyte (i) reabsorbed by renal tubules on day (j);

mmol excreted = total mmol electrolyte excreted in 24 hours.

* (60 min × 24-hours)/1000 ml – unit conversation to yield mmol/day used in ***Step 2***.

7.2.4.2. 'Arterialised' blood specimens

Arterialised blood samples were collected from the earlobe at baseline and on six mornings during the expedition to include the following (rest) days: 07, 09, 14, 16, 21 and 23 October, 2019 (**Figure 7.1**). Ears were warmed with a hot water bottle prior to ear pricks using sterile lancets (Sanguiletten®, ASID BONZ GmbH, Herrenberg, Germany). Blood was collected into a heparinised capillary tube (Safe-Wrap Combo Blood Collection tubes, RNA Medical, Devens, MA, USA,), transferred into an EG6$^+$ cartridge, and then analysed using the iSTAT point-of-care blood gas analyser (Abbott Laboratories, Lake Bluff, Illinois, USA). EG6$^+$ cartridges (Abbott Laboratories) yielded measurements of: haematocrit (Hct, %PCV), haemoglobin (Hb, g/dl), sodium (Na^+, mmol/l), potassium (K^+, mmol/l), bicarbonate (HCO_3^-, mmol/l), base excess (mmol/l), partial pressure of oxygen (PO_2, mm Hg), partial pressure of carbon dioxide (PCO_2,

mm Hg), total carbon dioxide (TCO_2, mmol/l), pH, and arterial oxygen saturation (SaO_2, %). The iSTAT analyser was calibrated each time a new box of EG6+ cartridges were opened (approximately every 25 tests).

Brain-natriuretic peptide (BNP, pg/ml) was also analysed using the iSTAT analyser with accompanying BNP cartridges (Abbott Laboratories, Lake Bluff, Illinois, USA). BNP was analysed on select days (09, 14, and 16 October) in a subset of participants (n = 4; all males) whom were known to have a history of high levels of serum NT pro-BNP upon previous exposure to high altitude (~3 years previous).

7.2.4.3. Venous blood specimens

Additional blood samples were collected by venipuncture once at baseline and each morning during the expedition. Approximately 10 ml of whole blood was drawn from the antecubital vein into a syringe and then transferred into a centrifuge tube (both, round and conical tips) containing 10 µl of thrombin*. Specimens were left to clot for approximately 45 minutes after which clots were manually removed using bamboo sticks. Clot-free specimens were centrifuged at 2,000 g (4,300 to 5,000 rpm, rotor arm 9.65 cm) for 10 minutes on the Heraeus® Labofuge® 200 Centrifuge (Thermo Scientific, Waltham, Massachusetts, USA). Following centrifugation, 1.5 ml of serum supernatant from each specimen was aliquoted into four repeat 2 ml cryovials (polypropylene, with screw cap) with the residual specimen volume discarded in accordance with Good Clinical Practices (GCP) for disposing of clinical waste. Aliquots were immediately frozen at –80 °C (using solid CO_2), where they remained for the

* Thrombin used for serum specimens was constituted and aliquoted into individual repeat 2 ml cryovials and frozen in the UK prior to departure for Sikkim. Aliquots remained frozen at –80 °C (using solid CO_2) during the expedition and once thawed, thrombin was pipetted into each individual serum centrifuge tube. The purpose of pre-departure constitution and aliquoting was to ensure that 'fresh' thrombin could be thawed and used each day during the expedition.

remainder of the expedition. Upon arrival back in Birmingham, UK specimens were replaced into long-term storage (at –80 °C), where they remained until analysis.

7.2.4.3.1. Serum analysis

All serum specimens were analysed on the Optilite™ immunoturbidimetric auto-analyser (The Binding Site, Ltd. Birmingham, UK) back-to-back for C-reactive protein (CRP), high-sensitivity CRP (hs-CRP), cystatin C, and α1-AGP using commercially available kits* (The Binding Site, Ltd., Birmingham, UK). Each kit contained reagent, calibrator, and high- and low-controls, which were stored at 4 °C throughout. Prior to analysis, kit calibrators and controls were spiramixed at room temperature for approximately 30 minutes and then used to: 1) calibrate each assay, and 2) analyse control samples for quality assurance. High- and low-control results were required to fall within the factory recommended reference ranges for each reagent prior to proceeding with any serum analyses.

Following calibration and quality checks, serum samples were thawed on a spiramixer for approximately 30 minutes[476]. As for urine specimens, individual participants' serum specimens from across the expedition were analysed together on a single day in order to prevent any potential confounding influence of between-day imprecision. No freeze-thaw cycles had occurred prior to serum analyses for cystatin C, CRP, and α1-AGP.

The hs-CRP assay (measuring range: 0.5 – 10.0 mg/l) was planned for use in the first instance as baseline CRP levels were expected to be below the low-end of the full-range CRP assay (measuring range: 5 – 1,425 mg/l). By comparison, the full range CRP assay was anticipated to be required for expedition specimens as serum CRP at altitude was expected to exceed the higher end of the hs-CRP assay[149]. Thus, specimens were analysed first using the

* The Binding Site, Ltd. product codes for serum assays: LK044.L.OPT (hs-CRP), NK044 (CRP), and NK063.OPT (α1-AGP).

hs-CRP assay and if unmeasurable (> above 10 mg/l), analysis was repeated in triplicate using the full range CRP assay (measuring range: 5 – 1,425 mg/l). α1-AGP (measuring range: 0.19 – 6.00 g/l) and cystatin C (measuring range: 0.4 – 12.0 mg/l) assays were expected to adequately cover a concentration range that would be suitable for baseline and altitude specimens. Cystatin C results were utilised to calculate eGFR (**Equation 7.1**).

7.2.5. Nocturnal pulse oximetry

Peripheral oxygenation (SpO_2) was assessed by pulse oximetry and recorded overnight at baseline (for two nights) and each night throughout the expedition. Portable wrist worn pulse oximeters (WristOx, Model 3150, Nonin Medical Inc., Plymouth, MN, USA) recorded peripheral oxygenation, which was sensed from the finger pulp using a flexible infrared finger sensor (Adult 8000J sensor, Nonin Medical Inc., Plymouth, MN, USA) and accompanying (disposable) adhesive finger wrap (**Image 7.1a – 7.1c**). An instructional video (by Nonin Medical Inc.) and detailed written instructions for self-placement of the device, sensor, and finger wrap were provided to all participants weeks prior to baseline collections to allow ample time for troubleshooting and questions.

Image 7.1a – c – Portable pulse oximeters and finger sensors. WristOx 3150 Model finger pulse oximeter and 8000J adult flexible finger wrap with disposable adhesive sticker (Nonin Medical). Photo credit to Dr Courtney Wheatley and Mr Jesse Schwarz of the Johnson Lab, Mayo Clinic, Scottsdale campus, Scottsdale, Arizona.

SpO_2 and heart rate (HR, bpm) were recorded continuously (second-by-second, 1 Hz) throughout the night and stored on-device until being offloaded using nVision (v6.5.1, Nonin Medical Inc., Plymouth, MN, USA). Baseline collections were offloaded prior to departure for Sikkim, with the device's internal timestamp reset to IST upon arrival in country. Nocturnal data were then offloaded every 2 to 3 days throughout the expedition along with replacement of batteries (as shown in **Image 7.2**).

Image 7.2 – Offloading of pulse oximetry data from portable devices during the expedition. Pictured offload took place at Jakthang camp (3,300 m). Photo credit to Dr Sam Lucas.

7.2.5.1. Preanalytical processing - artifact detection and removal

nVision and an *ad hoc* MATLAB function (R2019b, Mathworks, Natick, MA, USA) were used to process and analyse raw data files (.csv). Following offloading, artifacts were identified from the SpO_2 data using any one of the following criteria: 1) SpO_2 value < 30%; 2) arbitrary values > 100% (e.g., 500% for the WristOx oximeters), or 3) a deviation of > 4% from the SpO_2 of the preceding second[477]. After identification, artifacts were counted, used to calculate the artifact-index (**Equation 7.3**), and then removed.

Equation 7.3 – Artifact-index of nocturnal pulse oximetry recordings sampled at 1 Hz. Results presented as a percentage of the total recording length.

$$AI_{oximetry} = \frac{n}{recording\ length_{raw}} \times 100$$

Where:

n = number of artifacts counted from the entire recording (or number of points counted at 1 Hz);

$recording\ length_{raw}$ = length, in seconds, of the raw artifact-inclusive recording;

$AI_{oximetry}$ = artifact-index (AI) expressed as a percentage (or portion) of the nocturnal recording) relative to the recording length.

7.2.5.2. Time series analyses

7.2.5.2.1. Descriptive statistics and 1st statistical moment

Mean SpO_2 (1st statistical moment) and additional descriptive statistics including: minimum SpO_2, mean HR, and mean HR/SpO_2 ratio (beats/min/%) were calculated and identified from each artifact-free nocturnal recording using MATLAB (and confirmed with nVision). Mean SpO_2 and mean HR, were also calculated from nocturnal recordings for both basal (i.e., first 10 minutes of nocturnal recording; at the beginning of the night) and waking (i.e., last 3 minutes of nocturnal recording; in the morning) time periods.

7.2.5.2.2. 2nd – 4th statistical moments (variance, skewness, and kurtosis proper)

Frequency distribution plots (relative frequency and cumulative frequency) were constructed from the artifact-free recordings using a second *ad hoc* MATLAB function. Summations of total seconds spent at each SpO_2 level (e.g., 100%, 99%, 98%, and so on) during the night provided the basis for frequency plots (or histograms) with each SpO_2 representing a single bin. Absolute time spent at each SpO_2 was then divided by the total sleep time and plotted as a proportion (%) of total sleep time to produce the relative frequency distribution. Data from these plots were used to calculate the 2nd through 4th statistical moments (variance,

skewness, and kurtosis proper)[464] [465], which helped define the morphologic attributes of nocturnal recordings.

7.2.5.2.2.1. 2nd statistical moment – variance

Nocturnal SpO_2 variance was estimated in MATLAB using **Equation 7.4a** and **7.4b.** Nocturnal variance represented 'fluctuations' in SpO_2 across the night and was secondary to the oxygen desaturation index (ODI; see section **7.2.5.3**).

Equation 7.4a – Variance equation applied to nocturnal pulse oximetry recordings using MATLAB. Syntax 'var' was used to call this function in MATLAB.

$$V = \frac{1}{N-1}\sum_{i=1}^{N}|A_i - \mu|^2$$

Equation 7.4b – Calculation of mean used for variance calculations (Equation 7.4a).

$$\mu = \frac{1}{N}\sum_{i=1}^{N} A_i$$

Where:

V	= variance;
A	= $SpO_{2nocturnal}$ made up of N scalar observations (1 observation/ sec);
N	= integers between 30 – 100% SpO_2;
μ	= mean result.

7.2.5.2.2.2. 3rd statistical moment – skewness

Skewness was assessed using MATLAB using **Equation 7.5a** and **7.5b** for each nocturnal recording. Skewness was used to define the relationship between the mean and median for each nocturnal SpO_2 recording. Median SpO_2 was defined as the SpO_2 at which the most time (seconds) was spent throughout the night compared to other SpO_2 values (i.e., SpO_2 bin from histogram plot with greatest frequency). Skewness results could be either negative or positive, which referenced the directional inflection of the peak (when visualising) and further allowed for the determination of the location of the mean in relation to the remaining portion of nocturnal SpO_2 values (or the tails). For example, a positive skew indicates that the 'tail' on

the right side of the 'peak' is longer than the one on the left and thus, indicated that the majority of the nocturnal SpO_2 values being analysed were located to the left of the mean[478]. Alternatively, a negative skew indicates that the 'tail' on the left side is longer than that on the right and that a majority of the nocturnal SpO_2 values being analysed were located to the right of the mean[478]. An absolute skew of ≥ 2 was used to identify substantial asymmetry in the data[478 479].

Equation 7.5a – Skewness syntax utilised in MATLAB.

Y = skewness(X)

Where:

y	= the skewness of x;
x	= SpO_2 data from a single night (a vector) recorded at 1 Hz;
skewness	= **Equation 7.5b** applied to x.

Equation 7.5b – Skewness equation utilised in MATLAB for nocturnal oxygen saturation (SpO_2) data.

$$s = E(x-\mu)^3 \times \sigma^3$$

Where:

x	= median of an array (i.e., SpO_2 values for that nocturnal recording);
μ	= mean of an array (i.e., SpO_2 values for that nocturnal recording);
σ	= the standard deviation of x;
$E(t)$	= the expected value of the quantity t;
s	= skewness of x.

7.2.5.2.2.3. 4th statistical moment – kurtosis (proper)

Kurtosis was calculated using traditional methods (**Equation 7.6a** and **7.6b**), which normally serve to measure the tendency of a dataset to contain outliers. For the purposes of this study however, kurtosis served as a measure of the 'peakedness' (or 'flatness') of the nocturnal oximetry dataset and functioned to assess the magnitude of the relationship between the SpO_2 at which the most time was spent relative to the remaining portion of the night. Thus, higher values for kurtosis reflected greater 'peakedness' (on visual inspection) and indicated

that the magnitude (in seconds) of time spent at the SpO_2 in question was greater compared to the remaining duration at alternate SpO_2. For example, at sea-level in healthy individuals a high skew would be expected as most of the night is spent at a select few saturations (i.e., 95% – 100%). Alternatively, at altitude when the SpO_2 may fluctuate more, a lower skew would be expected as the time throughout the night is spread across a wider range of saturations ('flatter' morphology on visual inspection). Due to the high number of data points per recording (sampled at 1 Hz × ~8 hours), a 'significant' kurtosis (proper) was considered to be a value > 7[478 479].

Equation 7.6a – Kurtosis syntax utilised in MATLAB.

K = kurtosis(x)

Where:

x	= single night of continuous SpO_2 data (a vector) recorded at 1 Hz;
k	= kurtosis of the dataset from night x.

Equation 7.6b – Kurtosis equation utilised in MATLAB.

$$k = E(x-\mu)^4 \times \sigma^4$$

Where:

x	= median of an array (i.e., SpO_2 values for that nocturnal recording);
μ	= mean of an array (i.e., SpO_2 values for that nocturnal recording);
σ	= the standard deviation of x;
$E(t)$	= the expected value of the quantity t;
k	= kurtosis of x.

7.2.5.2.3. Cumulative frequency of nocturnal saturation

Cumulative frequencies in the present study were calculated and plotted using *ad hoc* MATLAB functions and were examined separately for each individual and each night. Cumulative frequency plots were used to assess nocturnal hypoxaemia[464 465 466 467] and referred to the (cumulative) total time spent across the night at or below a given %SpO_2 (e.g., cumulative time < 90% SpO_2, CT90[480]). Similar to the altitude-adjusted desaturation criteria described

next, cumulative sleep times were adapted for altitude collections based on past altitude-adjusted cut-offs (TST SpO_2 < 80%[460]). Only TST < 80% values were reported and analysed although, an example of the entire cumulative frequency plot will be provided for two individuals' nightly data (separately) in order to demonstrate the utility and functionality of these plots.

7.2.5.3. Desaturation characteristics

7.2.5.3.1. Desaturation length and frequency

nVision software was used to calculate desaturation characteristics to include: total number of desaturations, desaturation length, total time spent in desaturations, and desaturation frequency (or oxygen desaturation index, ODI; desaturations/hour). Desaturations were defined using the following criteria[477]:

1) event onset marked by a point 'a', where a fall in SpO_2% occurred at a rate > 0.1% per second, but < 4% per second, from a preceding 20 second baseline;
2) event nadir[477], occurring at point 'b', was achieve where the SpO_2 at the nadir was reduced by at least 4% (an altitude-corrected nadir; and opposed to the standard 3%[460]) from the 20-second baseline SpO_2;
3) the ending of the event, marked by a point 'c' where SpO_2 returned to within 1% of the SpO_2 at point 'a' (onset) OR where SpO_2 was > 3% above the nadir (point, b); and
4) the entire event (from point 'a' to 'c') lasted at least ten seconds (≥ 10 seconds).

7.2.5.3.2. Desaturation area (or hypoxaemic burden)

Desaturation area is but one method used to quantify the severity of nocturnal desaturations during the night and uniquely enables the evaluation of the 'cumulative' nocturnal desaturation severity across[481 482]. During ascent, these methods could help to evaluate the impact of nocturnal hypoxaemia in relation to alternative physiologic manifestations (e.g., proteinuria). Calculations of nocturnal 'hypoxaemic burden' in the present

study were performed using a modified version of desaturation area derivations, (see **Equation 7.7**) which have previously demonstrated clinical significance in relation to the severity of nocturnal events[483 484]. For the purposes of the present study and to avoid over-complication, hypoxic burden was calculated relative to a baseline of 100% SpO_2[483] (or the 'theoretical' saturation; **Equation 7.7, *Steps 1 – 4***), although it is understood that the hypoxic burden can also be calculated relative to each individual desaturation event or relative to sequential moving SpO_2 means throughout the night[484]. Estimations of hypoxic burden were provided in units of %min/hour and were not indicative of the method by which the burden was achieved (e.g., 30%min/hour can be achieved with 30 minutes of 1% desaturation or 6 minutes of 5% desaturation occurring over the course of 1 hour)[484].

Equation 7.7 – Hypoxic burden calculations. ***Steps 1 – 4*** were used to calculate the hypoxic burden of the night from pulse oximetry recordings collected during ascent to and descent from 4,800 m. Estimations of nocturnal hypoxic burden are provided in units of %min/hour. By example, 20%min/hour reflects a hypoxic burden that may occur by various dimensions (e.g., 5 minutes × 4% desaturation or 10 minutes × 2% desaturation) occurring each hour of the night. * Note: denominator (i.e., 60 seconds) converts the units for recording length from seconds to minutes; desat $mins_{theoretical}$ refers to a hypoxic burden calculated relative to the theoretical saturation (100% SpO_2).

Step 1: $sat\ mins_{theoretical} = \frac{SpO_2\ 100\% \times recording\ length_{\ seconds}}{60\ secs}$

Step 2: $sat\ mins_{actual} = \frac{\sum (n \times t_n)}{60\ secs}$

Step 3: $desat\ mins_{theoretical} = sat\ mins_{theoretical} - sat\ mins_{actual}$

Step 4: $hypoxic\ burden_{theoretical} = \frac{desat\ mins_{theoretical}}{60 \times recording\ length_{hours}}$

Where:

recording length = duration of the artifact-free nocturnal recording in units specified; by subscript (i.e., seconds or minutes);
n = each integer from 50 – 100 (reflecting SpO_2 50 – 100%);
t = the time spent (in seconds) at an 'n' %SpO_2.

7.2.5.4. Methods comparison

Arterial oxygenation (SaO_2) measured using the iSTAT (refer to section **7.2.4**) was compared to peripheral oxygenation obtained by pulse oximetry overnight ($SpO_{2nocturnal}$) and

momentarily (30 – 90 seconds) each morning ($SpO_{2morning}$) during daily medical evaluations. Both, $SpO_{2nocturnal}$ and $SpO_{2morning}$ were measured utilising WristOx devices however, $SpO_{2morning}$ data were manually recorded (in a de-identified chart) by the attending GPs during medical examinations.

Comparisons between SaO_2 and $SpO_{2nocturnal}$ or $SpO_{2morning}$ were performed utilising Bland-Altman (B-A) plots. B-A plots were constructed from 70 pairs of SaO_2 and $SpO_{2nocturnal}$ data and 84 pairs of SaO_2 and $SpO_{2morning}$ data. The differences between SaO_2 and $SpO_{2nocturnal}$ or $SpO_{2morning}$ (y-axis) values were plotted against the average (x-axis) of the two measurements (i.e. (SaO_2 – $SpO_{2nocturnal}$)/average or (SaO_2 – $SpO_{2morning}$)/average)) as opposed to the difference being plotted against SaO_2 as a 'standard'[310 311]. Agreement and bias between the arterial and peripheral (nocturnal or morning) measurements were estimated from the B-A plots. The best fit line for the simple linear regression of the differences between measurements was also plotted along with the 95% limits of agreement (95% LOAs). Slope, x-intercept, and goodness of fit, which was evaluated using r-squared (R^2) and standard deviation of the residuals (Sy.x), of the best fit line were presented.

Further comparisons between $SpO_{2nocturnal}$ and $SpO_{2morning}$ measurements were performed for 16 night-morning pairings (n = 258 pairs) using mixed effects analysis with Holm-Šidák correction for multiple predetermined pairwise comparisons (e.g., $SpO_{2nocturnal}$ from 06 October vs $SpO_{2morning}$ from 07 October). B-A plot was also constructed for the differences between $SpO_{2nocturnal}$ and $SpO_{2morning}$, albeit only for measurements that had been validated against SaO_2 (i.e., n = 70 pairs) with bias and agreement calculated and the best fit line and LOAs plotted from the simple linear regression as described above.

7.2.6. Statistical analysis

A priori hypotheses to be tested were: 1) the impact of exposure to altitude (compared to baseline or compared across ascent) on physiologic responses (e.g., SBP, DBP, or HR), metrics derived from nocturnal recordings (e.g., nocturnal SpO_2 or desaturation index), and urine or serum biomarkers (e.g., urine α1-AGP or electrolytes; serum CRP, α1-AGP, or cystatin C) and 2) the relationships between these variables and urinary α1-AGP excretion (24-hour and EMU α1-AGP:CREA) across the expedition (e.g., nocturnal ODI vs 24-hour α1-AGP excretion or SBP vs EMU α1-AGP:CREA). Secondary exploratory analyses were also conducted between various physiologic variables, derivatives of nocturnal recordings, and urine or serum biomarkers (e.g., SBP vs nocturnal ODI) to further evaluate the mechanisms contributing to any observed changes in urinary α1-AGP excretion during the expedition.

Statistical analysis was performed using Prism (v8.3.0 for Mac iOS, Graphpad Software LLC, San Diego, CA, USA) and MATLAB (R2019b, Mathworks, Natick, MA, USA) where specified. Tests for normality or lognormality and outlier (± 3 SDs) removal were performed prior to conducting statistical analysis. Equivocal non-parametric tests were performed if abnormal distributions were exhibited following outlier removal.

Descriptive statistics for all data were presented as mean ± standard deviation (SD) unless otherwise specified (e.g., median ± interquartile range, IQR, for non-parametric data). Repeated measures ANOVA (parametric) and mixed models (restricted maximum likelihood; for normally distributed data containing missing values) were used to compare values between days of the expedition for all variables of interest (e.g., urinary α1-AGP, mean nocturnal SpO_2 or nocturnal skew) unless otherwise specified. Corrections for these analyses were utilised as follows: 1) Dunnett's *post-hoc* test for repeat-comparisons against baseline; 2) Tukey's

correction for repeat comparisons between days of the expedition; and 3) Holm-Šidák correction for multiple (predetermined) pairwise comparisons between two variables across days. For any data that were nonparametric, Friedman's test was used in place of repeated measures (where noted in results). Mann-Whitney U test was used to perform unpaired comparison of ranks between AMS^+ and AMS^- individuals for urinary α1-AGP measurements, as well as, derivatives of nocturnal recordings (i.e., TST < 80% SpO_2).

Pearson (or Spearman where appropriate) correlations were used determine whether relationships existed between altitude-induced changes in urinary α1-AGP excretion (24-hour and EMU) and other physiologic measurements (e.g., SBP, DBP, LLS, serum biomarkers, or nocturnal oxygenation) across expedition days. Given the potential for urinary α1-AGP to exhibit a large degree of between-individual variation and small degree of within-individual variation (as discussed in **Chapter 4**), a model compared against the altitude-induced between-day differences (e.g., comparison of daily means) would likely be most appropriate to further the understanding of overarching relationships with other variables. Thus in consideration of any such relationships in the context of HA hypoxia, it was decided that correlations would be plotted using the daily group means of the measures in question[485]. Correlation coefficients (Pearson r or Spearman *rho*) were reported and used to interpret the size of r values; specifically: values ranging from 0.00 to 0.30 (or –0.30) were considered representative of a negligible positive (or negative) correlation; values from 0.30 to 0.50 (or –0.30 to –0.50) representative of a low positive (or negative) correlation; and values from 0.70 to 0.90 (or –0.70 to –0.90) representative of a high positive (or negative) correlation[486]. Coefficients of determination (R^2) were additionally reported for Pearson correlations (only) with $R^2 > 0.5$ desired.

Exploratory analyses were conducted between secondary variables with these results presented in-text wherever possible and any remaining results presented in **Appendix 8.** All statistical tests were two-tailed with significance set to $\alpha \leq 0.05$.

7.3. RESULTS

7.3.1. Participants and study design

Baseline characteristics are presented in **Table 7.1** (mean ± SD). Estimated glomerular filtration rate was normal (> 60 ml/min/1.73 m^2) at baseline in all individuals. Only one individual reported having altitude exposure within the preceding 3 to 5 months. Only one (male) individual reported a history of severe altitude illness (high-altitude cerebral oedema, HACE) during a past ascent. Three individuals reported a history of AMS during past ascents above 3,500 m (occurring minimum 2 years prior to current expedition to Sikkim).

Table 7.1– Baseline characteristics and physiologic measures.

Age (years)	36 ± 16
Body mass (kg)	72.2 ± 11.6
Height (cm)	175.0 ± 10.5
Body mass index (BMI)	23.4 ± 1.8
Heart rate (bpm)	63 ± 10
Respiratory rate (breaths/min)	14.7 ± 2.4
Resting SpO_2(%)	95.0 ± 2.0
SBP (mm Hg)	113 ± 8
DBP (mm Hg)	69 ± 7
eGFR (ml/min/1.73 m^2)	132.5 ± 16.9

Values are presented as mean ± standard deviation. Baseline characteristics included, age, height, body mass, and body mass index (BMI) and were measured along with resting SpO_2, HR (beats per minute), and estimated glomerular filtration rate (eGFR, ml/min/1.73 m^2) prior to departure from Birmingham. Data for the additional physiologic measurements to include systolic and diastolic blood pressures (SBP and DBP, respectively; mm Hg), and respiratory rate (RR; breaths per minute, breaths/min) are presented from data collected on 07 October, 2019 (in Gangtok).

7.3.2. Daily physiologic measurements and Lake Louise Scores

All 18 participants successfully ascended to the top camp (4,800 m) with the assistance of 12 guiding staff and 50 local porters. Only one individual required premature descent*. Two individuals reported sudden onset severe gastrointestinal distress during the night at Jakthang camp (night 12 October and morning of 13 October, 2019) with others reporting mild symptoms, albeit still with sudden onset in the night and along the same time course. There was a significant effect of time on morning LLS ($p = 0.009$) and evening LLS ($p < 0.001$) with morning LLS being greatest on the 1st morning at the top camp (mean score, 1.50 ± 1.79; group score sum, 27) and evening LLS scores on the same day being the worst (mean

*A single female required descent on 17 October and was accompanied by two other females from the group back to the Yabuk camp (3,850 m) where they were met by the rest of the expedition team the following day during the normal ascent. Oximetry data from the night 17 October for these individuals was not included in analyses.

score, 2.00 ± 2.142; group score sum, 36), despite it being the 2nd evening at the top camp. The incidence of AMS (determined by LLS) for the group across the expedition was 50% (9 out of 18 individuals scoring positive on at least one morning) with the greatest prevalence for any one day being 33% (6 of 18 individuals on morning October 17; **Figure 7.3**).

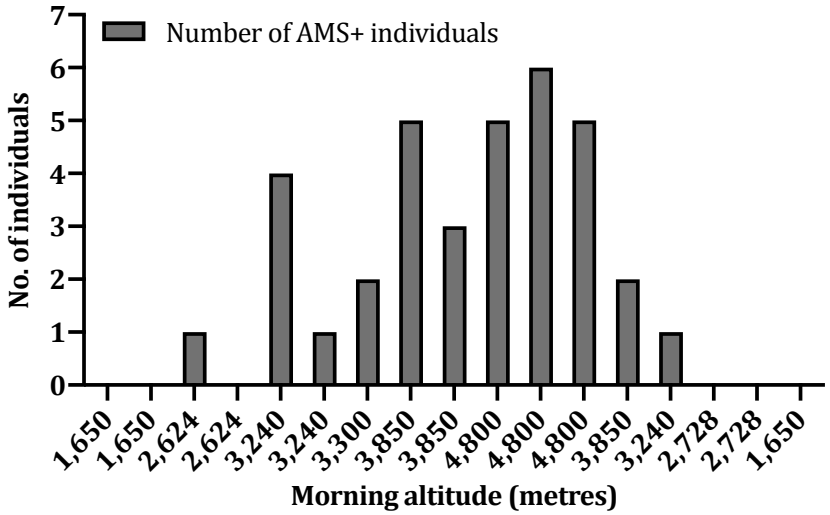

Figure 7.3 – Prevalence and incidence of acute mountain sickness (AMS) by Lake Louise Score (LLS) during ascent to 4,800 m. Prevalence of AMS (determined by number of individuals scoring positive for AMS from morning LLS) was greatest (33%) on the 2nd morning at the top camp (4,800 m, October 17) when 6 out of 18 individuals scored positive for AMS (AMS+). Incidence of AMS across the entire expedition was 50% with 9 out of 18 individuals scoring positive for AMS (by morning LLS) on at least one morning throughout.

Daily means for physiologic response measurements (e.g., SBP, DBP, HR, and RR) across the expedition are presented in **Table 7.2.** Average body mass measurements were not significantly different compared to baseline during the ascent phase of the expedition (all *p*-values > 0.05)*.

DBP was significantly increased ($p = 0.003$) during the expedition when compared to the first day of the expedition (07 October, 2019; 69 ± 7 mm Hg) and was highest on the final

* Scales used for measurements of body mass were accidentally dropped during the day on 19 October, 2019 after which there was a noticeable drop in individuals body masses that did not coincide with concomitant changes in fluid output, food intake, or gastrointestinal illness.

morning at the top camp (18 October, 2019; 81 ± 9 mm Hg). These significant increases were also observed for SBP, which was greatest on the final morning at the top camp (18 October, 2019; 130 ± 11 mm Hg) compared to the first expedition day (07 October, 2019; 113 ± 8 mm Hg, $p < 0.001$).

RR data were nonparametric and thus, Friedman's test was utilised in order to evaluate across days of the expedition. RR was significantly altered over the course of the expedition ($p < 0.001$), with the greatest increase from 07 October, 2019 measures on the first morning at the top camp (16 October, 19 ± 4). The observed increases in RR with ascent did not entirely resolve with descent, as evident from the difference between ascent vs descent values from Gangtok (15 ± 2 breaths/min vs 18 ± 3 breaths/min, $p = 0.033$).

HR from morning medical examinations was significantly different during the expedition compared to baseline ($p < 0.001$), with the greatest difference from baseline observed on the 2nd morning Yabuk camp (on average, 9 ± 3 bpm higher).

Table 7.2 – Daily heart and respiratory rates collected during morning medical examinations with ascent to 4,800 m.

Day of October	Altitude (m)	BM (kg)	SBP (mm Hg)	DBP (mm Hg)	HR (bpm)	RR (br/min)
7	1,650	73.5 ± 73.7	113 ± 8	69 ± 7	61 ± 10	15 ± 2
8	1,650	73.7 ± 12.0	112 ± 11	72 ± 8	65 ± 13	15 ± 2
9	2,624	71.8 ± 10.9	113 ± 11	73 ± 9	62 ± 13	15 ± 2
10	2,624	71.8 ± 11.8	113 ± 10	74 ± 5	69 ± 13	15 ± 2
11	3,240	72.7 ± 12.4	112 ± 9	70 ± 6	68 ± 16	16 ± 3
12	3,240	71.6 ±11.8	117 ± 9	72 ± 6	70 ± 15	17 ± 3
13	3,300	70.9 ±11.6	117 ± 9	74 ±6	66 ± 14	15 ± 2
14	3,850	71.2 ± 11.4	117 ± 7	77 ± 6	67 ± 9	16 ± 2
15	3,850	71.8 ±12.0	117 ± 10	75 ± 6	72 ± 14	18 ± 3
16	4,800	73.2 ± 12.1	120 ± 10	74 ± 7	70 ± 10	19 ± 4
17	4,800	73.4 ± 11.8	118 ± 11	73 ± 8	67 ± 12	19 ± 4
18	4,800	75.7 ± 13.0	130 ± 11	81 ± 9	67 ± 12	19 ± 4
19	3,850	78.5 ± 12.5	120 ± 13	76 ± 9	66 ± 15	17 ± 3
20	3,240	70.3 ± 11.7	117 ± 11	76 ± 7	72 ± 13	18 ± 3
21	2,728	69.1 ± 10.7	117 ± 11	73 ± 7	67 ± 16	18 ± 2
22	2,728	69.5 ± 11.5	113 ± 10	70 ± 9	62 ± 12	18 ± 3

Data are presented as the group mean ± standard deviation. Day of October reflected the expedition date and indicated altitudes (m) reflected the waking altitude (not sleep altitude). HR, heart rate (beats per min, bpm); respiratory rate (RR, breaths/min); SBP, systolic blood pressure (mmHg); DBP, diastolic blood pressure (mm Hg); and BM, body mass (kg).

7.3.3. Biological specimens

7.3.3.1. Arterialised blood gases

Arterialised earlobe specimens were well tolerated by most, albeit not by all, due to difficulties with blood-letting from the earlobe. The iSTAT analyser temperature was difficult to equilibrate at higher altitudes making calibration and analysis difficult at the highest camps (e.g., increased rate of cartridge failure and greater propensity for clotting in the capillary tubes

(SafeWrap® Blood Collection Tubes). These issues only increased data collection times and did not result in any missing sample points.

iSTAT results are presented in **Table 7.3**. Typical changes in blood gas measures were observed, with PCO_2 ($p < 0.001$), PO_2 ($p < 0.001$), TCO_2 ($p < 0.001$), SaO_2 ($p < 0.001$), base excess ($p < 0.001$), HCO_3^- ($p < 0.001$), and potassium ($p < 0.001$) significantly decreased with ascent, and pH ($p = 0.017$), haemoglobin ($p = 0.010$), and haematocrit ($p = 0.005$) significantly increased with ascent. BNP also increased with ascent among the subset of individuals (see **Table 7.4**).

Table 7.3 – Results for arterialised blood gases.

	Baseline (~130 m)	07 Oct (1,650 m)	09 Oct (2,624 m)	14 Oct (3,850 m)	16 Oct (4,800 m)	21 Oct (2,728 m)	23 Oct (1,650 m)
PO_2 (mm Hg)	75.8 ± 13.4	63.0 ± 6.7*	56.2 ± 4.7*	39.1 ± 4.1*	35.1 ± 3.6*	54.3 ± 5.0*	67.7 ± 6.6
PCO_2 (mm Hg)	34.4 ± 4.3	36.4 ± 3.8	35.0 ± 3.7	30.8 ± 4.0	28.1 ± 4.5*	31.5 ± 3.5	33.5 ± 2.9
TCO_2 (mmol/l)	25.89 ± 2.14	25.06 ± 1.67	24.63 ± 2.85	22.53 ± 3.14*	20.59 ± 1.80*	21.88 ± 2.20*	22.71 ± 2.14*
SaO_2 (%)	95.0 ± 2.6	92.0 ± 2.2	89.9 ± 2.3	76.7 ± 5.7	71.2 ± 7.1	88.4 ± 3.1	93.4 ± 2.0
HCO_3^- (mmol/l)	25.13 ±1.57	23.91 ± 2.14*	23.72 ± 1.94*	21.82 ± 2.86*	19.81 ± 3.10*	20.79 ± 1.66*	21.68 ± 2.02*
pH	7.468 ± 0.042	7.426 ± 0.013*	7.438 ± 0.025	7.456 ± 0.025	7.456 ± 0.053	7.426 ± 0.024*	7.415 ± 0.020*
BE (mmol/l)	1.40 ± 1.69	−0.53 ± 2.00*	−0.24 ± 1.89	−2.24 ± 2.77*	−4.06 ± 3.58*	−3.65 ± 1.84*	−2.88 ± 2.23*
K^+ (mmol/l)	5.65 ± 1.07	5.13 ± 0.82	4.85 ± 0.66	4.21 ± 0.22*	4.67 ± 0.58*	5.42 ± 0.64	4.91 ± 0.51
Na^+ (mmol/l)	137.8 ± 3.9	136.7 ± 1.4	138.6 ± 1.5	138.7 ± 1.9	138.5 ± 2.2	136.6 ± 1.4	137.9 ± 3.9
Hb (g/dl)	14.61 ± 1.57	14.82 ± 1.49	15.11 ± 1.58	14.76 ± 1.19	14.75 ± 1.04	15.88 ± 1.76*	15.28 ± 1.49
Hct (%PV)	43.00 ± 4.59	43.13 ± 4.22	44.41 ± 4.65	43.41 ± 3.50	43.35 ± 3.04	46.71 ± 5.21*	44.94 ± 4.38

Arterialised specimens were collected from the earlobe and analysed utilising the iSTAT point-of-care blood gas analyser (Abbott Laboratories). Data are presented as mean ± standard deviation by date of collection (October 2019) and collection altitude (in parenthesis). Expedition results were compared to baseline measurements using a mixed-effects model with Dunnett's *post hoc* test. All statistical tests were two-tailed with significance set to $\alpha < 0.05$. Significant difference compared to baseline is marked by an asterisk, *. PO_2, partial pressure of oxygen; PCO_2, partial pressure of carbon dioxide; TCO_2, total carbon dioxide; SaO_2, arterial oxygen saturation; HCO_3^-, bicarbonate; BE, base excess; K^+, potassium; Na^+, sodium; Hb, haemoglobin; and Hct, haematocrit.

Table 7.4 – Brain-natriuretic peptide (BNP) during ascent.

Participant No.	09 October	14 October	16 October
04	64 (79)	78 (93)	106 (121)
05	< 15 (15)	< 15 (15)	< 15 (15)
10	76 (91)	82 (97)	92 (107)
11	< 15 (15)	35 (50)	20 (35)
Mean	**50.00**	**63.75**	**69.50**

Individual BNP data (in a subset, n = 4) are presented for arterialised measurements (pg/ml) performed using the iSTAT analyser during ascent to 4,800 m (on select days). Normalised BNP data are noted in parenthesis (normalised to the lower limit of the measuring range, 15 pg/ml) with the normalised mean indicated in bold at the bottom of the table.

7.3.3.2. Venous specimens

A total of 324 venous whole blood specimens, totaling approximately 3,240 ml overall for the group, were successfully collected (from baseline and during the expedition) with cumulative volumes removed from each individual (~180 ml) being well tolerated among all. Serum was successfully isolated from the collected specimens (1,620 to 1,944 ml harvested as serum).

7.3.3.2.1. Serum cystatin C and eGFR

Serum cystatin C was significantly greater than baseline throughout the expedition, being greatest (0.720 ± 0.076 mg/l) on the final morning of residence at the top camp (18 October, 2019; 4,800 m), and decreased with descent to near baseline levels upon arrival back to 1,650 m in Gangtok (0.645 ± 0.093 mg/l).

Estimated glomerular filtration rate was significantly lower compared to baseline (132.5 ± 16.9 ml/min/1.73 m^2) on several days throughout the expedition as shown in **Figure 7.4**, albeit remained > 85 ml/min/1.73 m^2 in all individuals throughout. The lowest mean daily eGFR (116.1 ± 16.8 ml/min/1.73 m^2) was exhibited on the 3rd and final morning at 4,800 m and,

like cystatin C, returned to near to baseline levels (132.5 ± 22.4 ml/min/1.73 m^2) upon return to 1,650 m in Gangtok.

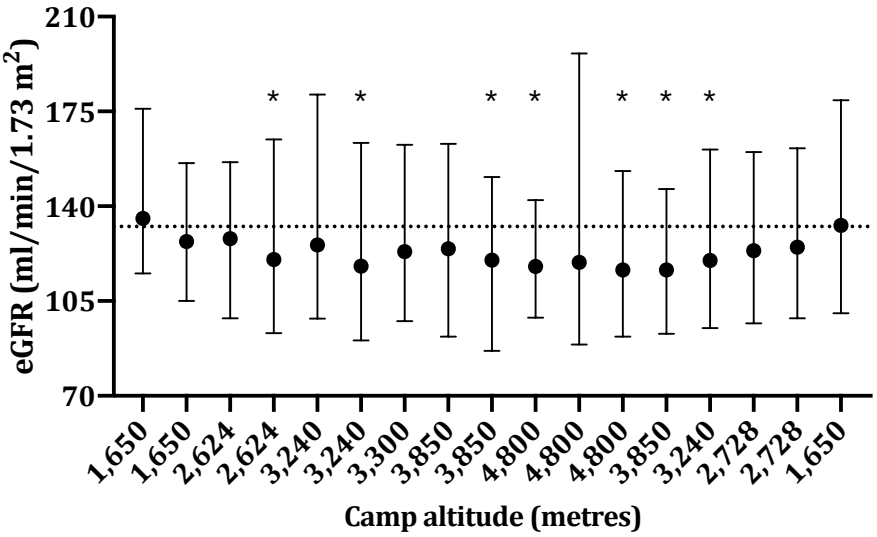

Figure 7.4 – Estimated glomerular filtration rate (eGFR). eGFR (ml/min/1.73 m^2) was estimated using a cystatin C-based equation (refer to **Equation 7.1**) with cystatin C analysis performed for serum specimens collected at the indicated morning altitudes (x-axis). Daily data are plotted as group mean with bars representative of the range (minimum – maximum). Dotted horizontal line represents mean eGFR of the group at baseline. Repeated measures ANOVA with Dunnett's *post hoc* test was used to compare daily eGFR to baseline. All test statistical tests were two-tailed with significance set to $\alpha < 0.05$ and marked by asterisk, *.

7.3.3.2.2. Serum C-reactive protein (CRP)

Serum CRP results are presented in **Figure 7.5a** and **7.5b**. There was a significant effect of time on CRP across the expedition ($p = 0.033$). Justification for presenting the data separately, with and without outliers, was to demonstrate the sensitivity of serum CRP measurements and highlight the potential for hypoxic effects to be overshadowed by alternative inflammatory stimulators during ascent. This was most notable for data from 12 October, which coincidentally also preceded two cases of severe gastrointestinal distress. When outliers were removed, the trend between altitude and serum CRP emerged with the 1st morning at 4,800 m (16 October) exhibiting the highest mean CRP (2.89 ± 0.64 mg/l) compared to all other days.

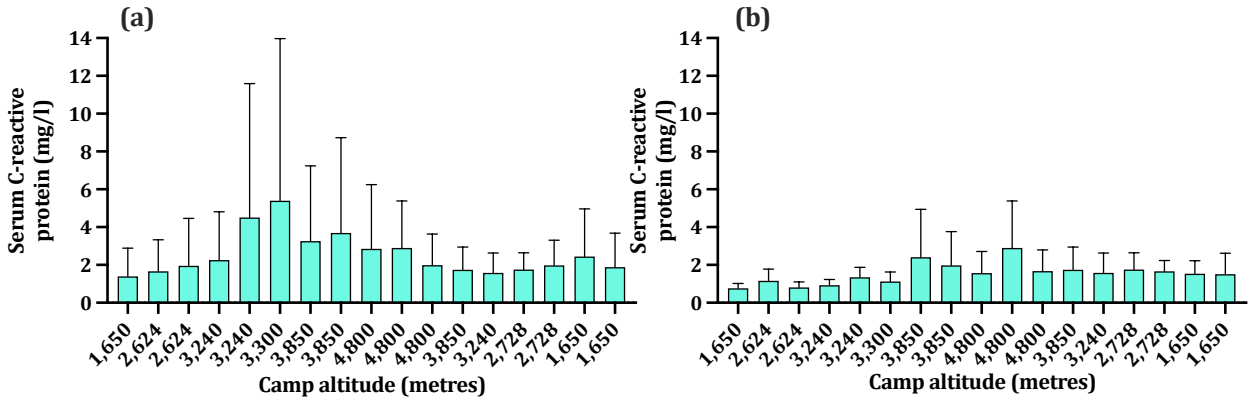

Figure 7.5 – Serum C-reactive protein (CRP) across days of the expedition. Fig. 7.5a (left) – Serum CRP (mg/l) plotted using data from all participants with notable elevations (i.e., outliers) in CRP observed morning of 13 October (3,300 m) and coinciding with the reported gastrointestinal distress exhibited during the preceding night; **Fig. 7.5b (right)** – Serum CRP plotted without outliers, eliminating the potential confound of alternative inflammatory factors. Columns represented the group mean with vertical error bars representative of the + SD. Camp altitude (x-axis) was representative of the altitude at which participants slept and blood specimens were collected.

7.3.3.2.3. Serum α1-AGP

Serum α1-AGP (g/l) data are presented in **Figure 7.6**. Serum α1-AGP was elevated in comparison to baseline throughout, with a significant effect of time ($p < 0.001$) observed over the course of the expedition. Although serum [α1-AGP] remained elevated during descent compared to baseline (p-values > 0.05), exploratory analysis demonstrated that serum [α1-AGP] upon return back to Gangtok (1,650 m; at the end of the expedition) was comparable to serum [α1-AGP] from the initial days of the expedition at the same altitude (all p-values > 0.05).

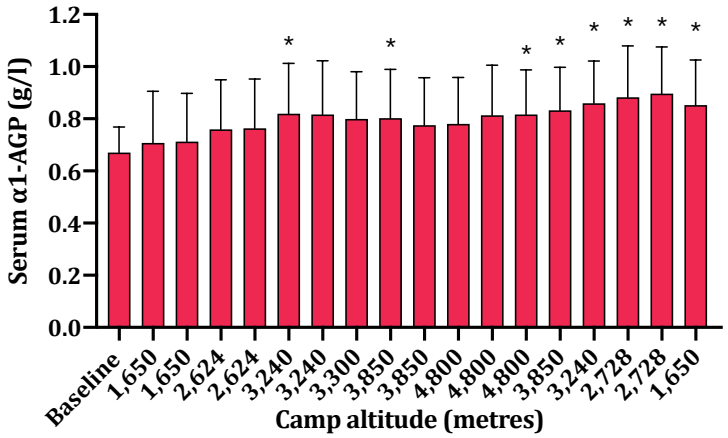

Figure 7.6 – Serum alpha-1 acid glycoprotein (α1-AGP, g/l) at baseline and throughout the expedition. Daily data are presented as group mean (column) + standard deviation (vertical error bars) for blood specimens collected at the indicated (x-axis) morning altitudes (beginning morning 07 October, 2019 and ending morning 23 October, 2019; refer to **Figure 7.1**). Mixed-effects model (with Dunnett's *post-hoc* test) was utilised to compare daily expedition measurements to baseline values while mixed-effects model (with Tukey's correction) was utilised to determine whether values were comparable between days of the expedition (i.e., ascent vs descent values from same camp). All statistical tests were two-tailed with significance set to $\alpha < 0.05$. * Indicates significant difference compared to baseline.

7.3.3.3. Urine specimens

Twenty-four-hour and EMU specimens were well tolerated in all participants throughout the expedition despite the extreme environment. Strategic planning was successful in avoiding overt urine leakage (< 5% volume) from the 3,000 ml containers. Accidental and premature emptying occurred for two specimens (on a single day), albeit the gaps in the datasets remained limited. A total of 2,576 urine aliquots (to include 4 repeats) were successfully kept at –80 °C throughout the expedition and transported back to Birmingham, UK for urinalysis.

7.3.3.3.1. Urine volumes and weights

Eighteen days' worth of early morning and 24-hour urine specimens (611.57 litres* or 649.58 kilograms) were collected between baseline and days of the expedition. Daily 24-hour specimen volumes and weights are presented in **Figures 7.7**.

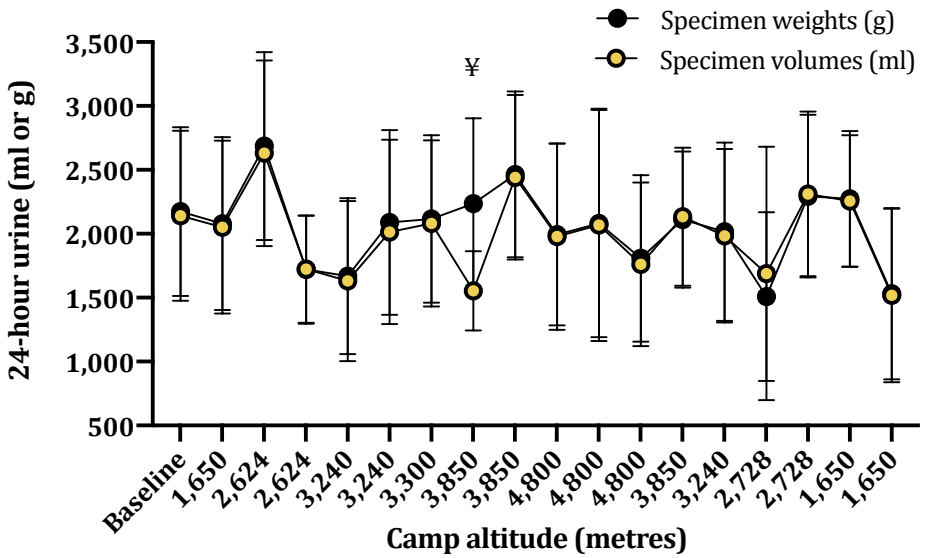

Figures 7.7 – Twenty-four-hour urine specimen weights (g) and volumes (ml). Daily data are plotted as the group mean ± standard deviation (error bars) for specimens measured (and aliquots frozen) at the indicated altitudes (x-axis). ¥ On 13 October, 2019 (Yabuk camp, 3,850 m), specimen volume was successfully recorded for only 3 specimens (due to lack of flat surface) although, weights were successfully measured for all specimens.

7.3.3.3.2. Urinalysis

7.3.3.3.2.1. Urinary alpha-acid glycoprotein (24-hour and EMU)

Six hundred forty-four specimens (to include both, 24-hour and EMU specimens) were analysed in triplicate (totaling 1,932 tests) for urinary α1-AGP with approximately 88% of all samples analysed at neat and the remaining 12% analysed at 1 + 5 dilution. Urinary α1-AGP fell below the lower limit of detection (< 0.08 mg/l) for only a single test out of all 1,932 tests. Within-run imprecision was lower for 24-hour urine specimens compared to EMU (SDs, 0.087

* On 13 October, 2019 urine volume was successfully recorded for only three specimens (due to lack of flat surface) while weight was successfully recorded for all specimens that day.

vs 0.099; and variances, 0.008 vs 0.010, respectively). Similarly, within-run %CV was lower for 24-hour specimens compared to EMUs (4.29% vs 6.63%, respectively), albeit still did not exceed allowable imprecision. Surprisingly, the uncorrected* mean [α1-AGP] (mg/l) values from EMU specimens were lower compared to the uncorrected [α1-AGP] values from 24-hour specimens (**Table 7.5**), although measurements correlated well ($p < 0.001$, r = 0.816).

* EMU [α1-AGP] uncorrected for urinary creatinine and 24-hour [α1-AGP] uncorrected for sample volume and collection duration.

Table 7.5 – Mean urinary alpha-1 acid glycoprotein concentration [α1-AGP] from 24-hour and early morning urine (EMU) specimens.

Camp altitude (m)	Day	24-hour [α1-AGP] (mg/l)	EMU [α1-AGP] (mg/l)
130	Baseline	0.520 ± 0.201	0.349 ± 0.210
1,650	07	0.994 ± 0.639	0.660 ± 0.362
2,624	08	0.531 ± 0.184	0.323 ± 0.113
2,624	09	0.840 ± 0.230	0.648 ± 0.329
3,240	10	1.766 ± 1.138	0.830 ± 0.363
3,240	11	1.587 ± 1.088	0.976 ± 0.460
3,300	12	1.106 ± 0.559	0.602 ± 0.283
3,850	13	1.096 ± 0.576	0.735 ± 0.293
3,850	14	1.752 ± 1.018	0.945 ± 0.568
4,800	15	2.289 ± 1.384	0.971 ± 0.521
4,800	16	2.671 ± 1.605	2.561 ± 1.941
4,800	17	3.302 ± 2.792	1.950 ± 1.430
3,850	18	2.817 ± 2.160	1.472 ± 1.160
3,240	19	1.724 ± 0.914	1.400 ± 1.072
2,728	20	2.012 ± 1.585	1.309 ± 0.981
2,728	21	1.573 ± 1.334	1.928 ± 1.486
1,650	22	1.958 ± 1.323	1.401 ± 0.810
1,650	23	2.003 ± 1.516	1.084 ± 0.846

Urinary [α1-AGP] data (uncorrected for specimen volume, collection duration, or creatinine) are presented as the mean ± standard deviation for the group for specimens collected at baseline and days of the expedition (October, 2019), which corresponded to the camp altitudes indicated in **Figure 7.1**.

Compared to baseline values from 24-hour and EMU specimens (1.093 ± 0.582 mg/24-hours and 0.025 ± 0.016 mg/mmol$_{\alpha1\text{-AGP:CREA}}$, respectively), α1-AGP excretion was significantly increased during the expedition (both, $p < 0.001$), although only mg/24-hours was correlated with altitude ($p < 0.001$, r = 0.824). Twenty-four-hour α1-AGP excretion was greatest (6.461 ± 5.212 mg/24-hours) during the first full 24-hours at 4,800 m (from 15 to 16 October; **Figure**

7.8) while α1-AGP:CREA from EMUs was greatest (0.205 ± 0.169 mg/mmol$_{α1\text{-AGP:CREA}}$) upon waking the first morning at 4,800 m (on 16 October; as shown in **Figure 7.9a** and **7.9b**). Individual measurements of 24-hour (mg/24-hours) and early morning (mg/mmol$_{α1\text{-AGP:CREA}}$) urinary α1-AGP correlated well ($p < 0.001$, r = 0.632).

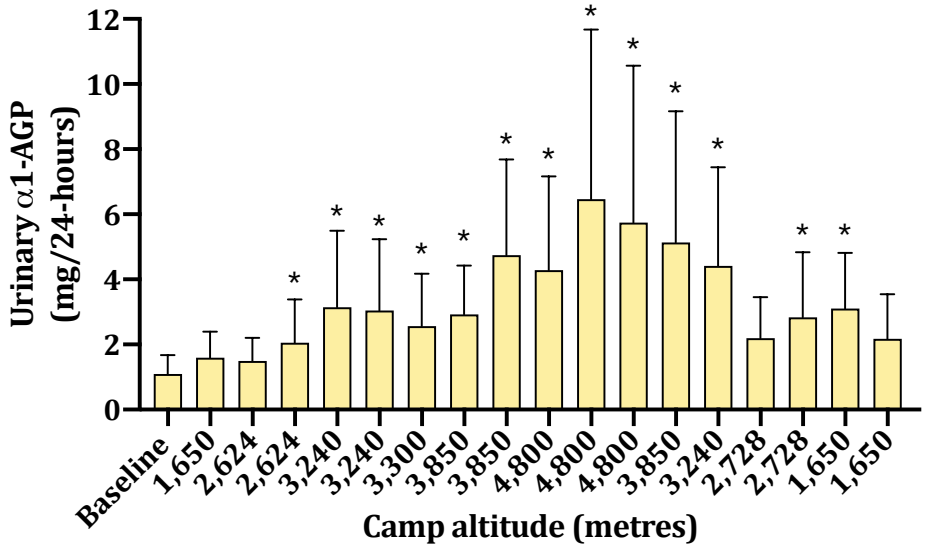

Figure 7.8 – Urinary alpha-1 acid glycoprotein (α1-AGP) from 24-hour urine specimens collected across the expedition. α1-AGP (mg/24-hours) data are plotted as the group mean + standard deviation (+SD, represented by vertical error bars) for 24-hour specimens completed (initiated the preceding day; 4 pm to 4 pm^{+1}) and processed at the indicated altitudes (x-axis). Mixed model with Dunnett's *post-hoc* test was used to compare daily urinary α1-AGP excretion (mg/24-hours) to baseline values with differences marked by an asterisk, *. Twenty-four-hour α1-AGP (mg/24-hours) was greatest (6.461 ± 5.212) during the first full 24-hours at 4,800 m (from 4pm 15 October through 4pm^{+1} 16 October, 2019). All statistical tests were two-tailed with significance set to $α < 0.05$.

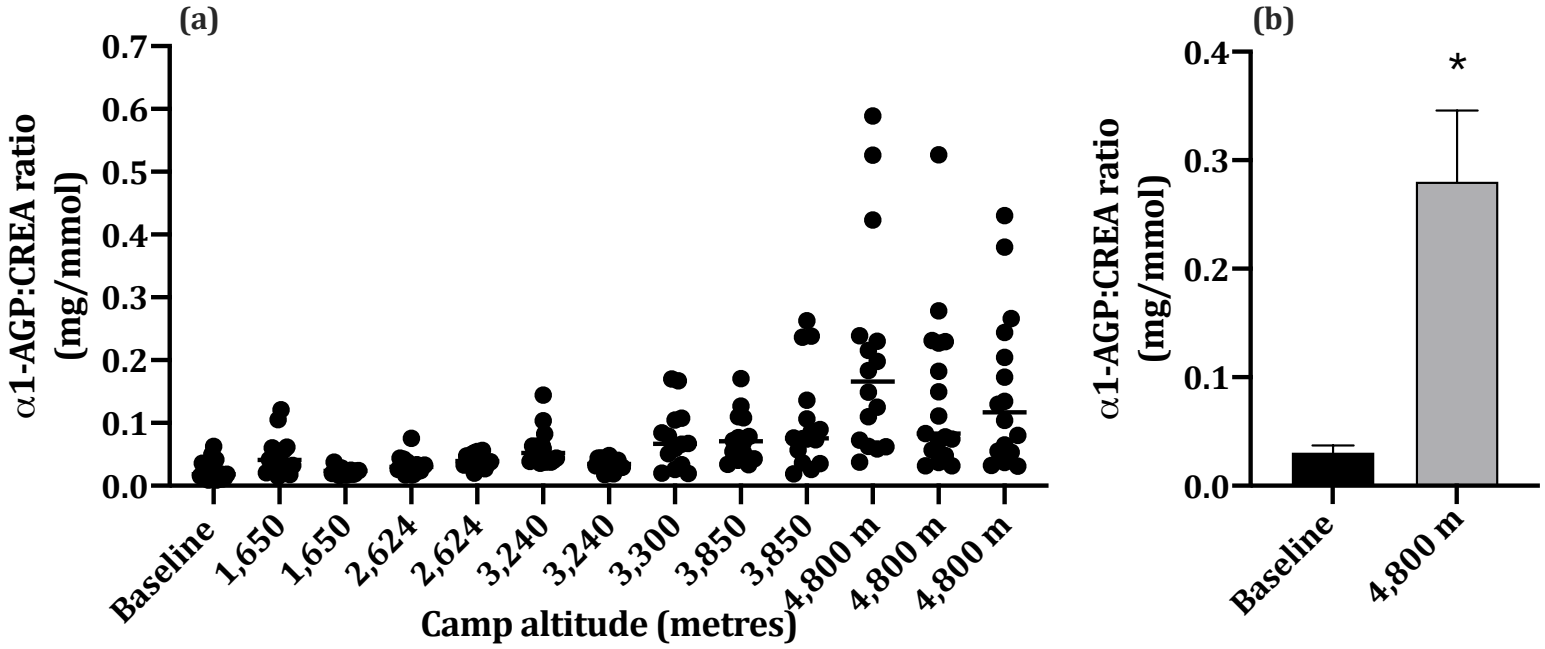

Figure 7.9 – Urinary alpha-1 acid glycoprotein (α1-AGP)-to-creatinine ratio(mg/mmol$_{α1\text{-AGP:CREA}}$) from early morning urine (EMU) specimens during ascent. Fig. 7.9a (left) – Individual α1-AGP:CREA measurements (for EMU specimens collected at the indicated morning altitudes, x-axis) are plotted for ascent only, albeit analysis included all days of the expedition with a significant difference observed between days ($p < 0.001$); **Fig. 7.9b (right)** – The greatest difference (0.181 mg/mmol$_{α1\text{-AGP:CREA}}$ [CIs: 0.046 to 0.315]) compared to baseline (0.025 ± 0.016 mg/mmol$_{α1\text{-AGP:CREA}}$) was exhibited on the 1st morning (0.205 ± 0.169 mg/mmol$_{α1\text{-AGP:CREA}}$) at the top camp (16 October, 4,800 m) with this difference being significant ($p = 0.009$; marked by an asterisk, *). Mixed model with Dunnett's *post-hoc* test was used to compare daily values to baseline. All statistical tests were two-tailed with significance set to $α < 0.05$.

Twenty-four-hour urinary excretion rates (mg/24-hours) were significantly different between AMS$^+$ vs AMS$^-$ individuals as shown in **Figure 7.10**.

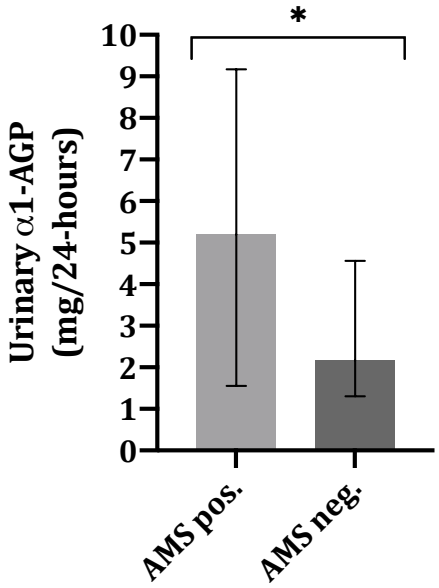

Figure 7.10 – Urinary alpha-1 acid glycoprotein (α1-AGP) compared between days when individuals scored positive or negative for acute mountain sickness (AMS) via Lake Louise Scores. Data are plotted as median (columns) ± interquartile ranges (25 – 75%; error bars). Mann-Whitney U test for unpaired comparison of ranks between the urinary α1-AGP excretion rates (mg/24-hours) of AMS positive vs AMS negative individuals. A significant difference between ranks in AMS$^+$ (1.985 [1.261 – 3.673] mg/24-hours) and AMS$^-$ (5.914 [1.553 – 9.173] mg/24-hours) individuals was observed for 24-hour α1-AGP excretion. All statistical tests were two-tailed with significance set to $\alpha < 0.05$ (marked by asterisk, *).

7.3.3.3.2.2. Twenty-four-hour urine electrolytes

Compared to baseline (96.49 ± 33.50 mmol/24-hour), Na^+ excretion was significantly higher on 14 out of 17 expedition days (all adj. *p*-values < 0.01), being greatest on 08 October (223.9 ± 105.4 mmol/l) after arriving in Lachung from Gangtok (**Figure 7.11a**). Comparison of Na^+ excretion between days of the expedition demonstrated a significant effect of time on Na^+ excretion ($p < 0.001$). Estimations for the percentages of Na^+ reabsorbed are presented in **Table 7.6** with significant reductions compared to baseline observed on all days except at top camp.

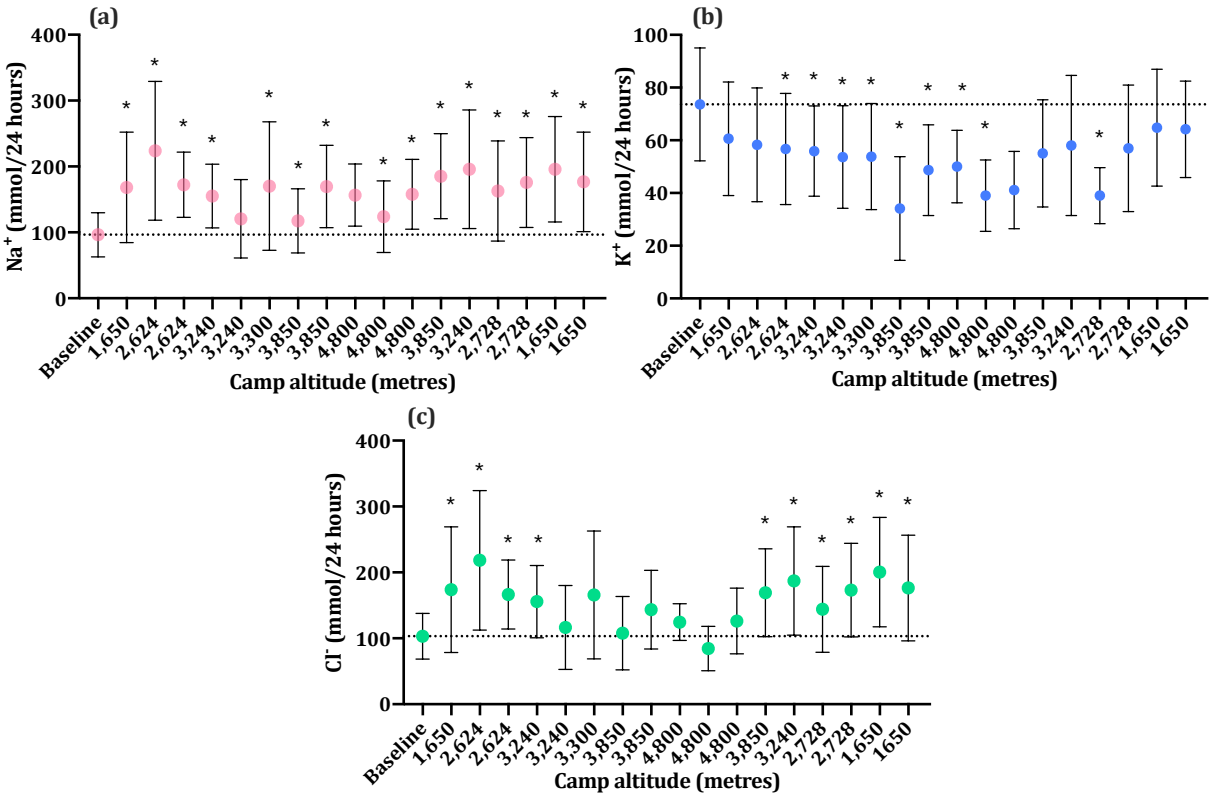

Figure 7.11 – Twenty-four-hour electrolyte excretion. Fig. 7.11a (top left) – Total urinary sodium (Na^+) excreted per 24-hours (mmol/24-hours); **Fig. 7.11b (top right) –** Total urinary potassium (K^+) excreted per 24-hours (mmol/24-hours); **Fig. 7.11c (bottom)** – Total urinary chloride (Cl^-) excreted per 24-hours (mmol/24-hours). Twenty-four-hour data (mmol/24-hour), calculated by correcting the measured [electrolyte] (mmol/l) for collection duration and specimen volume (litres), are plotted as mean ± standard deviation (for the group) for specimens processed at the indicated altitudes (x-axis). It should be noted that data from the first day at 3,850 (13 October, 2019) is only representative of three individuals as volumes were not successfully recorded for all individuals due to lack of a flat surface. Mixed effects analysis using Dunnett's *post hoc* test was conducted to compare daily values to baseline with significant difference compared to baseline marked by asterisk, *. All statistical tests were two-tailed with significance set to $\alpha < 0.05$.

Table 7.6 – Percent of filtered electrolyte load reabsorbed.

	Baseline (~130 m)	07 Oct (1,650 m)	09 Oct (2,624 m)	14 Oct (3,850 m)	16 Oct (4,800 m)	21 Oct (2,728 m)	23 Oct (1,650 m)
Na^+ reabsorbed (%)	99.6 ± 0.2	99.3 ± 0.3	99.2 ± 0.4	99.3 ± 0.2	99.5 ± 0.5	99.3 ± 0.3	99.3 ± 0.3
p-value	-	0.002*	0.001*	0.001*	0.072	< 0.001*	0.002*
K^+ reabsorbed (%)	89.7 ± 3.7	90.9 ± 3.1	90.6 ± 3.4	90.9 ± 3.2	92.1 ± 4.0	91.4 ± 3.6	89.7 ± 3.2
p-value	-	0.620	0.811	0.643	0.033*	0.122	> 0.999

Estimated percentages of the electrolyte filtered loads that were reabsorbed are presented as the mean ± standard deviation for the group. Individual values were estimated using the: cystatin C-based calculation of glomerular filtration rate (eGFR); blood [electrolyte], and urine [electrolyte] from 24-hour specimens. Mixed effects model with Dunnett's *post* hoc test was used to compare estimates between baseline and expedition days. All statistical tests were two-tailed with significance set to $\alpha < 0.05$ and marked by asterisk, *. K^+, potassium; and Na^+, sodium.

Mean K^+ excretion was significantly lower than baseline (73.62 ± 21.44 mmol/24-hour) on several days of the expedition as shown in **Figure 7.11b** and was lowest during the first 24-hours at the top camp (39.00 ± 13.57 mmol/l). A significant effect of time was observed on K^+ excretion when excretion was compared between days of expedition ($p < 0.001$). Estimations for the percentages of K^+ reabsorbed are presented in **Table 7.6** with a significant increase compared to baseline evident at the top camp only ($p = 0.033$).

Urinary Cl^- was elevated compared to baseline (103.2 ± 34.6 mmol/24-hour) on all days of the expedition (see **Figure 7.11c**) except during the first 24-hours at the top camp (84.5 ± 33.7 mmol/l, adj. $p = 0.406$). A significant effect of time on urinary Cl^- was observed across days the expedition ($p < 0.001$). Urinary Cl^- remained elevated compared to baseline upon arrival back to Gangtok, although compared to excretion at Gangtok from ascent, there was no difference ($p = 0.896$) indicating equilibration, nonetheless.

7.3.4. Nocturnal pulse oximetry

A total of 2,378.3 artifact-free hours of nocturnal SpO_2 data were collected across all days for the entire group. Mean recording length across all nights was 7.9 hours with the mean percent artifact being 3.54%. Device failure (e.g., fail to offload or fail to sense) and operator error were minimal throughout, with a total of 315 out of 339 recordings successfully collected throughout the expedition (93% success rate). Most issues were limited to the finger sensors due to regular wear and tear, although battery life was noticeably shorter at altitude compared to the factory specifications.

7.3.4.1. Time series analyses

7.3.4.1.1. Descriptive statistics and 1st statistical moment

Mean nocturnal SpO_2 from altitude recordings was significantly lower throughout ascent compared to baseline and was lowest (76.9 ± 3.0; $p < 0.001$)* during the 2nd night at the top camp (4,800 m; **Figure 7.12**).

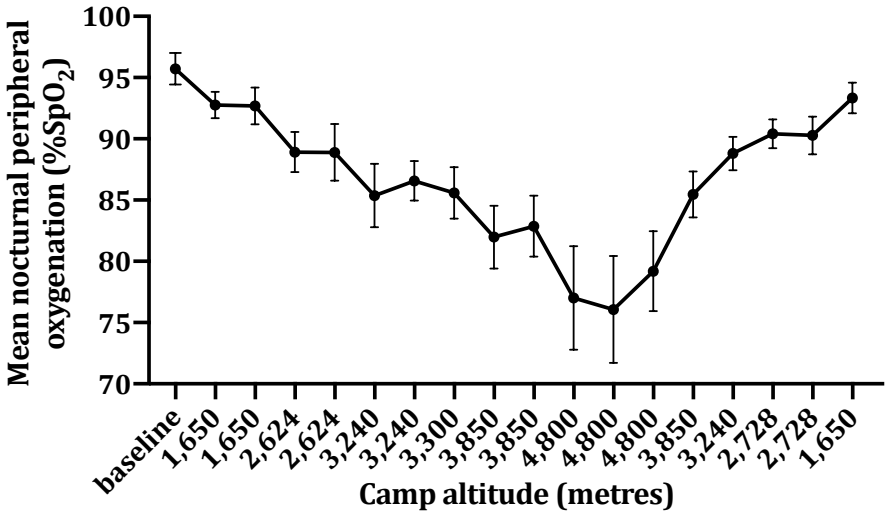

Figure 7.12 – Nocturnal peripheral oxygen saturation obtained by finger pulse oximetry (%SpO_2) during ascent to and descent from 4,800 m. Data are plotted as nocturnal mean ± standard deviation for the group at each indicated altitude (x-axis). Mixed effects analysis was conducted to compare nightly data to baseline (using Dunnett's *post hoc* test), as well as, between days of the expedition (using Tukey's correction). Nocturnal SpO_2 was significantly lower on all days of the expedition compared to baseline ($p < 0.001$) and was lowest (76.9% ± 3.0%) during the 2nd night at the top camp (4,800 m; 16 October, 2019). A significant effect of time (i.e., between days of the expedition) was also observed ($p < 0.001$). All statistical tests were two-tailed with significance set to $\alpha < 0.05$.

* Observed even despite the removal of the from the descendants on the night of 17 October, 2019.

Nocturnal HR/SpO_2 ratio increased with increasing altitude ($p < 0.001$, $R^2 = 0.750$), which was also reflected by the significant effect of time ($p < 0.001$) across the expedition. HR/SpO_2 ratio was greatest during the 2nd night at the top camp (16 October, 2019; 0.885 ± 0.138 beats/min/%) and appeared to recover with descent (see **Figure 7.13**).

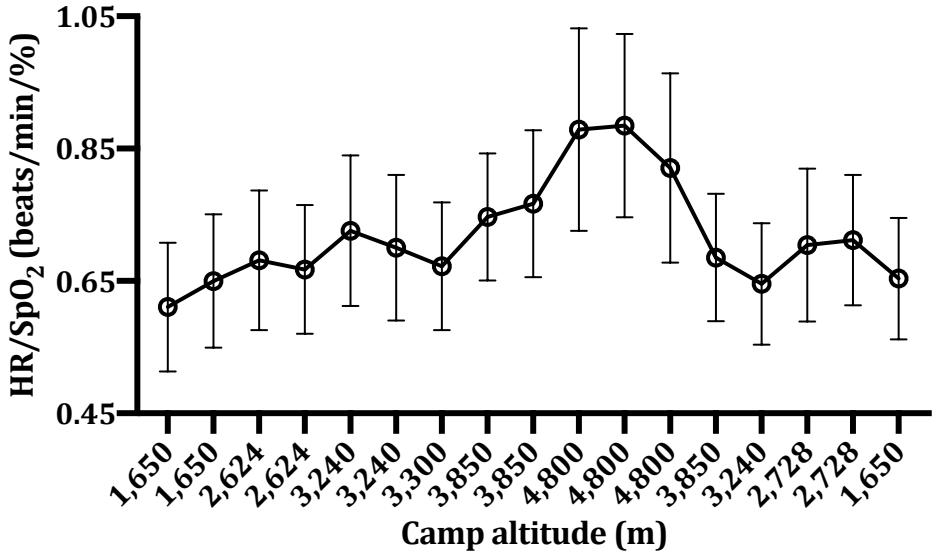

Figure 7.13 – Nocturnal HR/SpO_2 (beats/min/%) across the expedition. Data are plotted as group mean ± standard deviation (error bars) for each night of the expedition at the altitudes stated (x-axis). HR, heart rate; and SpO_2, peripheral oxygenation by finger pulse oximetry.

Basal vs waking results for SpO_2 and HR are presented in **Figure 7.14a – 7.14d**. There was a significant effect of time on basal and waking SpO_2 (both, $p < 0.001$) and HR (both, $p < 0.001$). Despite differences being small between basal and waking SpO_2, a significant difference was observed between the two measurements across the expedition (time × measurement, $p = 0.034$). A similar significant difference between basal and waking measurements was also evident for HR across the expedition (time × measurement, $p < 0.001$).

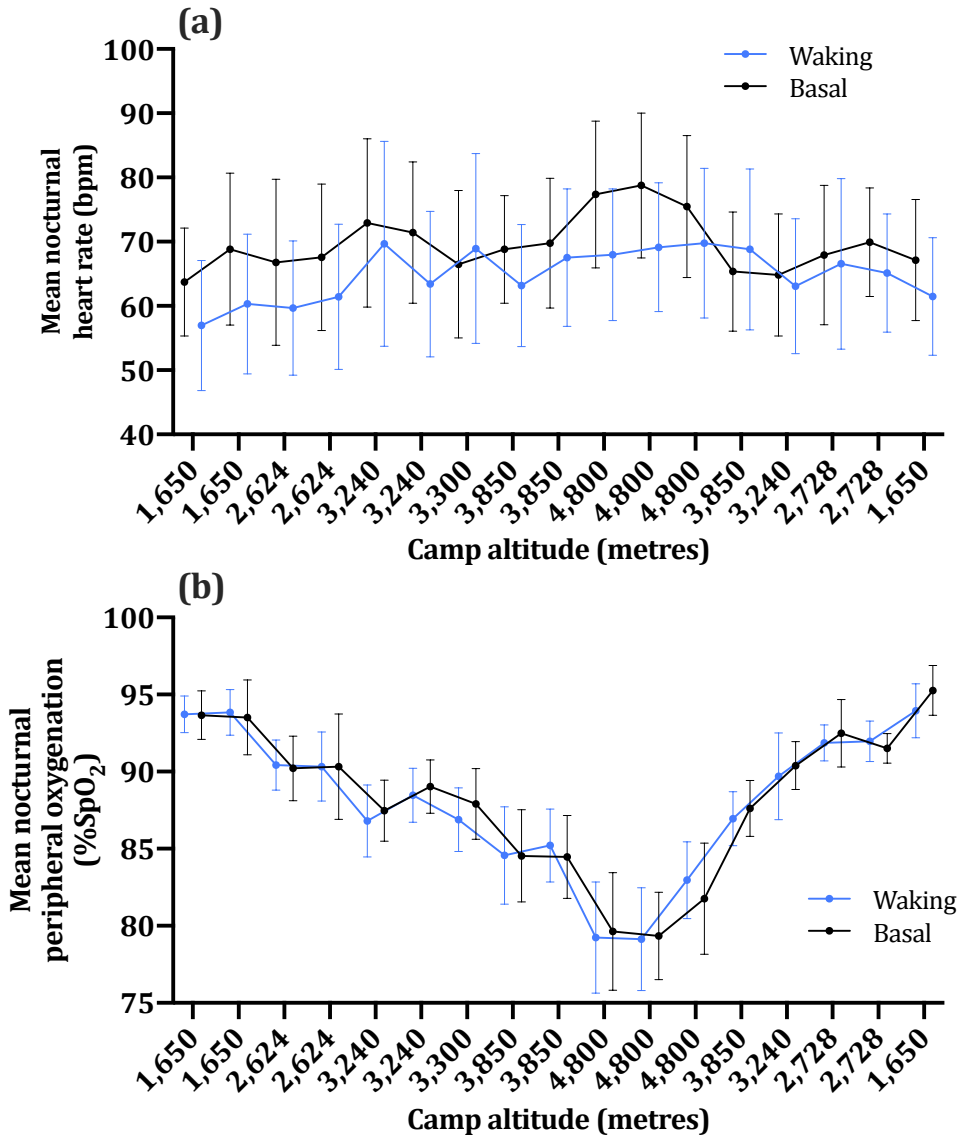

Figure 7.14 – Basal and waking physiologic responses during ascent. Fig. 7.14a (top) – Basal and waking heart rate (HR, bpm); and **Fig. 7.14b (bottom)** – Basal and waking peripheral oxygen saturation (%SpO_2). Basal and waking SpO_2 measurements are plotted as group mean ± standard deviation (error bars) while basal and waking HR were plotted as the median ± interquartile range (error bars) given the distribution of these data. Basal measurements were derived from the first 10 minutes of the nocturnal pulse oximetry recording, while waking measurements were derived from the last 3 minutes of the nocturnal recording (i.e., the morning).

7.3.4.1.2.2nd statistical moment – variance

Figure 7.15 – Figure 7.19 provide visual representations for the range of results presented for statistical moments in proceeding sections. Nocturnal SpO_2 variance was increased when SpO_2 was reduced (**Figure 7.15a**) and when altitude was increased (**Figure 7.15b**). Nocturnal SpO_2 variance was significantly greater throughout ascent compared to

baseline ($p < 0.001$) with the greatest difference compared to baseline (3.597 ± 2.525) exhibited on the 2nd night at the top camp (7.794 ± 4.323; mean difference, 4.197 [CIs: 0.63 to 8.330]), as shown in **Figure 7.15b.** A significant effect of time ($p < 0.001$) on nocturnal SpO_2 variance was also observed. Nocturnal SpO_2 variance was reduced (returning to 'normal') with descent and upon return to Gangtok (06 October vs 22 October, 2019) reached similarly low levels as to initial values observed for ascent ($p = 0.774$, mean difference, 0.212 [CIs: –0.444 to 0.868]). Exploratory analysis demonstrated a significant negative correlation between mean nocturnal SpO_2 variance and morning LLS ($p = 0.003$, $r = -0.701$, and $R^2 = 0.491$).

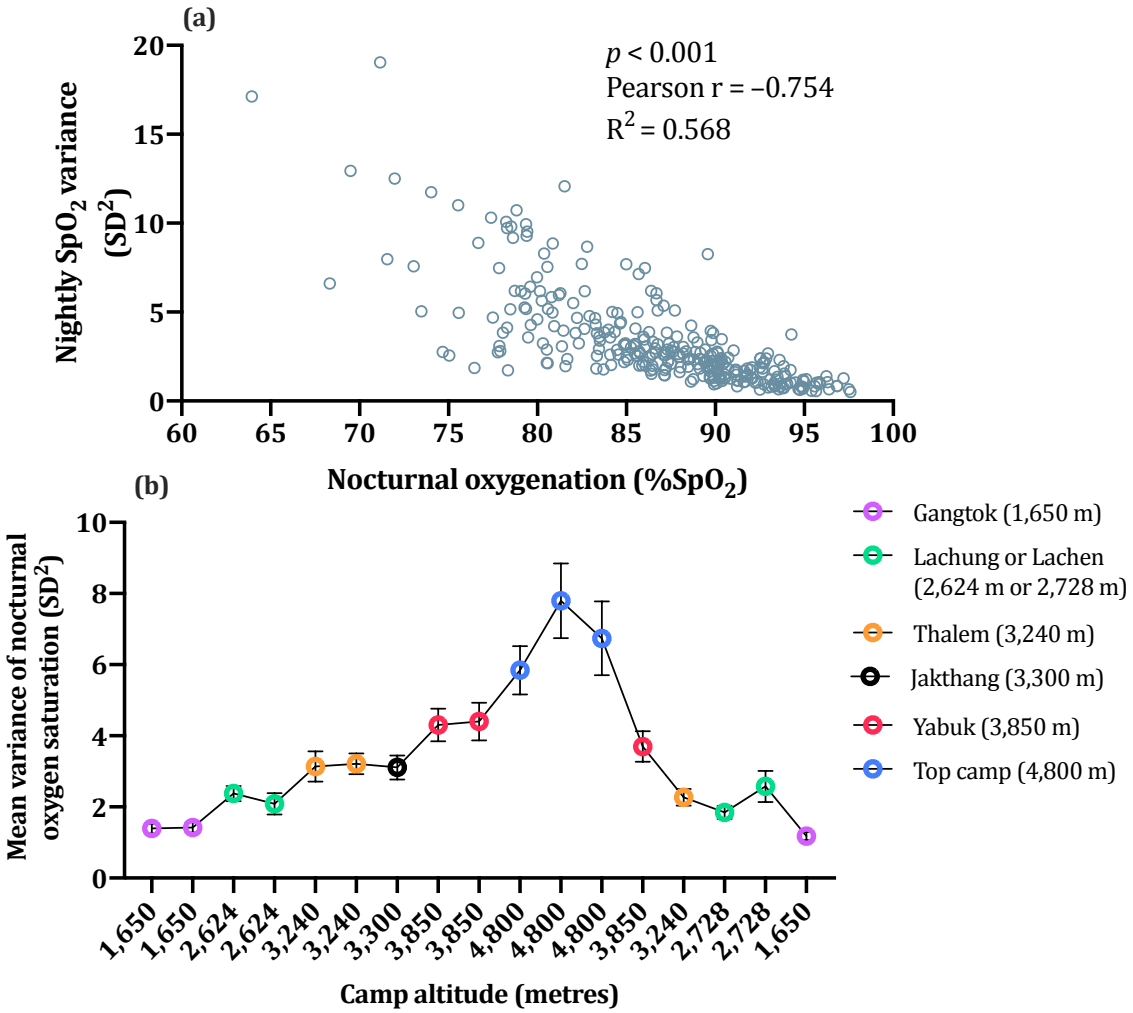

Figure 7.15 – Variance of nocturnal oxygenation (%SpO_2) during ascent to (and descent from) 4,800 m. Fig. 7.15a (top) – Scatter plot for nocturnal %SpO_2 variance (y-axis) vs mean nocturnal %SpO_2 from each nocturnal recording for all participants and all nights of the expedition; **Fig. 7.15b (bottom)** –Variance of nocturnal %SpO_2 plotted as mean variance ± standard deviation (SD; for the group) across all nights of the expedition. Nocturnal SpO_2 variance was greatest (7.794 ± 4.323) on the 2nd night at the top camp (4,800 m; 16 October, 2019). Nocturnal SpO_2 was recorded (at 1 Hz) using finger pulse oximetry. All statistical tests were two-tailed with significance set to $\alpha < 0.05$. Pearson r, correlation efficient; and R^2, coefficient of determination.

7.3.4.1.3.3rd statistical moment – skewness

Figure 7.16, **Figure 7.17a** and **Figure 7.18a** provide visual representations of relative frequency plots that were used to represent skewness and kurtosis results. **Figure 7.16** depicts a generalised version of these data, primarily, for visualisation and conceptualisation purposes, and was derived from the mean group data on select days.

Baseline nocturnal skew (for the group) was negative (–0.305 ± 0.847) whilst skew from all nights during ascent and descent was positive. Nocturnal skew was significantly elevated (p = 0.047) compared to baseline throughout the expedition, with the greatest difference from baseline exhibited on the 1st night at the Yabuk camp (3,850 m; mean difference, –0.763 [CIs: –1.568 to 0.043]).

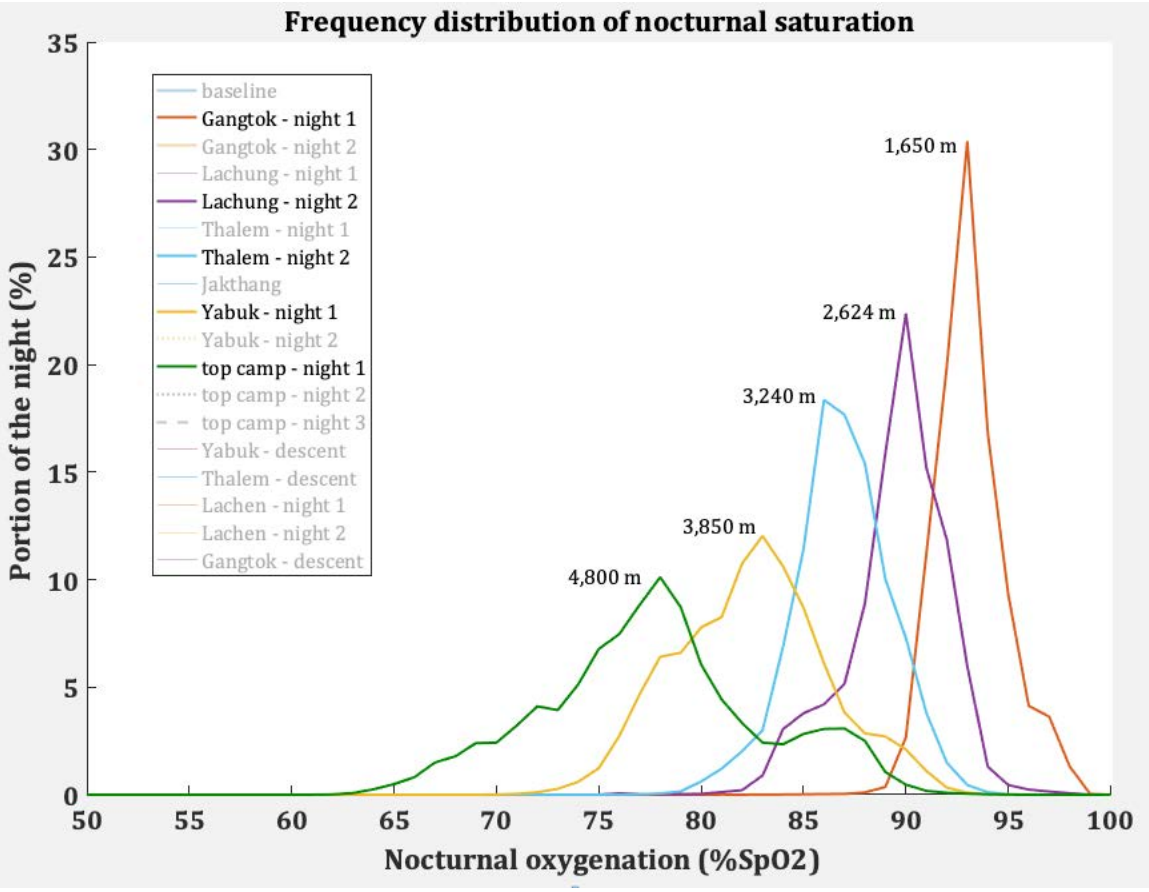

Figure 7.16 – Relative frequency distributions for nocturnal peripheral oxygen saturation (SpO_2) from 5 nights of ascent. Nightly data are represented by different colours and are plotted as the mean relative frequency (of the group) for each SpO_2 between 30% – 100. Indicated altitudes referred to the elevation (metres) at which the data were collected and corresponded to the 1st night at the following camps: Gangtok (1,650 m), Lachung (2,624 m), Thalem (3,240 m), Yabuk (3,850 m), and top camp (4,800 m). Kurtosis proper (or 'peakedness') of nocturnal SpO_2 is reduced (as a function of a portion of the night, %) with increasing altitude – representing a wider distribution of SpO_2 (a flattening of the frequency distribution). Mean relative frequency for all SpO_2 values < 50% was 0. Therefore, these data are not plotted.

By contrast, **Figure 7.17** and **Figure 7.18** show data from separate individuals on select nights with these figures being representative of plots that were derived for each individual and for each nocturnal recording. Data from **Figure 7.17** were representative of an individual who scored positive for AMS during residence at the top camp. A 'worsening' in skewness was observed during successive nights at the top camp (green vs purple lines), which were accompanied by increases in LLS. By comparison, **Figure 7.18** represented an alternate individual who scored negative for AMS during the same time period (and throughout).

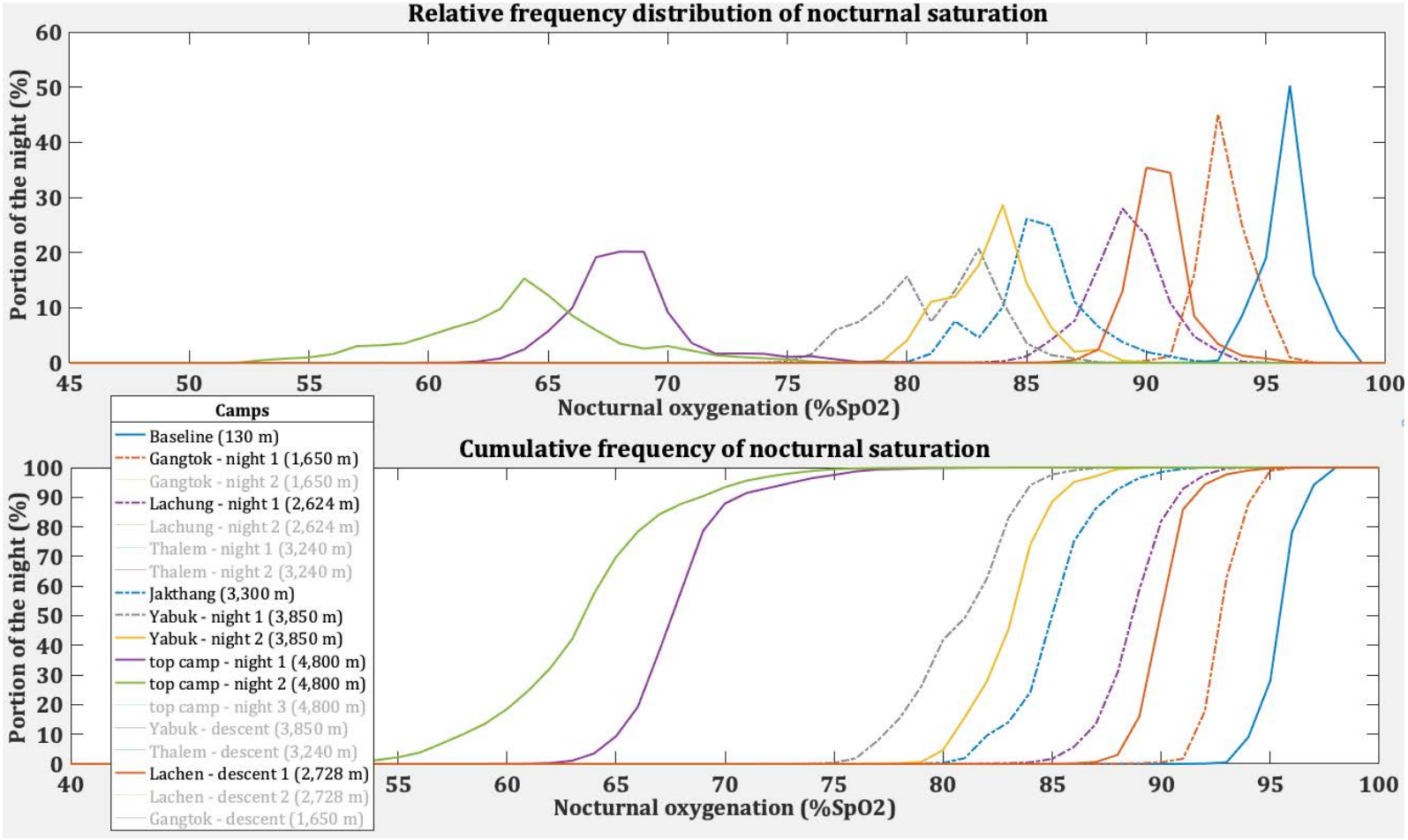

Figure 7.17 – Frequency distribution plots of nocturnal oxygenation (SpO_2). Fig. 7.17a (top) – Relative frequency; and **Fig. 7.17b (bottom) –** Cumulative frequency. Plots are presented for one individual from select nights (for clarity), albeit all nights were collected. 'Worsened' skewness (1st vs 2nd night at top camp: 1.28 vs 0.20; indicated by green and purple lines) and kurtosis were observed during successive nights at the top camp (4,800 m) and were evident from the change in 'peakedness' and inflection of the peak. These data coincided with similar changes in mean SpO_2 for the 1st (68.3% SpO_2, purple) and 2nd night (63.9% SpO_2, green) at 4,800 m. These data were representative of an individual who scored positive for acute mountain sickness twice during residence at 4,800 m and was later identified as the individual who required premature descent. Taken together, these data illustrate, and uniquely depict, altitude.

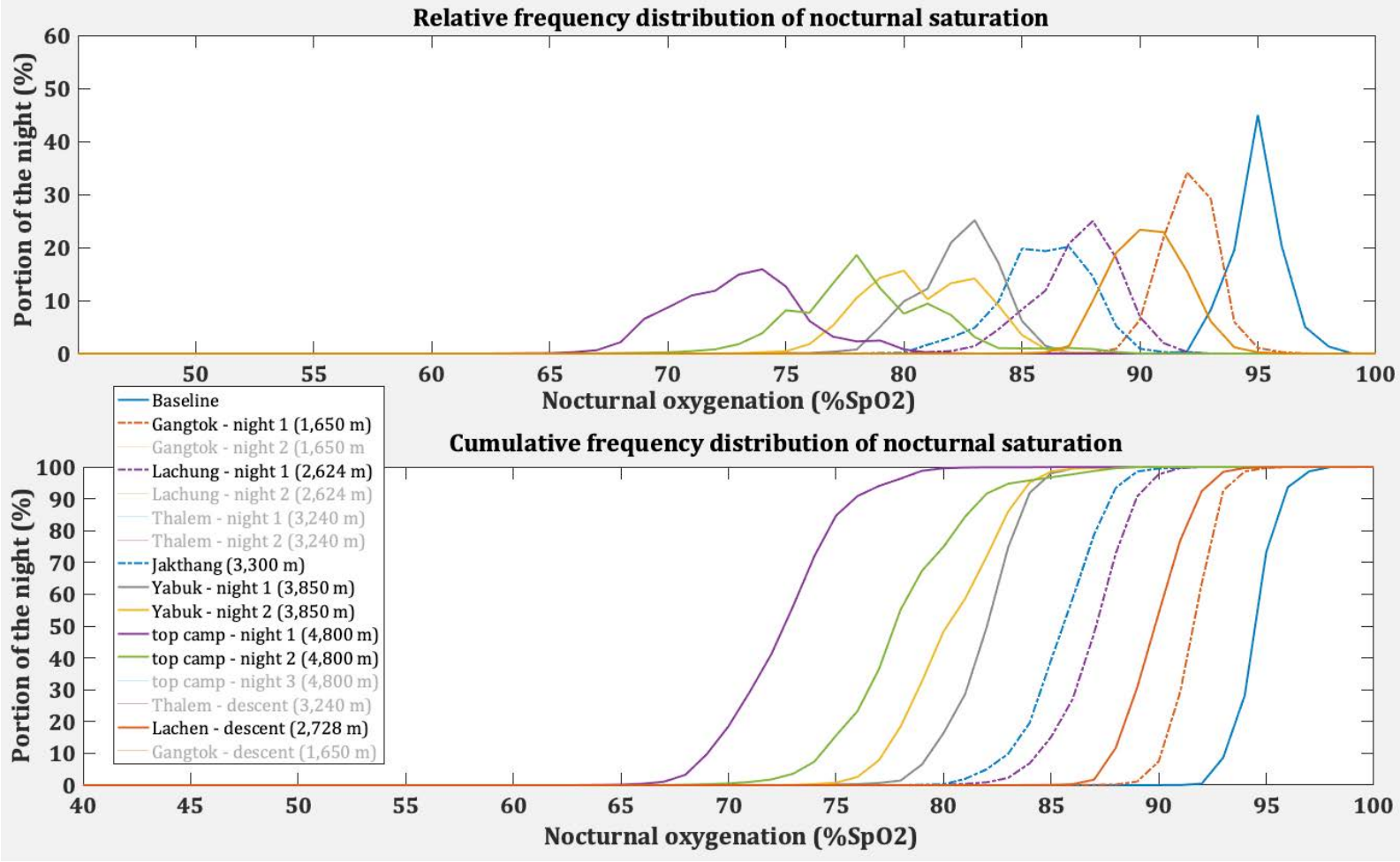

Figure 7.18 – Frequency distribution plots of nocturnal oxygenation (%SpO_2). Fig. 7.18a (top) – Relative frequency; and **Fig. 7.18b (bottom)** – Cumulative frequency. As with **Figure 7.17**, plots are presented for a single individual from select nights (for clarity), albeit for an individual who scored negative for acute mountain sickness throughout. Improvement in skewness and kurtosis were observed on the 2nd night at the top camp (4,800; purple vs green lines) opposed to the progressive worsening observed in **Figure 7.17**. Thus, these data illustrate, and uniquely depict, altitude tolerance.

7.3.4.1.4.4th statistical moment – kurtosis

Kurtosis proper for the group was greatest at baseline (5.909 ± 3.754) and 'flattest' (lowest) for the 2nd night at the top camp (16 October, 3.525 ± 0.894), although the differences between baseline and expedition nights did not reach significance (p = 0.059). There was, however, a significant effect of time on kurtosis proper when compared between days of the expedition (06 October – 22 October, 2019, p = 0.032). Kurtosis proper was also observed to improve with acclimatisation and descent, which was evident from the comparison of relative frequency plots between nights at the same camp (e.g ascent vs descent nights at Thalem). Specifically, upon return to Thalem camp (3,240 m) during descent, nocturnal kurtosis proper (4.471 ± 0.805) was significantly greater compared to the 2nd night at Thalem during ascent (4.003 ± 0.986, p = 0.025; **Figure 7.19**).

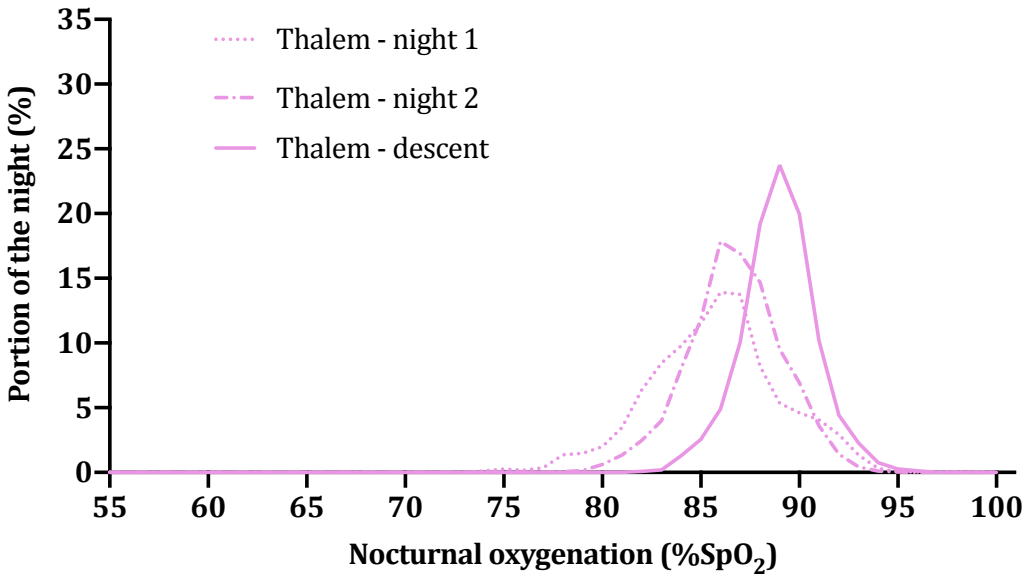

Figure 7.19 – Relative frequency distributions compared between ascent and descent nights at Thalem camp. Relative frequency distributions of nocturnal oxygenation (SpO_2) for the group are plotted for three separate nights at Thalem camp (3,240 m) from recordings obtained on successive nights of ascent (represented by two different dashed lines) and a single night of descent (solid line). Differences between nights are visually demonstrated (e.g., for kurtosis proper and skewness) and uniquely represent acclimatisation.

7.3.4.1.5. Cumulative frequency of nocturnal saturation

Cumulative frequency plots were successfully constructed in MATLAB (see bottom panels of **Figure 7.17** and **Figure 7.18**) for conceptualisation and feasibility purposes of TSTs, which were estimated at or below a range of saturations (e.g., TST < 80% SpO_2). A significant effect of time on TST < 80% SpO_2 was observed with ascent ($p < 0.001$). Analysis of successfully collected pairs of nocturnal recordings and morning LLS, from when AMS symptomology was greatest (refer to **Figure 7.3**), revealed that TST < 80% SpO_2 to be different between individuals based on AMS status (positive vs negative). Specifically, Mann-Whitney U comparison of ranks, demonstrated that TST < 80% SpO_2 was significantly different ($p < 0.001$) between AMS^- (0.05% [0.00 – 2.61%])* and AMS^+ (70.0% [6.6 – 91.5%]), as shown in **Figure 7.20**.

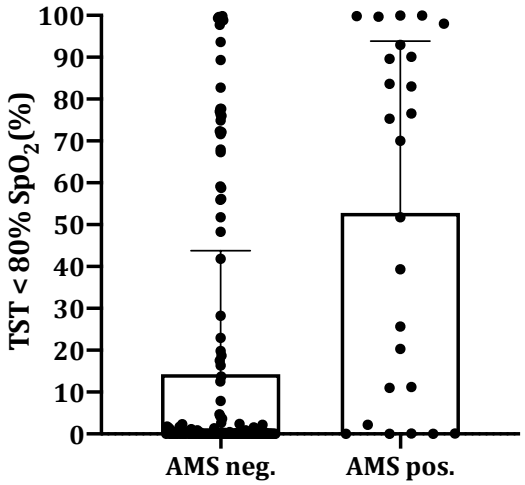

Figure 7.20 – Total sleep time (TST) spent < 80% oxygen saturation (SpO_2). Individual data are plotted with the mean ± standard deviation indicated (by columns and error bars, respectively) despite the non-normal distribution. Only ascent days are included, with plotted points requiring both successful collection of a nocturnal recording and LLS. TST < 80% SpO_2* is compared between individuals scoring positive or negative for acute mountain sickness (AMS) by Lake Louise Scores (LLS). Mann-Whitney-U test (unpaired comparison of ranks) demonstrated that TST < 80% SpO_2 was significantly different between AMS^- and AMS^+ individuals. All statistical tests were two-tailed with significance was set to $\alpha < 0.05$. * TST < 80% SpO_2 represents the proportion of the night spent at an oxygen saturation of 80% or lower.

* Values for TST < 80% (for AMS–and AMS+ individuals) are presented as median [lower – upper IQRs]) in-text.

7.3.4.2. Desaturation characteristics

7.3.4.2.1. Length and frequency

A significant effect of time was observed for both the length and number of desaturations (both $p < 0.001$). Lengths of desaturations were reduced with increasing altitude with the shortest desaturation lengths (17.8 ± 3.4 seconds) observed on the 3rd and final night at 4,800 m. Consequently, there was a significant effect of time ($p < 0.001$) on desaturation frequency characterised by ODI (desaturations per hour), which was greatest during the 2nd night at the top camp (40.8 ± 31.0 desats/hr; **Figure 7.21**).

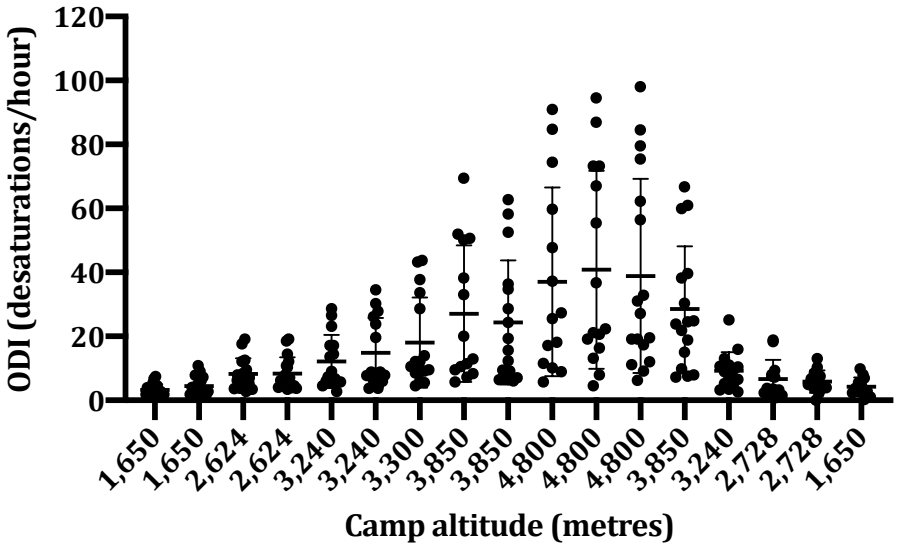

Figure 7.21 – Nocturnal oxygen desaturation index (ODI; desaturations/hour). Nightly individual data are plotted with the mean ± standard deviation for the group also represented (error bars). Mean ODI was greatest (40.8 ± 31.0 desats/hour) during the 2nd night at 4,800 m (16 October, 2019). There was a significant effect of time on ODI ($p < 0.001$). Desaturations were identified as a drop in saturation (decreasing by 0.1% per second) with a nadir at least 4% lower than a preceding 20-second baseline and lasting ≥ 10 seconds[460]. Mixed effects analysis (with Tukey's correction) was used to determine the effect of time on ODI with ascent. Significance was set to $\alpha < 0.05$.

Exploratory analysis demonstrated that mean ODI of the night (for the group) was correlated with morning LLS (by new criteria) ($p = 0.003$, r = 0.690), nocturnal SpO_2 variance ($p < 0.001$, r = 0.967; see **Figure 7.22**) and HR/SpO_2 ($p < 0.001$, r = –0.886) but not serum CRP ($p = 0.225$) or serum α1-AGP ($p = 0.296$).

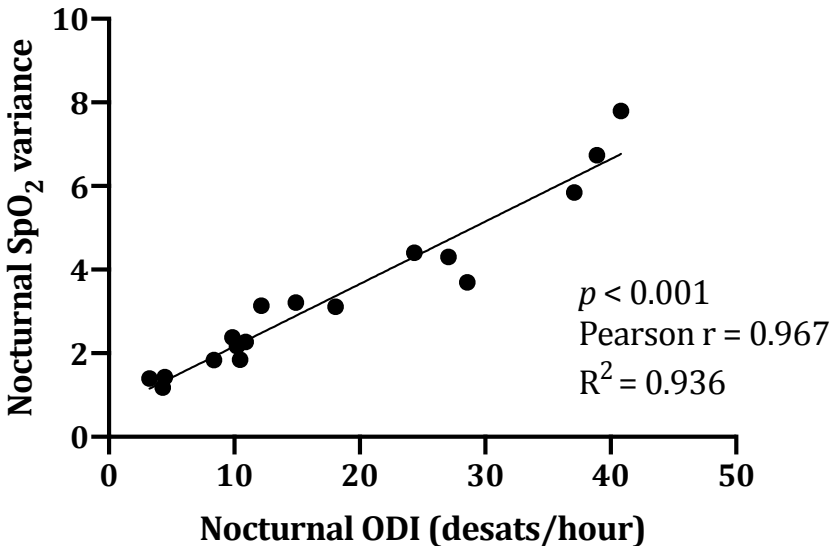

Figure 7.22 – Correlation between nocturnal oxygenation (SpO_2) variance and nocturnal oxygen saturation index (ODI, desaturations per hour). Pulse oximetry data were collected continuously (1 Hz) overnight throughout the expedition with data plotted from the nightly group means of each measure and for each day of the expedition. The three data points lying farthest to the right correspond to the three nights at this top camp (4,800 m). All statistical tests were two-tailed with significance set to $\alpha < 0.05$. Pearson r, correlation coefficient; and R^2, coefficient of determination.

7.3.4.2.2. Desaturation area (or hypoxic burden)

Nocturnal hypoxic burdens calculated relative to the 'theoretical' SpO_2 of 100% are presented in **Figure 7.23** with two individuals whom presented poorly at the top camp and scored positive for AMS highlighted. There was a significant effect of time across the expedition on nocturnal hypoxic burden ($p < 0.001$), which was greatest during the three nights at the top camp (15 October, 22.98 ± 4.22 %min/hr; 16 October, 23.12 ± 3.04 %min/hr; and 17 October, 20.16 ± 3.44 %min/hr). Exploratory analysis demonstrated that hypoxic burden was correlated with morning LLS ($p < 0.001$, r = 0.816, and $R^2 = 0.792$), SBP ($p = 0.005$, r = 0.660, and $R^2 = 0.436$), DBP ($p = 0.049$, r = 0.499, and $R^2 = 0.249$), RR ($p = 0.003$, r = 0.692, and $R^2 = 0.479$), and HR/SpO_2 ($p < 0.001$, r = –0.914, and $R^2 = 0.836$).

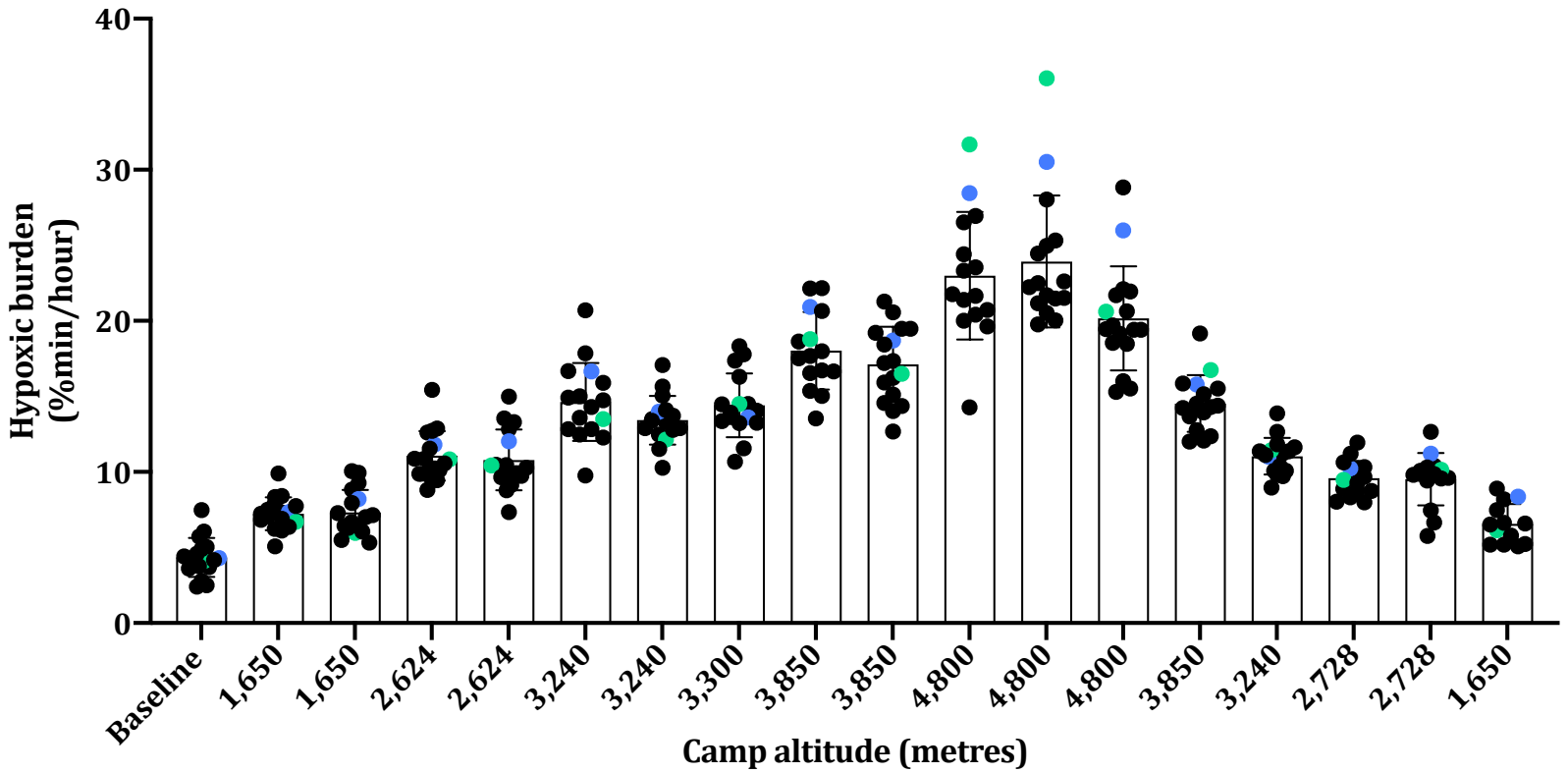

Figure 7.23 – Nocturnal hypoxic burden derived from pulse oximetry during ascent to and descent from 4,800 m. Individual data are plotted across days of the expedition with group means (columns) and standard deviations (errors bars) also represented. Coloured (blue and green) individual data corresponded to the nocturnal hypoxic burdens of two individuals whom presented poorly during residence at top camp relative to the group and scored positive for acute mountain sickness (via Lake Louise Scores). The individual in green required premature descent on the 3rd day at 4,800 m and therefore descended to Yabuk camp to spend the night at 3,850 (instead of a 3rd night at 4,800 m).

7.3.4.3. Methods comparisons

7.3.4.3.1. SaO_2 vs SpO_2

Bias was calculated for both SaO_2 vs $SpO_{2nocturnal}$ (–2.038 ± 4.403) and SaO_2 vs $SpO_{2morning}$ (–5.560 ± 5.559) with the limits of agreement (LOAs, 95% CIs) indicated on the B-A plots shown in **Figure 7.24a** (SaO_2 vs $SpO_{2nocturnal,}$ –10.670 to 6.592) and **Figure 7.24b** (SaO_2 vs $SpO_{2morning}$, –16.450 to 5.336). No significant deviations in linearity were identified by runs test for SaO_2 vs $SpO_{2nocturnal}$ (p = 0.229). Slopes of the best fit lines for the simple regressions (SaO_2 vs $SpO_{2nocturnal}$, 0.345 [CIs: 0.220 to 0.470] and SaO_2 vs $SpO_{2morning}$, 0.547 [CIs: 0.426 to 0.667]) significantly deviated from zero (both, $p < 0.001$). The x-intercept was lower for SaO_2 vs $SpO_{2nocturnal}$ (91.3% [CIs: 88.5 to 95.8%]) compared to SaO_2 vs $SpO_{2morning}$, (96.5% [CIs: 94.2 to 99.9%]).

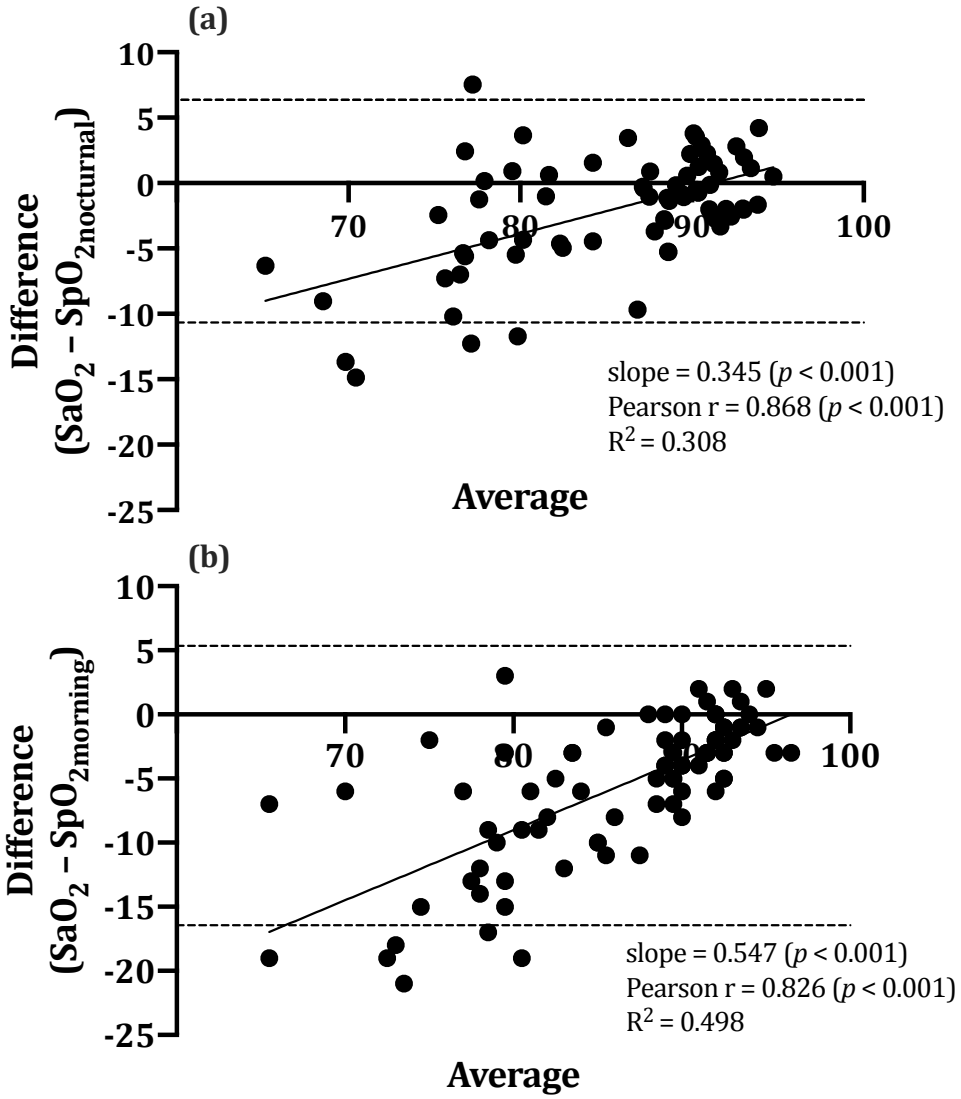

Figure 7.24 – Bland-Altman (B-A) plot comparing arterial oxygen saturation (SaO_2) and peripheral oxygen saturation (SpO_2). Fig. 7.24a (top) – B-A plot for the bias and agreement between arterial oxygenation (SaO_2) and nocturnal oxygen saturation by pulse oximetry ($SpO_{2nocturnal}$) with difference (SaO_2 – $SpO_{2nocturnal}$) plotted against the average of SaO_2 and mean nocturnal SpO_2 from the previous night (n = 70 pairs); **Fig. 7.24b (bottom)** – B-A plot for the bias and agreement between SaO_2 and morning pulse oximetry ($SpO_{2morning}$) (n = 84 pairs) with the difference (SaO_2 – $SpO_{2morning}$) plotted against the average of SaO_2 and $SpO_{2morning}$ measurements from the same morning. Best fit line of the linear regression is plotted to the differences and averages on each figure. Horizontal dashed lines represent the 95% limits of agreement (95% LOAs; top, –10.670 to 6.592; bottom, –16.450 to 5.336). SaO_2 was analysed from arterialised blood (from the earlobe) on the iSTAT blood gas analyser (Abbott Laboratories).

7.3.4.3.2. $SpO_{2nocturnal}$ vs $SpO_{2morning}$

For the 16 occasions when $SpO_{2nocturnal}$ and $SpO_{2morning}$ could be matched, mean $SpO_{2nocturnal}$ was consistently lower (14 out of 16 nights) and significantly different compared to momentary $SpO_{2morning}$ measurements (for 13 out of 16 days; all adj. $p < 0.05$)

obtained the following morning. The lack of differences in SpO_2 measurements occurred on rest days only (e.g., 2nd night and morning at Lachung and 2nd night and morning at Yabuk) with the exception of the night and morning at Jakthang camp (3,300 m), albeit a camp that was not much higher than the two previous nights at Thalem camp (3,240 m). By contrast, the greatest mean difference (± 9.10% SpO_2) occurred between the 3rd and final night and preceding morning at the top camp (night of 17 October and morning 18 October*).

The above differences between $SpO_{2morning}$ and $SpO_{2nocturnal}$ measurements were echoed in the B-A plot presented in **Figure 7.25** (95% LOAs, –2.285 to 8.488), which compared only measurements that had been validated against SaO_2. Linear regression plotted for the difference ($SpO_{2morning}$ – $SpO_{2nocturnal}$) vs the averages of these data had a slope (–0.204 ± 0.057) that significantly deviated from zero ($p < 0.001$). Plotted values were largely exhibited to be positive (> 0) with the overall mean difference ($SpO_{2morning}$ – $SpO_{2nocturnal}$) being 3.0% [CIs: 2.5 to 3.8%], indicating that $SpO_{2morning}$ measurements may overestimate SpO_2 and underestimate the degree of desaturation exhibited overnight.

* This relationship was observed despite the removal of the datasets belonging to the individual who required premature descent on the afternoon of October 17, 2019.

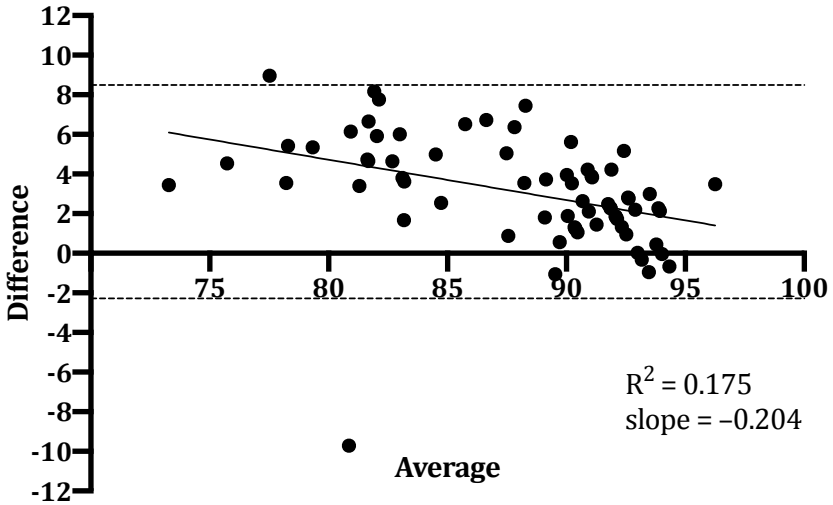

Figure 7.25 – Bland-Altman (B-A) plot comparing peripheral oxygenation from nocturnal ($SpO_{2nocturnal}$) and morning ($SpO_{2morning}$) pulse oximetry. Data are plotted as the difference ($SpO_{2morning} - SpO_{2nocturnal}$) vs the average SpO_2 of the two measurements (n = 70 pairs). Bias was 3.101 ± 2.748 and the 95% limits of agreement (–2.285 to 8.488) are represented by dashed horizontal lines. Simple linear regression applied to these data had a slope (–0.204 ± 0.057) that significantly deviated from zero ($p < 0.001$), albeit the goodness of fit was low ($R^2 = 0.175$). These results confirm that $SpO_{2morning}$ measurements may overestimate SpO_2 and thereby, underestimate the degree of desaturation exhibited during the night. All statistical tests were two tailed with significance set to $\alpha < 0.05$.

7.3.5. Correlations for urinary α1-AGP

Results from correlation analysis for relationships with 24-hour and early morning urinary α1-AGP (mg/24-hours and $mg/mmol_{\alpha1\text{-}AGP:CREA}$, respectively) are presented in **Table 7.7** with results from exploratory analysis between secondary variables presented in **Appendix 8.**

Table 7.7 – Correlation analysis for urinary alpha-1 acid glycoprotein excretion (α1-AGP).

	mg/24-hours		$mg/mmol_{\alpha 1\text{-}AGP:CREA}$	
	p-value	***r***	***p-value***	***r***
Physiologic responses				
Systolic BP	< 0.001*	0.673	0.009	0.628
Diastolic BP	0.057	-	0.215	-
Resting heart rate	< 0.001*	0.913	0.006*	0.641
Respiratory rate	< 0.001*	0.750	< 0.001*	0.864
Lake Louise Score	< 0.001*	0.749	0.248	-
eGFR*	0.004*	–0.663	0.034*	–0.517
Serum and urine biomarkers				
Serum cystatin C	0.003	0.682	0.038*	0.507
Serum CRP	0.710	-	0.358	-
Serum α1-AGP	0.576	-	0.033*	0.518
Urinary Na^+	0.777	-	0.728	-
Urinary K^+	0.006*	–0.640	0.102	-
Urinary Cl^-	0.143	-	0.656	-
Arterial blood measurements				
Haemoglobin	0.100	-	0.336	-
Haematocrit	0.072	-	0.301	-
Na^+	0.045*	0.187	0.343	-
K^+	0.121	-	0.022*	–0.214
pH	0.640	-	0.956	-
PO_2	< 0.001*	–0.451	< 0.001*	–0.497
PCO_2	0.014*	–0.226	< 0.001*	–0.431
TCO_2	< 0.001*	–0.327	< 0.001*	–0.521
Base excess	0.001*	–0.335	< 0.001*	–0.520
Bicarbonate	< 0.001*	–0.317	< 0.001*	–0.489
SaO_2	< 0.001*	–0.460	< 0.001*	–0.501
Nocturnal oximetry metrics				
Mean SpO_2	< 0.001*	–0.932	0.023*	–0.548
Kurtosis proper	0.019*	–0.548	0.024*	–0.530
Skewness	0.150	-	0.151	-
Variance	< 0.001*	0.825	0.026*	0.523
No. of desaturations	< 0.004*	0.927	0.004	0.665
Desaturation length	0.002*	–0.685	0.334	-

Table 7.7 – Correlation analysis for urinary α1-AGP (continued).

	mg/24-hours		mg/mmol$_{α1\text{-}AGP:CREA}$	
	p-value	***r***	***p-value***	***r***
Nocturnal oximetry metrics				
Oxygen desaturation index	< 0.001*	0.945	0.004*	0.665
Hypoxic burden	< 0.001*	0.928	0.025*	0.542
HR/SpO_2	< 0.001*	0.913	0.006*	0.641

Correlation analysis was performed for urinary measurements of α1-AGP from 24-hour (mg/24-hours) or early morning (mg/mmol$_{α1\text{-}AGP:CREA}$) urine specimens between all other physiologic measurements. Statistical tests were two-tailed with significance set to $\alpha < 0.05$. Correlation coefficients (Pearson r or Spearman *rho*); eGFR, estimate glomerular filtration rate; BP, blood pressure; CRP, C-reactive protein; Na^+, sodium; K^+, potassium; Cl^-, chloride; PO_2, partial pressure of oxygen; PCO_2, partial pressure of carbon dioxide; TCO_2, total carbon dioxide; HR, heart rate; SaO_2, arterial oxygen saturation; and SpO_2, peripheral oxygen saturation. * eGFR was estimated using a cystatin C-based equation.

7.3.5.1. Physiologic responses

Twenty-four-hour α1-AGP excretion (mg/24-hours) was correlated with metres of absolute altitude ($p < 0.001$, r = 0.824, and $R^2 = 0.679$), morning LLS ($p = 0.001$, r = 0.749, and $R^2 = 0.561$), RR ($p < 0.001$, r = 0.750, and $R^2 = 0.562$), eGFR ($p = 0.004$, r = –0.663, and $R^2 = 0.439$), and SBP ($p < 0.001$, r = 0.673, and $R^2 = 0.454$) but not DBP ($p = 0.057$).

Similarly, α1-AGP:CREA measurements from EMU specimens (mg/mmol$_{α1\text{-}AGP:CREA}$) were correlated with RR ($p < 0.001$, r = 0.864, and $R^2 = 0.746$), eGFR ($p = 0.034$, r = –0.517, and $R^2 = 0.268$; see **Figure 7.26**), and SBP ($p = 0.009$, r = 0.628, and $R^2 = 0.394$) but not DBP ($p = 0.215$) or LLS ($p = 0.248$).

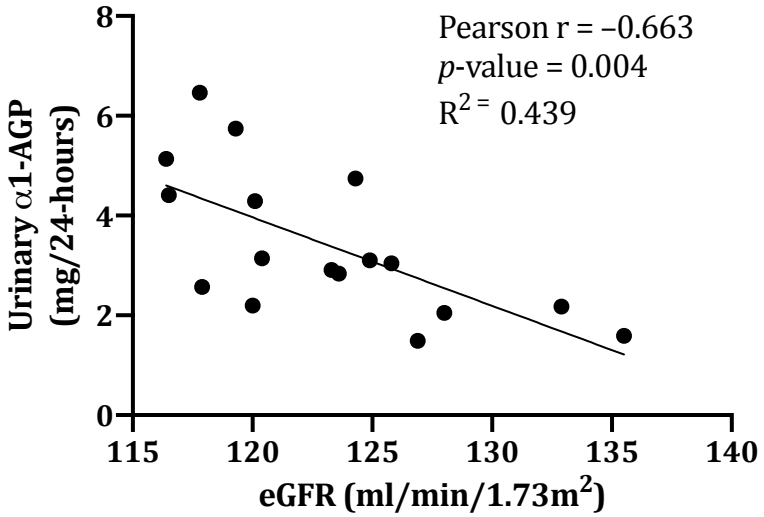

Figure 7.26 – Correlation between urinary alpha-1 acid glycoprotein (α1-AGP) and estimated glomerular filtration rate (eGFR) during ascent. Data are plotted from daily group means of 24-hour urinary α1-AGP and eGFR. eGFR was estimated utilising a cystatin C-based equation[473]. All statistical tests were two-tailed with significance set to $\alpha < 0.05$. Pearson r, correlation coefficient; and R^2, coefficient of determination.

7.3.5.2. Serum and urinary biomarkers

Increases in serum [α1-AGP] (g/l) observed during the expedition were not correlated with 24-hour urinary α1-AGP (mg/24-hours; $p = 0.576$) but were correlated with α1-AGP:CREA ratio from EMU specimens ($p = 0.033$, r = 0.518, and $R^2 = 0.268$). Serum CRP, however, was not related to 24-hour or early morning α1-AGP excretion (mg/24-hours, $p = 0.710$; and or $mg/mmol_{\alpha 1\text{-}AGP:CREA}$, $p = 0.358$, respectively). Similarly, serum CRP was not related to serum α1-AGP nor any other physiologic responses, LLS, or derivatives of nocturnal saturation.

Urinary Na^+ and Cl^- excretion were not correlated with 24-hour α1-AGP ($p = 0.777$ and $p = 0.143$, respectively) or α1-AGP:CREA excretion from EMUs ($p = 0.728$ and $p = 0.656$, respectively). By contrast, a significant negative correlation was observed between K^+ excretion and 24-hour α1-AGP excretion ($p = 0.006$, r = –0.640, and $R^2 = 0.410$), albeit no relationship was with between urinary K^+ and $mg/mmol_{\alpha 1\text{-}AGP:CREA}$ ($p = 0.102$).

7.3.5.3. Arterialised measures

Significant correlations were also evident between 24-hour α1-AGP excretion (mg/24-hours) and arterialised measures; specifically: Na^+ ($p = 0.045$, r = 0.187), PCO_2 ($p = 0.014$, r = –0.226), PO_2 ($p < 0.001$, r = –0.451), TCO_2 ($p < 0.001$, r = –0.327), base excess ($p = 0.001$, r = –0.335), HCO_3^- ($p < 0.001$, r = –0.317), and SaO_2 ($p < 0.001$, r = –0.460), although Spearman *rho* results were predominantly negligible or low (i.e., all between 0.00 ± 0.50).

Similarly, α1-AGP:CREA from EMUs ($mg/mmol_{\alpha1\text{-}AGP:CREA}$) was correlated with K^+ ($p = 0.022$, r = –0.214), PO_2 ($p < 0.001$, r = –0.497), PCO_2 ($p < 0.001$, r = –0.431), TCO_2 ($p < 0.001$, r = –0.521), base excess ($p < 0.001$, r = –0.520), HCO_3^- ($p < 0.001$, r = –0.489), and SaO_2 ($p < 0.001$, r = –0.501).

7.3.5.4. Nocturnal oxygen saturation

Urinary 24-hour α1-AGP excretion (mg/24-hours) was correlated with nocturnal pulse oximetry metrics; specifically: mean SpO_2 ($p < 0.001$, r = –0.932, $R^2 = 0.868$), SpO_2 variance ($p < 0.001$, r = 0.825, and $R^2 = 0.680$), kurtosis proper ($p = 0.019$, r = –0.548, and $R^2 = 0.300$), ODI ($p < 0.001$, r = 0.945; and $R^2 = 0.893$; see **Figure 7.27**), HR/SpO_2 ($p < 0.001$, r = 0.913, and $R^2 = 0.834$), and hypoxic burden ($p < 0.001$, r = 0.928, and $R^2 = 0.861$).

Similarly, α1-AGP:CREA was associated with nocturnal pulse oximetry metrics; specifically: mean SpO_2 ($p = 0.023$, r = –0.548, and $R^2 = 0.300$), SpO_2 variance ($p = 0.026$, r = 0.523, and $R^2 = 0.273$), kurtosis proper ($p = 0.024$ r = –0.530, and $R^2 = 0.280$), ODI ($p = 0.004$, r = 0.665, and $R^2 = 0.442$), HR/SpO_2 ($p = 0.006$, r = 0.641, and $R^2 = 0.441$) and hypoxic burden ($p = 0.025$, r = 0.542, and $R^2 = 0.294$).

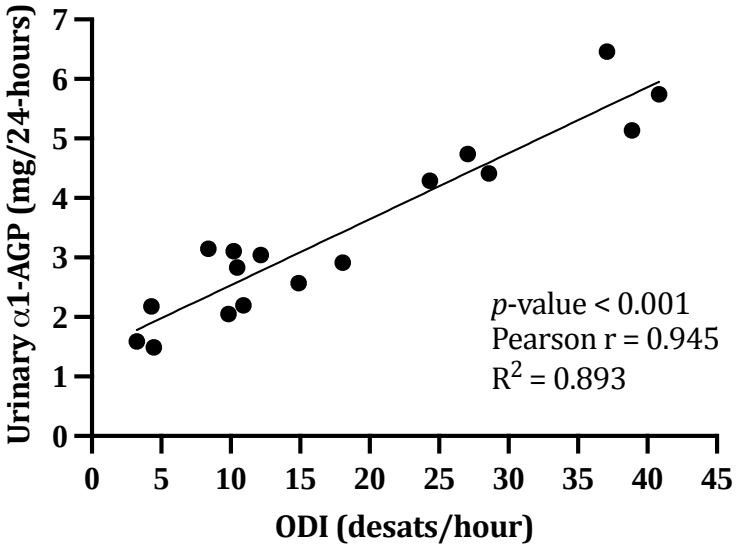

Figure 7.27– Correlation between 24-hour urinary alpha-1 acid glycoprotein (α1-AGP; mg/24-hours) and nocturnal oxygen desaturation index (ODI; desaturations/hour). Data are plotted for daily group means (from 18 individuals) for the two variables during ascent to and descent from 4,800 m. All statistical tests were two-tailed with significance set to $\alpha < 0.05$. Pearson r, correlation coefficient; and R^2, coefficient of determination.

7.4. DISCUSSION

The objective of this study was to examine the impact of hypoxia on urinary α1-AGP excretion during ascent to and descent from 4,800 m. To facilitate this, α1-AGP was analysed from 24-hour and EMU urine specimens collected during an expedition to HA with subsequent statistical analysis performed between urinary α1-AGP results and other physiologic measurements (e.g., SBP, DBP, HR, serum inflammatory markers, and nocturnal SpO_2, to name a few). Specifically, this study examined, in detail, the morphology of nocturnal oxygenation (used as markers of hypoxia) from finger pulse oximetry[470] with the aim to determine whether these measurements were related to urinary α1-AGP excretion. An additional aim was to determine whether these measured physiologic responses during ascent (e.g., increases in urinary α1-AGP excretion or changes in nocturnal oxygenation patterns) were indicative of AMS. A final aim was to

determine whether altitude-induced urinary α1-AGP measurements were comparable between 24-hour and EMU urine specimens.

7.4.1. Urinary α1-AGP during ascent

Twenty-four hour and EMU specimens were successfully collected during a 18-day expedition to HA with observed increases in 24-hour urinary α1-AGP excretion being both significant and consistent with previous ascents[7]. A strong positive correlation was observed between [α1-AGP] from 24-hour and EMU specimens however, [α1-AGP] was consistently lower in EMU specimens compared to 24-hour specimens (refer to **Table 7.5**). This difference was somewhat unexpected given the running hypothesis that hypoxia, being worst overnight during ascent, would contribute to a substantial amount of altitude-induced proteinuria. Given that EMU volume is unquestionably always less than (or equivocal to; for arguments sake) the total 24-hour urine volume, a lower [α1-AGP] in the smaller volume of EMU (vs larger [α1-AGP] in the total 24-hour volume) would suggest lower α1-AGP excretion overnight compared to the day.

This observation however, was based on [α1-AGP] values that had not yet been corrected for specimen volume, collection duration, or [creatinine] and made conclusions tenuous. Nevertheless, $mg/mmol_{\alpha 1\text{-}AGP:CREA}$ did significantly increase during ascent with measurements being positively correlated with mg/24-hours refer to section **7.3.3.3.2.1**). This suggested that EMU specimens may be sufficient for assessment of urinary α1-AGP with regards to altitude-induced glomerular leak.

7.4.2. Nocturnal pulse oximetry

Investigations of nocturnal pulse oximetry were designed to highlight the impact of hypoxia on urinary α1-AGP excretion (i.e., altitude-induced proteinuria) in the context of other (patho)physiologic manifestations of altitude (in)tolerance (e.g., elevations in

SBP, DBP, HR, or RR). These experiments built upon previous exercise experiments related to this question (refer to **Chapter 6**). Derivatives of nocturnal recordings along with additional biomarkers of physiologic response(s) to altitude were expected to, specifically, help assess the mechanism(s) contributing to altitude-induced increases in glomerular leak (as discussed in section **7.4.3**).

7.4.2.1. Time series analyses

As with urine specimens, nocturnal oximetry recordings were reasonably incorporated during ascent and successfully enabled the collection of many large time-series datasets that were consistent with previous yields[460]. As expected, mean nocturnal SpO_2 progressively decreased with increasing altitude and exploratory analysis demonstrated a relationship between these changes and AMS scores. While this was consistent with previous studies[454], and despite the utility of (momentary) daytime SpO_2 variance relating to hypoxic symptoms (e.g., dyspnea[487]), the present study appears to be one of the first to evaluate any relationship(s) between nocturnal measurements and multiple (patho)physiologic manifestations of exposure to HA (e.g., proteinuria and AMS symptomology) during ascent.

Previous studies assessing pulse oximetry during ascent to altitude[457] have failed to capture or report changes in (nocturnal) SpO_2 morphology (i.e., variance, skewness, and kurtosis proper), which occur during the night[14] and have provided clinically relevant information[467]. This is, in part, due to insufficient recording durations (e.g., 15 minutes)[468] and also, potentially, due to the difficulty in (visually) assessing data traces provided by the manufacturer's software for measures, such as, SpO_2 variance. Frequency plots presented in the present study demonstrate a novel method for visualising these data (variance, skewness, and kurtosis) and present the data in a way

that assists in the understanding of nocturnal SpO_2 variation in the context of increasing altitude.

Specifically, relative frequency plots of nocturnal SpO_2 in this study provided a unique advantage over existing SpO_2 traces by enabling not only visualisations of a single nocturnal recording, but also by allowing for the simultaneous comparison between multiple time series of SpO_2 data (e.g., between multiple nights), which is not currently possible using the existing manufacturer's software (e.g., nVision). **Figure 7.17a** demonstrated this functionality and successfully depicted the unique and distinct information that skewness and kurtosis can provide in comparison to only a mean SpO_2 value. Skewness and kurtosis results, depicted in the relative frequency plots, were also successful in highlighting acclimatisation for the group. This was evident from the comparison between successive nights at the same camp (e.g., top night 1 vs top camp night 2; see purple and green lines in **Figure 7.17** and **Figure 7.18**), as well as, the comparison between ascent and descent nights at the same camp (e.g., Thalem ascent night 1 vs Thalem ascent night 2 vs Thalem descent; see **Figure 7.19**). Moreover, skewness and kurtosis among individuals with poor LLS were different to the group, which indicates that these metrics may be useful in identifying individuals who are acclimatising poorly during ascent. The significant relationships between kurtosis and various physiologic responses and biomarkers during ascent (e.g., α1-AGP excretion) were consistent with those observed by Terrill and colleagues[464], whom reported a relation between kurtosis and obstructive sleep apnoea (OSA), and therefore further implicate the utility of these metrics and associated graphical representations.

Cumulative frequency plots offered the additional benefit of pairing data visualisations with nocturnal derivatives (e.g., TST < 80%) that have proven to be clinically meaningful in relation to AMS[468]. Although a significant difference between

AMS^+ vs AMS^- was observed for TST < 80% SpO_2 (refer to **Figure 7.20**), such evaluation could not afford simple or rapid intra- and inter-individual comparisons that were enabled by cumulative frequency plots (as shown in **Figure 7.17** and **Figure 7.18**). Considering findings from relative and cumulative plots it can be argued that the morphological analysis and graphical representation of nocturnal SpO_2 could help marry the utility and practicality of pulse oximetry measurements at HA, which stands to further improve data literacy in such environment.

7.4.2.2. Desaturation characteristics and hypoxic burden

Previous altitude studies have demonstrated strong agreement between ODI and apnoea-hypopnea index (AHI)[488], a quantitative marker of the occurrence and severity of sleep disordered breathing patterns known to occur with ascent to HA[489]. Such pathophysiologic (cyclical) breathing patterns, as well as, changes in nocturnal HR (via pulse oximetry) have, in the past, served as useful surrogates for measurements of 'loop-gain' within the ventilatory control system during ascent[490] and, furthermore, have been related to the incidence of altitude illnesses (e.g., AMS[491] and HAPE[492]) at HA. In support of this evidence were the observed results for ODI (refer to **Figure 7.21**) and HR/SpO_2 in the present study, which were indicative of acclimatisation status (via LLS). Similarly, hypoxic burden, which was successfully estimated from nocturnal recordings (relative to an SpO_2 of 100%[483]) in the present study, has demonstrated clinical significance among various populations[493]. Thus, the relationship between hypoxic burden and LLS was no surprise, albeit confirmed its relevance in relation to acclimatisation status during ascent. Therefore, several measures (e.g., ODI, HR/SpO_2, or hypoxic burden) may be worthy of consideration in regards to the presentation of and mechanisms for altitude-induced glomerular leak (as discussed in section **7.4.3**).

7.4.2.3. Methods comparison ($SpO_{2nocturnal}$ vs $SpO_{2morning}$)

Results from the B-A plots made it clear that peripheral oxygen saturation by pulse oximetry (both, $SpO_{2morning}$ and $SpO_{2nocturnal}$) may overestimate arterial oxygenation (SaO_2; refer to **Figure 7.24** and **Figure 7.25**). Disagreements were particularly evident below SpO_2 80%, albeit predictably linear[494] for both $SpO_{2nocturnal}$ and $SpO_{2morning}$ and consistent with previous results[455], thereby, supporting the use of a less conservative approach (i.e., SpO_2 values < 50%[495]) in regards to exclusion criteria for SpO_2 measurements at HA. Also consistent with recent HA comparisons[496], and the day-night differences (i.e., $SpO_{2nocturnal}$ < $SpO_{2morning}$) observed in respiratory disease (e.g., chronic obstructive pulmonary disease, COPD[480]), relative agreements between $SpO_{2nocturnal}$ (long-duration) and $SpO_{2morning}$ (momentary) revealed that $SpO_{2nocturnal}$ measurements were significantly lower than $SpO_{2morning}$. In addition, the disagreement between $SpO_{2nocturnal}$ and SaO_2 was less than that for SaO_2 vs $SpO_{2morning}$ (refer to **Figure 7.24a** and **Figure 7.24b**, respectively).

The nocturnal nature of $SpO_{2nocturnal}$ recordings could have, in part, resulted in the closer proximity of these measurements with SaO_2 compared to $SpO_{2morning}$) by limiting interruptions due to physical activity (or excessive movement) that contribute to signal noise[455] and reducing (oximeters') exposure to extreme environmental conditions associated with HA (e.g., cold, wet, and excessive external light sources), which can also contribute to erroneous estimations[455 470]. However, morning measurements were performed in similar conditions, albeit could not be used to assess additional nocturnal derivatives. Thus, these comparisons affirmed the superiority of nocturnal recordings for evaluations of oxygenation, which has not been explicated outlined in previous altitude studies. Further, these results provide support for the utilisation of

nocturnal over morning (short duration) pulse oximetry measurements in order to avoid underestimations of hypoxaemia during ascent to altitude.

7.4.3. Nocturnal hypoxia and altitude-induced proteinuria

Thorough reviews of renal responses to hypobaric hypoxia have highlighted both direct and indirect mechanisms for altitude-induced proteinuria. Plausible mechanisms for altitude-induced increases in urinary α1-AGP excretion observed in the present study will be discussed in the preceding subsections in the context of the observed physiologic responses with a specific focus on nocturnal pulse oximetry measurements. A schematic for mechanisms to be discussed is presented in **Figure 7.28**.

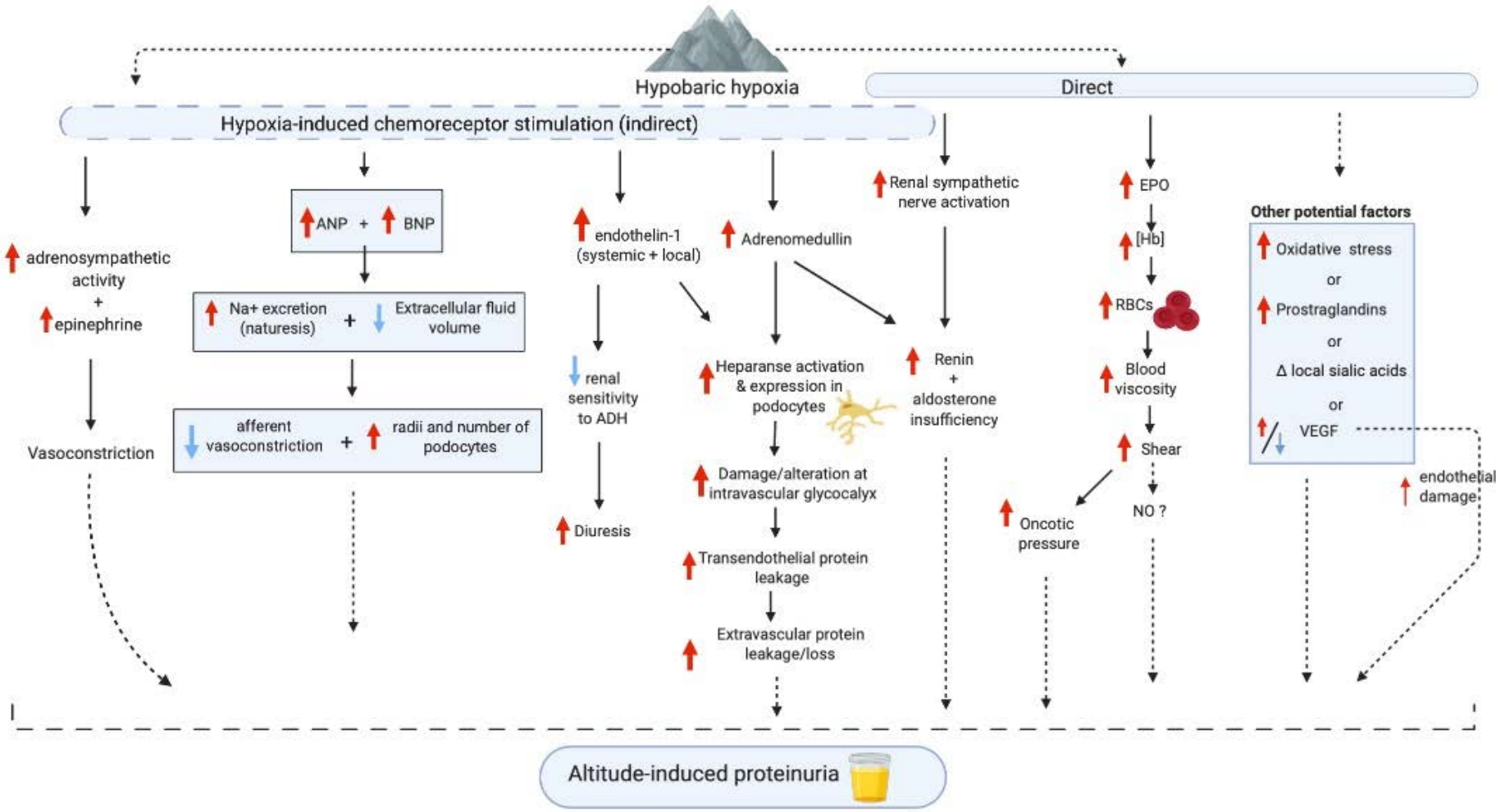

Figure 7.28 – Schematic of potential mechanisms for altitude-induced glomerular proteinuria. Solid lines are representative of established pathways while dotted lines indicate a potential mechanistic link between altitude-induced proteinuria. Potential factors with limited evidence, and requiring additional investigation, are contained in the text box (far right). Figure created with Biorender.com.

7.4.3.1. Diurnal variation and circadian rhythm

Evidence of diurnal variation for urinary α1-AGP and nocturnal SpO_2 was exhibited during ascent. For SpO_2, this was evident in the differences between morning and nocturnal SpO_2 measurements (i.e., $SpO_{2nocturnal}$ vs $SpO_{2morning}$; refer to **Figure 7.25**) and for urinary α1-AGP, in the differences between 24-hour and EMU specimens for [α1-AGP]. The observations for SpO_2 have been hypothesised as products of postural (upright vs supine)[497] or hormonal influences (e.g., cortisol)[498] , to name a few. Such postural impact could conceivably explain, in part, the day-night differences for urinary [α1-AGP][499] [500] however, given the consistency of postural factors across the expedition (supine each night; upright each day), and the progressive nature of increases in urinary α1-AGP by days, the contribution of postural factors to altitude-induced urinary α1-AGP excretion is unlikely. Thus, hormonal factors exhibiting diurnal patterns that may be further altered during ascent (e.g., cortisol, renin, angiotensin II, aldosterone, prostaglandin E_2, anti-diuretic hormone, adrenomedullin, endothelin-1) should be preferentially considered.

7.4.3.2. Inflammation and reactive oxygenated species (ROS)

The relationship between altitude-induced increases in urinary α1-AGP (24-hour α1-AGP and α1-AGP:CREA from EMUs) and increases in ODI (refer to **Figure 7.27**) and nocturnal SpO_2 variance were consistent with observations among patients exhibiting OSA[230] [501], and may provide clues regarding the underlying mechanisms for the altitude-induced rises. Worsening perturbations in nocturnal oxygenation with ascent[229], such as, the repetitive desaturation-reoxygenation events associated with increasing ODI, promote inflammation and the formation of reactive oxygen species (ROS), which can both cause endothelial dysfunction[452] [502] that may lead to proteinuria. Thus, increases in ODI with ascent were

expected to elicit increases in inflammatory markers, such as, serum CRP[149 503] and α1-AGP with the increases potentially dependent on the severity of ODI during ascent. This expectation made the observed rises in serum inflammatory markers (i.e., serum CRP and α1-AGP) unsurprising, however, the absence of any relationship between serum CRP and serum α1-AGP or serum CRP and metrics derived from nocturnal recordings was curious. The additional absence of any relationship between serum CRP and urinary α1-AGP, as well as, the confirmation of the dissociation between serum and urinary α1-AGP[7] creates further intrigue. These results implicate the likelihood of local (intra-renal) over systemic inflammatory mechanisms in the progression of urinary α1-AGP excretion during ascent, albeit the impact of systemic inflammation by a mechanism other than increases in ODI cannot be excluded.

Also of note, were the differences between the group and a subset of individuals with the highest LLS (and highest gastrointestinal scores throughout) nearest to the top camp (see). Individuals with high LLS (and being AMS^{+}) exhibited opposite changes in serum α1-AGP and CRP compared to the group and also exhibited some of the lowest urinary α1-AGP excretion rates, which were also in opposition to the rest of the group (i.e., progressive reductions vs progressive increases with ascent). These results were counterintuitive to the original hypotheses yet, the additional similarities between 2 out of the 4 individuals (later revealed to be genetically related, brother and sister) make these findings even more curious. A blunted inflammatory response to hypoxia (via blunted hypoxic chemosensitivity or attenuated hypoxic ventilatory response) could, in part, explain attenuated increases in circulating α1-AGP and CRP, however, would fail to explain additional decreases in serum [α1-AGP] with increasing altitude. Therefore, it must be considered that an alternate mechanism may be at play.

It remains plausible that decreasing [α1-AGP] in serum and urine with increasing altitude among these individuals was a product of: 1) increasing amounts of bound α1-AGP (making it undetectable or molecularly larger and thus less likely to leak); 2) increasing amounts of serum protein loss[504]; or 3) differential degrees and types of glycosylation of α1-AGP rendering its capture by immunoassays less effective (similar to the glycosylation-induced limitations in function[505]). Regardless, the potential implications would be similar with vascular integrity compromised and vascular permeability[21] and the leakage of proteins (e.g., α1-AGP) and other molecules (including fluid) into the extravascular space[506] promoted. While one may expect this to also drive increases in urinary α1-AGP, it is possible that leakage occurs disproportionately in different tissues (e.g., leakage predominating in the gastrointestinal tract; **Figure 7.29**). Nevertheless, attenuated altitude-induced rises in serum α1-AGP (and urinary α1-AGP in more severe cases) may reflect altitude intolerance and, similar to other markers of systemic inflammation (e.g., IL-1β, IL-6, and TNF-α), may confer increased susceptibility to altitude-related illnesses[469]. To conclude, a certain degree of increases in urinary α1-AGP excretion with ascent are likely normal, albeit excessive increases or decreases are likely reflective of a misappropriated response to hypoxia. The relationship between oppositional changes in serum and urinary α1-AGP with ascent require further investigation with the aetiology potentially important to altitude illness.

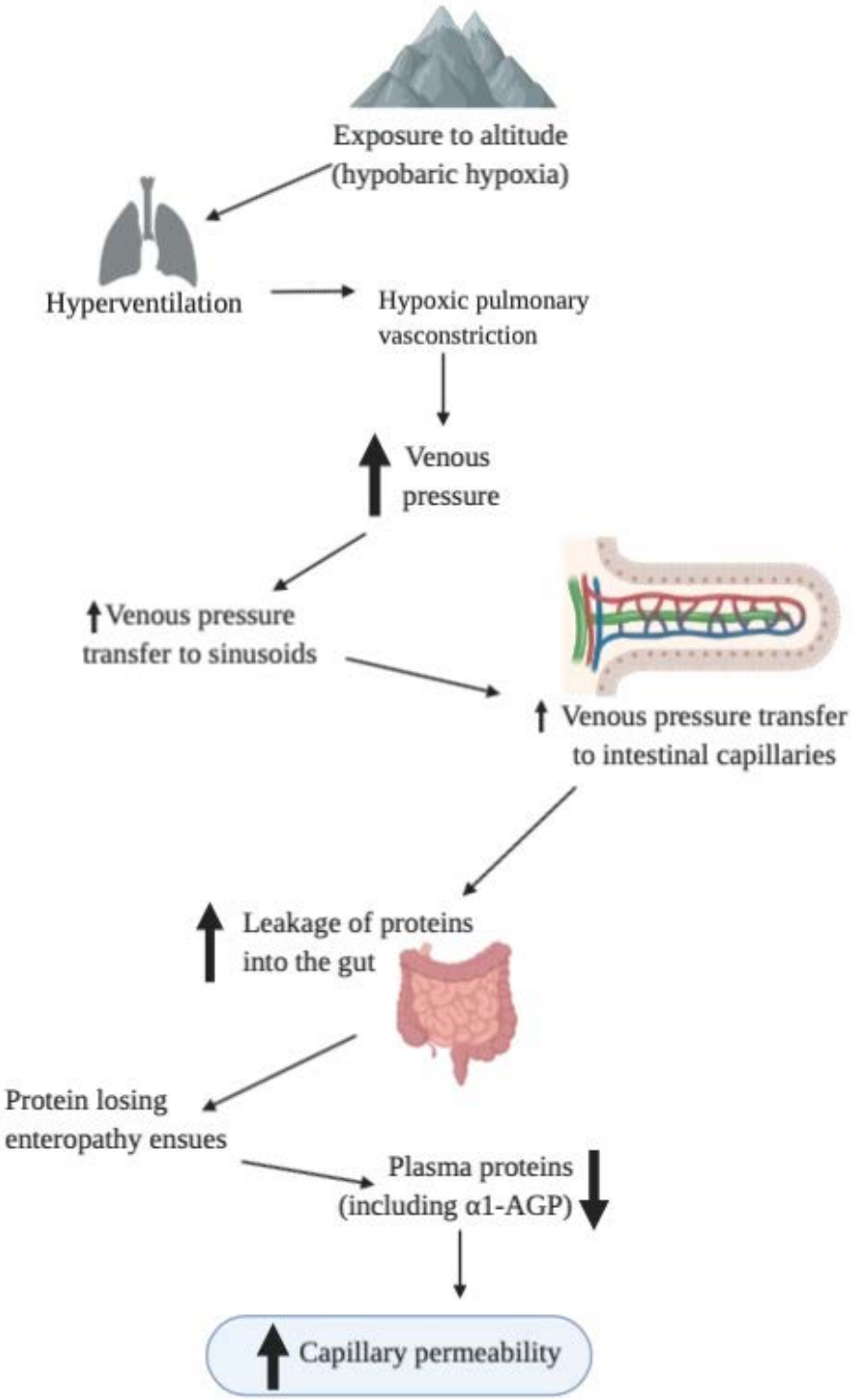

Figure 7.29 – Possible explanation for attenuated urinary alpha-1 acid glycoprotein (α1-AGP) and simultaneous hypoproteinemia (serum C-reactive protein and α1-AGP). Attenuated urinary α1-AGP and hypoproteinemia were primarily observed among individuals presenting poorly at high altitude, who also exhibited acute mountain sickness (as determined by Lake Louise Score > 3 with at least 1 point for headache). Figure created with Biorender.com.

7.4.3.3. Altered endothelial function and microvascular permeability

Regardless of serum α1-AGP, direct effects of renal hypoxia on glomerular endothelial cells remained possible with the associated mechanisms able to explain increases in urinary α1-AGP exhibited during ascent. For example, increases in endothelin-1[507 508] and adrenomedullin[509] (in response to hypoxia) known to occur with ascent (refer to **Figure 7.28**) can increase activation and expression of heparanase in podocytes[510]. Such increases result in the cleavage of heparan sulphate, an integral component of the glomerular filter particularly during acute renal inflammation[511], which ultimately reduces the anionic charge at the glomerular basement membrane (GBM)[136]. This process has previously been implicated in the progression of proteinuria[512] due to modulation of glomerular charge-selectivity, although the discussion has remained controversial and recent focus has shifted towards the effects of the loss of heparan sulphate on glomerular endothelial cells[513 135]. The impact on glomerular endothelial cells appears to result in the remodelling of the intravascular glycocalyx[513] and promotes transendothelial passage of proteins (e.g., albumin)[510 514 515] which, in the case of ascent, could translate into proteinuria. Support for the involvement of endothelin-1 is also provided by observed reductions in proteinuria following treatment with endothelin-1 antagonists (ET-1 antagonists)[516]. Future investigations of altitude-induced proteinuria should aim to isolate this mechanism and would benefit from including trials of ET-1 antagonists, which are already used during ascent (e.g., bosentan[176]).

Indirect effects of hypoxia on proteinuria[164] may also relate to [electrolyte] and the potential downstream effects on glomerular permeability. In a majority of the group, increases in urinary α1-AGP excretion coincided with decreases in K^+ excretion (increases in reabsorption), as well as, the diuretic and natriuretic[517] responses known to accompany ascent[164]. This is particularly interesting given the different origins of electrolyte and α1-AGP

excretions (i.e., tubular vs glomerular, respectively) along with hyperfiltration observed in some (see **Appendix 7**). Physiologic evidence indicates that increases in K^+ reabsorption would promote the release of nitric oxide (NO) from endothelial cells[518], which should help scavenge ROS and preserve glomerular permeability to plasma proteins[519]. In contrast however, alternate studies have demonstrated the opposite effects, in which increases in NO resulted in further increases in glomerular permeability to proteins, such as, albumin[520]. Regardless, the observed increases in K^+ are reflective of additional mechanisms, such as, increased renal sympathetic nerve activation (RNSA) that is likely relevant to altitude-induced increases in proteinuria and is discussed in preceding sections (see section **7.4.3.5**).

Additional factors that increase with ascent may also result in increased glomerular endothelial permeability. Increases in prostaglandins[521], which are indicative of vascular permeability, during ascent are but one example. Future studies could benefit from analysing such biomarkers of vascular and glomerular capillary permeability to better assess the involvement of endothelial cells in the progression of urinary α1-AGP excretion during ascent.

7.4.3.4. Haemodynamic factors

The significant increases in SBP, DBP, and RR with increasing altitude were not surprising nor were the increases in LLS, which were consistent with existing literature[188]. The observed relationship between SBP and urinary α1-AGP could be used to argue that a pressure-related mechanism may, in part, contribute to altitude-induced proteinuria. Previous altitude studies exploring this theory by administering losartan[335] however, have highlighted a different, albeit related, mechanism (i.e., induction of hepranase via activation of angiotensin receptor type-1 on podocytes; refer to **Chapter 5**) that may be responsible. Thus, the observed relationship between SBP and urinary α1-AGP in the present study is not sufficient to draw

definitive conclusions, albeit important in further debate related to such a pathway and other haemodynamic factors.

In addition to local or systemic pressures dictated by the vasculature, the pressure exerted (outward) by the blood may also be influential in the progression of proteinuria. Increases in blood proteins (e.g., haemoglobin) and red blood cells with ascent[522] effectively increase blood viscosity[219], which can alter glomerular capillary oncotic pressure[523] and further contribute to proteinuria.

7.4.3.5. Sympathetic activation

Results from the present study were, in part, supportive of the involvement of sympathetic activation in the progression of altitude-induced proteinuria. Specifically, local sympathetic activation was observed indirectly via the altitude-induced natriuretic response[524] upon initial exposure, which was followed by both, the return of Na^+ reabsorption to near baseline levels (and associated fluid retention) and elevated K^+ reabsorption at higher altitudes. Progressive increases in BNP (among the subset) were also observed in parallel to this (and with increasing altitude), and also coincided with elevations in urinary α1-AGP (among most individuals). This relationship between BNP and urinary α1-AGP was similar to observations among heart failure (for NT-proBNP and α1-AGP[282]), which has been associated with changes in RSNA[525]. Taken together, the misappropriated electrolyte handling[526] and increases in BNP, were suggestive of RSNA[526 527] during ascent, particularly, during the first 24 to 48 hours at 4,800 m when simultaneous elevations in urinary α1-AGP were observed.

Extra-renal sympathetic activation was also evident in the nocturnal HR and SpO_2 results (i.e., HR/SpO_2 or $\Delta HR/\Delta SpO_2$[528]). HR/SpO_2 can be used to evaluate: 1) the degree of synchronicity between the activation of the respiratory and cardiovascular systems[529]

(particularly with periodic breathing[530]), and 2) the magnitude of ensuing sympathetic activation. Increases in HR/SpO_2 with ascent were likely a product of worsening hypoxaemia and respiratory-induced modulation of HR (and blood pressure)[531], with the correlation between HR/SpO_2 and urinary α1-AGP, potentially, indicative of sympathetic influence.

Elevated RSNA observed with ascent may be driven by progressive increases in ODI by way of alterations in nocturnal BP patterns (dipping vs non-dipping)[188 532] and elevations in intraglomerular pressures[533 534]. Simultaneous elevations in SBP and 24-hour α1-AGP excretion (mg/24-hours) observed in the present study provided preliminary support for this, although analysis of noradrenaline (or norepinephrine) could be useful to help confirm this link.

By contrast, blunted chemosensitivity to hypoxia, a potential risk factor for AMS in unacclimatised lowlanders[458], confers attenuated rises in RSNA[534] and, during ascent, could be expected to elicit concomitant attenuations in altitude-induced proteinuria. This would provide an explanation for the disparate pattern observed for the subset of the individuals who presented most poorly and exhibited severe AMS. Evaluation of hypoxic ventilatory responses among these individuals, however, would be required to confirm this hypothesis.

7.4.4. Limitations and future directions

An obvious limitation of the present study was the small sample size, albeit a common limitation of expeditionary studies at HA[409]. Despite the low numbers however, there were interesting observations that warrant further investigation, especially, a larger scale feasibility assessment of the derivatives from nocturnal oxygenation measures and their wider application to the understanding, management, and prediction of AMS. Sample size could not be accurately estimated prospectively due to the novel nature of altitude-induced urinary α1-AGP measurements (i.e., via novel turbidimetric immunoassay) together with the unknown degree of

variation in urinary α1-AGP among the population during ascent. The present results, however, can be used prior to future similar studies to estimate the appropriate sample size.

Estimates of total body water other than body mass measurements would have improved the strength of the present results. While bioelectrical impedance[535] was considered, it was ultimately excluded given its limited ability to detect changes in hydration status[536] and the known influences of electrolytes on these measurements[535]. Inclusion of alternative measurements of total body water (e.g., Dual-energy X-ray absorptiometry, DEXA) could strengthen future studies, but are not entirely feasible at HA. Thus, future field-based studies would largely benefit from adopting a simpler method to evaluate fluid balance and, therefore, may consider including measurements of hydration status (e.g., urine osmolality). Although the ratio of urine specimen weights to volumes could have been compared respectively with the results used as a surrogate for specific gravity, such estimations would first require validation. Future studies may benefit from including visual questionnaire-based fluid intake diaries, such as, the Liq.In7[537] to assist assessments of fluid balance, particularly, given that precise measurements of fluid intake are unrealistic during HA expeditions and that recall-based intake assessments are largely unreliable.

With respect to future investigations of glomerular leakage and renal haemodynamics, researchers may consider including Doppler ultrasound measurements (of renal blood flow and vascular resistance) together with measurements of renal oxygen delivery consistent with those recently described by Steele and colleagues[451]. Such future studies may also consider assessing local oxygenation (in renal tissue) using methods, such as, near-infrared spectroscopy (NIRS)[538 539]. Using NIRS during ascent to investigate renal tissue oxygenation at various timepoints throughout the day (morning vs evening; daytime vs night-time) and, potentially, in different positions (e.g., lying vs seated or standing) could help improve the

understanding of renal oxygenation dynamics (e.g., diurnal influences or renal perfusion) as they relate to altitude-induced proteinuria and several of the mechanisms described herein.

Analysis for additional biomarkers would also improve the strength of future studies. Elevations in hypoxia inducible factor-1 alpha (HIF-1α) known to occur with ascent[540] may induce the expression of a ZEB-2-natural antisense transcript[541] and further reduce expression of nephrin and podocin, which ultimately result in podocyte effacement, compromised perm-selective function, and proteinuria[542]. By contrast, increases in vascular endothelial growth factor (VEGF), which have been shown to accompany ascent[543], may promote nephrin[544] expression and thereby improve glomerular filter integrity [545]. In support of this are the links between both increased VEGF and glomerular capillary repair, as well as, VEGF blockade and endothelial damage as highlighted by Satchell and colleagues[546]. By contrast, however, VEGF blockade has also been shown to attenuate proteinuria and endothelial nitric oxide synthase in disease models[547]. Thus, the involvement of VEGF in the progression of altitude-induced proteinuria requires further investigation.

7.5. CONCLUSION

From the present experiments, it was evident that altitude-induced increases in urinary α1-AGP were strongly influenced by characteristics of nocturnal oxygenation, with cyclical desaturations possibly having both systemic and localised intra-renal effects that promoted proteinuria. In addition, urinary α1-AGP and derivatives of nocturnal oxygenation (e.g., ODI and TST < 80% SpO_2) were indicative of acclimatisation status and generalised (in)tolerance to altitude. However, further investigations are warranted to assess the wider application of urinary α1-AGP and nocturnal pulse oximetry in relation to the understanding,

management, and prediction of AMS during ascent to high altitude. The present study demonstrated that EMU specimens and nocturnal pulse oximetry recordings are practical additions for HA research with graphical representations of nocturnal oximetry promoting improved interpretation.

Chapter 8

CONCLUSIONS AND FUTURE DIRECTIONS.

The primary objective of this thesis was to investigate mechanisms of proteinuria during physiologic challenge (e.g., during ascent or with exercise) by analysing urinary alpha-1 glycoprotein (α1-AGP), a sensitive marker of glomerular (mal)adaption. Chapters were structured around individual aims that set out to:

1. Develop a novel particle- (latex-) enhanced immunoturbidimetric assay (for use on an auto-analyser) designed for the detection of low-concentration α1-AGP in human urine specimens and conduct preliminary validation experiments (e.g., imprecision, interference, linearity, and stability) for this assay (**Chapter 3**).

2. Utilise the newly developed immunoassay to analyse α1-AGP in human urine specimens of varying types (e.g., 24-hours, early morning, or short-duration timed) (**Chapter 4**), with experiments intended to: 1) assess various units of measure reported in the existing literature; 2) determine the impact of age and/or sex on the various units of measure often reported for urinary α1-AGP; and 3) provide the foundation for sensitive and updated reference ranges for urinary α1-AGP (across various units of measure reported in the existing literature) in healthy humans.

3. Utilise the newly developed immunoassay to analyse α1-AGP in human urine specimens collected pre/post altitude exercise tests (with and without losartan and acetazolamide administration) and during ascent to altitude with experiments intended to facilitate distinctions between the apparently

redundant mechanisms (e.g., systemic pressure and hypoxaemia) hypothesised for post-exercise and altitude-induced proteinuria (**Chapter 5**).

4. Utilise the newly developed immunoassay to analyse α1-AGP in human urine specimens collected pre- and post-exercise in order to: a) demonstrate the superior efficacy of urinary α1-AGP over albumin for investigations of exercise-induced proteinuria, and b) evaluate the influence of hypoxaemia on exercise-induced α1-AGP excretion (**Chapter 6**).

5. Investigate and distinguish between mechanisms surrounding exercise- and altitude-induced proteinuria, by: 1) analysing α1-AGP using the novel immunoassay in human urine specimens (e.g., early morning and 24-hour) collected during ascent to altitude, and 2) collecting and comparing urinary α1-AGP results with nocturnal pulse oximetry measurements, as well as, additional physiologic measurements (e.g., arterial blood gases, blood pressure, Lake Louise scores[422], and heart rate; **Chapter 7**).

8.1. Major contributions and implications

Experiments associated with the above aims have produced novel findings related to the mechanisms of proteinuria with acute physiologic challenge. These contributions along with associated implications for practitioners will be reviewed here.

Chapter 3 – The successful development and preliminary validation of the novel turbidimetric immunoassay (for use on an auto-analyser) designed for the detection of low-concentration α1-AGP in human urine provides a notable contribution from this thesis. Firstly, this contribution was significant considering the breadth of known and possible clinical

applications for urinary α1-AGP (biomarker of disease; as outlined in the next chapter; **Chapter 4**). Secondly, the developed immunoassay stands to considerably improve existing analytical methods for urinary α1-AGP by enhancing: 1) the range of detection levels in human urine; and 2) the precision of urinary results. Thirdly, the developed immunoassay stands to significantly improve the practicality of conducting urinalysis for α1-AGP by: 1) reducing the time required for analysis; 2) lowering the number of personnel and expertise required to conduct analysis; and, thereby, 3) reducing costs associated with analysis. These advantages are all the more impactful when considering the immunoassay's optimisation for use on the Optilite™, a widely utilised auto-analyser that is readily available in biochemistry labs worldwide (e.g., large hospitals and universities).

Chapter 4 – The novel immunoassay was successfully used to analyse α1-AGP in various types of human urine specimens (e.g., 24-hour, early morning, and timed-spot specimens) collected among healthy individuals. Results from experimental urinalysis in this chapter provide the foundation for an updated and more sensitive reference range for urinary α1-AGP in healthy humans. No significant effect of age or sex was observed on urinary α1-AGP from experimental urinalysis; however, from the reviewed literature the potential for age to impact urinary α1-AGP results was clear. Nevertheless, the present immunoassay may be utilised to help establish more precise cut-off ranges for those diseases in which urinary α1-AGP has proven to be clinically significant. Similarly, the present immunoassay may improve the diagnostic/predictive potential of urinary α1-AGP as a biomarker in these diseases (as outlined in **Chapter 4**), as well as, additional diseases in which it has not yet been analysed.

Chapter 5 – The novel immunoassay was successfully used to analyse α1-AGP in human urine specimens collected during ascent to altitude. Results enabled distinctions

between the relative mechanisms contributing to post-exercise and altitude-induced proteinuria. Experiments in this chapter, uniquely, incorporated both losartan and acetazolamide administration to modulate exercise- and altitude-induced physiologic responses, such as, attenuation of amplifications in systemic blood pressure or hypoxaemia, respectively. This design enabled in-depth investigations surrounding the relative impacts of these mechanisms on urinary α1-AGP and, ultimately, led to the determinations of the most probable mechanistic 'factor(s)' that contribute to exercise- and altitude-induced proteinuria. In addition to these methods, results produced by experiments outlined in this chapter (e.g., significance of exercise intensity opposed to hypoxaemia in relation to post-exercise urinary α1-AGP) were essential in setting the scene for the experiments outlined in the chapters that followed.

Chapter 6 – The novel immunoassay was successfully used to analyse α1-AGP in urine specimens collected around exercise tests conducted in normoxia and hypoxia. Urinary α1-AGP results confirmed that elevations in post-exercise urinary α1-AGP were largely attributable to exercise intensity rather than hypoxaemia. Results also showed that urinary α1-AGP was superior compared to urinary albumin for investigations related to post-exercise proteinuria. Findings for urinary α1-AGP and the methodology for experimentation outlined in this chapter add to the current understanding of renal physiologic changes that accompany exercise and could be utilised to assist future investigations related to mechanisms for, and significance of, post-exercise proteinuria (or other scenarios where physical exertion applies, such as, physically demanding occupations).

Chapter 7 – The newly developed immunoassay was successfully used to analyse α1-AGP from human urine specimens collected during ascent to and decent from altitude. Altitude-

induced increases in urinary α1-AGP results were observed to be related to derivatives of nocturnal pulse oximetry recordings exhibited during ascent. Additional novelties observed in this chapter included: 1) the relationship(s) between the incidence of AMS and urinary α1-AGP excretion (and total sleep time < 80% SpO_2, TST < 80% SpO_2), and 2) the techniques applied to nocturnal pulse oximetry recordings collected at high altitude. Despite remaining questions, data obtained from experiments in this chapter provide vital information for power analysis calculations that can be used to estimate the sample size required by future experiments (as discussed in the next section). Future experiments are required to definitively confirm the diagnostic/predictive value of urinary α1-AGP in relation to altitude illness.

8.2. Major improvements

Limitations of experiments outlined within this thesis have already been discussed in preceding chapters with several possible improvements also articulated. Nevertheless, to enhance the impact of this thesis, the recommended modifications that stand to considerably improve the outlined works will be reiterated here.

Chapter 3 – Preliminary validation experiments conducted for the turbidimetric immunoassay require expansion prior to commercialisation (if desired). Any such additional validation experiments should ensure the completion of a full 20-day trial period[298]. In addition, further investigation of assay interference is required and should include a more comprehensive panel of potential interferents (e.g., haemoglobin, bilirubin, or lipaemia)[303]. Although nonlinearity remained within allowable limits, future studies may consider repeating analyses conducted in this chapter given the 95% confidence interval observed for the lowest [α1-AGP] analysed.

Chapter 4 – As mentioned, no significant effect of age or sex was observed for urinary α1-AGP from experimental urinalysis; however, based on the literature reviewed, the potential impact of age on urinary α1-AGP measurements was clear. Age groups for which this was observed were not included as part of the experimental urinalysis of this chapter and, therefore, further investigations are required to fully understand the impact of age. Such investigations are also needed in order to determine whether age-specific normative values (for healthy and diseased populations) are required for urinary α1-AGP and whether the same relationship(s) with age exist in relation to disease cut-offs.

Chapter 5 – The complexity of the study design (administration of two drugs) was an admitted limitation of the experiments outlined in this chapter and was further complicated by additional factors (e.g., missing data points), which ultimately reduced the size of the placebo-acetazolamide group. Group size limitations imposed by the guiding team (for safety reasons) however, did not allow this to be mitigated in advance. By contrast, the potential of acclimatisation to be a confounding factor for repeat altitude exercise tests (separated by 48 hours of residence at 5,035 m) should have been better anticipated. A less complex and more controlled design (e.g., randomised controlled trial or randomised cross-over[548]) should be implemented in the future with further experiments required to confirm the observed results following the administration of losartan and acetazolamide. Future researchers may also consider comparing losartan with a different (i.e., more potent) angiotensin receptor blocker (e.g., telmisartan) or an alternative pharmacologic agent entirely (e.g., calcium channel blocker).

Chapter 6 – In efforts to mitigate problems encountered in **Chapter 5** experiments, a less complex design (randomised cross-over or randomised control trial) was adopted with repeat altitude exercise tests performed in normoxia and hypoxia (chamber-based) with ample time at sea-level to ensure 'wash out' between sessions. Despite exercise duration being

successfully controlled and participants achieving maximal effort in both NOR and HYP conditions, reduced power output in HYP was observed and could, arguably, be a major limitation. Nevertheless, the observed reductions in exercise power output in HYP coincided with reductions in urinary α1-AGP despite substantial hypoxaemia. This effectively demonstrated the significance of exercise intensity in relation to exercise-induced proteinuria (as opposed to the degree of hypoxaemia). Future studies may consider the administration of a submaximal exercise test using an intensity that: 1) significantly stimulates both urinary α1-AGP and hypoxaemia (in HYP conditions); and 2) can be maintained for equivocal durations in both environmental conditions.

It was additionally unclear whether (and to what degree) intra- (within-individual between days) and inter-individual (between-individual) variation of urinary α1-AGP could have influenced observed significant results for the comparisons of post-exercise urinary α1-AGP measurements (within-individual and between-conditions). Thus, future experiments may consider: 1) conducting repeat exercise tests in both environmental conditions, or 2) including repeat collections for 24-hour urine specimens in order to more precisely estimate change from baseline and better understand the impact of within-individual variation in post-exercise urinary α1-AGP excretion.

Despite the potential areas of improvement, data from this chapter could be utilised to perform rigorous power analysis (utilising appropriate methods eloquently reviewed by Gelman and Hill[549]) and to estimate the necessary sample size to ensure robust results for future investigations related to post-exercise urinary α1-AGP.

Chapter 7 – The repeated-measures nature of the data (e.g., daily collections during ascent) and the known intra- and inter-individual variability that exists for biological data[550] (e.g., urinary α1-AGP) made results somewhat difficult to interpret and communicate. Related

future studies (e.g., investigation of the diagnostic/predictive value of urinary α1-AGP in relation to AMS) and associated statistical analysis plans should aim to include: 1) a power analysis (estimated from data in **Chapter 7**) for the calculation of the appropriate sample size[551] and 2) repeated-measures correlations[552] for the assessment of relationships between urinary α1-AGP measurements and physiologic measurements (e.g., urinary α1-AGP and ODI).

In addition, observed urinary α1-AGP results among individuals with severe AMS were physiologically counterintuitive and contradicted the running hypothesis. Thus, additional analysis is also required to provide further insight regarding the discrepancy in urinary α1-AGP measurements between AMS positive and negative individuals. Given the potential clinical significance of this discrepancy (e.g., a potential biomarker of pathophysiologic response or altitude intolerance) it cannot be ignored. Future experiments investigating this may be strengthened by including: 1) methods that can identify and quantify the presence of sialic acids in urine; and 2) evaluation of the proportions of α1-AGP glycoforms present in the specimen. Such methods may include chromatography, electrophoresis, and a thiobarbituric acid assay (Warren assay[553]) as described by Treuheit and colleagues[554]. Results from these tests may be further evaluated in conjunction with LLS and could help to determine whether any changes in the structural characteristics of α1-AGP occur during ascent and whether such changes translate into functional changes (i.e., presentation of AMS). In addition to the primary outcomes focused around α1-AGP, **Chapter 7** highlighted how nocturnal pulse oximetry may be insightful for prediction of altitude illness. These preliminary observations indicated that nocturnal measures, such as, TST < 80% SpO_2, could be indicative of (and predictive for) AMS during ascent, albeit further investigation is warranted.

8.3. Conclusions and future directions

New research questions and future directions have arisen as products of the present research and have been highlighted in previous chapters. Nevertheless, those research questions whose answers stand to contribute significant developments related to further elucidation of the mechanism(s) that contribute to exercise- and altitude-induced proteinuria will be reviewed next in the form of a dialogue describing future directions.

Time-related considerations will also be presented for those research areas that stand to substantially benefit from including α1-AGP (serum and urinary) in addition to existing test/analyses. In the context of urinary α1-AGP, this sub-section will provide examples for novel applications of the newly developed immunoassay.

8.3.1. Exercise-induced proteinuria

Future studies investigating exercise-induced proteinuria should focus on the aetiology of the relationship between exercise intensity (power output) and urinary α1-AGP excretion. These investigations would be wise to include several additional measurements, such as, assessments of renovascular pressure (e.g., resistive index determined by doppler ultrasound[555]) opposed to just measurements of systemic pressure. These investigations may be further expanded to include comparisons of urinary α1-AGP with and without a more potent (high bioavailability or long-acting) pharmacologic agent used to target renovascular hypertension (e.g., angiotensin converting enzyme (ACE) inhibitors: lisinopril or enalapril[556]; or alternative ARBs: Irbesartan or telmisartan[557]). Additional comparisons in this context may be made between modes of exercise (e.g., running, cycling, or swimming; as previously reviewed by Poortmans and Vanderstraeten[187]) in order to further elucidate the contribution from alterations in renovasculature pressure to post-exercise proteinuria.

8.3.2. Altitude-induced proteinuria

8.3.2.1. Assessments of associated intra-glomerular mechanisms

Future investigations aiming to evaluate intra-glomerular origins of altitude- (or exercise-) induced proteinuria, may benefit from including additional urinary or serum markers (e.g., vascular endothelial growth factor, VEGF, or endothelin-1, to name a few) that may be indicative of vascular damage or endothelial permeability (as reviewed by Goncharov and colleagues[558]). Such analyses would be necessary to confirm or deny glomerular endothelial involvement and may also useful for distinguishing between the contributions of multiple, simultaneous, intra-glomerular mechanisms (e.g., endothelial permeability and GBM charge-selectivity).

In pursuit of a deeper understanding of the relationship between nocturnal ODIs and urinary α1-AGP, specifically, assessments of local (renal) desaturation and reoxygenation using near-infrared spectroscopy (NIRS) technology may be considered[538 539]. Measurement of any associated changes in renal haemodynamics may also be worthy of investigation and could benefit from including Doppler ultrasound, as recently described by Steele and colleagues[451].

8.3.2.2. Evaluations of the relationship(s) between α1-AGP and altitude illness.

Given the demonstrated relationship between urinary α1-AGP and AMS, further consideration may be given to the potential use of urinary α1-AGP as a diagnostic/predictive measure of AMS, as well as, other altitude illnesses (e.g., high-altitude cerebral or pulmonary oedema; HACE or HAPE, respectively). Comparisons of urinary α1-AGP and AMS (via LLS) during ascent between highland and lowland natives (with additional comparisons between natives of different mountain ranges; e.g., Andean vs Tibetan[559]) may further assist such investigations and would also enable an evaluation of the significance of genetic ancestry.

Inclusion of various serum or urinary biomarkers of oxidative stress[560 561], as well as, inclusion of local or systemic markers of antioxidant capacity[562] may also be considered for specimens collected during ascent. Analyses for such markers stand to lead to a deeper understand regarding the transient effects of hypoxia on renal physiology during ascent to altitude.

In the context of HACE, the modulation endothelial permeability by α1-AGP[143] in the brain is also worth mentioning along with the propensity for proteinuria to precede cerebral oedema (in animal models)[563]. Although it is unclear whether a direct association exists between HACE and brain or glomerular endothelial permeability, several pressure independent mechanisms have been proposed[564]. To that end, a double-blinded, age-matched, clinical trial assessing urinary α1-AGP excretion and cerebral changes detected by magnetic resonance imaging (MRI) among individuals exposed to 12.0% – 13.5% O_2 for a total of 26 hours with and without administration of dexamethasone[176] had been designed and was initiated, albeit remains incomplete (see for more details and an overview of this experiment). Additional supplementary information related to this experiment is provided in **Appendix 9** (see also **Supplement 4** and **Supplement 5**).

8.3.3. New and noteworthy applications of α1-AGP

8.3.3.1. Extreme environmental conditions

Despite the newly developed immunoassay for urinary α1-AGP not being clinically meaningful for prognosis of chronic kidney disease[565], novel applications for α1-AGP (urine or serum) as a biomarker of physiologic response to environmental extremes (other than exposure to altitude) remain possible. Specifically, urinary α1-AGP could be a useful biomarker of disease onset or progression among individuals working in the heat (e.g., Mesoamerican sugarcane workers[566]), whom often develop acute kidney injury of unknown origin (albeit with

both, tubular and glomerular components[567]). The developed assay could therefore help improve understanding surrounding renal responses and maladaptation that occur with heat exposure. Nevertheless, urine and serum α1-AGP, and additional biomarkers of glomerular (e.g., oxidative stress markers or endothelial permeability markers) and tubular involvement, analysed from specimens collected among affected and unaffected Mesoamerican sugarcane workers would be required to further elucidate the mechanistic elements for heat-induced proteinuria in this population.

APPENDICES

Appendix 1 – Overview of literature search strategy.

A literature search was conducted in accordance with The Cochrane Handbook and with modifications[568] applied where indicated. The search was not restricted to the English language nor any specific time interval. Cochrane CENTRAL, PubMed, and University of Birmingham Library Database were used to initiate bibliographic searches. Database searching was followed by handsearching, conference abstracts/proceedings, other reviews, and finally, web-searching. Database searches were conducted using variations of molecule name (e.g., 'alpha-1 acid glycoprotein', 'orosomucoid' or 'orosomucoid-1' (not 'orosomucoid-2') in addition to descriptors (e.g., 'urinary', 'urine', or 'serum'). Abstracts were reviewed in order to determine appropriateness for further inclusion. Database searches and preliminary screening (of abstracts) identified 270 studies for further consideration. From remaining studies, 165 full-length papers were reviewed with 105 ultimately included. Citations from these papers were reviewed to identify additional papers relevant for inclusion.

Appendix 2 – Certificate of Analysis for European Reference Material (ERM®) DA470k/IFCC.

The first page of the certificate from the European Commission's Joint Research Centre (JRC) is presented here (listing the concentration of human serum proteins in the reconstituted material) with the remaining pages, as well as, a full catalogue available on the JRC website.

JOINT RESEARCH CENTRE
Institute for Reference Materials and Measurements

CERTIFICATE OF ANALYSIS

ERM®- DA470k/IFCC

HUMAN SERUM

Proteins in the reconstituted material [1]	Mass concentration	
	Certified value [2] [g/L]	Uncertainty [3] [g/L]
α_2 macroglobulin (A2M)	1.43 [4]	0.06
α_1 acid glycoprotein (AAG)	0.617 [5]	0.013
α_1 antitrypsin (AAT)	1.12 [5]	0.03
albumin (ALB)	37.2 [4]	1.2
β-2-microglobulin (B2M)	0.00217 [6]	0.00007
complement 3c (C3c)	1.00 [4]	0.04
complement 4 (C4)	0.162 [4]	0.007
haptoglobin (HPT)	0.889 [4]	0.021
immunoglobulin A (IgA)	1.80 [4]	0.05
immunoglobulin G (IgG)	9.17 [4]	0.18
immunoglobulin M (IgM)	0.723 [4]	0.027
transferrin (TRF)	2.36 [5]	0.08
transthyretin (TTR)	0.220 [5]	0.018

1) When the material is reconstituted according to the specified procedure (see page 3).
2) The certified values are the unweighted means of 6-14 accepted mean values, independently obtained by 5-14 laboratories, using ERM-DA470 as calibrant (Baudner et al., EUR reports 15423 and 16882 European Communities, Luxembourg (1993)) or a pure protein preparation.
3) Expanded uncertainty with a coverage factor $k = 2$ corresponding to a level of confidence of about 95 % estimated in accordance with the Guide to the Expression of Uncertainty in Measurement (GUM), ISO, 1995.
4) This certified mass concentration is traceable to the stated value of the mass concentration in USNRP 12-0575C (Reimer et al., Am. J. Clin. Pathol. 77 (1982) 12-19) used as calibrant for assigning values to ERM-DA470, applying the procedures described for the certification of ERM-DA470 and in the report for ERM-DA470k/IFCC.
5) The certified value in the calibrant ERM-DA470 was obtained by calibration with a pure protein preparation (Blirup-Jensen, Clin. Chem. Lab. Med. 39 (2001) 1090-1097). Consequently, the certified value in ERM-DA470k/IFCC is traceable to the International System of Units (SI) via ERM-DA470, applying the procedures described in the certification report of ERM-DA470 (see point 2) and in the certification report for ERM-DA470k/IFCC.
6) The certified value in the pure protein preparation was obtained by amino-acid analysis (A. Muñoz, et al., Anal. Biochem. 408 (1) (2011), 124-131) and confirmed by dry mass determination (S. Blirup-Jensen, Clin. Chem. Lab. Med. 39 (2001) 1090-1097). Consequently, the certified value in ERM-DA470k/IFCC is traceable to the International System of Units (SI) through the pure protein preparation

This certificate is valid for one year after purchase.
Sales date:
The minimum amount of sample to be used is 2 μL.

Accepted as an ERM®, Geel, July 2008
Latest revision Geel, April 2015

Signed:

Prof. Dr. Hendrik Emons
European Commission
Joint Research Centre
Institute for Reference Materials and Measurements
Retieseweg 111
B-2440 Geel, Belgium

Registration No. 268-RM
ISO Guide 34 for the
production of reference materials

All following pages are an integral part of the certificate.

Page 1 of 4

Appendix 3 – Equation for nonlinear 4-parameter logistic (4-PL) curve.

Limits of blank (LOB), detection (LOD), and quantification (LOQ), were estimated individually first using the relevant equations outlined in the chapter text with results (in units for absorbance) then input (individually) into the below equation along with parameters (*a* – *d*) from the 4-PL non-linear regression model that was applied to assay responses from standard dilutions. Outputs were further log-transformed to yield a final result for the corresponding alpha-1 acid glycoprotein concentration (mg/l) that was associated with the response (abs) value (*x*).

$$x = c \times \left(\frac{a-d}{y-d} - 1\right)^{\frac{1}{b}}$$

Where:

- *a* = bottom; minimum value that can be obtained (what happens with dose of 0);
- *b* = Hill's slope; the slope of the curve at the inflection point;
- *c* = point of inflection, halfway between *a* and *d*;
- *d* = top; maximum value that can be obtained (what happens with infinite dose);
- *x* = the log(concentration) results to be transformed to yield final concentration (mg/l);
- *y* = absorbance results for LOB, LOD, or LOQ equations from analyses of blank samples (n = 26).

Appendix 4 – List of search terms.

Search terms and Boolean operators utilised for database searches are presented here. The search formula began with "(('urine' OR 'urinary') AND…" and was completed with the additional terms listed below:

- 'orosomucoid' OR
- 'orosomucoid-1' OR
- 'ORM1' OR
- 'ORM-1' OR
- 'alpha-1 acid glycoprotein' OR
- 'α1-AGP' OR
- 'a1-AGP' OR
- 'AGP'.

Appendix 5 – Estimation of oxygen concentration for hypoxic sessions.

To avoid undue illness upon acute exposure to altitude, albeit still provide a potent hypoxic stimulus for proteinuria (e.g., 5,085 m, consistent with Whymper Hut, **Chapter 5**), a target altitude of 4,000 m was chosen for HYP sessions. In order to set the environmental chamber, a general barometric pressure equation was used to estimate the barometric pressure exhibited at 4,000 m (i.e., 463.37 mm Hg; calculation not shown). The alveolar gas equation (**Supplemental Equation 1**) was then used to estimate the associated partial pressure of inspired oxygen (P_IO_2) for this altitude (***Step 2***). The result was utilised to estimate the fraction of O_2 needed for delivery by the chamber ($F_IO_{2chamber}$) in order to elicit a P_IO_2 equivocal to 4,000 m (***Steps 3***). This result (i.e., 0.122 or 12.2% O_2) was set as the target $F_IO_{2chamber}$ for all HYP sessions with the allowable O_2 concentration (or percent O_2) deviation set to ± 5% of the target elevation (i.e., 3,800 – 4,200 m), which was estimated as $F_IO_{2chamber}$ = 0.120 to 0.127 (or 12.0% – 12.7% O_2; as shown in ***Steps 4a*** and ***4b***).

Supplemental Equation 1 – Alveolar gas equation.

$$P_IO_2 = (P_B - PH_2O) \times F_IO_2$$

Where:

- P_B = barometric pressure;
- P_0 = barometric pressure at sea-level;
- P_IO_2 = partial pressure of inspired oxygen;
- PH_2O = partial pressure of water (47 mm Hg);
- F_IO_2 = fraction of inspired oxygen (or concentration of O_2).

Step 1 – Calculate P_IO_2 for sea-level conditions (where P_0 = the P_B at sea-level; ~760 mm Hg and F_IO_2 at sea-level = ~0.209).

$$P_IO_2 = (P_0 - 47) \times 0.209$$
$$P_IO_2 = (760 - 47) \times 0.209$$
$$P_IO_2 = 149.0 \text{ mm Hg at sea level}$$

Step 2 – From a generalised barometric pressure equation use P_B estimates for 4,000 m (463.37 mm Hg; equations and calculation not shown), to calculate P_IO_2 for 4,000 m.

$$P_IO_2 = (463.37 - 47) \times 0.209$$
$$P_IO_2 = 87 \text{ mm Hg at 4,000 m}$$

Step 3 – Calculate F_IO_2 required for delivery by the chamber ($F_IO_{2chamber}$) to that will equilibrate to P_IO_2 exhibited at 4,000 m.

$$87 = (760 - 47) \times F_IO_{2chamber}$$
$$F_IO_{2chamber} = 87 \div (760 - 47)$$
$$F_IO_{2chamber} = 0.122 \text{ or } 12.2\%$$

Step 4 – Estimate the allowable $F_IO_{2chamber}$ deviation consistent with a ± 5% deviation in 4,000 m of elevation (i.e., 3,800 – 4,200 m).

Step 4a – Using generalised P_B estimates for 3,800 m (479.31 mm Hg) and 4,200 m (455.49 mm Hg) calculate P_IO_2 for the altitude range.

$$P_B = (479.31 - 47) \times 0.209$$
$$P_B = 90.35 \text{ mm Hg (at 3,800 m)}$$

and

$$P_B = (455.49 - 47) \times 0.209$$
$$P_B = 85.37 \text{ mm Hg (at 4,200 m)}$$

Step 4b – Substitute P_IO_2 results from ***Step 4a*** into alveolar equation to produce corresponding $F_IO_{2chamber}$ limits corresponding to ± 5% deviation from 4,000 m (by elevation).

$$90.35 = (760 - 47) \times F_IO_{2chamber}$$
$$F_IO_{2chamber} = 90.35 \div (760 - 47)$$
$$F_IO_{2chamber} = 0.1267; \text{ or } 12.7\% \text{ (for 3,800 m)}$$

and

$$85.37 = (760 - 47) \times F_IO_{2chamber}$$
$$F_IO_{2chamber} = 85.37 \div (760 - 47)$$
$$F_IO_{2chamber} = 0.1197; \text{ or } 12.0\% \text{ (for 4,200 m)}$$

Appendix 6 – Physiologic responses and α1-AGP excretion for a subset of participants.

Physiologic response outcomes (e.g., SBP, DBP, SpO_2 and HR) and α1-AGP excretion measured at 30-minute intervals pre- and post-exercise for the subset of participants (n = 7) are presented in **Supplement 1.** Among the subset, significant effects of time (p = 0.002), condition (p < 0.001), and interaction (condition × time; p < 0.001) were observed for SpO_2 (**Supplement 1a**). Similarly, significant effects of time (p < 0.001) and interaction (p = 0.006; **Supplement 1b**) were observed for HR. No significant effects of time, condition, nor interaction were evident for SBP or DBP (**Supplement 1c** and **Supplement 1d**).

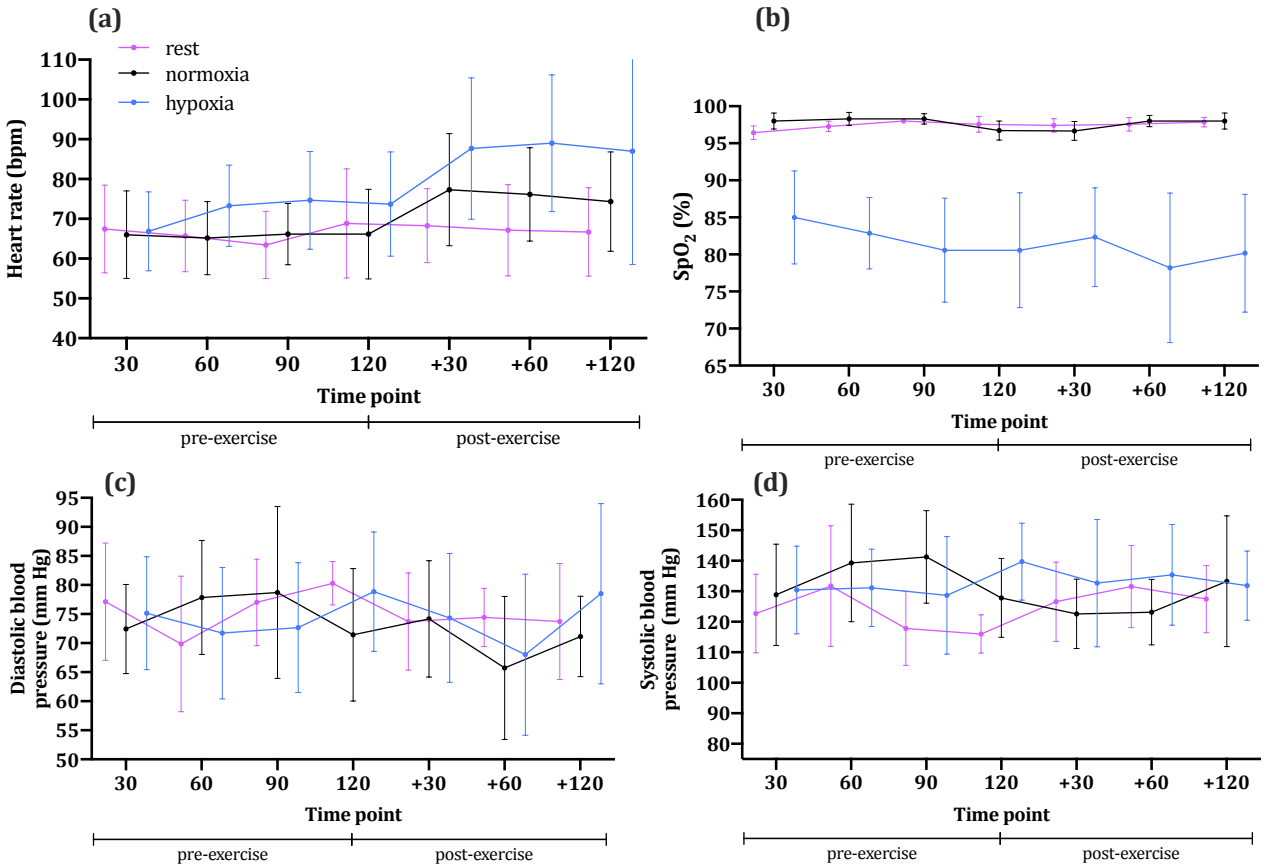

Supplement 1 – Physiologic response outcomes for a subset of participants. Supp. 1a (top left) – Heart rate (HR). Significant main effects of time ($p < 0.001$) and interaction ($p = 0.006$) but not condition ($p = 0.104$) were observed for HR; **Supp. 1b (top right)** – Peripheral oxygen saturation (%SpO_2). Significant main effect of time ($p = 0.002$), condition ($p < 0.001$), and interaction ($p < 0.001$) was observed for SpO_2; **Supp. 1c (bottom left)** – Diastolic blood pressure (DBP). No main effect of condition ($p = 0.879$), time ($p = 0.107$), or interaction ($p = 0.149$) were observed for DBP; **Supp. 1d (bottom right)** – Systolic blood pressure (SBP). No main effect of condition ($p = 0.167$), time ($p = 0.663$), or interaction ($p = 0.179$) was observed for SBP. Data are plotted (mean ± 95% confidence intervals) for a subset of participants (n = 7) who completed resting control, normoxia, and hypoxia trials (sessions differentiated by line colour, see legend). Interval measurements are interleaved (by condition). The leftmost timepoint on the x-axis ('30') referred to time elapsed after entering the chamber while '+30' referred to time elapsed after exercise completion. Mixed effects analysis (see section **6.2.7**) was used to evaluate main effects of conditions and time with all statistical tests being two-tailed and significance set to $\alpha < 0.05$.

Urinary α1-AGP excretion rates during resting control trials and experimental sessions completed in the subset (n = 7) are presented in **Supplement 2** Unsurprisingly, significant effects of condition ($p = 0.021$) and time ($p = 0.015$) were evident for α1-AGP with an additional interaction effect (time × condition; $p = 0.010$) also observed. Urinary α1-AGP at

post-30 minutes was greater than pre-exercise in NOR (p= 0.008) and HYP (p = < 0.001) but not in the resting control trial (p = 0.997) with post-30-minute excretion rates being greater in NOR and HYP compared the same timepoint in the resting control trial (p = 0.004 and p = 0.013, respectively; **Supplement 2**).

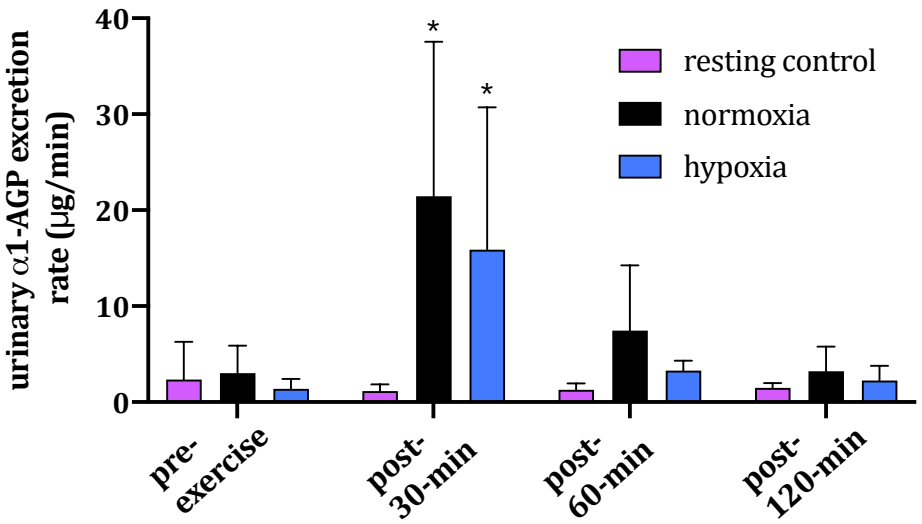

Supplement 2 – Urinary alpha-1 acid glycoprotein (α1-AGP) excretion rates (μg/min) for the subset of participants. Urinary α1-AGP excretion data (mean ± standard deviation, SD; error bars) are presented for those participants whom completed: resting control, normoxic (NOR), and hypoxic sessions (indicated by column colour; see legend). Significant effects of time (p = 0.015), condition (p = 0.021), and interaction (p = 0.010) were observed. Post-exercise α1-AGP 30 minutes after exercise was significantly greater compared to pre-exercise (as indicated by asterisk, *) in NOR (p = 0.008) and HYP (p < 0.001) but in the resting control trial (p = 0.997). Mixed effects analysis was applied to corresponding log-transformed values. All statistical tests were two-tailed with significance set to α < 0.05.

Appendix 7 – Estimated glomerular filtration (eGFR) rate during ascent to altitude.

In addition to the correlations presented in **Table 7.7**, exploratory analysis of daily means demonstrated that eGFR was correlated with metres of altitude ($p < 0.001$, r = –0.805), nocturnal HR/SpO_2 ($p = 0.015$, r = –0.577), and variables presented in **Supplement 3** Also of note from individual eGFR data, was the disparate pattern observed among AMS positive (AMS^+) and AMS negative (AMS^-) individuals during residence at the top camp. In contrast to AMS^-, AMS^+ individuals (not undergoing pharmacologic treatment; n = 4) displayed elevated eGFRs (3 out of 4) relative to pre-ascent levels (1 of 4 showing no change) on at least one morning during residence at 4,800 m.

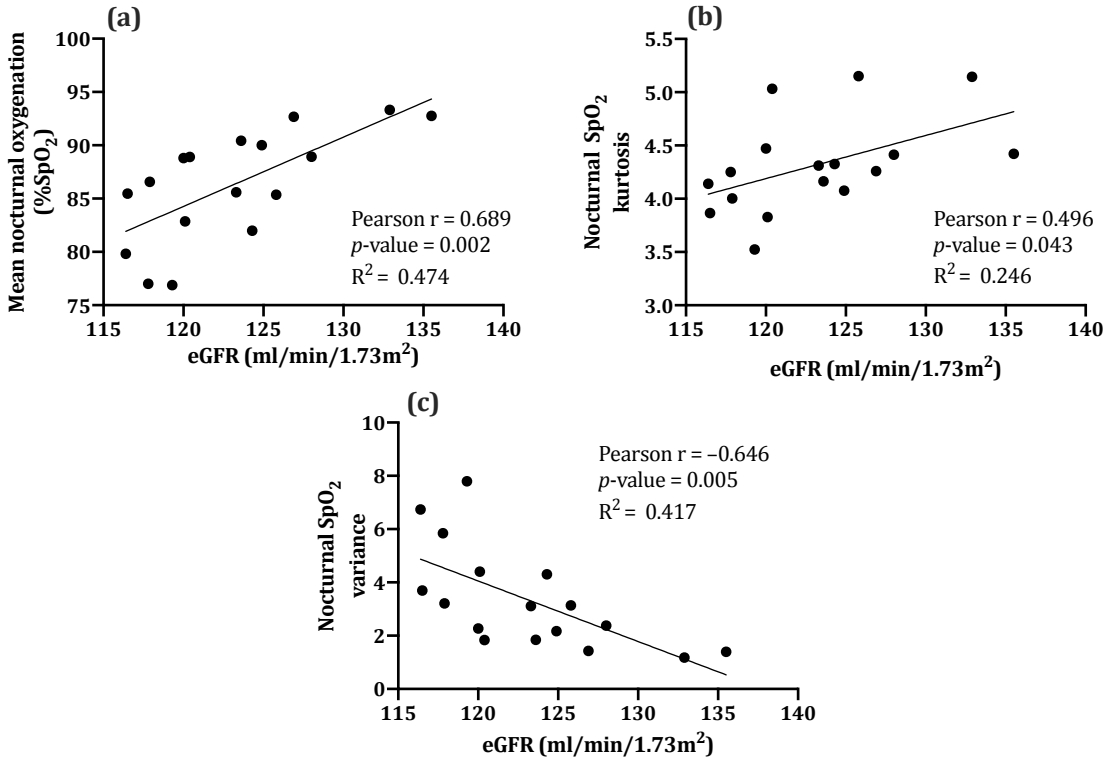

Supplement 3 – Correlations between estimated glomerular filtration rate (eGFR, ml/min/1.73 m²) and nocturnal SpO_2 derivatives. Supp. 3a (top left) – Correlation between eGFR and mean nocturnal SpO_2; **Supp. 3b (top right)** – Correlation between eGFR and kurtosis; and **Supp. 3c (bottom left)** – Correlation between eGFR and nocturnal variance. Data are plotted from daily group means for each variable. eGFR was estimated from serum [cystatin C] measurements using **Equation 7.1**. All statistical tests were two-tailed with significance was set to $\alpha < 0.05$. Pearson r, correlation coefficient; and R^2, coefficient of determination.

Estimated glomerular filtration rate is routinely used in place of GFR to evaluate renal function and can be calculated using serum and urinary markers (e.g., creatinine and cystatin C)[473]. Estimated glomerular filtration is largely reflective of the efficiency of molecular (e.g., protein or electrolyte) reabsorption in renal tubules with reductions oftentimes accompanying proteinuria, particularly, in the later stages of kidney disease. Estimated glomerular filtration has also been demonstrated to increase upon initial exposure to high-altitude and further followed by a return to baseline within several days[569]. Changes in eGFR thereafter are discrepant between studies with the topic remaining controversial[164]. Provided that normal tubular function is not associated with α1-AGP reabsorption[155], increases in urinary α1-AGP with ascent are considered products of (patho)physiologic responses within the glomerulus and, therefore, would not be expected to relate to any changes in tubular function or eGFR during ascent.

The results presented above were consistent with the study conducted by Pichler and colleagues whom demonstrated reductions in filtration among most participants, albeit hyperfiltration among a select few individuals with results correlating with AMS scores[569]. Given the propensity for cystatin C equations to overestimate eGFR above values of 90 ml/min/1.73 m^2 when using the present cystatin C-based equation[2 473], it would be inappropriate to hyper focus on this result alone. Curiously, hyperfiltration exhibited in the present study occurred among individuals exhibiting high hypoxic burdens, and elevated AMS scores. Most interesting however, were the concomitant changes in serum inflammatory markers among these individuals, which were oppositional to that of the group. It is possible that increases in eGFR (i.e., reductions in cystatin C) among these individuals were disguised as hyperfiltration by hypoxia-induced immunosuppression of cystatin C, which can occur for serum markers on exposure to altitude. Increases in cystatin C and concomitant reductions in

eGFR in the rest of the group would have thus, been reflective of a more appropriated immune response to hypoxia[570]. This potential for overestimation of eGFR (by cystatin C-based equations) was not addressed by the only other similar altitude study. The above explanation is supported by the lack evidence in the literature (publications[571] and preprints[572]) for any renal dysfunction with ascent. The only plausible physiologic connection between eGFR and urinary α1-AGP would relate to the alteration in electrical forces facilitated by changes in blood flow through the glomerulus[169], albeit a weak explanation and unable to account for disparities between individuals.

Appendix 8 – Exploratory analysis results.

Exploratory analysis revealed that both 24-hour urinary K^+ and Cl^- excretion were positively correlated with nocturnal mean SpO_2 (K^+: $p = 0.002$, r = 0.704; Cl^-: $p = 0.003$, r = 0.677) and negatively correlated with additional nocturnal measurements; specifically: ODI (K^+: $p = 0.016$, r = –0.590; Cl^-: $p = 0.046$, r = –0.490), SpO_2 variance (K^+: $p = 0.039$, r = –0.505; Cl^-: $p = 0.036$, r = –0.496), and HR/SpO_2 (K^+: $p = 0.016$, r = –0.590; Cl^-: $p = 0.026$, r = –0.539). Twenty-four-hour urinary Na^+ and K^+ excretion, but not Cl^-, were correlated with nocturnal: skewness (Na^+: $p = 0.032$, r = 0.505; K^+: $p = 0.031$, r = –0.523) and kurtosis proper (Na^+: $p = 0.033$, r = –0.505; K^+: $p = 0.029$, r = 0.529).

Correlations for nocturnal HR/SpO_2 were also observed between: RR ($p < 0.001$, r = 0.780), LLS ($p = 0.002$, r = 0.710), and SBP ($p = 0.015$, r = 0.594). HR/SpO_2 ratio was not correlated with serum CRP ($p = 0.546$) or serum α1-AGP ($p = 0.634$).

Appendix 9 – Ongoing clinical trial utilising urinary alpha-1 acid glycoprotein (α1-AGP).

Experiments were aimed at assessing abnormal changes in cerebral (assessed via magnetic resonance imaging, MRI) and renal (assessed via urine collection and subsequent urinalysis) markers among individuals exposed to hypoxia with and without dexamethasone administration (as discussed in the next paragraph). The overall clinical trial designed can be referenced in **Supplement 4**.

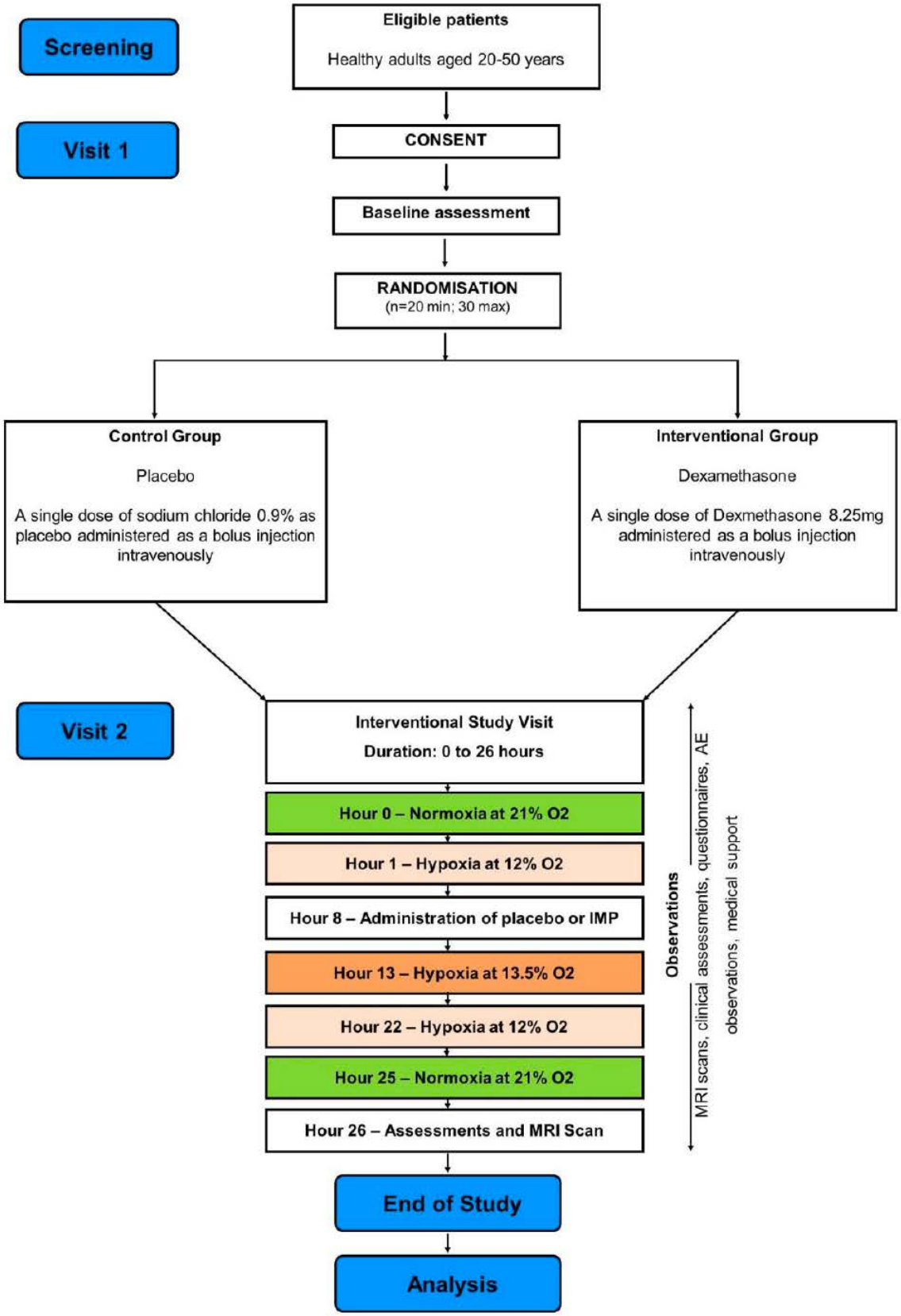

Supplement 4 – Clinical trial study design. Diagram shows the progression of the study from the time screening through analysis. MRI, magnetic-resonance imaging.

Intervention visits (refer to **Supplement 5** for complete timeline) were conducted in pairs with individuals age and sex matched. Prior to exposure to hypoxia for interventional sessions, all individuals underwent MRI of the head (at T = 0;). Following this, participants entered a hypoxic tent outfitted with a hypoxicator (supplying 12% O_2 until T = 13; refer to the table) at T = 1. The tent-based hypoxic exposure was substituted with mask-based delivery of the hypoxic gas mixture at times when the participant exited the tent (e.g., for MRI). A single dose of either placebo (sodium chloride 0.9%, 8.2 ml) or dexamethasone 8.25 mg (2.5 ml; made up to 8.2 ml with sodium chloride 0.9%) was administered as a bolus injection over 5 minutes at T = 8. MRI was repeated at T = 7, 11, 22 and 26.

Timed urine collections (not shown in table) were collected throughout with aliquots obtained in parallel with measurements for vitals (peripheral oxygenation, blood pressure, and heart rate), acute mountain sickness scores (via Lake Louise scores[422], LLS), and serum biomarkers at the following timepoints: T = 4, 8, 12, 22, and 26. To initiate urine collections and start the clock for timed collections, participants were asked to urinate upon arrival for visit 2 (intervention visit at T = 0). All urine thereafter was collected into 3,000 ml vesicles designed for 24-hour urine collections with timed collections occurring from: T = 0 to T = 4; T = 4 to T = 8; T = 8 to T = 12; and T = 12 to T = 26. Volume and actual collection duration (to the minute) were recorded for each timed urine collection with a specimen (~20 ml) then obtained, centrifuged, aliquoted, and stored on ice until transported to long-term storage (–80°C) where specimens would remain until analysis. Preliminary analyses had been planned following the completion of 8 interventional sessions (n = 16) however, due to the emergence of SARS-CoV-2[573] the MRI scanner was reprioritised for COVID-19 patients and, therefore, the study has been postponed indefinitely.

Supplement 5 – Clinical trial timeline.

Observations & Assessments	Visit 1 - Screening	Randomisation	Visit 2 - Intervention (in hours)																												ET
			T=0	1*	2	3	4	5	6	7	8	9	10	11	12	13	14	15	16	17	18	19	20	21	22	23	24	25	26	After T=0
Eligibility confirmation	X																													
Informed consent	X																													
Medical History	X																													
Current Medications	X																													
Demographics	X																													
MRI safety questionnaire	X		X																											
Vital Signs	X		X		X		X		X		X			X										X		X		X	X	
Blood test	X		X								X			X										X				X		
Randomisation		X																												
Urine pregnancy test (females only)**			X																											
Venous cannulation			X																											
Finger prick test			X								X			X										X				X		
MRI Scan			X							X				X										X				X		
Lake Louise Score			X		X		X		X		X			X										X						
Administration of IMP or placebo											X																			
Normoxia at 21% O2			X																								X	X		
Hypoxia at 12% O2				X	X	X	X	X	X	X	X	X	X	X	X										X	X	X				
Hypoxia at 13.5% O2																X	X	X	X	X	X	X	X	X							
Inspired O2 & CO2			X	←Every 15 mins→									←Every 30 mins→															X			
AEs/SAEs			←Monitored throughout participation→																											X	
End of Study																													X		
Early Termination																														X	

* Observations will be conducted ± 30 minutes of the stated hour wherever possible with any deviations reported on the protocol deviation log. ** A urine pregnancy test is required for all females at visit 2 (intervention visit) prior to initiation of any study procedures. ET, early termination of study participation anytime after T = 0 at visit 2 (intervention visit).

REFERENCES

1. Putnam FW. The Plasma Proteins. 2nd Edition ed. Orlando, FL: Academic Press 1987.

2. Fournier T, Medjoubi NN, Porquet D. Alpha-1-acid glycoprotein. *Biochim Biophys Acta* 2000;1482(1-2):157-71. [published Online First: 2000/11/04]

3. Hochepied T, Berger FG, Baumann H, et al. Alpha(1)-acid glycoprotein: an acute phase protein with inflammatory and immunomodulating properties. *Cytokine Growth Factor Rev* 2003;14(1):25-34. doi: 10.1016/s1359-6101(02)00054-0 [published Online First: 2002/12/18]

4. Kustán P, Köszegi T, Miseta A, et al. Urinary Orosomucoid A Potential Marker Of Inflammation In Psoriasis. *Int J Med Sci* 2018;15(11):1113-17.

5. Kustán P, Szirmay B, Horváth-Szalai Z, et al. Urinary orosomucoid: validation of an automated immune turbidimetric test and its possible clinical use. *Biochemia Medica* 2016;26(3):421-30.

6. Poortmans J, Jeanloz RW. Quantitative immunological determination of 12 plasma proteins excreted in human urine collected before and after exercise. *J Clin Invest* 1968;47(2):386-93. doi: 10.1172/JCI105735 [published Online First: 1968/02/01]

7. Talks B, Bradwell S, Delamere J, et al. Urinary alpha-1-acid glycoprotein is a sensitive marker of glomerular protein leakage at altitude. *High Alt Med Biol* 2018;19(3):295-98.

8. Javitt NB, Miller AT. Mechanism of Exercise Proteinuria. *J Appl Physiol* 1952;4(11):834-39.

9. Suzuki M, Ikawa S. The mechanisms of exercise-induced proteinuria--relationship between urinary excretion of proteins and lactate after exhaustive exercise. *Japanese Society of Nephrology* 1991;33(4):357-64.

10. Bradwell A, Brearey S, Harris S, et al. Effect of hard exercise on proteinuria at high altitude. *High Altitude Medicine and Biology* 2003; 3(31):436.

11. Poortmans JR. Postexercise proteinuria in humans. Facts and mechanisms. *JAMA* 1985;253(2):236-40. [published Online First: 1985/01/11]

12. Senturk UK, Kuru O, Kocer G, et al. Biphasic pattern of exercise-induced proteinuria in sedentary and trained men. *Nephron Physiol* 2007;105(2):p22-32. doi: 10.1159/000097953 [published Online First: 2006/12/21]

13. Kohanpour MA, Sanavi S, Peeri M, et al. Effect of submaximal aerobic exercise in hypoxic conditions on proteinuria and hematuria in physically trained young men. *Iran J Kidney Dis* 2012;6(3):192-7. [published Online First: 2012/05/05]

14. Ainslie PN, Lucas SJ, Burgess KR. Breathing and sleep at high altitude. *Respir Physiol Neurobiol* 2013;188(3):233-56. doi: 10.1016/j.resp.2013.05.020 [published Online First: 2013/06/01]

15. Hudnall SD. Hematology: a pathophysiologic approach / S. David Hudnall. Philadelphia, PA: Mosby/Elsevier 2012:1-2.

16. Schreiber G. The synthesis and secretion of plasma proteins in the liver. *Pathology* 1978;10(4):394. doi: https://doi.org/10.1016/S0031-3025(16)39817-8

17. Baumann H, Gauldie J. Regulation of hepatic acute phase plasma protein genes by hepatocyte stimulating factors and other mediators of inflammation. *Mol Biol Med* 1990;7(2):147-59. [published Online First: 1990/04/01]

18. Peters TJ. All about albumin: biochemistry, genetics, and medical applications. 1st Edition ed. San Diego, CA: Academic Press 1995.

19. Bteich M. An overview of albumin and alpha-1-acid glycoprotein main characteristics: highlighting the roles of amino acids in binding kinetics and molecular interactions. *Heliyon* 2019;5(11):e02879. doi: 10.1016/j.heliyon.2019.e02879 [published Online First: 2019/12/18]

20. Schmid K, Burgi W, Collins JH, et al. The disulfide bonds of alpha1-acid glycoprotein. *Biochemistry* 1974;13(13):2694-7. doi: 10.1021/bi00710a006 [published Online First: 1974/06/18]

21. Van Dijk W, Do Carmo S, Rassart E, et al. The Plasma Lipocalins α1-Acid Glycoprotein, Apolipoprotein D, Apolipoprotein M and Complement Protein C8γ. Madame Curie Bioscience Database [Internet]. Austin, TX: Landes Biosciences 2000-2013.

22. van Dijk W, Havenaar EC, Brinkman-van der Linden EC. Alpha 1-acid glycoprotein (orosomucoid): pathophysiological changes in glycosylation in relation to its function. *Glycoconj J* 1995;12(3):227-33. doi: 10.1007/bf00731324 [published Online First: 1995/06/01]

23. De Graaf TW, Van der Stelt ME, Anbergen MG, et al. Inflammation-induced expression of sialyl Lewis X-containing glycan structures on alpha 1-acid glycoprotein (orosomucoid) in human sera. *J Exp Med* 1993;177(3):657-66. doi: 10.1084/jem.177.3.657 [published Online First: 1993/03/01]

24. Huang RY, Hudgens JW. Effects of desialylation on human alpha1-acid glycoprotein-ligand interactions. *Biochemistry* 2013;52(40):7127-36. doi: 10.1021/bi4011094 [published Online First: 2013/09/18]

25. Mackiewicz A, Mackiewicz K. Glycoforms of serum alpha 1-acid glycoprotein as markers of inflammation and cancer. *Glycoconj J* 1995;12(3):241-7. doi: 10.1007/bf00731326 [published Online First: 1995/06/01]

26. Biou D, Chanton P, Konan D, et al. Microheterogeneity of the carbohydrate moiety of human alpha 1-acid glycoprotein in two benign liver diseases: alcoholic cirrhosis and acute hepatitis. *Clin Chim Acta* 1989;186(1):59-66. doi: 10.1016/0009-8981(89)90204-0 [published Online First: 1989/12/29]

27. Yazawa S, Takahashi R, Yokobori T, et al. Fucosylated Glycans in α1-Acid Glycoprotein for Monitoring Treatment Outcomes and Prognosis of Cancer Patients. *PLOS ONE* 2016;11(6):e0156277. doi: 10.1371/journal.pone.0156277

28. Iijima S, Shiba K, Kimura M, et al. Changes of alpha1-acid glycoprotein microheterogeneity in acute inflammation stages analyzed by isoelectric focusing using serum obtained postoperatively. *Electrophoresis* 2000;21(4):753-9. doi: 10.1002/(sici)1522-2683(20000301)21:4<753::Aid-elps753>3.0.Co;2-y [published Online First: 2000/03/25]

29. van Dijk W, Turner GA, Mackiewicz A. Changes in glycosylation of acute-phase proteins in health and disease: occurrence, regulation and function *Glycosylation & Disease* 1994;1(1):5-14.

30. Lowe JB. Glycan-dependent leukocyte adhesion and recruitment in inflammation. *Curr Opin Cell Biol* 2003;15(5):531-8. doi: 10.1016/j.ceb.2003.08.002 [published Online First: 2003/10/02]

31. Schmid K. Preparation and properties of an acid glycoprotein prepared from human plasma. *J Am Chem Soc* 1950;72(6):2816-16.

32. Schmid K. Preparation and Properties of Serum and Plasma Proteins. XXIX. Separation from Human Plasma of Polysaccharides, Peptides and Proteins of Low Molecular Weight. Crystallization of an Acid Glycoproteinl. *J Am Chem Soc* 1953;75(1):60-68.

33. Tokita K, Schmid K. Variants of Alpha-1-Acid Glycoprotein. *Nature* 1963;200:266. doi: 10.1038/200266a0 [published Online First: 1963/10/19]

34. Johnson AM, Schmid K, Alper CA. Inheritance of human alpha-1-acid glycoprotein (orosomucoid) variants. *J Clin Invest* 1969;48(12):2293-9. doi: 10.1172/JCI106195 [published Online First: 1969/12/01]

35. Dente L, Pizza MG, Metspalu A, et al. Structure and expression of the genes coding for human alpha 1-acid glycoprotein. *EMBO J* 1987;6(8):2289-96. [published Online First: 1987/08/01]

36. Yuasa I, Umetsu K, Vogt U, et al. Human orosomucoid polymorphism: molecular basis of the three common ORM1 alleles, ORM1*F1, ORM1*F2, and ORM1*S. *Hum Genet* 1997;99(3):393-8. doi: 10.1007/s004390050378 [published Online First: 1997/03/01]

37. Sebetan IM, Oshida S, Yuasa I, et al. Genetic polymorphisms of orosomucoid ORM1 and ORM2 in Egyptians, Sudanese, and Qataris: occurrence of two new alleles. *Hum Biol* 1997;69(1):121.

38. Mastana SS, Jayasekara R, Fisher P, et al. Genetic polymorphism of orosomucoid (ORM) in populations of the United Kingdom, Indian subcontinent, and Cambodia. *Jpn J Hum Genet* 1993;38(3):289-96. doi: 10.1007/BF01874139 [published Online First: 1993/09/01]

39. Eap CB, Cuendet C, Baumann P. Binding of amitriptyline to alpha 1-acid glycoprotein and its variants. *J Pharm Pharmacol* 1988;40(11):767-70. doi: 10.1111/j.2042-7158.1988.tb05169.x [published Online First: 1988/11/01]

40. Bree F, Houin G, Barre J, et al. Pharmacokinetics of intravenously administered 125I-labelled human alpha 1-acid glycoprotein. *Clin Pharmacokinet* 1986;11(4):336-42. doi: 10.2165/00003088-198611040-00006 [published Online First: 1986/07/01]

41. Kremer JM, Wilting J, Janssen LH. Drug binding to human alpha-1-acid glycoprotein in health and disease. *Pharmacol Rev* 1988;40(1):1-47. [published Online First: 1988/03/01]

42. Taguchi K, Nishi K, Chuang V, et al. Molecular Aspects of Human Alpha-1 Acid Glycoprotein — Structure and Function2013.

43. Easton JA, Hardwicke J, Whitehead PH. The estimation of two alpha(1) glycoproteins (orosomucoid and another alpha(1) acid glycoprotein) in health and disease. *J Clin Pathol* 1962;15(6):585-90. doi: 10.1136/jcp.15.6.585 [published Online First: 1962/11/01]

44. Wong W, Aoki FY, Friesen AD, et al. Effect of acute experimental influenza a virus pneumonia on concentration of alpha1-acid glycoprotein in mouse serum. *Inflammation* 1989;13(6):659-72. doi: 10.1007/BF00914310

45. Pos O, Moshage HJ, Yap SH, et al. Effects of monocytic products, recombinant interleukin-1, and recombinant interleukin-6 on glycosylation of alpha 1-acid glycoprotein: studies with primary human hepatocyte cultures and rats. *Inflammation* 1989;13(4):415-27. doi: 10.1007/bf00914925 [published Online First: 1989/08/01]

46. Gendler SJ, Dermer GB, Silverman LM, et al. Synthesis of alpha 1-antichymotrypsin and alpha 1-acid glycoprotein by human breast epithelial cells. *Cancer Res* 1982;42(11):4567-73. [published Online First: 1982/11/01]

47. Sörensson J, Matejka GL, Ohlson M, et al. Human endothelial cells produce orosomucoid, an important component of the capillary barrier. *Am J Physiol* 1999;45:H530-H34.

48. Azuma Y, Murata M, Matsumoto K. Alteration of sugar chains on alpha(1)-acid glycoprotein secreted following cytokine stimulation of HuH-7 cells in vitro. *Clin Chim Acta* 2000;294(1-2):93-103. doi: 10.1016/s0009-8981(99)00248-x [published Online First: 2000/03/23]

49. Wigmore SJ, Fearon KC, Maingay JP, et al. Interleukin-8 can mediate acute-phase protein production by isolated human hepatocytes. *Am J Physiol* 1997;273(4):E720-26. doi: 10.1152/ajpendo.1997.273.4.E720.

50. Mouthiers A, Mejdoubi N, Baillet A, et al. Retinoids increase alpha-1 acid glycoprotein expression at the transcriptional level through two distinct DR1 retinoic acid responsive elements. *Biochim Biophys Acta* 2004;1678(2-3):135-44. doi: 10.1016/j.bbaexp.2004.03.005 [published Online First: 2004/05/26]

51. Boudreau F, Yu S-J, Asselin C. CCAAT/Enhancer Binding Proteins Beta and Delta Regulate α1-Acid Glycoprotein Gene Expression in Rat Intestinal Epithelial Cells. *DNA and Cell Biology* 1998;17(8):669-77. doi: 10.1089/dna.1998.17.669

52. Nevo S, Picornell A, Miguel A, et al. Orosomucoid (ORM1) polymorphism in Arabs and Jews of Israel: more evidence for a middle eastern origin of the Jews. *Hum Biol* 1996;68(2):217-29. [published Online First: 1996/04/01]

53. García-Ortiz L, Vargas-Alarcón G, Fragoso JM, et al. A/G Gln20Arg (exon 1) and G/A Val156Met (exon 5) polymorphisms of the human orosomucoid 1 gene in Mexico. *Genet Mol Res* 2008;7(1):7-15. doi: 10.4238/vol7-1gmr348 [published Online First: 2008/02/15]

54. Picornell A, Castro JA, Ramon MM. Serum protein polymorphism in Chuetas (Majorcan Jews)--GC, A2HS, ORM, ITI and HP. *Gene Geogr* 1994;8(2):137-45. [published Online First: 1994/08/01]

55. Escallon MH, Ferrell RE, Kamboh MI. Genetic studies of low-abundance human plasma proteins. V. Evidence for a second orosomucoid structural locus (ORM2) expressed in plasma. *American journal of human genetics* 1987;41(3):418-27.

56. Montiel MD, Carracedo A, Blazquez-Caeiro JL, et al. Orosomucoid (ORM1 and ORM2) types in the Spanish Basque Country, Galicia and northern Portugal. *Hum Hered* 1990;40(6):330-4. doi: 10.1159/000153956 [published Online First: 1990/01/01]

57. Scacchi R, Corbo RM, Rickards O, et al. The Cayapa Indians of Ecuador: a population study of seven protein genetic polymorphisms. *Annals of Human Biology* 1994;21(1):67-77. doi: 10.1080/03014469400003082

58. Yuasa I, Umetsu K, Suenaga K, et al. Orosomucoid (ORM) typing by isoelectric focusing: evidence of two structural loci ORM1 and ORM2. *Hum Genet* 1986;74(2):160-1. doi: 10.1007/bf00282080 [published Online First: 1986/10/01]

59. Scacchi R, Corbo RM, Cossu G, et al. Distribution of ORM1, C6, C7 and APO C-II allele frequencies in populations from mainland Italy and Sardinia. *Hum Hered* 1992;42(5):309-15. doi: 10.1159/000154088 [published Online First: 1992/01/01]

60. Dülmer M, Reker G, Nguyen TT, et al. Human orosomucoid (ORM1) subtyping: further population genetic data and reports on the feasibility to type aged blood samples and stains. *J Forensic Sci* 1998;43(2):413-6. [published Online First: 1998/04/17]

61. Luckenbach C, Kömpf J, Ritter H. Orosomucoid (ORM 1) subtyping and formal genetics. *Human Genetics* 1991;87(4):429-32. doi: 10.1007/BF00197162

62. Thymann M, Eiberg H. Orosomucoid polymorphism: Determination by Separator Isoelectric Focusing and Demonstration of ORM*F subtypes. *11th Congress of the Society for Forensic Haemogenetics (Gesellschaft für forensische Blutgruppenkunde eV)* 1986:162-66.

63. Weidinger S, Hallwachs R, Paoli G, et al. Genetic structure in the Garfagnana (Tuscany, Italy): a study of eight protein markers by isoelectric focusing. *Hum Hered* 1993;43(3):186-9. doi: 10.1159/000154175 [published Online First: 1993/05/01]

64. Eap CB, Baumann P. Isoelectric focusing of alpha-1 acid glycoprotein (orosomucoid) in immobilized pH-gradients with 8M urea: detection of its desialylated variants using an alkaline phosphatase-linked secondary antibody system. *Electrophoresis* 1988;9(10):650-4. doi: 10.1002/elps.1150091005 [published Online First: 1988/10/01]

65. Cerri N, De Ferrari F. Genetic polymorphism of orosomucoid (ORM1 and ORM2) in Lombardy (Italy). *Int J Legal Med* 1992;104(6):325-8. doi: 10.1007/bf01369551 [published Online First: 1992/01/01]

66. Corbo RM, Scacchi R, Cossu G, et al. Genetic Studies on the Senegal Population. II. Polymorphisms of the Plasma Proteins F13A, F13B, ORM1, AHSG, C6, C7, and APOC2. *Human Biology* 1994;66(5):885-903.

67. Metzner D, Scheil HG. Polymorphism of human orosomucoid in populations of western Germany and Switzerland. *Gene Geogr* 1988;2(2-3):119-22. [published Online First: 1988/08/01]

68. Weidinger S, Müller T, Schwarzfischer F, et al. Three new orosomucoid (ORM) variants revealed by isoelectric focusing and print immunofixation. *Human Genetics* 1987;77(3):286-88. doi: 10.1007/BF00284488

69. Moral P, Esteban E, Vives S, et al. Genetic study of the population of Tenerife (Canary Islands, Spain): Protein markers and review of classical polymorphisms. *Am J Phys Anthropol* 1997;102(3):337-49. doi: 10.1002/(SICI)1096-8644(199703)102:3<337::AID-AJPA4>3.0.CO

2-S

70. Alonso A, Visedo G, Sancho M, et al. Isoelectric Focusing in Miniaturized Gels: Application to GC, PI, Tf and ORM Subtyping in Central Spain. *13th Congress of the International Society for Forensic Haemogenetics (Internationale Gesellschaft für forensische Hämogenetik eV)* 1990:255-59.

71. Saha N, Undevia JV, Juneja RK, et al. Polymorphisms of alpha-1-acid (orosomucoid), alpha-2-HS-glycoproteins and alpha-1-B among the Parsis of India. *Hum Hered* 1992;42(6):367-71. doi: 10.1159/000154099 [published Online First: 1992/01/01]

72. Yuasa I, Umetsu K, Suenaga K. Orosomucoid (ORM) typing by isoelectric focusing: evidence for an additional duplicated ORM1 locus haplotype and close linkage of two ORM loci. *American journal of human genetics* 1988;43(2):165-69.

73. Umetsu K, Yuasa I, Yamashita T, et al. Genetic polymorphisms of orosomucoid and alpha-2-HS-glycoprotein in Thai, Sri Lankan and Paraguayan populations. *Jinrui Idengaku Zasshi* 1989;34(3):195-202. doi: 10.1007/bf01900721 [published Online First: 1989/09/01]

74. Sebetan IM, Sagisaka K. Genetic polymorphisms of orosomucoid ORM1 and ORM2 in Libyans: occurrence of ORM1*2.1 and three new ORM2 alleles. *Jinrui Idengaku Zasshi* 1988;33(4):439-43. doi: 10.1007/bf01897784 [published Online First: 1988/12/01]

75. Sebetan IM, Sagisaka K. Genetic polymorphisms of orosomucoid ORM1 and ORM2 in a Japanese population: occurrence of new ORM1 alleles. *Zeitschrift für Rechtsmedizin* 1989;102(1):5-9. doi: 10.1007/BF00201256

76. Brega A, Scacchi R, Cuccia M, et al. Study of 15 Protein Polymorphisms in a Sample of the Turkish Population. *Human Biology* 1998;70(4):715-28.

77. Yuasa I, Umetsu K, Suenaga K, et al. Orosomucoid (ORM) typing by isoelectric focusing: an analysis of ORM haplotypes. *Hum Hered* 1990;40(5):267-71. doi: 10.1159/000153943 [published Online First: 1990/01/01]

78. Yiping H, Qing G, Meiyun W. Genetic Polymorphisms of Alpha-2-HS-Glycoprotein, Group-Specific Component and Orosomucoid in the Han Population, Chengdu, China. *Human Heredity* 1992;42(6):380-83. doi: 10.1159/000154101

79. Salzano FM, Umetsu K, Yuasa I, et al. Isoelectric focusing studies in Brazilian Indians--uncovering variation of ORM, AHSG and IF. *Jinrui Idengaku Zasshi* 1990;35(4):283-90. doi: 10.1007/bf01883750 [published Online First: 1990/12/01]

80. Li J, Xu J, Li Y, et al. [Genetic polymorphisms of serum orosomucoid in Han population in Nanjing of China]. *Zhonghua Yi Xue Yi Chuan Xue Za Zhi* 1999;16(4):236-8. [published Online First: 1999/08/04]

81. Umetsu K, Yuasa I, Chen ER, et al. Orosomucoid 1 and orosomucoid 2 types in the Taiwanese and Japanese: evidence for five new orosomucoid variants. *Electrophoresis* 1988;9(5):224-6. doi: 10.1002/elps.1150090506 [published Online First: 1988/05/01]

82. Umetsu K, Ikeda N, Kashimura S, et al. Orosomucoid (ORM) typing by print lectinofixation: a new technique for isoelectric focusing. Two common alleles in Japan. *Hum Genet* 1985;71(3):223-4. doi: 10.1007/bf00284578 [published Online First: 1985/01/01]

83. Abe S, Kurisaki E, Kuroda Y, et al. Distribution of orosomucoid (ORM1) phenotypes in Cook Islanders: analysis by six-band patterns. *Gene geography : a computerized bulletin on human gene frequencies* 1988;2(2-3):85-88.

84. Umetsu K, Yuasa I, Nishimura H, et al. Genetic polymorphisms of orosomucoid and alpha-2-HS-glycoprotein in a Philippine population. *Hum Hered* 1988;38(5):287-90. doi: 10.1159/000153801 [published Online First: 1988/01/01]

85. Friedman MJ. Control of malaria virulence by alpha 1-acid glycoprotein (orosomucoid), an acute-phase (inflammatory) reactant. *Proc Natl Acad Sci U S A* 1983;80(17):5421-4. doi: 10.1073/pnas.80.17.5421 [published Online First: 1983/09/01]

86. Snyder S, Coodley EL. Inhibition of platelet aggregation by alpha1-acid glycoprotein. *Arch Intern Med* 1976;136(7):778-81. [published Online First: 1976/07/01]

87. Costello M, Fiedel BA, Gewurz H. Inhibition of platelet aggregation by native and desialised alpha-1 acid glycoprotein. *Nature* 1979;281(5733):677-8. doi: 10.1038/281677a0 [published Online First: 1979/10/25]

88. Williams JP, M.R. W, Pechet TTV, et al. α1-Acid glycoprotein reduces local and remote injuries after intestinal ischemia in the rat. *American Journal of Physiology-Gastrointestinal and Liver Physiology* 1997;273(5):G1031-G35. doi: 10.1152/ajpgi.1997.273.5.G1031

89. Vasson MP, Roch-Arveiller M, Couderc R, et al. Effects of alpha-1 acid glycoprotein on human polymorphonuclear neutrophils: influence of glycan microheterogeneity. *Clin Chim Acta* 1994;224(1):65-71. doi: 10.1016/0009-8981(94)90121-x [published Online First: 1994/01/14]

90. Bories PN, Guenounou M, Féger J, et al. Human alpha 1-acid glycoprotein-exposed macrophages release interleukin 1 inhibitory activity. *Biochemical and biophysical research communications* 1987;147(2):710-15. doi: 10.1016/0006-291x(87)90988-0

91. Sorensson J, Ohlson M, Bjornson A, et al. Orosomucoid has a cAMP-dependent effect on human endothelial cells and inhibits the action of histamine. *Am J Physiol Heart Circ Physiol* 2000;278(5):H1725-31. doi: 10.1152/ajpheart.2000.278.5.H1725 [published Online First: 2000/04/25]

92. Shiyan SD, Bovin NV. Carbohydrate composition and immunomodulatory activity of different glycoforms of alpha1-acid glycoprotein. *Glycoconj J* 1997;14(5):631-8. doi: 10.1023/a:1018544711767 [published Online First: 1997/08/01]

93. Pos O, Oostendorp RA, van der Stelt ME, et al. Con A-nonreactive human alpha 1-acid glycoprotein (AGP) is more effective in modulation of lymphocyte proliferation than Con A-reactive AGP serum variants. *Inflammation* 1990;14(2):133-41. doi: 10.1007/bf00917452 [published Online First: 1990/04/01]

94. Haraldsson B, Rippe B. Serum factors other than albumin are needed for the maintenance of normal capillary permselectivity in rat hindlimb muscle. *Acta Physiol Scand* 1985;123(4):427-36. doi: 10.1111/j.1748-1716.1985.tb07609.x [published Online First: 1985/04/01]

95. Muchitsch EM, Teschner W, Linnau Y, et al. In vivo effect of alpha 1-acid glycoprotein on experimentally enhanced capillary permeability in guinea-pig skin. *Arch Int Pharmacodyn Ther* 1996;331(3):313-21. [published Online First: 1996/05/01]

96. Haraldsson BS, Johnsson EKA, Rippe B. Glomerular permselectivity is dependent on adequate serum concentrations of orosomucoid. *Kidney International* 1992;41(2):310-16. doi: 10.1038/ki.1992.43

97. Johnsson E, Haraldsson B. Addition of purified orosomucoid preserves the glomerular permeability for albumin in isolated perfused rat kidneys. *Acta Physiol Scand* 1993;147(1):1-8. doi: 10.1111/j.1748-1716.1993.tb09466.x [published Online First: 1993/01/01]

98. Haraldsson B, Nystrom J, Deen WM. Properties of the glomerular barrier and mechanisms of proteinuria. *Physiol Rev* 2008;88(2):451-87. doi: 10.1152/physrev.00055.2006 [published Online First: 2008/04/09]

99. Betteridge KB, Arkill KP, Neal CR, et al. Sialic acids regulate microvessel permeability, revealed by novel in vivo studies of endothelial glycocalyx structure and function. *J Physiol* 2017;595(15):5015-35. doi: 10.1113/jp274167 [published Online First: 2017/05/20]

100. Curry FE, Rutledge JC, Lenz JF. Modulation of microvessel wall charge by plasma glycoprotein orosomucoid. *Am J Physiol-Heart C* 1989;257(5):H1354-H59. doi: 10.1152/ajpheart.1989.257.5.H1354

101. Muchitsch E, Pichler L, Schwarz HP, et al. Effects of human alpha-1-acid glycoprotein on aminonucleoside-induced minimal change nephrosis in rats. *Nephron* 1999;81(2):194-9. doi: 10.1159/000045276 [published Online First: 1999/02/06]

102. Logdberg L, Wester L. Immunocalins: a lipocalin subfamily that modulates immune and inflammatory responses. *Biochim Biophys Acta* 2000;1482(1-2):284-97. doi: 10.1016/s0167-4838(00)00164-3 [published Online First: 2000/11/04]

103. Matsumoto K, Sukimoto K, Nishi K, et al. Characterization of ligand binding sites on the alpha1-acid glycoprotein in humans, bovines and dogs. *Drug Metab Pharmacokinet* 2002;17(4):300-6. doi: 10.2133/dmpk.17.300 [published Online First: 2004/12/25]

104. Huang Z, Ung T. Effect of alpha-1-acid glycoprotein binding on pharmacokinetics and pharmacodynamics. *Curr Drug Metab* 2013;14(2):226-38. [published Online First: 2012/10/25]

105. Israili ZH, Dayton PG. Human alpha-1-glycoprotein and its interactions with drugs. *Drug Metab Rev* 2001;33(2):161-235. doi: 10.1081/DMR-100104402 [published Online First: 2001/08/10]

106. Scott BJ, Bradwell AR, Schneider RE, et al. Propranolol binding to serum orosomucoid. *Lancet* 1979;1(8122):930. doi: 10.1016/s0140-6736(79)91415-6 [published Online First: 1979/04/28]

107. Tiula E, Elfving S. Serum protein binding of phenytoin, diazepam and propranolol in age-related decrease in renal function. *Ann Clin Res* 1987;19(3):163-9. [published Online First: 1987/01/01]

108. Bilello JA, Bilello PA, Prichard M, et al. Reduction of the in vitro activity of A77003, an inhibitor of human immunodeficiency virus protease, by human serum alpha 1 acid glycoprotein. *J Infect Dis* 1995;171(3):546-51. [published Online First: 1995/03/01]

109. Zhang X-Q, Schooley RT, Gerber JG. The Effect of Increasing α1-Acid Glycoprotein Concentration on the Antiviral Efficacy of Human Immunodeficiency Virus Protease Inhibitors. *The Journal of Infectious Diseases* 1999;180(6):1833-37. doi: 10.1086/315123

110. Koeppen BM, Stanton BA. Renal Physiology. 5th Edition ed. Philidelphia, PA: Elsevier Mosby 2013.

111. Deigner HP, Friedrich E, Sinn H, et al. Scavenging of lipid peroxidation products from oxidizing LDL by albumin alters the plasma half-life of a fraction of oxidized LDL particles. *Free Radic Res Commun* 1992;16(4):239-46. doi: 10.3109/10715769209049177 [published Online First: 1992/01/01]

112. Keller F, Maiga M, Neumayer HH, et al. Pharmacokinetic effects of altered plasma protein binding of drugs in renal disease. *Eur J Drug Metab Pharmacokinet* 1984;9(3):275-82. doi: 10.1007/bf03189651 [published Online First: 1984/07/01]

113. Gounden V, Vashisht R, Jialal I. Hypoalbuminemia. Trease Island, FL: StatPearls Publishing; 2021 [Available from: https://www.ncbi.nlm.nih.gov/books/NBK526080/2021.

114. Hall CL, Hardwicke J. Low molecular weight proteinuria. *Annu Rev Med* 1979;30:199-211. doi: 10.1146/annurev.me.30.020179.001215 [published Online First: 1979/01/01]

115. Murakami T, Kawakami H, Matsuyama S, et al. Asymptomatic low molecular weight proteinuria: studies in five patients. *Clin Nephrol* 1987;28(2):93-8. [published Online First: 1987/08/01]

116. Lazzara MJ, Deen WM. Model of albumin reabsorption in the proximal tubule. *American Journal of Physiology-Renal Physiology* 2007;292(1):F430-F39. doi: 10.1152/ajprenal.00010.2006

117. Ohlson M, Sörensson J, Lindström K, et al. Effects of filtration rate on the glomerular barrier and clearance of four differently shaped molecules. *American Journal of Physiology-Renal Physiology* 2001;281(1):F103-F13. doi: 10.1152/ajprenal.2001.281.1.F103

118. Perkins SJ, Kerckaert JP, Loucheux-Lefebvre MH. The shapes of biantennary and tri/tetraantennary alpha 1 acid glycoprotein by small-angle neutron and X-ray scattering. *Eur J Biochem* 1985;147(3):525-31. doi: 10.1111/j.0014-2956.1985.00525.x [published Online First: 1985/03/15]

119. Koshimura J, Narita T, Sasaki H, et al. Urinary excretion of transferrin and orosomucoid are increased after acute protein loading in healthy subjects. *Nephron Clin Pract* 2005;100(2):c33-7. doi: 10.1159/000085030 [published Online First: 2005/04/09]

120. Christensen EI, Birn H, Storm T, et al. Endocytic receptors in the renal proximal tubule. *Physiology (Bethesda)* 2012;27(4):223-36. doi: 10.1152/physiol.00022.2012 [published Online First: 2012/08/10]

121. Tencer J, Frick IM, Oquist BW, et al. Size-selectivity of the glomerular barrier to high molecular weight proteins: upper size limitations of shunt pathways. *Kidney Int* 1998;53(3):709-15. doi: 10.1046/j.1523-1755.1998.00797.x [published Online First: 1998/03/21]

122. Deen WM. What determines glomerular capillary permeability? *Journal of Clinical Investigation* 2004;114(10):1412–14. doi: https://doi.org/10.1172/JCI23577

123. Reiser J, Kriz W, Kretzler M, et al. The glomerular slit diaphragm is a modified adherens junction. *Journal of the American Society of Nephrology* 2000;11(1):1-8.

124. Olson JL, Rennke HG, Venkatachalam MA. Alterations in the charge and size selectivity barrier of the glomerular filter in aminonucleoside nephrosis in rats. *Lab Invest* 1981;44(3):271-9. [published Online First: 1981/03/01]

125. Abu Hamad R, Berman S, Hachmo Y, et al. Response of Renal Podocytes to Excessive Hydrostatic Pressure: a Pathophysiologic Cascade in a Malignant Hypertension Model. *Kidney and Blood Pressure Research* 2017;42(6):1104-18. doi: 10.1159/000485774

126. Miner JH. The glomerular basement membrane. *Exp Cell Res* 2012;318(9):973-8. doi: 10.1016/j.yexcr.2012.02.031 [published Online First: 2012/03/14]

127. Kanwar YS, Danesh FR, Chugh SS. Contribution of proteoglycans towards the integrated functions of renal glomerular capillaries: a historical perspective. *Am J Pathol* 2007;171(1):9-13. doi: 10.2353/ajpath.2007.070356 [published Online First: 2007/06/27]

128. Kubosawa H, Kondo Y. Reevaluation of anionic sites in the rat glomerular basement membrane. *Nephron* 1997;76(4):445-51. doi: 10.1159/000190227 [published Online First: 1997/01/01]

129. Miner JH. Glomerular basement membrane composition and the filtration barrier. *Pediatr Nephrol* 2011;26(9):1413-7. doi: 10.1007/s00467-011-1785-1 [published Online First: 2011/02/18]

130. Bohrer MP, Baylis C, Humes HD, et al. Permselectivity of the glomerular capillary wall. Facilitated filtration of circulating polycations. *J Clin Invest* 1978;61(1):72-8. doi: 10.1172/JCI108927 [published Online First: 1978/01/01]

131. Harvey SJ, Cunningham J, Rops A, et al. Disruption of glomerular basement membrane charge through podocyte-specific mutation of agrin does not alter glomerular permselectivity. *American Journal of Pathology* 2007;171:139-52.

132. Goldberg S, Harvey SJ, Cunningham J, et al. Glomerular filtration is normal in the absence of both agrin and perlecan-heparan sulfate from the glomerular basement membrane. *Nephrol Dial Transplant* 2009;24(7):2044-51. doi: 10.1093/ndt/gfn758 [published Online First: 2009/01/16]

133. van de Hoven MJ, Wijnhoven T, Li J-P, et al. Reduction of anionic sites in the glomerular basement membrane by heparanase does not lead to proteinuria. *Int Soc of Nephr* 2008;73:278-87.

134. Axelsson J, Sverrisson K, Rippe A, et al. Reduced diffusion of charge-modified, conformationally intact anionic Ficoll relative to neutral Ficoll across the rat glomerular filtration barrier in vivo. *Am J Physiol Renal Physiol* 2011;301(4):F708-12. doi: 10.1152/ajprenal.00183.2011 [published Online First: 2011/07/22]

135. Fridén V, Oveland E, Tenstad O, et al. The glomerular endothelial cell coat is essential for glomerular filtration. *Int Soc of Nephr* 2011;79:1322-30.

136. Raats CJ, Van Den Born J, Berden JH. Glomerular heparan sulfate alterations: mechanisms and relevance for proteinuria. *Kidney Int* 2000;57(2):385-400. doi: 10.1046/j.1523-1755.2000.00858.x [published Online First: 2000/01/29]

137. Tisher C.C., Madsen K.M. The Kidney Philadelphia, PA: Saunders 1991:3–75.

138. Predescu D, Predescu S, McQuistan T, et al. Transcytosis of α₁-acidic glycoprotein in the continuous microvascular endothelium. *Proceedings of the National Academy of Sciences* 1998;95(11):6175-80. doi: 10.1073/pnas.95.11.6175

139. JIANG H, GUAN G, ZHANG R, et al. Increased urinary excretion of orosomucoid is a risk predictor of diabetic nephropathy. *Nephrology* 2009;14(3):332-37. doi: 10.1111/j.1440-1797.2008.01053.x

140. Kreisberg JI, Venkatachalam M, Troyer D. Contractile properties of cultured glomerular mesangial cells. *Am J Physiol* 1985;249(4 Pt 2):F457-63. doi: 10.1152/ajprenal.1985.249.4.F457 [published Online First: 1985/10/01]

141. Kagami S. Involvement of glomerular renin-angiotensin system (RAS) activation in the development and progression of glomerular injury. *Clinical and experimental nephrology* 2012;16(2):214-20. doi: 10.1007/s10157-011-0568-0 [published Online First: 2011/12/02]

142. Qin Z, Hoh CK, Olson ES, et al. Molecular Imaging of the Glomerulus via Mesangial Cell Uptake of Radiolabeled Tilmanocept. *J Nucl Med* 2019;60(9):1325-32. doi: 10.2967/jnumed.118.223727 [published Online First: 2019/02/24]

143. Yuan W, Li G, Zeng M, et al. Modulation of the blood-brain barrier permeability by plasma glycoprotein orosomucoid. *Microvasc Res* 2010;80(1):148-57. doi: 10.1016/j.mvr.2010.03.011 [published Online First: 2010/04/07]

144. Hackett PH, Yarnell PR, Hill R, et al. High-Altitude Cerebral Edema Evaluated With Magnetic Resonance ImagingClinical Correlation and Pathophysiology. *JAMA* 1998;280(22):1920-25. doi: 10.1001/jama.280.22.1920

145. Swenson ER, Maggiorini M, Mongovin S, et al. Pathogenesis of High-Altitude Pulmonary EdemaInflammation Is Not an Etiologic Factor. *JAMA* 2002;287(17):2228-35. doi: 10.1001/jama.287.17.2228

146. Staub NC. Pulmonary edema due to increased microvascular permeability to fluid and protein. *Circ Res* 1978;43(2):143-51. doi: 10.1161/01.res.43.2.143 [published Online First: 1978/08/01]

147. Lewis DM, Bradwell AR, Shore AC, et al. Capillary filtration coefficient and urinary albumin leak at altitude. *European journal of clinical investigation* 1997;27(1):64-8,Coates G, Gray GW, Nahmias C, et al. High Altitude Physiology and Medicine. New York, NY: Springer 1982:pp 176-178.

148. Hansen JM, Olsen NV, Feldt-Rasmussen B, et al. Albuminuria and overall capillary permeability of albumin in acute altitude hypoxia. *Journal of applied physiology (Bethesda, Md : 1985)* 1994;76(5):1922-7.

149. Bradwell AR. Birmingham Medical Research Expeditionary Society 1977 Expedition: serum and urine proteins during a high altitude trek. *Postgrad Med J* 1979;55(645):478-82. doi: 10.1136/pgmj.55.645.478 [published Online First: 1979/07/01]

150. Rennie I, Joseph B. Urinary protein excretion in climbers at high altitude. *The Lancet* 1970;i:1247-51.

151. Chen W, Liu Q, Wang H, et al. Prevalence and risk factors of chronic kidney disease: a population study in the Tibetan population. *Nephrol Dial Transplant* 2011;26(5):1592-9. doi: 10.1093/ndt/gfq608 [published Online First: 2010/10/14]

152. Rennie D, Marticorena E, Monge C, et al. Urinary protein excretion in high-altitude residents. *J Appl Physiol* 1971;31(2):257-9. doi: 10.1152/jappl.1971.31.2.257 [published Online First: 1971/08/01]

153. Wada K, Mizuguchi Y, Wada Y, et al. Hyperlipidaemia, lack of sleep and smoking as risk factors for proteinuria among high altitude mountain trekkers. *Nephrology (Carlton)* 2006;11(2):131-6.

154. Urinary orosomucoid (alpha-1 acid glycoprotein) latex immunoassay is effective for the detection of increased proteinuria associated with altitude and sea-level exercise. . Europhysiology; 2018; London, UK. Proceedings Physiological Society.

155. Winterborn MH, Bradwell AR, Chesner IM, et al. The origin of proteinuria at high altitude. *Postgrad Med J* 1987;63(737):179-81.

156. Mogensen CE, Vittinghus E, Sølling K. Abnormal albumin excretion after two provocative renal tests in diabetes: physical exercise and lysine injection. *Kidney Int* 1979;16(3):385-93. doi: 10.1038/ki.1979.141 [published Online First: 1979/09/01]

157. Christiansen MS, Hommel E, Magid E. Orosomucoid in urine is a powerful predictor of cardiovascular mortality in normoalbuminuric patients with type 2 diabetes at five years of follow-up. *Diabetologia* 2005;48:386-93.

158. Coppel J, Hennis P, Gilbert-Kawai E, et al. The physiological effects of hypobaric hypoxia versus normobaric hypoxia: a systematic review of crossover trials. *Extreme Physiology & Medicine* 2015;4(1):2. doi: 10.1186/s13728-014-0021-6

159. Loeppky JA, Roach RC, Maes D, et al. Role of hypobaria in fluid balance response to hypoxia. *High Alt Med Biol* 2005;6(1):60-71. doi: 10.1089/ham.2005.6.60 [published Online First: 2005/03/18]

160. Palubiski LM, O'Halloran KD, O'Neill J. Renal Physiological Adaptation to High Altitude: A Systematic Review. *Frontiers in Physiology* 2020;11(756) doi: 10.3389/fphys.2020.00756

161. Dempsey JA, Forster HV, DoPico GA. Ventilatory acclimatization to moderate hypoxemia in man. The role of spinal fluid (H+). *J Clin Invest* 1974;53(4):1091-100. doi: 10.1172/jci107646 [published Online First: 1974/04/01]

162. Forster HV, Dempsey JA, Chosy LW. Incomplete compensation of CSF [H+] in man during acclimatization to high altitude (48300 M). *J Appl Physiol* 1975;38(6):1067-72. doi: 10.1152/jappl.1975.38.6.1067 [published Online First: 1975/06/01]

163. Severinghaus JW, Mitchell RA, Richardson BW, et al. Respiratory control at high altitude suggesting active transport regulation of CSF pH. *Journal of Applied Physiology* 1963;18(6):1155-66. doi: 10.1152/jappl.1963.18.6.1155

164. Goldfarb-Rumyantzev AS, Alper SL. Short-term responses of the kidney to high altitude in mountain climbers. *Nephrol Dial Transplant* 2014;29(3):497-506. doi: 10.1093/ndt/gft051 [published Online First: 2013/03/26]

165. Milledge JS. Acid-base changes associated with respiratory acclimatization to altitude. *Postgraduate medical journal* 1979;55(645):468-70. doi: 10.1136/pgmj.55.645.468

166. Poortmans JR, Vanderstraeten J. Kidney function during exercise in healthy and diseased humans. An update. *Sports Med* 1994;18(6):419-37. doi: 10.2165/00007256-199418060-00006 [published Online First: 1994/12/01]

167. Poortmans JR. Exercise and renal function. *Exerc Sport Sci Rev* 1977;5:255-94. [published Online First: 1977/01/01]

168. Pujar NS, Zydney AL. Electrostatic and electrokinetic interactions during protein transport through narrow pore membranes. *Engin Chem Res* 1994;33:2473-82.

169. Hausmann R, Kuppe C, Egger H, et al. Electrical forces determine glomerular permeability. *J Am Soc Nephrol* 2010;21(12):2053-8. doi: 10.1681/ASN.2010030303 [published Online First: 2010/10/16]

170. Vehaskari VM, Chang CT, Stevens JK, et al. The effects of polycations on vascular permeability in the rat. A proposed role for charge sites. *The Journal of clinical investigation* 1984;73(4):1053-61.

171. Vehaskari VM, Root ER, Germuth FG, Jr., et al. Glomerular charge and urinary protein excretion: Effects of systemic and intrarenal polycation infusion in the rat. *Kidney International* 1982;22(2):127-35. doi: 10.1038/ki.1982.144

172. Sörensson J, Ohlson M, Haraldsson B. A quantitative analysis of the glomerular charge barrier in the rat. *American Journal of Physiology-Renal Physiology* 2001;280(4):F646-F56. doi: 10.1152/ajprenal.2001.280.4.F646

173. Ciarimboli G, Schurek HJ, Zeh M, et al. Role of albumin and glomerular capillary wall charge distribution on glomerular permselectivity: studies on the perfused-fixed rat kidney model. *Pflugers Arch* 1999;438(6):883-91. [published Online First: 1999/12/11]

174. Singh MV, Salhan AK, Rawal SB, et al. Blood gases, hematology, and renal blood flow during prolonged mountain sojourns at 3500 and 5800 m. *Aviat Space Environ Med* 2003;74(5):533-6. [published Online First: 2003/05/20]

175. Winslow RM, Samaja M, West JB. Red cell function at extreme altitude on Mount Everest. *J Appl Physiol Respir Environ Exerc Physiol* 1984;56(1):109-16. doi: 10.1152/jappl.1984.56.1.109 [published Online First: 1984/01/01]

176. Joyce KE, Lucas SJE, Imray CHE, et al. Advances in the available non-biological pharmacotherapy prevention and treatment of acute mountain sickness and high altitude cerebral and pulmonary oedema. *Expert Opinion on Pharmacotherapy* 2018:1-12. doi: https://doi.org/10.1080/14656566.2018.1528228

177. Bärtsch P, Swenson ER. Acute high-altitude illnesses. *N Engl J Med* 2013;369(17):1666-7. doi: 10.1056/NEJMc1309747 [published Online First: 2013/10/25]

178. Cain SM, James E. Dunn I. Increase of arterial oxygen tension at altitude by carbonic anhydrase inhibition. *Journal of Applied Physiology* 1965;20(5):882-84. doi: 10.1152/jappl.1965.20.5.882

179. Leaf DE, Goldfarb DS. Mechanisms of action of acetazolamide in the prophylaxis and treatment of acute mountain sickness. *J Appl Physiol (1985)* 2007;102(4):1313-22. doi: 10.1152/japplphysiol.01572.2005 [published Online First: 2006/10/07]

180. Maren TH. Carbonic anhydrase: chemistry, physiology, and inhibition. *Physiological Reviews* 1967;47(4):595-781. doi: 10.1152/physrev.1967.47.4.595

181. Höhne C, Pickerodt PA, Francis RC, et al. Pulmonary vasodilation by acetazolamide during hypoxia is unrelated to carbonic anhydrase inhibition. *American Journal of Physiology-Lung Cellular and Molecular Physiology* 2007;292(1):L178-L84. doi: 10.1152/ajplung.00205.2006

182. Balanos GM, Teppema LJ, Steinback CD, et al. Acetazolamide reduces hypoxic pulmonary vasoconstriction in humans. *The FASEB Journal* 2006;20(5):LB31-LB31. doi: https://doi.org/10.1096/fasebj.20.5.LB31-b

183. Bradwell AR, Delamere JP. The effect of acetazolamide on the proteinuria of altitude. *Aviat Space Environ Med* 1982;53(1):40-3. [published Online First: 1982/01/01]

184. Wang C, Wang R, Xie H, et al. Effect of acetazolamide on cytokines in rats exposed to high altitude. *Cytokine* 2016;83:110-17. doi: 10.1016/j.cyto.2016.04.003 [published Online First: 2016/04/23]

185. Zambraski EJ, Bober MC, Goldstein JE, et al. Changes in renal conical sialic acids and colloidal iron staining associated with exercise. *Medicine and Science in Sports and Exercise* 1981;13:229-32.

186. Rennke HG, Denker BM, Rose BD. Renal pathophysiology: The essentials. . Philadelphia: Lippincott Williams & Wilkins 2007.

187. Poortmans JR. Exercise and renal function. *Sports Med* 1984;1(2):125-53. [published Online First: 1984/03/01]

188. Parati G, Bilo G, Faini A, et al. Changes in 24 h ambulatory blood pressure and effects of angiotensin II receptor blockade during acute and prolonged high-altitude exposure: a randomized clinical trial. *Eur Heart J* 2014;35(44):3113-22. doi: 10.1093/eurheartj/ehu275 [published Online First: 2014/08/28]

189. Hansen JM, Kanstrup IL, Richalet JP, et al. High altitude-induced albuminuria in normal man is enhanced by infusion of low-dose dopamine. *Scandinavian journal of clinical and laboratory investigation* 1996;56(4):367-72.

190. Hayashi K, Ozawa Y, Fujiwara K, et al. Role of actions of calcium antagonists on efferent arterioles--with special references to glomerular hypertension. *Am J Nephrol* 2003;23(4):229-44. doi: 10.1159/000072054 [published Online First: 2003/07/04]

191. Cantone A, Cerretelli P. Effect of training on proteinuria following muscular exercise. *International Zeitschift für Angewandte Physiologie und Arbeitsphysiologie* 1960;18:324-29,Taylor A. Some characteristics of exercise proteinuria. *Clin Sci* 1960;18:209-17.

192. Rostrup M. Catecholamines, hypoxia and high altitude. *Acta Physiol Scand* 1998;162(3):389-99. doi: 10.1046/j.1365-201X.1998.00335.x [published Online First: 1998/05/13]

193. Matovinović MS. Podocyte Injury in Glomerular Diseases. *EJIFCC* 2009;20(1):21-27.

194. Alexander JK, Grover RF. Mechanism of reduced cardiac stroke volume at high altitude. *Clin Cardiol* 1983;6(6):301-3. doi: 10.1002/clc.4960060612 [published Online First: 1983/06/01]

195. Wilson MH, Imray CH. The cerebral venous system and hypoxia. *J Appl Physiol (1985)* 2016;120(2):244-50. doi: 10.1152/japplphysiol.00327.2015 [published Online First: 2015/08/22]

196. Wilson MH, Imray CH, Hargens AR. The headache of high altitude and microgravity--similarities with clinical syndromes of cerebral venous hypertension. *High Alt Med Biol* 2011;12(4):379-86. doi: 10.1089/ham.2011.1026 [published Online First: 2011/11/18]

197. Lund U, Rippe A, Venturoli D, et al. Glomerular filtration rate dependence of sieving of albumin and some neutral proteins in rat kidneys. *Am J Physiol Renal Physiol* 2003;284:F1226-F34.

198. Xu F, Mao C, Liu Y, et al. Losartan chemistry and its effects via AT1 mechanisms in the kidney. *Curr Med Chem* 2009;16(28):3701-15. [published Online First: 2009/09/15]

199. Heeg JE, de Jong PE, van der Hem GK, et al. Reduction of proteinuria by angiotensin converting enzyme inhibition. *Kidney Int* 1987;32(1):78-83. doi: 10.1038/ki.1987.174 [published Online First: 1987/07/01]

200. Plata R, Cornejo A, Arratia C, et al. Angiotensin-converting-enzyme inhibition therapy in altitude polycythaemia: a prospective randomised trial. *Lancet (London, England)* 2002;359(9307):663-6.

201. Bilo G, Villafuerte FC, Faini A, et al. Ambulatory blood pressure in untreated and treated hypertensive patients at high altitude: the High Altitude Cardiovascular Research-Andes study. *Hypertension* 2015;65(6):1266-71.

202. Arestegui AH, Fuquay R, Sirota J, et al. High altitude renal syndrome (HARS). *Journal of the American Society of Nephrology : JASN* 2011;22(11):1963-8.

203. Deyneli O, Yavuz D, Velioglu A, et al. Effects of ACE inhibition and angiotensin II receptor blockade on glomerular basement membrane protein excretion and charge selectivity in type 2 diabetic patients. *J Renin Angiotensin Aldosterone Syst* 2006;7(2):98-103. doi: 10.3317/jraas.2006.016 [published Online First: 2006/11/04]

204. Parving HH, de Zeeuw D, Cooper ME, et al. ACE gene polymorphism and losartan treatment in type 2 diabetic patients with nephropathy. *J Am Soc Nephrol* 2008;19(4):771-9. doi: 10.1681/ASN.2007050582 [published Online First: 2008/01/18]

205. Bigham AW, M. K, F. L-V, et al. Angiotensin-converting enzyme genotype and arterial oxygen saturation at high altitude in Peruvian Quechua. *High Alt Med Biol* 2008;9(2):167-78.

206. Liljefors I, Piscator M, Risinger C. Exercise proteinuria in monozygotic and dizygotic twins. Biochemistry of Exercise. Basel: Karger 1969:333-39.

207. Deodhar SD, Cuppage FE, Gableman E. STUDIES ON THE MECHANISM OF EXPERIMENTAL PROTEINURIA INDUCED BY RENIN. *J Exp Med* 1964;120(4):677-90. doi: 10.1084/jem.120.4.677 [published Online First: 1964/10/01]

208. Segall L, Covic A, Goldsmith DJA. Direct renin inhibitors: the dawn of a new era, or just a variation on a theme? *Nephrology Dialysis Transplantation* 2007;22(9):2435-39. doi: 10.1093/ndt/gfm363

209. Keynes RJ, Smith GW, Slater JD, et al. Renin and aldosterone at high altitude in man. *J Endocrinol* 1982;92(1):131-40. doi: 10.1677/joe.0.0920131 [published Online First: 1982/01/01]

210. Krämer BK, Ritthaler T, Schweda F, et al. Effects of hypoxia on renin secretion and renal renin gene expression. *Kidney International* 1998;54:S155-S58. doi: https://doi.org/10.1046/j.1523-1755.1998.06732.x

211. Milledge JS, Beeley JM, McArthur S, et al. Atrial natriuretic peptide, altitude and acute mountain sickness. *Clin Sci (Lond)* 1989;77(5):509-14. doi: 10.1042/cs0770509 [published Online First: 1989/11/01]

212. Bärtsch P, Shaw S, Franciolli M, et al. Atrial natriuretic peptide in acute mountain sickness. *J Appl Physiol (1985)* 1988;65(5):1929-37. doi: 10.1152/jappl.1988.65.5.1929 [published Online First: 1988/11/01]

213. McMurray J, Seidelin PH, Howey JE, et al. The effect of atrial natriuretic factor on urinary albumin and beta 2-microglobulin excretion in man. *J Hypertens* 1988;6(10):783-6. [published Online First: 1988/10/01]

214. Axelsson J, Rippe A, Rippe B. Transient and sustained increases in glomerular permeability following ANP infusion in rats. *Am J Physiol Renal Physiol* 2011;300(1):F24-30. doi: 10.1152/ajprenal.00347.2010 [published Online First: 2010/10/15]

215. Curry F-RE. Atrial natriuretic peptide: an essential physiological regulator of transvascular fluid, protein transport, and plasma volume. *The Journal of clinical investigation* 2005;115(6):1458-61. doi: 10.1172/JCI25417

216. Malpas SC, Shweta A, Anderson WP, et al. Functional response to graded increases in renal nerve activity during hypoxia in conscious rabbits. *Am J Physiol* 1996;271(6 Pt 2):R1489-99. doi: 10.1152/ajpregu.1996.271.6.R1489 [published Online First: 1996/12/01]

217. Duplain H, Vollenweider L, Delabays A, et al. Augmented Sympathetic Activation During Short-Term Hypoxia and High-Altitude Exposure in Subjects Susceptible to High-Altitude Pulmonary Edema. *Circulation* 1999;99(13):1713-18. doi: doi:10.1161/01.CIR.99.13.1713

218. Siebenmann C, Robach P, Lundby C. Regulation of blood volume in lowlanders exposed to high altitude. *Journal of Applied Physiology* 2017;123(4):957-66. doi: 10.1152/japplphysiol.00118.2017

219. Simpson LO. Blood Viscosity Induced Proteinuria. *Nephron* 1984;36:280-81.

220. Simpson LO. A hypothesis proposing increased blood viscosity as a cause of proteinuria and increased vascular permeability. *Nephron* 1982;31(1):89-93. doi: 10.1159/000182623 [published Online First: 1982/01/01]

221. Kaysen GA, Myers BD, Couser WG, et al. Mechanisms and consequences of proteinuria. *Lab Invest* 1986;54(5):479-98. [published Online First: 1986/05/01]

222. Ferenbach DA, Bonventre JV. Kidney tubules: intertubular, vascular, and glomerular cross-talk. *Current opinion in nephrology and hypertension* 2016;25(3):194-202. doi: 10.1097/mnh.0000000000000218

223. Koçer G, Barcrali F, Kuru O, et al. The Renin–Angiotensin System, Not the Kinin–Kallikrein System, Affects Post-Exercise Proteinuria. *Nephron* 2018;139:299-304.

224. Masmura S, Mizuta K, Nakata K. Note on some urinary components in exercise proteinuria. Part 2. Quantitative analyses of urinary kininases and kinin-releasing enzymes. *Mie Medical Journal* 1970;20:105-12.

225. Klausen T, Olsen NV, Poulsen TD, et al. Hypoxemia increases serum interleukin-6 in humans. *European Journal of Applied Physiology and Occupational Physiology* 1997;76(5):480-82. doi: 10.1007/s004210050278

226. Lundeberg J, Feiner JR, Schober A, et al. Increased Cytokines at High Altitude: Lack of Effect of Ibuprofen on Acute Mountain Sickness, Physiological Variables, or Cytokine Levels. *High Alt Med Biol* 2018;19(3):249-58. doi: 10.1089/ham.2017.0144 [published Online First: 2018/06/21]

227. Hartmann G, Tschöp M, Fischer R, et al. HIGH ALTITUDE INCREASES CIRCULATING INTERLEUKIN-6, INTERLEUKIN-1 RECEPTOR ANTAGONIST AND C-REACTIVE PROTEIN. *Cytokine* 2000;12(3):246-52. doi: https://doi.org/10.1006/cyto.1999.0533

228. Molmenti EP, Ziambaras T, Perlmutter DH. Evidence for an acute phase response in human intestinal epithelial cells. *J Biol Chem* 1993;268(19):14116-24. [published Online First: 1993/07/05]

229. Burgess KR, Lucas SJE, Shepherd K, et al. Worsening of central sleep apnea at high altitude—a role for cerebrovascular function. *Journal of Applied Physiology* 2013;114(8):1021-28. doi: 10.1152/japplphysiol.01462.2012

230. Gozal D, Jortani S, Snow AB, et al. Two-dimensional differential in-gel electrophoresis proteomic approaches reveal urine candidate biomarkers in pediatric obstructive sleep apnea. *Am J Respir Crit Care Med* 2009;180(12):1253-61. doi: 10.1164/rccm.200905-0765OC [published Online First: 2009/10/03]

231. Lemos Vde A, dos Santos RV, Lira FS, et al. Can high altitude influence cytokines and sleep? *Mediators Inflamm* 2013;2013:279365. doi: 10.1155/2013/279365 [published Online First: 2013/05/22]

232. Nakuluri K, Mukhi D, Mungamuri SK, et al. Stabilization of hypoxia-inducible factor 1alpha by cobalt chloride impairs podocyte morphology and slit-diaphragm function. *J Cell Biochem* 2018 doi: 10.1002/jcb.28041 [published Online First: 2018/11/06]

233. Fournier C, Bouach N, Delafosse C, et al. Inducible expression and regulation of the alpha 1-acid glycoprotein gene by alveolar macrophages: prostaglandin E2 and cyclic AMP act as new positive stimuli. *J Immunol* 1999;163(5):2883-90.

234. Haase VH. Mechanisms of hypoxia responses in renal tissue. *J Am Soc Nephrol* 2013;24(4):537-41. doi: 10.1681/asn.2012080855 [published Online First: 2013/01/22]

235. Jefferson JA, Simoni J, Escudero E, et al. Increased Oxidative Stress Following Acute and Chronic High Altitude Exposure. *High Altitude Medicine & Biology* 2004;5(1):61-69. doi: 10.1089/152702904322963690

236. Dosek A, Ohno H, Acs Z, et al. High altitude and oxidative stress. *Respiratory Physiology & Neurobiology* 2007;158(2):128-31. doi: https://doi.org/10.1016/j.resp.2007.03.013

237. Raats CJ, Bakker MA, van den Born J, et al. Hydroxyl radicals depolymerize glomerular heparan sulfate in vitro and in experimental nephrotic syndrome. *J Biol Chem* 1997;272(42):26734-41. doi: 10.1074/jbc.272.42.26734 [published Online First: 1997/10/23]

238. Vilar RE, Ghael D, Li M, et al. Nitric oxide degradation of heparin and heparan sulphate. *Biochem J* 1997;324 (Pt 2):473-9. [published Online First: 1997/06/01]

239. Mohamed EI, Fahmi NM, El Kholy SM, et al. Effects of Reactive Oxygen Species on in vitro Filtration of Water and Albumin across Glomerular Basement Membrane. *Int J Biomed Sci* 2006;2(2):121-34. [published Online First: 2006/06/01]

240. Baillie JK, Bates MG, Thompson AA, et al. Endogenous urate production augments plasma antioxidant capacity in healthy lowland subjects exposed to high altitude. *Chest* 2007;131(5):1473-8. doi: 10.1378/chest.06-2235 [published Online First: 2007/05/15]

241. Hurtado A, Escudero E, Pando J, et al. Cardiovascular and renal effects of chronic exposure to high altitude. *Nephrol Dial Transplant* 2012;27 Suppl 4:iv11-6. doi: 10.1093/ndt/gfs427 [published Online First: 2013/01/04]

242. Jefferson JA, Escudero E, Hurtado ME, et al. Hyperuricemia, hypertension, and proteinuria associated with high-altitude polycythemia. *Am J Kidney Dis* 2002;39(6):1135-42. doi: 10.1053/ajkd.2002.33380 [published Online First: 2002/06/05]

243. Attia DM, Ni ZN, Boer P, et al. Proteinuria is preceded by decreased nitric oxide synthesis and prevented by a NO donor in cholesterol-fed rats. *Kidney Int* 2002;61(5):1776-87. doi: 10.1046/j.1523-1755.2002.00313.x [published Online First: 2002/04/23]

244. Levett DZ, Fernandez BO, Riley HL, et al. The role of nitrogen oxides in human adaptation to hypoxia. *Scientific Reports* 2011;1(1):109. doi: 10.1038/srep00109

245. Lei H, Sun Y, Luo Z, et al. Fatigue-induced Orosomucoid 1 Acts on C-C Chemokine Receptor Type 5 to Enhance Muscle Endurance. *Scientific Reports* 2016;6(1):18839. doi: 10.1038/srep18839

246. Qin Z, Wan J-J, Sun Y, et al. ORM Promotes Skeletal Muscle Glycogen Accumulation via CCR5-Activated AMPK Pathway in Mice. *Frontiers in Pharmacology* 2016;7(302) doi: 10.3389/fphar.2016.00302

247. Poortmans JR, Engels MF, Labilloy D, et al. The influence of the type of activity upon post-exercise proteinuria in man. *Medicine and Science in Sports and Exercise* 1982;14(118)

248. Poortmans JR, Brauman H, Staroukine M, et al. Indirect evidence of glomerular/tubular mixed-type postexercise proteinuria in healthy humans. *Am J Physiol* 1988;254(2 Pt 2):F277-83. doi: 10.1152/ajprenal.1988.254.2.F277 [published Online First: 1988/02/01]

249. Poortmans JR, Jeanloz RW. Quantitative Immunological Determination of 12 Plasma Proteins Excreted in Human Urine Collected before and after Exercise. *Journal of Clinical Investigation* 1968;47:386-93.

250. Gardner KD, Jr. THE EFFECT OF pH ON THE FILTRATION, REABSORPTION, AND EXCRETION OF PROTEIN BY THE RAT KIDNEY. *The Journal of Clinical Investigation* 1961;40(3):525-35. doi: 10.1172/JCI104280

251. Fisher M. NEPHRITIS: An Experimental and Critical Study of Its Nature, Cause and the Principles of Its Relief. *Archives of Internal Medicine* 1912;IX(5):637-40. doi: 10.1001/archinte.1912.00060170114008

252. Tomino Y, Inoue W, Watanabe S, et al. Detection of glomerular sialic acids in patients with diabetic nephropathy. *Am J Nephrol* 1988;8(1):21-6. doi: 10.1159/000167548 [published Online First: 1988/01/01]

253. Hartley LH, Mason JW, Hogan RP, et al. Multiple hormonal responses to prolonged exercise in relation to physical training. *Journal of Applied Physiology* 1972;33(5):607-10. doi: 10.1152/jappl.1972.33.5.607

254. Staessen J, Fagard R, Hespel P, et al. Plasma renin system during exercise in normal men. *J Appl Physiol (1985)* 1987;63(1):188-94. doi: 10.1152/jappl.1987.63.1.188 [published Online First: 1987/07/01]

255. Olsen NV. Effect of hypoxaemia on water and sodium homeostatic hormones and renal function. *Acta Anaesthesiol Scand Suppl* 1995;107:165-70. doi: 10.1111/j.1399-6576.1995.tb04352.x [published Online First: 1995/01/01]

256. Huang Y, Border WA, Noble NA. Functional renin receptors in renal mesangial cells. *Current Hypertension Reports* 2007;9(2):133-39. doi: 10.1007/s11906-007-0024-4

257. van den Hoven MJ, Waanders F, Rops AL, et al. Regulation of glomerular heparanase expression by aldosterone, angiotensin II and reactive oxygen species. *Nephrol Dial Transplant* 2009;24(9):2637-45. doi: 10.1093/ndt/gfp182 [published Online First: 2009/05/12]

258. Cosenzi A, Carraro M, Sacerdote A, et al. Involvement of the renin angiotensin system in the pathogenesis of postexercise proteinuria. *Scand J Urol Nephrol* 1993;27(3):301-4. doi: 10.3109/00365599309180438 [published Online First: 1993/01/01]

259. Gündüz F, Kuru O, Sentürk UK. Angiotensin II inhibition attenuates postexercise proteinuria in rats. *Int J Sports Med* 2005;26(9):710-3. doi: 10.1055/s-2004-830559 [published Online First: 2005/10/21]

260. Paeng J, Park J, Um JE, et al. The locally activated renin-angiotensin system is involved in albumin permeability in glomerular endothelial cells under high glucose conditions. *Nephrol Dial Transplant* 2017;32(1):61-72. doi: 10.1093/ndt/gfw089 [published Online First: 2016/07/01]

261. Kone BC, Baylis C. Biosynthesis and homeostatic roles of nitric oxide in the normal kidney. *American Journal of Physiology-Renal Physiology* 1997;272(5):F561-F78. doi: 10.1152/ajprenal.1997.272.5.F561

262. Symons JD, Stebbins CL, Musch TI. Interactions between angiotensin II and nitric oxide during exercise in normal and heart failure rats. *J Appl Physiol (1985)* 1999;87(2):574-81. doi: 10.1152/jappl.1999.87.2.574 [published Online First: 1999/08/13]

263. Gündüz F, Kuru O, Sentürk UK. Effect of nitric oxide on exercise-induced proteinuria in rats. *J Appl Physiol (1985)* 2003;95(5):1867-72. doi: 10.1152/japplphysiol.00599.2003 [published Online First: 2003/07/23]

264. Mittleman KD, Zambraski EJ. Exercise-induced proteinuria is attenuated by indomethacin. *Med Sci Sports Exerc* 1992;24(10):1069-74. [published Online First: 1992/10/01]

265. Farquhar WB, Kenney WL. Age and renal prostaglandin inhibition during exercise and heat stress. *Journal of Applied Physiology* 1999;86(6):1936-43. doi: 10.1152/jappl.1999.86.6.1936

266. Srivastava T, McCarthy ET, Sharma R, et al. Prostaglandin E(2) is crucial in the response of podocytes to fluid flow shear stress. *J Cell Commun Signal* 2010;4(2):79-90. doi: 10.1007/s12079-010-0088-9 [published Online First: 2010/04/08]

267. McCarthy ET, Sharma M. Indomethacin protects permeability barrier from focal segmental glomerulosclerosis serum. *Kidney Int* 2002;61(2):534-41. doi: 10.1046/j.1523-1755.2002.00172.x [published Online First: 2002/02/19]

268. Dempsey JA, Hanson PG, Henderson KS. Exercise-induced arterial hypoxaemia in healthy human subjects at sea level. *The Journal of physiology* 1984;355:161-75. doi: 10.1113/jphysiol.1984.sp015412

269. Powers SK, Deminice R, Ozdemir M, et al. Exercise-induced oxidative stress: Friend or foe? *Journal of Sport and Health Science* 2020;9(5):415-25. doi: https://doi.org/10.1016/j.jshs.2020.04.001

270. Singh A, Ramnath RD, Foster RR, et al. Reactive oxygen species modulate the barrier function of the human glomerular endothelial glycocalyx. *PLoS One* 2013;8(2):e55852. doi: 10.1371/journal.pone.0055852 [published Online First: 2013/03/05]

271. Schrijvers BF, Flyvbjerg A, De Vriese AS. The role of vascular endothelial growth factor (VEGF) in renal pathophysiology. *Kidney Int* 2004;65(6):2003-17. doi: 10.1111/j.1523-1755.2004.00621.x [published Online First: 2004/05/20]

272. Sharma R, Suzuki K, Nagase H, et al. Matrix metalloproteinase (stromelysin-1) increases the albumin permeability of isolated rat glomeruli. *J Lab Clin Med* 1996;128(3):297-303. doi: 10.1016/s0022-2143(96)90031-1 [published Online First: 1996/09/01]

273. Wu D, Cao W, Xiang D, et al. Exercise induces tissue hypoxia and HIF-1α redistribution in the small intestine. *Journal of sport and health science* 2020;9(1):82-89. doi: 10.1016/j.jshs.2019.05.002 [published Online First: 2019/05/09]

274. Roberts WG, Palade GE. Increased microvascular permeability and endothelial fenestration induced by vascular endothelial growth factor. *J Cell Sci* 1995;108 (Pt 6):2369-79. [published Online First: 1995/06/01]

275. Eremina V, Sood M, Haigh J, et al. Glomerular-specific alterations of VEGF-A expression lead to distinct congenital and acquired renal diseases. *J Clin Invest* 2003;111(5):707-16. doi: 10.1172/jci17423 [published Online First: 2003/03/06]

276. Onions KL, Gamez M, Buckner NR, et al. VEGFC Reduces Glomerular Albumin Permeability and Protects Against Alterations in VEGF Receptor Expression in Diabetic Nephropathy. *Diabetes* 2019;68(1):172. doi: 10.2337/db18-0045

277. Satchell SC, Braet F. Glomerular endothelial cell fenestrations: an integral component of the glomerular filtration barrier. *American journal of physiology Renal physiology* 2009;296(5):F947-F56. doi: 10.1152/ajprenal.90601.2008 [published Online First: 2009/01/07]

278. Szirmay B, Tarnok A, Sarlos P, et al. Elevated urinary orosomucoid excretion as a novel biomarker in Crohn's disease. *Eur J Clin Invest* 2019;49(3):e13054. doi: 10.1111/eci.13054 [published Online First: 2018/11/20]

279. Li F, Yu Z, Chen P, et al. The increased excretion of urinary orosomucoid 1 as a useful biomarker for bladder cancer. *Am J Cancer Res* 2016;6(2):331-40.

280. Christiansen MS, Hesse D, Ekbom P, et al. Increased urinary orosomucoid excretion predicts preeclampsia in pregnant women with pregestational type 1 diabetes. *Diabetes Res Clin Pract* 2010;89(1):16-21. doi: 10.1016/j.diabres.2010.03.018 [published Online First: 2010/04/16]

281. Kustan P, Szirmay B, Horvath-Szalai Z, et al. Urinary orosomucoid: a novel, early biomarker of sepsis with promising diagnostic performance. *Clin Chem Lab Med* 2017;55(2):299-307. doi: 10.1515/cclm-2016-0840 [published Online First: 2016/11/07]

282. Hou L, Li F, Zeng Q, et al. Excretion of Urinary Orosomucoid 1 Protein Is Elevated in Patients with Chronic Heart Failure. *PLoS ONE* 2014;9(9)

283. Vittinghus E. Preanalytical handling of stored urine samples, and measurement of β2-microglobulin, orosomucoid, albumin, transferrin and immunoglobulin G in urine by enzyme-linked immunosorbent assays (ELISA). *Scand J Clin Lab Invest* 1990;50(8):843-49.

284. Khalaf AN, Bocker J, Kerp L, et al. Urine screening in outdoor volunteers: day versus night versus 24 hour collection. *Eur J Clin Chem Clin Biochem* 1991;29(3):185-8. [published Online First: 1991/03/01]

285. Jerebstova M, Saraf SL, Soni S, et al. Urinary orosomucoid is associated with progressive chronic kidney disease stage in patients with sickle cell anemia. *Am J Hematology* 2018;93(4):E107-E09.

286. Cahen R, Francois B, Sabot JF, et al. [Comparative study of urine immunoelectrophoresis and 4 indexes of glomerular selectivity in chronic glomerulopathies]. *Pathol Biol (Paris)* 1985;33(1):23-6. [published Online First: 1985/01/01]

287. Sviridov D, Owen WE, Roberts WL, et al. Proteinuria without albuminuria: urinary protein excretion by a subset of patients with burn injuries. *Clin Chim Acta* 2009;403(1-2):42-46. doi: 10.1016/j.cca.2009.01.012 [published Online First: 2009/04/14]

288. Christiansen MS, Blirup-Jensen S, Foged L, et al. A particle-enhanced turbidimetric immunoassay for quantitative determination of orosomucoid in urine: development, validation and reference values. *Clin Chem Lab Med* 2004;42(10):1168-77. doi: 10.1515/CCLM.2004.237 [published Online First: 2004/11/24]

289. Newman DJ, Henneberry H, Price CP. Particle enhanced light scattering immunoassay. *Ann Clin Biochem* 1992;29 (Pt 1):22-42. doi: 10.1177/000456329202900104 [published Online First: 1992/01/01]

290. Price CP, Spencer K, Whicher J. Light-scattering immunoassay of specific proteins: a review. *Ann Clin Biochem* 1983;20 Pt 1:1-14. doi: 10.1177/000456328302000101 [published Online First: 1983/01/01]

291. Freund J. The Agglutination of Tubercle Bacilli. *American Review of Tuberculosis* 1925;12(2):pp. 124–41.

292. Gavin JJ. Microbiological process report. Analytical microbiology. I. The test organism. *Appl Microbiol* 1956;4(6):323-31. [published Online First: 1956/11/01]

293. Class 2 Device Recall N PROT STANDARD SL. In: Services USDoHH, ed. Marburg Germany CSL Behring GmbH, 2017.

294. ISO Guide 34 for the production of reference materials. Certificate of Analysis for ERM - DA70k/IFCC: Joint Research Centre - Institute for Reference Materials and Measurements, 2015.

295. Armbruster DA, Pry T. Limit of blank, limit of detection and limit of quantitation. *Clin Biochem Rev* 2008;29 Suppl 1(Suppl 1):S49-52. [published Online First: 2008/10/15]

296. CLSI Approved Guideline EP17-A2. Evaluation Of Detection Capability For Clinical Laboratory Measurement Procedures; Approved Guideline *Clinical and Laboratory Standards Institute* 2012;32(8)

297. Tencer J, Thysell H, Andersson K, et al. Stability of albumin, protein HC, immunoglobulin G, kappa- and lambda-chain immunoreactivity, orosomucoid and alpha 1-antitrypsin in urine stored at various conditions. *Scand J Clin Lab Invest* 1994;54(3):199-206. doi: 10.1080/00365519409088425 [published Online First: 1994/05/01]

298. NCCLS Approved Guideline EP5-A. Evaluation of Precision Performance of Clinical Chemistry Devices. Wayne, PA1999.

299. Chesher D. Evaluating assay precision. *The Clinical biochemist Reviews* 2008;29 Suppl 1(Suppl 1):S23-S26.

300. Westgard JO, Burnett RW. Precision requirements for cost-effective operation of analytical processes. *Clinical Chemistry* 1990;36(9):1629-32. doi: 10.1093/clinchem/36.9.1629

301. CLSI Approved Guideline EP6-A. Evaluation of the Linearity of Quantitative Measurement Procedures: A Statistical Approach. *Clinical and Laboratory Standards Institute* 2003;23(29)

302. Glick MR, Ryder KW, Jackson SA. Graphical comparisons of interferences in clinical chemistry instrumentation. *Clinical Chemistry* 1986;32(3):470-75. doi: 10.1093/clinchem/32.3.470

303. Dimeski G. Interference testing. *The Clinical biochemist Reviews* 2008;29 Suppl 1(Suppl 1):S43-S48.

304. Preissner CM, Dodge LA, O'Kane DJ, et al. Prevalence of Heterophilic Antibody Interference in Eight Automated Tumor Marker Immunoassays. *Clinical Chemistry* 2005;51(1):208-10. doi: 10.1373/clinchem.2004.040501

305. CLSI Approved Guideline EP25-A. CLSI Approved Guideline EP17-A2. Evaluation Of Detection Capability For Clinical Laboratory Measurement Procedures; Approved Guideline. . *Clinical and Laboratory Standards Institute* 2009;29(20)

306. NCCLS Approved Guideline EP9-A2. Method Comparison and Bias Estimation Using Patient Samples. 2002

307. Grubbs FE. Procedures for Detecting Outlying Observations in Samples. *Technometrics* 1969;11(1):1-21. doi: 10.1080/00401706.1969.10490657

308. OECD. Testing and Assessment2018:131.

309. Altman DG, Bland JM. Measurement in Medicine: The Analysis of Method Comparison Studies. *Journal of the Royal Statistical Society Series D (The Statistician)* 1983;32(3):307-17. doi: 10.2307/2987937

310. Bland J, Altman D. Comparing methods of measurement: why plotting difference against standard method is misleading. *Lancet* 1995;346:1085–87.

311. Chhapola V, Kanwal SK, Brar R. Reporting standards for Bland-Altman agreement analysis in laboratory research: a cross-sectional survey of current practice. *Ann Clin Biochem* 2015;52(Pt 3):382-6. doi: 10.1177/0004563214553438 [published Online First: 2014/09/13]

312. Chan JF, Yuan S, Kok KH, et al. A familial cluster of pneumonia associated with the 2019 novel coronavirus indicating person-to-person transmission: a study of a family cluster. *Lancet* 2020;395(10223):514-23. doi: 10.1016/s0140-6736(20)30154-9 [published Online First: 2020/01/28]

313. Gottschalk PG, Dunn JR. The five-parameter logistic: a characterization and comparison with the four-parameter logistic. *Anal Biochem* 2005;343(1):54-65. doi: 10.1016/j.ab.2005.04.035 [published Online First: 2005/06/15]

314. Magnusson B, Örnemark U. Eurachem Guide: The Fitness for Purpose of Analytical Methods – A Laboratory Guide to Method Validation and Related Topics. . 2nd ed ed: Eurachem 2014.

315. NCCLS Proposed Guideline EP6-P. Evaluation of the linearity of quantitative analytical methods. Wayne, PA1986.

316. NCCLS Approved Guideline EP15-A. User demonstration of performance for precision and accuracy. Wayne, PA2000.

317. NCCLS Approved Guideline EP9-A. Method comparison and bias estimation using patient samples. Wayne, PA1995.

318. Andreasson U, Perret-Liaudet A, van Waalwijk van Doorn LJ, et al. A Practical Guide to Immunoassay Method Validation. *Front Neurol* 2015;6:179. doi: 10.3389/fneur.2015.00179 [published Online First: 2015/09/09]

319. Schiettecatte J, Anckaert E, Smitz J. Interferences in Immunoassays2012.

320. Tate J, Ward G. Interferences in immunoassay. *The Clinical biochemist Reviews* 2004;25(2):105-20.

321. Bouatra S, Aziat F, Mandal R, et al. The human urine metabolome. *PLoS One* 2013;8(9):e73076. doi: 10.1371/journal.pone.0073076 [published Online First: 2013/09/12]

322. Medicine ABoI. ABIM Laboratory Test Reference Ranges 2020.

323. Hoppin JA, Ulmer R, Calafat AM, et al. Impact of urine preservation methods and duration of storage on measured levels of environmental contaminants. *Journal of Exposure Science & Environmental Epidemiology* 2006;16(1):39-48. doi: 10.1038/sj.jea.7500435

324. Hogan MC, Lieske JC, Lienczewski CC, et al. Strategy and rationale for urine collection protocols employed in the NEPTUNE study. *BMC Nephrol* 2015;16:190. doi: 10.1186/s12882-015-0185-3 [published Online First: 2015/11/19]

325. Feres MC, Bini R, De Martino MC, et al. Implications for the use of acid preservatives in 24-hour urine for measurements of high demand biochemical analytes in clinical laboratories. *Clin Chim Acta* 2011;412(23-24):2322-5. doi: 10.1016/j.cca.2011.08.033 [published Online First: 2011/09/14]

326. Neims AH. Clinical Pharmacology & Therapeutics. . London: Palgrave Macmillan 1980.

327. Taylor TP, Janech MG, Slate EH, et al. Overcoming the effects of matrix interference in the measurement of urine protein analytes. *Biomark Insights* 2012;7:1-8. doi: 10.4137/BMI.S8703 [published Online First: 2012/02/01]

328. Holland M, Kraght P, Akbas N, et al. Improved Statistical Methods for Evaluation of Stability of In Vitro Diagnostic Reagents. *Statistics in Biopharmaceutical Research* 2017;9(3):272-78. doi: 10.1080/19466315.2017.1305287

329. Tencer J, Thysell H, Andersson K, et al. Long-term Stability of Albumin, Protein HC, Immunoglobulin G, κ- and λ-chainimmunoreactivity, Orosomucoid and α1-antitrypsin in Urine Stored at -20°C. *Scandanavian Journal of Urology and Nephrology* 1997;31(1):67-71.

330. Christiansen MS, Iversen K, Larsen CT, et al. Increased urinary orosomucoid excretion: a proposed marker for inflammation and endothelial dysfunction in patients with type 2 diabetes. *Scand J Clin Lab Invest* 2009;69(2):272-81. doi: 10.1080/00365510802531100 [published Online First: 2008/10/31]

331. Devarajan P, Krawczeski CD, Nguyen MT, et al. Proteomic identification of early biomarkers of acute kidney injury after cardiac surgery in children. *Am J Kidney Dis* 2010;56(4):632-42. doi: 10.1053/j.ajkd.2010.04.014 [published Online First: 2010/07/06]

332. Haj-Ahmad TA, Abdalla MAK, Haj-Ahmad Y. Potential Urinary Protein Biomarker Candidates for the Accurate Detection of Prostate Cancer among Benign Prostatic Hyperplasia Patients. *Journal of Cancer* 2014;5(2):103-14.

333. Kentsis A, Lin YY, Kurek K, et al. Discovery and validation of urine markers of acute pediatric appendicitis using high-accuracy mass spectrometry. *Ann Emerg Med* 2010;55(1):62-70.e4. doi: 10.1016/j.annemergmed.2009.04.020 [published Online First: 2009/06/27]

334. Christiansen MS, Hommel E, Magid E, et al. Orosomucoid in urine is a powerful predictor of cardiovascular mortality in normoalbuminuric patients with type 2 diabetes at five years of follow-up. *Diabetologia* 2005;48(2):386-93. doi: 10.1007/s00125-004-1630-1 [published Online First: 2005/01/13]

335. Joyce KE, Delamere J, Bradwell S, et al. Hypoxia is not the primary mechanism contributing to exercise-induced proteinuria. *BMJ Open Sport & Exercise Medicine* 2020;6(1):e000662. doi: 10.1136/bmjsem-2019-000662

336. Bernard A, Buchet JP, Roels H, et al. Renal excretion of proteins and enzymes in workers exposed to cadmium. *Eur J Clin Invest* 1979;9(1):11-22. doi: 10.1111/j.1365-2362.1979.tb01662.x [published Online First: 1979/02/01]

337. Tencer J, Thysell H, Grubb A. Analysis of proteinuria: reference limits for urine excretion of albumin, protein HC, immunoglobulin G, k- and Δ-immunoreactivity, orosomucoid and α1-antitrypsin. *Scandinavian Journal of Clinical and Laboratory Investigation* 1996;56(8):691-700. doi: 10.3109/00365519609088816

338. Wilson DW, Long WL, Thompson HC, et al. Changes in the composition of the urine after muscular exercise. *Proceedings of the Society for Experimental Biology and Medicine* 1924;21(8):425-26. doi: 10.3181/00379727-21-214

339. Bunjevac A, Gabaj NN, Miler M, et al. Preanalytics of urine sediment examination: effect of relative centrifugal force, tube type, volume of sample and supernatant removal. *Biochem Med (Zagreb)* 2018;28(1):010707. doi: 10.11613/bm.2018.010707 [published Online First: 2018/02/24]

340. O'brien RM. A Caution Regarding Rules of Thumb for Variance Inflation Factors. *Quality & quantity* 2007;41(5):673-90. doi: 10.1007/s11135-006-9018-6

341. Moher D, Liberati A, Tetzlaff J, et al. Preferred Reporting Items for Systematic Reviews and Meta-Analyses: The PRISMA Statement. *PLOS Medicine* 2009;6(7):e1000097. doi: 10.1371/journal.pmed.1000097

342. Higgins JPT, Thomas J, Chandler J, et al. Cochrane Handbook for Systematic Reviews of Interventions. v6.1 ed2020.

343. Hozo SP, Djulbegovic B, Hozo I. Estimating the mean and variance from the median, range, and the size of a sample. *BMC Medical Research Methodology* 2005;5(1):13. doi: 10.1186/1471-2288-5-13

344. Wan X, Wang W, Liu J, et al. Estimating the sample mean and standard deviation from the sample size, median, range and/or interquartile range. *BMC Medical Research Methodology* 2014;14(1):135. doi: 10.1186/1471-2288-14-135

345. Mu AK, Lim BK, Hashim OH, et al. Detection of differential levels of proteins in the urine of patients with endometrial cancer: analysis using two-dimensional gel electrophoresis and o-glycan binding lectin. *Int J Mol Sci* 2012;13(8):9489-501. doi: 10.3390/ijms13089489 [published Online First: 2012/09/06]

346. Bonde JP, Vittinghus E. Urinary excretion of proteins among metal welders. *Hum Exp Toxicol* 1996;15(1):1-4. doi: 10.1177/096032719601500101 [published Online First: 1996/01/01]

347. Phillips A, Rowell FJ. A competitive enzyme-linked immunosorbent assay for alpha 1-acid glycoprotein in serum and urine samples. *Clin Chem* 1988;34(8):1569-71. [published Online First: 1988/08/01]

348. Hjorth L, Helin I, Grubb A. Age-related reference limits for urine levels of albumin, orosomucoid, immunoglobulin G and protein HC in children. *Scand J Clin Lab Invest* 2000;60(1):65-73. [published Online First: 2000/04/11]

349. Selvaraju V, Ayine P, Fadamiro M, et al. Urinary Biomarkers of Inflammation and Oxidative Stress Are Elevated in Obese Children and Correlate with a Marker of Endothelial Dysfunction. *Oxidative Medicine and Cellular Longevity* 2019;2019:9604740. doi: 10.1155/2019/9604740

350. Smith EMD, Lewandowski LB, Jorgensen AL, et al. Growing international evidence for urinary biomarker panels identifying lupus nephritis in children - verification within the South African Paediatric Lupus Cohort. *Lupus* 2018;27(14):2190-99. doi: 10.1177/0961203318808376 [published Online First: 2018/10/24]

351. El-Beblawy NM, Andrawes NG, Ismail EA, et al. Serum and Urinary Orosomucoid in Young Patients With Type 1 Diabetes: A Link Between Inflammation, Microvascular Complications, and Subclinical Atherosclerosis. *Clin Appl Thromb Hemost* 2016;22(8):718-26. doi: 10.1177/1076029616637185 [published Online First: 2016/03/16]

352. Watson L, Midgley A, Pilkington C, et al. Urinary monocyte chemoattractant protein 1 and alpha 1 acid glycoprotein as biomarkers of renal disease activity in juvenile-onset systemic lupus erythematosus. *Lupus* 2012;21(5):496-501. doi: 10.1177/0961203311431249 [published Online First: 2011/12/08]

353. Jensen H, Henriksen K. PROTEINURIA IN NON-RENAL INFECTIOUS DISEASES. *Acta Medica Scandinavica* 1974;196(1 - 6):75-82. doi: https://doi.org/10.1111/j.0954-6820.1974.tb00971.x

354. Poortmans JR, Haralambie G. Biochemical changes in a 100 km run: Proteins in serum and urine. *European Journal of Applied Physiology and Occupational Physiology* 1979;40(4):245-54. doi: 10.1007/BF00421516

355. Ito S, Tsuda A, Momotsu T, et al. Urinary orosomucoid excretion rate in patients with non-insulin-dependent diabetes mellitus. *Acta Endocrinol (Copenh)* 1989;120(5):584-90. doi: 10.1530/acta.0.1200584 [published Online First: 1989/05/01]

356. Kustán P, Szirmay B, Kőszegi T, et al. Monitoring urinary orosomucoid in patients undergoing cardiac surgery: A promising novel inflammatory marker. *Clin Biochem* 2017;50(18):1002-06. doi: 10.1016/j.clinbiochem.2017.07.010 [published Online First: 2017/07/25]

357. Vasson MP, Baguet JC, Arveiller MR, et al. Serum and urinary alpha-1 acid glycoprotein in chronic renal failure. *Nephron* 1993;65(2):299-303. doi: 10.1159/000187492 [published Online First: 1993/01/01]

358. Narita T, Sasaki H, Hosoba M, et al. Parallel increase in urinary excretion rates of immunoglobulin G, ceruloplasmin, transferrin, and orosomucoid in normoalbuminuric type 2 diabetic patients. *Diabetes Care* 2004;27(5):1176-81. doi: 10.2337/diacare.27.5.1176 [published Online First: 2004/04/28]

359. Christiansen MS, Hommel E, Friberg L, et al. Increased urinary orosomucoid excretion is not related to impaired renal function in patients with type 2 diabetes. *Journal of Diabetes and Its Complcations* 2010;24:28-36.

360. Wang H, Bao X, Ma Y, et al. Urinary orosomucoid 1 protein to creatinine ratio as a potential biomarker for early screening of kidney impairment in type-2 diabetes patients. *Nephrology (Carlton)* 2020 doi: 10.1111/nep.13707 [published Online First: 2020/03/10]

361. Magid E, Guldager H, Hesse D, et al. Monitoring urinary orosomucoid in acute inflammation: observations on urinary excretion of orosomucoid, albumin, alpha1-microglobulin, and IgG. *Clin Chem* 2005;51(11):2052-8. doi: 10.1373/clinchem.2005.055442 [published Online First: 2005/09/17]

362. Prescott E, Hjardem-Hansen R, Dela F, et al. Exercise training in older patients with systolic heart failure: adherence, exercise capacity, inflammation and glycemic control. *Scand Cardiovasc J* 2009;43(4):249-55. doi: 10.1080/14017430802593427 [published Online First: 2008/12/23]

363. Németh B, Péter I, Boncz I, et al. Urinary orosomucoid: a new marker of cardiovascular risk in psoriatic patients? *Ther Clin Risk Manag* 2019;15:831-37. doi: 10.2147/tcrm.S197633 [published Online First: 2019/07/17]

364. Schlatzer D, Maahs DM, Chance MR, et al. Novel urinary protein biomarkers predicting the development of microalbuminuria and renal function decline in type 1 diabetes. *Diabetes care* 2012;35(3):549-55. doi: 10.2337/dc11-1491 [published Online First: 2012/01/11]

365. Christiansen MS, Hommel E, Magid E, et al. Orosomucoid in urine predicts cardiovascular and over-all mortality in patients with Type II diabetes. *Diabetologia* 2002;45(1):115-20. doi: 10.1007/s125-002-8251-3

366. Inoue K, Wada J, Eguchi J, et al. Urinary fetuin-A is a novel marker for diabetic nephropathy in type 2 diabetes identified by lectin microarray. *PLoS One* 2013;8(10):e77118. doi: 10.1371/journal.pone.0077118 [published Online First: 2013/10/22]

367. Zhan Z, Guan Y, Mew K, et al. Urine α-fetoprotein and orosomucoid 1 as biomarkers of hepatitis B virus-associated hepatocellular carcinoma. *American Journal of Physiology-Gastrointestinal and Liver Physiology* 2020;318(2):G305-G12. doi: 10.1152/ajpgi.00267.2019

368. Milani L, Gatta A, Merkel C, et al. Proteinuria in patients with cirrhosis: relationship between renal and hepatic function. *Clin Sci (Lond)* 1982;63(4):387-92. doi: 10.1042/cs0630387 [published Online First: 1982/10/01]

369. Jerebtsova M, Taye A, Smith N, et al. Association between plasma and urinary orosomucoid and chronic kidney disease in adults with sickle cell disease. *Brit J Haematol* 2020;190(1):e45-e48. doi: https://doi.org/10.1111/bjh.16702

370. Suzuki M, Wiers K, Brooks EB, et al. Initial validation of a novel protein biomarker panel for active pediatric lupus nephritis. *Pediatr Res* 2009;65(5):530-6. doi: 10.1203/PDR.0b013e31819e4305 [published Online First: 2009/02/17]

371. Brunner HI, Bennett MR, Gulati G, et al. Urine Biomarkers to Predict Response to Lupus Nephritis Therapy in Children and Young Adults. *The Journal of Rheumatology* 2017;44(8):1239. doi: 10.3899/jrheum.161128

372. Bennett MR, Pleasant L, Haffner C, et al. A Novel Biomarker Panel to Identify Steroid Resistance in Childhood Idiopathic Nephrotic Syndrome. *Biomark Insights* 2017;12:1177271917695832-32. doi: 10.1177/1177271917695832

373. Scherzer R, Lin H, Abraham A, et al. Use of urine biomarker-derived clusters to predict the risk of chronic kidney disease and all-cause mortality in HIV-infected women. *Nephrol Dial Transplant* 2016;31(9):1478-85. doi: 10.1093/ndt/gfv426 [published Online First: 2016/01/13]

374. Nickolas TL, O'Rourke MJ, Yang J, et al. Sensitivity and specificity of a single emergency department measurement of urinary neutrophil gelatinase-associated lipocalin for diagnosing acute kidney injury. *Ann Intern Med* 2008;148(11):810-9. doi: 10.7326/0003-4819-148-11-200806030-00003 [published Online First: 2008/06/04]

375. Beilby JP, O'Leary BA. Alpha 1-acid glycoprotein decreases recovery of total protein in urine when trichloroacetic acid is used to precipitate the proteins. *Clin Chem* 1990;36(3):565-7. [published Online First: 1990/03/01]

376. Miller WG, Bruns DE, Hortin GL, et al. Current issues in measurement and reporting of urinary albumin excretion. *Clin Chem* 2009;55(1):24-38. doi: 10.1373/clinchem.2008.106567 [published Online First: 2008/11/26]

377. Suzuki M, Ikawa S. [Circadian variations of urinary excretions of microproteins and N-acetyl-beta-D-glucosaminidase (NAG) during the ordinary activity day]. *Nihon Jinzo Gakkai Shi* 1990;32(6):673-82. [published Online First: 1990/06/01]

378. Buzio C, Mutti A, Capani F, et al. Circadian Rhythm of Proteinuria: Effects of an Evening Meat Meal. *Nephrology Dialysis Transplantation* 1989;4(4):266-70. doi: 10.1093/oxfordjournals.ndt.a091870

379. Koopman MG, Arisz L. Spectrum of diurnal rhythms in glomerular permeability in patients with membranous nephropathy. *Nephrol Dial Transplant* 1997;12 Suppl 2:47-52. [published Online First: 1997/01/01]

380. Barr DB, Wilder LC, Caudill SP, et al. Urinary creatinine concentrations in the U.S. population: implications for urinary biologic monitoring measurements. *Environ Health Perspect* 2005;113(2):192-200. doi: 10.1289/ehp.7337 [published Online First: 2005/02/03]

381. Baxmann AC, Ahmed MS, Marques NC, et al. Influence of muscle mass and physical activity on serum and urinary creatinine and serum cystatin C. *Clinical journal of the American Society of Nephrology : CJASN* 2008;3(2):348-54. doi: 10.2215/CJN.02870707 [published Online First: 2008/01/30]

382. Tynkevich E, Flamant M, Haymann J-P, et al. Decrease in urinary creatinine excretion in early stage chronic kidney disease. *PloS one* 2014;9(11):e111949-e49. doi: 10.1371/journal.pone.0111949

383. Jain RB. An improved approach to report creatinine-corrected analyte concentrations in urine. *Cogent Environmental Science* 2016;2(1):1259880. doi: 10.1080/23311843.2016.1259880

384. Lieberthal JG, Cuthbertson D, Carette S, et al. urinary biomarkers in relapsing antineutrophil cytoplasmic antibody-associated vasculitis. *J Rheumatol* 2013;40(5):674-83. doi: 10.3899/jrheum.120879 [published Online First: 2013/04/03]

385. Nagaraj N, Mann M. Quantitative analysis of the intra- and inter-individual variability of the normal urinary proteome. *J Proteome Res* 2011;10(2):637-45. doi: 10.1021/pr100835s [published Online First: 2010/12/04]

386. Denic A, Glassock RJ, Rule AD. Structural and Functional Changes With the Aging Kidney. *Adv Chronic Kidney Dis* 2016;23(1):19-28. doi: 10.1053/j.ackd.2015.08.004

387. Wuerzner G, Firsov D, Bonny O. Circadian glomerular function: from physiology to molecular and therapeutical aspects. *Nephrology Dialysis Transplantation* 2014;29(8):1475-80. doi: 10.1093/ndt/gft525

388. Jolly SE, Burrows NR, Chen S-C, et al. Racial and ethnic differences in albuminuria in individuals with estimated GFR greater than 60 mL/min/1.73 m(2): results from the Kidney Early Evaluation Program (KEEP). *American journal of kidney diseases : the*

official journal of the National Kidney Foundation 2010;55(3 Suppl 2):S15-S22. doi: 10.1053/j.ajkd.2009.09.034

389. Jarad G, Miner JH. Update on the glomerular filtration barrier. *Curr Opin Nephrol Hypertens* 2009;18(3):226-32. [published Online First: 2009/04/18]

390. Wolyniec W, Kasprowicz K, Rita-Tkachenko P, et al. Biochemical Markers of Renal Hypoperfusion, Hemoconcentration, and Proteinuria after Extreme Physical Exercise. *Medicina (Kaunas)* 2019;55(5) doi: 10.3390/medicina55050154 [published Online First: 2019/05/22]

391. Luks AM, Johnson RJ, Swenson ER. Chronic Kidney Disease at High Altitude. *J Am Soc Nephrol* 2008;19:2262-71.

392. Caravita S, Faini A, Baratto C, et al. Upward Shift and Steepening of the Blood Pressure Response to Exercise in Hypertensive Subjects at High Altitude. *J Am Heart Assoc* 2018;7:1-7.

393. West JB, Lahiri S, Gill MB, et al. Arterial oxygen saturation during exercise at high altitude. *Journal of Applied Physiology* 1962;17(4):617.

394. Jonk AM, van den Berg IP, Olfert IM, et al. Effect of acetazolamide on pulmonary and muscle gas exchange during normoxic and hypoxic exercise. *J Physiol* 2007;579(Pt 3):909-21. doi: 10.1113/jphysiol.2006.120949 [published Online First: 2007/01/16]

395. Levey AS, Bosch JP, Lewis JB, et al. A more accurate method to estimate glomerular filtration rate from serum creatinine: a new prediction equation. Modification of Diet in Renal Disease Study Group. *Ann Intern Med* 1999;130(6):461-70. [published Online First: 1999/03/13]

396. Bradwell AR, Myers SD, Beazley M, et al. Exercise Limitation of Acetazolamide at Altitude (3459 m). *Wilderness Environ Med* 2014;25:272-77.

397. Thompson PD, Arena R, Riebe D, et al. ACSM's new preparticipation health screening recommendations from ACSM's guidelines for exercise testing and prescription, ninth edition. *Curr Sports Med Rep* 2013;12(4):215-7. doi: 10.1249/JSR.0b013e31829a68cf [published Online First: 2013/07/16]

398. Poortmans JR, Labilloy D. The influence of work intensity on postexercise proteinuria. *Eur J Appl Physiol Occup Physiol* 1988;57(2):260-3. [published Online First: 1988/01/01]

399. Rangemark C, Lind H, Lindholm L, et al. Lisinopril reduces postexercise albuminuria more effectively than atenolol in primary hypertension. *Eur J Clin Pharmacol* 1996;49(4):267-71.

400. Esnault VLM, Potironjosse M, Testa A, et al. Captopril but Not Acebutolol, Prazosin or Indomethacin Decreases Postexercise Proteinuria. *Nephron* 1991;58(4):437-42. doi: Doi 10.1159/000186476

401. Kramer A, van den Hoven M, Rops A, et al. Induction of glomerular heparanase expression in rats with adriamycin nephropathy is regulated by reactive oxygen species and the renin-angiotensin system. *J Am Soc Nephrol* 2006;17:2513-20.

402. Brinkkoetter PT, Holtgrefe S, van der Woude FJ, et al. Angiotensin II type 1-receptor mediated changes in heparan sulfate proteoglycans in human SV40 transformed podocytes. *J Am Soc Nephrol* 2004;15(1):33-40. [published Online First: 2003/12/25]

403. van Det NF, Tamsma JT, van den Born J, et al. Differential effects of angiotensin II and transforming growth factor beta on the production of heparan sulfate proteoglycan by mesangial cells in vitro. *J Am Soc Nephrol* 1996;7(7):1015-23. [published Online First: 1996/07/01]

404. van Ginkel S, de Haan A, Woerdeman J, et al. Exercise intensity modulates capillary perfusion in correspondence with ACE I/D modulated serum angiotensin II levels. *Appl Transl Genom* 2015;4:33-7. doi: 10.1016/j.atg.2015.03.002 [published Online First: 2016/03/05]

405. Joyce KE, Balanos GM, Fountain A, et al. Hypoxia does not influence post-exercise proteinuria. *European Database of Sport Science* 2019(abstract)

406. Bradwell AR, Ashdown K, Rue C, et al. Acetazolamide reduces exercise capacity following a 5-day ascent to 4559 m in a randomised study. *BMJ Open Sport Exerc Med* 2018;4(1):e000302. doi: 10.1136/bmjsem-2017-000302 [published Online First: 2018/02/02]

407. Elisabeth E, Hannes G, Johannes B, et al. Effects of low-dose acetazolamide on exercise performance in simulated altitude. *Int J Physiol Pathophysiol Pharmacol* 2017;9(2):28-34. [published Online First: 2017/05/24]

408. Joyce KE, Lucas SJE, Bradwell AR. Acetazolamide can impair exercise performance; it depends upon the cohort studied. *Journal of Applied Physiology* 2020;128(5):1457-57. doi: 10.1152/japplphysiol.00173.2020

409. Ainslie PN. On the nature of research at high altitude: packing it all in! *Experimental Physiology* 2014;99(5):741-42. doi: https://doi.org/10.1113/expphysiol.2013.077362

410. Poortmans JR, Engels MF, Sellier M, et al. Urine protein excretion and swimming events. *Med Sci Sports Exerc* 1991;23(7):831-5. [published Online First: 1991/07/01]

411. Poortmans JR, Haralambie G. Biochemical changes in a 100 km run: proteins in serum and urine. *Eur J Appl Physiol Occup Physiol* 1979;40(4):245-54. [published Online First: 1979/03/01]

412. Flood FB. ALBUMINURIA AND HEMATURIA IN BOXERS. *Journal of the American Medical Association* 1959;171(12):1678-79. doi: 10.1001/jama.1959.73010300001014

413. Poortmans JR, Jourdain M, Heyters C, et al. Postexercise proteinuria in rowers. *Can J Sport Sci* 1990;15(2):126-30. [published Online First: 1990/06/01]

414. Montelpare WJ, Klentrou P, Thoden J. Continuous versus intermittent exercise effects on urinary excretion of albumin and total protein. *Journal of Science and Medicine in Sport* 2002;5(3):219-28. doi: 10.1016/S1440-2440(02)80006-8

415. Powers SK, Williams J. Exercise-induced hypoxaemia in highly trained athletes. *Sports Med* 1987;4(1):46-53. doi: 10.2165/00007256-198704010-00005 [published Online First: 1987/01/01]

416. Poortmans JR, Haggenmacher C, Vanderstraeten J. Postexercise proteinuria in humans and its adrenergic component. *J Sports Med Phys Fitness* 2001;41(1):95-100. [published Online First: 2001/04/24]

417. Koçer G, Sentürk UK, Kuru O, et al. Potential sources of oxidative stress that induce postexercise proteinuria in rats. *J Appl Physiol (1985)* 2008;104(4):1063-8. doi: 10.1152/japplphysiol.00581.2007 [published Online First: 2008/02/09]

418. Schoene RB, Lahiri S, Hackett PH, et al. Relationship of hypoxic ventilatory response to exercise performance on Mount Everest. *J Appl Physiol Respir Environ Exerc Physiol* 1984;56(6):1478-83. doi: 10.1152/jappl.1984.56.6.1478 [published Online First: 1984/06/01]

419. Riebe D, Franklin BA, Thompson PD, et al. Updating ACSM's Recommendations for Exercise Preparticipation Health Screening. *Med Sci Sports Exerc* 2015;47(11):2473-9. doi: 10.1249/mss.0000000000000664 [published Online First: 2015/10/17]

420. Whelton P, Carey R, Aronow W, et al. 2017 ACC/AHA/AAPA/ABC/ACPM/AGS/APhA/ASH/ASPC/NMA/PCNA Guideline for the Prevention, Detection, Evaluation, and Management of High Blood Pressure in Adults: A Report of the American College of Cardiology/American Heart Association Task Force on Clinical Practice Guidelines. *Hypertension* 2018;71(6):e13-e115. doi: 10.1161/HYP.0000000000000065

421. Netzer NC, Chytra R, Küpper T. Low intense physical exercise in normobaric hypoxia leads to more weight loss in obese people than low intense physical exercise in normobaric sham hypoxia. *Sleep Breath* 2008;12:129-34.

422. Roach RC, Hackett PH, Oelz O, et al. The 2018 Lake Louise Acute Mountain Sickness Score. *High Altitude Medicine & Biology* 2018;19(1):4-6. doi: 10.1089/ham.2017.0164

423. Borg GA. Psychophysical bases of perceived exertion. *Med Sci Sports Exerc* 1982;14(5):377-81. [published Online First: 1982/01/01]

424. Riebe D, Ehrman JK, Liguori G, et al. ACSM's guidelines for exercise testing and prescription. 10th ed. Philadelphia: Wolters Kluwer 2018.

425. Adachi J, Kumar C, Zhang Y, et al. The human urinary proteome contains more than 1500 proteins, including a large proportion of membrane proteins. *Genome Biol* 2006;7(9):R80. doi: 10.1186/gb-2006-7-9-R80 [published Online First: 2006/09/05]

426. Weil JV, Byrne-Quinn E, Sodal IE, et al. Hypoxic ventilatory drive in normal man. *The Journal of clinical investigation* 1970;49(6):1061-72. doi: 10.1172/JCI106322

427. Swanson GD, Bellville JW. Step changes in end-tidal CO2: methods and implications. *Journal of Applied Physiology* 1975;39(3):377-85. doi: 10.1152/jappl.1975.39.3.377

428. Katayama K, Sato K, Matsuo H, et al. Changes in ventilatory responses to hypercapnia and hypoxia after intermittent hypoxia in humans. *Respiratory Physiology & Neurobiology* 2005;146(1):55-65. doi: https://doi.org/10.1016/j.resp.2004.11.007

429. Goldberg S, Ollila HM, Lin L, et al. Analysis of Hypoxic and Hypercapnic Ventilatory Response in Healthy Volunteers. *PloS one* 2017;12(1):e0168930-e30. doi: 10.1371/journal.pone.0168930

430. Rebuck AS, Campbell EJ. A clinical method for assessing the ventilatory response to hypoxia. *Am Rev Respir Dis* 1974;109(3):345-50. doi: 10.1164/arrd.1974.109.3.345 [published Online First: 1974/03/01]

431. Peeri M, Kohanpour M-A, Sanavi S, et al. Effects of different intensities of aerobic exercise on proteinuria in hypoxia and normoxia conditions in young football players. *Diálisis y Trasplante* 2012;33(3):84-88. doi: https://doi.org/10.1016/j.dialis.2011.10.001

432. Lundby C, Sander M, Van Hall G, et al. Maximal exercise and muscle oxygen extraction in acclimatizing lowlanders and high altitude natives. *The Journal of Physiology* 2006;573(2):535-47. doi: 10.1113/jphysiol.2006.106765

433. O'Neill J, Jasionek G, Drummond SE, et al. Renal Cortical Oxygen Tension is Decreased Following Exposure to Long-term but not Short-term Intermittent Hypoxia in the Rat. *Am J Physiol Renal Physiol* 2019 doi: 10.1152/ajprenal.00254.2018 [published Online First: 2019/01/17]

434. Bernardi L, Schneider A, Pomidori L, et al. Hypoxic ventilatory response in successful extreme altitude climbers. *European Respiratory Journal* 2006;27(1):165-71. doi: 10.1183/09031936.06.00015805

435. Cibella F, Cuttitta G, Romano S, et al. Respiratory energetics during exercise at high altitude. *J Appl Physiol (1985)* 1999;86(6):1785-92. doi: 10.1152/jappl.1999.86.6.1785 [published Online First: 1999/06/16]

436. Schoene RB. Limits of human lung function at high altitude. *J Exp Biol* 2001;204(Pt 18):3121-7. [published Online First: 2001/10/03]

437. Tadida Meli I, Tankeu A, Dehayem M, et al. Exercise-induced albuminuria vs circadian variations in blood pressure in type 1 diabetes. *World J Diabetes* 2017;8(2):74-79. doi: 10.4239/wjd.v8.i2.74

438. Middlekauff Holly R, Nitzsche Egbert U, Hoh Carl K, et al. Exaggerated Renal Vasoconstriction During Exercise in Heart Failure Patients. *Circulation* 2000;101(7):784-89. doi: 10.1161/01.CIR.101.7.784

439. van Someren K, Howatson G, Nunan D, et al. Comparison of the Lactate Pro and Analox GM7 blood lactate analysers. *International journal of sports medicine* 2005;26(8):657-61.

440. Pyne DB, Boston T, Martin DT, et al. Evaluation of the Lactate Pro blood lactate analyser. *European Journal of Applied Physiology* 2000;82(1):112-16. doi: 10.1007/s004210050659

441. Bonaventura JM, Sharpe K, Knight E, et al. Reliability and accuracy of six hand-held blood lactate analysers. *Journal of sports science & medicine* 2015;14(1):203-14.

442. Rao F, Wessel J, Wen G, et al. Renal Albumin Excretion. *Hypertension* 2007;49(5):1015-31. doi: 10.1161/HYPERTENSIONAHA.106.081679

443. Masuo K, Lambert GW, Esler MD, et al. The role of sympathetic nervous activity in renal injury and end-stage renal disease. *Hypertens Res* 2010;33(6):521-28. doi: 10.1038/hr.2010.35

444. Sun X, Li L, Overdier KH, et al. Analysis of Total Human Urinary Glycosaminoglycan Disaccharides by Liquid Chromatography-Tandem Mass Spectrometry. *Anal Chem* 2015;87(12):6220-7. doi: 10.1021/acs.analchem.5b00913 [published Online First: 2015/05/26]

445. Schmidt EP, Overdier KH, Sun X, et al. Urinary Glycosaminoglycans Predict Outcomes in Septic Shock and Acute Respiratory Distress Syndrome. *American journal of respiratory and critical care medicine* 2016;194(4):439-49. doi: 10.1164/rccm.201511-2281OC

446. Gyurászová M, Gurecká R, Bábíčková J, et al. Oxidative Stress in the Pathophysiology of Kidney Disease: Implications for Noninvasive Monitoring and Identification of Biomarkers. *Oxidative Medicine and Cellular Longevity* 2020;2020:5478708. doi: 10.1155/2020/5478708

447. Yoshioka T, Ichikawa I, Fogo A. Reactive oxygen metabolites cause massive, reversible proteinuria and glomerular sieving defect without apparent ultrastructural abnormality. *J Am Soc Nephrol* 1991;2(4):902-12. [published Online First: 1991/10/01]

448. Sanders M, Rasmussen S, Cooper D, et al. Renal and intrarenal blood flow distribution in swine during severe exercise. *J Appl Physiol* 1976;40(6):932-5. doi: 10.1152/jappl.1976.40.6.932 [published Online First: 1976/06/01]

449. Prinzen FW, Bassingthwaighte JB. Blood flow distributions by microsphere deposition methods. *Cardiovasc Res* 2000;45(1):13-21. doi: 10.1016/s0008-6363(99)00252-7

450. Ruf B, Bonelli V, Balling G, et al. Intraoperative renal near-infrared spectroscopy indicates developing acute kidney injury in infants undergoing cardiac surgery with cardiopulmonary bypass: a case-control study. *Crit Care* 2015;19(1):27-27. doi: 10.1186/s13054-015-0760-9

451. Steele AR, Tymko MM, Meah VL, et al. Global REACH 2018: Renal oxygen delivery is maintained during early acclimatization to 4330 m. *American Journal of Physiology-Renal Physiology* 2020 doi: 10.1152/ajprenal.00372.2020

452. Hwu D-W, Lin K-D, Lin K-C, et al. The association of obstructive sleep apnea and renal outcomes—a systematic review and meta-analysis. *BMC Nephrology* 2017;18(1):313. doi: 10.1186/s12882-017-0731-2

453. Burgess KR, Johnson PL, Edwards N. Central and obstructive sleep apnoea during ascent to high altitude. *Respirology* 2004;9(2):222-29. doi: 10.1111/j.1440-1843.2004.00576.x

454. Burgess KR, Johnson P, Edwards N, et al. Acute mountain sickness is associated with sleep desaturation at high altitude. *Respirology* 2004;9(4):485-92. doi: 10.1111/j.1440-1843.2004.00625.x [published Online First: 2004/12/23]

455. Luks AM, Swenson ER. Pulse Oximetry at High Altitude. *High Alt Med Biol* 2011;12(2):109-20.

456. Tannheimer M, Thomas A, Gerngross H. Oxygen saturation course and altitude symptomatology during an expedition to broad peak (8047 m). *Int J Sports Med* 2002;23(5):329-35. doi: 10.1055/s-2002-33144 [published Online First: 2002/08/08]

457. Kidd LR, Duncan C, Mason NP. Variations in Pulse Oximetry at High Altitude. *High Alt Med Biol* 2013;14(1):87.

458. Nespoulet H, Wuyam B, Tamisier R, et al. Altitude illness is related to low hypoxic chemoresponse and low oxygenation during sleep. *European Respiratory Journal* 2012;40(3):673. doi: 10.1183/09031936.00073111

459. Erba P, Anastasi S, Senn O, et al. Acute mountain sickness is related to nocturnal hypoxemia but not to hypoventilation. *European Respiratory Journal* 2004;24(2):303. doi: 10.1183/09031936.04.00006504

460. Cross TJ, Ross-Keller M, Issa A, et al. The Impact of Averaging Window Length on the "Desaturation" Indexes Obtained Via Overnight Pulse Oximetry at High Altitude. *SLEEP* 2015; 38(8):1331-34.

461. Tannheimer M, Kirsten J, Treff G, et al. Usability of Pulse Oximetry During Severe Physical Exercise at High Altitude. *Deutsche Zeitschrift f¸r Sportmedizin* 2018;Volume 69(No. 11):351-54.

462. Lin SH, Branson C, Leung J, et al. Oximetry as an Accurate Tool for Identifying Moderate to Severe Sleep Apnea in Patients With Acute Stroke. *J Clin Sleep Med* 2018;14(12):2065-73. doi: 10.5664/jcsm.7538

463. Marcos JV, Hornero R, Alvarez D, et al. Assessment of four statistical pattern recognition techniques to assist in obstructive sleep apnoea diagnosis from nocturnal oximetry. *Med Eng Phys* 2009;31(8):971-8. doi: 10.1016/j.medengphy.2009.05.010 [published Online First: 2009/07/14]

464. Terrill PI. A review of approaches for analysing obstructive sleep apnoea-related patterns in pulse oximetry data. *Respirology* 2019 doi: 10.1111/resp.13635 [published Online First: 2019/06/28]

465. Terrill PI, Dakin C, Edwards BA, et al. A graphical method for comparing nocturnal oxygen saturation profiles in individuals and populations: Application to healthy infants and preterm neonates. *Pediatr Pulmonol* 2018;53(5):645-55. doi: 10.1002/ppul.23987 [published Online First: 2018/03/27]

466. Terrill PI, Dakin C, Hughes I, et al. Nocturnal oxygen saturation profiles of healthy term infants. *Arch Dis Child* 2015;100(1):18-23. doi: 10.1136/archdischild-2013-305708 [published Online First: 2014/07/27]

467. Harigopal S, Satish HP, Taktak AF, et al. Oxygen saturation profi le in healthy preterm infants. *Arch Dis Child Fetal Neonatal Ed* 2011;96:F339–F42.

468. Mandolesi G, Avancini G, Bartesaghi M, et al. Long-term monitoring of oxygen saturation at altitude can be useful in predicting the subsequent development of moderate-to-severe acute mountain sickness. *Wilderness Environ Med* 2014;25(4):384-91.

469. Wang C, Jiang H, Duan J, et al. Exploration of Acute Phase Proteins and Inflammatory Cytokines in Early Stage Diagnosis of Acute Mountain Sickness. *High Altitude Medicine & Biology* 2018;19(2):170-77. doi: 10.1089/ham.2017.0126

470. Seifi S, Khatony A, Moradi G, et al. Accuracy of pulse oximetry in detection of oxygen saturation in patients admitted to the intensive care unit of heart surgery: comparison of finger, toe, forehead and earlobe probes. *BMC Nurs* 2018;17:15. doi: 10.1186/s12912-018-0283-1 [published Online First: 2018/04/26]

471. Roach RC, Hackett PH, Oelz O, et al. The 2018 Lake Louise Acute Mountain Sickness Score. *High Alt Med Biol* 2018;19(1):4-6. doi: 10.1089/ham.2017.0164 [published Online First: 2018/03/28]

472. Brodmann Maeder M, Brugger H, Pun M, et al. The STAR Data Reporting Guidelines for Clinical High Altitude Research. *High Alt Med Biol* 2018;19(1):7-14. doi: 10.1089/ham.2017.0160 [published Online First: 2018/03/30]

473. Stevens LA, Coresh J, Schmid CH, et al. Estimating GFR using serum cystatin C alone and in combination with serum creatinine: a pooled analysis of 3,418 individuals with CKD. *Am J Kidney Dis* 2008;51(3):395-406. doi: 10.1053/j.ajkd.2007.11.018 [published Online First: 2008/02/26]

474. Delanghe J, Speeckaert M. Preanalytical requirements of urinalysis. *Biochem Med (Zagreb)* 2014;24(1):89-104. doi: 10.11613/bm.2014.011 [published Online First: 2014/03/15]

475. Herrington W, Illingworth N, Staplin N, et al. Effect of Processing Delay and Storage Conditions on Urine Albumin-to-Creatinine Ratio. *Clin J Am Soc Nephrol* 2016;11(10):1794-801. doi: 10.2215/cjn.13341215 [published Online First: 2016/09/23]

476. Aziz N, Fahey JL, Detels R, et al. Analytical Performance of a Highly Sensitive C-Reactive Protein-Based Immunoassay and the Effects of Laboratory Variables on Levels of Protein in Blood. *Clinical and Diagnostic Laboratory Immunology* 2003;10(4):652-57. doi: 10.1128/cdli.10.4.652-657.2003

477. Taha BH, Dempsey JA, Weber SM, et al. Automated detection and classification of sleep-disordered breathing from conventional polysomnography data. *Sleep* 1997;20(11):991-1001. doi: 10.1093/sleep/20.11.991 [published Online First: 1998/02/11]

478. Kim H-Y. Statistical notes for clinical researchers: assessing normal distribution (2) using skewness and kurtosis. *Restorative Denstistry & Endodontics* 2013:52-54. doi: http://dx.doi.org/10.5395/rde.2013.38.1.52

479. West S, Finch J, Curran P. Structural equation modeling: Concepts, issues, and applications. Newbery Park, CA: Sage 1995:p56-75.

480. Buekers J, Theunis J, De Boever P, et al. Wearable Finger Pulse Oximetry for Continuous Oxygen Saturation Measurements During Daily Home Routines of Patients With Chronic Obstructive Pulmonary Disease (COPD) Over One Week: Observational Study. *JMIR Mhealth Uhealth* 2019;7(6):e12866. doi: 10.2196/12866 [published Online First: 2019/06/15]

481. Kulkas A, Duce B, Leppanen T, et al. Severity of desaturation events differs between hypopnea and obstructive apnea events and is modulated by their duration in obstructive sleep apnea. *Sleep Breath* 2017;21(4):829-35. doi: 10.1007/s11325-017-1513-6 [published Online First: 2017/06/07]

482. Muraja-Murro A, Kulkas A, Hiltunen M, et al. The severity of individual obstruction events is related to increased mortality rate in severe obstructive sleep apnea. *J Sleep Res* 2013;22(6):663-9. doi: 10.1111/jsr.12070 [published Online First: 2013/08/14]

483. Jaffray DA, ed. Desaturation event characteristics and mortality risk in severe sleep apnea. World Congress on Medical Physics and Biomedical Engineering, June 7-12, 2015, Toronto, Canada; 2015 2015//; Cham. Springer International Publishing.

484. Azarbarzin A, Sands SA, Stone KL, et al. The hypoxic burden of sleep apnoea predicts cardiovascular disease-related mortality: the Osteoporotic Fractures in Men Study and the Sleep Heart Health Study. *European heart journal* 2019;40(14):1149-57. doi: 10.1093/eurheartj/ehy624

485. Within-group and between-group correlation : Illustration on noninvasive estimation of intracranial pressure.

486. Mukaka MM. Statistics corner: A guide to appropriate use of correlation coefficient in medical research. *Malawi Med J* 2012;24(3):69-71.

487. Costello J, Bhogal AS, Williams TB, et al. Effects of Normobaric Hypoxia on Oxygen Saturation Variability. *High Altitude Medicine & Biology* 2020;21(1):76-83. doi: 10.1089/ham.2019.0092

488. Torre-Bouscoulet L, Castorena-Maldonado A, Banos-Flores R, et al. [Agreement between oxygen desaturation index and apnea-hypopnea index in adults with suspected obstructive sleep apnea at an altitude of 2240 m]. *Arch Bronconeumol* 2007;43(12):649-54. doi: 10.1016/s1579-2129(07)60150-5 [published Online First: 2007/12/07]

489. Johnson PL, Edwards N, Burgess KR, et al. Sleep architecture changes during a trek from 1400 to 5000 m in the Nepal Himalaya. *J Sleep Res* 2010;19(1 Pt 2):148-56. doi: 10.1111/j.1365-2869.2009.00745.x [published Online First: 2009/08/12]

490. Bloch KE, Latshang TD, Turk AJ, et al. Nocturnal periodic breathing during acclimatization at very high altitude at Mount Muztagh Ata (7,546 m). *Am J Respir Crit Care Med* 2010;182(4):562-8. doi: 10.1164/rccm.200911-1694OC [published Online First: 2010/05/06]

491. Nussbaumer-Ochsner Y, Ursprung J, Siebenmann C, et al. Effect of short-term acclimatization to high altitude on sleep and nocturnal breathing. *Sleep* 2012;35(3):419-23. doi: 10.5665/sleep.1708 [published Online First: 2012/03/02]

492. Clarenbach CF, Senn O, Christ AL, et al. Lung function and breathing pattern in subjects developing high altitude pulmonary edema. *PLoS One* 2012;7(7):e41188. doi: 10.1371/journal.pone.0041188 [published Online First: 2012/07/26]

493. Chen F, Chen K, Zhang C, et al. Evaluating the clinical value of the hypoxia burden index in patients with obstructive sleep apnea. *Postgrad Med* 2018;130(4):436-41. doi: 10.1080/00325481.2018.1465326 [published Online First: 2018/04/21]

494. Ross EM, Matteucci MJ, Shepherd M, et al. Measuring Arterial Oxygenation in a High Altitude Field Environment: Comparing Portable Pulse Oximetry With Blood Gas Analysis. *Wilderness & Environmental Medicine* 2013;24(2):112-17. doi: 10.1016/j.wem.2012.11.009

495. Glanfield M. High altitude testing of pulse oximeter. *Bmj* 1988;297(6662):1516. doi: 10.1136/bmj.297.6662.1516 [published Online First: 1988/12/10]

496. Tannheimer M, Lechner R. The correct measurement of oxygen saturation at high altitude. *Sleep and Breathing* 2019;23(4):1101-06. doi: 10.1007/s11325-019-01784-9

497. Arias RS, Etienne B, Polotsky VY, et al. Upright posture increases oxyhemoglobin saturation in Peruvian highlanders. *Respir Physiol Neurobiol* 2019;266:138-43. doi: 10.1016/j.resp.2019.04.015 [published Online First: 2019/05/03]

498. Tannheimer M, van der Spek R, Brenner F, et al. Oxygen saturation increases over the course of the night in mountaineers at high altitude (3050–6354 m). *Journal of Travel Medicine* 2017;24(5):1-6.

499. Robinson RR, Glenn WG. Fixed and reproducible orthostatic proteinuria IV. Urinary albumin excretion by healthy human subjects in the recumbent and upright postures. *The Journal of Laboratory and Clinical Medicine* 1964;64(5):717-23. doi: 10.5555/uri:pii:0022214364900964

500. Montagna G, Buzio C, Calderini C, et al. Relationship of proteinuria and albuminuria to posture and to urine collection period. *Nephron* 1983;35(2):143-4. doi: 10.1159/000183064 [published Online First: 1983/01/01]

501. Elsharkawi I, Gozal D, Macklin EA, et al. Urinary biomarkers and obstructive sleep apnea in patients with Down syndrome. *Sleep Med* 2017;34:84-89. doi: 10.1016/j.sleep.2017.02.005 [published Online First: 2017/03/07]

502. Turek NF, Ricardo AC, Lash JP. Sleep disturbances as nontraditional risk factors for development and progression of CKD: review of the evidence. *Am J Kidney Dis* 2012;60(5):823-33. doi: 10.1053/j.ajkd.2012.04.027 [published Online First: 2012/06/26]

503. Yao M, Tachibana N, Okura M, et al. The relationship between sleep-disordered breathing and high-sensitivity C-reactive protein in Japanese men. *Sleep* 2006;29(5):661-5. [published Online First: 2006/06/16]

504. Johnson JT, Lindsay I, Day RW, et al. Living at Altitude Adversely Affects Survival Among Patients With a Fontan Procedure. *Journal of the American College of Cardiology* 2013;61(12):1283-89. doi: https://doi.org/10.1016/j.jacc.2013.01.008

505. Sumanth MS, Jacob SP, Abhilasha KV, et al. Differential glycosylation of alpha-1-acid glycoprotein (AGP-1) contributes to its functional diversity. *bioRxiv* 2020:2020.02.27.968974. doi: 10.1101/2020.02.27.968974

506. Hamilton SM, Johnston MG, Fong A, et al. Relationship between increased vascular permeability and extravascular albumin clearance in rabbit inflammatory responses induced with Escherichia coli. *Lab Invest* 1986;55(5):580-7. [published Online First: 1986/11/01]

507. Morganti A, Giussani M, Sala C, et al. Effects of exposure to high altitude on plasma endothelin-1 levels in normal subjects. *J Hypertens* 1995;13(8):859-65. doi: 10.1097/00004872-199508000-00006 [published Online First: 1995/08/01]

508. Modesti PA, Vanni S, Morabito M, et al. Role of endothelin-1 in exposure to high altitude: Acute Mountain Sickness and Endothelin-1 (ACME-1) study. *Circulation* 2006;114(13):1410-6. doi: 10.1161/CIRCULATIONAHA.105.605527 [published Online First: 2006/09/20]

509. Haditsch B, Roessler A, Hinghofer-Szalkay HG. Renal adrenomedullin and high altitude diuresis. *Physiol Res* 2007;56(6):779-87. [published Online First: 2006/11/08]

510. Garsen M, Lenoir O, Rops ALWMM, et al. Endothelin-1 Induces Proteinuria by Heparanase-Mediated Disruption of the Glomerular Glycocalyx. *Journal of the American Society of*

Nephrology : JASN 2016;27(12):3545-51. doi: 10.1681/ASN.2015091070 [published Online First: 2016/03/29]

511. Rops ALWMM, van der Vlag J, Lensen JFM, et al. Heparan sulfate proteoglycans in glomerular inflammation. *Kidney International* 2004;65(3):768-85. doi: https://doi.org/10.1111/j.1523-1755.2004.00451.x

512. van den Born J, van den Heuvel LP, Bakker MA, et al. Distribution of GBM heparan sulfate proteoglycan core protein and side chains in human glomerular diseases. *Kidney Int* 1993;43(2):454-63. doi: 10.1038/ki.1993.67 [published Online First: 1993/02/01]

513. Salmon AH, Ferguson JK, Burford JL, et al. Loss of the endothelial glycocalyx links albuminuria and vascular dysfunction. *J Am Soc Nephrol* 2012;23(8):1339-50. doi: 10.1681/asn.2012010017 [published Online First: 2012/07/17]

514. Woodcock TE, Woodcock TM. Revised Starling equation and the glycocalyx model of transvascular fluid exchange: an improved paradigm for prescribing intravenous fluid therapy. *BJA: British Journal of Anaesthesia* 2012;108(3):384-94. doi: 10.1093/bja/aer515

515. McCurdy TR, Bhakta V, Eltringham-Smith LJ, et al. In vivo Clearance of Alpha-1 Acid Glycoprotein Is Influenced by the Extent of Its N-Linked Glycosylation and by Its Interaction with the Vessel Wall. *Journal of Biomedicine and Biotechnology* 2012;2012:292730. doi: 10.1155/2012/292730

516. Barton M. Therapeutic potential of endothelin receptor antagonists for chronic proteinuric renal disease in humans. *Biochimica et Biophysica Acta (BBA) - Molecular Basis of Disease* 2010;1802(12):1203-13. doi: https://doi.org/10.1016/j.bbadis.2010.03.012

517. Zaccaria M, Rocco S, Noventa D, et al. Sodium regulating hormones at high altitude: basal and post-exercise levels. *J Clin Endocrinol Metab* 1998;83(2):570-4. doi: 10.1210/jcem.83.2.4578 [published Online First: 1998/02/19]

518. Oberleithner H, Callies C, Kusche-Vihrog K, et al. Potassium softens vascular endothelium and increases nitric oxide release. *Proc Natl Acad Sci U S A* 2009;106(8):2829-34. doi: 10.1073/pnas.0813069106 [published Online First: 2009/02/10]

519. Sharma M, McCarthy ET, Savin VJ, et al. Nitric oxide preserves the glomerular protein permeability barrier by antagonizing superoxide. *Kidney Int* 2005;68(6):2735-44. doi: 10.1111/j.1523-1755.2005.00744.x [published Online First: 2005/12/01]

520. Li B, Yao J, Morioka T, et al. Nitric oxide increases albumin permeability of isolated rat glomeruli via a phosphorylation-dependent mechanism. *J Am Soc Nephrol* 2001;12(12):2616-24. [published Online First: 2001/12/01]

521. Richalet JP, Hornych A, Rathat C, et al. Plasma prostaglandins, leukotrienes and thromboxane in acute high altitude hypoxia. *Respiration Physiology* 1991;85(2):205-15. doi: https://doi.org/10.1016/0034-5687(91)90062-N

522. Brahmachari HD, Malhotra MS, Joseph S, et al. Effects of stay at high altitude on the serum proteins of man. *Indian J Physiol Pharmacol* 1973;17(4):365-9. [published Online First: 1973/10/01]

523. Smolichev EP. The effect of high altitude on the protein composition of human blood. *Bulletin of Experimental Biology and Medicine* 1961;50(4):1053-55. doi: 10.1007/BF00784878

524. Feddersen B, Ausserer H, Haditsch B, et al. Brain natriuretic peptide at altitude: relationship to diuresis, natriuresis, and mountain sickness. *Aviat Space Environ Med* 2009;80(2):108-11. doi: 10.3357/asem.2390.2009 [published Online First: 2009/02/10]

525. Ramchandra R, Barrett CJ. Regulation of the renal sympathetic nerves in heart failure. *Frontiers in physiology* 2015;6:238-38. doi: 10.3389/fphys.2015.00238

526. Li J, He Q, Wu W, et al. Role of the renal sympathetic nerves in renal sodium/potassium handling and renal damage in spontaneously hypertensive rats. *Exp Ther Med* 2016;12(4):2547-53. doi: 10.3892/etm.2016.3669 [published Online First: 2016/09/06]

527. Salman IM, Sattar MA, Abdullah NA, et al. Role of renal sympathetic nervous system in the control of renal potassium handling. *J Nephrol* 2010;23(3):291-6. [published Online First: 2010/03/30]

528. Yamamoto M. [Mechanism of ventilatory and heart-rate responses during sustained hypoxia in humans--role of endogenous adenosine]. *Hokkaido Igaku Zasshi* 1997;72(6):583-96. [published Online First: 1998/02/18]

529. Kato H, Menon AS, Slutsky AS. Mechanisms mediating the heart rate response to hypoxemia. *Circulation* 1988;77(2):407-14. doi: 10.1161/01.cir.77.2.407 [published Online First: 1988/02/01]

530. Masuyama S, Shinozaki T, Kohchiyama S, et al. Heart rate depression during sleep apnea depends on hypoxic chemosensitivity. A study at high altitude. *The American review of respiratory disease* 1990;141(1):39-42. doi: 10.1164/ajrccm/141.1.39

531. Leung RST, Bradley TD. Respiratory modulation of heart rate and blood pressure during Cheyne-Stokes respiration. *Journal of Electrocardiology* 2003;36:213-17. doi: https://doi.org/10.1016/j.jelectrocard.2003.09.062

532. Selcoki Y, Uz B, Baybek N, et al. The effects of nocturnal dipping on cardiovascular outcomes and proteinuria in essential hypertensive patients. *Central European Journal of Medicine* 2008;3(3):279-86. doi: 10.2478/s11536-008-0009-y

533. Sakaguchi Y, Shoji T, Kawabata H, et al. High prevalence of obstructive sleep apnea and its association with renal function among nondialysis chronic kidney disease patients in Japan: a cross-sectional study. *Clin J Am Soc Nephrol* 2011;6(5):995-1000. doi: 10.2215/cjn.08670910 [published Online First: 2011/03/19]

534. Schmidt M, Ledderhos C, Honig A. Kidney function during arterial chemoreceptor stimulation. I. Influence of unilateral renal nerve section, bilateral cervical vagotomy, constant artificial ventilation, and carotid body chemoreceptor inactivation. *Biomed Biochim Acta* 1985;44(5):695-709. [published Online First: 1985/01/01]

535. Lukaski HC, Johnson PE, Bolonchuk WW, et al. Assessment of fat-free mass using bioelectrical impedance measurements of the human body. *Am J Clin Nutr* 1985;41(4):810-7. doi: 10.1093/ajcn/41.4.810 [published Online First: 1985/04/01]

536. Saunders MJ, Blevins JE, Broeder CE. Effects of hydration changes on bioelectrical impedance in endurance trained individuals. *Med Sci Sports Exerc* 1998;30(6):885-92. doi: 10.1097/00005768-199806000-00017 [published Online First: 1998/06/13]

537. Morin C, Gandy J, Brazeilles R, et al. Fluid intake patterns of children and adolescents: results of six Liq.In7 national cross-sectional surveys. *European Journal of Nutrition* 2018;57(3):113-23. doi: 10.1007/s00394-018-1725-y

538. Beck J, Loron G, Masson C, et al. Monitoring Cerebral and Renal Oxygenation Status during Neonatal Digestive Surgeries Using Near Infrared Spectroscopy. *Front Pediatr* 2017;5:140-40. doi: 10.3389/fped.2017.00140

539. Harer MW, Chock VY. Renal Tissue Oxygenation Monitoring-An Opportunity to Improve Kidney Outcomes in the Vulnerable Neonatal Population. *Front Pediatr* 2020;8:241-41. doi: 10.3389/fped.2020.00241

540. Höpfl G, Ogunshola O, Gassmann M. Hypoxia and high altitude. The molecular response. *Adv Exp Med Biol* 2003;543:89-115. doi: 10.1007/978-1-4419-8997-0_7 [published Online First: 2004/01/10]

541. Nakuluri K, Mukhi D, Nishad R, et al. Hypoxia induces ZEB2 in podocytes: Implications in the pathogenesis of proteinuria. *J Cell Physiol* 2019;234(5):6503-18. doi: 10.1002/jcp.27387 [published Online First: 2018/09/22]

542. Nakuluri K, Mukhi D, Mungamuri SK, et al. Stabilization of hypoxia-inducible factor 1α by cobalt chloride impairs podocyte morphology and slit-diaphragm function. *J Cell Biochem* 2018 doi: 10.1002/jcb.28041 [published Online First: 2018/11/06]

543. Walter R, Maggiorini M, Scherrer U, et al. Effects of high-altitude exposure on vascular endothelial growth factor levels in man. *Eur J Appl Physiol* 2001;85(1-2):113-7. doi: 10.1007/s004210100419 [published Online First: 2001/08/22]

544. Izzedine H, Massard C, Spano JP, et al. VEGF signalling inhibition-induced proteinuria: Mechanisms, significance and management. *European Journal of Cancer* 2010;46(2):439-48. doi: https://doi.org/10.1016/j.ejca.2009.11.001

545. Singh A, Satchell SC, Neal CR, et al. Glomerular Endothelial Glycocalyx Constitutes a Barrier to Protein Permeability. *Journal of the American Society of Nephrology* 2007;18(11):2885. doi: 10.1681/ASN.2007010119

546. Satchell SC, Anderson KL, Mathieson PW. Angiopoietin 1 and Vascular Endothelial Growth Factor Modulate Human Glomerular Endothelial Cell Barrier Properties. *Journal of the American Society of Nephrology* 2004;15(3):566. doi: 10.1097/01.ASN.0000115397.22519.03

547. Flyvbjerg A, Dagnæs-Hansen F, De Vriese AS, et al. Amelioration of Long-Term Renal Changes in Obese Type 2 Diabetic Mice by a Neutralizing Vascular Endothelial Growth Factor Antibody. *Diabetes* 2002;51(10):3090. doi: 10.2337/diabetes.51.10.3090

548. Grimes DA, Schulz KF. An overview of clinical research: the lay of the land. *Lancet* 2002;359(9300):57-61. doi: 10.1016/s0140-6736(02)07283-5 [published Online First: 2002/01/26]

549. Gelman A, Hill J. Sample size and power calculations. In: Gelman A, Hill J, eds. Data Analysis Using Regression and Multilevel/Hierarchical Models. Cambridge: Cambridge University Press 2006:437-56.

550. Harris EK. Effects of Intra-and Interindividual Variation on the Appropriate Use of Normal Ranges. *Clinical Chemistry* 1974;20(12):1535-42. doi: 10.1093/clinchem/20.12.1535

551. Buderer NM. Statistical methodology: I. Incorporating the prevalence of disease into the sample size calculation for sensitivity and specificity. *Acad Emerg Med* 1996;3(9):895-900. doi: 10.1111/j.1553-2712.1996.tb03538.x [published Online First: 1996/09/01]

552. Bakdash JZ, Marusich LR. Repeated Measures Correlation. *Frontiers in psychology* 2017;8:456-56. doi: 10.3389/fpsyg.2017.00456

553. Warren L. The thiobarbituric acid assay of sialic acids. *J Biol Chem* 1959;234(8):1971-5. [published Online First: 1959/08/01]

554. Treuheit MJ, Costello CE, Halsall HB. Analysis of the five glycosylation sites of human alpha 1-acid glycoprotein. *The Biochemical journal* 1992;283 (Pt 1)(Pt 1):105-12. doi: 10.1042/bj2830105

555. Viazzi F, Leoncini G, Derchi LE, et al. Ultrasound Doppler renal resistive index: a useful tool for the management of the hypertensive patient. *Journal of hypertension* 2014;32(1):149-53. doi: 10.1097/HJH.0b013e328365b29c

556. Sun W, Zhang H, Guo J, et al. Comparison of the Efficacy and Safety of Different ACE Inhibitors in Patients With Chronic Heart Failure: A PRISMA-Compliant Network Meta-Analysis. *Medicine* 2016;95(6):e2554-e54. doi: 10.1097/MD.0000000000002554

557. Abraham HMA, White CM, White WB. The comparative efficacy and safety of the angiotensin receptor blockers in the management of hypertension and other cardiovascular diseases. *Drug Saf* 2015;38(1):33-54. doi: 10.1007/s40264-014-0239-7

558. Goncharov NV, Nadeev AD, Jenkins RO, et al. Markers and Biomarkers of Endothelium: When Something Is Rotten in the State. *Oxidative medicine and cellular longevity*

2017;2017:9759735-35. doi: 10.1155/2017/9759735 [published Online First: 2017/11/23]

559. Beall CM. Two routes to functional adaptation: Tibetan and Andean high-altitude natives. *Proceedings of the National Academy of Sciences* 2007;104(suppl 1):8655-60. doi: 10.1073/pnas.0701985104

560. Il'yasova D, Scarbrough P, Spasojevic I. Urinary biomarkers of oxidative status. *Clinica chimica acta; international journal of clinical chemistry* 2012;413(19-20):1446-53. doi: 10.1016/j.cca.2012.06.012 [published Online First: 2012/06/07]

561. Frijhoff J, Winyard PG, Zarkovic N, et al. Clinical Relevance of Biomarkers of Oxidative Stress. *Antioxid Redox Signal* 2015;23(14):1144-70. doi: 10.1089/ars.2015.6317 [published Online First: 2015/10/26]

562. Cao G, Prior RL. Comparison of different analytical methods for assessing total antioxidant capacity of human serum. *Clin Chem* 1998;44(6 Pt 1):1309-15. [published Online First: 1998/06/13]

563. Blezer ELA, Schurink M, Nicolay K, et al. Proteinuria Precedes Cerebral Edema in Stroke-Prone Rats. *Stroke* 1998;29(1):167-74. doi: doi:10.1161/01.STR.29.1.167

564. Blezer EL, Nicolay K, Koomans HA, et al. Losartan versus enalapril on cerebral edema and proteinuria in stroke-prone hypertensive rats. *Am J Hypertens* 2001;14(1):54-61. [published Online First: 2001/02/24]

565. Babiker M, Joyce KE, Fenton A, et al. Urinary alpha-1 acid glycoprotein and progression to end stage renal disease in chronic kidney disease. . UK Kidney Week. Brighton, UK, 2019.

566. Wesseling C, Glaser J, Rodríguez-Guzmán J, et al. Chronic kidney disease of non-traditional origin in Mesoamerica: a disease primarily driven by occupational heat stress. *Rev Panam Salud Publica* 2020;44:e15. doi: 10.26633/rpsp.2020.15 [published Online First: 2020/01/31]

567. Wijkström J, Leiva R, Elinder C-G, et al. Clinical and Pathological Characterization of Mesoamerican Nephropathy: A New Kidney Disease in Central America. *American Journal of Kidney Diseases* 2013;62(5):908-18. doi: 10.1053/j.ajkd.2013.05.019

568. Cooper C, Booth A, Varley-Campbell J, et al. Defining the process to literature searching in systematic reviews: a literature review of guidance and supporting studies. *BMC Medical Research Methodology* 2018;18(1):85. doi: 10.1186/s12874-018-0545-3

569. Pichler J, Risch L, Hefti U, et al. Glomerular filtration rate estimates decrease during high altitude expedition but increase with Lake Louise acute mountain sickness scores. *Acta Physiol (Oxf)* 2008;192(3):443-50. doi: 10.1111/j.1748-1716.2007.01758.x [published Online First: 2007/11/01]

570. Mishra KP, Ganju L. Influence of High Altitude Exposure on the Immune System: A Review. *Immunological Investigations* 2010;39(3):219-34. doi: 10.3109/08820131003681144

571. Olsen NV, Kanstrup IL, Richalet JP, et al. Effects of acute hypoxia on renal and endocrine function at rest and during graded exercise in hydrated subjects. *J Appl Physiol (1985)* 1992;73(5):2036-43. doi: 10.1152/jappl.1992.73.5.2036 [published Online First: 1992/11/01]

572. Biollaz J, Buclin T, Hildebrandt W, et al. No role for renal dysfunction and fluid imbalance in acute mountain sickness at 4,559 m. preprint

573. Huang C, Wang Y, Li X, et al. Clinical features of patients infected with 2019 novel coronavirus in Wuhan, China. *Lancet* 2020;395(10223):497-506. doi: 10.1016/s0140-6736(20)30183-5 [published Online First: 2020/01/28]